CHARACTERISING THE ROLE OF INFLAMMATORY PROCOAGULANT PHOSPHOLIPIDS IN ARTERIAL THROMBOSIS

MAJD BASHAR PROTTY

A THESIS SUBMITTED TO

CARDIFF UNIVERSITY

IN ACCORDANCE WITH THE REQUIREMENTS FOR THE

DEGREE OF

DOCTOR OF PHILOSOPHY (PHD)

2021

Acknowledgments

This PhD thesis has been one of the most challenging academic endeavours that I have had to face in my career so far. As I write this acknowledgement, I reflect on the journey that led me here today to achieve this lifelong ambition. Without the support, patience and guidance of the following people, it would not have been possible to complete this body of work. It is to them that I owe my deepest gratitude.

- My supervisors, Professor Valerie O'Donnell and Professor Peter Collins who guided me on this journey through all the highs and lows, and for being always available and approachable.
- My collaborators and enablers, Professor Zaheer Yousef, Dr Anirban Choudhury, Dr Rito Mitra, Mr Dave Bosanquet, Dr Vince Jenkins and Professor Alastair Poole. Without them and their teams, the study would not have taken off nor expanded the way it did.
- Members of the Cardiff Lipidomics group who listened to my rants and helped me re-focus when I most needed it ! Vikki, Daniela, James, Ali, Anastasia and Patricia to name a few.
- Clinical mentors and supporters who enabled me to continue being in contact with the cardiology cath lab and the clinical world, reminding me of why I was doing this research in the first place.
- All the participants who took part in the study, who always thanked me for taking an interest in advancing medical research and wished me luck on this journey.
- My funders, the Wellcome Trust GW4-CAT scheme, for their generous financial support and the numerous mentorship and training workshops organized by Jayne, Tracey and the programme directors.
- My parents, Bashar and Ban, for being the inspiration behind academic achievements in medicine and for providing motivational speeches when I needed them.
- My brother, Salam, who kept me abreast of the latest Netflix developments to facilitate much-needed headspace.
- Last, but by no means least, my wife, Sahar, and my two boys, Thomas and Peter, to whom I dedicate this thesis. You were always patient when I babbled on about recruitment, lab experiments, and seemingly endless writing. Without your support, I would not have achieved half of what I have so far.

SUMMARY

Arterial thrombosis is an inflammatory response triggered by atherosclerotic plaque rupture causing acute coronary syndromes (ACS), strokes and death. Clotting reactions require interactions of coagulation proteins with aminophospholipids (aPL) and enzymatically oxidized phospholipids (eoxPL) on the surface of blood cells. This thesis investigates the role of aPL and eoxPL in arterial thrombosis.

Using liquid chromatography with tandem mass spectrometry (LC-MS/MS), I quantified eoxPL generated in thrombin-activated platelets from a healthy cohort and demonstrated a large degree of inter- and intra-individual variation. Aspirin supplementation *in-vivo* reduced the amount of COX-1 derived eoxPL, but increased diacyl 12-hydroxyeicosatetraenoic acid (12-HETE) containing eoxPL (12-HETE-PL) generation without affecting the levels of free 12-HETE. This suggests that aspirin interferes with re-esterification pathways of 12-HETE to acyl lysophospholipids.

Lipidomic analysis of arterial thrombi extracted from patients undergoing clot retrieval procedures demonstrated the presence of HETE-PL, with a predominance of platelet-derived 12-HETE-PL. Using a clinical cohort, I demonstrated elevated thrombin generation on the surface of isolated EV and leukocytes, but not platelets, from patients with ACS versus healthy controls (HC). Lipidomic analysis demonstrated no differences between groups in HETE-PL amounts from resting platelets, leukocytes and EV. Nevertheless, as seen with the healthy cohort, thrombin-activated platelets from patients supplemented with aspirin had higher diacyl 12-HETE-PL generation. Finally, there were no differences in the fraction (%) externalized

phosphatidylethanolamine (%PE) on the surface of platelets and leukocytes across the groups. However, EV samples had lower %PE in ACS versus HC which, unlike platelets and leukocytes, correlated inversely with thrombin generation.

In summary, eoxPL were detected within arterial thrombi and their synthesis is increased with aspirin. Thrombin generation is higher on the surface of EV from ACS patients, which may be explained by differences in the aPL lipidome between groups. Further studies examining therapeutic agents targeting procoagulant lipids are needed.

ABBREVIATIONS

a.m.u	Atomic mass unit
AA	Arachidonic acid
AAA	Abdominal aortic aneurysm
ACD	Acid-citrate-dextrose
ACN	Acetonitrile
ACS	Acute coronary syndrome
ACSL	Long-chain fatty-acid CoA ligase
aPL	Aminophospholipids
ATP	Adenosine triphosphate
BHT	Butylated hydroxytoluene
Ca^{2+}	Calcium ion
CAD	Coronary artery disease
CoA	Co-enzyme A
COX	Cyclooxygenase
CRP	C-reactive protein
CVD	Cardiovascular disease
DHA	Docosahexaenoic acid
DiEHEDA	8,9-11,12-diepoxy-13-hydroxy-eicosadienoic acid
DMPC	1,2-dimyristoyl-sn-glycero-3-phosphocholine
DMPE	1,2-dimyristoyl-sn-glycero-3-phosphoethanolamine
DMPS	1,2-dimyristoyl-sn-glycero-3-phosphoserine
DMSO	Dimethyl sulfoxide
DOAC	Direct-acting oral anti-coagulant
DOPS	Dioleoyl-sn-glycero-3-phospho-L-serine
DTPA	Diethylenetriaminepentaacetate
EDTA	Ethylenediaminetetraacetic acid
EoxPL	Enzymatically oxidized phospholipids
EPA	Eicosapentaenoic acid
EV	Extracellular vesicles
FA	Fatty acid
GL	Glycerolipids
GP	Glycoprotein
GPX	Glutathione peroxidase
HC	Healthy control
HDOHE	Hydroxydocosahexaenoic acid
HETE	Hydroxytetraenoic acid
HPETE	Hydroperoxytetraenoic acid
HPLC	High performance liquid chromatography
IPA	Propan-2-ol
IS	Internal standard
KETE	Ketoeicosatetraenoic acid
LA	Linoleic acid
LC	Liquid chromatography
LC-MS/MS	Liquid chromatography coupled to tandem mass spectrometry
LDL	Low density lipoprotein
LOX	Lipoxygenase

LPAT	Lysophospholipid acyl transferase
m/z	Mass/charge ratio
MAPK	Mitogen-activated protein kinase
MBOAT	Membrane bound O-acyl transferase
MeOH	Methanol
MI	Myocardial infarction
MRM	Multiple reaction monitoring
MS	Mass spectrometry
MW	Molecular weight
NSAID	Non-steroidal anti-inflammatory drugs
NTA	Nanoparticle tracking analysis
OxLDL	Oxidized low density lipoprotein
oxPL	Oxidized phospholipids
PAR	Protease activated receptor
PBS	Phosphate-buffered saline
PC	Phosphatidylcholine
PCA	Principal component analysis
PCET	Proton-coupled electron transfer mechanism
PE	Phosphatidylethanolamine
PFP	Platelet-free plasma
PGH_2	Prostaglandin H_2
PGI_2	Prostaglandin I_2
PL	Phospholipids
PLA_1	Phospholipase A_1
PLA_2	Phospholipase A_2
PLC	Phospholipase C
PPP	Platelet-poor plasma
PRP	Platelet-rich plasma
PS	Phosphatidylserine
PUFA	Polyunsaturated fatty acids
RF	Risk Factor patient group (with no obstructive CAD)
SAPE	1-stearoyl-2-arachidonoyl-sn-glycero-3-phosphoethanolamine
SAPS	1-stearoyl-2-arachidonoyl-sn-glycero-3-phosphoserine
SEC	Size exclusion chromatography
SL	Sphingolipids
sn1/sn2	Stereospecific numbering
SOPS	1-stearoyl-2-oleoyl-sn-glycero-3-phospho-L-serine
SpAPE	1-(1Z-octadecenyl)-2-arachidonoyl-sn-glycero-3-phosphoethanolamine
TBS	Tris-buffered saline
TF	Tissue factor
TLR	Toll-like receptor
TxA_2	Thromboxane A_2
TxB_2	Thromboxane B_2
VSMC	Vascular smooth muscle cells
VWF	Von Willebrand factor

TABLE OF CONTENTS

CHAPTER 1 GENERAL INTRODUCTION

1.1 THE BURDEN OF CARDIOVASCULAR DISEASE ON MORBIDITY AND MORTALITY

Cardiovascular disease (CVD) is the biggest killer in the Western world and is responsible for 47% of all deaths in Europe every year[1]. In the United Kingdom, it is estimated that CVD is responsible for an average of 200 deaths on a daily basis, costing the economy £29 billion per year due to premature death, hospital treatment, prescriptions, and lost productivity[2]. These figures highlight the scope of the problem posed by CVD, despite the reductions in morbidity and mortality achieved over the last few decades in modifying population behaviour[3]. Research in this field therefore is critical in allowing us to better understand the underlying pathology and to establish strategies to aid its prevention and treatment.

The term CVD encompasses all disorders of the heart and the circulatory system, with the two main forms being coronary heart disease and cerebrovascular disease (stroke)[2]. Both these disease groups manifest with reduced blood flow to the heart or the brain as a result of arterial stenosis or arterial occlusion leading to ischaemia and/or infarction. The consequences of these may include disability, heart failure or indeed death[4].

Arterial stenosis is caused by atherosclerosis which is a chronic inflammatory disease process affecting the endothelial lining of arteries[5] and will be described in more details in section **1.4**. This process is responsible for conditions such as stable coronary artery disease (angina pectoris) and peripheral vascular disease. The presence of atherosclerosis paves the way for further morbidity caused by plaque rupture and thrombus formation. The formation of this thrombus may occlude the vessel in situ or embolize to a distant organ obstructing blood flow and causing subsequent tissue death, also known as 'infarction'. The process of thrombus formation as a consequence of atherosclerotic plaque rupture is known as 'athero-thrombosis' or 'arterial thrombosis' and is responsible for causing acute coronary syndrome (ACS) and the

majority of ischaemic strokes[6]. The pathophysiology underlying atherosclerosis and arterial thrombosis will be described in more details in sections **1.4.1** and **1.4.2**.

Despite recent advances in the treatment of arterial thrombosis, approximately 10-20% of patients receiving best medical therapy will go on to develop another myocardial infarction (MI), stroke or die from cardiovascular causes in the following few years[7,8]. At the current time, the best therapies for arterial thrombosis lie in antiplatelet and anticoagulant agents, the evidence base for which will be described in more detail in section **1.5**. However, it is recognized that platelets and other immune cells are important for providing a phospholipid (PL) membrane surface for the interaction of coagulation factors, as will be described in section **1.3**. In spite of this, the contribution of procoagulant PL membranes to arterial thrombosis or whether they vary between health and disease remains unexplored. To address this, one aim of my PhD will be to characterise the procoagulant PL within arterial thrombi as well as on the surface of platelets, leukocytes and extracellular vesicles (EVs) in patients with arterial thrombosis.

1.2 CELLULAR LIPIDS

Lipids are hydrophobic molecules found in all cell types and required for structural support, energy storage and signalling. They are derived from dietary sources or generated endogenously within the cell and exist in several forms including free fatty acids (FA), glycerolipids (GL), sphingolipids (SL) and sterols. Each of these categories contains large numbers of lipids with distinct molecular structures and basic properties. Thus they are classified according to common functional groups, structural motifs and other differences such as FA chain length and hydrocarbon saturation[9]. Their metabolism and transport is highly regulated by cellular proteins which include phospholipases, oxidases and lipid transports.

Of importance to this thesis are FA and PL. FA form the fundamental category of biological lipids and therefore the basic building blocks of more complex lipids. They comprise a hydrocarbon chain with a terminal carboxylic acid group and can be saturated or unsaturated depending on the number of double bonds [10,11]. Recent work by the LIPID MAPS consortium has agreed a notation for FA to describe the number of carbons and double bonds in a molecule[12]. For instance, stearic acid is described as FA 18:0 reflecting a fatty acid with 18 carbons and no double bonds. In contrast, arachidonic acid is described as FA 20:4 reflecting a fatty acid with 20 carbons and 4 double bonds, hence unsaturated. PL consist of a glycerol molecule which acts as the backbone for attachment to two fatty acyl chains forming a hydrophobic tail, and a phosphate headgroup forming a hydrophilic head, providing it with an 'amphipathic' structure that is essential in maintaining the integrity of cell membranes[13]. More details on the subtypes and nomenclature of PL will be described in section **1.2.1**.

Agonist-activation of circulating blood cells leads to significant changes to lipid composition and the formation of new biologically significant "bioactive" lipids which play a

key role in mediating signalling pathways both within the cell and with other cells[14]. In platelets for instance, stimulation with thrombin or collagen leads to structural alterations to the membrane including shape change, spreading and degranulation. Of relevance to this thesis, PL and oxylipins (oxygenated FA) have been demonstrated to be instrumental to inflammation, coagulation and haemostasis[9], as will be described in the sections below.

1.2.1 Phospholipids (PL)

In common with mammalian cells, the predominant group of structural lipids in platelets are PL. These amphiphatic lipids form the membranes of cells and organelles with the hydrophobic FA portion orientated to the core and polar phosphate-containing head groups facing the aqueous phase (**Figure 1.1**)[9,13]. Their presence was described in the 'fluid mosaic model' of plasma membranes where they form the fluid lipid-rich phase containing a mosaic of membrane proteins[15].

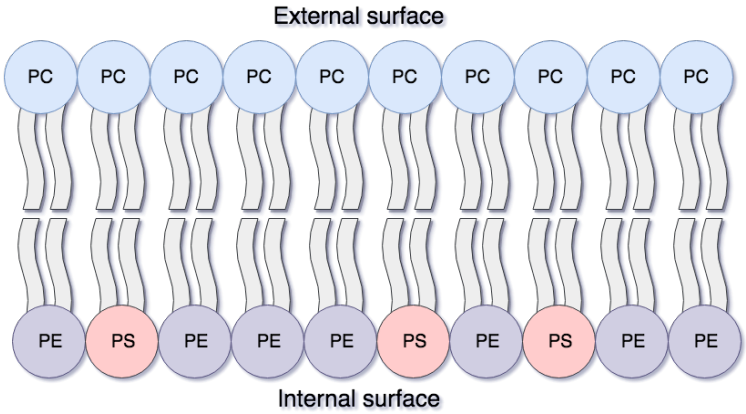

Figure 1.1. The phospholipid (PL) plasma membrane (a generic illustration).

Polarised PLs make up the membrane bilayer of all mammalian cells with phosphate head groups facing the aqueous phase, and hydrophobic fatty acids facing the core. Other lipids and proteins line the membrane, but are not shown in this figure. PS: phosphatidylserine, PE: phosphatidylethanolamine, PC: phosphatidylcholine.

Glycerol forms the backbone that links the PL head groups to the FA, with the latter attaching at the *sn1* and *sn2* positions (**Figure 1.2**). Generally, the *sn1* FA are saturated or monounsaturated and can be linked to the backbone with an acyl, alkyl (ether) group or alkenyl group (plasmalogen)[16]. In innate immune cells, plasmalogens with a phosphatidylethanolamine (PE) head-group are abundant and are reported to form just over 10% of total membrane PL molecules[17,18]. The vinyl ether bond is particularly vulnerable to reactive oxygen species, thus suggesting a protective role for plasmalogens in limiting oxidative damage to other lipid species and cells[18,19]. However, it remains unknown whether plasmalogens have a role in diseases known to generate oxygen free radicals, such as atherosclerosis.

The *sn2* FA are typically polyunsaturated (PUFA) with longer acyl chains[9,13]. A combination of these variations and the different FA can result in hundreds of unique PL species of which the most abundant contain palmitic acid (FA 16:0), stearic acid (FA 18:0), or oleic acid (FA 18:1) at *sn1*; and linoleic acid (LA; FA 18:2), arachidonic acid (AA; FA 20:4), eicosapentaenoic acid (EPA; FA 20:5), or docosahexaenoic acid (DHA; FA 22:6) at *sn2*. The agreed notation for PL is to start with the headgroup, and describe the *sn1* FA, include the type of bond ('a' for acyl, 'p' for plasmalogen, 'e' for ether), and the sn2 FA separated by a forward slash (/) character. An example of this is PE 18:0a/20:4 which describes 1-stearoyl-2-arachidonyl-phosphatidylethanolamine. When the *sn1/sn2* positions are uncertain, the slash is replaced with an underscore (_)[12].

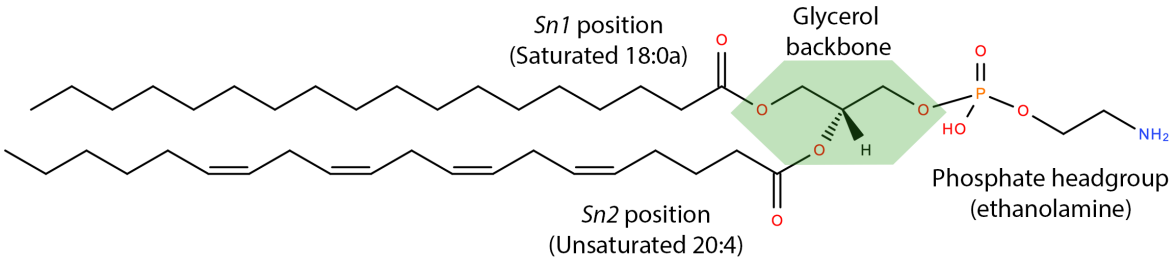

Figure 1.2. Example of a phospholipid molecule demonstrating the *sn1*/*sn2*/headgroup positions on the glycerol backbone.

In this example, 1-stearoyl-2-arachidonyl-phosphatidylethanolamine, or PE 18:0a/20:4, is demonstrated with the glycerol backbone highlighted in a green polygon. Structures drawn with the aid of tools on the LIPID MAPS resource.

Of note, AA is present in mammalian PLs with up to 10-fold higher concentrations than other PUFA in circulating blood cells such as platelets [13]. This is of particular relevance to this thesis as there is evidence that PL with longer unsaturated fatty acid chains support coagulation reactions somewhat better than shorter fatty acid chains[20]. The role of PL in supporting coagulation will be discussed in section **1.3.4**. In mammalian cells, there are five main classes of PL based on the polar head group (**Figure 1.3**), specifically PE, phosphatidylcholine (PC), phosphatidylglycerol (PG), phosphatidylinositol (PI) and phosphatidylserine (PS)[13]. The most common of these are PC and PE, which together amount to approximately two thirds of total PLs in innate immune cells[21].

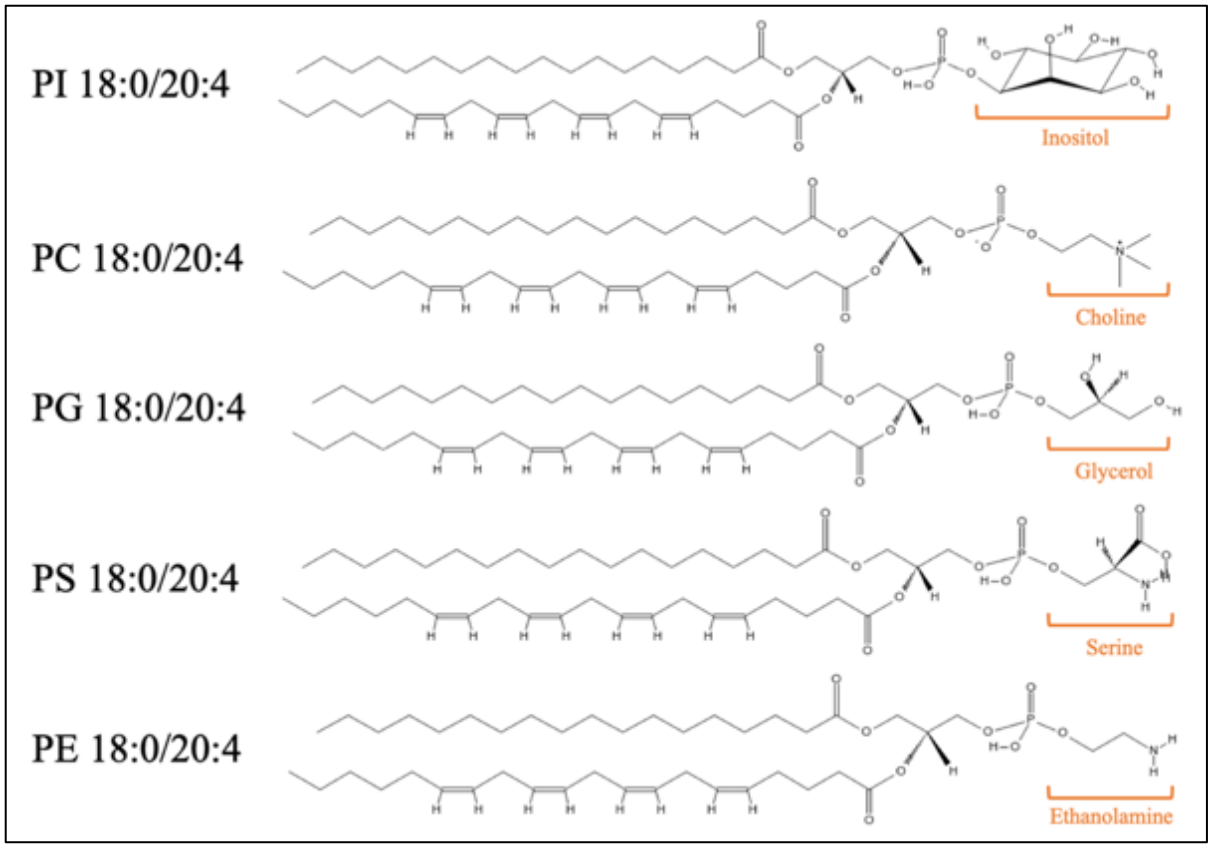

Figure 1.3. Phospholipid classes and chemical structures highlighting the phosphate head groups.

In these images, the *sn1* fatty acid is stearic acid (FA 18:0) and the *sn2* fatty acid is arachidonic acid (FA 20:4). The structures of the five head groups can also be seen (PI: phosphatidylinositol, PC: phosphatidylcholine, PG: phosphatidylglycerol, PS: phosphatidylserine, PE: phosphatidylethanolamine). Structures drawn with the aid of tools on the LIPID MAPS resource.

1.2.2 Native PL and membrane asymmetry

The PL membrane of resting circulating immune cells is asymmetric. Its external leaflet is composed predominantly of PC, which also makes up 40 % of total PL. In contrast, the cytosolic facing leaflet is enriched in PE and also PS, which is present at lower abundance[22,23] (**Figure 1.1**). This asymmetry of mostly neutral PL in the outer membrane and negatively charged PL in the inner membrane generates an electrical gradient which is regulated by transmembrane lipid transporters. The ATP-dependent flippase or translocase keep the negatively-charged aminophospholipids (aPL) PE and PS internally facing, whereas the activity of floppase, another ATP-dependent transporter, regulates the translocation of PC to the outer membrane[24].

Upon cell activation or apoptosis, PL membrane asymmetry is disrupted as a result of the rapid flux of negatively charged aPL to the outer surface. This is the result of activation of calcium-dependent scramblase which mediates bidirectional movement of PL[25]. Concurrently, the rise in intracellular calcium leads to the inactivation of both flippase and floppase which halts the processes responsible for maintaining asymmetry[22,24]. The net effect is the externalisation of aPL which alters the biophysical composition of the membrane and provides a negatively charged surface. This facilitates the binding of coagulation factors on the surface enabling generation of thrombin and fibrin (described below). Defects in this process are exemplified by Scott syndrome, a rare genetic disorder caused by a mutation to the TMEM16F scramblase protein, which causes an inability of platelets to externalise aPL, leading to a bleeding phenotype[13,26,27]. Despite an established role in promoting thrombin formation as part of haemostasis, it remains unknown whether PL alterations contribute to the pathology of arterial thrombosis, where persistent thrombin formation is noted[28].

1.2.3 Oxylipin generation

Activation of immune cells leads to hydrolysis of membrane PL via the action of phospholipase enzymes, such as phospholipase A_2 (PLA_2). These generate free polyunsaturated FA (PUFA) which can be oxygenated by one of three enzymatic pathways: cyclooxygenase (COX), lipoxygenase (LOX) or cytochrome p450 enzymes (CYP), resulting in the generation of oxylipins[9]. AA is one of the most abundant PUFA precursors for oxylipin generation in immune cells, playing a significant role in inflammation, thrombosis and haemostasis[13]. Group IV cytosolic isoforms of PLA_2 ($cPLA_2$) are highly specific for AA-containing PL and are regulated by the mitogen-activated protein kinase (MAPK) signalling pathway[29-31]. **Figure 1.4** depicts a simplified version of this pathway highlighting COX and LOX pathways.

There are two COX isoforms, the constitutively-expressed COX-1 and the inflammation-inducible COX-2[32]. Both convert AA to prostaglandin H_2 (PGH_2) which is then further metabolised by several cell-specific CYP enzymes. In platelets, the CYP enzyme thromboxane synthase converts PGH_2 to thromboxane A2 (TxA_2) which itself is a potent secondary activator of platelets[33]. It is worth noting that aspirin and non-steroidal anti-inflammatory medications (NSAIDs) work predominantly by inhibiting COXs. The effect of aspirin on platelet COX-1 will be described in section **1.5.1**.

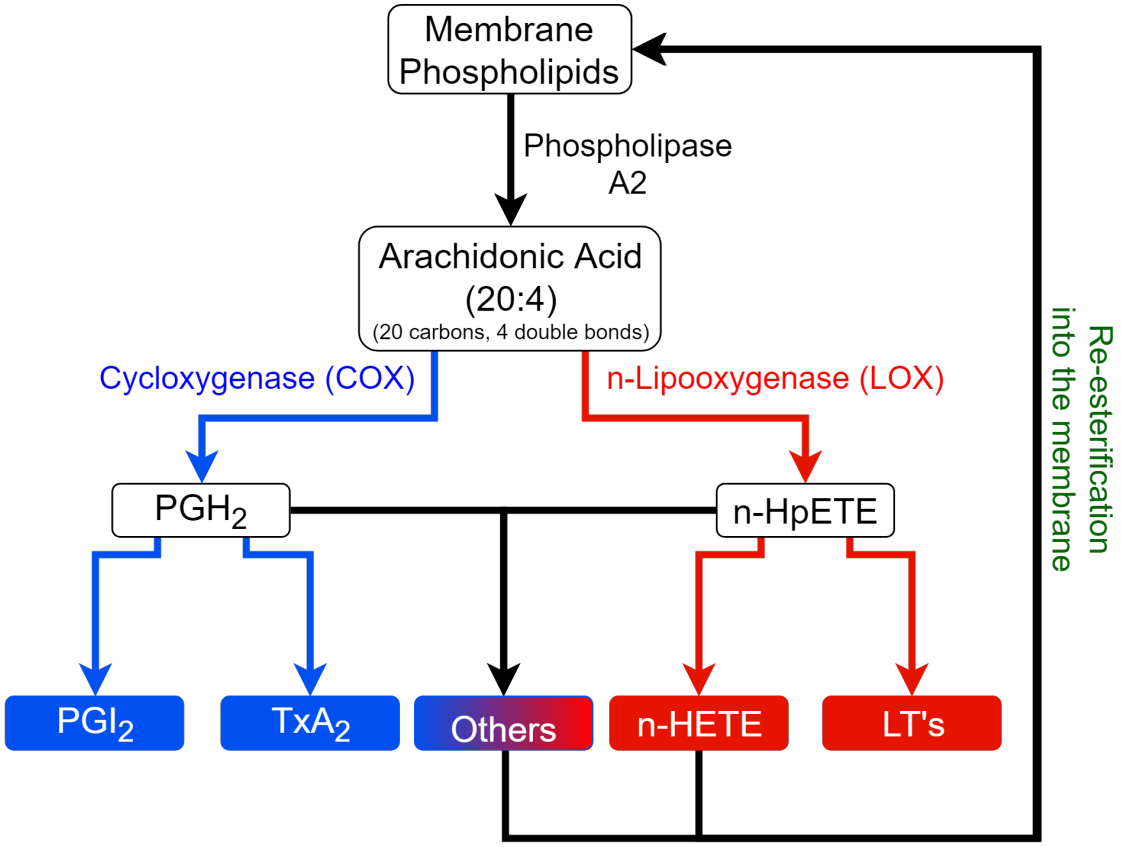

Figure 1.4. The typical oxylipin and enzymatically oxidized phospholipid pathway in circulating blood cells.

Membrane phospholipids can be cleaved by phospholipase A2 (PLA_2) into polyunsaturated fatty acids (PUFA), such as arachidonic acid (FA 20:4). These PUFA are oxygenated via the action of cyclooxygenase (COX) or lipoxygenase (LOX) enzymes to generate oxylipins, which are referred to as 'eicosanoids' if generated from 20-carbon PUFA such as arachidonic acid (AA). Some oxylipins may be re-esterified back to the membrane to form enzymatically oxidized phospholipids. The 'n-' prefix denotes the enzyme isoforms which are responsible for generating oxylipin positional isomers at the corresponding 'n-' carbon on AA (eg: 12-LOX in platelets generating 12-hydroxyeicosatetranoeic acids, or 12-HETE).

LOXs are a group of non-heme iron-containing enzymes which are expressed in a cell/tissue-specific manner [34]. They oxygenate AA to form hydroperoxyeicosatetranoeic acids (HPETEs) which are then reduced by glutathione peroxidases (GPXs) to form hydroxyeicosatetranoeic acids (HETEs). The oxygenation process begins with hydrogen abstraction from the PUFA, followed by radical migration and the stereospecific addition of dioxygen (**Figure 1.5**)[35]. The position of the oxygen insertion is dictated by the cell-specific LOX isoform which is named based on the most prominent oxygenation site on AA [36]. Using platelets as an example, stimulation with potent agonists such as thrombin leads to the release of AA into the cytoplasm which is then oxygenated by 12-LOX on carbon 12 (C12) to generate 12-HPETE[37-39]. This is then rapidly reduced via GPX to 12-HETE, which may be released by activated platelets or re-esterified back to the membrane[40] as will be described below in section **1.2.4**.

Other than 12-LOX in platelets, a number of other LOX enzymes are expressed in immune cells. Monocytes and neutrophils express 5-LOX which generates 5-HPETE, a precursor of 5-HETE and a number of leukotrienes with potent inflammatory properties[36]. There are two 15-LOX isoforms in humans, 15-LOX1 and 15-LOX2. These oxygenate AA to 15-HPETE. 15-LOX1 is found in eosinophils, reticulocytes and peripheral blood monocytes[35,41], while 15-LOX2 is found predominantly in the epidermis[37,38]. Unique to 15-LOX1 is the ability to directly oxygenate intact membrane PL, as will be described in section **1.2.4**.

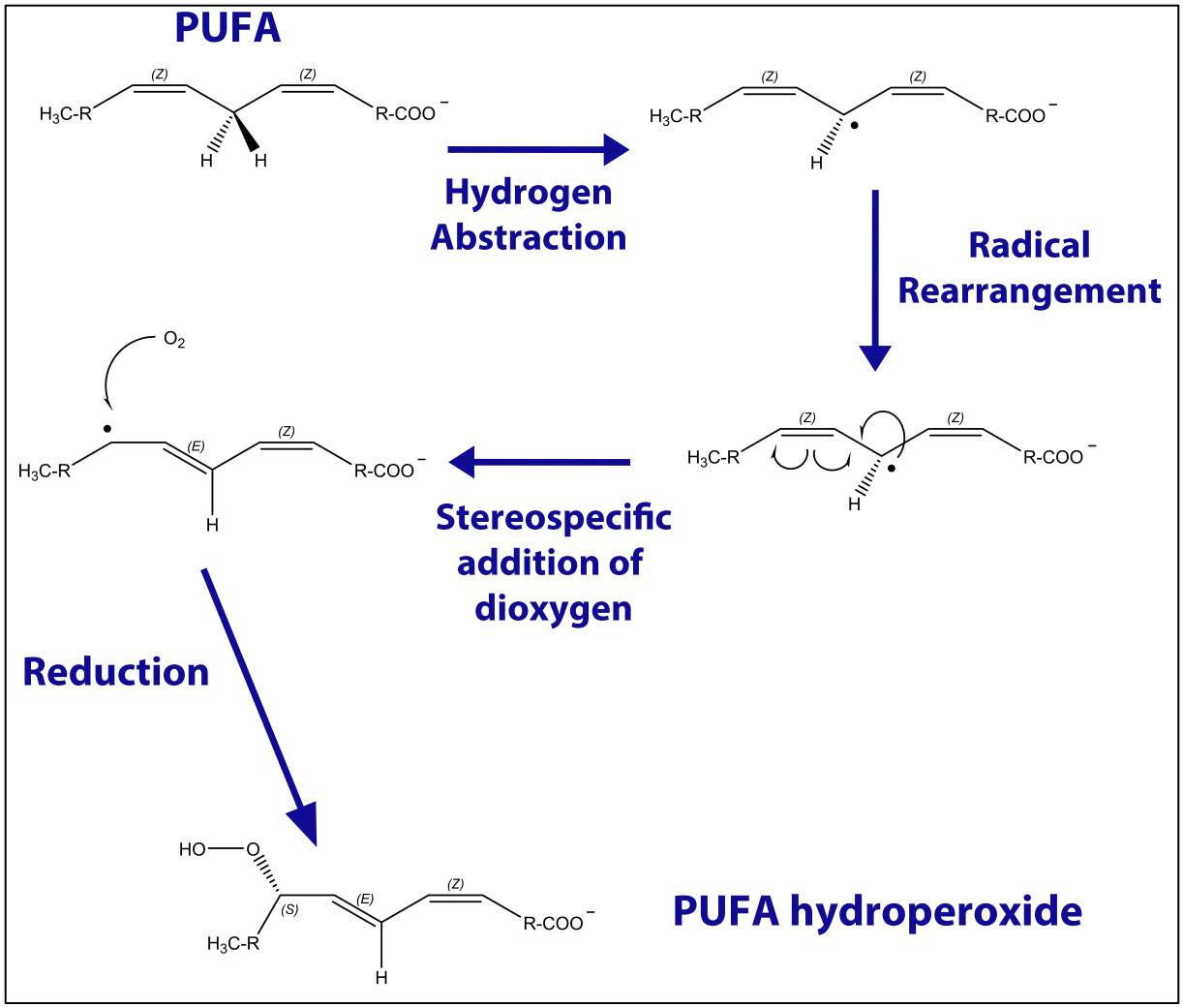

Figure 1.5. The mechanism of action of LOXs.

Hydrogen atom abstraction from the PUFA substrate proceeds through a proton-coupled electron transfer mechanism (PCET), with simultaneous transfer of electron and proton via a concerted mechanism. Subsequently, radical rearrangement takes place with stereospecific dioxygen insertion. This is followed by a further PCET step to generate a PUFA hydroperoxide which can then be reduced by glutathione peroxidase (GPX) enzymes to the hydroxide forms. In the case of AA, the hydroperoxides are known as HPETEs, hydroxides known as HETEs and the position of the oxygen insertion (forming (S) stereoisomers) is dictated by the cell-specific LOX isoform. LOX: Lipoxygenase, PUFA: polyunsaturated fatty acid, AA: arachidonic acid, HPETE: hydroperoxyeicosatetraenoic acid, HETE: hydroxyeicosatetraenoic acid.

It is worth noting that COX can also catalyse a LOX-type reaction which leads to formation of HETEs. This occurs when the COX dioxygenase activity, where one dioxygen molecule is introduced to AA, is not followed by a subsequent endoperoxide formation[42,43]. This is the result of the reduction of peroxyl radicals into a hydroperoxide instead of undergoing cyclization. Consequently, this incomplete catalytic cycle leads to oxygenation at C11 or C15, followed by reduction, with resultant formation of 11-HETE or 15-HETE, respectively[44,45] (**Figure 1.6**).

Both LOX and COX exhibit stereospecificity when it comes to oxygenating AA. This is in contrast to non-enzymatic oxygenation (e.g. by chemical oxidants) of AA which generates equal amounts of *(S)* and *(R)* enantiomers. For LOX-generated 12-, 15- and 5-HETEs in immune cells, the hydroxyl group occurs in the *(S)* configuration, whereas COX-generated 11-HETE forms in the *(R)* configuration. Both *(S)* and *(R)* 15-HETE enantiomers can be formed by COX, but with a predominance of the *(R)* stereochemistry[44].

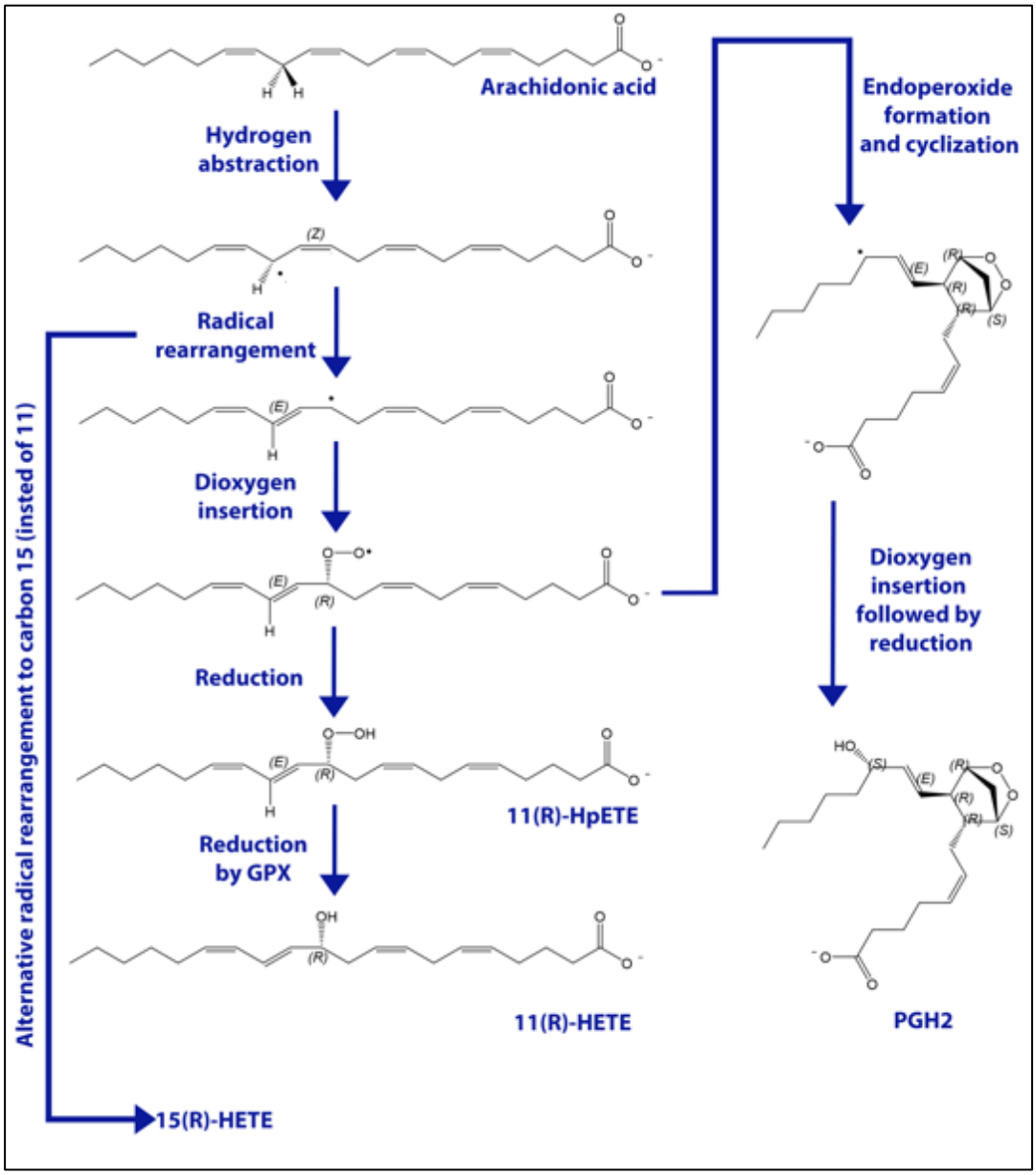

Figure 1.6. Reaction mechanism of cyclooxygenase (COX) and the generation of 11-HETE and 15-HETE as biproducts of the dioxygenase reactions.

Arachidonic acid (AA) undergoes hydrogen atom abstraction followed by radical rearrangement to allow for the insertion of a dioxygen molecule. The resultant product undergoes endoperoxide formation and cyclization to ultimately generate prostaglandin H2 (PGH2) - the intermediary product of COX-derived prostaglandins and thromboxanes. The dioxygenated AA may also undergo reduction instead of cyclization, leading to the generation of 11(R)-HPETE and subsequent reduction by glutathione peroxidase (GPX) enzymes to 11(R)-HETE. Alternative radical rearrangement to carbon 15 (instead of 11) can lead to the generation of 15(R)-HETE downstream of COX metabolism of AA. HPETE: hydroperoxyeicosatetraenoic acid, HETE: hydroxyeicosatetraenoic acid.

1.2.4 Enzymatic formation of oxidized PL (oxPL)

In addition to their role as bioactive mediators, oxylipins can be re-esterified into the membrane to form enzymatically-oxidised PLs (eoxPLs) which alter the biophysical structure of the platelet PL surface and modify its functions[9,13]. A prime example of this is the re-esterification of HETEs back to the PL membrane to generate HETE-containing PLs (HETE-PLs). Over the last two decades, a number of HETE-PL species generated downstream of LOX enzymes have been identified as a consequence of cellular activation of human immune cells including platelets[40,46,47]. These were discovered by studies from our group which utilised precursor scanning electrospray ionization/tandem spectroscopy for the HETE product ion (*m/z* 319.2), identifying a number of large precursor ions corresponding to HETE-PL species[46]. The recent eoxPL discoveries will be described in more detail in sections **1.2.5-1.2.7** for both LOX/COX pathways. The role of HETE-PL is yet to be fully elucidated in health and disease, although there is an increasing body of evidence to suggest that these eoxPL are important in mediating coagulation reactions[14], as will be described in section **1.3.5**. The eoxPL synthesis pathways are described in this section with a focus on oxylipin modification and re-esterification to the PL membrane[9,13].

Following the formation of oxylipins, as described above in section **1.2.3**, acylation with coenzyme A (CoA) may take place via the action of long-chain fatty acyl-CoA synthase (ACSL). There are numerous isoforms of ACSL catalysing the same type of reaction, yet they are functionally differentiated by preference for specific FA chain length, tissue distribution, and subcellular location[48]. Focusing on 20 carbon oxylipins (also known as eicosanoids) generated from AA, there are at least 5 ACSL isoforms (ACSL-1,-3,-4,-5 and -6) implicated in their conversion from FA to FA-CoA[48]. Using *in-vitro* studies, Klett *et al* demonstrated that all 5 isoforms were able to convert HETEs to HETE-CoAs, but at differing rates and amounts[49].

The differences in expression profiles and FA preference for individual ACSL isoenzymes enables them to channel specific fatty acids toward distinct metabolic fates in different tissues[49,50]. Nevertheless, studies on the specific roles of ACSL, their regulation and substrate preference in immune cells are lacking.

Following the activity of ACSL described above, the resultant acyl-CoA can be re-esterified into a membrane lysophospholipid (lysoPL) via the action of an *sn2* acyltransferase (also known as lysophospholipid acyltransferase, or LPAT), as depicted in **Figure 1.7**. This pathway is well-documented in immune cells where HETE-PL can be generated acutely on activation of neutrophils and platelets[40,46,51]. The requirement for hydrolysis and re-esterification for HETE-PL was demonstrated in both neutrophils and platelets using ^{18}O-H_2O stable isotope dilution MS and/or the LPAT inhibitor thimerosal to block oxPUFA re-esterification[40,47]. The cycle of PL hydrolysis by PLA_2 into FA/lysoPL and subsequent re-esterification of free FA to a lysoPL by LPATs is known as Lands' cycle and has been shown to occur in several immune cell types[14 40,47].

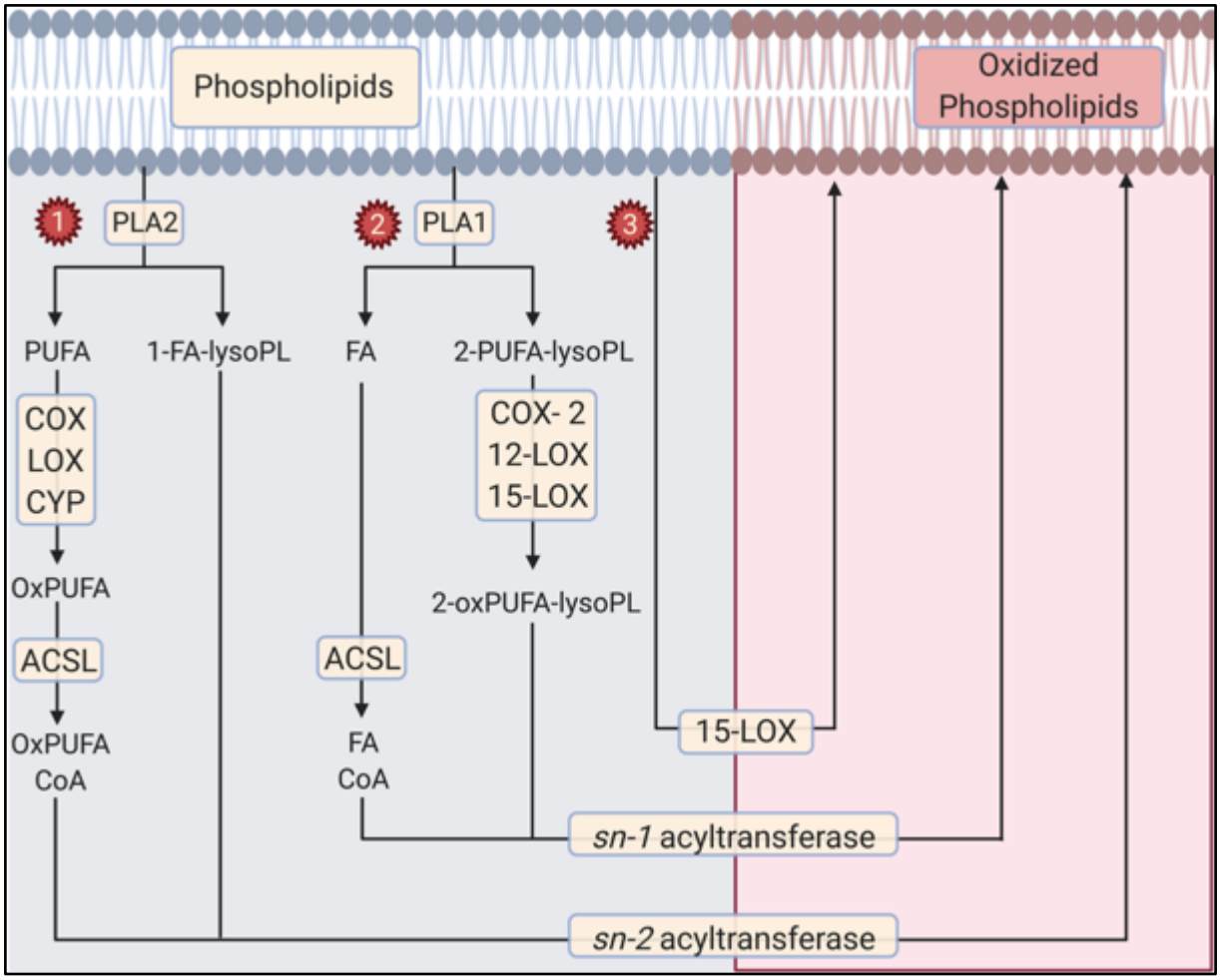

Figure 1.7. The enzymatic pathways of eoxPL biosynthesis.

(1) PLA_2 hydrolyses membrane PL releasing the *sn2* PUFA which is then oxygenated by COX-1/2, LOXs or cytochrome p450 enzymes to generate oxylipins (oxPUFA). These undergo the addition of coenzyme A (CoA) via acyl-CoA synthase (ACSL), prior to being re-esterified into a lysophospholipid (lysoPL) by any one of a series of *sn2* acyltransferases (also known as LPATs). (2) The phospholipase PLA_1 hydrolyses membrane PL to release 2-PUFA-lysophospholipids which may be oxygenated by COX-2, 12S-LOX and 15-LOX prior to being re-esterified with a fatty acid CoA (FA-CoA). (3) Unique to 15-LOX is the ability to directly oxygenate membrane PL to form eoxPL.

There are numerous LPAT enzymes described in the literature with specific re-esterification substrates within Lands' Cycle which vary by cell type and organism. For instance, LPCAT demonstrates selectivity for lysoPC (hence the L**PC**AT nomenclature), whereas LPEAT is selective for lysoPE[52,53]. Another family of LPATs is the membrane bound O-acyltransferase (MBOAT), to whom the majority of LPCAT enzymes belong[54-56]. MBOAT is primarily localised within the endoplasmic reticulum and mitochondria, with 11 human genes for the different isoforms which are present in a variety of tissues[55]. To complicate further, some MBOAT enzymes have a preference for specific acyl donors. For instance, MBOAT 5 and 7 preferentially utilise arachidonyl-CoA [55,57]. Despite being selective for lysoPC, MBOAT 5 (or LPCAT 3) has been shown to esterify acyls into lysoPS and lysoPE, indicating the complexity of these enzyme cycles[58]. It is not known however which of these enzymes is responsible for the re-esterification of oxylipins and whether specificity varies by the position of the hydroxyl group in the case of HETEs.

A second pathway for the generation of eoxPL is mediated via the action of 15-LOX which can oxygenate membrane PL directly without the need for PLA_2 activity to release the PUFA[46]. This was demonstrated by Maskrey et al using monocytes incubated in buffer containing ^{18}O-H_2O and activated with calcium ionophore (A23187). In this experiment, the authors observed no uptake of 15-HETE-^{18}O into HETE-PEs, implying direct oxygenation of PE by 15-LOX[46]. Additionally, 15-LOX maybe able to generate eoxPL by acting on the PUFA moiety of cholesterol esters (CE) which may then be hydrolysed to oxPUFA before being re-esterified to lysoPL[46,59,60]. Last, recent studies showed that oxygenation of 2-AA-lysoPL by COX-2, 15-LOX2 and platelet 12-LOX forms a 2-oxylipin-lysoPL which can be converted to eoxPL via the action of *sn1* acyltransferase[61-63] (**Figure 1.7**).

It is worth noting that oxPL and oxPUFA can be formed non-enzymatically through uncontrolled oxidation via free radical mechanisms during cell stress or inflammation. The initial reactions generate peroxyl radicals which can abstract hydrogens from a bismethylene group on PUFA to form hydroperoxides. Intermediates formed during this process can escape to react in an uncontrolled manner, leading non-enzymatic rearrangements of enzymatic pathway intermediates and generating a range of non-enzymatic oxPL products[64]. An example of where these processes take place in human disease is during atherosclerotic plaques formation as a result of chronic inflammation. In these plaques, a range of non-enzymatically generated oxPL has been described with possible effects on vascular endothelial cell and macrophage functions[65-68].

1.2.5 Platelet eoxPL species generated by 12-LOX

As described above, human platelets express 12-LOX and COX-1 which mediate oxidation of PUFA, ultimately leading to eoxPL generation. In this section, 12-LOX generated eoxPL products in agonist-activated platelets will be introduced. The COX-1 derived eoxPL in platelets and immune cells will be described in a subsequent section (**1.2.7**).

Agonist-activation of platelets leads to the 12-LOX driven synthesis of 12-HETE-PL. Initial studies from our group demonstrated four molecular species of 12-HETE-PE and two 12-HETE-PC generated in response to thrombin stimulation. These are PE 18:0a/12-HETE, PE 18:0p/12-HETE, PE 18:1p/12-HETE, PE 16:0p/12-HETE, PC 18:0a/12-HETE and PC 16:0a/12-HETE. Their formation has been observed within minutes of platelet activation and is sustained for up to 3 hours[40]. Thrombin receptors were confirmed to be implicated in 12-HETE-PL formation with experiments utilising peptide agonists of the thrombin receptors PAR-1 and PAR-4 on human platelets[40]. Furthermore, the formation of 12-HETE-PL required

several intracellular signalling mediators such as calcium, *src* tyrosine kinase, protein kinase C (PKC) and secretory PLA_2 ($sPLA_2$) as demonstrated by experiments utilising inhibitors to these mediators[40]. To confirm 12-LOX as the enzymatic pathway responsible for the formation of these lipids, platelets from 12-LOX deficient mice were studied and demonstrated undetectable levels of 12-HETE-PL upon agonist-activation[69].

Several other esterified oxPUFA generated by 12-LOX have been reported in agonist-activated human platelets. These include 14-hydroxydocosahexaenoic acid (14-HDOHE) generated from oxidation of DHA and re-esterified into plasmalogen (16:0p, 18:0p) or diacyl (16:0a, 18:0a) PE species[51]. These HDOHE-PE are generated acutely within 2 minutes of thrombin-activation of platelets by 12-LOX in the same way as 12-HETE-PL, albeit at lower levels[51]. The role of HDOHE-PL in platelets remains uncharacterised. Finally, a recent study from our group used targeted and untargeted lipidomic approaches to discover many previously unknown eoxPL generated in agonist-activated platelets[70]. The majority of these oxPL were monohydroxy lipids derived from AA, DHA, EPA and other PUFA. Up to now, the enzymatic pathways responsible for formation of many of these lipids remain unknown. How the platelet eoxPL lipidome varies between individuals remains unstudied, and will form the focus of **Chapter 3** in this thesis.

1.2.6 LOX-generated eoxPL species in leukocytes

As described previously, human monocytes express 15-LOX and can therefore oxidize AA to 15-HETE. This enzyme is constitutively active, but can be further enhanced by stimulation of monocytes with IL4, IL13 or calcium ionophore[46,59,71]. Using precursor ion scanning, our group uncovered 15-HETE-PL in resting human monocytes, and showed they increase upon stimulation with calcium ionophore[46]. Characterisation of these demonstrated four 15-HETE-

PE species with either acyl (18:0a) or plasmalogens (18:0p, 18:1p, 16:0p) at the *sn1* position[46]. Furthermore, the enzymatic origin was confirmed with chiral LC-MS/MS demonstrating a predominance of 15(S)-HETE attached to the PL[46,59], with 15-LOX directly oxidizing PE, as described above in section **1.2.4**[46,59]. An anti-inflammatory role for 15-HETE-PL has been shown through binding to toll-like receptor 4 (TLR4) accessory proteins such as CD14 and lipopolysaccharide binding protein (LPB), and thus impairing the activation of TLR4[59]. Furthermore, 15-HETE-PL on the surface of eosinophils have recently been demonstrated to participate in coagulation reactions, as will be described in section **1.3.5**[72].

In addition to 15-HETE-PL, other 15-LOX generated eoxPL have been reported in ionophore stimulated human monocytes. These include ketoeicosatetraenoic acid (KETE) containing PL. Specifically, KETE-PE containing acyl (18:0a) or plasmalogen (18:0p, 18:1p and 16:0p) lipids at the *sn1* position were detected in these cells[73]. To confirm their enzymatic origin, studies on macrophages from 12/15-LOX deficient mice, the murine analogue to human 15-LOX, demonstrated an absence of KETE-PE[73]. The generation of KETE-PE is thought to involve both 15-LOX and 15-hydroxyprostaglandin dehydrogenase (15-PGDH), the latter responsible for oxidizing 15-HETE-PE to 15-KETE-PE[73].

Human neutrophils express 5-LOX which can generate 5-HETE-PL upon agonist activation with bacterial peptides, chemokines or calcium ionophore[47]. The main 5-HETE-PL species identified in neutrophils are PC 16:0a/5-HETE, PE 18:0p/5-HETE, PE 18:1p/5-HETE and PE 16:0p/5-HETE. These PL are generated in a coordinated mechanism involving calcium, phospholipase C (PLC), $cPLA_2$ and $sPLA_2$, as demonstrated by studies utilising inhibitors to these mediators. In addition to the role of 5-HETE-PL in enhancing coagulation reactions, which will be described in section **1.3.5**, *in-vitro* studies demonstrated a role for 5-HETE-PL

in regulating neutrophil activities including superoxide generation and the release of neutrophil extracellular traps[47].

Finally, it is worth noting that there are no studies to date examining LOX-derived eoxPL in lymphocytes. This is despite reports that T-lymphocytes express 5-LOX confirmed by transcriptomic and western blot studies[74]. This may suggest that T-lymphocytes are capable of generating oxPUFA and eoxPL, although that remains unconfirmed.

1.2.7 COX-generated eoxPL species

COX-1 is ubiquitously and constitutively expressed in both leukocytes and platelets. In contrast, COX-2 is an inducible enzyme found in leukocytes but not platelets[32,75]. For decades, the role of these COX isoforms in generating oxPUFA and mediating cellular processes has been recognized[75]. However, only recently have COX-generated eoxPL been described in the literature.

Studies from our group were the first to report the generation of eoxPL which contain COX-derived prostaglandins[76]. Lipid extracts from human platelets activated with thrombin, collagen or calcium ionophore were analysed using precursor LC-MS/MS for eoxPL incorporating PGE_2 or PGD_2. This demonstrated the presence of these prostaglandins in PE lipids containing 16:0p, 18:1p, 18:0p and 18:0a at the *sn1* position. Their formation occurred within 2 to 5 minutes of platelet activation and required calcium mobilisation, PLC, $cPLA_2$ and *src* tyrosine kinases[76]. Aspirin supplementation (*in vivo*) and inhibitors of re-esterification (*in vitro*) inhibited their generation, indicating that they form via COX-1 activity, and downstream LPAT-dependent esterification [76]. During identification of these lipids, other previously unknown COX-1 eoxPL were also identified. The characterisation of these lipids led to the

identification of eoxPL which contain 8,9-11,12-diepoxy-13-hydroxy-eicosadienoic acid (DiEHEDA) generated by COX-1 oxidation of AA[77,78]. These novel COX-1 derived eoxPL utilise the same generation machinery described above for prostaglandin-containing eoxPL, leading to the generation of four PE eoxPL species containing 16:0p, 18:0p, 18:1p and 18:0a at the *sn1* position. The function of these lipids is yet unknown, but they appear to activate neutrophil integrin expression *in-vitro,* which may suggest a role in modulating inflammation[79]. Finally, COX-derived 15(R)-HETE may be re-esterified into 15-HETE-PL which has been demonstrated to facilitate coagulation reactions *in vitro*[63,80,81].

1.3 HAEMOSTASIS

The physiological process of preventing or stopping bleeding is known as haemostasis[82]. It consists of a highly regulated balance between procoagulant and anticoagulant mechanisms which provide a rapid and localised response to vessel injury. Defects in this process, such as dysfunction or absence of the key players involved, leads to excessive bleeding or unwanted thrombosis.

The overall outcome of the haemostatic process is to seal the vascular injury by forming an occlusive clot – also known as a 'haemostatic plug'. Key contributors to this process are circulating platelets which mediate the formation of a platelet plug [83]. Coagulation is initiated by tissue factor (TF) on extravascular cells such as fibroblast and is amplified on the surface of activated platelets to generate thrombin and form a fibrin clot. The integrated interactions of platelets and the coagulation system will be discussed below. It is important to emphasise however that the link between activated platelets and thrombin formation is provided by the procoagulant PL membrane. Whilst both platelets and coagulation factors have been investigated and targeted in thrombotic diseases such as ACS, the role procoagulant PLs in ACS remains unexplored and forms the focus of this thesis.

1.3.1 Platelets

Platelets are anucleate discoid cells which are responsible for haemostasis as well as wound healing, vessel integrity and inflammatory processes. They are derived from megakaryocytes in the bone marrow and circulate in the blood stream in a quiescent state at a count of 150-450 x 10^9 per litre and have a life span of up to ten days[84]. Platelets play an important role in binding to areas of damaged vessel wall and initiating haemostasis and wound

repair. At the site of vascular injury they become active through multiple mechanisms which lead to the generation of a procoagulant environment that aims to seal the injury to prevent blood loss[85]. This process is essential to survival. However, dysregulated activation of this system in disease may lead to excessive activity and formation of clots in intact blood vessels which obstruct blood flow and lead to end organ damage. This pathological state is known as thrombosis, and is responsible for conditions such as heart attacks and strokes[86].

1.3.2 Physiological role of platelets in haemostasis

Platelets are critical for haemostasis as part of the physiological process of wound healing. When the vessel wall is damaged, von Willebrand factor (VWF) is exposed and unravels in the high shear conditions. The VWF recruits unactivated platelets to the vessel wall (adhesion) which are exposed to extracellular matrix proteins (e.g. collagen) and TF-generated thrombin at the site of blood vessel injury activating surface receptors on the platelet membrane (**Figure 1.8**)[87]. This triggers a secondary signalling cascade which causes platelet shape changes (from discoid to spiny) by altering the actin cytoskeleton. It also leads to activation of integrin glycoprotein (GP) receptors (e.g. GP IIbIIIa) which allow platelets to bind to each other (aggregation), and secretion of stored granules containing mediators that activate other platelets through surface receptors (e.g. adenosine diphosphate, ADP). This leads to the formation of a "platelet plug" which seals the injured vessel[85]. This plug supports coagulation reactions and fibrin clot formation, stabilising the platelet plug. Defects that interfere with platelet function or number are known to cause bleeding disorders, particularly of muco-cutaneous tissue [88].

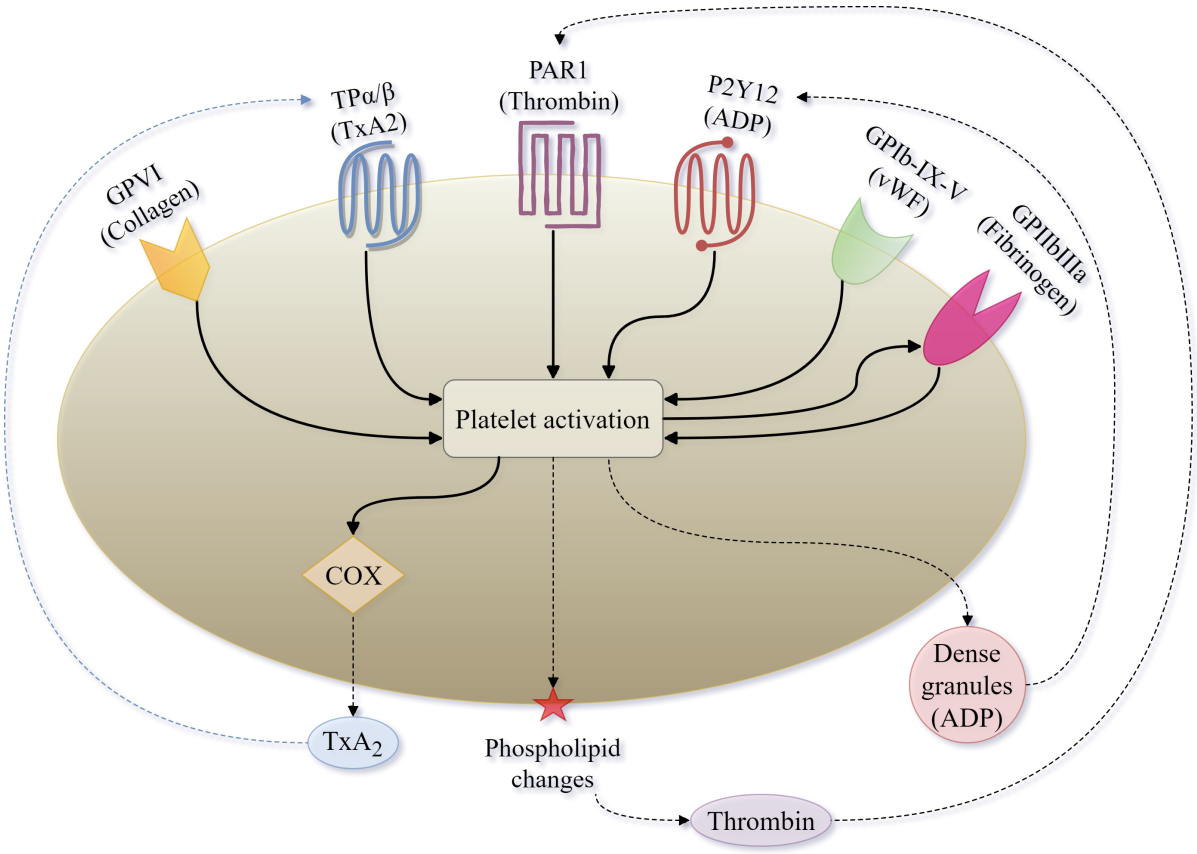

Figure 1.8. Platelet activation by different ligands through a number of surface receptors (key targets illustrated).

Platelet receptors facilitate their response to a number of ligands. The initial activation leads to a secondary signalling cascade which causes the release of stored or synthesis newly synthesized secondary mediators which augment the platelet response. Changes to the phospholipid surface also take place promoting thrombin generation.

1.3.3 The coagulation system

Our understanding of the coagulation system has evolved considerably from the originally described "coagulation cascade" to the currently accepted "cell-based model" of coagulation[89]. Whilst both describe reactions that involve proteins known as coagulation factors, the latter model places a significant emphasis on interactions of these proteins with cell membranes. To simplify the description of this model, three overlapping phases of coagulation were proposed: initiation, amplification and propagation[90]. These reactions require the presence of calcium ions, coagulation factors and aPL on the external leaflet of cell membranes[91,92]. The end result of this is the formation of fibrin which stabilises the platelet plug and forms a clot to seal the site of the vessel injury and stop the blood loss. The different phases and contributors to this process will be detailed below and are shown in **Figure 1.9**.

In the initiation phase, expression of TF on extravascular cells is critical for the activation of coagulation. This transmembrane protein serves as a receptor for factor VII (FVII) and its activated form (FVIIa) and is constitutively expressed on the surface of cells surrounding blood vessels such as smooth muscle cells and fibroblasts[93]. Disruption to vascular endothelial architecture exposes the blood to TF-expressing cells leading to the formation of the TF:FVIIa complex which activates the coagulation system.

Activation of TF from its encrypted to decrypted conformation is influenced by co-expression of PS on the PL membrane, formation of disulphide bonds between cysteine residues at positions 186 and 209, and interactions with cholesterol-containing lipid rafts[92,94]. The mechanism for this is not entirely defined, but is thought to relate to interactions between PS and TF which expose the substrate binding sites for other coagulation factors[95]. These

interfaces may be direct physical interactions between the polar PS headgroup and lysine residues on the TF extracellular domain[96,97], or relate to an electrostatic contact caused by the PS negative charge which may align the TF quaternary structure on the membrane surface to expose the enzymatic active site[96,97]. In both cases, the end result is activation of the TF:FVIIa extrinsic tenase complex which initiates coagulation reactions[98,99]. The activation of FVII to FVIIa is mediated by the presence of low levels of proteases in the circulation which include thrombin, factor IXa (FIXa), factor Xa (FXa) and factor XIIa (FXIIa)[100-102]. Upon formation of the TF:FVIIa complex in response to vessel injury, FVII conversion to FVIIa is significantly increased by a process of autoactivation[103]. This leads to generation of more TF:FVIIa complexes which enzymatically cleave factor X to Xa (FXa) and factor IX to IXa (FIXa). Small scale generation of thrombin takes place as a result of the action of FXa on prothrombin[104]. FXa binds to TFPI and the FXa/TFPI complex inhibits the TF/FVIIa complex, terminating the initiation process (see below), after which coagulation is dependent on the amplification phase.

The amplification phase takes place on the PL surface of platelets activated by collagen and the small amount of thrombin generated in the initiation phase. Activation of factor VIII to FVIIIa and factor V to FVa takes place a result of enzymatic cleavage by thrombin. These serve as co-factors for FIXa and FXa, respectively which in turn lead to the accelerated generation of FXa by the FIXa:FVIIIa "intrinsic tenase" complex and of thrombin by the FXa:FVa "prothrombinase" complex[90,104].

Loss of membrane asymmetry and exposure of negatively charged aPL following platelet activation is critical to both of the above phases as it strongly accelerates the reactions of the extrinsic tenase (TF:FVIIa), intrinsic tenase and prothrombinase complexes[105]. Exposure of the negatively charged PS leads to electrostatic and hydrophobic interactions which increase the

binding of GLA-domain containing coagulation factors (VIIa, IXa, Xa and II) to the membranes[106]. This is facilitated by calcium ions which bind to the GLA domains and expose a hydrophobic region within the omega loop which can then allow the coagulation factor to penetrate the PL membrane[107]. It is thought that each GLA domain has a single binding site specific for the carboxyl group on the PS head-group as well as additional calcium binding sites for interactions with the phosphates on any PL other than PC. Nuclear magnetic resonance (NMR) analysis has demonstrated that the PL head-group bends in order to allow its phosphate to associate with GLA-bound calcium. Lipids with a PE headgroup can interact with the GLA domains and enhance the function of PS, whereas the bulky methyl residues of the PC choline head-group make it unable to participate in this process[107,108]. The increased local concentration of coagulation factors on the PL surface enhance the function and interactions of these proteins. It also facilitates transfer of substrate and product between the coagulation complexes and helps to restrict the activity of the coagulation process to areas of injury[105].

The accumulated enzyme complexes (tenase and prothrombinase) on the platelet surface support large scale thrombin generation as part of the propagation phase[90]. This phase ensures continuous generation of thrombin and subsequently fibrin to form a sufficiently large clot. Finally, the fibrin clot is stabilized via the thrombin-mediated activation of factor XIII to FXIIIa (fibrin stabilizing factor) which covalently links fibrin polymers[104].

The coagulation system is tightly regulated at various stages by a number of inhibitors which prevent inappropriate activation. Tissue factor pathway inhibitor (TFPI) is a single-chain polypeptide associated with uninjured endothelium bound to glycosaminoglycans[109,110]. It acts as a protease inhibitor blocking FVIIa and FXa activity and can also bind protein S which enhances its anti-FXa activity[111]. Therefore, the balance between levels of TF (increased with

injury) and TFPI (bound to uninjured endothelium) regulate the initiation phase of coagulation[90]. Healthy endothelium also expresses high levels of thrombomodulin (TM) which binds circulating thrombin and changes its specificity to prevent it from activating platelets or forming fibrin[90]. The resultant thrombin:TM complex becomes an activator of protein C, which regulates the amplification phase of coagulation alongside its co-factor protein S by proteolytic inactivation of FVa and FVIIIa[112]. Other regulators of the coagulation system include circulating inhibitors of thrombin such as anti-thrombin (ATIII) and alpha-2-macroglobulin[90]. It is worth noting that for protein C and protein S to function, they also require the presence of a negatively-charged membrane surface provided by PS externalisation[113].

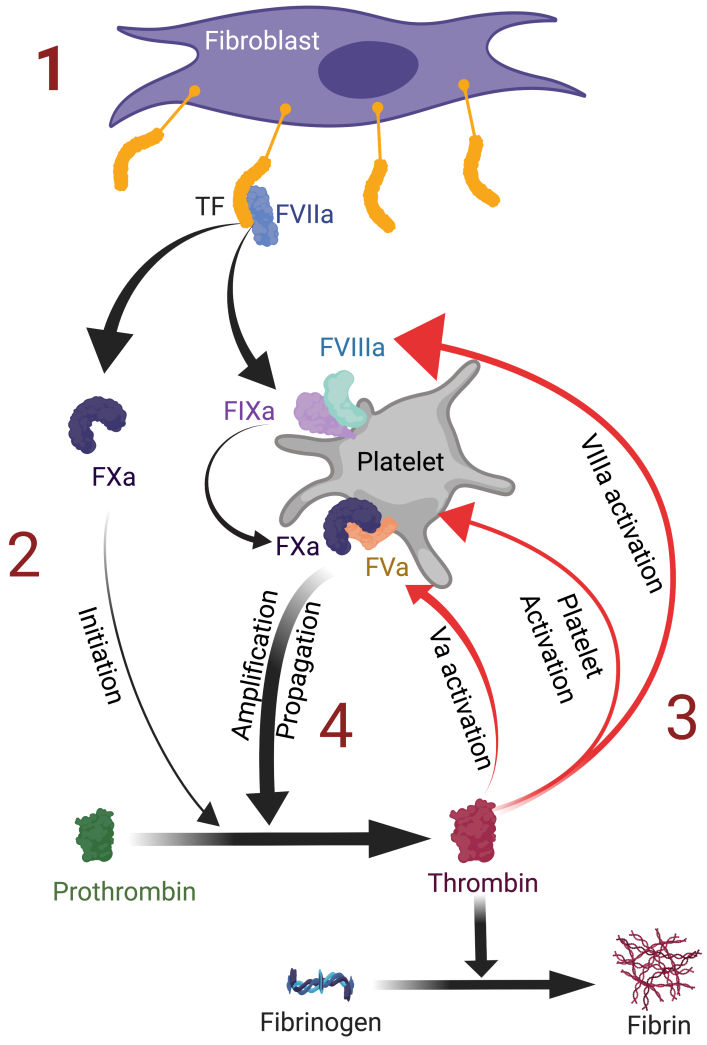

Figure 1.9. The coagulation system (cell-based model).

Activation of coagulation is driven by tissue factor (TF) expressing cells in the subendothelial space (1). The TF:FVIIa complex activation of FX to FXa and FIX to FIXa is termed the 'initiation phase' which generates small amounts of thrombin (2). This is sufficient to activate FV to FVa and FVIII to FVIIIa leading to the formation of FIXa:FVIIIa and FXa:FVa complexes on the platelet PL surface (3). These complexes lead to the formation of more FXa and more thrombin, respectively, as part of the 'amplification phase'. More thrombin leads to more activated platelets and coagulation factors locally, creating a thrombin-forming 'propagation phase' loop (4) which leads to the formation of fibrin.

1.3.4 Externalised aPL species in platelets and leukocytes

The externalisation of aPL is a calcium dependent process which takes place during cell activation or apoptosis. Furthermore, the presence of external facing aPL on the surface of cells is critical in facilitating coagulation reactions. In the majority of the literature, aPL externalisation is detected using flow cytometry techniques that rely on the use of annexin V or lactadherin to label the PS/PE headgroups[114-116]. These techniques however are incapable of distinguishing between PS and PE, determining their absolute quantities or defining their FA composition.

To tackle the limitations inherent to flow cytometry techniques, our group developed a mass spectrometry based assay to allow the detection and the discrimination between total (throughout the membrane) and externalised (outer leaflet) aPL species in the membrane surface of platelets and leukocytes[117]. This assay utilises amine chemistry and relies on derivatising aPL by labelling the primary amines on the serine and ethanolamine portions of the headgroups using N-hydroxysuccinimide (NHS) biotin and sulfo-NHS biotin. These two types of biotinylation reagents allow labelling of total aPL throughout the cell membranes (NHS-biotin) or on the external facing membrane leaflet only (sulfo-NHS-biotin). This is due to the hydrophobicity of NHS-biotin which allows it to penetrate the cell membrane, unlike sulfo-NHS-biotin which remains on the outer surface owing to its water soluble properties[118]. Beyond this difference, the biotinylation process is identical for the two reagents which react spontaneously with amines to form an amide bond between biotin and the aPL. This processes leads to a mass shift of 226 a.m.u which can be measured using a sensitive and specific LC-MS/MS method to distinguish external aPL from internal forms.

Using this biotin derivatisation LC-MS/MS method, our group demonstrated that human platelets externalise 5 molecular species of PE and 3 species of PS, with the majority containing AA at the *sn2* position[20,117]. These species are PE 16:0p/20:4, PE 18:0a/20:4, PE 18:0p/20:4, PE 18:1p/20:4, PE 18:0a/18:1, PS 18:0a/18:1, PS 18:1a/18:1 and PS 18:0a/20:4. It is worth noting that apart from Scott syndrome, no published studies to date have examined potential variations in aPL species on the surface of platelets and/or leukocytes in bleeding or thrombotic disorders.

The FA composition of aPL appears to influence their procoagulant function. Specifically, coagulation activity was lower in PE containing shorter chain FA (14:0) compared with PE with AA at *sn2*[20]. Similarly, replacing AA with docosahexanoic acid (DHA) at *sn2* resulted in reduced procoagulant activity[20]. The authors of the study hypothesize that the influence of FA on PE procoagulant activity may relate to differential interaction with coagulation factors through their GLA domains driven by length of FA chain[20]. Overall, these findings highlight the importance of FA characterisation in studies investigating the procoagulant activity of aPL, and suggest that simply examining aPL headgroup externalisation (e.g. with Annexin V) is insufficient.

1.3.5 The role of eoxPL in coagulation

In addition to native aPL, eoxPL have been implicated in supporting coagulation. Of particular interest to this thesis are the HETE-PL eoxPL which are made via the action of LOX enzymes in innate immune cells[14]. All positional isomers of HETE-PL have been shown to be able to facilitate coagulation reactions *in vitro* leading to enhanced thrombin generation in a dose-dependent manner[81]. Specifically, in thrombin generation assays, the addition of liposomes containing TF and varying amounts of 12-HETE-PE to platelet poor plasma

enhanced production of thrombin, compared to unoxidized PE[81]. The amount of thrombin formed correlated with the increase in the amount of 12-HETE-PE (1-10% of total liposome composition)[69]. This is thought to be related to an eoxPL-induced change in the biophysical properties of the activated cell membrane which results in a more negative charge on the anionic surface, enhancing the binding of coagulation factors to the surface[69,81].

Of interest, native (unoxidized) PC cannot support coagulation factor binding, and its presence on the external leaflet ensures that the coagulation system remains inactive in resting cells. This is in contrast to 12-HETE-PC, which can directly enhance thrombin generation. For example, inclusion of 12-HETE-PC to the TF-liposomes enhanced PS-mediated thrombin generation[69], contrary to native unoxidized PC which does not support coagulation[22,108]. This finding is thought to relate to a change in the biophysical properties of PC where the hydrophilic hydroxyl group added to the AA bends-up to the hydrophilic surface of the membrane which facilitates interaction with calcium, the phosphate groups of other lipids and the carboxylate group on PS[40,69]. In addition to these spatial changes, 12-HETE-PC may provide increased electronegativity to the outer membrane leaflet by virtue of the hydroxyl group on C12[69]. Indeed, using both molecular dynamics simulations and calcium binding assays, studies from our group demonstrated that increasing the proportion of HETE-PL on liposomal surfaces increased calcium binding, which may be due to providing a more negative charge on the membrane surface[69,81].

Recently, the role of HETE-PL in supporting coagulation was further examined in mice lacking the platelet *Alox12* gene which encodes the platelet 12-LOX enzyme. Compared to wild type controls, *Alox12*$^{-/-}$ mice exhibit a bleeding phenotype and generated smaller clots in response to venous injury[69]. Subcutaneously injecting 12-HETE-PL containing liposomes into

the tail rescued this phenotype in a tail-bleeding assay[69]. Furthermore, the role of 12- and 15-HETE-PL in eosinophils has also been described as important to propagating coagulation, haemostasis, and thrombotic disease[72]. This was examined in mice lacking the *Alox15* gene which is responsible for the expression of 12/15-LOX in murine eosinophils. Compared to wild type controls, *Alox15*$^{-/-}$ mice demonstrated defective fibrin clot formation and reduced thrombin generation on the surface of eosinophils[72]. This defect was rescued by the addition of liposomes containing 12-HETE-PL to eosinophil mixtures which, in addition to 15-HETE-PL, is a product of murine 12/15-LOX. The pro-thrombotic role of 12/15-LOX was demonstrated using a venous injury model which demonstrated smaller clot formation in *Alox15*$^{-/-}$ mice compared with wild type controls[72]. Finally, HETE-PL were also demonstrated to play a role in murine models of abdominal aortic aneurysm (AAA), a condition that causes thrombus-containing arterial aneurysms. In these angiotensin-II treated *ApoE*$^{-/-}$ mice, deletion of *Alox15* or *Alox12* resulted in protection against aneurysm formation. [119]. These findings suggest an *in vivo* role for HETE-PL in mediating thrombosis and haemostasis.

The role of eoxPL in coagulation was also examined in human studies. Patients with antiphospholipid syndrome who had experienced a venous thrombotic event had higher levels of circulating eoxPL on the surface of platelets and leukocytes as well as elevated plasma levels of IgG that recognised eoxPL. This was seen for both platelet 12-HETE-PL as well as leukocyte 15- and 5-HETE-PL[69]. Furthermore, patients undergoing cardio-pulmonary bypass surgery, who are known to be susceptible to elevated risk of bleeding post-procedure, were found to have lower platelet 12-HETE-PL post operatively, compared to their preoperative levels[81]. This reduction in 12-HETE-PL was hypothesized to be a contributing factor to their bleeding phenotype. These findings in human disease further support a potential association of

HETE-PL with thrombosis and haemostasis. To date however, there have not been any human studies to investigate the role of HETE-PL in arterial thrombosis.

1.4.1 Atherogenesis

Understanding the disease process of atherosclerosis is central to understanding the pathophysiology of arterial thrombosis. Atherosclerosis describes the deposition of fatty and fibrous material in the innermost lining of the artery, the intima, which when disrupted acutely provokes the formation of a thrombus that occludes the lumen[120]. The pathogenesis of atheromata (plural) will be described in this section and is depicted in **Figure 1.10**.

Initiation of atherosclerosis appears to be related to low-density lipoprotein (LDL) particles, responsible for the transport of lipids through the circulation. It is thought that the levels of LDL in most contemporary human societies are much higher than the physiologically needed amounts, and are consequently chronically exposed to arteries in excess amounts[121-123]. This exposure is recognized as the principal determinant of atherosclerosis initiation and progression, where LDL particles can deposit in the arterial wall[124,125]. To complicate matters, modified LDL particles termed oxidized LDL (oxLDL) have been reported to promote atherogenesis [126,127]. OxLDL particles are formed by oxidative modification of LDL altering their structure and content, leading to a more atherogenic phenotype[128]. Mechanisms for their formation are predominantly non-enzymatic, caused by reactive oxygen species which are formed by metal ion catalysis[126,127]. LDL/oxLDL particles enter intimal macrophages via scavenger receptors and overload them with cholesterol esters, leading to the formation of foam cells. These lipid-rich cells are the hall mark of atherosclerotic lesions, leading to their characteristic histological appearance which gives it the Greek name ‘athero-‘, meaning ‘gruel’ or ‘porridge’ (**Figure 1.10**) [129]. Of relevance to this thesis, these foam cells are rich in TF on their membrane surface which makes them highly prothrombotic if exposed to flowing blood[130].

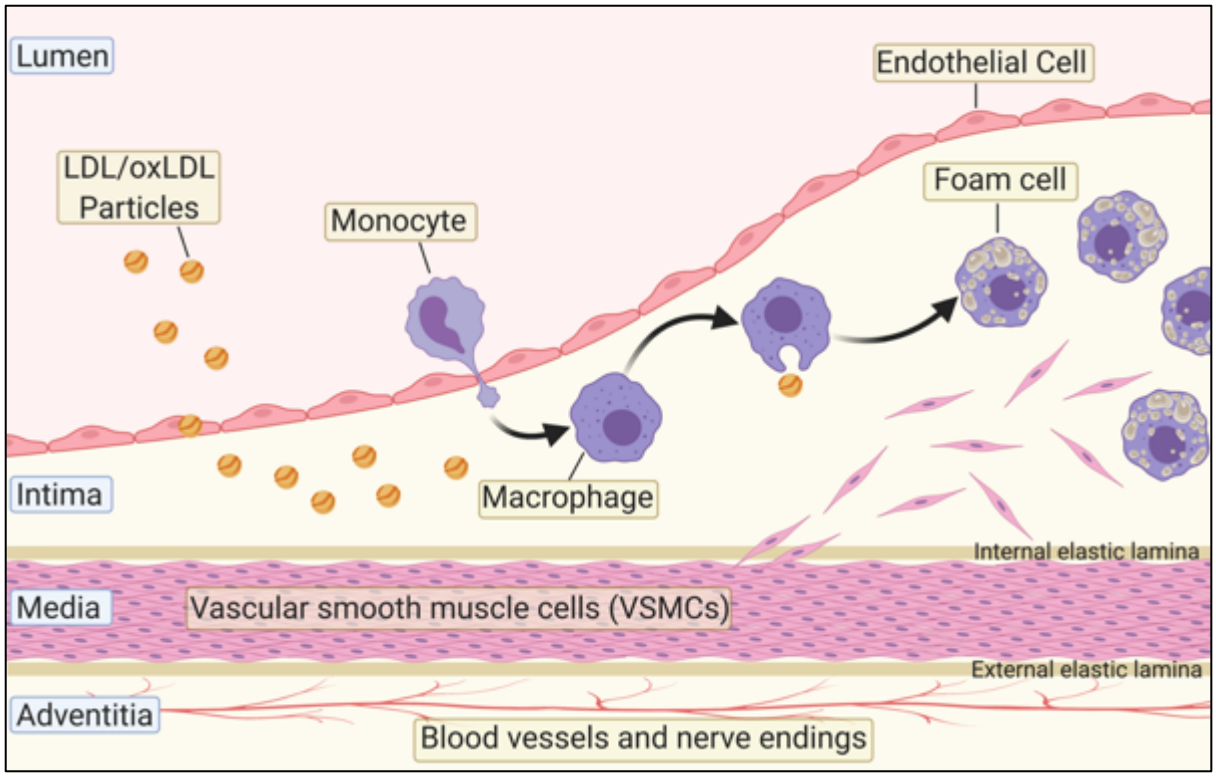

Figure 1.10. The process of atherosclerosis within arterial walls - the accumulation of foam cells carrying prothrombotic properties.

Arterial walls consist of three layers ('tri-laminar'): the intima is the innermost layer which is separated from the vascular lumen with a layer of endothelial cells. The media is the middle layer which consists of vascular smooth muscle cells and is separated from the other two layers by a lamina which consists of extracellular matrix proteins such as collagen and elastin. The outermost layer is the adventitia which consists of fibrous connective tissue and contains blood vessels ('vasa vasorum') and nerve endings. The atherosclerotic process implicates the intimal layer, and starts by the deposition of (oxidized) low density lipoprotein (LDL/oxLDL) particles which causes disruption in the endothelial barrier and expression of adhesion molecules. Over time (left to right), this damage to the endothelial allows inflammatory cells (primarily monocytes) to infiltrate the intimal layer and to differentiate into tissue resident macrophages. Intimal oxLDL/LDL particles enter these macrophages via scavenger receptors and overload them with cholesterol esters, leading to the formation of foam cells which are the hallmark of atherosclerotic lesions.

The entry of oxLDL/LDL into the intima and the initiation of atherosclerosis is thought to be related to a defective endothelial barrier between circulating blood and the vessel intima. The endothelium plays a pivotal role in regulating the arterial circulation which is under continuous friction from the circulatory shear stress exerted by arterial pressures[131]. Factors such as hypertension, smoking and diabetes mellitus have been implicated in damage to the endothelium by inducing oxidative to arterial walls and inactivating regulatory pathways such as those provided by nitric oxide leading to endothelial dysfunction[132-135]. The consequence of these processes is disruption to the endothelial barrier with subsequent atheroma initiation which encroach on the arterial lumen causing turbulent flow and disturbance to arterial shear stress[131]. The result is non-laminar flow which promotes oxidative and inflammatory states in the arterial wall, disrupting the homeostatic protective functions of the endothelium and reversing its anti-inflammatory properties[131,136,137]. Thus, a vicious circle of endothelial damage followed by atheroma formation leads to more damage, atherosclerosis and propagation of this pathological process.

After a number of years, these early atheromata progress via the continued accumulation of lipid-rich inflammatory cells and subsequent modification to the extracellular matrix (ECM). In addition to macrophages, vascular smooth muscle cells (VSMC) have also been described to give rise to foam cells via a process of metaplasia[138]. These cells migrate to the intima from the media, undergo phenotypic switching to macrophage-like cells and contribute to the growth of the plaque, formation of ECM macromolecules and inflammation[138]. Examples of ECM molecules include collagen, elastin and glycosaminoglycans which can entrap LDL/oxLDL particles and leads to further lipid accumulation and foam cell formation[138]. These macrophages and macrophage-like cells can undergo programmed cell death with defective clearance (efferocytosis), leading to the accumulation of a lipid-rich necrotic cores in advanced

atheromas, which are highly thrombogenic by virtue of containing TF on their membrane surface (**Figure 1.11**) [130,139-142]. Finally, in the advanced stages of atherosclerosis, dysregulated deposition and impaired clearance of calcium leads to the development of regions of calcifications which cause mechanical instability of plaques, with a higher risk of disruption and subsequent arterial thrombosis[143,144].

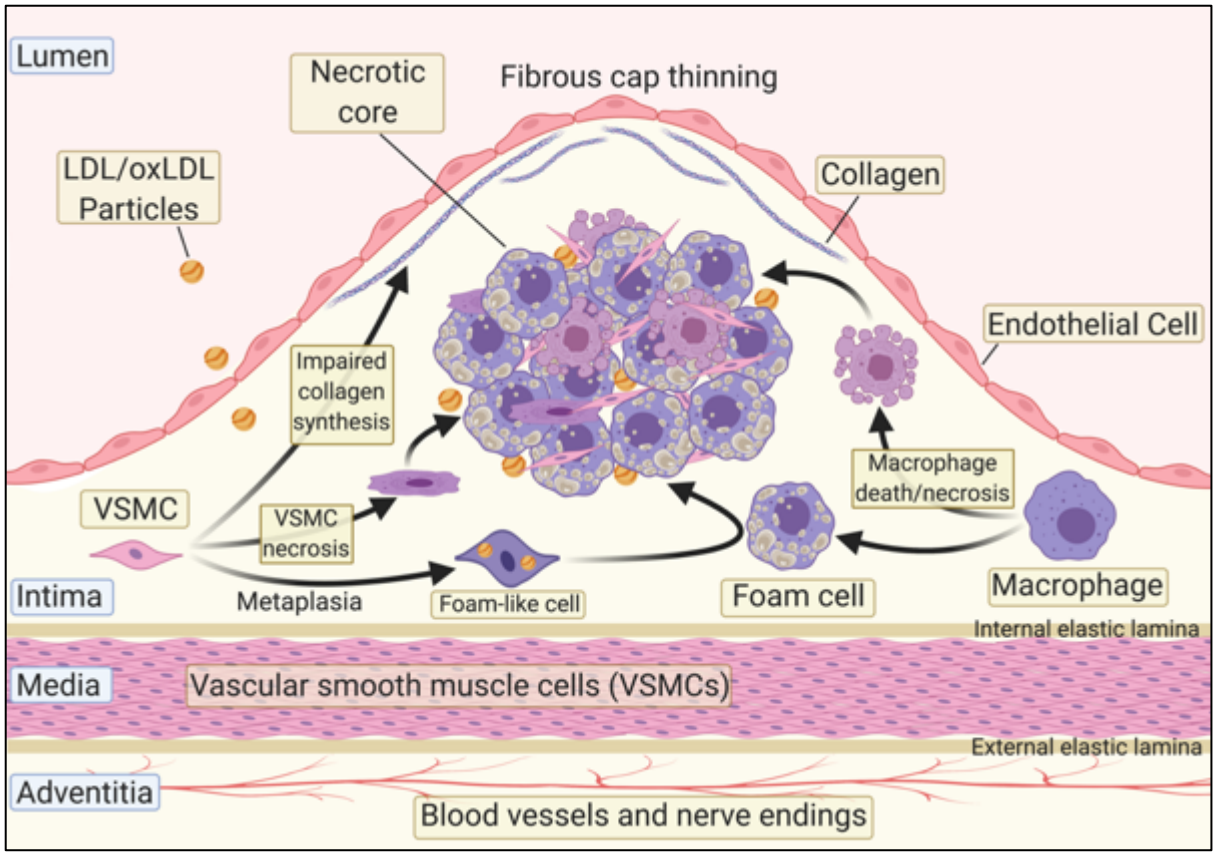

Figure 1.11. Formation of necrotic cores within atheromas which are rich in TF and carry a prothrombotic burden when exposed to the circulation upon plaque rupture.

As part of atheroma progression, vascular smooth muscle cells (VSMC) resident within the innermost layer of the arterial wall (the intima) produce extracellular matrix (ECM) molecules such as collagen in a dysregulated fashion which leads to formation of a fibrous cap. This cap is weakened and undergoes thinning as a result of matrix metalloproteinases released by activated macrophages. Furthermore, VSMC can undergo a process of metaplasia to form foam-like cells which are deposited in the intima alongside foam cells formed by macrophage engulfment of (oxidized) low density lipoproteins (LDL/oxLDL) particles. As the lesions advance, VSMCs and macrophages can undergo cell death by apoptosis, necrosis or efferocytosis which leads to the accumulation of dead or dying cells within the intima.

Of particular interest to this thesis is the contribution of the coagulation system to atherogenesis and plaque progression. The plasma membranes of foam cells are rich in TF co-localising with FVII, demonstrated by studies examining human atherosclerotic lesions and associated with early atheroma formation[145,146]. TF:FVIIa is responsible for formation of FXa and thrombin on procoagulant surfaces rich in procoagulant PL. Together, FXa and thrombin can signal through activation of proteinase activated receptors (PARs) which are present on the surface of platelets and endothelial cells[147]. In addition to their roles in haemostasis (PAR1 and PAR4), PAR receptors have also been implicated in inflammation and atherogenesis. The FXa and thrombin receptor, PAR1, has been implicated in atheroma formation in ApoE$^{-/-}$ mice [148]. In a study by Rana et al, inhibition of PAR1 with pepducin PZ-128 led to decreased formation of atheromas in thoracic and abdominal aortic sections from ApoE$^{-/-}$ mice[148]. This was thought to be due to a reduction in monocyte transmigration and macrophage infiltration by interfering with the expression of vascular adhesion molecules[148]. In another study utilising a separate model of atherosclerosis, Jones et al demonstrated that deletion of PAR2, a receptor for FXa, attenuates atherosclerotic lesion development in LDLR$^{-/-}$ mice[149]. This was thought to be related to reduced levels of pro-atherosclerotic chemokines which drove monocyte chemotaxis[149]. These studies demonstrate that the protease activity of coagulation factors may influence formation of atherosclerotic lesions by activating the inflammatory PAR pathways.

Adding to this, interfering with procoagulant phospholipid generation in murine models of abdominal aortic aneurysms lead a decrease in aneurysm formation[119]. These aortic lesions are atherosclerotic in nature with the added presence of intramural thrombi[150]. In a study from our group, genetic deletion of *Alox12* or *Alox15*, impairing the synthesis of the procoagulant 12- and 15-HETE-PL, resulted in reduced aneurysm formation[119]. These lipids were shown to be present within human aneurysmal aortic tissue and are known to be essential for normal

haemostatic mechanisms as described in section **1.3.5**[81,119]. Taken together, these studies suggest that the coagulation system and procoagulant membranes are also implicated in atherogenesis, taking them one step further from their role in driving thrombus formation. It remains unknown however whether circulating cells in patients with arterial thrombosis, such as ACS, possess a more procoagulant surface which may drive excessive thrombin generation. To address this, I will test the membrane procoagulant potential in circulating platelets, leukocytes and plasma EVs from patients with ACS versus healthy controls.

1.4.2 Plaque disruption and arterial thrombosis

The defective ECM that overlies the lipid-rich core of atheromas can form an overlying fibrous cap. These can fissure or erode exposing the circulation to the highly thrombogenic lipid-rich plaque which contain high levels of TF[130,151]. Disruption of these plaques can take place in coronary arteries (heart attacks or ACS), cerebral arteries (strokes) or peripheral limb arteries (critical limb ischaemia)[152,153]. The process of thrombosis on the surface of disrupted plaques is termed 'athero-thrombosis' or 'arterial thrombosis'[6].

Histological examination of ruptured plaques has demonstrated the presence of a thin fibrous cap with a very large necrotic lipid-rich core[153]. Plaques with these characteristics are traditionally described as 'vulnerable plaques', whereas those with thicker fibrous caps are termed 'stable plaques'. This classification attempts to simplify the complex spectrum of plaque destabilisation, with the aim of providing a framework that allows clinicians to decide which plaque requires treatment and which does not[154,155]. This however remains a challenge despite advances in intravascular imaging[156].

Whilst it remains unclear what process influences plaque stability, it is thought that inflammatory cells play a key role in impeding the synthesis of collagen by VSMC and consequently impairing the ability of these cells to maintain the skeleton of the fibrous cap[157,158]. These inflammatory processes include activation of interstitial collagenases by activated cells which degrade key components within the structure of the fibrous cap[159]. Weakening of these caps leads to atherosclerotic plaque rupture exposing the blood compartment to the thrombogenic plaque core. Another proposed mechanism for plaque disruption is erosion. Lesions implicated in plaque erosion seem to have a distinct morphology which distinguishes them from typical ruptured plaques. Specifically, they have a rich ECM composition, fewer inflammatory leukocytes, less lipid and no thin friable fibrous cap, yet remain capable of promoting thrombosis by exposing the inner core[160]. In both plaque rupture and erosion, the substances exposed to the circulation include TF produced by VSMC and macrophages which can activate the coagulation system leading to formation of thrombin and subsequently fibrin[161]. Thrombin also activates platelet aggregation, a major contributor to thrombus formation, which will be described below. What remains unknown is whether procoagulant PL on the surface of platelets, leukocytes or plasma EV are altered in patients in the acute stages of arterial thrombosis, and whether eoxPL contribute to the clot architecture. Here, I will address this by characterising the lipidomic composition of arterial thrombi as well as the membranes of circulating platelets, leukocytes and plasma EVs from patients with ACS versus healthy controls.

1.4.3 The role of platelets in arterial thrombosis

Rupture or erosion of atherosclerotic plaques exposes the blood vessel lumen to significant amounts of ECM proteins, such as collagen, and leads to platelet activation of platelets. This is followed by platelet aggregation on the surface of disrupted plaques which represents the

initial step in thrombus formation[162]. The exposure of collagen to the circulation leads to platelet activation both directly, through GP Ia/IIa and GP VI receptors, or indirectly via VWF bridges which form under high shear conditions between collagen and the platelet GP Ib-IX-V receptor[163]. This leads to platelet shape changes and subsequent release of ADP and TxA_2 which promote the activation and recruitment of further platelets to the site of the aggregate. Ligands such as adenosine triphosphate (ATP) released by leukocytes at the site of plaque disruption can also lead to platelet activation, indicating a possible role for non-platelet immune cells[164].

The presence of high shear velocity within arteries and the driving influence this has on VWF-mediated platelet activation had traditionally led to the belief that arterial thrombi are composed predominantly of platelets ('white clots') with little involvement from the coagulation system[165]. This however is untrue as these thrombi have been shown to contain a large amount of fibrin, which has been reported to occupy 43% of thrombus volume compared with 31% platelets, 17% red blood cells, 5% leukocytes and 2% microvesicles[165,166]. The high proportion of fibrin is thought to form and accumulate as a result of activation of the coagulation system by virtue of exposure to TF contained within plaques [162]. Therefore, it is evident that platelet-activation is not the sole contributor to this process and that the coagulation system is implicated as well. As described above in section **1.3**, the link between activation of the coagulation system and activated cells, such as platelets, is a procoagulant phospholipid surface. Despite this, no studies to date have investigated differences in the platelet procoagulant PL surface between patients with arterial thrombosis and healthy controls to test whether platelets provide a more prothrombotic PL reaction surface. This thesis will address this knowledge gap by studying the procoagulant lipidome of platelets from ACS patients compared with healthy controls.

1.4.4 Leukocytes, inflammation and arterial thrombosis

The same risk factors for endothelial dysfunction and the initiation of atherosclerosis described above, such as hyperlipidaemia, hypertension or diabetes, have been implicated in the activation of inflammatory pathways[120]. These pathways can then go on to alter arterial intimal cells causing further endothelial dysfunction and propagation of atherosclerosis. Using hypertension as an example, high levels of angiotensin II activate inflammatory pathways governed by the nuclear factor-κB (NF-κB) pathway[167]. Hypertension has also been implicated in the activation of adaptive T cell immunity leading to the release of a number of inflammatory cytokines such as tumour necrosis factor alpha (TNFα) and interferon gamma (IFNγ) causing further vascular dysfunction and damage[168]. T lymphocytes have also been shown to be present within human atheromas with varying roles in atherogenesis[169]. Another example of risk factors causing inflammatory propagation of atherosclerosis is insulin resistance and diabetes mellitus. In these conditions, changes in visceral adiposity have been shown to cause activation of inflammatory cells resident within adipose tissue[170,171]. This extravascular inflammation can still affect distant arterial walls by virtue of generating soluble inflammatory cytokines which lead to intimal cell activation and damage[172,173]. These data suggest that activation of inflammatory pathways and cells is central to the process of atherosclerosis, the precursor to arterial thrombosis. How this is linked with the processes of coagulation is not well understood currently.

In addition to adaptive immune cell activation, innate immune cells have been shown to contribute to athero-thrombotic process. In addition to the previously described roles of platelets and macrophage, granulocytes have also been shown to contribute to this process. Specifically, recent work on neutrophil extracellular traps (NETs) has implicated these cells in the process of vascular thrombosis[174]. NETs are released by neutrophils that undergo a

specialised form of cell death known as NETosis and consist of DNA strands that bind to proteins, such as TF, and leukocyte enzymes. They are present in blood clots where they propagate thrombosis and amplify intimal injury[175,176]. Other innate immune cells that are associated with arterial thrombosis include eosinophils. Activation of these cells, as measured by the levels of eosinophilic cationic protein, predicts cardiovascular outcomes such as stroke and myocardial infarction[72]. Histological sections of arterial and venous thrombi have shown the presence of eosinophils within the architecture of the clot. The mechanisms involved in the prothrombotic contribution of eosinophils are thought to relate to the presence of endogenous TF on their surface, the presence of procoagulant PLs (15-HETE-PL) as well as the formation of eosinophil extracellular traps where are thought to work in a similar way to NETs[72,177,178]. However, it remains unknown whether other procoagulant lipids, such as aPL and eoxPL, on the surface of leukocytes are dysregulated in ACS patients.

Given the evidence of immune cell activation described above, it is no surprise that markers of inflammation, such as C-reactive protein (CRP) rise in patients with arterial thrombosis and can predict cardiovascular risk[179]. These findings have become the foundation of the increasingly popular 'inflammatory hypothesis' which is thought to drive arterial thrombosis[180]. This hypothesis lead to a number of recent land mark clinical trials examining the effects of anti-inflammatory therapies for the secondary prevention of further heart attacks and strokes with positive preliminary results[181,182]. Whether the presence of inflammation in arterial thrombosis translates into activation of lipid metabolism pathways and generation of bioactive inflammatory procoagulant lipids on the surface of immune cells remains unstudied. This will be addressed in this thesis by studying the aPL and eoxPL lipidome of leukocytes from patients with ACS compared with healthy controls.

1.4.5 Extracellular vesicles (EV)

EVs are PL membrane-bound structures which bud off activated cells containing antigens specific to the parent cell, but no nucleus[183-185]. Whilst all EV's are defined as vesicles less than 1 μm in diameter, a number of subtypes exist within this all-encompassing definition[98]. The main two subtypes are exosomes and ectosomes, but it is worth noting that experimental EV isolates may also include apoptotic bodies and lipoproteins, which are also submicron PL-bound particles. Exosomes are released from cells by exocytosis of endocytic and multivesicular bodies, whereas ectosomes originate directly from the membrane surface of the parent cell (**Figure 1.12**) [186,187]. Both of these EV subgroups are characterised by the presence of aPL on their membrane surface, with the additional presence of tetraspanin proteins in the case of exosomes[188]. Having said that, many variations exist in definitions and nomenclature with significant overlap in the literature making it very difficult to reliably restrict published findings to one EV subtype or the other. For the purposes of this thesis, the introductory focus will be describing ectosomal EVs (also known as microvesicles) and their formation, though going forward, assays employed in this thesis to isolate EVs face the same challenges encountered by the literature in isolating a pure subtype.

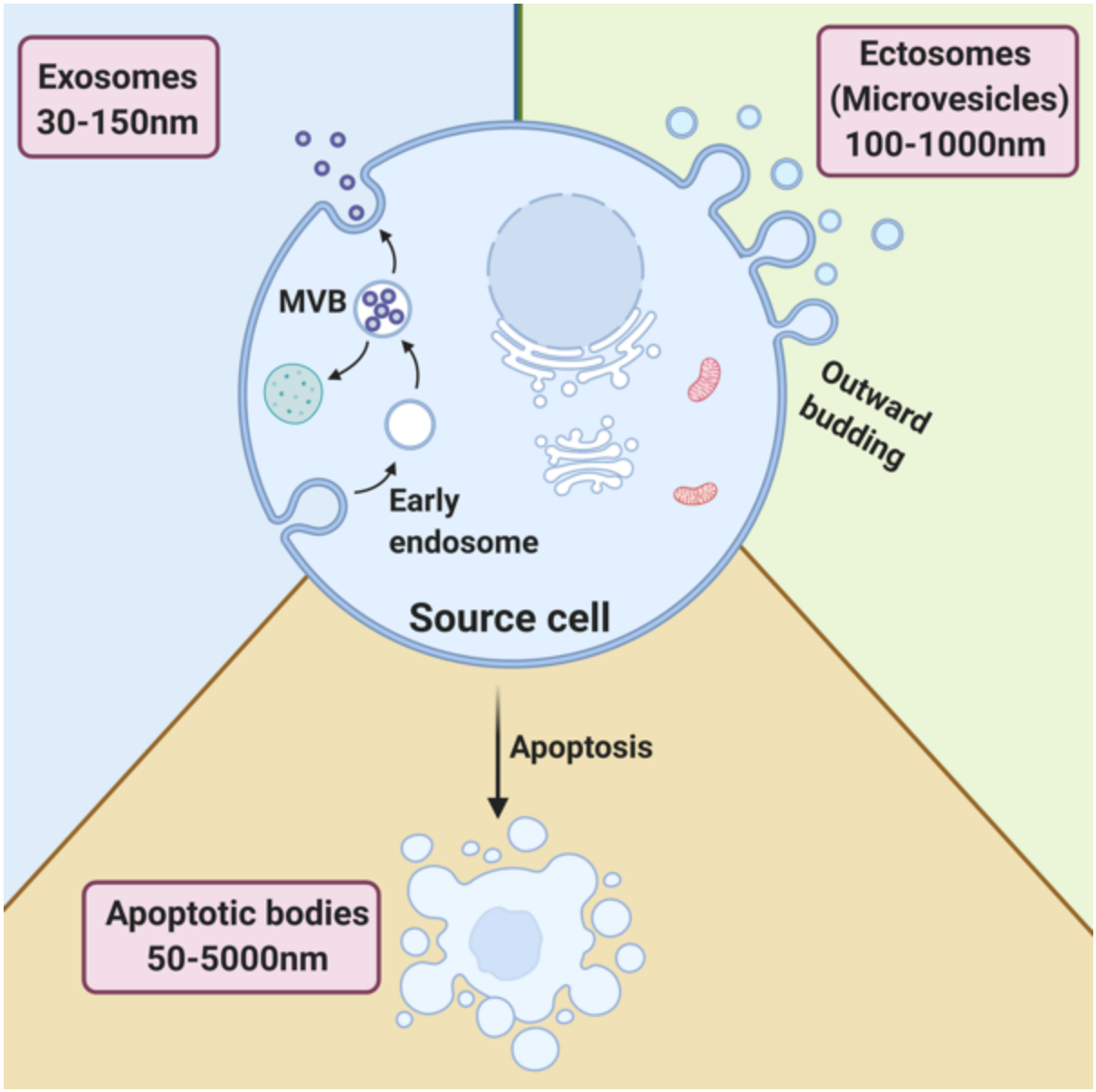

Figure 1.12. Schematic representation of subtypes of extracellular vesicles (EV) released by a cell and their respective diameters.

EV isolates contain three main subtypes: exosomes, ectosomes and apoptotic bodies. Exosomes are released by exocytosis, whereas ectosomes (also known as shedding microvesicles) are secreted by outward budding of the plasma membrane. Apoptotic bodies are released by dying cells during the later stages of apoptosis so that cell debris can be phagocytosed and cleared by immune cells. MVB: multivesicular body.

In order for blood cells to initiate EV formation, cell activation or apoptosis needs to take place. This starts by calcium mobilisation within the endoplasmic reticulum which leads to loss of membrane asymmetry and exposure of aPL to the surface via the scramblase enzymes. This is accompanied by activation of calpain and gelsolin, two enzymes that are critical for EV formation by disrupting the actin cytoskeleton resulting in membrane budding and EV shedding[189]. Calpain severs the association of actin with membrane proteins by disrupting actin-binding proteins, whereas gelsolin achieves similar results by cleaving actin capping proteins[190-192]. The end result is release of EV enriched in aPL on their membrane, with estimates derived from high-performance thin layer chromatography (HPTLC) on EV from healthy human plasma describing 60% PC, 9% PE and 4% PS with the remainder consisting of other lipids[193]. What remains unknown about EV membranes is whether they contain eoxPL. Several studies have reported the presence of truncated oxPL on the surface of EV budding off apoptotic cells. These include oxPC which has been demonstrated using the E0 monoclonal antibody with flow cytometry studies of EVs released from *in-vitro* activated endothelial cells[194]. However, no studies to date have examined the presence of eoxPL on plasma EV membranes. This gap in the knowledge will be examined in this thesis using lipidomic studies on plasma EV from patients with ACS and healthy controls.

EVs in the circulation originate from different cells including platelets, leukocytes, erythrocytes and endothelial cells, with platelet EVs thought to represent 70-90% of all circulating particles[195]. Differences in their total amount or relative proportions relate to the rate of their release from cells and subsequent clearance from the circulation[98]. Mechanisms for EV removal are not well understood, making it difficult to define their lifespan after formation. Reports of murine models of platelet-derived EV *in vivo* describe a 30 minute lifespan[196]. Possible clearance mechanisms include phospholipases, phagocytosis or

opsonization and subsequent clearance[197,198]. The gap in our knowledge of how EVs are cleared makes it difficult to determine whether the persistently high EV levels found in patients with conditions such as ACS relate to the index event or are a consequence of ongoing inflammatory cell activation and EV turnover[199].

Similar to activated platelets and immune cells, EVs expose procoagulant aPL on their surface, giving it a potential role in the process of coagulation. The involvement of EV in coagulation was first described in 1967, when Wolf et al described 'platelet dust' in reference to EV aggregates that were noted in human plasma coagulation assays[200]. Subsequent research groups identified EV formation following platelet stimulation by collagen and thrombin, with a 10-fold more abundance in serum compared to plasma indicating that they are produced in the course of clotting[201,202]. Of interest to this thesis, exposing whole blood to high shear stress similar to that seen in severe atherosclerosis has been shown to activate platelets and generate platelet-derived EVs, unlike normal arterial shear stress[203]. The mechanistic basis for this is thought to relate to VWF-GP Ib-IX-V activity, and results in the deposition of potentially procoagulant EVs at the stenotic site which are not dislodged under extreme flow conditions akin to those present in atherosclerotic arteries[204]. These observations have led to an increasing interest in the involvement of EVs in thrombotic processes which will be described below. Whilst the presence of aPL on the external membrane leaflet is characteristic of EV, it remains unknown what proportion of aPL is externalised compared to total aPL (throughout the membrane). In this thesis, I will be quantifying the fraction (percentage) of aPL externalised to the EV surface in patients with arterial thrombosis as well as healthy controls.

1.4.6 Role of plasma EV in thrombosis and haemostasis

The presence of procoagulant aPL and TF on the surface of EVs is reported to provide around 50 to 100-times more procoagulant properties than an identical surface area unit of an activated platelet[205]. TF-positive EVs have a leukocyte origin and are present within thrombi, as detected by intravital microscopy[206]. It is thought that the small size of TF-positive EVs allows them to access the centre of the thrombus and interact with platelet P-selectins much quicker than the much larger TF-bearing leukocyte[207]. Conflicting reports exist describing the presence of TF on the surface of some platelet-derived EVs, despite the fact that platelets lack the machinery to generate TF themselves[98,99,208]. Such TF-positive platelet EVs may have acquired TF as a result of transfer from monocytes and granulocytes to platelets[99,209]. It is worth noting that outside of their role in TF decryption, EV membrane aPLs have received little attention in how they contribute to TF-independent coagulation reactions and whether their composition differs between health and disease. To address this, I will measure coagulation reactions on the surface of plasma EV using a purified mixture of FXa:FVa and prothrombin, thereby analysing the contribution of the lipid membrane independent of TF status.

The role of EVs in haemostasis is illustrated by defects in their production in patients with Castaman's and Scott syndrome, resulting in a bleeding phenotype. Patients with Castaman's syndrome have normal platelet prothrombinase activity, but lack the ability to generate EVs due to an unknown mechanism and demonstrate a bleeding tendency as a result[210,211]. A similar phenotype is observed in patients with Scott syndrome who lack the 'scramblase' functionality described in section **1.2.2**, and therefore have impaired platelet prothrombinase activity due to defective aPL externalisation[212]. Of interest to this section, EV formation is also defective in patients with Scott syndrome, highlighting the importance of aPL externalisation as a pivotal prerequisite step in the formation of EVs[213-215]. Interestingly, patients suffering from

Stormorken's syndrome (also known as 'inverse Scott syndrome') also exhibit a bleeding tendency despite having a constitutive activation of platelets with elevation of circulating platelet-derived EVs[216]. These observations of a bleeding phenotype at extremes of EV counts suggest a complex non-linear relationship between EV formation and procoagulant phenotypes.

The pathological role of EVs in driving thrombosis has been described in models of arterial and venous thrombosis[217]. In murine models of arterial thrombosis, thrombus formation was supported by the accumulation of EVs which participated in fibrin deposition[206,218,219]. Similarly, models of venous thrombosis demonstrated enhanced thrombosis when TF-positive EVs derived from thrombosed mice were injected into healthy mice [220]. In a hybrid model utilising EVs from humans and introducing them into venous stasis models in rats demonstrated higher thrombogenicity in TF positive EVs from patients undergoing cardiac surgery compared to healthy controls[221]. Finally, human diseases implicating EVs in thrombosis have focused mainly on their role in cancer-associated thrombosis where evidence of increased thrombogenicity was demonstrated for EVs derived from tumour cells[222,223]. These studies confirm that EV are prothrombotic, but it remains unclear whether this is due to the presence of TF, procoagulant PL or indeed both on the EV surface.

Of particular interest to this thesis is the presence of higher numbers of EVs in patients suffering from arterial thrombosis and its risk factors[224-230]. Patients suffering from hypertension have higher levels of circulating EVs which correlate with their blood pressure readings and are thought to be generated as a consequence of higher shear pressures[224]. Similarly, diabetes mellitus is associated with higher levels of EVs released as a consequence of stimuli such as advanced glycation products and oxidative stress, with a higher procoagulant

phenotype in patients with poor glycaemic control[225,226]. Patients with dyslipidaemias have upregulated EV levels as a consequence of LDL-induced membrane blebbing[227]. Indeed, the development of atherosclerosis may be influenced by EVs, generated as a result of the mechanisms described above, which alter the profile of adhesion molecules on endothelial cells and promote monocyte transmigration and vascular inflammation[98,231]. In addition, the presence of high amounts of EVs within the atherosclerotic plaque may contribute to the thrombotic process that follows plaque rupture[232]. This may implicate EVs in ACS where elevated numbers were demonstrated in comparison to CAD patients[228-230], and shown to positively correlate with high-risk coronary angiographic features[233].

It is worth noting that beyond their proposed use as biomarkers and presence in higher amounts, the exact role and regulation of EVs in human arterial thrombosis remains largely unstudied. Furthermore, it is not known whether higher levels of aPL are exposed on the EV membrane in patients with ACS compared to healthy controls, whether eoxPL are present and if the lipid membrane contribute to a prothrombotic phenotype independent of TF activity. These questions will be addressed as part of this thesis by using thrombin generation assays and lipidomic studies on plasma EV from ACS patients and healthy controls.

1.5.1 Aspirin

Given the role of platelets in promoting thrombosis, a number of pharmacological inhibitors have been developed, the first of which was aspirin. Initially used as an anti-inflammatory and analgesic, it was not until the 1960s and 1970s that research established aspirin as an effective anti-thrombotic agent associated with a reduction in the rates of myocardial infarctions[234,235]. Since then, aspirin has been shown to have marked benefits in the management of arterial thrombosis (e.g. myocardial infarction and stroke) and secondary prevention of cardiovascular disease, with some potential for primary prevention in healthy people[236].

Aspirin is a potent irreversible inhibitor of COXs which works by acetylating serine residues within the active site, thus preventing the binding of PUFA substrates and blocking oxylipin synthesis [237]. Given that platelets are anucleate and thus, are unable to synthesise more COX-1, the aspirin inhibitory effect persists for the entirety of their lifespan (10 days) and leads to a reduction in TxA_2 synthesis. By doing so, continuous low dose aspirin supplementation (at 75mg once daily) will generate an anti-platelet effect by reducing secondary aggregation downstream of TxA_2 receptors (TPα and TPβ)[237].

The impact of aspirin on eoxPL generated downstream of platelet 12-LOX remains not characterised. This is of particular importance given that both COX-1 and 12-LOX share the same PUFA substrates, and therefore aspirin supplementation may interfere with the 12-LOX pathway indirectly. This thesis addresses this gap in the literature by studying the effect of aspirin on 12-LOX generated eoxPL in a healthy cohort of 28 individuals (**Chapter 3).**

1.5.2 Anti-coagulant agents and arterial thrombosis

Up until recently, the use of anticoagulants in the management of arterial thrombosis has been limited. This was the result of an absence of net clinical benefit when warfarin, the oldest and most commonly used oral anticoagulant, was used in the management of arterial thrombosis (e.g. acute coronary syndrome - ACS). Warfarin works by blocking vitamin K epoxide reductase, interfering with the synthesis of coagulation factors FII, FVII, FIX and FX and leading to an anti-coagulant effect[28]. Despite being significantly beneficial in the treatment of venous thrombosis and atrial fibrillation, studies examining its effectiveness in treating arterial thrombosis, such as in ACS, have demonstrated mixed results with a substantial risk of bleeding offsetting any anti-ischaemic benefits[238-240]. This reinforced the traditional view that arterial thrombosis occurring under high shear flow conditions is a platelet-driven event with limited contribution from the coagulation system[28].

Newer direct-acting oral anti-coagulant (DOAC) medications were developed in the last decade with seemingly better safety profiles that warfarin[28]. Given this and their ease of dosing with no requirement for monitoring, these agents gained rapid popularity[28,241]. This also facilitated their testing in patients with ACS, where there is convincing evidence of increased thrombin production and therefore involvement of the coagulation cascade[28]. The most significant demonstration of their effectiveness in this context was shown in the ATLAS ACS 2-TIMI 51 trial in 2012[242]. This study showed that low dose rivaroxaban (2.5 mg twice daily, as opposed to the venous thrombosis dose of 20 mg once daily) reduced the occurrence of the primary outcome of cardiovascular death, myocardial infarction or stroke by 16%, with a small increase in the risk of bleeding (2.1% versus 0.6% compared to placebo). Rivaroxaban works by directly inhibiting FXa, a coagulation factor that is responsible for the generation of thrombin. Therefore, the finding of a beneficial role with an anti-coagulant in ACS has strongly

re-ignited interest in the role of thrombin generation and the coagulation system in the pathophysiology of ACS.

In order for FXa to be synthesized and to function as a prothrombinase (along with its co-factor FVa), it requires the presence of a procoagulant PL membrane. Despite this, the role of the PL surface in the context of arterial thrombosis remains undefined. I will address this gap in the literature by studying the procoagulant lipidome (both aPL and eoxPL) and its ability to generate thrombin on the surface of circulating platelets, leukocytes and plasma EV from a clinical cohort of patients with ACS and healthy controls.

1.6 LIPIDOMICS

Lipidomics refers to the comprehensive, large-scale analysis of lipids in biological systems. This is possible owing to recent advances in liquid chromatography (LC) followed by soft ionisation tandem mass spectrometry (MS/MS) techniques. LC-MS/MS has high sensitivity for detecting large numbers of molecular species within a sample based on separation of lipids by structural differences such as double bond position using LC, followed by separation by mass/charge ratios (*m/z*) using MS/MS[9]. In my studies, LC-MS/MS will be used for the lipidomic analysis of cells, plasma EVs and clots.

1.6.1 Liquid chromatography with tandem mass spectrometry (LC-MS/MS)

The use of reverse phase LC prior to MS allows the user to separate lipids based on their lipophilicity. In simple terms, the sample is injected into a stream of mobile phase consisting of a mixture of aqueous and organic solvents, which then passes through an LC column containing a non-polar stationary phase at a specified flow rate. The lipids within the sample will interact with both the mobile and stationary phases leading to adsorbance followed by elution at varying times, known as retention time (RT). Given the range of lipids that may be present within a biological sample, the choice of column and mobile phases will vary and the method may require optimisation to enable detection of the lipid species of interest.

Following separation with LC, samples are passed to the MS for detection and further chemical characterisation. Using an electrospray ionisation (ESI) chamber, compounds resolved by LC are ionised through a hypodermic needle maintained at a high voltage. The result is the creation of positively charged ions by the addition of cations such as hydrogen

([M+H]+), or negatively charged ions by the subtraction of a hydrogen nucleus ([M-H]-). These ions are then passed through a mass filter based on their mass to charge ratio (*m/z*) prior to reaching a mass detector. An example of a mass filter is a quadrupole, which is made of four equidistant parallel rods through which an oscillating radiofrequency field is applied. The charged ions pass through the quadrupole and their paths are selectively stabilized or destabilized based on the radiofrequency field generated by a pre-specified voltage passing through the four rods. This allows the instrument to define the range of *m/z* filter which can then reach the detector, whereas ions with unstable trajectories will collide with the rods and are eliminated.

The detection of precursor ions and their product fragments may be accomplished using individual MS elements separated in space (such as with a triple quadrupole instrument) or a single MS element separated in time (such as an ion trap) [243]. Tandem MS/MS with a triple quadrupole allows for the analysis of precursor and product ions in separate regions of the instrument, and is thus tandem in space. In contrast, using MS with an ion trap utilises the same physical space for the detection of precursor and product ions with a timing sequence[243]. For the purposes of this thesis, the MS/MS instrument utilised will be a triple quadrupole which consists of three separate quadrupole chambers, the first and third of which are mass analysers that house four parallel gold-plated rods (quadrupoles). The second is a collision cell where nitrogen or argon fragment the molecule for MS/MS analysis. The first quadrupole (Q1) acts as a mass filter for precursor/parent ions. These are then passed to the collision cell (Q2) where a neutral gas (e.g. argon) is used to induce multiple collisions resulting in fragmentation. In the third chamber (Q3), the product ions are passed to scan for a range *m/z* ratios to allow for the recognition of parent and daughter ions of a specific *m/z* through a detector[9]. **Figure 1.13** demonstrates the typical configuration of a triple quadrupole LC-MS/MS instrument.

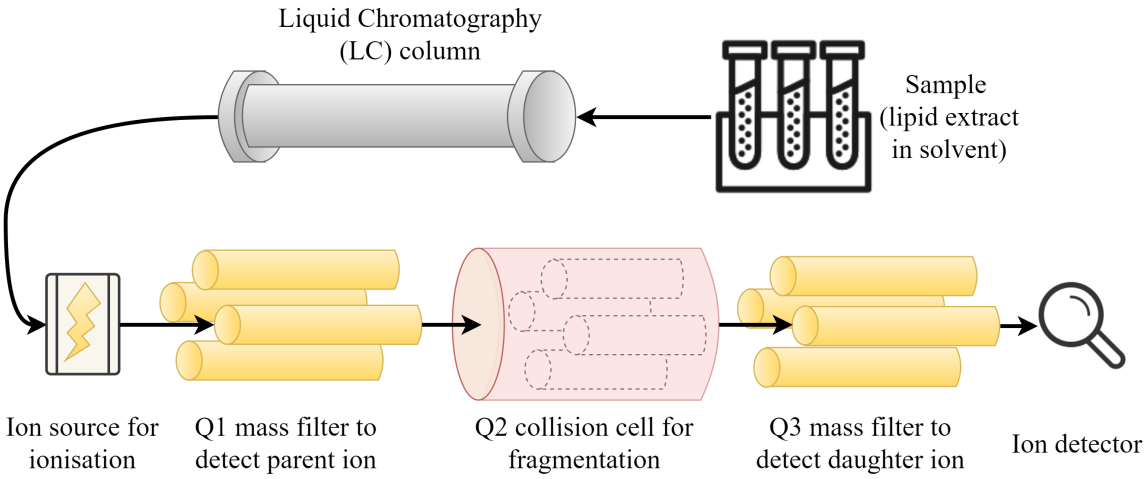

Figure 1.13. The typical configuration of a liquid chromatography with tandem mass spectrometry (LC-MS/MS) device.

Processed samples which are dissolved in solvent are injected into the LC column to facilitate separation by structural differences based on retention times. Separated lipids are then fed into the MS/MS and ionised to generate an *m/z* ratio for each precursor lipid. These may be filtered in the first set of quadrupoles (Q1) prior to passing into the collision cell (Q2). Fragmented product ions are filtered in the third set of quadrupole (Q3). Transitions of Q1 mass to Q3 mass coupled to LC retention time facilitate accurate detection of lipid species.

1.6.2 Targeted lipidomics with LC-MS/MS

In targeted LC-MS/MS, lipids eluting at different times from the LC are passed to the MS/MS and monitored using multiple reaction mode (MRM). In this setting, parent (precursor) and daughter (product) *m/z* for lipids of interests are prespecified in the machine which optimizes the time spent acquiring data and provides sufficient data points across peaks. This method maximizes sensitivity which allows the detection of small amounts of analytes with good precision[9]. The choice of parent and daughter ions is based on knowledge of the fragmentation pattern of the analyte and the resulting mass spectrum. For instance, 12-HETE fragmentation in negative ion mode results in a specific product ion with an *m/z* of 179.1. This could be targeted with MRM scanning for the transition from 319.2 (parent) to 179.1 (daughter) to detect 12-HETE in analysed samples (**Figure 1.14**).

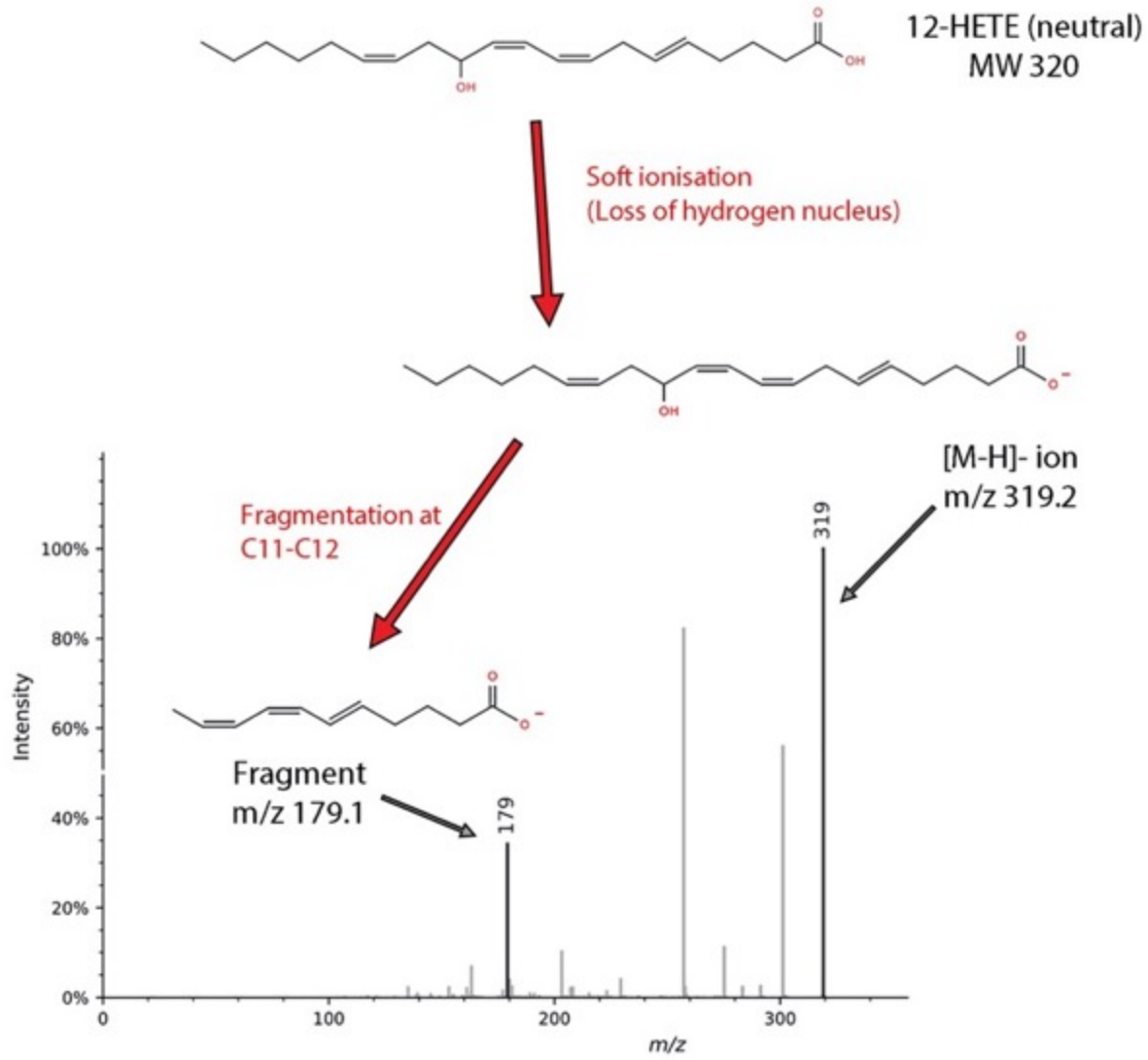

Figure 1.14. Mass spectrometry fragmentation pattern for 12-HETE in negative mode.

The molecular weight (MW) of 12-HETE is 320. This undergoes 'soft ionisation' in the ion source of the mass spectrometer (MS) by removal of a proton. The resultant [M-H]- precursor ion carries a mass to charge ratio (*m/z*) of 319.2 in negative ion mode. Following fragmentation in the collision cell, multiple product ions may be detected in the resultant mass spectrum, with the 179.1 *m/z* ion being described as being specific for 12-HETE[244]. Chemical structures were adapted from LIPID MAPS. The mass spectrum was obtained from Metabolomics Spectrum Resolver as fragmented on a Qtrap 4000 MS/MS instrument (UCSD, mzspec:MASSBANK::accession:UT000029).

1.7 HYPOTHESIS AND AIMS

The evidence presented above describes what is currently known about eoxPL generation in response to inflammation and agonist-activation of immune cells (section **1.2.4**). Nevertheless, no studies to date have examined how eoxPL generation in platelets varies in response to differences in gender or aspirin supplementation. This thesis tackles this gap in the literature by presenting the largest study to date on how eoxPL generation varies by gender, aspirin and over time in platelets from a healthy cohort.

Despite the literature review presented above which indicates an essential role for membrane PLs in driving effective coagulation (section **1.3**), it is not known whether the procoagulant potential of PL membranes from platelets, leukocytes and plasma EV varies between ACS and healthy controls. This question will be addressed as part of this thesis using a TF-independent chromogenic thrombin generation assay to determine whether differences exist in the ability of PL membranes to facilitate coagulation reactions. In addition, this thesis will present the first lipidomic analysis of human arterial thrombi quantifying the amounts of HETE-PL, whose role in arterial thrombosis remains unknown.

Finally, there is increasing evidence for aPL and eoxPL in promoting coagulation reactions *in-vitro* and in murine and human models of disease. Nevertheless, it remains unknown whether procoagulant PL profiles on the surface of circulating platelets, leukocytes and plasma EVs vary between patients with arterial thrombosis, such as ACS, and healthy controls. This gap in the knowledge will be addressed by the presented thesis by comparing aPL and eoxPL amounts on circulating membrane surfaces from patients with ACS versus healthy controls. This will utilise contemporary lipidomic techniques relying on the use of LC-MS/MS and derivatisation methods to facilitate the detection and quantification of these lipids.

On the whole, characterizing the procoagulant lipidome from ACS patients will improve our understanding of the role of membrane PL in these conditions and their influence on membrane procoagulant potential. This may lead to the identification of PL-based therapeutic targets for the prevention and treatment of pathological clotting.

1.7.1 Hypothesis

An altered procoagulant surface of circulating blood cells contributes to the underlying mechanisms of thrombosis in ACS.

1.7.2 Aims

Aim 1: To characterise the eoxPL composition of platelets collected from healthy people, and investigate the influence of gender and aspirin on levels and composition.

Aim 2: To determine the eoxPL composition of arterial thrombi from patients with coronary or peripheral vascular disease.

Aim 3: To determine the capacity of the platelet, leukocyte and plasma EV membrane surfaces to support coagulation in patients with ACS compared to healthy and disease-matched controls.

Aim 4: To determine the membrane surface aPL and eoxPL composition of platelets, leukocytes and plasma EV in patients with ACS compared to healthy and disease-matched controls.

CHAPTER 2 MATERIALS AND METHODS

2.1.1 Chemicals

Solvents and solutions were purchased from ThermoFisher Scientific (Massachusetts, USA) as follows: HPLC grade water (H_2O), glacial acetic acid, propan-2-ol (IPA), hexane, chloroform, methanol (MeOH), acetonitrile (ACN), tissue culture grade phosphate buffered saline (PBS), NHS-biotin and EZ-Link Sulfo-NHS-biotin.

Chemical powders were from Sigma Aldrich (Missouri, USA) as follows: diethylenetriaminepentaacetate (DTPA), acetaminophen, butylated hydroxytoluene (BHT), pentamethylchromanol, stannous chloride ($SnCl_2$), trisodium citrate dihydrate, citric acid monohydrate, sodium chloride (NaCl), sodium hydrogen carbonate ($NaHCO_3$), potassium chloride (KCl), di-sodium hydrogen orthophosphate, sodium hydroxide (NaOH), hydrochloric acid (HCl), sodium dihydrogen orthophosphate dihydrate, magnesium chloride hexahydrate, HEPES, glucose, dimethyl sulfoxide (DMSO), L-lysine, calcium chloride ($CaCl_2$), bovine thrombin, calcium ionophore (A23187), trypan blue, triethylamine, trisaminomethane base (tris) and ethylenediaminetetraacetic acid (EDTA).

Hetasep was purchased from StemCell Technologies, Canada.

2.1.2 Coagulation factors and chromogenic substrates

Coagulation factors and chromogenic substrate were obtained from Enzyme Research Laboratories (Swansea, UK), except for Human Factor Va which was obtained from Haematologic/Cambridge Bioscience (Cambridge, UK). Coagulation factors were reconstituted in H_2O and aliquoted as follows: Human Prothrombin (Factor II) 20 μM, Human

Factor Va 1 μm, Human Factor Xa 10 μM, Human Alpha Thrombin (Factor IIa) for standard curve generation 10 μM. The chromogenic substrate S-2238 (Pefachrome TH 8198) was reconstituted in H_2O at 2.8 mM.

2.1.3 Lipids

Phospholipid standards were purchased from Avanti Polar Lipids (Alabama, USA): 1,2-dimyristoyl-*sn*-glycero-3-phosphoethanolamine (DMPE), 1,2-dimyristoyl-*sn*-glycero-3-phosphatidylcholine (DMPC), 1,2-dimyristoyl-*sn*-glycero-3-phosphatidylserine (DMPS), 1-stearoyl-2-arachidonoyl-*sn*-glycero-3-phosphoethanolamine (SAPE), 1-stearoyl-2-arachidonoyl-*sn*-glycero-3-phosphoethanolamine (SAPC), 1-stearoyl-2-arachidonoyl-*sn*-glycero-3-phosphoserine (SAPS), 1-stearoyl-2-oleoyl-*sn*-glycero-3-phospho-L-serine (SOPS), 1-(1Z-octadecenyl)-2-arachidonoyl-*sn*-glycero-3-phosphoethanolamine (SpAPE) and 1,2-dioleoyl-*sn*-glycero-3-phospho-L-serine (DOPS),

Deuterated eicosanoid standards 12(S)-hydroxyeicosatetraenoic acid (12(S)-HETE-d8) and thromboxane B2 (TxB_2-d4) were purchased from Cayman Chemical (Michigan, USA).

2.2 BUFFERS

2.2.1 Buffers for platelet isolation and activation

Acid Citrate Dextrose (ACD)

25g of Trisodium citrate, 13.7 g citric acid and 20 g glucose were dissolved in 900 ml of H_2O. The pH was adjusted to 5.4 and the solution was made up to 1 L with H_2O to give a final concentration of 85 mM trisodium citrate, 65 mM citric acid and 100mM glucose. The solution was syringe filtered through a 0.22 μm filter, dispensed into 15 ml aliquots, and stored at -20 °C.

Tyrodes buffer

7.84 g NaCl, 1.02 g $NaHCO_3$, 0.22 g KCl, 0.09 g di-sodium hydrogen orthophosphate, 0.3 g magnesium chloride hexahydrate, 2.38 g HEPES and 0.9 g glucose were dissolved in 900 ml H_2O. The pH was adjusted to 7.4 and the solution was made up to 1 L with H_2O to give a final concentration of 134 mM NaCl, 12 mM $NaHCO_3$, 2.9mM KCl, 0.34 mM di-sodium hydrogen orthophosphate, 1 mM magnesium chloride hexahydrate, 10mM HEPES and 5 mM glucose. The solution was vacuum filtered through a 0.22 μm filter, dispensed into 50 ml aliquots, and stored at -20 °C.

Stock bovine thrombin (20 U/ml)

Lyophilized bovine thrombin powder (100 U) was reconstituted in 5 ml sterile PBS to give a stock of 20 U/ml. The solution was dispensed into 20 μl aliquots and stored at -80 °C.

2.2.2 Buffers for leukocyte isolation and activation

Krebs buffer

5.8 g NaCl, 11.37 g HEPES, 0.37 g KCl, 0.16 g sodium dihydrogen orthophosphate dihydrate and 0.36 g glucose were dissolved in 900 ml H_2O. The pH was adjusted to 7.4 and the solution was made up to 1 L with H_2O to give a final concentration of 100 mM NaCl, 48 mM HEPES, 5 mM KCl, 1 mM sodium dihydrogen orthophosphate dihydrate and 2 mM glucose. The solution was vacuum filtered through a 0.22 μm filter, dispensed into 10 ml aliquots, and stored at -20 °C.

PBS/0.4% tricitrate (w/v)

4 g trisodium citrate was dissolved in 900 ml PBS. The pH was adjusted to 7.4 and the solution was made up to 1 L with PBS. It was then vacuum filtered through a 0.22 μm filter, dispensed into 50 ml aliquots, and stored at -20 °C.

2% Citrate (w/v)

20 g trisodium citrate was dissolved in 900 ml H_2O. The pH was adjusted to 7.4 and the solution was made up to 1 L with H_2O. It was then vacuum filtered through a 0.22 μm filter, dispensed into 50 ml aliquots, and stored at -20 °C.

RBC lysis buffer (0.2% hypotonic saline)

2 g NaCl was dissolved in 1 L H_2O. The solution was vacuum filtered through a 0.22 μm filter, dispensed into 50 ml aliquots, and stored at -20 °C.

Stock A23187 (2 mM)

5 mg of A23187 powder was reconstituted in 4.8 ml DMSO to give a stock of 2 mM. The solution was dispensed into 10 µl aliquots and stored at -80 °C.

2.2.3 Buffers for prothrombinase assay

Tris-buffered saline (TBS)

24 g Tris and 88 g NaCl were dissolved in 900 ml H_2O. The pH was adjusted to 7.4 and the solution was to 1 L with H_2O. This created a 10x TBS stock to be diluted 1:10 (v/v) with H_2O immediately prior to use to give a final TBS composition of 20mM Tris and 150 mM NaCl. The stock was vacuum filtered through a 0.22 µm filter, dispensed into 1 ml aliquots, and stored at -20 °C.

Stock 5% BSA (w/v)

5 g of BSA was dissolved in 100 ml TBS. The solution was filter sterilised through a 0.22 µm filter, and stored at -20 °C.

TBS/BSA Prothrombinase buffer

100 µl of stock 5 % BSA was added to 1 ml of 10x TBS and the volume was made up to 10 ml with H_2O. The final composition therefore was 0.05 % BSA (w/v) in TBS. The solution was vacuum filtered through a 0.22 µm filter and stored at 4 °C for up to 2 weeks.

Stock $CaCl_2$ (1 M)

7.35 g $CaCl_2$ was dissolved in 50 ml H_2O. The solution was filter sterilised with 0.22 µm filter, dispensed into 1.5 ml aliquots and stored at -20 °C.

EDTA (35 mM)

1.02 g EDTA was dissolved in 100 ml H_2O. The solution was filter sterilised with 0.22 µm filter, dispensed into 100 µl aliquots and stored at -20 °C.

2.2.4 Buffers for lipid extraction and sample processing

Pentamethylchromanol (10 mM)

220 mg of pentamethylchromanol was dissolved in 100 ml chloroform. The solution was prepared immediately before use.

DTPA stock solution (10 mM)

DTPA stock solution (10 mM) was made by dissolving 3.93 mg of DTPA in 1 ml H_2O, followed by the addition of 30 µl NaOH (1 M) to facilitate dissolving at 37 ºC.

Acetaminophen stock (7.5 mM)

Acetaminophen stock solution (7.5 mM) was made by dissolving 1.13 mg in 1 ml H_2O.

BHT Stock (10 mM)

BHT 10 mM stock was made by dissolving 2.20 mg in 1 ml of MeOH.

$SnCl_2$ stock solution (7.5 mM)

$SnCl_2$ 100 mM stock was made by dissolving 18.9 mg into 1 ml of H_2O. All stocks were prepared fresh on the day of lipid extraction.

Anti-oxidant buffer

This was made as a stock of 25 ml of cold PBS (4 ^{o}C) containing DTPA (100 μM), BHT (100 μM) and acetaminophen (7.5 μM). This was prepared fresh on the day of lipid extraction and placed on ice.

2.3 HEALTHY COHORT FOR PLATELET EOXPL CHARACTERISATION

A total number of 28 healthy volunteers were recruited from the workplace (14 male, 14 female) for a study that utilised untargeted platelet lipidomics to investigate differences amongst individuals (Brasher et al, unpublished). The recruitment took place between August 2016 to June 2017, and was completed prior to commencing my PhD. Information is provided below on the sampling and generation of samples, which were then available for me to carry out targeted LC-MS/MS to investigate platelet eoxPL lipidomics.

For this study, all participants signed written consent forms in line with the ethical approval obtained from Cardiff University (SMREC16/02). They then underwent phlebotomy from a peripheral vein to provide a blood sample for platelet isolation.

The entry criteria included a two-week washout period from any non-steroidal anti-inflammatory drugs (NSAIDs) use. Following the initial sample collection, participants were commenced on aspirin 75 mg once daily for seven days and sampled thereafter, before stopping the aspirin. Participants were invited to repeat this process after two months and four months of the initial sampling date. **Figure 2.1** describes the recruitment schedule and indicates recruitment rates and loss to follow up.

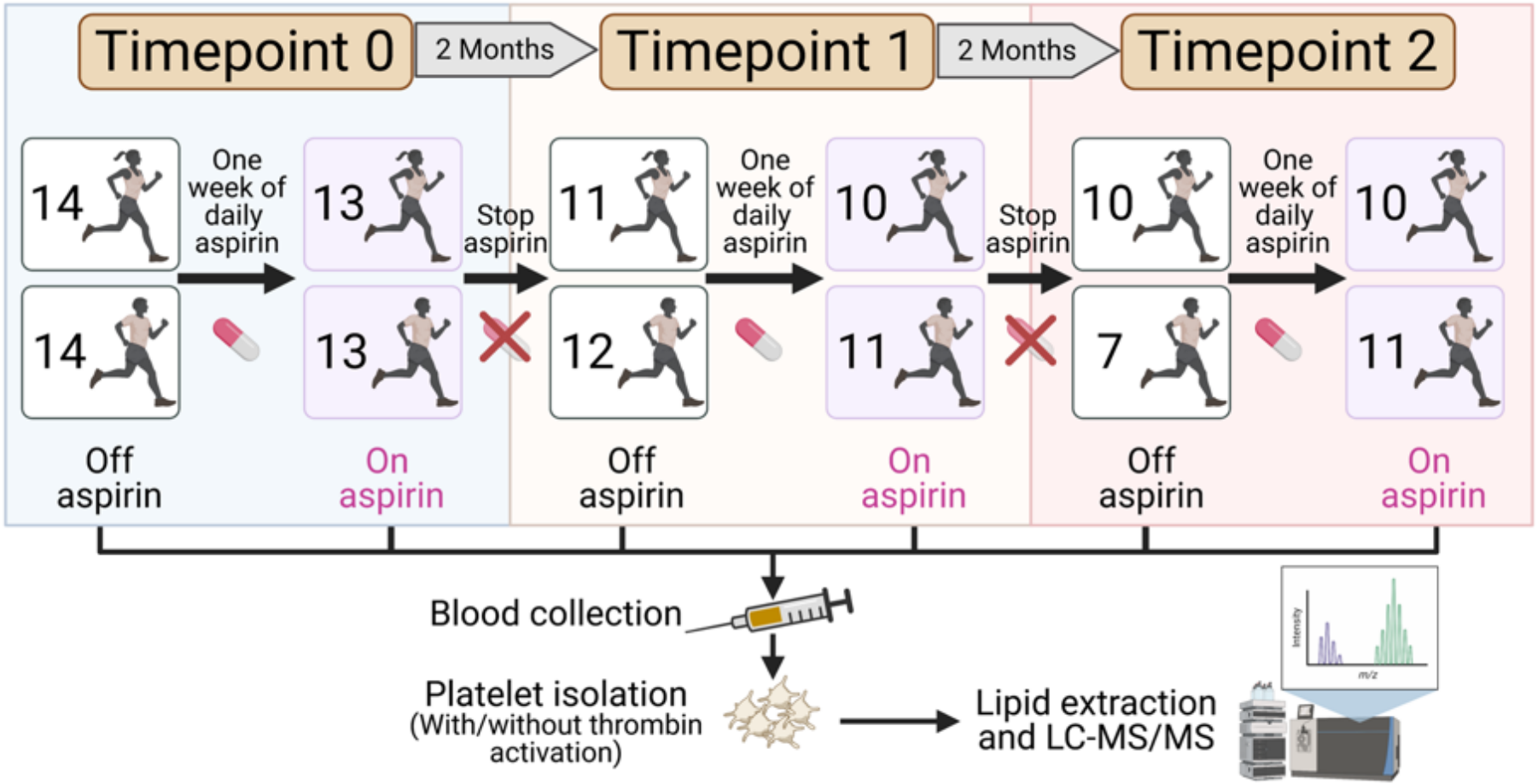

Figure 2.1. Recruitment schedule and number of healthy participants at each time point.

A cohort of 28 healthy volunteers (14 males, 14 females) with platelet lipid extracts stored in our laboratory was used for the purposes of this study. Participants underwent blood sampling off aspirin, and then following a one-week course of aspirin 75mg once daily. This process was repeated after two months and four months.

2.4 CLINICAL COHORT TO STUDY PLATELETS, LEUKOCYTES AND EV IN ARTERIAL THROMBOSIS

2.4.1 Ethical approval for patient participation (Clinical cohort)

The study took place across two sites: Cardiff University and Cardiff and Vale University Health Board. Ethical permission was obtained from Health and Care Research Wales (HCRW, IRAS 243701) and the designated research ethics committee (REC reference 18/YH/0502). The participant information leaflets and consent forms are in Appendices **10.3-10.4**.

2.4.2 Study participants and inclusion/exclusion criteria (Clinical cohort)

Patients with acute coronary syndrome, as a model for arterial thrombosis, and controls were recruited to investigate the phospholipid composition of platelets, leukocytes and extracellular vesicles (EV) and their prothrombotic potential. Participating age and gender-matched individuals were recruited into one of the following four groups:

- *Acute Coronary Syndrome (ACS)*: This group was identified on in-patient cardiology wards and defined clinically with the aid of diagnostic tests (ischaemic ECG changes and a raised troponin level) and clinical assessment by the cardiology team. All patients were recruited within 48 hours of the index event prior to any revascularisation/angioplasty.
- Controls (three groups to include a spectrum of atherosclerosis from healthy controls to patients with obstructive coronary disease), as follows:
    - *Significant coronary artery disease (CAD):* This group consisted of patients attending for an elective coronary angiogram to assess for symptoms of stable angina in the absence of a history of acute coronary syndrome. Patients were assigned to this group if coronary angiography

demonstrated lesions requiring revascularisation on anatomical/physiological criteria as defined by guidelines from the European society for cardiology (ESC, 2018)[245].

- *Risk-factor matched (RF):* This group includes patients attending for a diagnostic coronary angiogram with risk factors for ischaemic heart disease (hypertension, diabetes, hypercholesterolaemia, smoking, chronic kidney disease or combination thereof) but whose coronary angiogram demonstrates no significant coronary artery disease, defined as not requiring revascularisation on anatomical/physiological criteria as per the ESC 2018 guidelines[245].
- *Healthy controls (HC):* This group of patients had no significant history for ischaemic heart disease, its risk factors (as above), were never-smokers, and were not taking anti-platelets, anti-coagulants or statins. They were identified from the workplace or were volunteers from partner studies such as 'HealthWise Wales'[246].

Inclusion criteria

- Age 18 years or older
- Acute coronary syndrome in the patient group, or no history of acute coronary syndrome in the control groups.

Exclusion criteria

- A diagnosis of infective endocarditis
- A diagnosis of atrial fibrillation
- Inability to consent to study

2.4.3 Study procedures (Clinical cohort)

The recruitment schedule took place from March 2019 to March 2020. Patients recruited into this study were consented to donate a one-off blood sample of 50 ml and to allow researchers access to their medical records to document comorbidities and investigation results. I carried out the phlebotomy procedure on all participants using the same technique to collect blood into pre-prepared syringes containing anticoagulant as described in the cell isolation sections below. The blood was transferred to the laboratory within 10 min and processed to isolate washed platelets, leukocytes and EV's. The washed cells were divided into fractions to undergo lipid extraction and functional testing with the prothrombinase assay as described below.

A summary of study design can be seen in **Figure 2.2**.

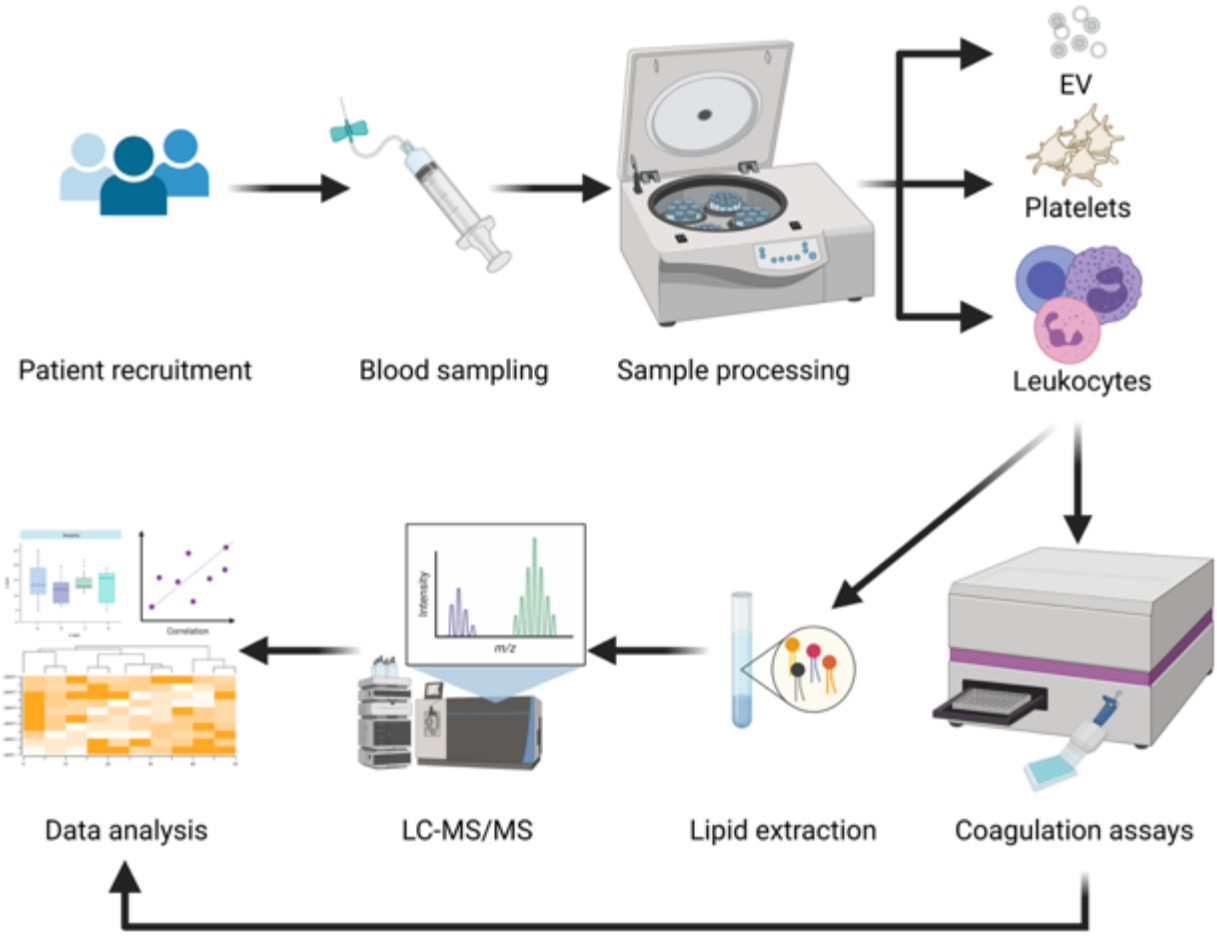

Figure 2.2. The experimental design of studies of arterial thrombosis in the clinical cohort.

Patients identified suitable for the study were recruited as described in the methods section. Blood sampling took place in a clinical area, and was transferred immediately to the laboratory. Cell isolation took place to separate platelets, leukocytes and extracellular vesicles (EV). The washed cells were divided into fractions to undergo functional testing with the prothrombinase assay and lipidomic extraction and processing with LC-MS/MS before bioinformatic analysis.

2.5.1 Ethical approval for patient participation (Clots cohort)

The study took place across three sites: Cardiff University, Cardiff and Vale University Health Board (CVUHB) and Aneurin Bevan University Health Board (ABUHB). Ethical permission was obtained from Health and Care Research Wales (HCRW, IRAS 243701) and the designated research ethics committee (REC reference 18/YH/0502). The participant information leaflet and consent forms are in **Appendix 10.5** and **10.6**, respectively.

2.5.2 Study participants and inclusion/exclusion criteria (Clots cohort)

Twenty patients with arterial thrombosis who underwent surgery/intervention to remove diseased tissue were recruited. Participating individuals were patients who underwent routine vascular surgery (embolectomies and endarterectomies) or percutaneous coronary intervention (PCI).

Patients were identified by the collaborating vascular/cardiology teams from their operating patient lists. There were no changes to the standard operating procedure and no additional surgical/interventional steps were carried out. Some of these procedures were time-critical, and ethical approvals allowed the research team to seek retrospective consent in the following 48 hours after the emergency procedure. This was in the form of written informed consent which also included permission to record the participants medical history from hospital notes. If consent was declined, stored samples were discarded as per local procedures.

Discarded clots were collected, immediately snap-frozen on dry ice and placed in an -80 ^{o}C ultralow temperature freezer on site pending transport on dry ice to the laboratory for analysis. All samples were processed in accordance with the Human Tissue Act 2004. More details are described below.

Inclusion criteria (Clots cohort)

- Age 18 years or older
- Undergoing vascular surgery or percutaneous transluminal intervention to treat arterial thrombotic disorders, where there is a clinical indication to remove and discard diseased tissue (e.g. clot)

Exclusion criteria (Clots cohort)

- Inability to consent to study within the specified time frame

A summary of study flow can be seen in **Figure 2.3**.

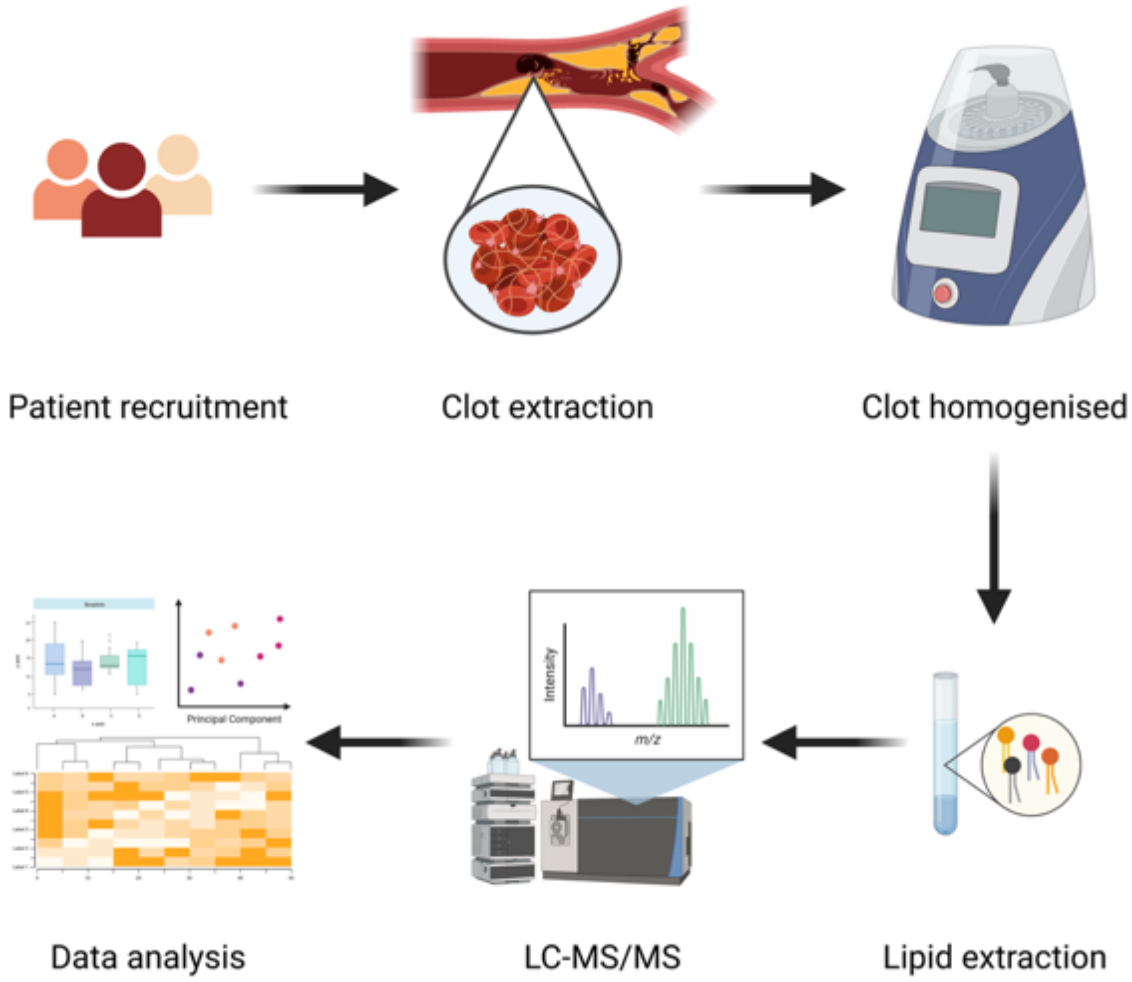

Figure 2.3. The experimental design of clot lipidomics utilised in this chapter.

Patients undergoing vascular/interventional procedures were identified by the clinical team and recruited into the study. Clots which were routinely extracted as part of this procedure are preserved and transferred to -80ºC storage facilities. Samples were extracted in two batches by undergoing homogenisation in the Bead Ruptor Elite™, lipid extraction and then lipidomic processing with LC-MS/MS before bioinformatic analysis.

2.5.3 Clot retrieval procedures

Coronary clots were collected from patients who presented with ST-elevation myocardial infarction (STEMI) to the cardiology department in the University Hospital of Wales and underwent emergent PCI. These patients were initially diagnosed by paramedics upon arrival based on electrocardiographic features of ST-segment elevation in more than 2 leads corresponding to a myocardial muscle territory. Following this, the emergency catheterisation laboratory ('cath lab') was activated and patients transferred immediately, bypassing the emergency department. Upon arrival, patients were prepared for coronary angioplasty to relieve the occlusion. As part of this procedure, a thrombus aspiration catheter (Export Advance^{TM}, Medtronic) was advanced through the peripheral vascular access (radial artery) to the coronary artery and the clot was retrieved by the collaborating interventional cardiologist (Dr Anirban Choudhury). This was then washed by a nurse assistant with saline over the cell sieve that accompanies the catheter kit, transferred to a sterile cryovial and immediately snap frozen on dry ice prior to transfer to -80^{o}C for storage.

Vascular clots were collected from patients who were managed by the Vascular Department at the Royal Gwent Hospital and were identified from routine operating lists. This included patients who underwent carotid endarterectomy following an ischaemic stroke with evidence of 70% stenosis in the internal carotid artery on ultrasonography, and in whom surgery revealed an adherent clot. Patients undergoing limb embolectomy were also recruited to this study. In this group of patients, the indication for surgery was limb ischaemia necessitating amputation or artery-to-artery bypass who required embolectomy as part of this procedure. In both the carotid endarterectomy and limb embolectomy groups, a research nursing member was contacted prior to surgery to attend with a box of dry ice on standby. Once the clot was retrieved by the collaborating vascular surgeon (Mr David Bosanquet) using

standard open surgical technique, it was placed into cryovials and immediately snap frozen on dry ice prior to transfer to -80 ºC freezer for storage.

Once clots are retrieved and samples stored on site in -80 ºC freezers, the local research teams would contact me to collect the samples on dry ice and transfer to Cardiff university for storage and analysis, as will be described in section **2.11**.

2.6 PLATELET ISOLATION

Washed platelets were isolated as described[247]. Blood was drawn into 2 x 20 ml syringes each containing 3.6 ml of ACD with low tourniquet tension using a 21-gauge butterfly needle. A total volume of 15.15 ml of blood was collected from each participant into each syringe (blood:ACD ratio of 8.1:1.9 v/v) and processed within 10 min. This entailed running it very slowly down the wall of 15 ml polypropylene tubes and centrifuging at 250 x g for 10 minutes at room temp with no brake. The platelet rich plasma (PRP) was carefully aspirated and transferred gently to a fresh tube using a plastic Pasteur pipette. Particular care was taken not to draw up any of white blood cells at the interface with the red blood cells by leaving 1 ml of plasma undisturbed.

The PRP was centrifuged at 1,000 x g for 8 minutes at room temp with no brake. The platelet-poor plasma (PPP) supernatant was carefully aspirated and transferred to polypropylene tubes for extracellular vesicle (EV) isolation, described below in section **2.8**. The platelet pellet was suspended in 10 ml of Tyrodes Buffer and ACD (9:1 v/v). Platelets were very slowly and gently resuspended using a Pasteur pipette. This was followed by a final centrifugation step at 1,000 x g for 8 minutes at room temp with no brake.

The washed platelet pellet was re-suspended by gently running 1 ml of Tyrodes buffer down the side of the falcon tube and very slowly and gently resuspending the pellet. Platelets were then counted using a haemocytometer and their concentration adjusted to 2 x 10^8/ml by adding more Tyrodes buffer. The washed platelet isolate was allowed to rest at room temperature for 30 min whilst leukocyte isolation was taking place.

2.6.1 Thrombin activation of platelets

Duplicate aliquots of 1.5 ml washed human platelets, at a concentration of 2 x 10^8 per ml in Tyrodes buffer, were transferred into 1.5 ml reaction tubes. One sample remained unstimulated, whilst the other sample was recalcified in preparation for thrombin activation. This was achieved by adding 6 µl of stock 250 mM $CaCl_2$ to give a final concentration of 1 mM $CaCl_2$, followed by gentle tube inversion and incubation in a 37 °C water bath for 5 min. Samples were then activated by adding 15 µl of 20 U/ml stock bovine thrombin to give a final concentration of 0.2 U/ml. Samples were then placed in a 37 °C water bath for 30 min with gentle inversion every 5-10 min.

2.7 LEUKOCYTE ISOLATION

Leukocytes were isolated using dextran sedimentation as described[69]. Blood was drawn into a 50 ml syringe already containing 4 ml of HetaSep and 4 ml of 2 % citrate via a 21-gauge butterfly needle. A total volume of 20 ml of blood was collected from each participant and processed within 10 min. The syringe was kept upright at room temperature for 45 minutes to allow the red cells to sediment. The upper plasma layer was recovered and centrifuged at 250 g for 10 min at 4 °C. The pellet was resuspended in ice-cold PBS/0.4 % tricitrate, centrifuged at 250 g for 6 min at 4 °C and the supernatant containing platelets and plasma decanted.

Erythrocytes were removed by hypotonic lysis of the pellet by the addition of 5 ml of RBC lysis buffer, with gentle swirling for 30 - 60 seconds followed by the addition of 45 ml of ice-cold PBS/0.4 % tricitrate and centrifugation at 250 g for 6 min at 4 °C. A further RBC lysis was carried out by adding 5ml of RBC lysis buffer, gentle swirling, following by the addition of 45 ml of PBS (no citrate) and centrifugation at 250 g for 5 min at 4 °C. Leukocytes were resuspended in 1 ml of ice-cold Krebs buffer, counted using a haemocytometer, resuspended at 4 x 10^6/ml and placed on ice until use.

2.7.1 Calcium Ionophore activation of leukocytes

Duplicate aliquots of 1.5 ml washed leukocytes, at a concentration of 4 x 10^6 per ml in Krebs buffer, were transferred into 1.5 ml reaction tubes. One sample remained unstimulated, whilst the other sample was recalcified in preparation for calcium ionophore activation. This was achieved by adding 6 µl of stock 250 mM $CaCl_2$ to give a final concentration of 1 mM $CaCl_2$, followed by gentle tube inversion and incubation in a 37 °C water bath for 5 min. Samples were then activated by adding 7.5 µl of 2 mM stock A23187 to give a final concentration of 10 µM. Samples were placed in a 37 °C water bath for 30 min with gentle inversion every 5-10 min.

2.8 EXTRACELLULAR VESICLE PREPARATION

To prepare washed EV fractions, I adapted the methods described in recent literature and guidelines[248,249]. Specifically, the PPP supernatant recovered from the platelet isolation step in **2.6** above was transferred to a fresh polypropylene tube and used for EV preparation. This entailed a further centrifugation step at 1,000 g for 8 min to ensure that the resulting supernatant is 'platelet-free' plasma (PFP), which was then dispensed into 1 ml fractions in 1.5 ml reaction

tubes. Six of these fractions (6 ml total volume of PFP) were used for the EV wash and concentration step below, and the remaining PFP fractions snap frozen on dry-ice and stored at -80 °C for future quantification of EV, described in section **2.8.1** below, and analysis of plasma content.

The EV wash and concentration step was carried out using a bench-top ultracentrifuge with a 30 min centrifugation step at 16,000 g at 20 °C. The top 750 µl fraction was decanted, and a wash step carried out by adding 750 µl of Tyrodes buffer followed by gentle inversion of the tubes. A further ultracentrifugation step was carried out at 16,000 g for 30 min at 20 °C. The top 950 µl was decanted, 50 µl of Tyrodes added to the EV pellet, followed by mixing and pooling into a single tube by pipetting. This generated a washed EV-rich fraction which was used for the lipid extraction and prothrombinase assay.

2.8.1 Quantification of extracellular vesicles

Aliquots of PFP samples prepared in Section **2.8** above and stored at -80 °C were shipped on dry ice to a collaborator in the University of Reading (Dr Keith Allen-Redpath) to quantify plasma EV for all recruited participants. The collaborator carried out size exclusion chromatography (SEC) followed by nanoparticle tracking analysis (NTA), in line with current EV quantification guidelines[248,249]. The SEC columns used were the iZON qEV columns (Izon Science Ltd, Oxford, UK) containing beads with an estimated pore size of 75 nm. These were rinsed with 30 ml PBS as per manufacturer instructions. The time for 5ml of PBS to flow through was recorded, and a time of approximately 5 minutes indicated that the column was clean and ready to use. To process plasma fractions through the SEC column, excess PBS above the filter was pipetted out and 500 µl of PFP was loaded onto the column. The bottom luer tip cap was removed, and PBS was added until the last of the PFP just entered the column top-

filter to allow the collection of eluate in 30 sequential fractions of 0.5ml. Once eluted, 30ml of PBS and 10ml of 20% ethanol (Sigma-Aldrich, Gillingham, United Kingdom) were applied for cleaning, and columns were finally stored in 20 % ethanol at 4~8 °C.

Next, the collaborator quantified SEC fractions using NTA. This method allows the capture and recording of particles (EVs in the current study) moving under Brownian motion. The NanoSight 300 (Malvern, UK), equipped with a high sensitive sCMOS camera and a 488 nm blue laser, was used to assess the size distribution and concentrations of all types of particles. Fractions collected by SEC were diluted with PBS to maintain the numbers of particles in the field of view below 200/screen. For each analysis, five videos, each of 60 seconds duration, were captured with the camera level at 12. A higher camera level could detect more particles but also has a higher risk to introduce unexpected background noise. The setting up of camera level has been trialled by the collaborator's laboratory, and camera level at 12 or 13 is optimal for the detection of EVs (data not shown). Data were analysed using the instrument software NTA 3.20. The number of EVs per ml of analysed fractions was calculated as:

$$\frac{EVs}{ml} of\ neat\ fraction = \text{'}Events\ indicated\ in\ NTA\text{'}\ (\frac{particles}{ml}) \times dilution\ factor$$

The total EV concentration isolated from SEC was summed from the fractions containing the majority (> 90%) of particles (Fractions 7~9), and this value represented the total numbers of EVs per ml of PFP, and was used to normalise EV data.

2.9 PROTHROMBINASE ASSAY

The coagulation mix was prepared from stock solutions to contain final concentrations of 1 μM FII, 15 nM FVa, 50 nM FXa and 5 mM $CaCl_2$ in a 1.5 ml reaction tube and was placed on ice.

A standard curve was prepared by serial dilution of human FIIa at a starting concentration of 400 nM diluted in a 1:2 ratio with prothrombinase buffer in a 96-well half-area plate (Greiner, Germany) until the lowest concentration of 3.125 nM. Each standard curve well contained 50 μl volume.

Platelets, leukocytes and EV isolated as described above, were aliquoted in triplicate to wells of a 96-well plate, at defined amounts: platelets: 4 x 10^6 cells/20 μl, leukocytes: 8 x 10^4 cells/20 μl, EV: undiluted 20 μl. Next, the coagulation reaction was initiated by adding 20 μl of coagulation mix to each well including a triplicate of blank wells containing 20 μl of buffer. The reaction was stopped after 5 min, by adding 10 μl EDTA (35 mM) to give a final concentration of 7 mM, bringing the total reaction volume to 50 μl.

To measure the amount of thrombin generated, using the standard curve, I utilised a CLARIOstar Plus plate reader (BMG Labtech, Aylesbury, UK). The quantification reaction was started via addition (via a multi-channel pipette) of 20 μl S-2238 chromogenic thrombin substrate to yield a final concentration of 0.8 mM substrate in a volume of 70 μl per well. Thrombin cleavage of S-2238 frees the p-nitroaniline dye which is detected in a plate reader using absorbance at 405 nm. The plate was read for 15 minutes in kinetic mode, and the amount of thrombin formed was calculated against the standard curve and averaged across the triplicates. A graphic summary of the assay can be seen in **Figure 2.4**.

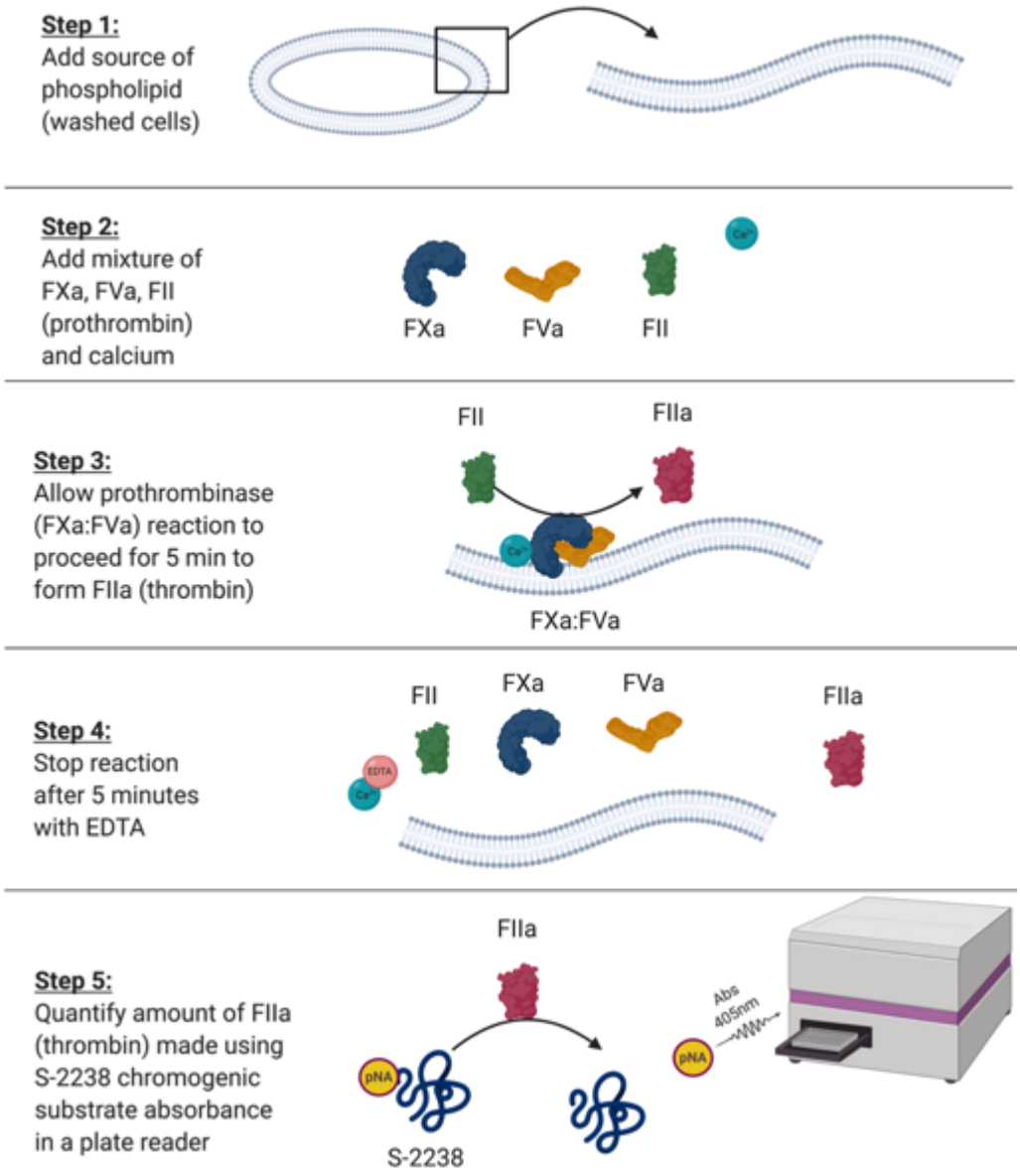

Figure 2.4. The workflow of the prothrombinase assay used to determine the procoagulant potential of washed cells and extra-cellular vesicles.

In step 1, a known number of cells (platelets, leukocytes or EV) was aliquoted into a 96-well half-area plate to provide a source of phospholipid membrane. In step 2, a fixed amount of coagulation factor mixture containing calcium, FII, FXa, FVa was added to the plate to start the prothrombinase reaction on the surface of cells. The reaction was allowed to proceed for 5 minutes only (step 3), before being quenched with EDTA (step 4). The amount of thrombin (FIIa) made was quantified using a p-nitroaniline (pNA) containing chromogenic substrate S-2238 and a plate reader in absorbance mode (405nm) against a standard curve of human thrombin (step 5).

2.10 LIPID EXTRACTION FOR WASHED CELLS/EV EOXPL

A stock mixture of lipid internal standards (IS) was pre-mixed at a concentration of 100 ng/µl (in MeOH) for each of DMPE/DMPC and aliquoted into multiple HPLC vials for storage at -80 ºC to use throughout the study. Immediately before extraction, the pre-mixed IS stock solution was diluted in MeOH to a final concentration of 1 ng/µl of each standard (DMPE/DMPC). Of this, 10 µl (10 ng of each standard) was added to each sample.

The volume of samples used in this extraction was 1 ml. Platelet samples therefore contained 2 x 10^8 cells (1 ml) whereas leukocyte samples contained 4 x 10^6 cells (1 ml). The EV sample was diluted with Tyrodes buffer 1:6 (v/v) in a total volume of 1.5 ml. Of this, 1 ml was used for EV eoxPL lipid extraction.

Lipids were extracted by adding 2.5 ml of solvent mixture (1 M acetic acid, IPA, hexane (2:20:30, v/v/v)) to 1 ml of sample (resting/activated platelets, resting/activated leukocytes or plasma EV), vortexing for 1 minute, and then adding 2.5 ml of hexane. After vortexing for 1 min and centrifugation at 250 g for 5 min at 4 °C, lipids were recovered in the upper hexane layer to a new extraction vial. The remaining samples were then re-extracted by addition of a further 2.5 ml of hexane, vortexed for 1 min and centrifuged at 250 g for 5 min at 4 ºC. The resulting upper hexane layer was combined with the previously recovered layer, and the mixture evaporated to dryness using a Rapidvap evaporation system (Labconco Corporation, USA). Once dry, lipids were resuspended in 200 µl MeOH and stored at -80 ºC until analysis with LC-MS/MS, as described in section **2.14**.

2.11 LIPID EXTRACTION FOR CLOT EOXPL

Immediately before extraction, the pre-mixed IS stock solution was diluted in MeOH to a final concentration of 1 ng/µl of each standard (DMPE/DMPC). Clots were retrieved from the -80 °C freezer onto dry ice and divided with a scalpel if deemed to be larger than 200 mg by visual estimate. Next, clots were weighted on a four-figure balance, transferred into 1.5 ml reaction tubes and placed on wet ice. Following this, 0.5 ml of anti-oxidant buffer, 10 µl of lipid IS mixture (10 ng DMPC/DMPE) and 8-10 ceramic beads (1.4 mm) was added. To reduce hydroperoxylipids in the sample, 10 µl of $SnCl_2$ (100 mM) was added to the mixture. The tubes were then placed in the Bead Ruptor Elite™ (Omni, USA) and tissue homogenisation was carried out at 4 m/s for 20 seconds at 4 °C.

Homogenised clot samples (0.5 ml) were transferred from the reaction tubes to extraction tube containing 2.5 ml ice-cold MeOH and placed on ice. To aid sample recovery, a further 0.5 ml anti-oxidant buffer was added to the reaction tubes and then combined with the sample in the extraction tubes. A modified Bligh and Dyer lipid extraction method was carried out by adding 1.25 ml of chloroform to each extraction tube. The mixture was vortexed for 1 min, and samples were placed on ice for 30 minutes. Following this, 1.25 ml of chloroform was added and the mixture was vortexed for 1 minute. 1.25 ml of H_2O was added, solvent mixture vortexed for 1 min and then centrifuged at 400 g for 5 min at 4 °C to support phase separation. The bottom layer was collected into fresh vials using glass Pasteur pipettes and samples were evaporated to dryness using a Rapidvap vacuum evaporation system (Labconco, USA). Lipids were resuspended in 100 µl of MeOH, transferred to HPLC vials, and stored at -80 °C until analysis using LC-MS/MS, as described in section **2.14**.

2.12 HETE-PL STANDARD GENERATION

To generate HETE-PL standard curves for quantification, positional isomer mixtures of PE 18:0a/HETE and PC 18:0a/HETE were synthesised as previously described[247]. This entailed incubation of 5 mg of SAPE/SAPC with 64 µl of 10 mM of pentamethylchromanol. The mixture was dried using a stream of nitrogen and incubated for 24 hours at 37 ^{o}C. Subsequently, the mixture was resuspended in 200 µl of MeOH followed by the addition of 10 µl of 100mM $SnCl_2$ and incubation for 10 minutes at room temperature to reduce the hydroperoxylipids and generate a racemic HETE-PL mixture containing 5-,8-,9-,11-,12- and 15-HETE-PL positional isomers.

The HETE-PL mixture was purified to remove secondary oxidation products and unoxidized substrate phospholipid. This was carried out using reverse phase HPLC with a Discovery C18 column (25 cm × 4.6 mm, 5 µm, Sigma Aldrich, USA) at a flow rate of 1 ml/min, and gradient of 50 % to 100 % mobile phase B (A: H_2O, 5 mM ammonium acetate, B: MeOH, 5 mM ammonium acetate) over 15 min, then held at 100 % B for 20 min. Elution was monitored at 205 nm (unoxidized lipid) and 235 nm (HETE-PL) and fractions of HETE-PL collected.

Purified lipids were dried using a stream of nitrogen, resuspended in MeOH, transferred to HPLC vials, and quantified using spectrophotometry at 235nm using the extinction coefficient, $\varepsilon = 28\ mM^{-1},cm^{-1}$. The relative amounts of individual HETE-PL isomers were determined by HPLC peak integration. Resultant vials were stored under nitrogen at -80 ^{o}C for use throughout the study.

2.13 STANDARD CURVE QUANTIFICATION OF EOXPL LIPIDS

Standard curves for HETE-PL positional isomers were generated as described previously[247]. This involved serial dilution of lipid standards generated in section **2.12** in MeOH that contains a fixed amount of IS per vial (DMPE/DMPC). The range of dilutions that were prepared had the following amounts: 10 ng, 5 ng, 1 ng, 500 pg, 100 pg, 50 pg, 10 pg, 5 pg, 1 pg of lipid standard with 100 pg IS per 10 µl. These vials were analysed using the same LC-MS/MS method as the samples, described in section **2.14**.

For each standard vial, lipid and IS peaks were integrated. Next, a ratio of the integrated lipid area to the integrated IS area was taken. This was plotted against the ratio of lipid amount (ng) to IS amount (ng) and the slope was computed using Microsoft Excel. In order to determine the amount of lipid (ng) present within analysed samples, the following equation was applied for each lipid within samples:

$$Lipid\ (ng) = \frac{Lipid\ (area) \times\ IS\ (ng)}{IS\ (area) \times\ slope}$$

2.14 MASS SPECTROMETRY OF EOXPL

Lipid extracts were separated using reverse-phase high performance liquid chromatography (HPLC) on a Luna, 3 µm C-18 150 mm × 2 mm column (Phenomenex, USA) with a gradient of 50 to 100 % solvent B for 10 min followed by 30 min at 100 % B (solvent A: MeOH/ACN/ H_2O (60:20:20) with 1 mM ammonium acetate; solvent B: MeOH with 1 mM ammonium acetate) with a flow rate of 200 µl/min. Products were analysed in multiple reaction monitoring (MRM) mode on a Qtrap 6500 (Sciex, USA) by monitoring transitions from precursor mass (Q1 m/z) to product ion mass (Q3 m/z) in negative ion mode. Settings were a dwell time of 75 msec, declustering potential (DP) of -50 volts, entrance potential (EP) of -10

volts, collision energy (CE) of -38 volts, and collision cell exit potential (CXP) of -11 volts for all lipids.

The list of MRM transitions used varied in the different cohorts described in this thesis. For platelet samples from the healthy cohort, the 49 most abundant platelet eoxPL, as described previously were investigated[70] (**Table 2.1**). Whereas in the clinical and clot cohorts, the focus was on HETE-PL known to be made by platelets and leukocytes (**Table 2.2**).

Table 2.1. Multiple reaction monitoring (MRM) transitions for the eoxPL analysed in negative ion mode as part of targeted lipidomic analysis of platelets from the healthy cohort.

Name (ID)	Precursor m/z (Q1)	Product ion m/z (Q3)
PE 16:0p_HETE	738.6	319.2
PE 16:0a_HETE	754.6	319.2
PE 16:0p_20:4;2O	754.6	335.2
PE 16:0p_HDoHE	762.6	343.2
PE 18:1p_12-HETE	764.6	179.1
PE 18:0p_20:5;O	764.6	317.2
PE 16:0p_22:5;O	764.6	345.2
PE 18:0p_12-HETE	766.6	179.1
PE 18:0p_15-HETE	766.6	219.1
PE 16:0e_22:5;O	766.6	345.2
PE 16:0p_22:4;O	766.6	347.2
PE 16:0a_20:4;2O	770.6	335.2
PE 16:0p_20:4;3O	770.6	351.2
PE 16:0p_Di-EHEDA	770.6	351.2
PE 18:2a_HETE	778.6	319.2
PE 16:0a_HDOHE	778.6	343.2
PE 18:1a_12-HETE	780.6	179.1
PE 18:0a_20:5;O	780.6	317.2
PE 18:1p_20:4;2O	780.6	335.2
PE 16:0a_22:5;O	780.6	345.2
PE 16:0p_22:5;2O	780.6	361.2
PE 18:0a_12-HETE	782.6	179.1
PC 16:0a_12-HETE	782.6	179.1
PE 18:0p_HDOHE	790.6	343.2
PE 18:1p_22:5;O	790.6	345.2
PE 18:0p_22:5;O	792.6	345.2
PE 18:1p_22:4;O	792.6	347.2
PE 20:0p_HETE	794.6	319.2
PE 18:0p_22:4;O	794.6	347.2
PE 18:1p_20:4;3O	796.6	351.2

PE 18:0p_20:4;3O	798.6	351.2
PE 18:1p_Di-EHEDA	796.6	351.2
PE 18:0p_Di-EHEDA	798.6	351.2
PE 18:1a_HDoHE	804.7	343.2
PC 18:2a_HETE	806.7	319.2
PC 16:0a_HDOHE	806.7	343.2
PE 18:0a_HDOHE	806.7	343.2
PE 18:1a_22:5;O	806.7	345.2
PE 20:1a_12-HETE	808.7	179.1
PC 18:1a_12-HETE	808.7	179.2
PC 16:0a_22:5;O	808.7	345.2
PE 18:0a_22:5;O	808.7	345.2
PE 18:1a_22:4;O	808.7	347.2
PC 18:0a_12-HETE	810.7	179.1
PE 18:0p_22:4;2O	810.7	359.2
PE 18:0a_20:4;3O	814.7	351.2
PE 18:0a_Di-EHEDA	814.7	351.2
PE 18:0p_20:4;2O	782.6	335.2
PE 16:0a_22:4;O	782.6	347.2
DMPC (PC 14:0/14:0)	662.5	227.1
DMPE (PE 14:0/14:0)	634.5	227.1

Table 2.2. Multiple reaction monitoring (MRM) transitions for the oxPL analysed in negative ion mode as part of targeted lipidomic analysis of clots extracted and cells isolated from the clinical cohort.

Analyte	Precursor m/z (Q1)	Product ion m/z (Q3)
DMPC (PC 14:0/14:0)	662.5	227.1
DMPE (PE 14:0/14:0)	634.5	227.1
PE 16:0p_5-HETE	738.6	115.1
PE 16:0p_12-HETE	738.6	179.1
PE 16:0p_15-HETE	738.6	219.1
PE 16:0p_11-HETE	738.6	167.1
PE 16:0p_8-HETE	738.6	155.1
PE 18:1p_5-HETE	764.6	115.1
PE 18:1p_12-HETE	764.6	179.1
PE 18:1p_15-HETE	764.6	219.1
PE 18:1p_11-HETE	764.6	167.1
PE 18:1p_8-HETE	764.6	155.1
PE 18:0p_5-HETE	766.6	115.1
PE 18:0p_12-HETE	766.6	179.1
PE 18:0p_15-HETE	766.6	219.1
PE 18:0p_11-HETE	766.6	167.1
PE 18:0p_8-HETE	766.6	155.1
PE 18:0a_5-HETE or PC 16:0a_5-HETE	782.6	115.1
PE 18:0a_12-HETE or PC 16:0a_12-HETE	782.6	179.1
PE 18:0a_15-HETE or PC 16:0a_15-HETE	782.6	219.1
PE 18:0a_11-HETE or PC 16:0a_11-HETE	782.6	167.1
PE 18:0a_8-HETE or PC 16:0a_8-HETE	782.6	155.1
PC 18:0a_5-HETE	810.7	115.1
PC 18:0a_12-HETE	810.7	179.1
PC 18:0a_15-HETE	810.7	219.1
PC 18:0a_11-HETE	810.7	167.1
PC 18:0a_8-HETE	810.7	155.1

2.15 LIPID EXTRACTION FOR WASHED CELL/EV APL (TOTAL AND EXTERNALISED)

Total and externalised aPL on the cell membrane of isolated platelets, leukocytes and EV were quantified as described[117]. This method utilises amine chemistry to label external and total aPL with biotin to aid detection on the LC-MS/MS, as will be described below. The ratio between externalised and total aPL was used in subsequent analyses to determine the fraction (%) aPL externalised.

The first step in this assay is the generation of biotinylated lipid standards including internl standards. Stocks of the following lipids were biotinylated: DMPE, DMPS, DOPS, SOPS, SAPS, SpAPE and SAPE. A total of 1 mg of each lipid was dried and reconstituted in 330 µl of chloroform:MeOH (2:1 v/v) and incubated with 52 mM of NHS-biotin and 3.3 µl of triethylamine for 30 min to allow biotinylation of primary amines on PS/PE head groups to take place. Biotinylated aPL standards were purified using reverse phase high performance LC (HPLC) with a Discovery C18 column (25 cm × 4.6 mm, 5 µm) at a flow rate of 1 ml/min, and gradient of 50 % to 100 % mobile phase B (A: H_2O, 5 mM ammonium acetate, B: MeOH, 5 mM ammonium acetate) over 15 min, then held at 100 % B for 20 min. Elution was monitored at 205 nm. HPLC Samples were dried using a Rapidvap vacuum evaporation system (Labconco, USA), resuspended with 100 µl of MeOH. They were subsequently transferred to fresh pre-weighed HPLC vials, dried under nitrogen and accurately weighed to determine the purified mass. All aPL lipids were then resuspended at 100 ng/µl stocks in MeOH and stored under nitrogen at -80 ^{o}C.

A stock mixture of biotinylated lipid IS (biotinylated DMPS/DMPE) was pre-mixed at a concentration of 100 ng/µl (in MeOH) for each lipid and aliquoted into multiple HPLC vials for storage at -80 ^{o}C to use throughout the study. Immediately before lipid extraction, the pre-

mixed stock solution of IS was diluted in MeOH to a final concentration of 1 ng/µl of each IS. Of this, 10 µl (10 ng of each standard) was added to each aPL extract.

Sample volumes used for this assay were 0.2 ml with a starting cell concentration of 2 x 10^8 cells/ml for platelets and 4 x 10^6 cells/ml for leukocytes. The final cell count used therefore was 4 x 10^7 platelets and 8 x 10^5 leukocytes. EV sample was diluted with Tyrodes buffer 1:6 (v/v) in a total volume of 1.5 ml of which 0.2 ml volume was used for this assay. For externalised (outer membrane leaflet) aPL, 0.2 ml of washed cells in resting and activated states and EV were incubated with 86 µl of 11 mM EZ-Link Sulfo-NHS-biotin for 10 min at room temperature. The reaction was quenched with 72 µl of 250 mM of L-lysine for 10 min at room temperature to remove all unreacted biotinylation reagent. The final volume was made up to 0.4 ml by adding 42 µl of PBS. To label total (throughout the membrane) aPL, 0.2 ml of washed cells in resting and activated states and EV were incubated with 20 µl of 20 mM NHS-biotin for 10 min at room temperature. The final volume was made up to 0.4 ml by adding 180 µl PBS.

Lipids were extracted by adding the 0.4 ml sample to 1.5 ml of solvent mixture chloroform:MeOH (1:2 v/v). Samples were vortexed for 1 min followed by the addition of 0.5 ml of chloroform. This is followed by a further vortex for 1 min and the addition of 0.5ml H_2O to achieve phase separation. After vortexing for a further minute and centrifugation at 250 g for 5 min at 4 °C, lipids were recovered in the lower chloroform layer using a glass Pasteur pipette. Samples were evaporated to dryness using a Rapidvap evaporation system (Labconco Corporation, USA), resuspended in 100 µl MeOH and stored at -80^{o}C until analysis by LC-MS/MS as described in section **2.17**.

2.16 STANDARD CURVE QUANTIFICATION OF APL LIPIDS

Standard curves for aPL were generated as described previously[117]. This involved serial dilution of lipid standards generated in section **2.15** in MeOH that contains a fixed amount of IS per vial (biotinylated DMPS/DMPE). The range of dilutions that were prepared had the following amounts: 10 ng, 5 ng, 1 ng, 500 pg, 100 pg, 50 pg, 10 pg, 5 pg, 1 pg of lipid standard with 100 pg IS per 10 µl. These vials were analysed using the same LC-MS/MS method as the samples, described in section **2.17**.

For each standard vial, lipid and IS peaks were integrated. Next, a ratio of the integrated lipid area to the integrated IS area was taken. This was plotted against the ratio of lipid amount (ng) to IS amount (ng) and the slope was computed using Microsoft Excel. In order to determine the amount of lipid (ng) present within analysed samples, the following equation was applied for each lipid within samples:

$$Lipid\ (ng) = \frac{Lipid\ (area) \times\ IS\ (ng)}{IS\ (area) \times\ slope}$$

2.17 MASS SPECTROMETRY OF APL LIPIDS

Lipid extracts were separated using reverse-phase high performance liquid chromatography (HPLC) on an Ascentis C-18 5 µm 150 mm × 2.1 mm column (Sigma Aldrich, USA) with an isocratic solvent (MeOH with 0.2 % w/v ammonium acetate) at a flow rate of 400 µl/min. Products were analysed in multiple reaction monitoring (MRM) mode on a Qtrap 4000 (Sciex, USA) by monitoring transitions from precursor mass (Q1 m/z) to product ion mass (Q3 m/z) in negative ion mode as previously described[117]. **Table 2.3** below lists the MRM transitions, lipid names and settings used for this analysis. The method also included MRM transitions for biotinylated DMPE/DMPS with a dwell time of 200 msec for all lipids.

Table 2.3. Multiple reaction monitoring (MRM) transitions for the aPL analysed in negative ion mode as part of targeted lipidomic analysis of cells isolated from patients with atherothrombosis.

Analyte	Mass	Biotinylated mass	*m/z* [M-H]$^-$	Biotinylated MRM transition	DP (V)	CE (V)	CXP (V)
PE 14:0/14:0 (DMPE)	635	861	860	860→227	−135	−60	−13
PS 14:0/14:0 (DMPS)	679	905	904	904→591	−150	−42	−17
PE 18:0p_20:4 (SpAPE)	751	977	976	976→303	−160	−60	−5
PE 18:0a_20:4 (SAPE)	767	993	992	992→303	−170	−58	−5
PE 16:0p_20:4 (PpAPE)	723	949	948	948→303	−160	−60	−5
PE 18:0a_18:1 (SOPE)	745	971	970	970→281	−170	−58	−5
PE 18:1p_20:4 (OpAPE)	749	975	974	974→303	−160	−60	−5
PS 18:0a_18:1 (SOPS)	789	1,015	1,014	1,014→701	−140	−44	−23
PS 18:1a/18:1 (DOPS)	787	1,013	1,012	1,012→699	−150	−46	−23
PS 18:0a_20:4 (SAPS)	811	1,037	1,036	1,036→723	−145	−42	−23

2.18 EICOSANOID ANALYSIS

Lipid extracts were separated on a C18 Spherisorb ODS2, 5 μm, 150 x 4.6-mm column (Waters, Hertfordshire, UK) using a gradient of 50 – 90 % B over 10 min (A, H_2O:ACN:acetic acid, 75:25:0.1; B, MeOH:ACN:acetic acid, 60:40:0.1) with a flow rate of 1 ml/min. Products were quantified by LC-MS/MS analysis on the Sciex Q-Trap 4000 using negative ion mode and MRM transitions for 12-HETE, TxB_2, and their respective deuterated IS 12-HETE-d8 and TxB_2-d4 as shown in **Table 2.4** [40].

Table 2.4. Multiple reaction monitoring (MRM) transitions for the eicosanoids analysed in the healthy cohort study of platelet lipids.

Analyte	MRM transition	DP (V)	CE (V)	CXP (V)
12-HETE	319.2→179.1	–65	–18	–12
TxB_2	369.1→169.1	–60	–22	–12
12-HETE-d8	327.2→184.1	–60	–20	–12
TxB_2-d4	373.3→173.3	–55	–22	–10

2.19 CHIRAL ANALYSIS OF HETE-PL

To distinguish between S and R stereoisomers for HETE-PL species, lipid extracts underwent alkaline hydrolysis followed by chiral LC-MS/MS as described previously[40,250]. The alkaline hydrolysis step was carried out by taking 80 µl of lipid extract into a new extraction tube, drying it under a gentle stream of nitrogen, resuspending in 1.5 ml IPA and vortexing for 1 min. Next, 1.5 ml of 1 M NaOH was added to each sample followed by vortexing for 10 sec. Samples were then placed in a 60 °C water bath for 30 minutes to undergo alkaline hydrolysis of esterified FAs. After this, 140 µl of concentrated (12 M) HCl was added to each sample to acidify to pH 3.0 (estimated with Litmus paper). Prior to undergoing re-extraction, 3 ng of 12(S)-HETE-d8 were added to each sample as an IS. This was followed by the addition of 3 ml hexane, vortexing for 1 minutes and centrifugation at 250 g for 5 minutes at 4 °C to aid phase separation. Lipids were recovered in the upper hexane layer to a new extraction vial. The remaining samples were then re-extracted by addition of a further 3 ml of hexane, vortexed for 1 min and centrifuged at 250 g for 5 min at 4 °C. The resulting upper hexane layer was combined with the previously recovered layer, and the mixture evaporated to dryness using a Rapidvap evaporation system (Labconco Corporation, USA). Once dry, lipids were resuspended in 60 µl MeOH and transferred to an LC-MS/MS vial.

The S and R stereoisomers for each HETE positional isomer were separated on a Chiralpak AD-RH, 5 µm, 150 x 4.6-mm column (Daicel, France) using an isocratic solvent (MeOH:H_2O:glacial acetic acid, 95:5:0.1 v/v) with a flow rate of 0.3 ml/min over 25 min. Products were quantified by LC-MS/MS on the Sciex Q-Trap 4000 using negative ion mode and MRM transitions for 15-, 12-, 11-, 8- and 5-HETE, as well as 12(S)-HETE-d8, as shown in **Table 2.5**.

Table 2.5. Multiple reaction monitoring (MRM) transitions for chiral analysis of hydrolysed HETE stereoisomers.

Analyte	MRM transition	DP (V)	CE (V)	CXP (V)
15-HETE	319.2→219.1	–70	–20	–13
12-HETE	319.2→179.1	–75	–22	–9
11-HETE	319.2→167.1	–75	–24	–1
8-HETE	319.2→155.1	–70	–22	–9
5-HETE	319.2→115.1	–70	–22	–7
12(S)-HETE-d8	327.2→184.1	–80	–22	–11

2.20 STATISTICAL ANALYSIS

Raw data was exported from Analyst (Sciex, USA) and analysed using MultiQuant (Sciex, USA). Peak integration was carried out for each lipid to calculate the area under the curve (AUC). The limit of detection (LOD) used for this analysis was a signal to noise ratio of 5:1. Where no (reliable) peak was detected, a value of zero was assigned. Peak areas were normalised to the relevant IS (DMPC for the PC lipids, DMPE for the PE lipids, DMPS for PS lipids) and exported as a comma separated values (CSV) file. Subsequent statistical and bioinformatics analysis was carried out in the coding environment R (Open source, version 3.5.3).

For generation of heatmaps, samples were averaged within their groups, and a log10 was applied to lipid amounts (ng) normalized to cell count or tissue weight (mg) for each lipid to allow row-wise and column-wise comparison. Next, lipid measurements were plotted as intensity values using the pheatmap package with lipid hierarchical clustering. Intensity levels were represented by a colour gradient ranging from blue (very low levels or absent) to red (high levels) with variations in between. Each lipid was annotated, using a colour code, according to its presumed enzymatic origin.

Statistical significance was determined with the Mann-Whitney-Wilcoxon Test for pairwise comparison and Kruskal-Wallis test for analysis of differences between more than two groups. All of these tests were done with base R and figures generated with the 'ggplot2' package. Correlation analysis was carried out with the 'corrplot' packages and utilised Pearson's correlation for linear dependence between variables. The cut-off value chosen for test significance was a p-value <0.05. Since no more than 50 variables (lipids) between

samples, multiple comparison testing was not required (confirmed by Dr John Watkins, Lecturer in Statistics, School of Medicine).

Volcano plots were created using a combination of fold change (FC) and Mann-Whitney-Wilcoxon p-value testing. The purpose of FC is to compare absolute value changes between two group means and is calculated as the ratio in group average lipid measurement for each variable. To maintain the same distance from the (0,0) baseline coordinates, FC values are plotted on a log2 scale (x-axis) and p-values are plotted on a -log10 scale (y-axis).

Principal component analysis (PCA) was utilised as a multivariate dimension-reduction tool to examine lipid patterns that differentiated biological samples. PCA aims to find the directions that best explain the variance in a data set (X) without considering class labels (Y), hence termed 'unsupervised'. It works by reducing a large number of variables (lipids) to a small set of principal components that account for variance between samples using eigenvector linear algebra algorithms. The method utilised for PCA analysis in this thesis was the singular value decomposition method provided by the base R 'prcomp' function. The variance explained by principal components in the data is organised in descending order such that PC1 accounts for most of the variance in the data, followed by PC2 and so on. These principal components are utilised to plot new coordinates for each sample, termed 'scores', and for each variable (lipid), termed loadings. The R package ggplot2 was utilised to create 'scores' and 'loadings' plots which describe the variance exhibited by samples and lipids and highlighting patterns of similarities or differences.

Graphical illustrations of assays, designs and pathways were carried out using the online platforms draw.io and biorender.com (premium subscription).

CHAPTER 3 ENZYMATICALLY OXIDIZED PHOSPHOLIPIDS IN PLATELETS FROM HEALTHY VOLUNTEERS VARY WITH TIME, ASPIRIN AND GENDER

3.1 INTRODUCTION

A recent pilot study from our group by Slatter et al discovered many previously unknown eoxPL generated in agonist-activated platelets[70]. Using untargeted screening of lipids from resting and thrombin-activated platelets from three genetically unrelated healthy donors, the authors demonstrated a prominent group of ions in both positive and negative mode at ~15–25 min in the non-polar datasets (*m/z* ~700–900). Database searching and matching assigned these ions to eoxPL. Given the large number of candidate ions found, the authors focused on the top 52 upregulated eoxPL in response to thrombin and carried out a targeted lipidomic analysis by acquiring mass spectra followed by further validation with MRM of precursor *m/z* to *sn2* carboxylate product ion. In addition to identifying the large group of unknown eoxPL, Slatter et al demonstrated diversity in the platelet lipidome between the three human participants who were recruited to the study[70]. Understanding the degree of variation between participants was limited by the small sample size, but was highlighted by the fact that only 63.7% of platelet lipids were common to all three participants. Indeed, thrombin-activation of platelets elevated groups of platelet lipids to different extents in the three participants suggesting variation in the response to thrombin. This variation may be due to factors such as inter-individual differences, gender influence or intra-individual variation in eoxPL amounts over time due to homeostatic influences. However, it was not possible to investigate the contribution of these factors to eoxPL variation in the pilot study due to the small sample size.

Given the important role of aspirin in primary/secondary cardiovascular prevention, an understanding of how this drug influences the formation of pro-coagulant and immuno-reactive lipids is warranted. Limited data is available on changes to eoxPL amounts in platelets in response to supplementation with aspirin, a potent COX-1 inhibitor. Additionally, it is not

known whether aspirin has any impact on products generated by 12-LOX, given that they share the same upstream pathway as COX-1 products. In the study described above by Slatter et al, *in vivo* aspirin supplementation led to a large reduction in COX-1 generated lipids, but it also appeared to affect 12-LOX generated lipids to varying degrees between participants. However, the small sample size of three participants limited any quantitative conclusions to how 12-LOX lipids are affected[70].

Taken together, the study by Slatter et al highlights a poorly understood variation in the platelet lipidome between individuals in response to thrombin and aspirin which requires a larger sample size for better characterisation[70]. Given that many of these eoxPL play a role in inflammation and coagulation, an understanding on how stable or variable they are between and within individuals, in response to aspirin and between males and females is essential[14,70].

In this chapter, I will expand on the pilot study described above by characterising the eoxPL generated by platelets in a larger cohort (28 individuals: 14 males, 14 females) using a targeted LC-MS/MS analysis of the 49 most abundant platelet eoxPL as described previously[70]. Samples from this larger cohort had been collected and processed prior to the start of my PhD by a previous member of the group, Dr Chris Brasher, who carried out an untargeted analysis on the platelet lipidome (unpublished). Details on the recruitment schedule is described in Materials and Methods (Section **2.3**). The aims of this chapter will be to:

1. Quantify inter-individual variation on platelet eoxPL generation using the larger cohort of 28 individuals.
2. Quantify intra-individual variation on platelet eoxPL generation over time. This was made possible with the longitudinal sampling schedule where participants were sampled three times over six months.

3. Assess the influence of gender on platelet eoxPL generation and whether the amounts generated vary between males and females. This was made possible by having a gender-balanced recruitment schedule with 14 males and 14 females.
4. Assess the influence of aspirin on thrombin-activated platelet eoxPL generation. This was made possible by the *in vivo* supplementation of participants with aspirin and sampling on and off the COX-1 inhibitor.

3.2 RESULTS

3.2.1 Correlation plot highlights enzymatic origin of unknown eoxPL

Throughout this study, information on the enzymatic origin of lipids known to be generated by 12-LOX were derived from previous work utilising genetically modified mice lacking platelet *Alox12* (e.g. 12-HETE-PL)[69]. For COX-1 generated eoxPL, information confirming the enzymatic origin are derived from human studies utilising aspirin supplementation (e.g. DiEHEDA-containing PL)[77]. Despite this, the enzymatic origin of many recently described platelet eoxPL remain unknown[70].

To investigate the enzymatic origin of unknown eoxPL measured in this study, I carried out a correlation plots for all 49 platelet lipids studied with LC-MS/MS (**Figure 3.1**). This analysis identifies clusters of eoxPL which correlate with each other reflecting common traits such as enzymatic origin. Based on this, one can infer the enzymatic origin of unknown eoxPL if they cluster in a block with known eoxPL. These results informed the categories assigned to the 'presumed enzymatic origin' throughout this chapter. Additionally, they demonstrate the presence of unknown platelet lipids generated by COX-1, 12-LOX as well as other as of yet unknown enzymatic pathways.

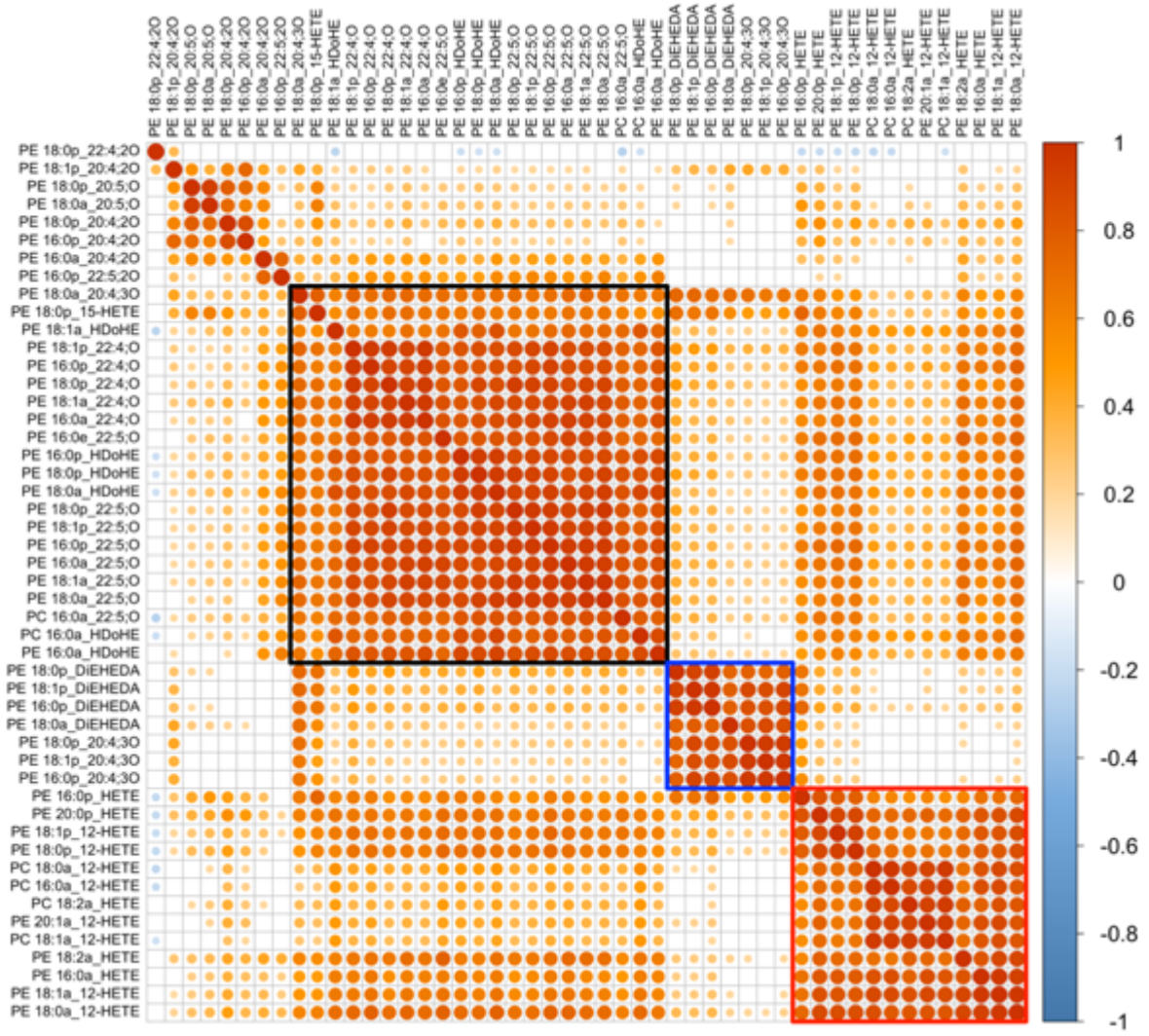

Figure 3.1. Correlation plot of thrombin-activated platelet eoxPL demonstrates clustering by *sn2* fatty acid with distinct clusters forming by presumed enzymatic origin.

Lipids were extracted from platelets (2 x 10^8) following thrombin activation (0.2 U/ml) as in Materials and Methods and quantified by LC-MS/MS. The ratio of analyte:internal standard was calculated for each lipid and averaged (mean) over the three timepoints for each donor (n=28). Next, Pearson's correlation coefficients were calculated and only significant ($p<0.05$) correlations were plotted with the corrplot R package. The colour intensity indicates effect size as measured by the R correlation coefficient value (dark blue -1, white 0, dark red 1; as indicated in the legend scale on the right). Lipids are boxed by hierarchical clustering of presumed enzymatic origin (Blue box: COX-1 cluster. Red box: 12-LOX cluster. Black box: unknown origin).

3.2.2 Thrombin activation of platelets leads to increased generation of eoxPL

Next, I plotted the eoxPL data from resting and thrombin-activated platelet samples on a heatmap to enable visualisation of all lipids (**Figure 3.2**). This confirmed that eoxPL amounts (determined by the ratio of analyte:IS) were higher in thrombin-activated samples compared to resting platelets.

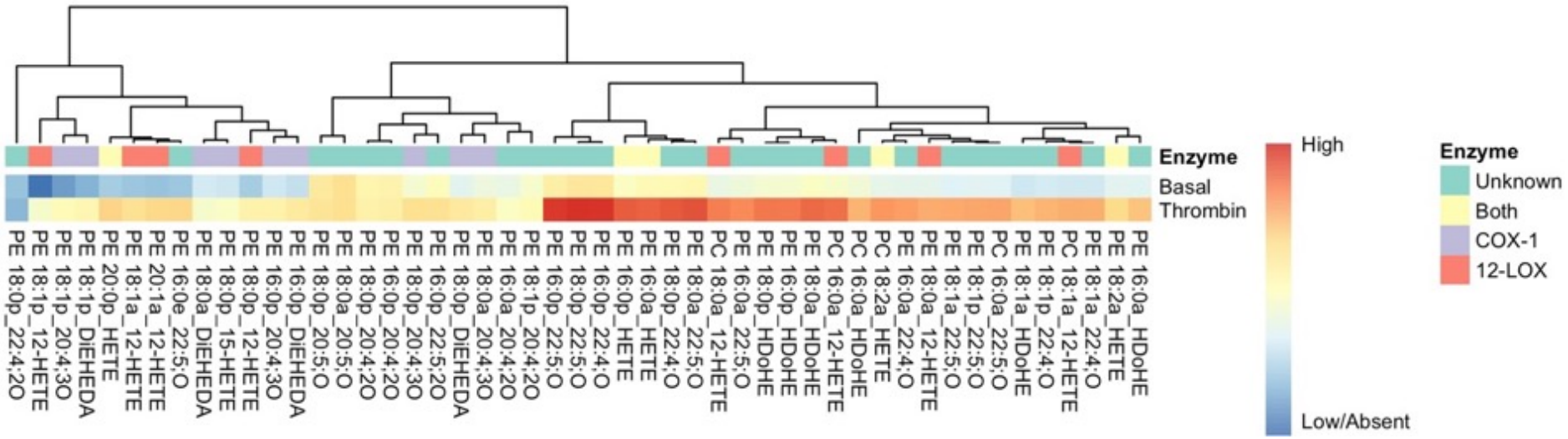

Figure 3.2. Thrombin stimulates healthy donor platelets to generate eoxPL.

Lipids were extracted from resting platelets (2 x 10^8) or following activation with thrombin (0.2 U/ml) as in Materials and Methods and quantified by LC-MS/MS. The ratio of analyte:internal standard was calculated for each lipid and averaged (mean) over the three timepoints for each donor (n=28). Next, values were averaged (mean) across donors separated by activation status (resting/thrombin-activated), log10 transformed and plotted as a heatmap with hierarchical clustering using the pheatmap R package. The presumed enzymatic origin of eoxPL is seen in the legend (COX-1: cyclooxygenase-1, 12-LOX: 12-lipoxygenase, Both: both COX-1/12-LOX can generate this lipid).

3.2.3 The amount of eoxPL generated by thrombin-activated platelets varies over time and between individuals

In the pilot study by Slatter et al, a large degree of variability in thrombin-activated platelet eoxPL amounts between individuals was described but no measure of variability was reported due to the small sample size and one-off sampling schedule[70]. The variability reported may arise from differences between individuals (inter-individual) or from differences for the same individual over time (intra-individual). The larger sample size and the three sampling time points in this healthy cohort will allow me to quantify both of these variations.

To investigate variations in the lipidome over time, I calculated the mean amount of eoxPLs generated in thrombin-activated platelets from all individuals for each of the three timepoints and plotted it as a line chart (**Figure 3.3**). Relative to the first time point, eoxPL varied over time by up to 4-fold difference (increase or decrease). Of the 49 eoxPL measured, 18 significantly varied in amount over time as demonstrated in **Figure 3.4**. To assess whether eoxPL variation occurred in groups of lipids with similar features, such as headgroup or enzymatic origin, I carried out an unsupervised hierarchical clustering analysis (**Figure 3.5**). This demonstrated possible clustering by *sn2* FA with distinct clusters for 12-HETE containing PL, monohydroxylipids generated from non-AA PUFA and COX-1 derived lipids. This suggests that the pattern of variation may differ by enzymatic pathway.

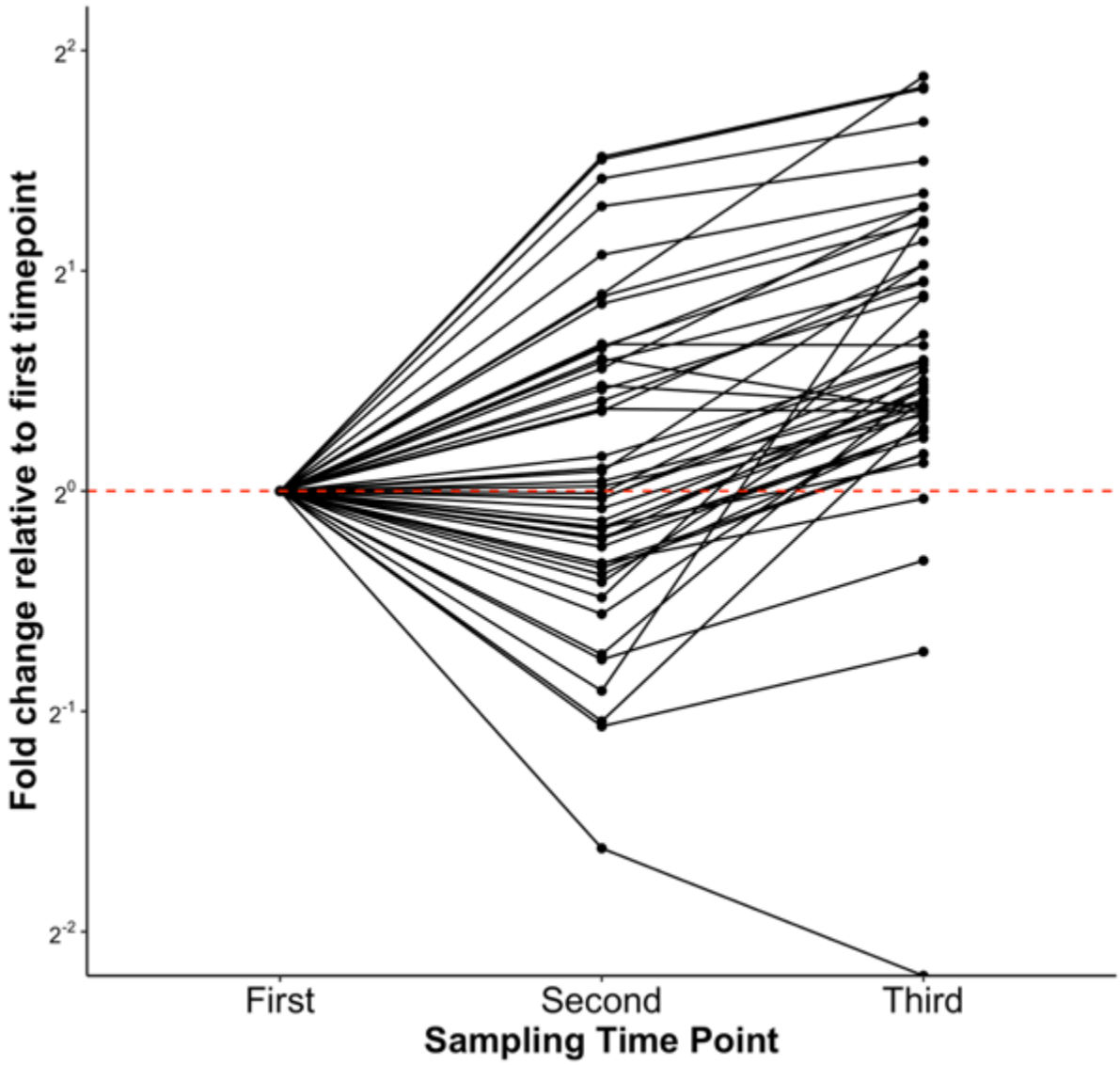

Figure 3.3. The amount of eoxPL generated in thrombin-activated platelets vary over time by up to four fold.

Lipids were extracted from platelets (2 x 10^8) following thrombin activation (0.2 U/ml) as in Materials and Methods and quantified by LC-MS/MS. Lipid to internal standard signal area ratio (lipid:IS) were calculated for each lipid across donors (n=28) over three sampling time points (2 monthly intervals). The lipid:IS for each eoxPL was averaged (mean) across all participants for each time point. Next, the data was normalised (divided by) the eoxPL lipid:IS for the first time point, and charted as a line plot where each line indicates a lipid amount over the three timepoints relative to the first time point.

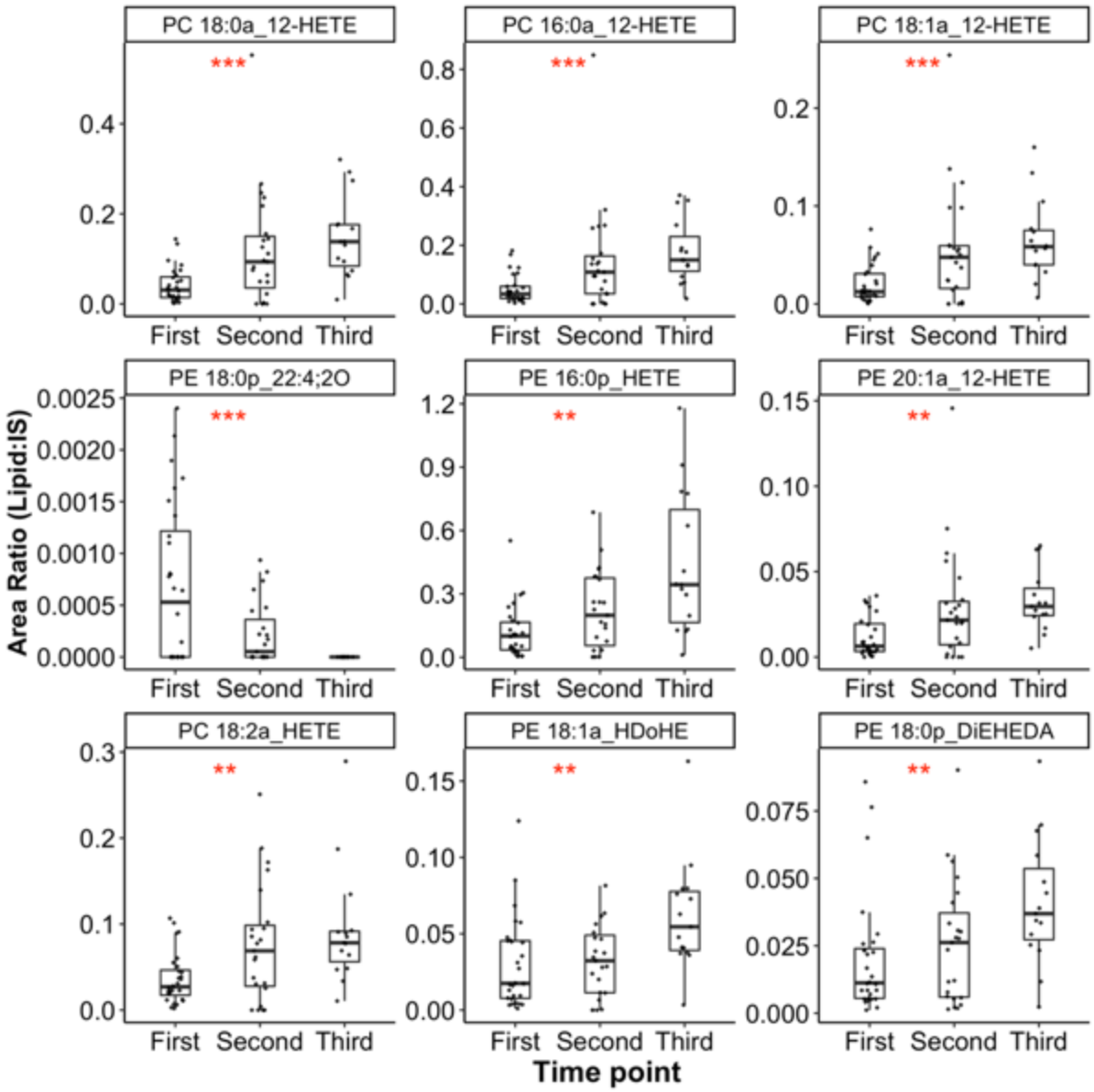

Figure 3.4A. Boxplots of eoxPL generated by thrombin-activated platelets which significantly vary over time (1 of 2).

Lipids were extracted from platelets (2 x 10^8) following thrombin activation (0.2 U/ml) as in Materials and Methods and quantified by LC-MS/MS. Lipid to internal standard signal area ratio (lipid:IS) were calculated for each lipid across donors (n=28) over three sampling time points (2 monthly intervals). Next, the data was charted as box plot with the ggplot2 R package over the three time points. Box edges indicate the interquartile range (IQR) with the median line inside the box. Whiskers indicate 1.5 times the IQR. Statistical difference across the three groups was tested with Kruskal-Wallis test (*: $p < 0.05$, **: $p < 0.01$, ***: $p < 0.001$).

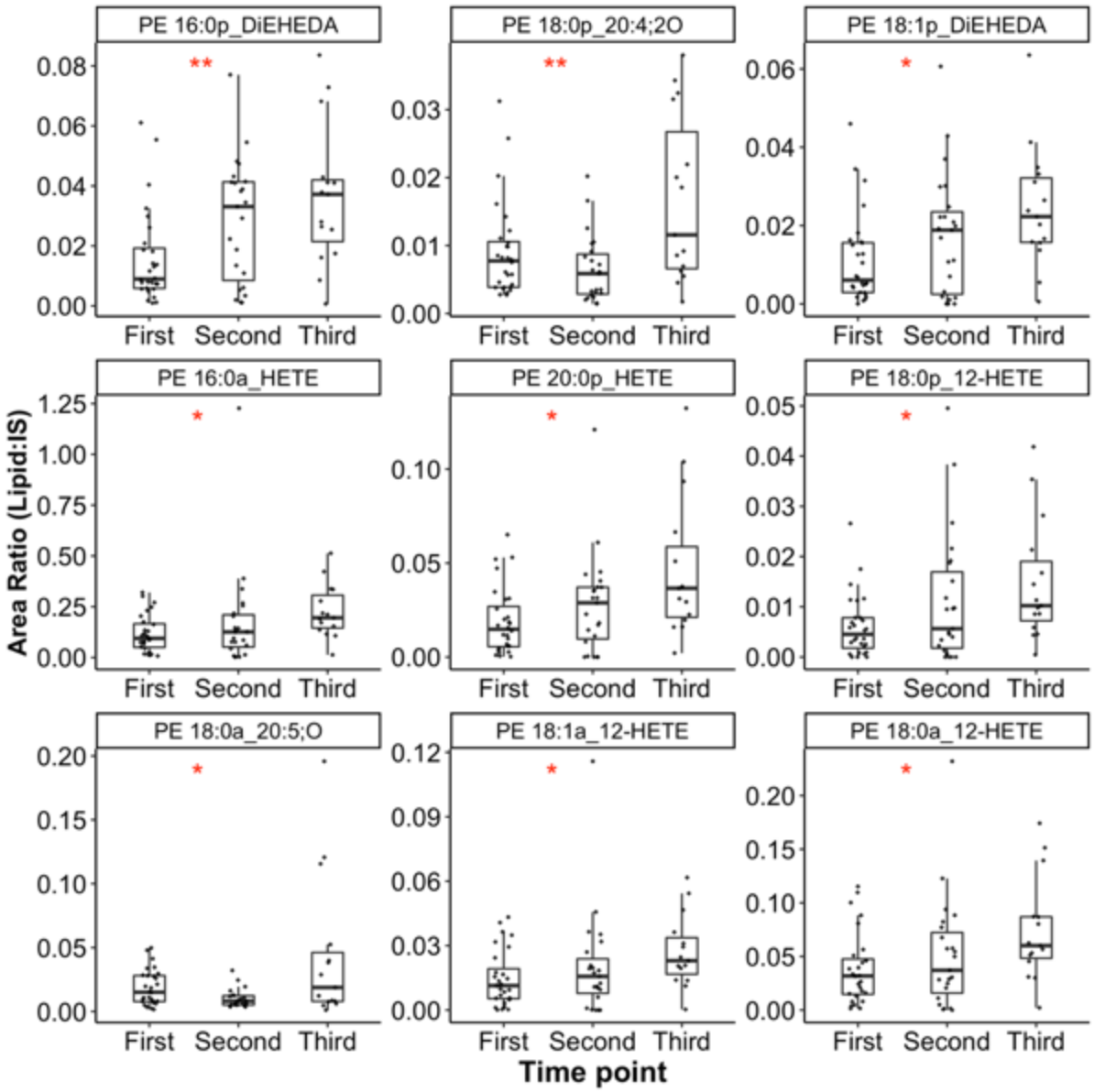

Figure 3.4B. Boxplots of the eoxPL generated by thrombin-activated platelets which significantly vary over time (2 of 2).

Lipids were extracted from platelets (2 x 10^8) following thrombin activation (0.2 U/ml) as in Materials and Methods and quantified by LC-MS/MS. Lipid to internal standard signal area ratio (lipid:IS) were calculated for each lipid across donors (n=28) over three sampling time points (2 monthly intervals). Next, the data was charted as box plot with the ggplot2 R package over the three time points. Box edges indicate the interquartile range (IQR) with the median line inside the box. Whiskers indicate 1.5 times the IQR. Statistical difference across the three groups was tested with Kruskal-Wallis test (*: $p < 0.05$, **: $p < 0.01$, ***: $p < 0.001$).

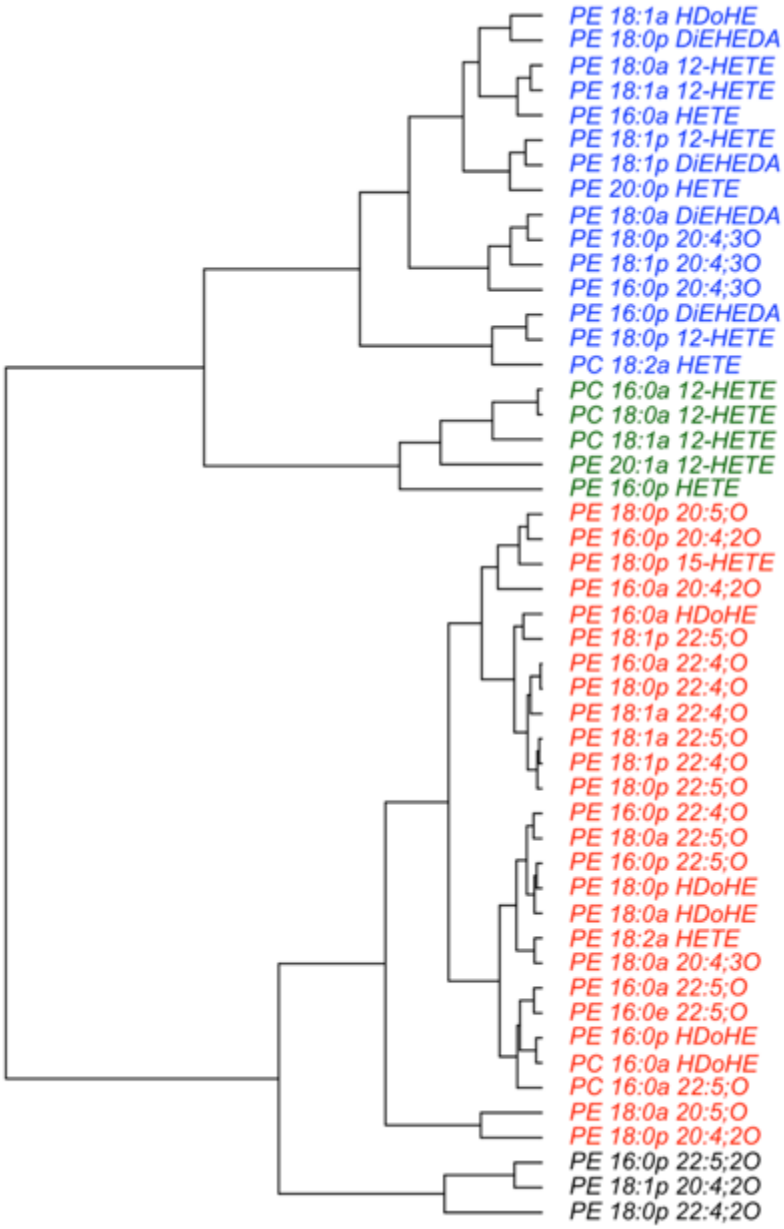

Figure 3.5. Hierarchical clustering of relative lipid amounts over time may indicate clustering by *sn2* FA.

Lipids were extracted from platelets (2 x 10^8) following thrombin activation (0.2 U/ml) as in Materials and Methods and quantified by LC-MS/MS. Lipid to internal standard signal area ratio (lipid:IS) were calculated for each lipid across donors (n=28) over three sampling time points (2 monthly intervals). The lipid:IS for each eoxPL was averaged (mean) across all participants for each time point. Next, the data was normalised (divided by) the eoxPL lipid:IS for the first time point, processed through hierarchical clustering (complete linkage) and charted as a dendrogram coloured for the four highest level clusters.

To investigate inter-individual variations, I took eoxPL data for the first time point and calculated the relative standard deviation (RSD, also known as coefficient of variation) for each lipid across the 28 participants (**Table 3.1**). This demonstrated a large degree of variation with a range of 71-139% RSD in eoxPL amounts between individuals.

Taken together, the findings from this section quantifying the variation in eoxPL amounts generated by thrombin-activated platelets (**Table 3.1**), and reflects a high degree of variability between individuals with up to 4-fold differences in eoxPL generation over time (**Figure 3.3**). The potential reasons for this will be addressed in the discussion section.

Table 3.1. The amounts of eoxPL generated in thrombin-activated platelets vary between individuals as indicated by the relative standard deviation (RSD)

Lipids were extracted from platelets (2 x 10^8) following thrombin activation (0.2 U/ml) as in Materials and Methods and quantified by LC-MS/MS. Lipid to internal standard signal area ratio were calculated for each product across donors (n=28). Using data from the first time point only, relative standard deviation (RSD: standard deviation (SD) ÷ mean × 100%) was calculated for each lipid across all participants to indicate inter-individual variability.

EoxPL	RSD %	EoxPL	RSD %
PE 18:1p_20:4;3O	139%	PE 20:1a_12-HETE	99%
PE 16:0a_20:4;2O	126%	PE 16:0p_DiEHEDA	99%
PE 16:0p_20:4;3O	118%	PE 16:0a_HDoHE	99%
PE 16:0p_22:5;2O	117%	PE 18:1a_HDoHE	97%
PE 18:0p_22:4;2O	113%	PC 18:1a_12-HETE	97%
PE 18:0p_22:5;O	112%	PE 16:0p_HDoHE	97%
PE 18:0p_HDoHE	111%	PC 16:0a_12-HETE	97%
PC 16:0a_22:5;O	110%	PE 18:1p_22:4;O	96%
PE 18:1p_22:5;O	108%	PC 16:0a_HDoHE	95%
PE 18:0p_DiEHEDA	108%	PE 20:0p_HETE	94%
PE 16:0p_22:4;O	108%	PE 18:0a_DiEHEDA	94%
PE 18:0a_HDoHE	106%	PC 18:0a_12-HETE	92%
PE 18:1p_12-HETE	106%	PE 18:1a_12-HETE	89%
PE 16:0e_22:5;O	106%	PE 18:0a_12-HETE	86%
PE 18:0a_22:5;O	105%	PE 18:0p_20:5;O	82%
PE 18:1a_22:4;O	105%	PC 18:2a_HETE	81%
PE 16:0p_22:5;O	105%	PE 16:0a_HETE	78%
PE 18:1a_22:5;O	104%	PE 18:0a_20:4;3O	77%
PE 18:0p_22:4;O	103%	PE 18:0p_20:4;2O	77%
PE 18:1p_DiEHEDA	103%	PE 18:2a_HETE	76%
PE 16:0p_HETE	103%	PE 18:1p_20:4;2O	76%
PE 16:0a_22:4;O	102%	PE 18:0a_20:5;O	74%
PE 18:0p_20:4;3O	101%	PE 16:0p_20:4;2O	72%
PE 18:0p_12-HETE	101%	PE 18:0p_15-HETE	71%
PE 16:0a_22:5;O	100%		

3.2.4 Aspirin reduces the amounts of COX-1-derived eoxPL in thrombin-activated platelets, but increases 12-LOX-derived eoxPL

Next, to investigate the effect of aspirin on eoxPL amounts in thrombin-activated platelets, a volcano plot analysis was used (**Figure 3.6**). This demonstrated that *in-vivo* aspirin supplementation significantly reduced the amount of COX-1-derived eoxPL in thrombin-activated platelets, but led to an increase in a group of 12-LOX-derived eoxPL. A box plot analysis demonstrated that this group was composed of 12-HETE-PL with an acyl group at the *sn1* position (**Figure 3.7**). In contrast, plasmalogen (ether bond) 12-HETE-PL were similar in samples from patients with or without aspirin supplementation (**Figure 3.8**).

This analysis demonstrates that in-*vivo* supplementation of aspirin has an impact on 12-LOX-derived eoxPL generated in thrombin-activated platelets, but only for those with an acyl, not a plasmalogen, bond at the *sn1* position. The mechanism for this is unknown, but will be discussed in section **3.3** of this chapter.

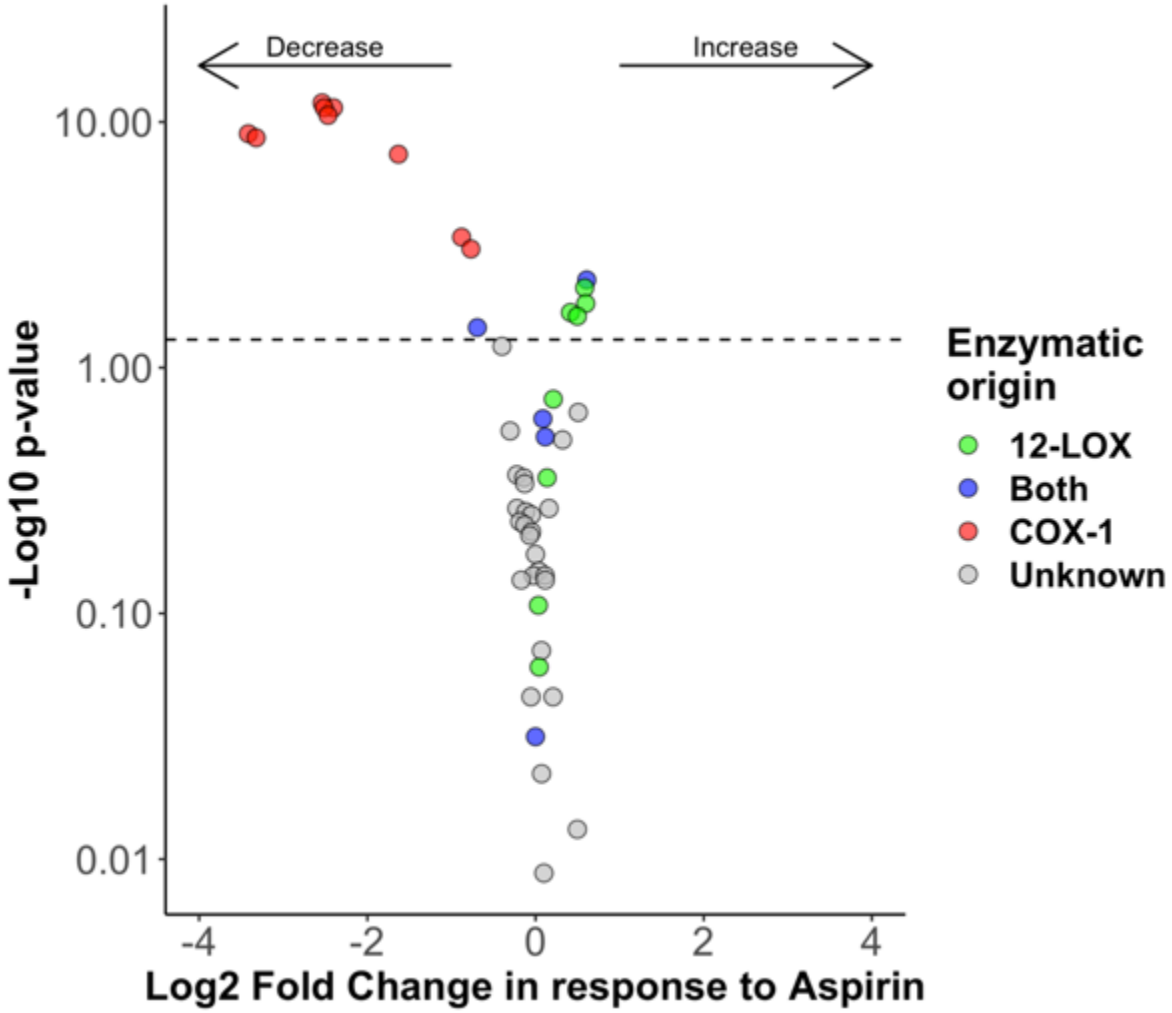

Figure 3.6. Aspirin significantly reduced the amount of COX-1 generated eoxPL in thrombin-activated platelets compared with resting platelets, but led to an increase in some 12-LOX generated eoxPL.

Lipids were extracted from platelets (2 x 10^8) following activation with thrombin (0.2 U/ml) as in Materials and Methods and quantified by LC-MS/MS. Lipid to internal standard signal area ratio were calculated for each product and averaged across all 'healthy cohort' participants and timepoints, separated only by aspirin. Next, log2 fold changes were calculated between aspirin (n=27) and no aspirin (n=28) and plotted on the X-axis (each dot represents a lipid). P-values were calculated with the Mann-Whitney-Wilcoxon non-parametric test and plotted as -log10 (p value) on the Y-axis. The horizontal dashed line corresponds to p=0.05, with all points above the line having a $p < 0.05$. The presumed enzymatic origin of eoxPL is seen in the legend (COX-1: cyclooxygenase-1, 12-LOX: 12-lipoxygenase, Both: both COX-1/12-LOX can generate this product).

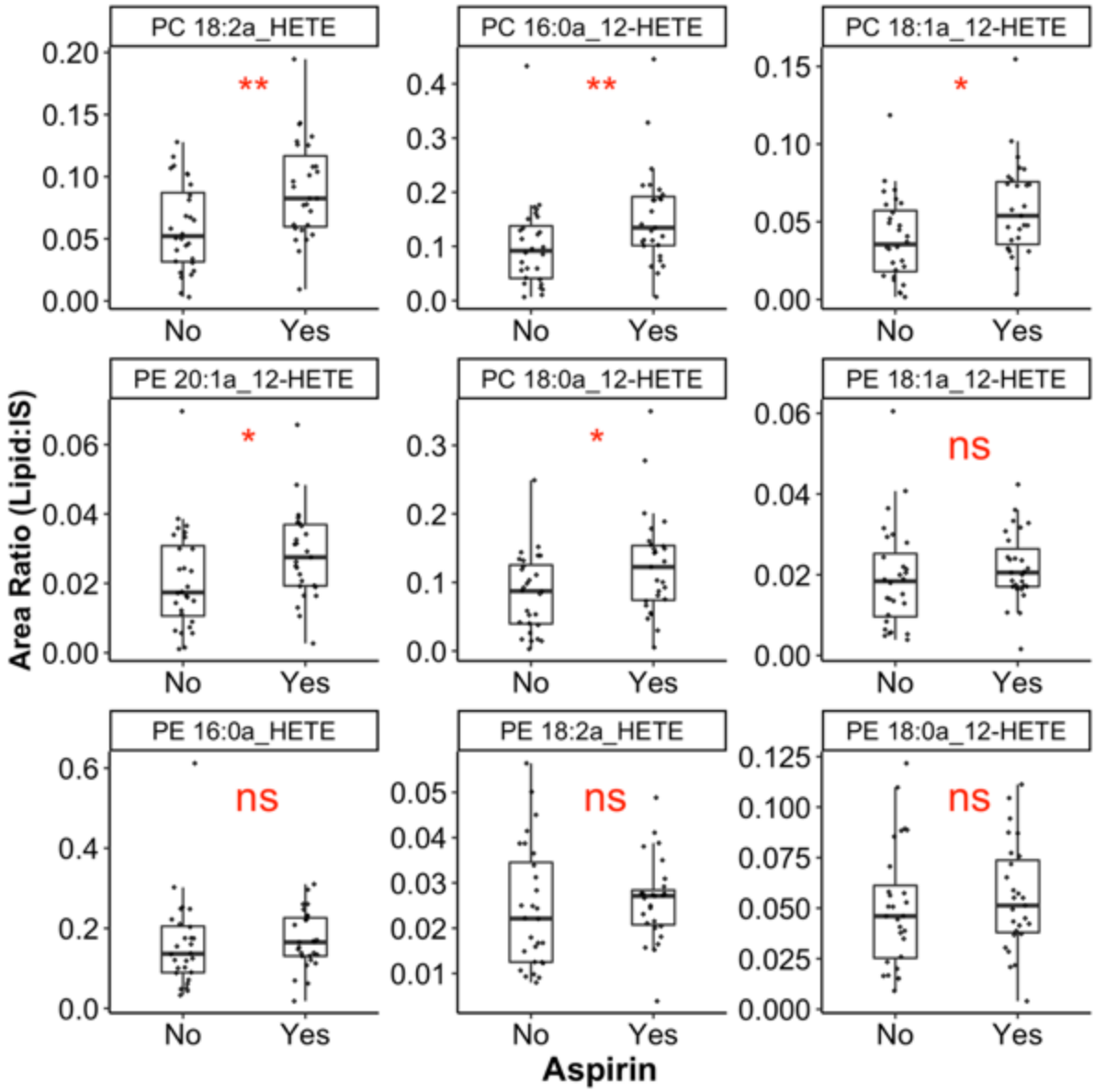

Figure 3.7. Higher amounts of diacyl 12-HETE-PL generated in thrombin-activated platelets from participants supplemented with aspirin *in-vivo*.

Lipids were extracted from platelets (2 x 10^8) following activation with thrombin (0.2 U/ml) as in Materials and Methods and quantified by LC-MS/MS. Lipid to internal standard signal area ratio were calculated for each product and averaged across all 'healthy cohort' participants and timepoints, separated only by aspirin. Next, data points were plotted for patients with (n=27) or without (n=28) *in-vivo* aspirin supplementation. P-values were calculated with the Mann-Whitney-Wilcoxon test (ns: not significant, *: p <0.05, **: p <0.01, ***: p <0.001).

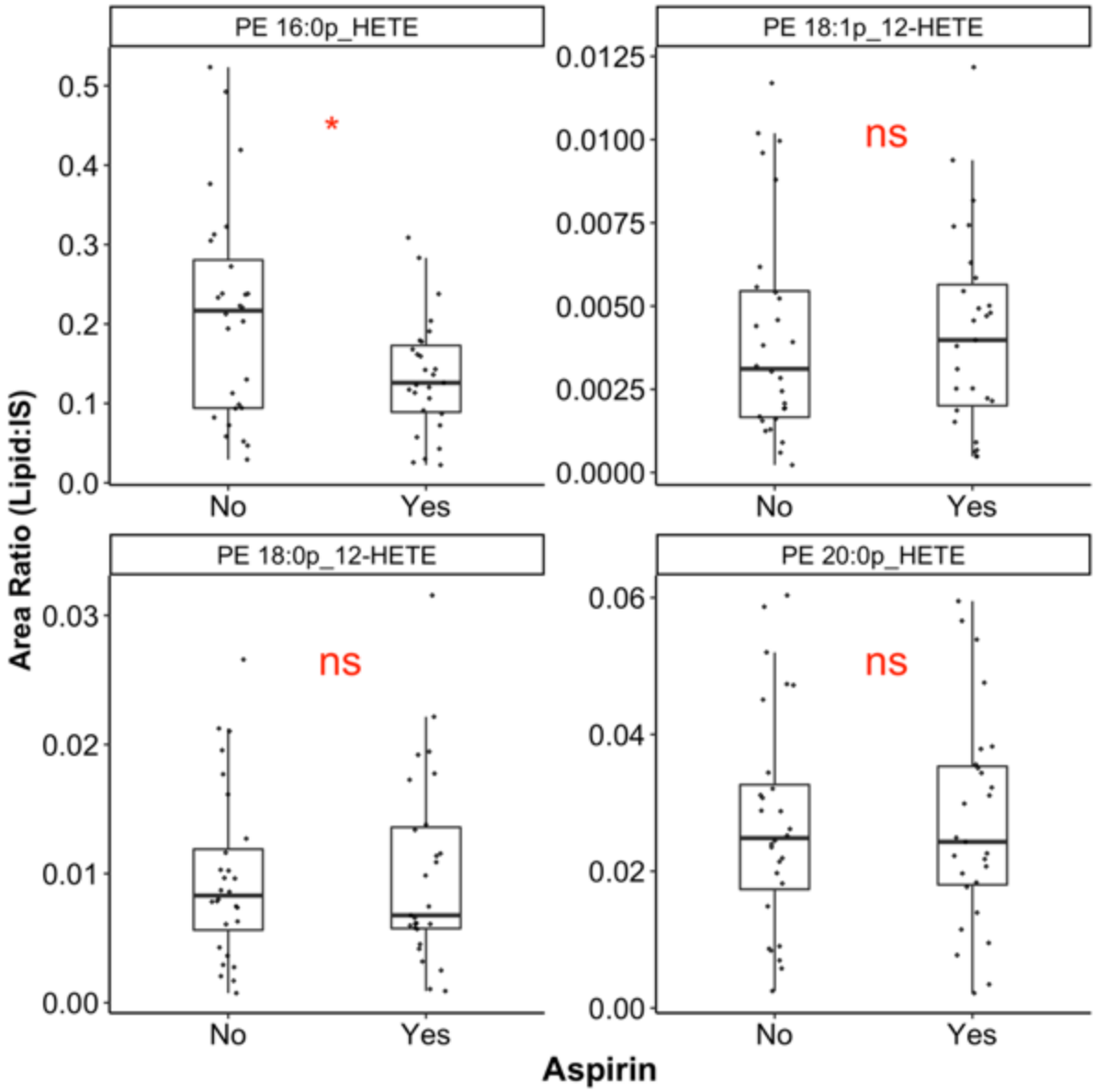

Figure 3.8. The amount of plasmalogen 12-HETE-PL generated in thrombin-activated platelets was similar between participants on or off aspirin.

Lipids were extracted from platelets (2 x 10^8) following activation with thrombin (0.2 U/ml) as in Materials and Methods and quantified by LC-MS/MS. Lipid to internal standard signal area ratio were calculated for each product and averaged across all 'healthy cohort' participants and timepoints, separated only by aspirin. Next, data points were plotted for patients with (n=27) or without (n=28) *in-vivo* aspirin supplementation. P-values were calculated with the Mann-Whitney-Wilcoxon test (ns: not significant, *: p <0.05, **: p <0.01, ***: p <0.001).

3.2.5 Thrombin-activated platelets generate less eoxPL in males versus females.

Next, to examine the influence of gender on eoxPL generation in thrombin-activated platelets, I carried out a volcano plot analysis looking at fold-changes driven by male gender (compared to females). This demonstrated a trend towards lower levels of eoxPL in males compared with females (**Figure 3.9**), demonstrating that gender differences in eoxPL-generation exist, though the mechanism for this is unknown.

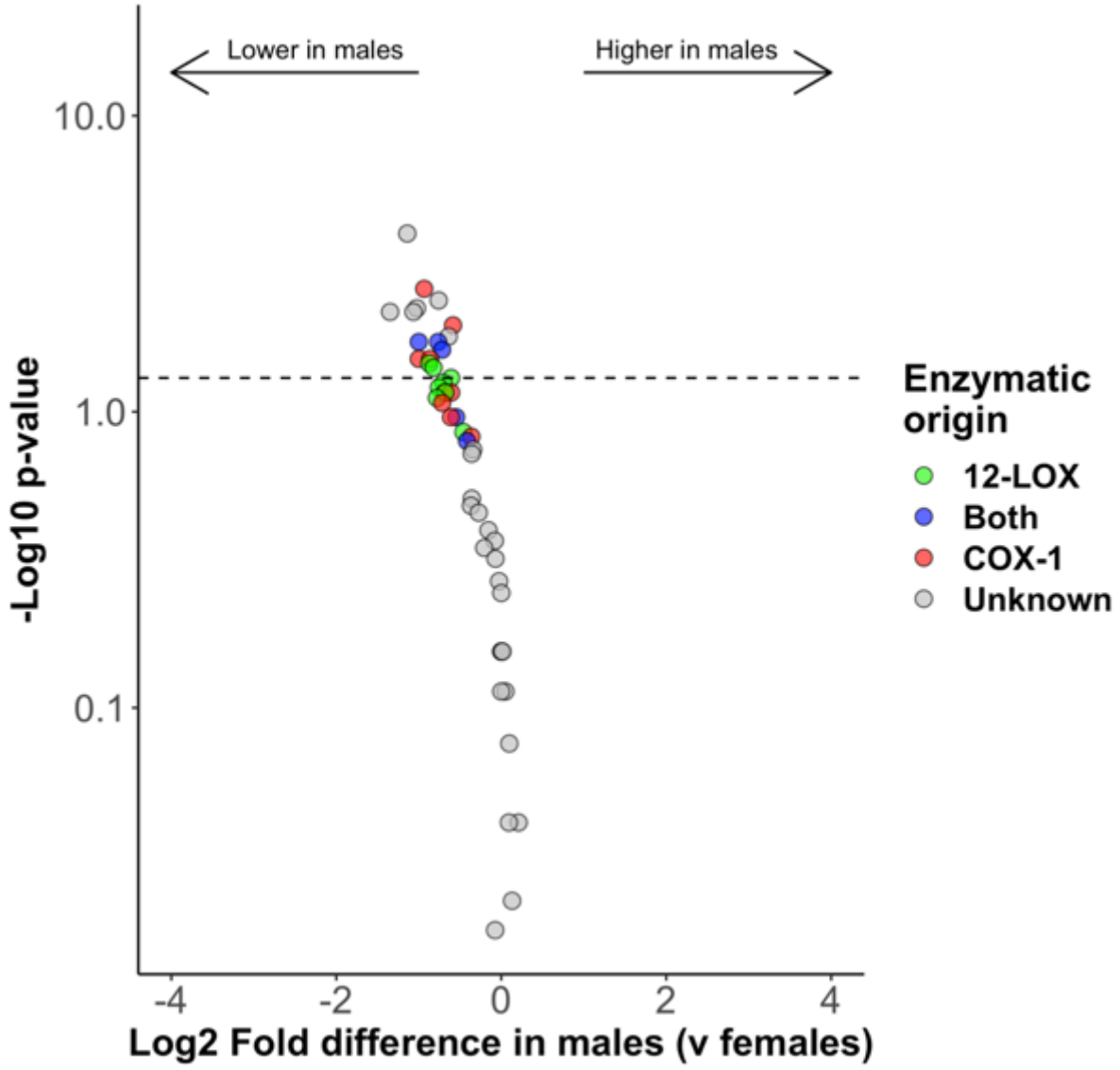

Figure 3.9. The amount of eoxPL generated in thrombin-activated platelets had a lower trend in males (compared to females).

Lipids were extracted from platelets (2 x 10^8) following activation with thrombin (0.2 U/ml) as in Materials and Methods and quantified by LC-MS/MS. The ratio of analyte:internal standard was calculated for each lipid and averaged (mean) over the three timepoints for each donor. Next, log2 fold changes were calculated between males (n=14) and females (n=14) and p-values calculated with the Mann-Whitney-Wilcoxon non-parametric test. The horizontal dashed line corresponds to p=0.05, with all points above the line having a $p < 0.05$. The presumed enzymatic origin of eoxPL is seen in the legend (COX-1: cyclooxygenase-1, 12-LOX: 12-lipoxygenase, Both: both COX-1/12-LOX can generate this product).

3.2.6 The impact of aspirin on eoxPL generation in males and females is similar for COX-1, but different for 12-LOX

Next, to examine whether the effect of aspirin on eoxPL generation in thrombin-activated platelets is different between males and females, a gender-specific subgroup analysis was carried out (**Figure 3.10** and **Figure 3.11**). This shows that the reduction of COX-1-derived eoxPL in response to aspirin is consistent irrespective of gender, whereas the observed increase in 12-LOX-generated eoxPL is observed in males only.

Box plots of individual eoxPL from thrombin-activated platelets show lower amounts of diacyl 12-HETE-PL off aspirin in males compared to females, which then increase in patients supplementation with aspirin *in-vivo* (**Figure 3.12**). This is consistent with the observed trend of lower eoxPL generation in males compared with females described in section **3.2.5** above.

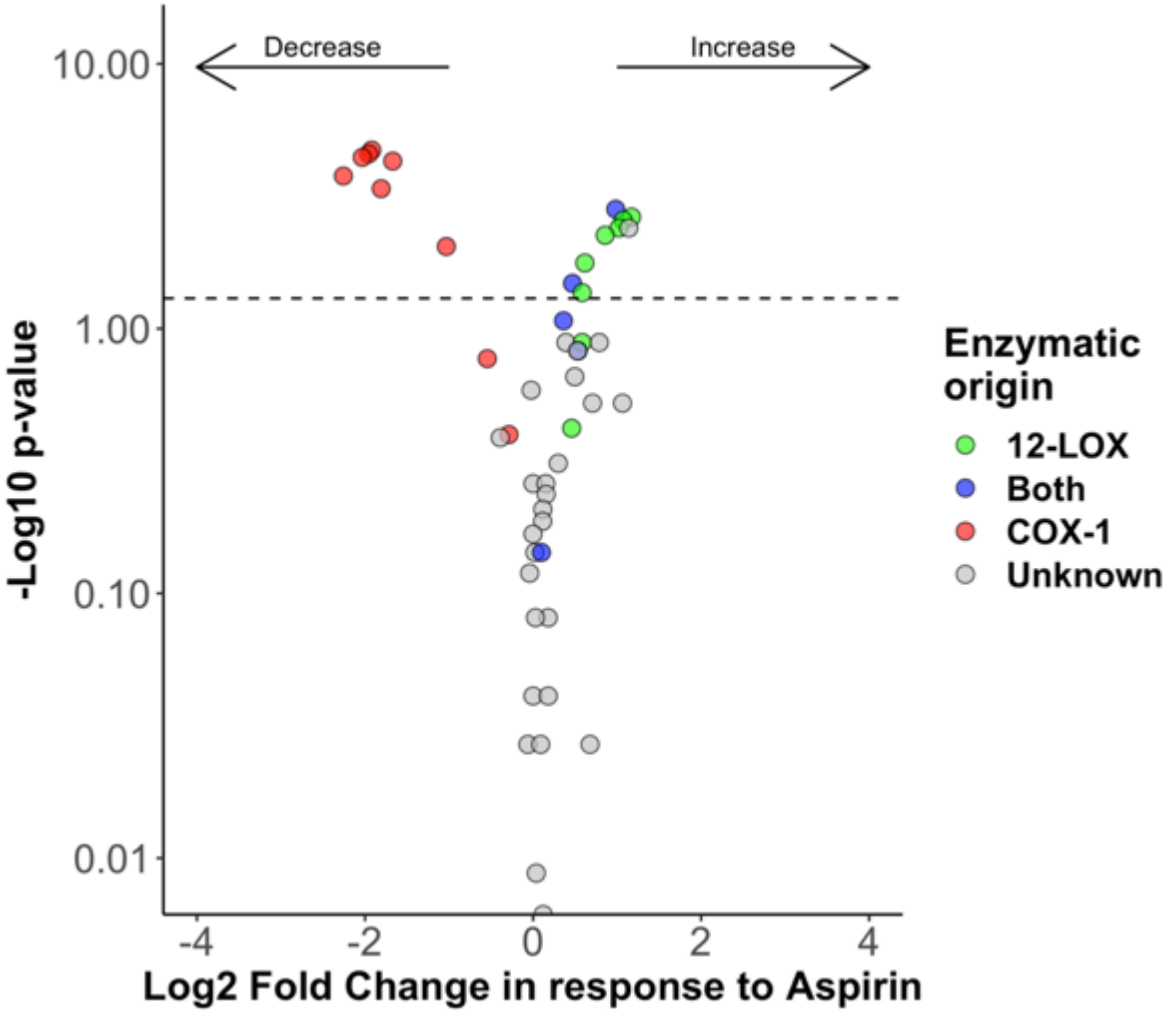

Figure 3.10. In males, aspirin significantly reduced the amount of COX-1 generated eoxPL in thrombin-activated platelets compared with resting platelets, but led to an increase in some 12-LOX generated eoxPL.

Lipids were extracted from platelets (2 x 10^8) following activation with thrombin (0.2 U/ml) as in Materials and Methods and quantified by LC-MS/MS. The ratio of analyte:internal standard was calculated for each lipid and averaged (mean) over the three timepoints for each male donor. Next, log2 fold changes were calculated between aspirin (n=13) and no aspirin (n=14) and p-values calculated with the Mann-Whitney-Wilcoxon non-parametric test. The horizontal dashed line corresponds to p=0.05, with all points above the line having a $p < 0.05$. The presumed enzymatic origin of eoxPL is seen in the legend (COX-1: cyclooxygenase-1, 12-LOX: 12-lipoxygenase, Both: both COX-1/12-LOX can generate this product).

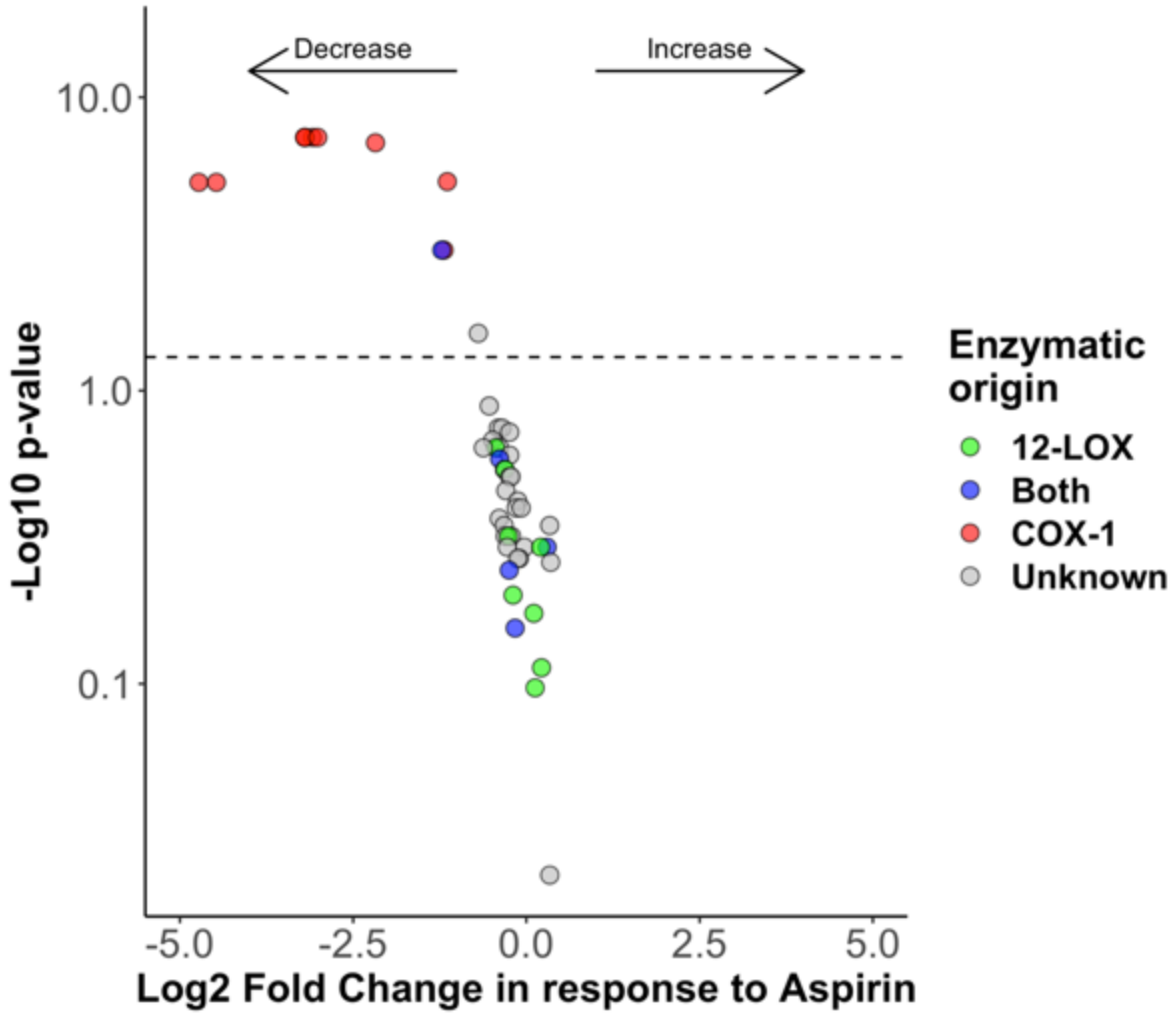

Figure 3.11. In females, aspirin significantly reduced the amount of COX-1 generated eoxPL in thrombin-activated platelets compared with resting platelets, but unlike in males, aspirin had no impact on 12-LOX generated eoxPL.

Lipids were extracted from platelets (2 x 10^8) following activation with thrombin (0.2 U/ml) as in Materials and Methods and quantified by LC-MS/MS. The ratio of analyte:internal standard was calculated for each lipid and averaged (mean) over the three timepoints for each female donor. Next, log2 fold changes were calculated between aspirin (n=14) and no aspirin (n=14) and p-values calculated with the Mann-Whitney-Wilcoxon non-parametric test. The horizontal dashed line corresponds to p=0.05, with all points above the line having a $p < 0.05$. The presumed enzymatic origin of eoxPL is seen in the legend (COX-1: cyclooxygenase-1, 12-LOX: 12-lipoxygenase, Both: both COX-1/12-LOX can generate this product).

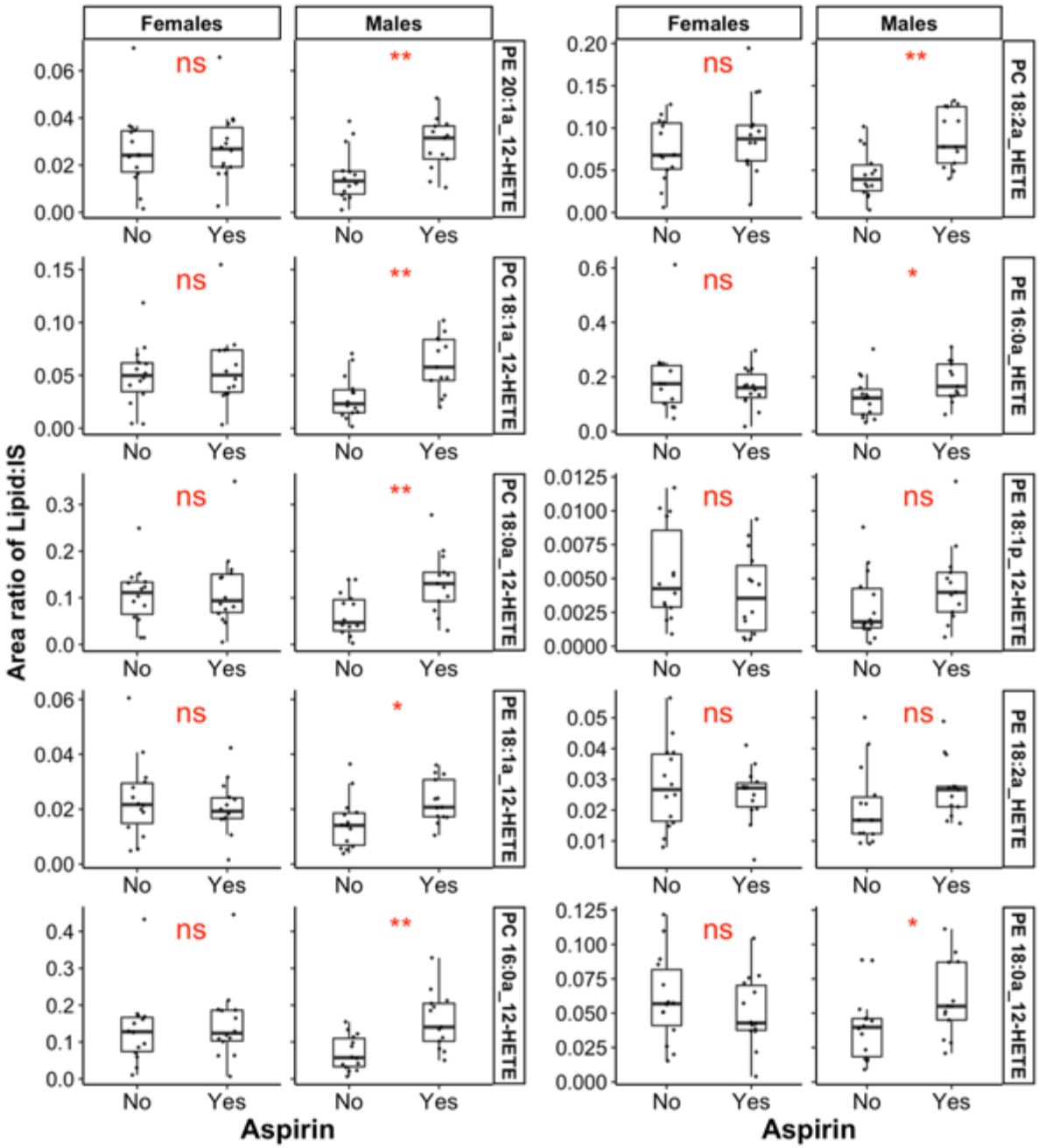

Figure 3.12. *In-vivo* supplementation of aspirin in males, but not females, leads to higher diacyl 12-HETE-PL generation in thrombin-activated platelets.

Lipids were extracted from platelets (2 x 10^8) following activation with thrombin (0.2 U/ml) as in Materials and Methods and quantified by LC-MS/MS. Lipid to internal standard signal area ratio were calculated for each product and averaged across all 'healthy cohort' participants and timepoints, separated by aspirin and gender (n aspirin = 27 [13 males, 14 females], n no aspirin = 28 [14 males, 14 females]). Next, box plots of all data points were plotted for all eoxPL, compared by aspirin and gender status and tested with the Mann-Whitney-Wilcoxon non-parametric test (ns: not significant, * $p < 0.05$, ** $p < 0.01$, *** $p < 0.001$).

3.2.7 Aspirin reduces TxB_2 generation but has no impact on free 12-HETE in platelets from either males or females

Finally, to investigate whether aspirin supplementation affects free oxylipin generation differently for males or females, free 12-HETE (12-LOX) and TxB_2 (COX-1) were measured in all samples. The initial study design did not include internal standards for the measurement of eicosanoids as this was not planned in the original study. Therefore, this analysis was carried out *post hoc* by adding 5 ng of each deuterated eicosanoid internal standard (12-HETE-d8 and TxB_2-d4) to samples in an additional targeted lipidomics run as described in Materials and Methods, to give a reasonable estimate of amounts generated.

There were no differences seen in the levels of 12-HETE with aspirin supplementation for both males and females. As expected, TxB_2 levels were significantly lower with aspirin supplementation and this was the same for both males and females (**Figure 3.13**).

These findings demonstrate that the higher levels of 12-HETE-PL generated by thrombin-stimulated platelets following aspirin supplementation (described in sections **3.2.4** and **3.2.6**) are not matched by higher levels of free 12-HETE.

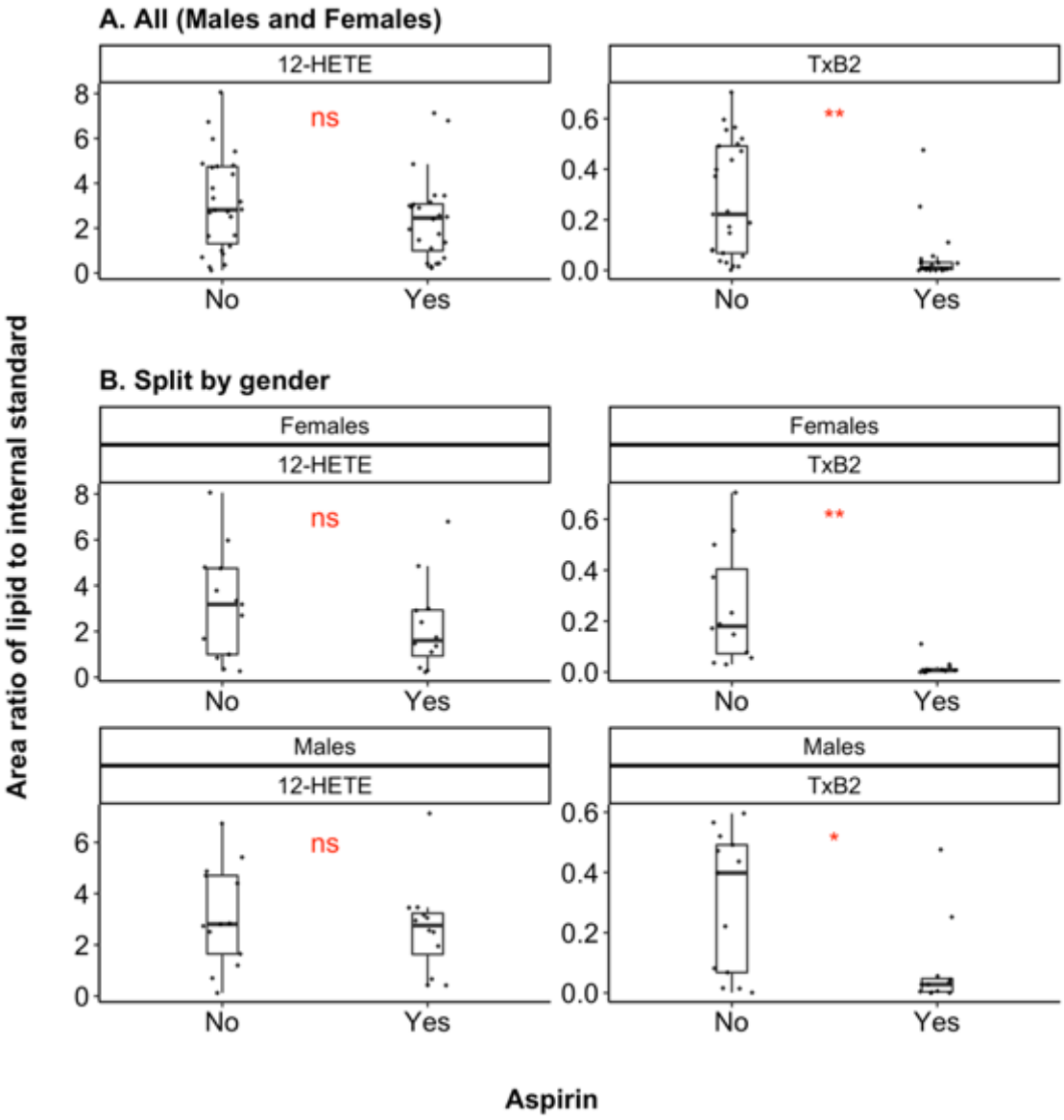

Figure 3.13. Aspirin supplementation significantly reduced the amounts of thrombin-activated platelet TxB_2 (COX-1 product) in all participants irrespective of gender, but had no impact on the levels of 12-LOX-derived free 12-HETE.

Lipids were extracted from platelets (2 x 10^8) following activation with thrombin (0.2 U/ml) as in Materials and Methods and quantified by LC-MS/MS. The ratio of analyte:internal standard was calculated for each lipid and averaged (mean) over the three timepoints for each donor. These values were separated by aspirin and subgrouped by gender (n aspirin = 27 [13 males, 14 females], n no aspirin = 28 [14 males, 14 females]). Next, box plots of all data points were plotted for 12-HETE and TxB_2 for all patients (A) and gender subgroups (B). P-values were calculated with the Mann-Whitney-Wilcoxon non-parametric test (ns: not significant, * $p < 0.05$, ** $p < 0.01$, *** $p < 0.001$).

3.3 DISCUSSION

In this chapter, I expanded on previous studies into platelet eoxPL generation by using a larger cohort of healthy volunteers to examine variations between individuals and over time as well as assess the influence of gender and *in-vivo* aspirin supplementation. The findings add to our understanding on how eoxPL generation varies, which is of importance given the role that these lipids play in mediating inflammation and coagulation[14].

The amounts of eoxPL generated in thrombin-activated platelets varied across the three sampling time points indicating intra-individual variation (**Figure 3.3**). Factors which could be responsible for driving differences over time include seasonal variation in lipid synthesis, akin to the diurnal and seasonal variation noted with cortisol and immune system parameters[251-253]. This is particularly relevant to this study as participant samples were collected over a period of 6 months, which may have introduced such seasonal variation. However, it was not possible to determine such seasonal effect with the current cohort due to the continuous weekly recruitment schedule which makes it difficult to subgroup participants by season. Furthermore, the pattern of change over time varied between the individual lipids, with many lipids rising in the second and third timepoints, whereas others decreased in amounts (**Figure 3.4**). Hierarchical clustering analysis demonstrated possible grouping of eoxPL variation over time by *sn2* FA (**Figure 3.5**). This may imply that the pattern of intra-individual variation in eoxPL is affected by the enzymatic pathway and the metabolised PUFA as suggested in the pilot study[70]. Alternatively, the clustering may relate to the relative abundance of these lipids in platelets over time, whereby lipids of high abundance group together and separate from lipids of low overall abundance.

In addition to intra-individual variation, eoxPL amounts also varied between individuals as demonstrated by high RSD values (**Table 3.1**). This may relate to genetic or environmental influences on enzymatic pathways in this unrelated group of humans. In fact, genetic polymorphisms in COX-1 have been previously shown to significantly modify the amount of serum thromboxane generation[254]. It is of course possible that some of the variation, both inter- and intra-individuals, may relate to sampling and processing variables, although seeing as all assays, including phlebotomy, were carried out by the same individual with the same protocol, the contribution of this is likely limited. Indeed, despite the high RSD values, the thrombin-induced eoxPL generation (**Figure 3.2**) and the COX-1 inhibition in response to aspirin (**Figure 3.6**) seem to be consistent across individuals with eoxPLs reliably clustering in groups by enzymatic origin (**Figure 3.1**). These findings suggest that despite inter- and intra-individual variations in the amount of eoxPL generated, there's relative stability in the patterns of synthesis.

The response to *in-vivo* aspirin supplementation confirmed that COX-1-generated eoxPL in thrombin-activated platelets were the most consistently affected lipids in the analysed set with significantly reduced levels in response to the drug in both males and females (separately or in combination) (**Figure 3.6**). However, the most striking finding of this study is the differences in the levels of 12-LOX-generated eoxPL in response to aspirin. These were elevated in thrombin-activated platelets when participants were supplemented with aspirin compared to not being on the drug. Furthermore, upon subgrouping this analysis by gender, only males demonstrated this increase in 12-HETE-PL generation with aspirin, whereas females had little or no change with aspirin in this group of eoxPL (**Figure 3.10** and **Figure 3.11**). These findings are of particular relevance to this thesis given the role that 12-HETE-PL play in enhancing coagulation. This raises the question as to whether aspirin could have an

impact on coagulation by interfering with procoagulant lipid generation, which will be discussed below.

To investigate the mechanism behind the increased levels of 12-HETE-PL with aspirin, I hypothesized that this could be related to aspirin-induced sparing of PUFA from undergoing metabolism with COX-1. This could lead to increased substrate (e.g. AA) availability which could be utilised by 12-LOX to generate free 12-HETE which may then be re-esterified. However, this was not supported by analysis of free 12-HETE which was present in similar amounts in samples from patients on or off aspirin (**Figure 3.13**). This suggests that the most likely mechanism therefore relates to the re-esterification of 12-HETE to the acyl lysoPL in the membrane. Specifically, it may suggest that the likely mechanistic location is LPAT pathways implicated in re-esterifying free 12-HETE to acyl lysoPL (**Figure 3.14**), which remains to be tested.

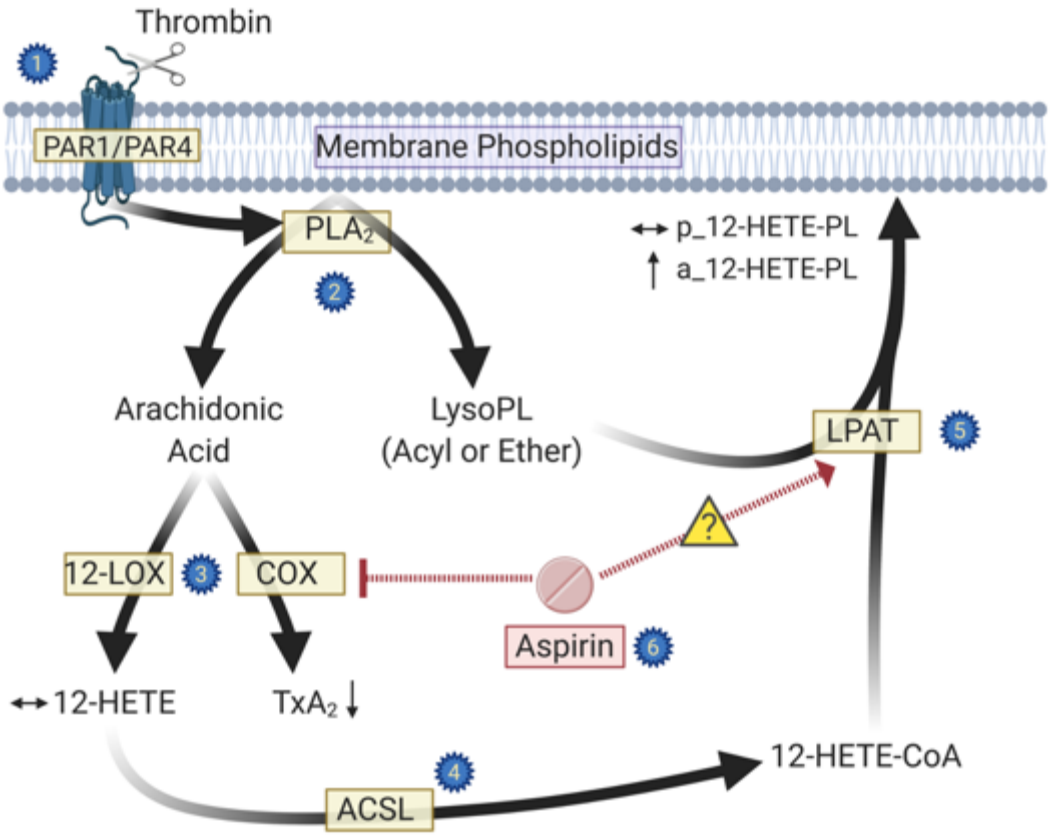

Figure 3.14. Effect of aspirin on 12-HETE-PL synthesis in thrombin-activated platelets.

1) Stimulation of platelets with thrombin activates the protease activated receptors PAR1 and PAR4 in humans. 2) This leads to activation of phospholipase A_2 (PLA_2) which metabolises membrane phospholipids at the *sn2* position releasing polyunsaturated fatty acids (PUFA) and lysophospholipids, which may have an acyl or ether bond at the *sn1* position. 3) Arachidonic Acid is a PUFA which undergoes modification via 3) 12-lipoxygenase (12-LOX) or cyclooxygenase (COX) to generate oxylipins. 4) The first step of re-esterification of oxylipins, such as 12-HETE, is to create a fatty acyl-CoA via the action of acyl Co-A synthetase (ACSL). 5) Lysophospholipid acyl transferase (LPAT) enzymes re-esterify 12-HETE-CoA to the membrane surface which modifies native phospholipids. This generates 12-HETE-PL which may have an acyl (a_12-HETE-PL) or an ether (p_12-HETE-PL) bond at *sn1*. 6) The results from this chapter show that Aspirin blocks COX activity which results in less TxB_2 (a stable metabolite of TxA_2) generation, but does not affect the levels of free 12-HETE. Despite this, aspirin supplementation appears to result in more a_12-HETE-PL generation but does not affect the levels of p_12-HETE-PL. This observation suggests that aspirin may have a role in interfering with LPAT re-esterification pathways specific to diacyls but not plasmalogens, either directly or indirectly (through reducing TxA_2 amounts).

Aspirin has traditionally been viewed as an antithrombotic with no effect on *in vitro* coagulation assays. A number of studies have shown that clinical assays for coagulation markers, levels of thrombin-antithrombin (TAT) complexes, prothrombin fragments 1 + 2 (F1+2) and fibrinopeptide A (FPA) are not altered in response to aspirin[255-257]. Studies examining thrombin generation by virtue of the calibrated automated thrombin (CAT) system demonstrated lower levels of thrombin formation, as determined by a fluorogenic substrate, when patients were supplemented with aspirin[258,259]. However, given the platelet-driven feedback loop with CAT assays and the depressed platelet activity as a result of COX-1 inhibition, the effects on thrombin formation have been attributed to the lower platelet reactivity in response to aspirin[260]. These suggest that aspirin has no significant clinical effect on coagulation and is consistent with studies which have noted no difference in clinical outcomes in conditions that are driven by the coagulation cascade as opposed to platelets (such as venous thrombosis and atrial fibrillation)[261]. This makes it difficult to infer a clinical role for our findings, and suggests no impact on overall coagulation. Alternatively, it may be that the effect that aspirin has on reducing TxA_2 levels far outweighs any increase in coagulation mediated by HETE-PL lipids. It is interesting to note that none of the clinical studies above were powered or designed to detect differences in response to aspirin between men and women and certainly most (if not all) of the original aspirin trials in 1960s-1980s recruited men only, and inferred the clinical benefit to women by extrapolation[262].

3.4 CONCLUSION

In conclusion, this chapter expanded on existing literature and utilised a larger cohort of healthy volunteers to examine variations in the profiles of platelet eoxPL in response to time, gender and aspirin supplementation. It demonstrated up to four-fold variation in the amounts of eoxPL generated over time with a large degree of variation between participants. In addition, there were overall lower levels of eoxPL generated in thrombin-activated platelets from male compared to female participants. Furthermore, aspirin supplementation was associated with a decrease in COX-1-derived eoxPL, but an increase in 12-LOX derived 12-HETE-PL. This observation was unique to male participants and only affected diacyl 12-HETE-PL.

The findings of this chapter therefore raise questions as to whether aspirin alters the procoagulant surface of platelets, particularly in males, by affecting re-esterification pathways and highlights the need for more studies to elucidate the mechanism for this. Specifically, to investigate whether *in-vivo* aspirin supplementation interferes with LPAT activity on acyl lysoPL in the platelet membrane which may be studied using platelet/megakaryocyte transcriptomics supported by genetically modified mice lacking one or more LPAT enzyme isoforms.

CHAPTER 4 CHARACTERISING THE HETE-PL

COMPOSITION OF ARTERIAL THROMBI IN PATIENTS WITH CORONARY AND PERIPHERAL VASCULAR DISEASE.

4.1 INTRODUCTION

The formation of thrombi under arterial shear stress on the surface of disrupted atherosclerotic plaques is responsible for myocardial infarction, ischaemic stroke and peripheral limb ischaemia[263]. The initial steps in this process consist of platelet activation in response to exposure of extracellular matrix proteins in the disrupted plaque leading to the development of platelet-rich thrombi classically associated with acute cardiovascular events[264]. Despite the use of antiplatelet agents however, 10-20% of patients continue to experience re-infarction, stroke or re-intervention, suggesting that other factors are at play[265-267]. These likely include leukocytes as well as the coagulation system, whose role in arterial thrombosis is evidenced by the presence of large amounts of fibrin in arterial thrombi and high amounts of tissue factor (TF) expression in human atherosclerotic lesions[145,268,269]. To date however, it is unknown whether procoagulant PLs are associated with arterial thrombi. This is particularly important given the recently emerging evidence of the role that procoagulant PLs, particularly HETE-PL generated by both platelets and leukocytes, play in linking activated cells to the initiation of coagulation[69,119].

The coagulation cascade is initiated by TF, which is normally expressed in subendothelial fibroblasts and becomes exposed to the circulation upon endothelial injury. The expression of TF in atherosclerotic plaques is enhanced, with evidence that macrophages and VSMC express high levels of TF on their surface, in EV populations and in extracellular matrix deposits[145,269-271]. This is thought to be driven by pro-inflammatory cytokines such as interleukin-1 (IL-1), interferon gamma (IFNγ), and tumour necrosis factor-alpha (TNFα)[272]. Indeed, histological staining of coronary clots has demonstrated TF at the sites of deposition of fibrin fibrils[273]. Taken together, this evidence supports the involvement of the coagulation system in arterial thrombosis and may explain the benefit seen with the addition of rivaroxaban (Factor Xa

inhibitor) to standard antiplatelet therapy by reducing ischaemic outcomes in patients with ACS when compared to antiplatelets alone[242]. A key contributor to FXa-driven coagulation and thrombin formation is the presence of negatively charged cell surfaces such as those provided by an activated platelet[163,274]. To date however, it remains unknown whether platelet-derived eoxPL form part of arterial thrombi.

Central to inflammation are leukocytes, which have also been implicated in atherothrombosis by being components of both plaques and the clot itself[273]. Previous studies that utilised coronary thrombus aspiration in ST-elevation myocardial infarction (STEMI), a condition which is caused by total thrombotic occlusion of a coronary artery, have demonstrated the presence of leukocytes within the clot histopathology [273,275]. In addition, elevated markers of systemic leukocyte activation were seen in ACS with evidence of increased trans-cardiac granulocyte and monocyte activation demonstrated by CD11b/CD18 expression profiles, activation of neutrophils demonstrated by lower myeloperoxidase (MPO) content and activation of lymphocytes with higher levels of serum IL-2 and increased HLA-D expression[276-278]. Therefore, it is likely that inflammation and leukocytes also play a role in arterial thrombus formation. However, it remains unclear whether leukocyte-derived eoxPL contribute to this process.

Procoagulant PLs contribute to thrombosis and haemostasis by facilitating the assembly of coagulation factor complexes, leading to activation and propagation of the clotting cascade[108,279]. HETE-PL are generated in leukocytes and platelets by cell-specific LOX isoforms[14]. A number of studies have examined their prothrombotic role *in vitro*, in animal models, and in human diseases such as antiphospholipid syndrome and abdominal aortic aneurysms[69,119]. However, no studies have examined their role in atherothrombosis of the

coronary arteries or the peripheral vasculature. If shown to be present, they may provide a new therapeutic target to complement current therapy targeted to coagulation factors.

4.1.1 Rationale for this study

Recent studies have identified networks of eoxPL implicated in the formation of clots and generated by different isoforms of the lipoxygenase (LOX) enzymes which vary depending on cell type[69,81]. The majority of these studies however examined individual cell types in isolation, limiting the applicability to the overall process in a formed human thrombus. In this chapter, I will study whole clots extracted from patients with coronary and peripheral vascular disease, undergoing percutaneous intervention or surgery. By using LC-MS/MS, I will measure the eoxPL present within these clots to profile the range of HETE-PL associated with atherothrombosis. Studying these pathological clots may shed some light on the cellular and molecular drivers of thrombosis in this life-threatening condition, and may reveal the involvement of eoxPL which are not targeted by current therapeutic agents.

4.1.2 The aim of this chapter

To characterise the HETE-PL composition of arterial thrombi from patients with coronary and peripheral vascular disease.

4.2 RESULTS

4.2.1 Participant baseline characteristics

Twenty participants were recruited comprising six emergency STEMI, eight carotid endarterectomy and six limb embolectomy patients. The age range was 50 - 85 years with 14/20 being male (70 %). The majority had one or more cardiovascular risk factors and were medicated on a combination of anti-platelet and anti-coagulant therapies. Baseline clinical characteristics of participants including their vascular comorbidities as defined by the study protocol are shown in **Table 4.1**.

The biochemical (renal profile) and haematological (full blood count with cell differentials) features of the participants are in **Table 4.2**. Clot age is defined as the estimated time from clinical diagnosis of atherothrombotic condition (i.e. STEMI, limb ischaemia or stroke) to the time of clot retrieval. This was estimated from medical records and electronic healthcare records by the local teams. All STEMI clots were collected within 3 hours of formation, whereas the carotid clots were more commonly older than 6 days since formation, as determined by time since stroke diagnosis. Limb clots are more heterogenous in terms of clot age ranging from 3 days to more than 6 weeks.

Table 4.1. Baseline clinical characteristics of patients with atherothrombosis who underwent surgical/interventional clot retrieval. (P2Y12 inhibitors: clopidogrel, prasugrel or ticagrelor, CKD: chronic kidney disease)

Clot ID	Tissue origin	Age	Gender	Aspirin	P2Y12 inhibitor	Anticoagulant	Statin	Hypertension	Diabetes	Smoker	CKD
STEMI1	Left anterior descending artery	67	Male	Yes	Yes	Warfarin	No	Yes	No	Never	No
STEMI2	Left anterior descending artery	59	Male	Yes	Yes	Heparin	No	No	No	Never	No
STEMI3	Right coronary artery	60	Male	Yes	Yes	Heparin	Yes	Yes	No	Ex	No
STEMI4	Left anterior descending artery	85	Male	Yes	Yes	Heparin	Yes	Yes	No	Never	Yes
STEMI5	Left anterior descending artery	59	Male	Yes	Yes	Heparin	Yes	Yes	Yes	Never	No
STEMI6	Right coronary artery	79	Female	Yes	Yes	Heparin	No	No	No	Ex	No
Carotid1	Left Carotid artery	71	Female	No	No	No	No	No	No	Ex	No
Carotid2	Left Carotid artery	69	Male	Yes	Yes	No	Yes	Yes	Yes	Ex	No
Carotid3	Right Carotid artery	75	Female	No	Yes	No	Yes	No	No	Never	No
Carotid4	Left Carotid artery	63	Male	Yes	Yes	Warfarin	Yes	Yes	No	Never	No
Carotid5	Right Carotid artery	76	Male	No	Yes	No	Yes	Yes	No	Never	No
Carotid6	Left Carotid artery	69	Male	No	Yes	No	Yes	Yes	No	Ex	No
Carotid7	Right Carotid artery	61	Male	Yes	Yes	No	Yes	Yes	No	Never	No
Carotid8	Left Carotid artery	58	Female	Yes	Yes	No	Yes	No	No	Current	No
Limb1	Right Femoral Embolectomy	59	Male	Yes	Yes	Heparin	No	No	No	Never	No
Limb2	Left Popliteal (Pop-Ped bypass)	50	Male	No	Yes	No	Yes	No	No	Current	No
Limb3	Left Femoral (Fem-Pop bypass)	62	Female	Yes	No	No	No	Yes	Yes	Ex	No
Limb4	Left Popliteal Below-Knee amputation	58	Male	No	No	Rivaroxaban	No	Yes	Yes	Ex	No
Limb5	Right Brachial Embolectomy	77	Female	Yes	No	Heparin	No	Yes	No	Never	No
Limb6	Right Popliteal (Fem-Pop bypass with embolectomy)	63	Male	No	Yes	No	Yes	No	No	Ex	No

Table 4.2. Baseline biochemical and haematological characteristics of patients with atherothrombosis who underwent surgical/interventional clot retrieval.

Clot age is the estimated time from diagnosis (clot formation/plaque disruption) to retrieval time. (Creat: serum creatinine μmol/L, Hb: haemoglobin g/dL, Plt: platelet count x 10^9/L, WCC: total white cell count x 10^9/L, Neutrophils/Eosinophils/Basophils/Lymphocytes/Monocytes: respective count x 10^9/L, RBC: red blood cell count x 10^{12}/L)

Clot ID	Clot age	Creat	Hb	Plt	WCC	Neutrophils	Eosinophils	Basophils	Lymphocytes	Monocytes	RBC
STEMI1	<3hr	137	172	168	12.1	10.7	0	0	0.9	0.5	5.3
STEMI2	<3hr	73	128	287	16.2	14.7	0.2	0	0.6	0.6	4.3
STEMI3	<3hr	96	149	301	7.1	5.4	0.1	0	1.1	0.4	4.5
STEMI4	<3hr	183	137	219	17	14.7	0.1	0	0.9	1.2	4.8
STEMI5	<3hr	92	132	283	14	12.5	0	0	0.5	1.5	4.4
STEMI6	<3hr	83	120	202	8.1	6.1	0	0	1.4	0.5	3.9
Carotid1	14 days	65	128	208	5.8	3.8	0.1	0.1	1.3	0.6	3.4
Carotid2	20 days	77	130	233	10.7	7.2	0.3	0.1	2.3	0.9	4.4
Carotid3	13 days	69	131	425	13.1	9.5	0	0	2.5	1.1	3.9
Carotid4	9 days	70	133	250	7.4	5.3	0.1	0	1.5	0.5	4.5
Carotid5	6 days	122	154	269	8.4	5.5	0.1	0	1.9	0.9	5.3
Carotid6	25 days	67	129	225	6	4.6	0.1	0	0.9	0.4	4.8
Carotid7	106 days	82	165	302	5.3	3.4	0.1	0	1.2	0.6	5.1
Carotid8	9 days	80	150	294	8.5	5.2	0.1	0	2.7	0.6	4.9
Limb1	3 days	69	125	501	10.5	7.5	0.1	0.1	2.2	0.8	4.0
Limb2	4 days	95	174	306	7.1	5.3	0.1	0	1.2	0.4	6.0
Limb3	>6 weeks	59	99	459	13.6	10.7	0	0	1.6	1.2	3.0
Limb4	6 days	70	83	163	8.3	6.1	0	0	1.5	0.6	2.7
Limb5	16 days	91	162	309	7.8	4.1	0.1	0.1	3.0	0.6	5.3
Limb6	15 days	63	179	313	9.2	6.3	0.5	0.1	1.0	1.3	5.8

4.2.2 Arterial clots contain eoxPL species

Lipids were normalised to ng per 100 mg clot for each sample and plotted on a heatmap (**Figure 4.1**). All had detectable levels of several HETE-PLs, but levels varied between samples. Overall, the highest levels of HETE-PL were seen in STEMI clots, followed by limb embolectomies and lastly by carotid endarterectomy samples. There were varying amounts of HETE-PL between limb clots with some samples having a similar profile to STEMI clots (Limb1, Limb2, Limb4, Limb5) whereas others were more similar to carotid clots (Limb3 and Limb6). Column-wise clustering demonstrates grouping of lipids by headgroups and the HETE positional isomer. Specifically, 15- and 11-HETE-PE formed one cluster, 5- and 11-HETE-PE forming another cluster, with a prominent cluster of 12-HETE-PLs. There were generally low levels detected of the non-enzymatically formed 8-HETE-PL (**Figure 4.1**). The clustering suggested by these findings indicate a likely involvement of COX (15- and 11-HETE-PL) and 12-LOX (12-HETE-PL) in generation of these lipids in arterial thrombi.

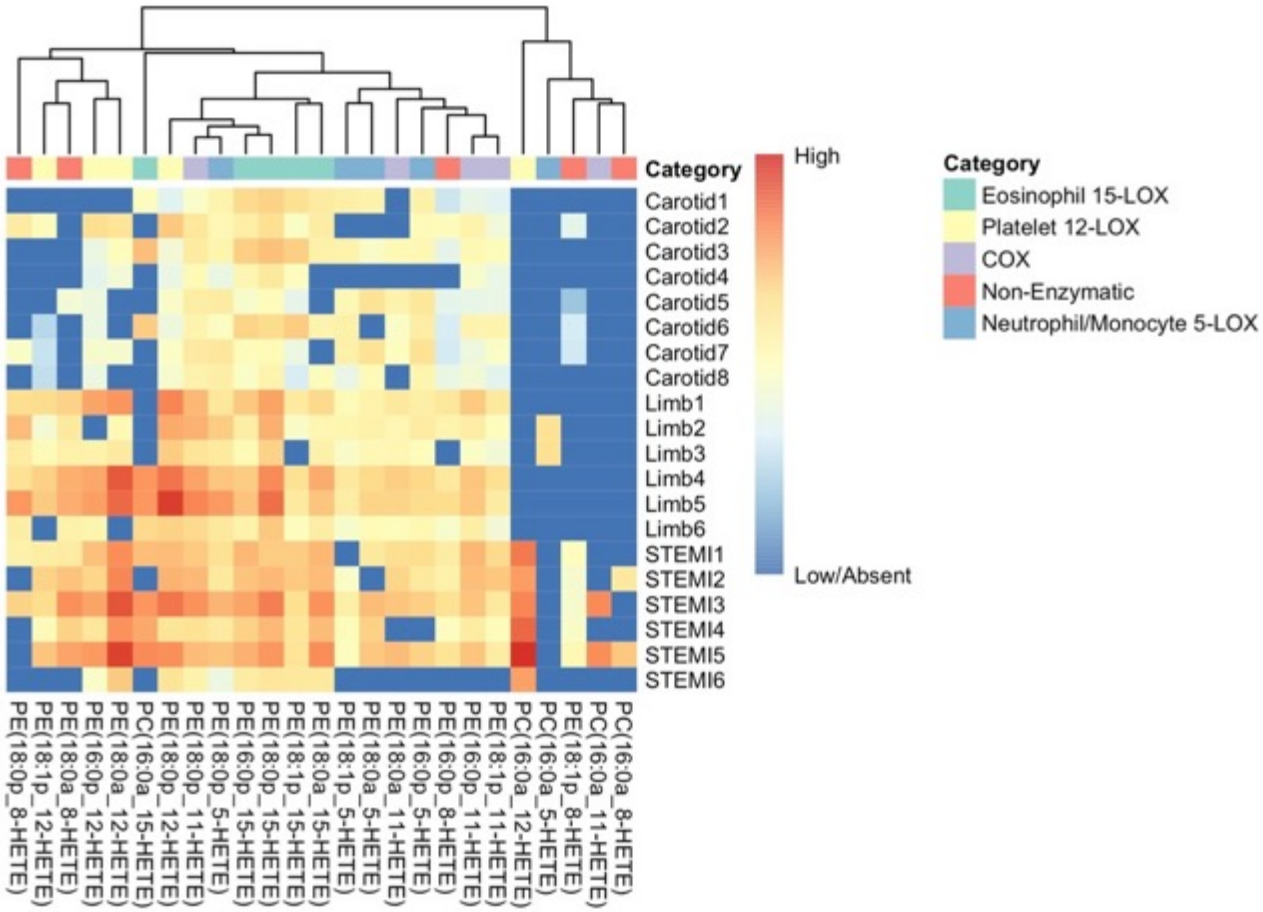

Figure 4.1. Arterial thrombi contain procoagulant HETE-PL with high amounts seen in STEMI compared with carotid clots.

Arterial thrombi were extracted, snap frozen on dry ice and frozen at -80 ^{o}C from patients undergoing angioplasty for ST-elevation myocardial infarction (STEMI), carotid endarterectomy (Carotid) or peripheral vascular embolectomy (Limb). Next, clots were homogenised using the BeadRuptor Elite and underwent lipid extraction as in Material and Methods. Lipids amounts (ng) were calculated by LC-MS/MS and normalised by clot weight (ng lipid/100 mg clot), log10 transformed and plotted as a heatmap with hierarchical clustering using the pheatmap R package. Category is the proposed enzymatic origin of HETE-PL species.

4.2.3 Multivariate analysis of clot OxPL profile demonstrates 12-HETE-PL as the key contributor to difference between samples

To visualise differences and similarities between samples based on their oxPL lipid profile, a multivariate analysis was carried out with a principal component analysis. In **Figure 4.2**, carotid endarterectomy samples are seen to be close to each other suggesting a high degree of similarity between samples. In contrast, STEMI samples are deviating away from carotid endarterectomy samples in the PC1 direction, suggesting that they possess different characteristics/lipid profile. Limb embolectomy samples were more heterogenous with some clustering with carotid clots (Limb3 and Limb6), whereas are others are deviating away in the PC1 and PC2 direction. The PC1 and PC2 principal components are responsible for 65% and 29% of variance, respectively, and therefore together they account for >94% of the difference between samples. This suggests that these are the two most important principal components that distinguish sample types from each other.

To investigate which HETE-PL are contributing to the difference between samples seen in this analysis, a loadings plot was generated (**Figure 4.3**). This demonstrates that the lipids having the largest effect on PC1 and PC2 are PE 18:0p_12-HETE, PE 18:0a_12-HETE and PC 16:0a_12-HETE. This is consistent with the intense signals seen in the heatmap described above and suggest that the presence of a 12-HETE fatty acyl attached to the PL (presumed to be of a platelet origin given the 12-LOX expression profile) is critical in differentiating between samples by being more abundant in STEMI and limb embolectomy samples compared with carotid clots.

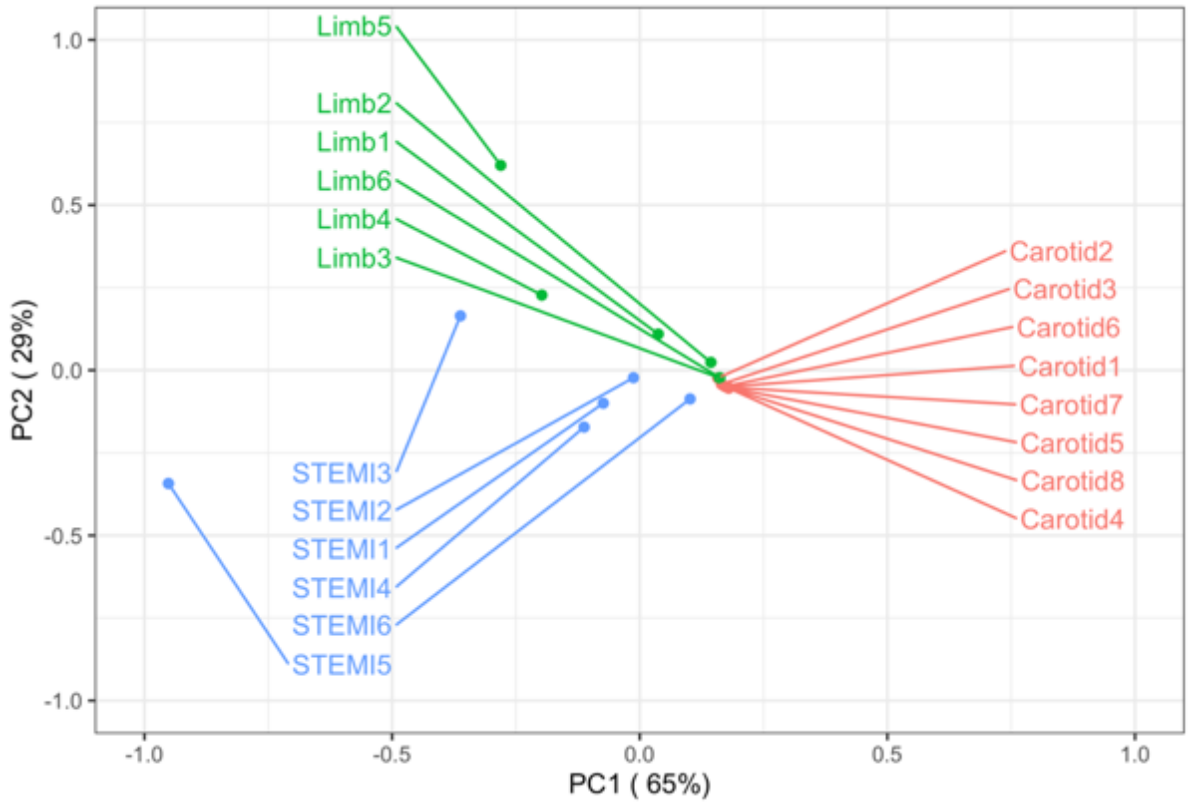

Figure 4.2. Principal component analysis of arterial thrombi by HETE-PL profile demonstrates grouping of samples by common features.

Arterial thrombi were extracted, snap frozen on dry ice and frozen at -80 ºC from patients undergoing angioplasty for ST-elevation myocardial infarction (STEMI), carotid endarterectomy (Carotid) or peripheral vascular embolectomy (Limb). Next, clots were homogenised using the BeadRuptor Elite and underwent lipid extraction as in Material and Methods. Lipids amounts (ng) were calculated by LC-MS/MS and normalised by clot weight (ng lipid/100 mg clot). Next, a principal component analysis was carried out using the prcomp() function in R, and the scores for two major components (PC1 and PC2) were used to plot the data. Each dot represents a sample.

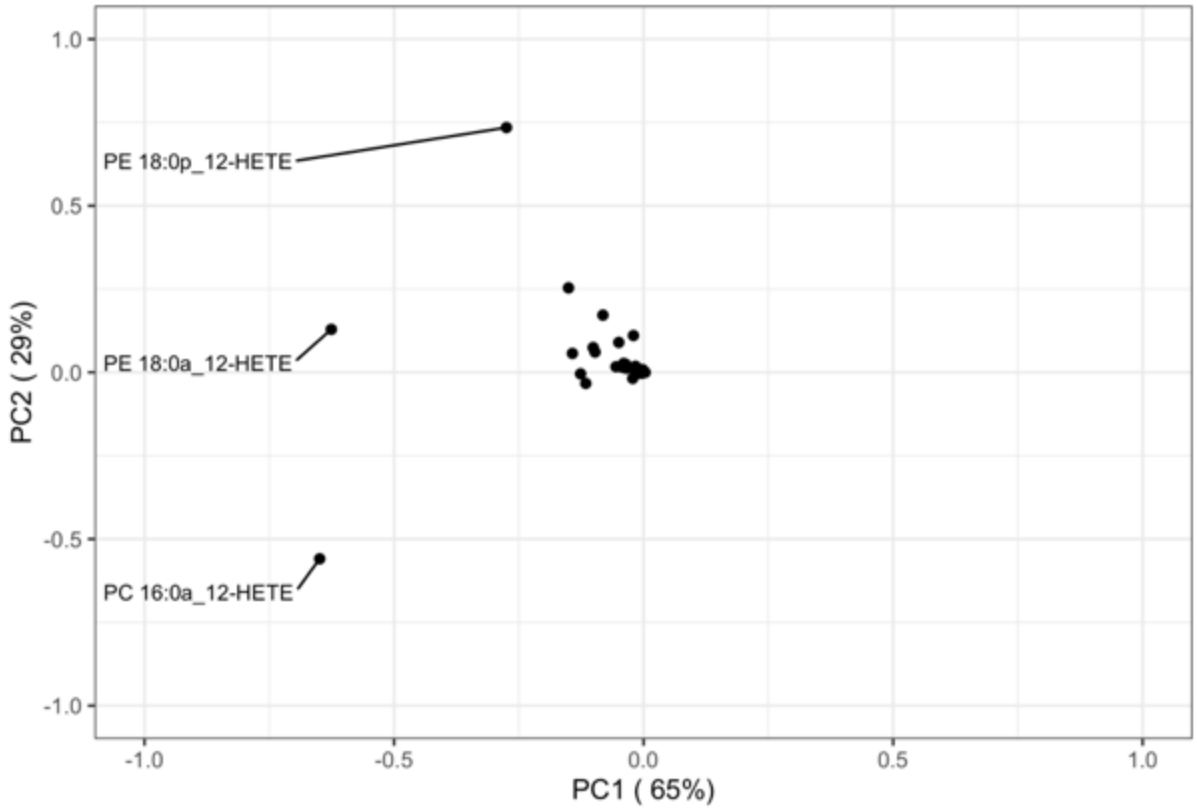

Figure 4.3. Loadings plot from the principal component analysis describing 12-HETE-PL as the variables most influential in explaining the difference between samples.

Arterial thrombi were extracted, snap frozen on dry ice and frozen at -80 ºC from patients undergoing angioplasty for ST-elevation myocardial infarction (STEMI), carotid endarterectomy (Carotid) or peripheral vascular embolectomy (Limb). Next, clots were homogenised using the BeadRuptor Elite and underwent lipid extraction as in Material and Methods. Lipids amounts (ng) were calculated by LC-MS/MS and normalised by clot weight (ng lipid/100 mg clot). Next, a principal component analysis was carried out using the prcomp() function in R, and the loadings for the two major components (PC1 and PC2) were used to plot the data. Each dot represents a lipid.

4.2.4 Quantitative analysis of HETE-PL isomers by clot type demonstrates variation in the amount of different positional isomers with a predominance of 12-HETE-PL

To quantify the magnitude of differences in HETE-PL within clot types, lipid amounts were grouped by HETE-PL positional isomer and sample type and plotted as a boxplot (**Figure 4.4**). The HETE-PL positional isomers are present in varying amount within samples. In carotid samples, the highest HETE-PL levels are seen for 15-HETE-PL with low levels seen for the other isomers. In contrast, STEMI samples had higher levels of 12-HETE-PL, followed by 15-HETE-PL, then 11-HETE-PL. This pattern is also observed in limb embolectomies, albeit with a larger degree of variability as shown by the large error bars (**Figure 4.4**). This suggests a likely enzymatic origin of formation, as non-enzymatic oxidation is expected to form equivalent amounts of the different positional isomers

These quantitative findings suggest that 12-HETE-PL, presumed to be of a platelet origin, are playing a key role in driving the variability between clot types and are the most predominant forms in STEMI and limb clots.

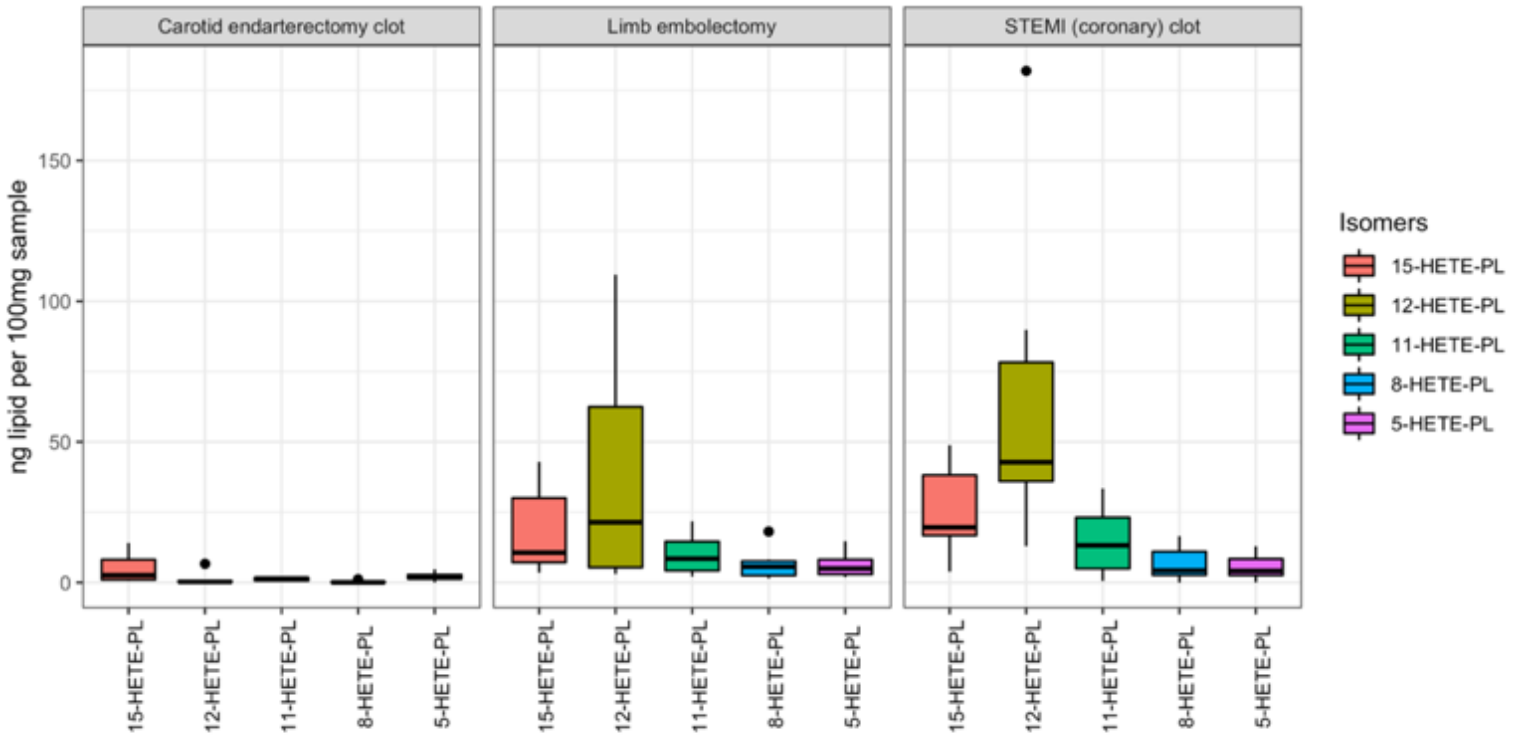

Figure 4.4. HETE-PL amounts expressed as ng lipid per 100mg clot sample, pooled by HETE-PL isomer, and grouped by clot type.

Arterial thrombi were extracted, snap frozen on dry ice and frozen at -80 ºC from patients undergoing angioplasty for ST-elevation myocardial infarction (STEMI), carotid endarterectomy (Carotid) or peripheral vascular embolectomy (Limb). Next, clots were homogenised using the BeadRuptor Elite and underwent lipid extraction as in Material and Methods. Lipids amounts (ng) were calculated by LC-MS/MS and normalised by clot weight (ng lipid/100 mg clot). Lipid species were summed up by positional isomer and plotted as box plots using the ggplot2 R package. Box edges indicate the interquartile range (IQR) with the median line inside the box. Whiskers indicate 1.5 times the IQR. Category is the proposed enzymatic origin of HETE-PL species.

4.2.5 Chiral analysis of clot lipid extracts confirms a likely enzymatic origin for 12-HETE-PL in STEMI and limb arterial thrombi.

Next, to investigate the proportion of HETE-PL generated enzymatically and non-enzymatically, lipid extract samples were alkaline hydrolysed to release the HETE fatty acyls from the eoxPL presumed *sn2* position, and analysed using chiral LC-MS/MS (as per Materials and Methods). The aim of this was to measure the amounts of R versus S stereoisomers for each HETE positional isomer, which are known to be preferentially different in enzymatic pathways given the stereospecificity of the LOX and COX enzymatic pathways, as described in section **1.2.4**. This demonstrated a >90% predominance of the 12(S)-HETE stereoisomer compared with 12(R)-HETE in STEMI and limb thrombi, confirming a likely enzymatic origin from platelet 12-LOX (**Figure 4.5**). Furthermore, limb thrombi also had higher levels of 11(R)-HETE which suggests they originate from COX activity. Finally, the results for 15-HETE are more difficult to interpret given that this lipid may be generated by 15-LOX or COX which can form 15(S)- and 15(R)-HETE, respectively. Nevertheless, there was slightly higher relative levels of 15(S)-HETE in all thrombi which suggests involvement of 15-LOX (eosinophils or monocytes). Taken together, these results confirm that the involvement of enzymatic pathways in the generation of HETE-PL within arterial thrombi.

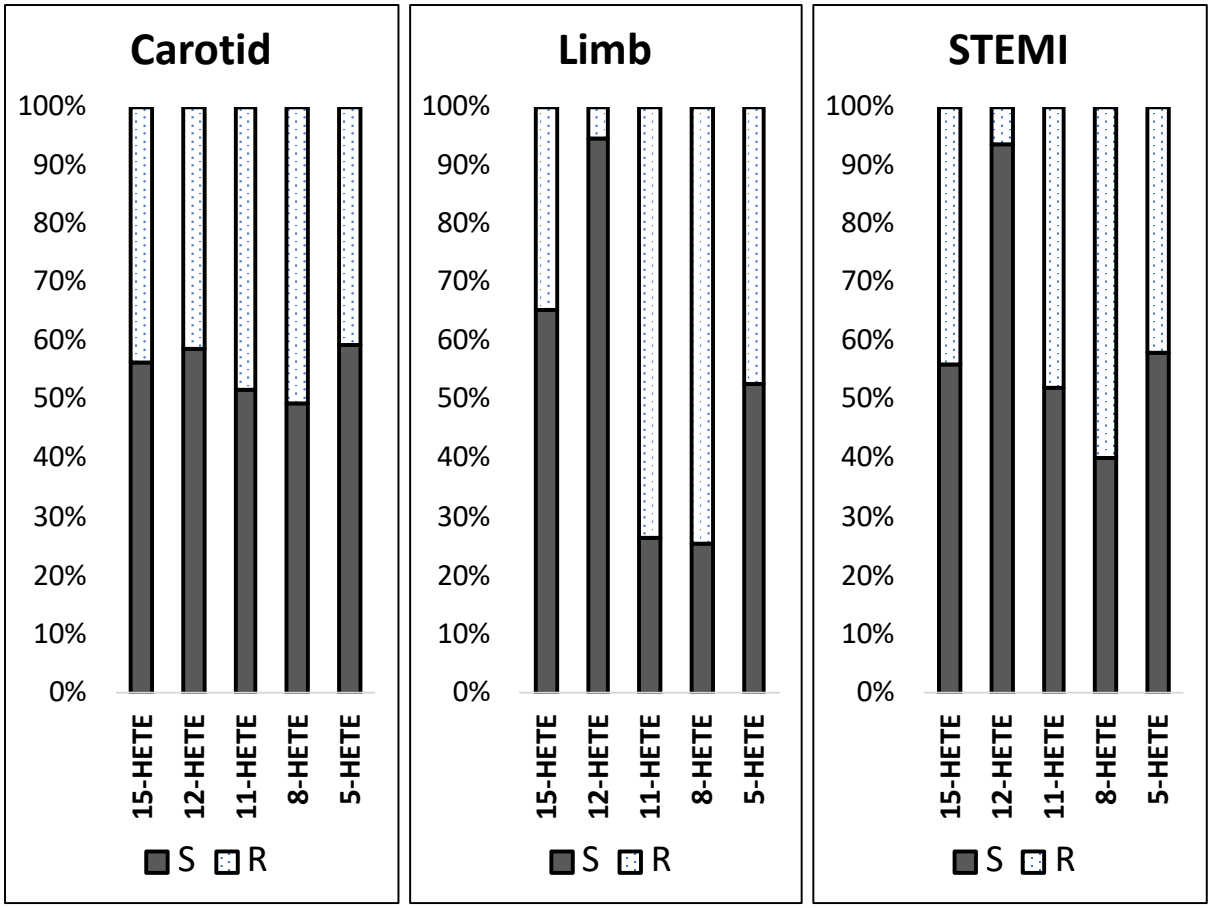

Figure 4.5. Chiral LC-MS/MS demonstrates higher amounts of 12(S)-HETE compared to 12(R)-HETE, suggesting a likely involvement of platelet 12-LOX.

Arterial thrombi were extracted, snap frozen on dry ice and frozen at -80 ^{o}C from patients undergoing angioplasty for ST-elevation myocardial infarction (STEMI), carotid endarterectomy (Carotid) or peripheral vascular embolectomy (Limb). Next, clots were homogenised using the BeadRuptor Elite and underwent lipid extraction as in Material and Methods. Samples (n=3 per tissue origin) were alkaline hydrolysed to release the HETE fatty acyl, followed by chiral LC-MS/MS to determine the relative proportions of S and R stereoisomers which were plotted above as 100% stacked bar charts.

4.3 DISCUSSION

In this chapter, I report a lipidomic analysis of atherothrombotic clots formed on disrupted plaque under shear stress in human atherothrombotic disease. Procoagulant HETE-PL were detectable and quantifiable in all analysed clots. The main driver of difference between clots was 12-HETE-PL, a product that is likely generated enzymatically by platelets evidenced by the presence of more of the 12(S)-LOX specific product stereoisomers. Indeed, coronary and limb clots had higher amounts of 12-HETE-PL compared to other isomers, whereas carotid clots had overall low amounts of HETE-PL with a predominance of 15-HETE-PL. The presence of HETE-PL within the clot architecture may contribute to the link between activated cells and the coagulation system in arterial thrombosis.

The amounts of HETE-PL were strikingly lower in the carotid endarterectomy samples compared to the STEMI/limb samples. Despite a similar pathophysiological process of formation under shear stress, the content of the clot could be influenced by other anatomical/pathological factors. For instance, carotid clot content may be contaminated by significant amount of plaque relative to clot. This is due to the nature of the surgical extraction technique which may explain the lower overall amounts of procoagulant oxPL. It could also provide an explanation for the predominance of 15-HETE-PL in carotid samples which may be a component of macrophage/foam cell content which are present in plaque lesions[275]. In fact, the presence of free 15-HETE has previously been reported as a component of human carotid plaques, but deemed to be non-enzymatically generated[280]. The chiral analysis seen in **Figure 4.5** indicates relatively similar proportions of S and R stereoisomers, which may indeed suggest that the source of HETE-PL in carotid samples is non-enzymatic oxidation. This is consistent with studies examining the enantiomeric composition of other eoxPL within advanced atherosclerotic plaques demonstrating a likely non-enzymatic origin[281].

The age of the analysed clots may be contributing factor to the differences observed between samples. STEMI clots were all retrieved within a short time from formation (<3 hours) compared to carotid clots (days/weeks). This could contribute to the higher observed amounts of HETE-PL owing to a possibly higher level of inflammatory cell activation in the acute phase[282]. This could also explain the 12-HETE-PL dominant profile in STEMI clots which may relate to the acute burst of platelet activation in the first few hours of thrombosis, compared to the carotid clots where sufficient time has passed since formation which allows for clot organisation to take place by the generation of an organised fibrin scaffold, modification to the cellular components and possible PL degradation[263,283,284]. Clots collected from limb embolectomies varied in retrieval time ('age') and this may explain the mixed picture observed in the multivariate analysis where despite an overall similar profile to STEMI, at least two of the 'oldest' clots were behaving in a way closer to carotid clots as seen on the heatmap (**Figure 4.1**). Other factors that may explain the variability within sample type may include inter-individual variability, co-morbidity profile, medications, or lifestyle choices. However, the current sample size is not sufficiently powered to investigate these factors in depth.

In the STEMI and limb samples collected, 15-HETE-PL was the second most abundant HETE-PL isomers. This oxPL may be enzymatically generated via 15-lipoxygenase, encoded by the *ALOX15* gene, which is found in eosinophils. Arterial thrombi were reported to contain eosinophils in the white/red transitional zone, with a positive correlation between the number of eosinophils detected histologically and the clot size[285]. Moreover, there is evidence that activation of eosinophils, as measured by proteomic markers, correlates with cardiovascular outcomes including myocardial infarction and strokes[72]. Furthermore, mice with a genetic deletion in *Alox15*, the equivalent murine gene to the human *ALOX15*, have defective

eosinophil-mediated thrombin generation and form smaller in-vivo clots in a venous injury model[72]. Consequently, it is likely that the source of 15-HETE-PL observed in the analysed STEMI and limb clots is eosinophils, particularly given their role in mediating thrombosis. Indeed, the higher proportion of 15(S)-HETE in the chiral analysis suggests that the likely source of 15-HETE-PL is 15-LOX, although the proportion of the S stereoisomer was between 55-65% (**Figure 4.5**). This is a relatively low proportion of overall 15-HETE-PL when compared to the >90% seen with 12(S)-HETE, and may therefore suggest a contribution from non-enzymatic pathways which are expected to generate equal amounts of S/R. However, it is worth recalling that COX enzymes can generate 15(R)-HETE-PL, and therefore it is possible that both COX and 15-LOX were actively synthesizing 15-HETE-PL, leading to only a modest predominance of S/R stereoisomers in the chiral analysis. Finally, a study on LA-derived eoxPL by Kühn et al suggests early involvement of 15-LOX in atherosclerotic plaques, which could be a reason why carotid samples, likely contaminated by large amounts of atherosclerotic plaques, had higher levels of 15-HETE-PL compared to other positional isomers[281].

The presence of procoagulant oxPL within the clot architecture may make them a novel therapeutic target with clinical implications on the management of patients with arterial thrombosis. There is emerging clinical evidence that the use of anticoagulants, such as rivaroxaban, carries beneficial effects in ACS and peripheral vascular disease, albeit with a higher risk of bleeding[242]. Genetically modified mice which lack *Alox12* and *Alox15* have been shown to have defective coagulation reactions and form smaller venous clots, suggesting that blocking the formation of HETE-PL may represent an anticoagulant target[69,72]. As of yet, there are no inhibiting agents in use clinically for 12-LOX and 15-LOX, and the inhibitor for 5-LOX, zileuton, has not been shown to carry any clinically significant impact on thrombosis or haemostasis[286,287]. The presence of leukocyte derived 5- or 15-HETE-PL highlights the role

that inflammatory cells other than platelets play in arterial thrombosis, which are not currently targeted in the treatment pathways.

There are a number of limitations that warrant discussion in this chapter. Firstly, the clot 'age' recorded is an estimate that relies on the onset of clinical symptoms and their detection by the clinical team. This may be prone to inaccuracies due to the 'silent' nature of some plaque ruptures. Secondly, the clot retrieval procedure varies between the three groups and may also vary by operator preference and clinical need, although this should not impact on the integrity of the clot. Finally, there will inevitably be some degree of non-enzymatic oxidation taking place both in-situ as part of free radical generation and ex-vivo as part of processing. However, when non-enzymatic oxidation takes place in isolation, the ratio of the HETE-PL positional isomers to each other is expected to be equivalent within samples. This is not the case with the analysed samples where variations in HETE-PL isomer amounts are observed within samples (**Figure 4.4**), suggesting a likely enzymatic involvement in their generation.

4.4 CONCLUSION

In conclusion, this chapter demonstrates the presence of procoagulant HETE-PL in arterial thrombi formed on disrupted plaque under shear stress. 12-HETE-PL is present at higher amounts than other positional isomers and is the main driver of difference between clot samples. As confirmed by a chiral analysis, the most likely source of 12-HETE-PL is platelets which are recognized as the main drivers of arterial thrombosis. The presence of 15-HETE-PL may indicate the involvement of cells other than platelets, particularly eosinophils, in the formation of arterial thrombi. The association of procoagulant HETE-PL with arterial thrombosis may present these lipids as future targets for the development of novel antithrombotic agents.

CHAPTER 5 DETERMINING THE ABILITY OF PLATELET, LEUKOCYTE AND EV MEMBRANES TO SUPPORT COAGULATION REACTIONS IN AN ARTERIAL THROMBOSIS COHORT.

5.1 INTRODUCTION

Patients suffering from ACS have higher levels of prothrombin fragments, thrombin:anti-thrombin complexes (TATs) and fibrin degradation products (FDP) compared to healthy controls[288]. This suggests a higher level of coagulation activity and more thrombin generation in patients with ACS. The process of thrombin generation requires activation of the prothrombinase complex (FXa:FVa) on a procoagulant PL surface[90]. Nevertheless, the contribution of the platelet, leukocyte and EV PL membranes to the procoagulant potential in ACS is unknown.

The aim of this chapter is to determine the procoagulant potential of PL membranes of platelets, leukocytes and EV in patients with acute coronary syndrome compared to healthy controls. To study this, I will utilise a clinical cohort of patients with ACS, CAD, RF and HC as described in Materials and Methods (section **2.4**) to study thrombin generation, and in later chapters carry out a lipidomic analysis and correlation. The hypothesis is that patients with ACS have altered procoagulant membranes on the surface of circulating membranes compared to healthy controls.

Here, I will use a prothrombinase assay that measures the ability of platelet, leukocyte and EV membranes to generate thrombin independent of plasma coagulation factors/inhibitors and importantly free of the influence of TF expression. This will be achieved by utilising and adapting previously described chromogenic prothrombinase assays (section **2.9**)[289-291]. The principle of the assay is to provide a standard mixture of purified FXa, FVa, FII and calcium which in the presence of a PL surface can generate thrombin. The only variable in the assay would therefore be the PL surface presented by platelets, leukocytes or EV. The assay will be

calibrated with a standard curve of human thrombin and optimised to detect thrombin amounts between 3 nM to 400 nM.

5.2 RESULTS

5.2.1 Participant baseline characteristics ('Clinical cohort')

Ninety participants were recruited to this study over a period of 12 months, consisting of 24 healthy controls (HC), 23 risk-factor matched (RF), 19 significant coronary artery disease (CAD) and 24 ACS patients. The mean age for all participants was 63.88 ± 9.63 years with a higher proportion of males than females (65.5%), but no significant difference between groups in age or gender. With the exception of healthy controls, patients had one or more risk factor for cardiovascular disease and were frequently medicated on a combination of anti-platelet and anti-coagulant therapy. Baseline clinical characteristics of participants including their vascular comorbidities as defined by the study protocol are shown in **Table 5.1**.

Patients with ACS had significantly higher leukocyte counts compared to RF and CAD control groups, which appear to be primarily due to higher neutrophil counts ($p<0.05$). All ACS patients received aspirin, a P2Y12 inhibitor (clopidogrel, prasugrel or ticagrelor) and an anticoagulant (fondaparinux or low molecular weight heparin). There were no differences in baseline cardiovascular risk factors and statin prescription between RF, CAD and ACS groups (**Table 5.1**).

Table 5.1. Baseline clinical characteristics of patients recruited in the clinical cohort. (WCC: white cell count, RBC: red blood cell count, P2Y12 inhibitors: clopidogrel, prasugrel or ticagrelor, CKD: chronic kidney disease, SD: standard deviation, p-value tests: Fisher exact (categorical) or Kruskal-Wallis (continuous), p-value comparators: all clinical groups (age, gender) or all except HC for other variables)

Variable	Healthy control (HC) (n=24)	Risk-factor matched (RF) (n=23)	Significant coronary artery disease (CAD) (n=19)	Acute coronary syndrome (ACS) (n=24)	p
Age, Mean ± SD	64.92 ± 10.79	61.43 ± 8.16	64.53 ± 9.65	64.67 ± 9.88	0.473
Male Gender (%)	14 (58.3)	12 (52.2)	16 (84.2)	17 (70.8)	0.133
Creatinine μmol/L, Mean ± SD	-	77.57 ± 12.60	88.39 ± 31.95	84.79 ± 18.64	0.318
Haemoglobin g/dL, Mean ± SD	-	146.04 ± 13.03	138.24 ± 17.95	144.46 ± 18.88	0.380
Platelets x 10^9/L, Mean ± SD	-	250.26 ± 44.01	261.94 ± 56.08	271.50 ± 82.72	0.869
WCC x 10^9/L, Mean ± SD	-	6.96 ± 1.57	7.92 ± 1.92	9.28 ± 2.90	0.011
Neutrophils	-	4.33 ± 1.17	5.02 ± 1.32	6.51 ± 2.49	0.003
Eosinophils	-	0.19 ± 0.09	0.25 ± 0.12	0.11 ± 0.08	<0.001
Basophils	-	0.02 ± 0.04	0.03 ± 0.05	0.00 ± 0.02	0.098
Lymphocytes	-	1.82 ± 0.68	1.89 ± 0.70	1.85 ± 0.71	0.818
Monocytes	-	0.57 ± 0.19	0.68 ± 0.21	0.73 ± 0.32	0.150
RBC x 10^{12}/L, Mean ± SD	-	4.80 ± 0.42	4.14 ± 1.26	4.64 ± 0.54	0.090
Aspirin use (%)	0 (0)	20 (87)	14 (73.7)	24 (100)	0.017
P2Y12 inhibitor use (%)	0 (0)	3 (13)	6 (31.6)	24 (100)	<0.001
Anticoagulant use (%)	0 (0)	3 (13)	0 (0)	24 (100)	-
Statin use (%)	0 (0)	15 (65.2)	15 (78.9)	19 (79.2)	0.532
Hypertension (%)	0 (0)	13 (56.5)	13 (68.4)	11 (45.8)	0.350
Diabetes (%)	0 (0)	7 (30.4)	3 (15.8)	6 (25)	0.554
Smoker (%)	0 (0)	7 (30.4)	9 (47.4)	13 (54.2)	0.244
CKD (%)	0 (0)	0 (0)	3 (15.8)	3 (12.5)	-

5.2.2 Prothrombinase activity is higher on the surface of leukocytes and plasma EV, but not platelets, in ACS patients compared to HC

To test for differences between groups in the procoagulant ability of platelet, leukocyte and plasma EV membranes, I used the prothrombinase assay described in Materials and Methods. This demonstrated that there were no significant differences in the ability of platelets from patients with ACS to support thrombin generation compared to HC (**Figure 5.1**). In leukocytes, there were significantly higher levels of thrombin generated in the ACS group compared with HC (**Figure 5.2**). In plasma EV, there were significantly higher levels of thrombin generated in ACS, CAD and RF compared to HC (**Figure 5.3**).

These findings demonstrate that the ability of leukocyte and EV membranes to support thrombin generation in ACS was higher than HC, whereas platelets did not demonstrate any differences between groups.

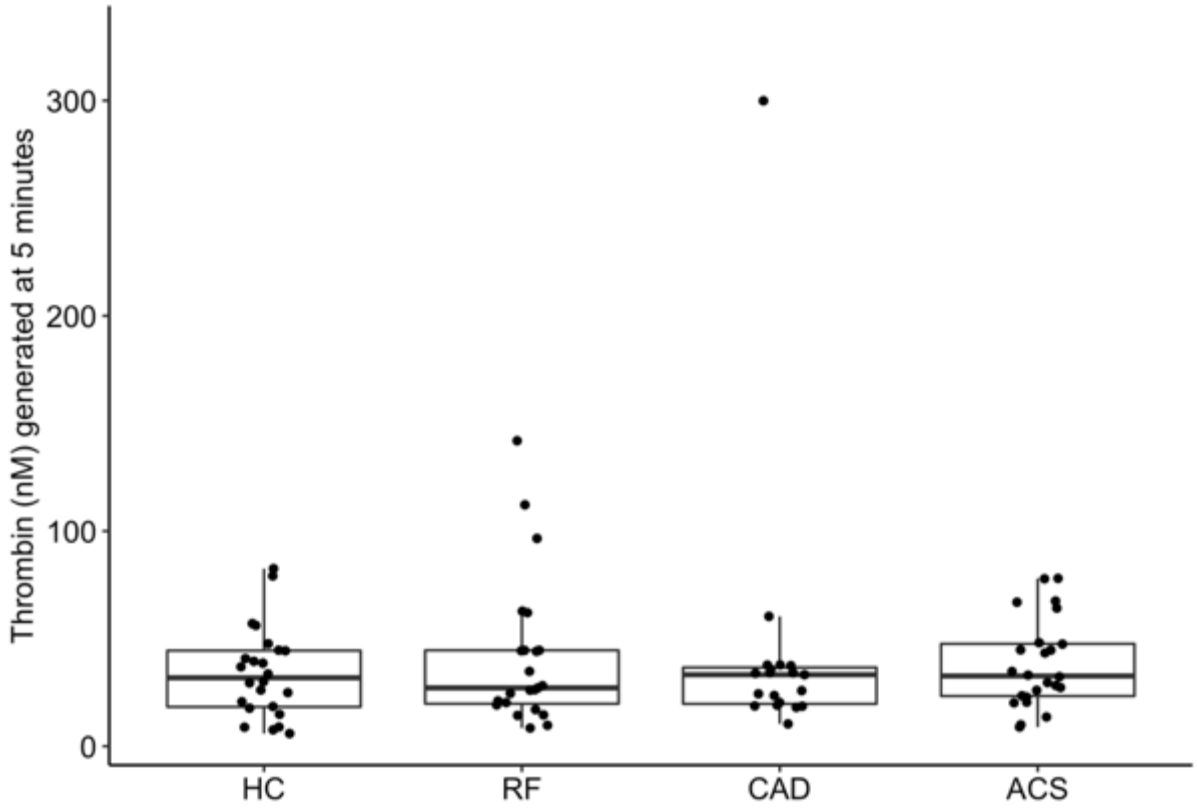

Figure 5.1. No difference in the amount of thrombin generated on the surface of platelets between groups.

The ability of platelet membranes to support thrombin generation was assessed using the prothrombinase assay as in Materials and Methods. Data was plotted as a box plot with the ggplot2 R package. Box edges indicate the interquartile range (IQR) with the median line inside the box. Whiskers indicate 1.5 times the IQR. Statistical significance was tested with Mann-Whitney-Wilcoxon test (*: $p < 0.05$, **: $p < 0.01$, ***: $p < 0.001$). ACS: acute coronary syndrome (n=24), CAD: coronary artery disease but no ACS (n=19), RF: Risk factors with no significant coronary artery disease (n=23), HC: Healthy control (n=24).

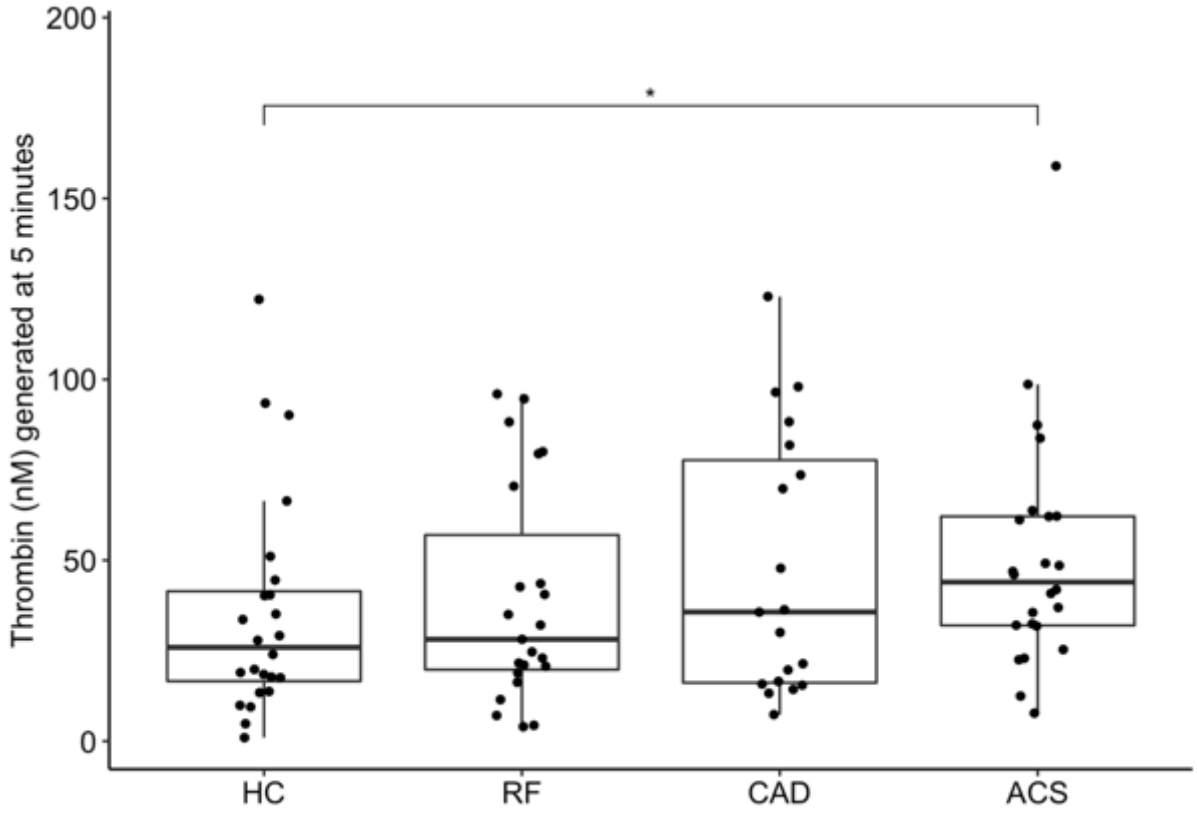

Figure 5.2. Higher amounts of thrombin generated on the surface of leukocytes from patients with ACS compared with HC.

The ability of leukocyte membranes to support coagulation reactions was assessed using the prothrombinase assay as in Materials and Methods. Data was plotted as a box plot with the ggplot2 R package. Box edges indicate the interquartile range (IQR) with the median line inside the box. Whiskers indicate 1.5 times the IQR. Statistical significance was tested with Mann-Whitney-Wilcoxon test (*: $p < 0.05$, **: $p < 0.01$, ***: $p < 0.001$). ACS: acute coronary syndrome (n=24), CAD: coronary artery disease but no ACS (n=19), RF: Risk factors with no significant coronary artery disease (n=23), HC: Healthy control (n=24).

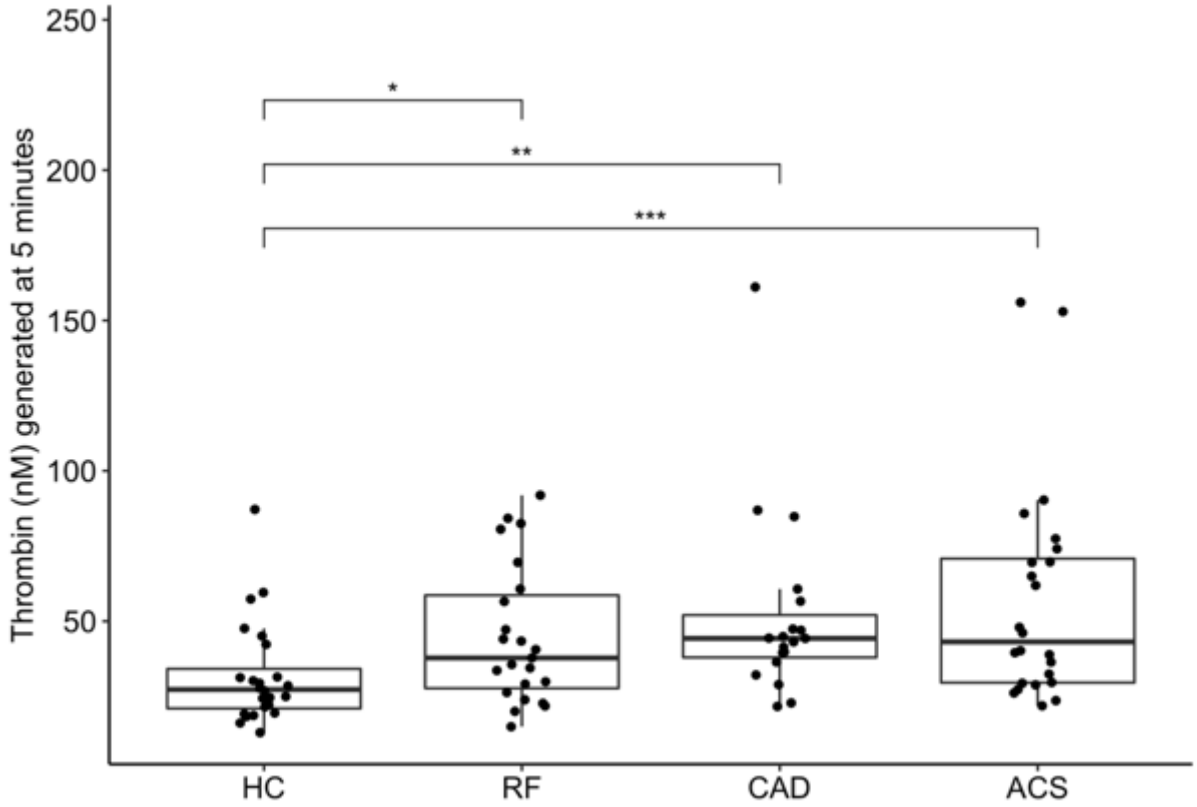

Figure 5.3. EV from patients with RF, CAD and ACS support more thrombin generation on their surface compared with HC.

The ability of EV membranes to support coagulation reactions was assessed using the prothrombinase assay as in Materials and Methods. Data was plotted as a box plot with the ggplot2 R package. Box edges indicate the interquartile range (IQR) with the median line inside the box. Whiskers indicate 1.5 times the IQR. Statistical significance was tested with Mann-Whitney-Wilcoxon test (*: $p < 0.05$, **: $p < 0.01$, ***: $p < 0.001$). ACS: acute coronary syndrome (n=24), CAD: coronary artery disease but no ACS (n=19), RF: Risk factors with no significant coronary artery disease (n=23), HC: Healthy control (n=24).

5.2.3 Significantly higher EV counts in CAD patients compared with HC, with an upward trend in RF and ACS patients

In order to quantify EV particles in plasma, samples taken from all participants underwent SEC/NTA quantification by a collaborator (Dr Keith Allen-Redpath) as described in Materials and Methods. This demonstrated significantly higher EV counts in CAD, and an increasing trend in RF and ACS patients, compared with HC (**Figure 5.4**). Furthermore, the size of EV particles (diameter) demonstrated significantly smaller particles in EV samples from CAD patients, and a downward trend in RF and ACS patients, compared with HC (**Figure 5.5**).

Coagulation reactions take place on the external surface of PL membranes, and therefore clotting factor enzyme kinetics may be affected by surface area. Therefore, I calculated the EV total surface area by combining the two parameters (count and size) using the surface area formula for a sphere:

$$EV\ total\ surface\ area\ =\ EV\ count\ \times\ EV\ surface\ area\ (4\pi r^2)$$

This demonstrated significantly larger total EV surface area in CAD patients, and an upward trend in RF and ACS patients, compared with HC (**Figure 5.6**).

Together, these data demonstrate that RF, CAD and ACS patients have a higher EV count and surface area compared with HC.

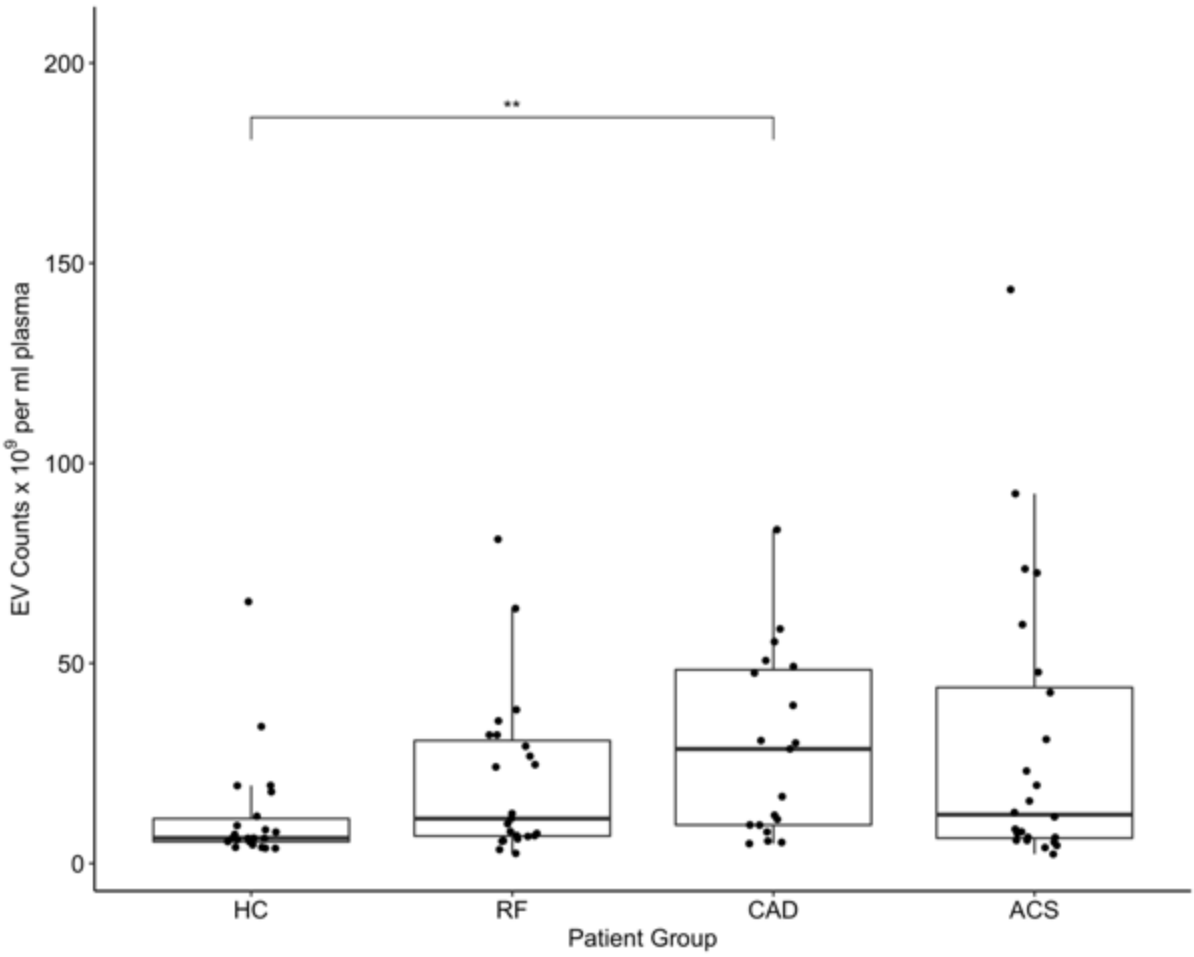

Figure 5.4. Significantly higher EV counts in CAD patients, and an upward trend in RF and ACS patients, compared with healthy controls.

Platelet-free plasma (0.5 ml) from each participant was processed through size exclusion chromatography (iZON qEV columns) and nanoparticle tracking analysis (Nanosight 300), as in Materials and Methods. This assessed the size distribution and concentrations of EV particles. Data was plotted as a box plot with the ggplot2 R package. Box edges indicate the interquartile range (IQR) with the median line inside the box. Whiskers indicate 1.5 times the IQR. Statistical significance was tested with Mann-Whitney-Wilcoxon test (*: $p < 0.05$, **: $p < 0.01$, ***: $p < 0.001$). ACS: acute coronary syndrome (n=24), CAD: coronary artery disease but no ACS (n=19), RF: Risk factors with no significant coronary artery disease (n=23), HC: Healthy control (n=24).

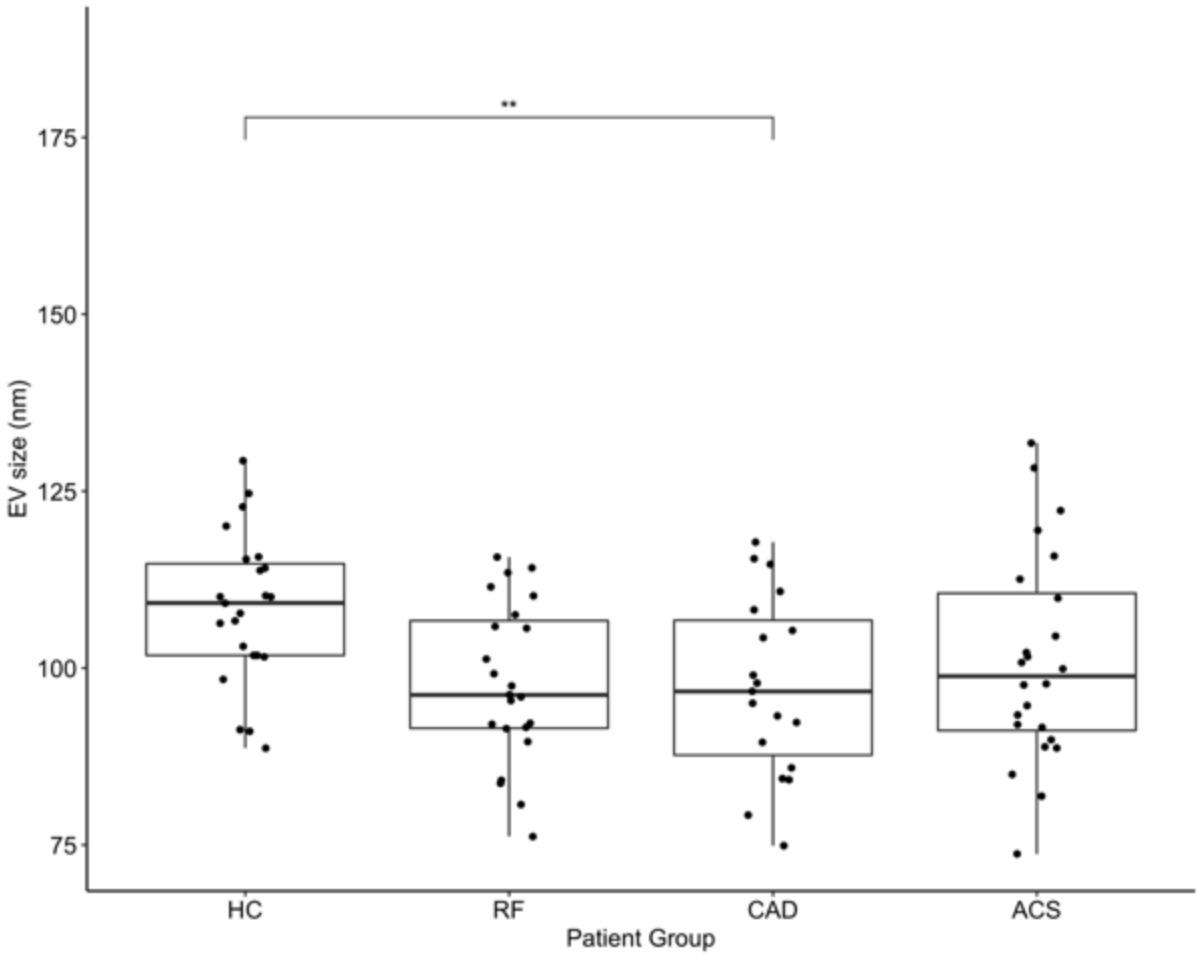

Figure 5.5. Significantly smaller EV particles (diameter) in CAD patients, and a downward trend in RF and ACS patients, compared with healthy controls.

Platelet-free plasma (0.5 ml) from each participant was processed through size exclusion chromatography (iZON qEV columns) and nanoparticle tracking analysis (Nanosight 300), as in Materials and Methods. This assessed the size distribution and concentrations of EV particles. Data was plotted as a box plot with the ggplot2 R package. Box edges indicate the interquartile range (IQR) with the median line inside the box. Whiskers indicate 1.5 times the IQR. Statistical significance was tested with Mann-Whitney-Wilcoxon test (*: $p < 0.05$, **: $p < 0.01$, ***: $p < 0.001$). ACS: acute coronary syndrome (n=24), CAD: coronary artery disease but no ACS (n=19), RF: Risk factors with no significant coronary artery disease (n=23), HC: Healthy control (n=24).

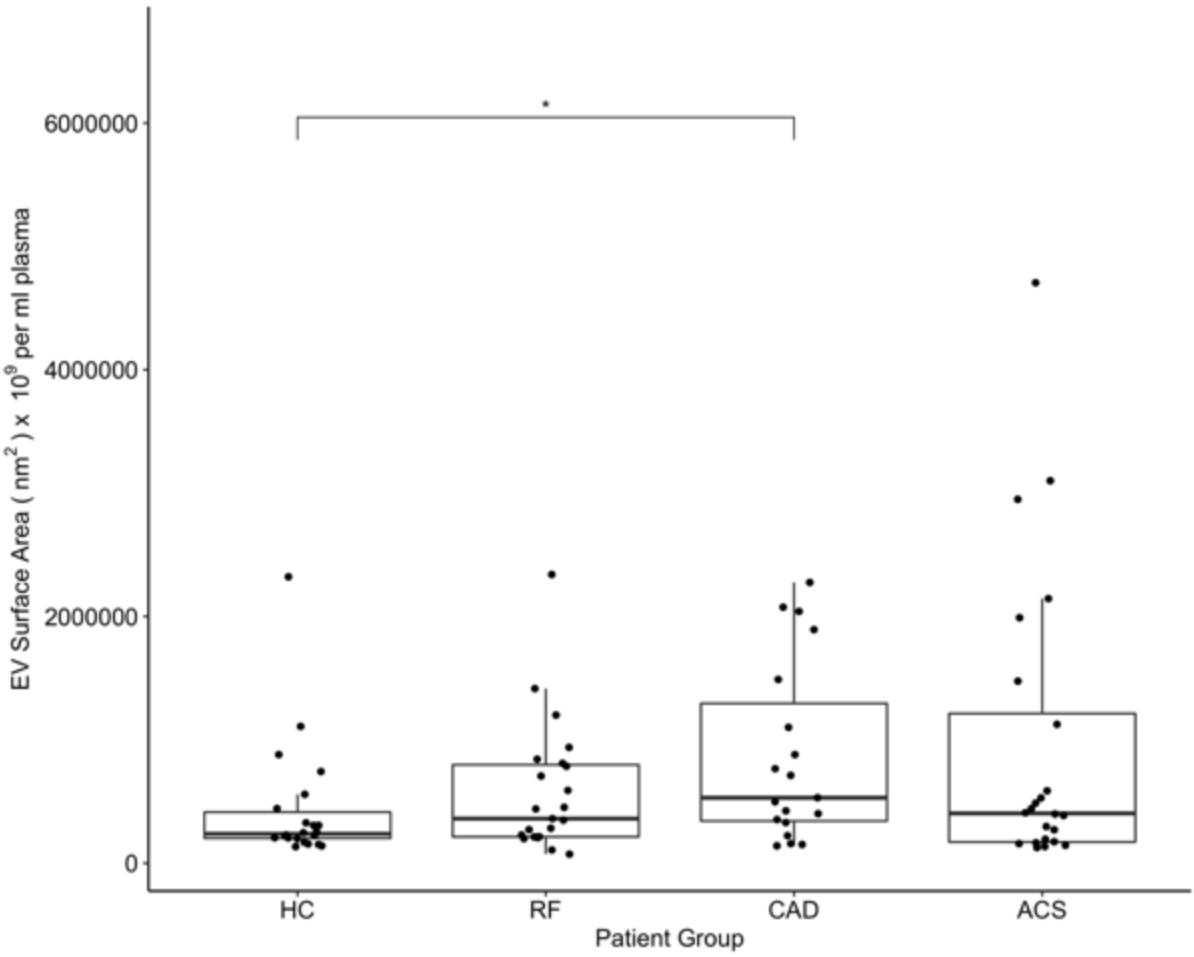

Figure 5.6. Significantly higher EV surface area in CAD patients, with an upward trend in RF and ACS patients, compared with healthy controls.

Platelet-free plasma (0.5 ml) from each participant was processed through size exclusion chromatography (iZON qEV columns) and nanoparticle tracking analysis (Nanosight 300), as in Materials and Methods. This assessed the size distribution and concentrations of EV particles. Surface area was calculated by multiplying count x sphere surface area ($4\pi r^2$). Data was plotted as a box plot with the ggplot2 R package. Box edges indicate the interquartile range (IQR) with the median line inside the box. Whiskers indicate 1.5 times the IQR. Statistical significance was tested with Mann-Whitney-Wilcoxon test (*: $p < 0.05$, **: $p < 0.01$, ***: $p < 0.001$). ACS: acute coronary syndrome (n=24), CAD: coronary artery disease but no ACS (n=19), RF: Risk factors with no significant coronary artery disease (n=23), HC: Healthy control (n=24).

5.2.4 Thrombin generation positively correlates with EV counts

In the previous section (**5.2.3**), I demonstrated that EV counts and surface area were higher in disease states compared to healthy controls. To investigate whether these physical differences influence coagulation activity on the surface of EV particles, I adjusted the thrombin generation data obtained from EV samples, and presented previously in section **5.2.2**, by EV count and total surface area.

After adjusting by EV count, the thrombin generation amounts were no longer different between clinical groups (**Figure 5.7**). The same applies following adjustment by EV surface area, where the previously observed differences in thrombin generation were no longer evident (**Figure 5.8**). This suggests that the higher thrombin generation in RF, CAD and ACS compared with HC is likely related to the higher EV counts. To test this, a correlation analysis was carried out, as seen in **Figure 5.9**, demonstrating a significant positive correlation between EV count and thrombin generation ($p<0.01$). Similarly, there was a significant positive correlation between EV surface area and thrombin generation ($p<0.001$), seen in **Figure 5.10**. Together therefore, it is likely that the higher thrombin generation observed in RF/CAD/ACS is a consequence of higher EV numbers and/or the higher amount of EV surface area in these groups compared with HC.

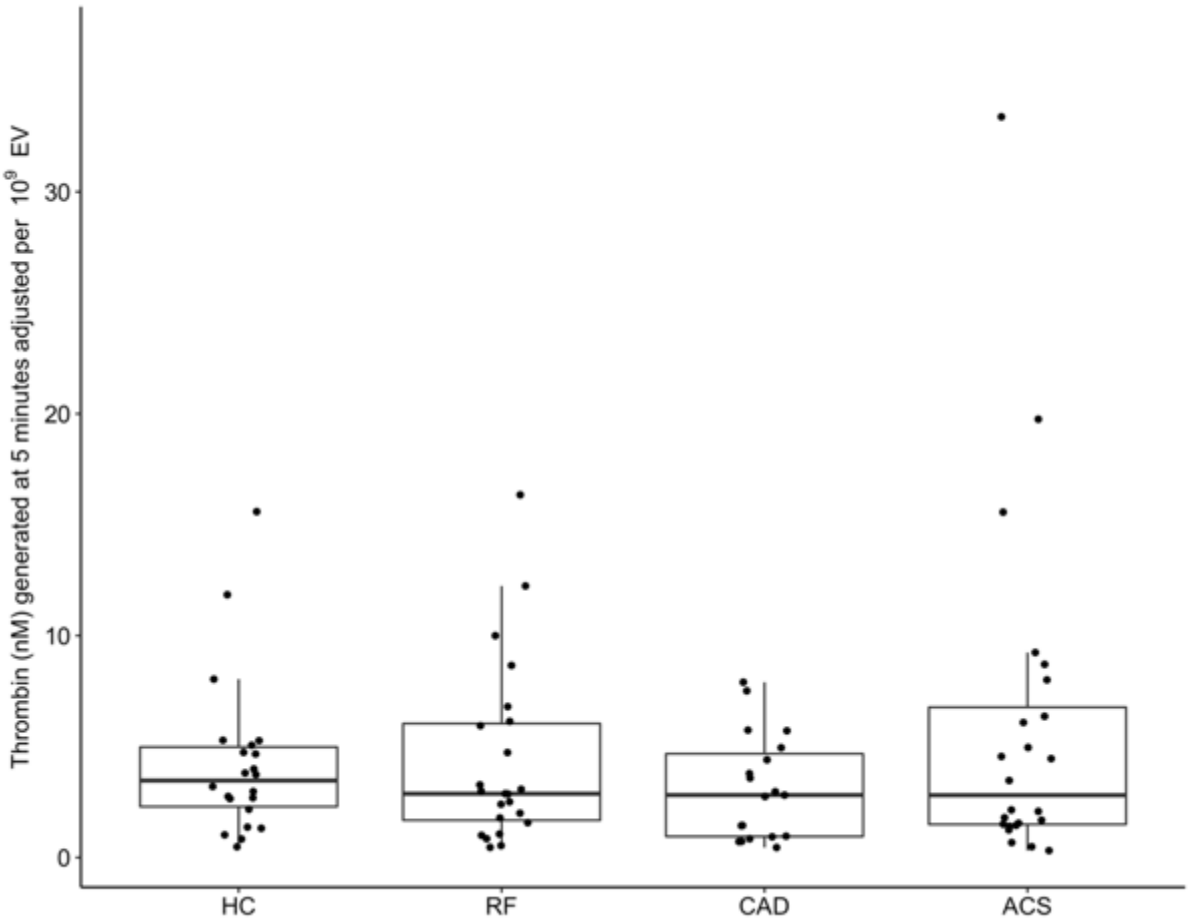

Figure 5.7. After adjusting for EV counts, thrombin generation was similar across clinical groups.

The ability of EV membranes to support coagulation reactions was assessed using the prothrombinase assay as in Materials and Methods. This was then adjusted by EV counts and normalised to 1 x 10^9 EV particles. Data was plotted as a box plot with the ggplot2 R package. Box edges indicate the interquartile range (IQR) with the median line inside the box. Whiskers indicate 1.5 times the IQR. Statistical significance was tested with Mann-Whitney-Wilcoxon test, and where significant differences exist, they are indicated by stars (*: $p < 0.05$, **: $p < 0.01$, ***: $p < 0.001$). ACS: acute coronary syndrome (n=24), CAD: coronary artery disease but no ACS (n=19), RF: Risk factors with no significant coronary artery disease (n=23), HC: Healthy control (n=24).

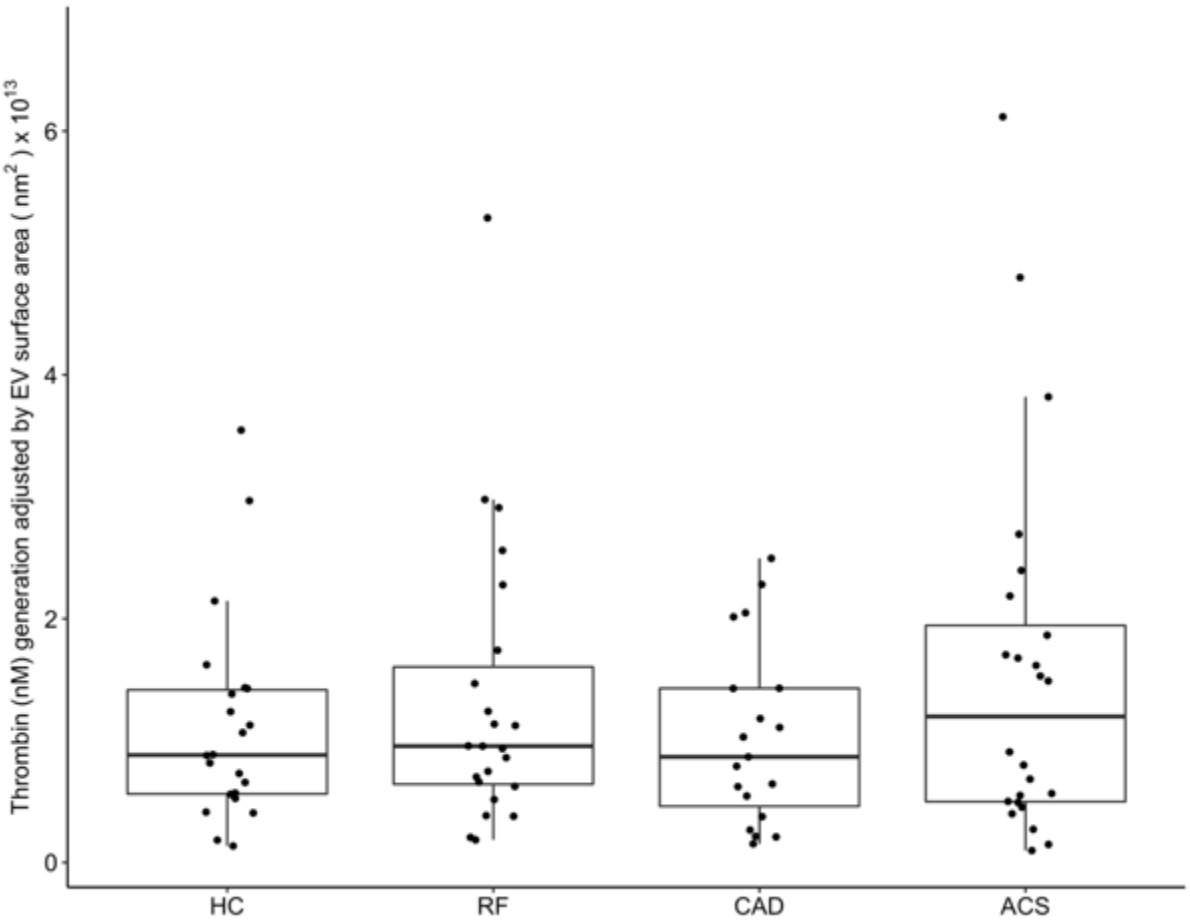

Figure 5.8. After adjusting for EV surface area, thrombin generation was similar across clinical groups.

The ability of EV membranes to support coagulation reactions was assessed using the prothrombinase assay as in Materials and Methods. This was then adjusted by EV counts and normalised to 1 x 10^9 EV particles. Data was plotted as a box plot with the ggplot2 R package. Box edges indicate the interquartile range (IQR) with the median line inside the box. Whiskers indicate 1.5 times the IQR. Statistical significance was tested with Mann-Whitney-Wilcoxon test, and where significant differences exist, they are indicated by stars (*: $p < 0.05$, **: $p < 0.01$, ***: $p < 0.001$). ACS: acute coronary syndrome (n=24), CAD: coronary artery disease but no ACS (n=19), RF: Risk factors with no significant coronary artery disease (n=23), HC: Healthy control (n=24).

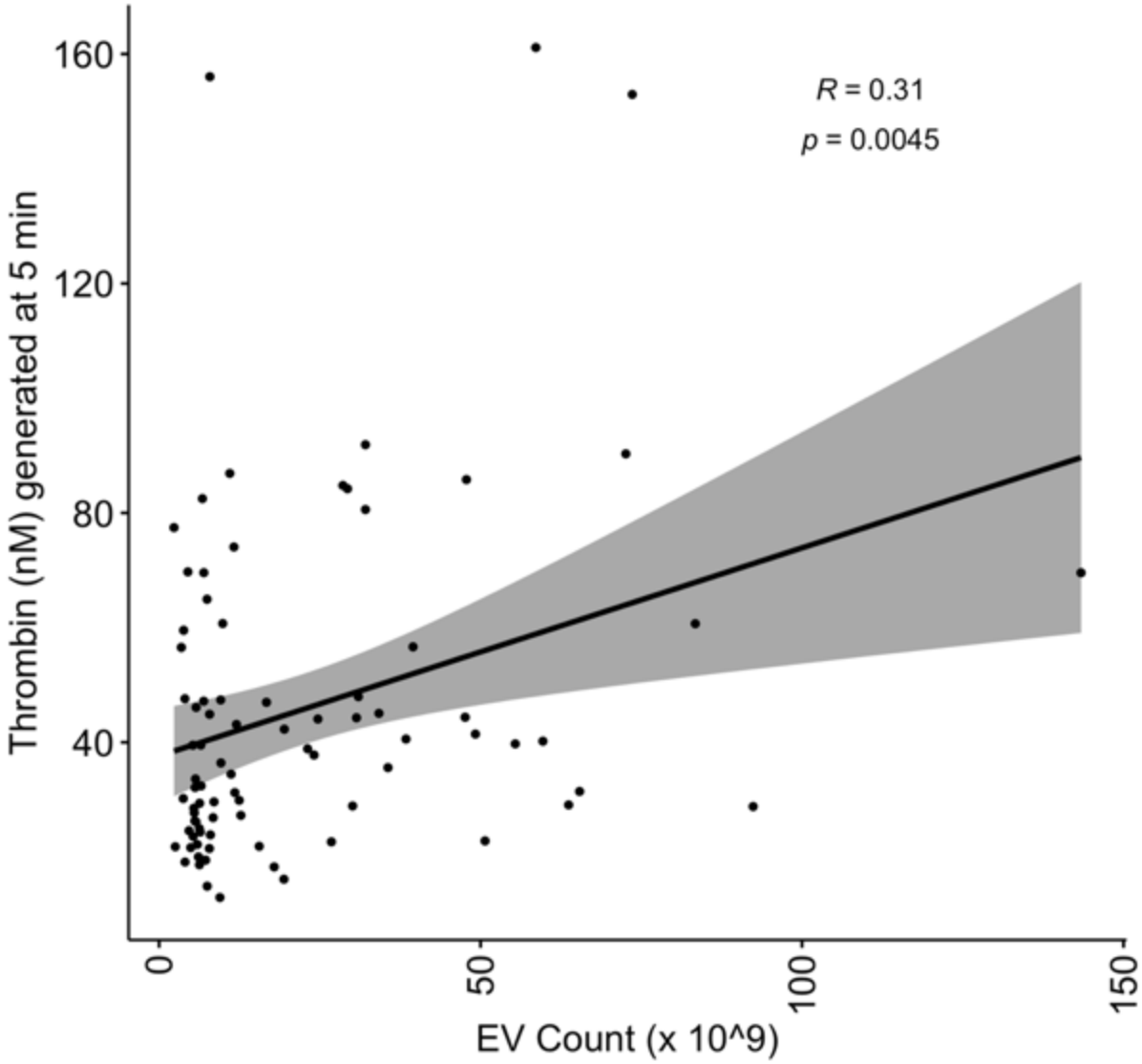

Figure 5.9. Thrombin generation on the EV membrane surface correlates positively with EV counts.

A correlation analysis of plasma EV count with thrombin generation on the surface of plasma EV is shown in this diagram. The correlated data was generated from the prothrombinase assay and EV quantification for all patients (as in Materials and Methods), Pearson's R correlation coefficients and significance was calculated and graphs plotted with the ggplot2 R package.

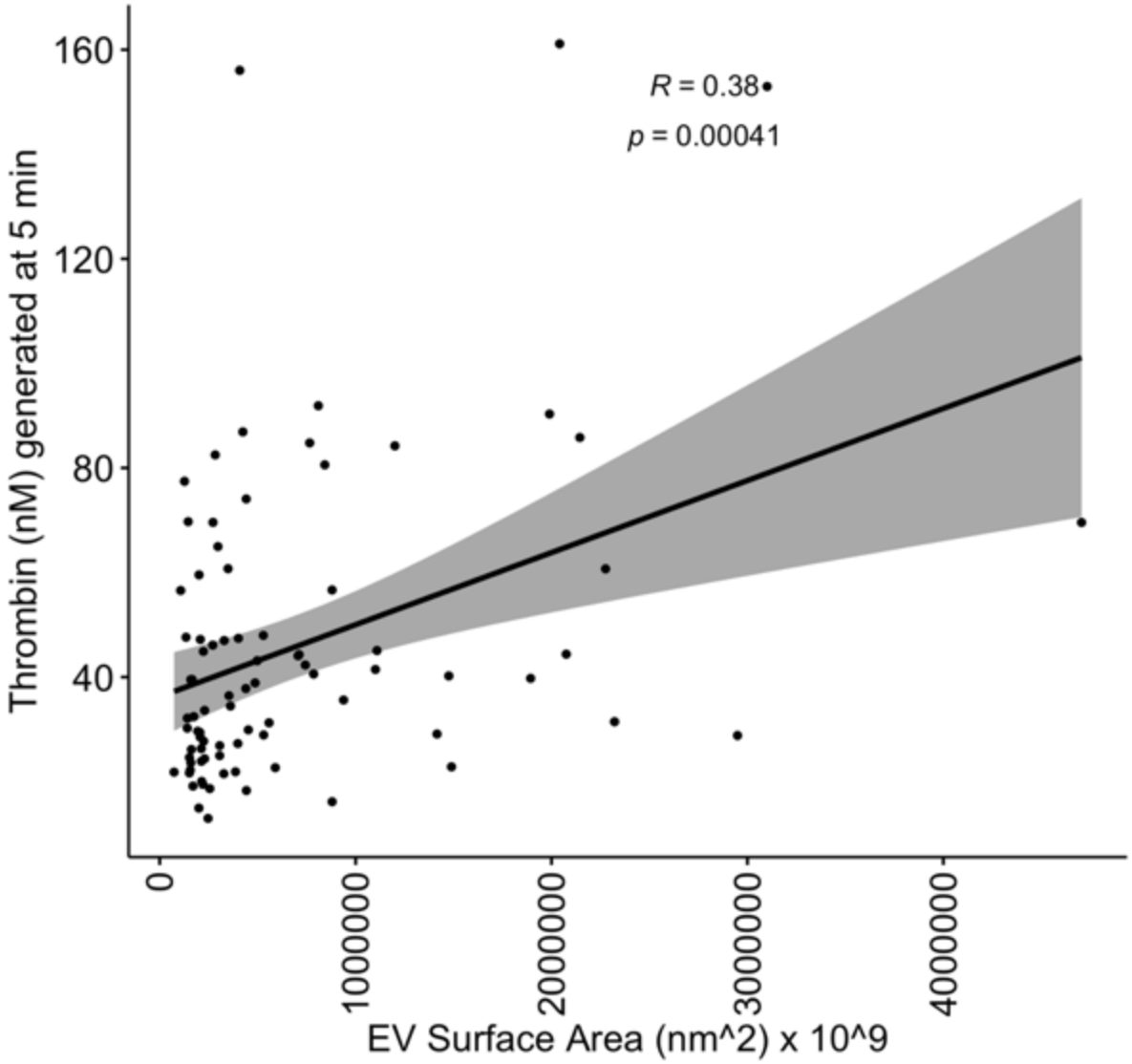

Figure 5.10. Thrombin generation on the surface of EV correlates positively with EV surface area.

A correlation analysis of plasma EV count with thrombin generation on the surface of plasma EV is shown in this diagram. The correlated data was generated from the prothrombinase assay and EV quantification for all patients (as in Materials and Methods), Pearson's R correlation coefficients and significance was calculated and graphs plotted with the ggplot2 R package.

5.3 DISCUSSION

The results presented in this chapter demonstrate that the surface of leukocytes and EV, but not platelets, in patients with ACS supports more thrombin generation compared with healthy controls. This suggests that the procoagulant membrane potential of leukocytes and plasma EV is greater in ACS, and presents a possible explanation for the previously reported higher activity of the coagulation system in this patient group[288]. Importantly, these findings highlight the PL membranes of leukocytes and EV as possible players which contribute to prothrombotic reactions in ACS.

Thrombin plays a critical role in inflammatory and thrombotic reactions with evidence of higher thrombin turnover in ACS and a therapeutic benefit in blocking its formation[292,293].The higher amount of thrombin generated on circulating membranes in ACS compared to HC may contribute to the increased coagulation activity in this condition and could represent a potential therapeutic target independent of coagulation factors or platelet activity, where current therapies lie. Here, I measured thrombin generation independently of TF expression or plasma modulators of coagulation (**Figure 2.4**). This is particularly relevant since TF expression is higher in patients with ACS on the surface of circulating monocytes and leukocyte-platelet aggregates[294,295]. In addition, patients with ACS have high levels of TF^+ EV in the circulation compared with healthy controls[296]. Consequently, studying thrombin generation in plasma from ACS patients using the Thrombinoscope™ assay[297] will likely be confounded by the presence of TF^+ EV which would augment thrombin generation through the extrinsic pathway. Overall, my data suggest that leukocyte and EV membranes may play a procoagulant role in ACS independently of TF or plasma.

There was a significantly higher amount of thrombin generation on the surface of leukocytes (per 8 x 10^4 cells) in patients with ACS compared with HC (**Figure 5.2**). This may be related to the reported increase in leukocyte activation as part of a systemic inflammatory response in ACS[298]. In fact, cardiovascular risk factors have also been shown to be individually associated with low grade inflammation, a process responsible for atherosclerosis, with evidence of leukocyte activation[299-304]. This could explain the significantly higher thrombin generation on the leukocyte surface in ACS patients, and the upward trend in RF/CAD, compared with HC (**Figure 5.2**). The mechanism for this however is not clear and may relate to difference in the procoagulant lipidome which will be examined in subsequent chapters. In addition, I observed higher total leukocyte counts, driven by neutrophils, in ACS patients compared with HC (**Table 5.1**). This is consistent with the literature where acute inflammation in ACS patients mobilizes neutrophils and predict poor outcomes[305,306]. In fact, it is known that higher total leukocyte counts, even when in the normal range, can predict future cardiovascular events in a healthy cohort[307]. When this higher leukocyte count in ACS is combined with the higher thrombin generation observed in **Figure 5.2**, it may suggest higher overall leukocyte procoagulant activity *in vivo*, however this remains untested.

EV are released into the circulation by activated or apoptotic cells, including leukocytes, platelets, erythrocytes, and endothelial cells[98,308]. Additionally, apoptotic cells within plaques can also generate EV, which enter the circulation following plaque rupture in ACS and may contribute to the thrombotic reactions via TF and PS expression[232,309-311]. Indeed, to explain the procoagulant properties in EV, the initial emphasis in the literature has been on TF positivity[98]. Earlier studies suggested that the presence of TF on the surface of EV, detected within thrombi, was the principal driver for procoagulant activity[99]. Whilst this may be true for monocyte-

derived EV which contain both TF and PS, it does not explain the procoagulant potential of platelet-derived EV which account for >25% of the procoagulant activity in blood and do not contain TF[206,312,313]. Despite initial reports of the ability of platelets to generate TF[314], the current literature refutes this and therefore it is likely that the main supporter for propagation of procoagulant reactions on the surface of platelet-derived EV is PS[313,315]. Such reactions are determined by the amount of EV generated by platelets, with a dose-dependent effect on thrombin generation *in vitro*[316]. Furthermore, in experiments that investigated thrombin generation on the surface of plasma EV using a fluorogenic substrate, addition of Annexin V to block PS had a more pronounced effect compared to the use of TF inhibitors[317]. Overall, this suggests that PS is a key facilitator for the propagation of coagulation reactions on the surface of EV.

Whilst a number of assays were developed to investigate the TF-driven procoagulant activity of EV, only a limited few are available to study the aPL contribution in isolation. The commercial assay Zymuphen™ MP Activity assay (Hyphen BioMed, France) measures the level of PS in the EV population using an ELISA-based kit coated with annexin V-streptavidin and incubated with FVa, FXa and FII to from the prothrombinase complex on the surface of isolated EV[318]. This is then quantified with a chromogenic prothrombinase substrate and values expressed as PS equivalents against a standard curve of lyophilized EV. Whilst this assay claims to quantify amount of PS using a standard curve, it does not account for physiological contribution of a biological membrane to thrombin generation. Another assay, called the STA®-Procoag-PPL (Stago, UK), measures EV procoagulant activity by mixing equal amounts of test plasma (containing EV) and phospholipid-free porcine plasma[319]. This mixture is then supplemented with FXa and clotting time is compared against a standard curve of synthetic phospholipids. The introduction of plasma, which contains natural or iatrogenic

inhibitors of coagulation, may interfere with the accuracy of the assay and forms a major limitation to studying procoagulant membrane properties. By using the assay employed in this chapter, I minimized the influence of plasma, calibrated the assay to a direct measure of human thrombin and measured TF-independent thrombin generation. Therefore, my approach was more tailored towards studying membrane procoagulant potentials than the alternatives.

EV numbers are known to be higher in people at elevated cardiovascular risk (hypertension, diabetes, chronic kidney disease, smoking) and in ACS[224,320-323]. This is in agreement with my results which show higher EV counts in RF, CAD and ACS patients compared with HC (**Figure 5.4**). This may explain the higher thrombin generation on the surface of EV seen in the patient groups compared to HC (**Figure 5.3**). In fact, once thrombin generation was adjusted by EV counts (**Figure 5.7**) and surface area (**Figure 5.8**), there were no longer any differences between groups. Taking this a step further, the findings of this chapter demonstrated a positive correlation between thrombin generation and EV count (**Figure 5.9**) and surface area (**Figure 5.10**). This suggests that the previously reported procoagulant phenotype in CAD/ACS patients may result from higher EV counts in CAD/ACS demonstrated in this study and others[224,288,320-323]. This may be a consequence of having more aPL circulating in the plasma which may facilitate thrombin generation reactions on the EV surface independently of TF. Finally, attempts to develop pharmacological inhibitors of EV generation have been limited to *in-vitro* and small pre-clinical studies[324]. If such agents enter clinical practice, they may serve as potential therapeutic agents to reduce the EV-mediated procoagulant phenotype seen in CAD/ACS.

5.4 CONCLUSION

In conclusion, I found higher amounts of thrombin generated on the surface of leukocytes and EV, but not platelets, from patients with ACS compared to healthy controls. This may be a possible contributor for the observed higher activity of the coagulation system in this patient group. The findings also highlight leukocytes and EV as possible players in driving prothrombotic reactions in ACS by virtue of the contribution of their procoagulant membranes.

Whilst it is not possible to determine whether the increased membrane procoagulant ability on the surface of leukocytes and plasma EV is a cause or a consequence of acute plaque rupture, the findings in this chapter could provide an explanation for the sustained increase in thrombin formation in ACS[288]. The underlying mechanism for this may relate to the aPL and eoxPL composition of these membranes which will be investigated in the subsequent chapters of this thesis.

CHAPTER 6 CHARACTERISING THE PROCOAGULANT EOXPL COMPOSITION OF PLATELETS, LEUKOCYTES AND EV IN AN ARTERIAL THROMBOSIS COHORT

6.1 INTRODUCTION

Procoagulant eoxPL, namely HETE-PL, are emerging as key players in the process of thrombosis and haemostasis[14]. Whilst a number of recent studies have examined their roles *in vitro*, *in vivo* murine models and in human disease such as anti-phospholipid syndrome, there are no studies to date examining their generation in arterial thrombosis[69,72,81]. The chapter herein addresses this by quantifying HETE-PL in platelets, leukocytes and plasma EV from patients with CAD and ACS.

It was previously shown that HETE-PL enhance PS/PE-dependent coagulation by augmenting the negative charge on the surface of cell membranes, further supporting coagulation reactions to take place in a calcium-dependent manner[69]. These lipids can be generated by innate immune cells through cell-specific LOX isoforms in response to activation by inflammatory ligands[14]. The combination of chronic and acute inflammation in arterial thrombosis leads to activation of immune cells and may contribute to a flux of HETE-PL that is yet to be defined[325-329]. Studying the HETE-PL composition of these cells in thrombo-inflammatory conditions such as arterial thrombosis may provide insight into their potential roles in driving the thrombotic phenotype in these diseases.

In the previous **Chapter 5**, I demonstrated that membrane surfaces of leukocytes and EV in patients with arterial thrombosis supported more thrombin generation in compared with HC. In addition, there's a large body of evidence to suggest sustained activation of the coagulation system in both CAD and ACS, with no clear mechanistic explanation yet. One potential contributor to this is the HETE-PL composition of the cell surface. Indeed, it was evident in **Chapter 4** that HETE-PL are present in clots extracted from patients with arterial thrombosis, suggesting that they may play a role in their formation.

In this chapter, I will compare the HETE-PL levels and species in platelets, leukocytes and plasma EV isolated from patients with arterial thrombosis (CAD and ACS) with controls (HC and RF). My hypothesis is that an altered HETE-PL composition on the surface of platelets, leukocytes and plasma EV is associated with this prothrombotic inflammatory condition.

6.2 RESULTS

6.2.1 The amount of 12-HETE-PL was elevated in thrombin-activated platelets from ACS patients compared with HC

First, I measured HETE-PL lipids in resting and thrombin-activated platelets from the clinical cohort and plotted them on a heatmap to visualise differences between groups (**Figure 6.1**). Thrombin-activated platelets generated higher levels of HETE-PL species than resting platelets, particularly for the platelet specific 12-HETE-PL as previously described (**Figure 6.1**)[40]. There were higher amounts of diacyl forms of 12-HETE-PL (both PC and PE) in thrombin-activated platelets from ACS compared with HC, but no difference in plasmalogens. This finding was examined further in section **6.2.6**.

Hierarchical clustering of the lipids showed grouping by *sn2* fatty acid, with 12-, 11- and 15-HETE-PL forming one cluster, alongside separate clusters of lower abundance for 5-HETE-PL and 8-HETE-PL (**Figure 6.1**). This is consistent with a predominance of 12-LOX and COX-1 derived HETE-PL in platelets.

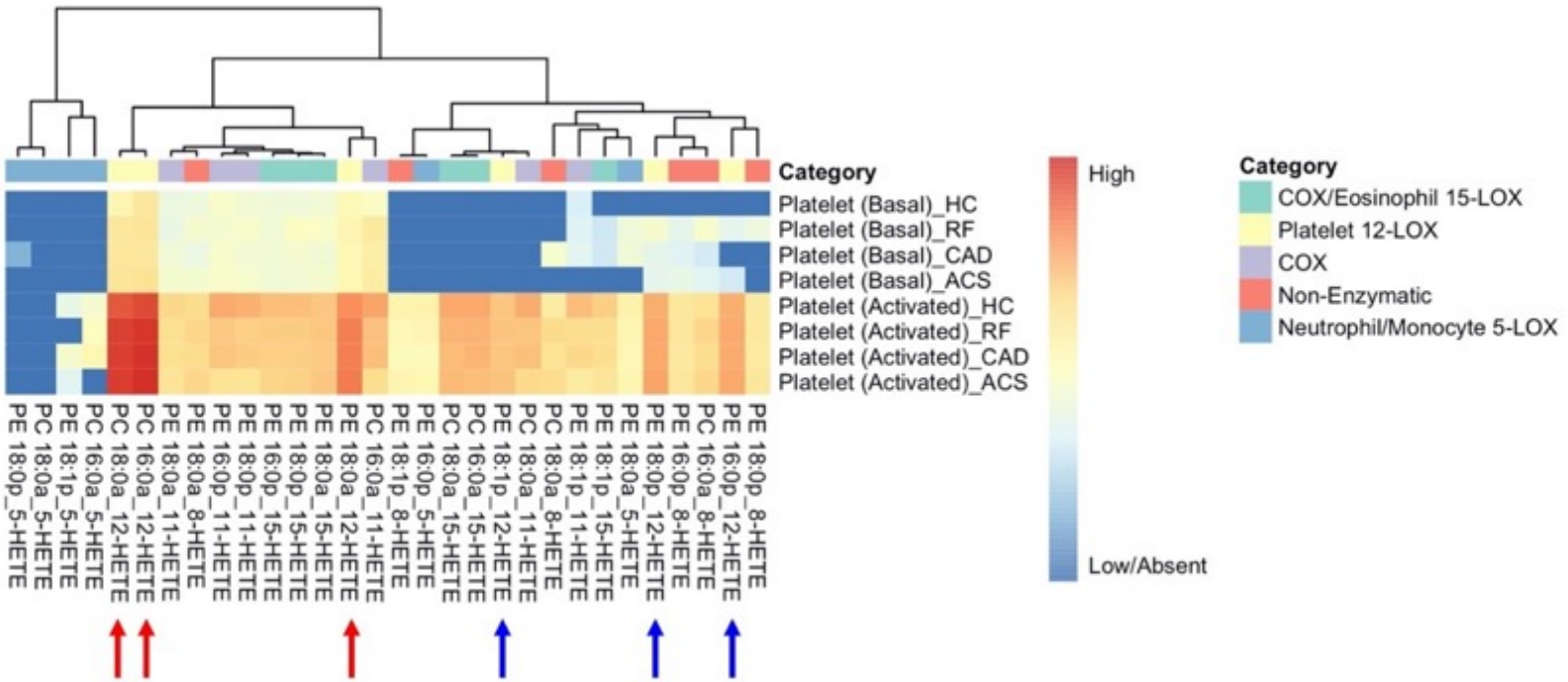

Figure 6.1. Heatmap of HETE-PL lipids in platelets from patients with arterial thrombosis shows higher levels of diacyl (red arrows), but not plasmalogen (blue arrows), 12-HETE-PL in thrombin-activated platelets from ACS compared with HC.

Lipids were extracted from resting platelets (2 x 10^8) or following activation with thrombin (0.2 U/ml) as in Materials and Methods. Lipids amounts (ng) were calculated by LC-MS/MS, log10 transformed and plotted as a heatmap with hierarchical clustering using the pheatmap R package. Category is the proposed enzymatic origin of HETE-PL species. ACS: acute coronary syndrome (n=24), CAD: coronary artery disease but no ACS (n=19), RF: Risk factors with no significant coronary artery disease (n=23), HC: Healthy control (n=24).

Next, to obtain an overview of differences in platelet HETE-PL between clinical groups and test for statistical significance, box plots were generated for measured lipids groupd by HETE positional isomer. For resting platelets, HETE-PL amounts were similar between groups (HC, RF, CAD and ACS) (**Figure 6.2**A). The exception was 8-HETE-PL, a non-enzymatic oxidation product, which was significantly elevated in CAD/ACS (v HC/RF), however compared with other HETE-PLs, this lipid was only detected in low amounts, less than 0.04 ng/2 x 10^8 platelets.

Following thrombin activation, levels of all platelet HETE-PL isomers increased with differences observed between groups (**Figure 6.2**B). Specifically, 15- and 11-HETE-PL were significantly lower in RF/CAD/ACS compared with HC. Generation of 12-HETE-PL, the main platelet HETE-PL, was higher in RF/CAD/ACS platelets compared with HC. There were no significant differences between ACS/CAD and HC patient groups for 8- and 5-HETE-PL species in thrombin-activated platelets which were generated in very low levels.

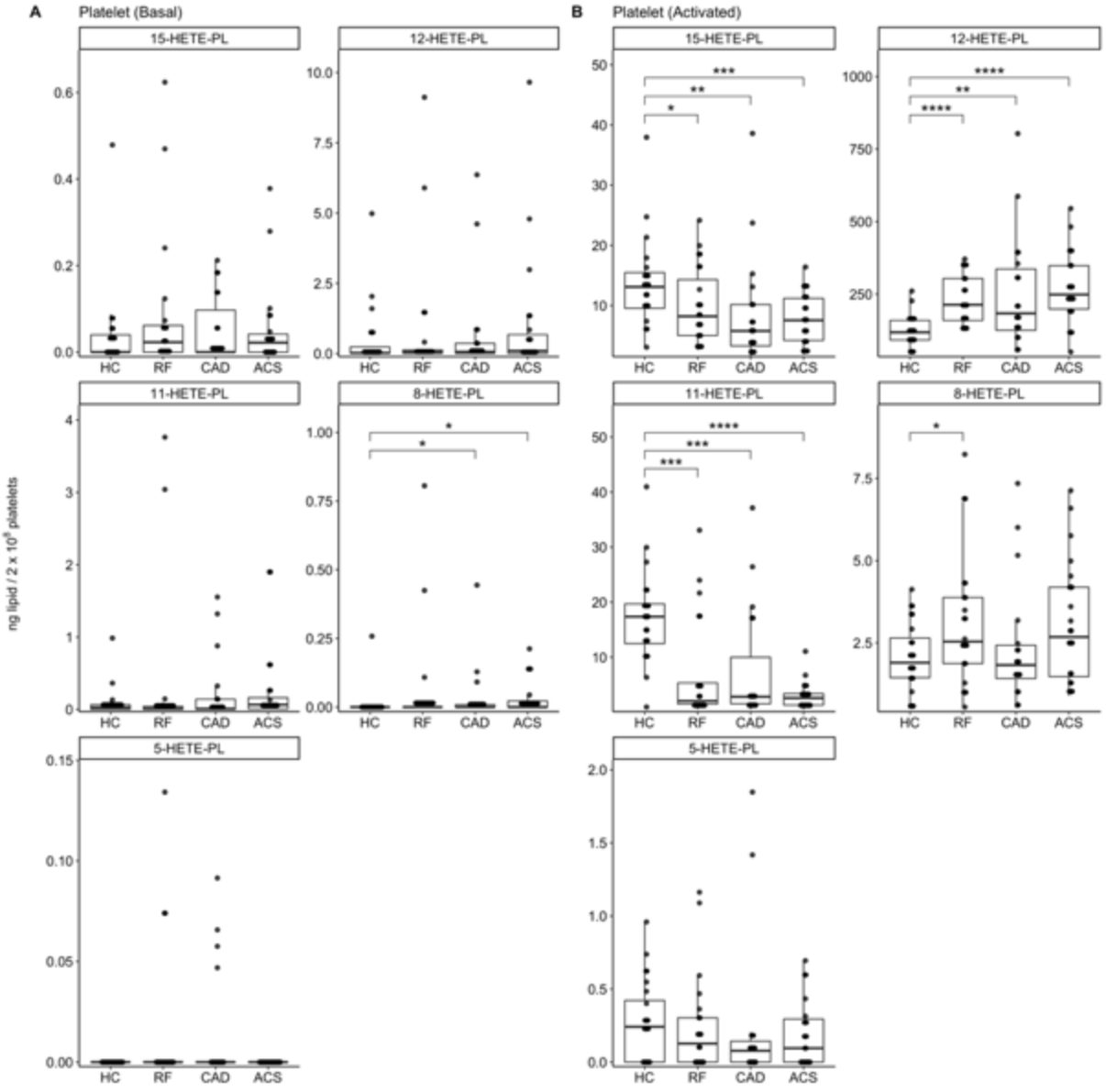

Figure 6.2. Pooling of platelet HETE-PL by *sn2* fatty acid confirmed higher 12-HETE-PL and lower 11-/15-HETE-PL levels in arterial thrombosis compared with healthy controls.

Lipids were extracted from platelets (2 x 10^8) in resting conditions (Panel A) or following activation with thrombin (0.2 U/ml, Panel B) as in Materials and Methods. Lipids amounts (ng) were calculated by LC-MS/MS for 6 lipids for each HETE-PL positional isomer (including 4 PE and 2 PC, as in Materials and Methods) and combined by *sn2* fatty acid. This was then plotted as a box plot with the ggplot2 R package. Box edges indicate the interquartile range (IQR) with the median line inside the box. Whiskers indicate 1.5 times the IQR. Statistical significance was tested with Mann-Whitney-Wilcoxon test, and where significant differences exist, they are indicated by stars (*: $p < 0.05$, **: $p < 0.01$, ***: $p < 0.001$). ACS: acute coronary syndrome (n=24), CAD: coronary artery disease but no ACS (n=19), RF: Risk factors with no significant coronary artery disease (n=23), HC: Healthy control (n=24).

Next, I expanded on the overview presented above by going on to examine individual lipid species which may drive the patterns observed with the combined HETE-PL positional isomers. To start with 15-HETE-PL, there were no significant differences between clinical groups in any of the 15-HETE-PL species measured from resting platelets (**Figure 6.3**A). Upon thrombin-activation, 15-HETE-PL species increase by 180-fold on average compared to resting amounts, with significantly lower levels of 15-HETE-PL species in thrombin-activated platelets from ACS/CAD/RF compared with HC (**Figure 6.3**B). This was the case for all 15-HETE-PL species irrespective of PC/PE headgroup, with the exception being PE 18:0a_15-HETE which demonstrated no significant differences between clinical groups. These findings likely reflect the inhibitory effect caused by aspirin, which was administered to none of the HC participants, some CAD/RF patients, and all ACS patients.

All 12-HETE-PL species measured, presumed to be 12-LOX products, were very low in resting platelets with no significant differences between clinical groups (**Figure 6.4**A). On thrombin activation, these lipids increased by almost 300-fold (**Figure 6.4**B). There were significantly higher levels of diacyl 12-HETE-PL species (18:0a, 16:0a) in thrombin-activated platelets from ACS/CAD/RF compared with HC, but plasmalogens (18:0p, 16:0p, 18:1p) were not significantly different . This was consistent for both PE or PC HETE-PL species.

11-HETE-PL (presumed to be a product of COX-1 in platelets) were detected in resting platelets at very low levels with no significant differences between patient groups (**Figure 6.5**A). Upon activation, platelets generated 11-HETE-PL, with an average increase of approximately 40-fold (**Figure 6.5**B). There were significantly lower levels of 11-HETE-PL in thrombin-activated platelets from ACS/CAD/RF compared with HC irrespective of PC/PE

headgroup. Thus, 11-HETE- and 15-HETE-PL behave similarly. The impact of aspirin on HETE-PL generation in this cohort will be examined later in section **6.2.2** of this chapter.

8-HETE-PL (non-enzymatically generated) were very low in resting platelets with no significant differences between clinical groups (**Figure 6.6**A). On thrombin activation of platelets, 8-HETE-PL were detected in small amounts across all groups, with significantly (but marginally) higher levels in ACS/RF versus HC in PC, but not PE, lipids irrespective of *sn1* FA (**Figure 6.6**B).

The amounts of 5-HETE-PL species generated by resting or thrombin-activated platelets were very low with no differences between groups (**Figure 6.7**).

Thus, the findings of this section so far indicate no differences in resting platelet HETE-PL amounts between groups. On thrombin activation, HETE-PL amounts increase which is expected given the mobilisation of PLA_2 and calcium within the cells. Differences were seen between patient groups for amounts of HETE-PL generated in thrombin-activated platelets. For COX-1 derived lipids (15- and 11-HETE-PL), the lower levels in ACS patients vs HC maybe related to aspirin supplementation which inhibits COX-1. The finding of higher levels of 12-HETE-PL in ACS v HC will be further explored in section **6.2.2** below.

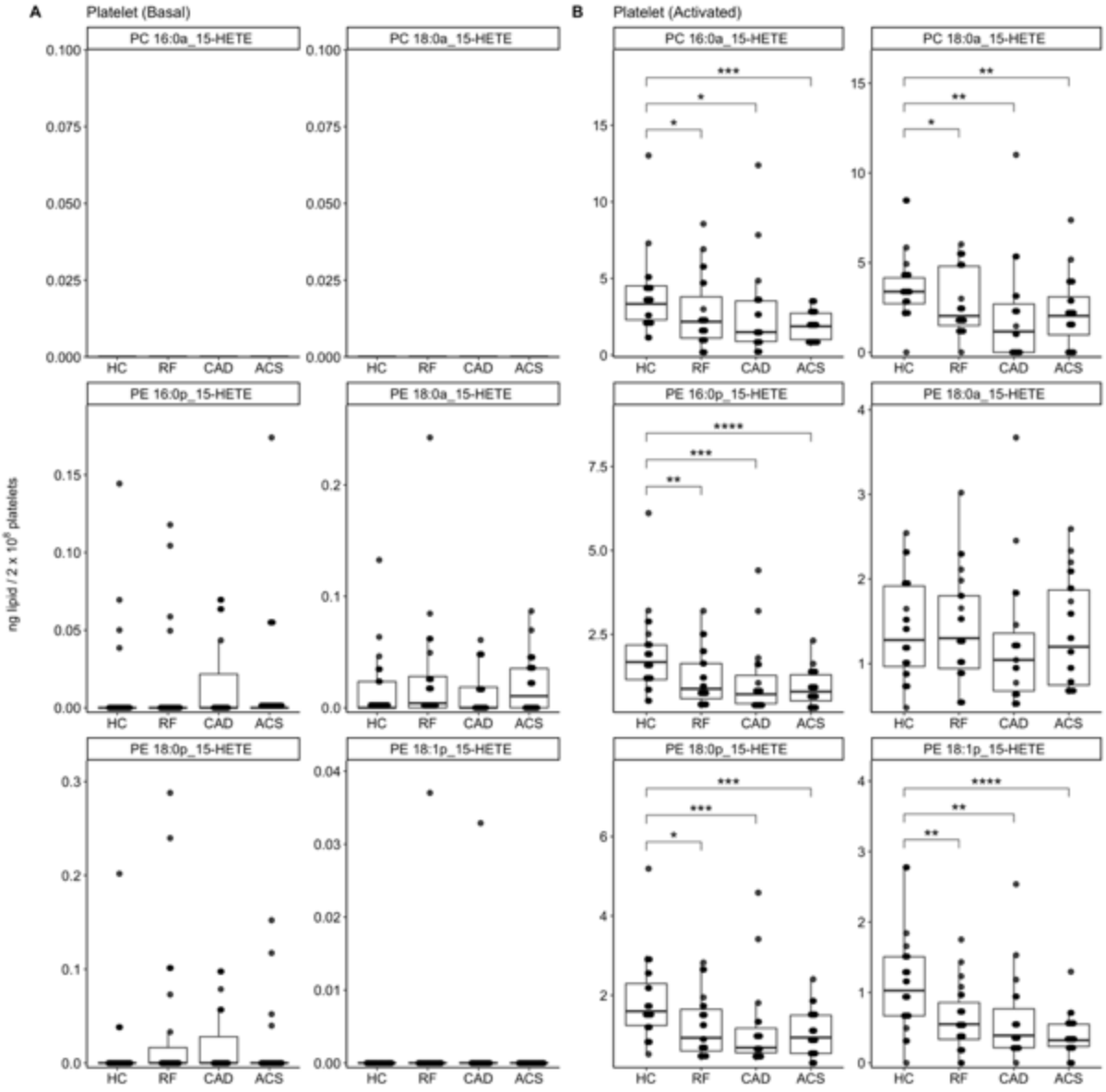

Figure 6.3. Levels of 15-HETE-PL in thrombin-stimulated platelets were lower in patients with arterial thrombosis compared with healthy controls.

Lipids were extracted from platelets (2 x 10^8) in resting conditions (Panel A) or following activation with thrombin (0.2 U/ml, Panel B) as in Materials and Methods. Lipids amounts (ng) were calculated by LC-MS/MS and plotted as a box plot with the ggplot2 R package. Box edges indicate the interquartile range (IQR) with the median line inside the box. Whiskers indicate 1.5 times the IQR. Statistical significance was tested with Mann-Whitney-Wilcoxon test, and where significant differences exist, they are indicated by stars (*: $p < 0.05$, **: $p < 0.01$, ***: $p < 0.001$). ACS: acute coronary syndrome (n=24), CAD: coronary artery disease but no ACS (n=19), RF: Risk factors with no significant coronary artery disease (n=23), HC: Healthy control (n=24).

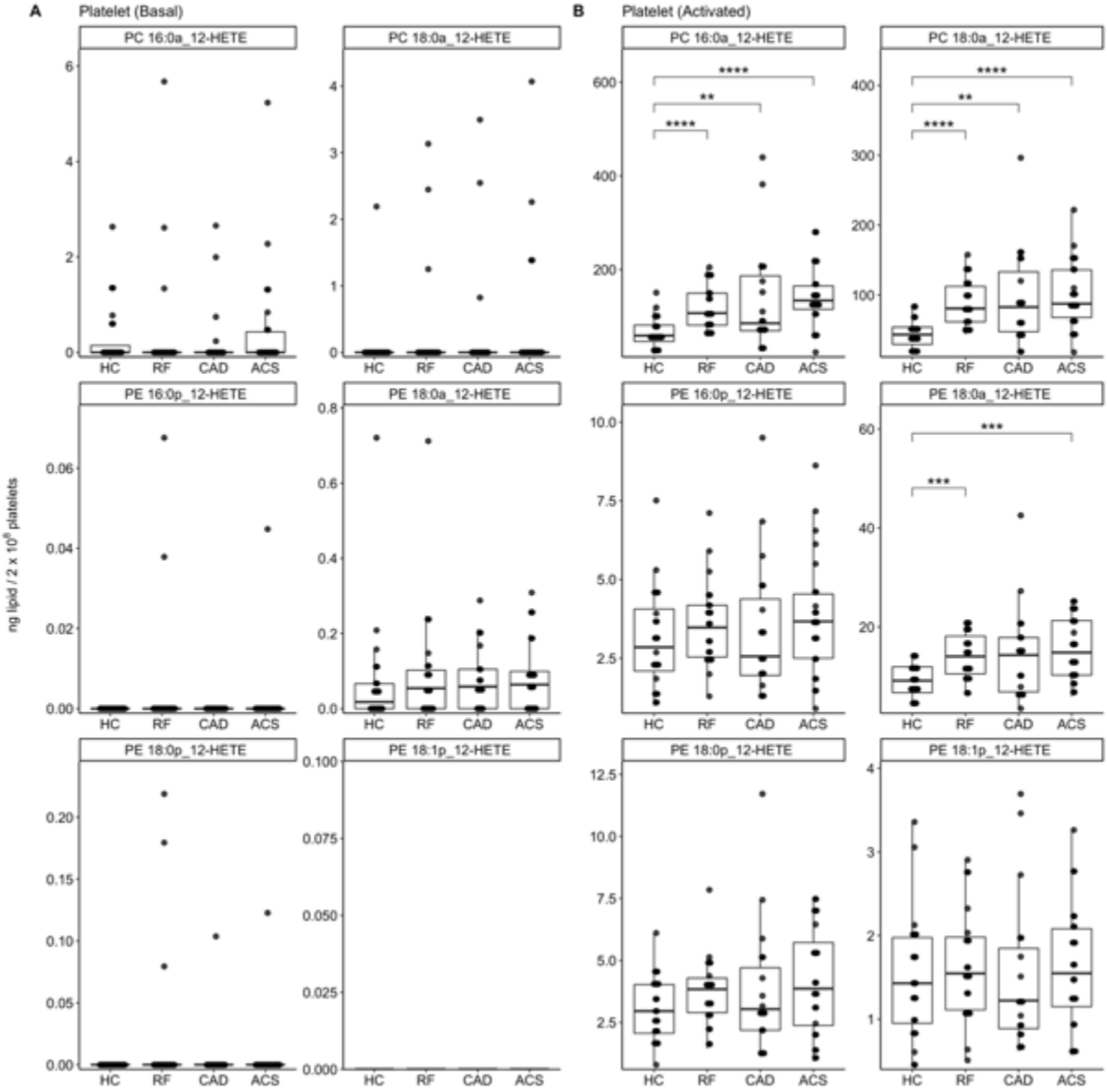

Figure 6.4. Levels of diacyl 12-HETE-PL in thrombin-stimulated platelets were higher in patients with arterial thrombosis compared with healthy controls.

Lipids were extracted from platelets (2 x 10^8) in resting conditions (Panel A) or following activation with thrombin (0.2 U/ml, Panel B) as in Materials and Methods. Lipids amounts (ng) were calculated by LC-MS/MS and plotted as a box plot with the ggplot2 R package. Box edges indicate the interquartile range (IQR) with the median line inside the box. Whiskers indicate 1.5 times the IQR. Statistical significance was tested with Mann-Whitney-Wilcoxon test, and where significant differences exist, they are indicated by stars (*: $p < 0.05$, **: $p < 0.01$, ***: $p < 0.001$). ACS: acute coronary syndrome (n=24), CAD: coronary artery disease but no ACS (n=19), RF: Risk factors with no significant coronary artery disease (n=23), HC: Healthy control (n=24).

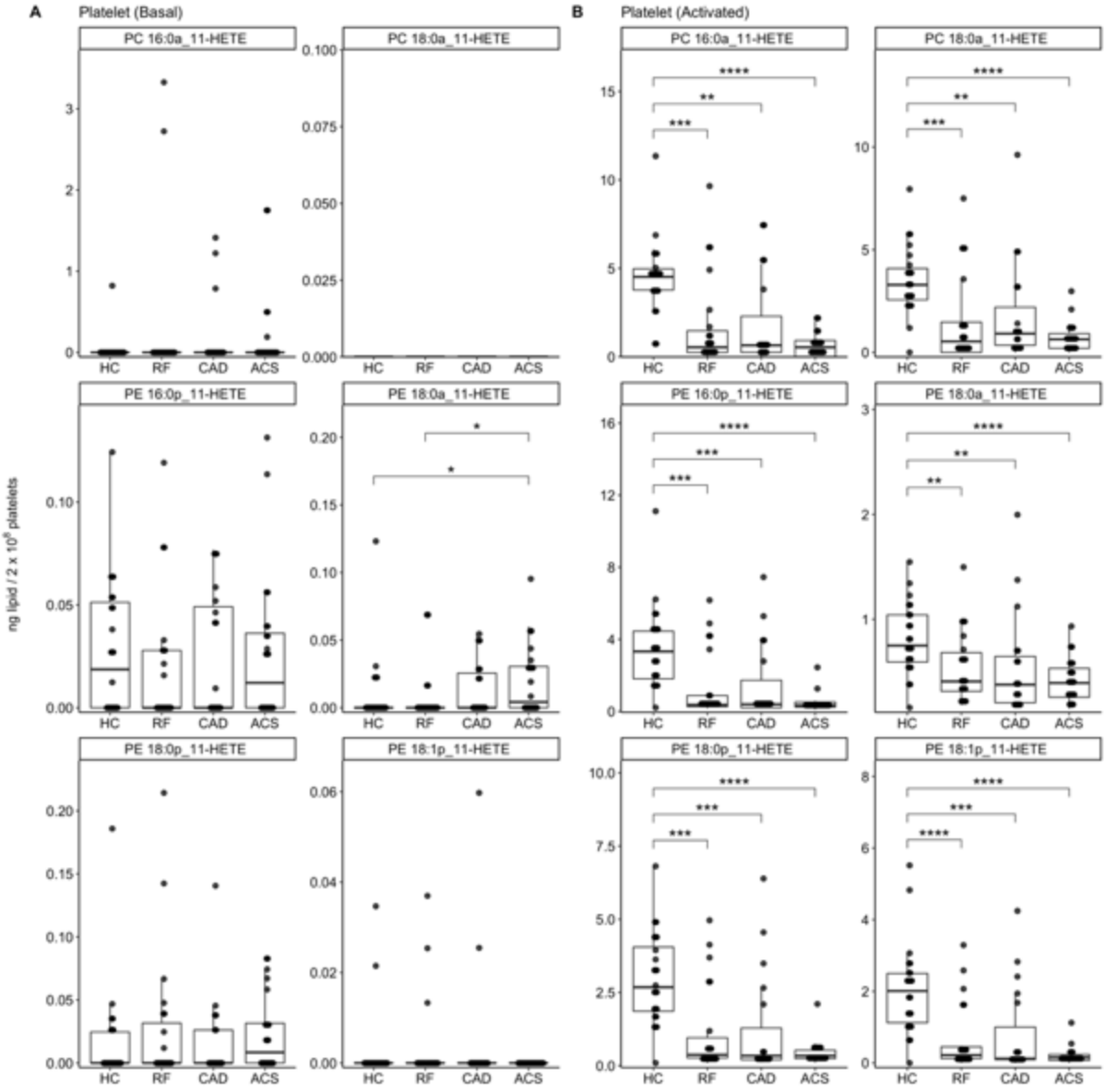

Figure 6.5. Levels of 11-HETE-PL in thrombin-stimulated platelets were lower in patients with arterial thrombosis compared with healthy controls.

Lipids were extracted from platelets (2 x 10^8) in resting conditions (Panel A) or following activation with thrombin (0.2 U/ml, Panel B) as in Materials and Methods. Lipids amounts (ng) were calculated by LC-MS/MS and plotted as a box plot with the ggplot2 R package. Box edges indicate the interquartile range (IQR) with the median line inside the box. Whiskers indicate 1.5 times the IQR. Statistical significance was tested with Mann-Whitney-Wilcoxon test, and where significant differences exist, they are indicated by stars (*: $p < 0.05$, **: $p < 0.01$, ***: $p < 0.001$). ACS: acute coronary syndrome (n=24), CAD: coronary artery disease but no ACS (n=19), RF: Risk factors with no significant coronary artery disease (n=23), HC: Healthy control (n=24).

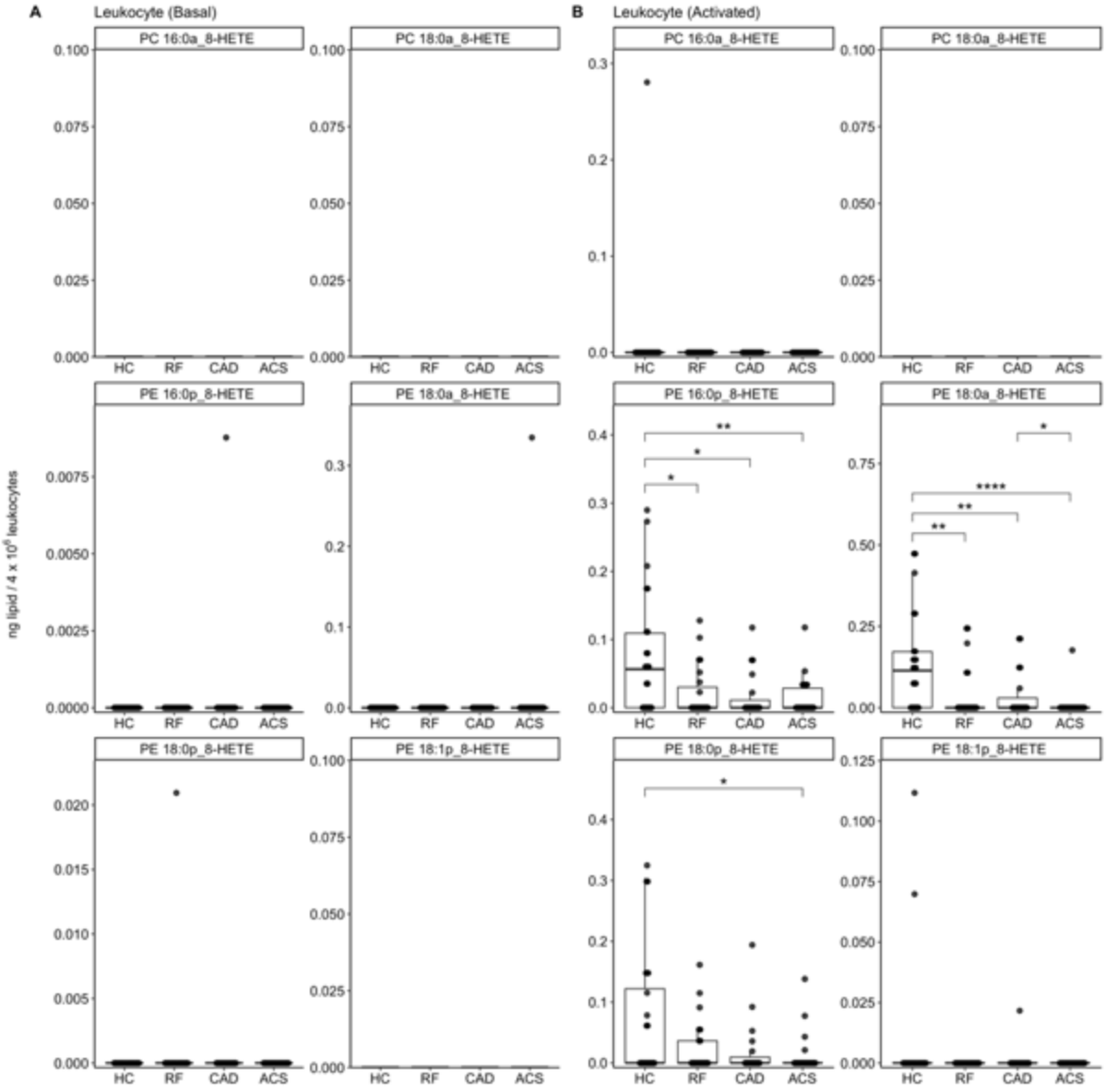

Figure 6.6. Non-enzymatic 8-HETE-PL were formed in small amounts upon stimulating platelets with thrombin.

Lipids were extracted from platelets (2 x 10^8) in resting conditions (Panel A) or following activation with thrombin (0.2 U/ml, Panel B) as in Materials and Methods. Lipids amounts (ng) were calculated by LC-MS/MS and plotted as a box plot with the ggplot2 R package. Box edges indicate the interquartile range (IQR) with the median line inside the box. Whiskers indicate 1.5 times the IQR. Statistical significance was tested with Mann-Whitney-Wilcoxon test, and where significant differences exist, they are indicated by stars (*: $p < 0.05$, **: $p < 0.01$, ***: $p < 0.001$). ACS: acute coronary syndrome (n=24), CAD: coronary artery disease but no ACS (n=19), RF: Risk factors with no significant coronary artery disease (n=23), HC: Healthy control (n=24).

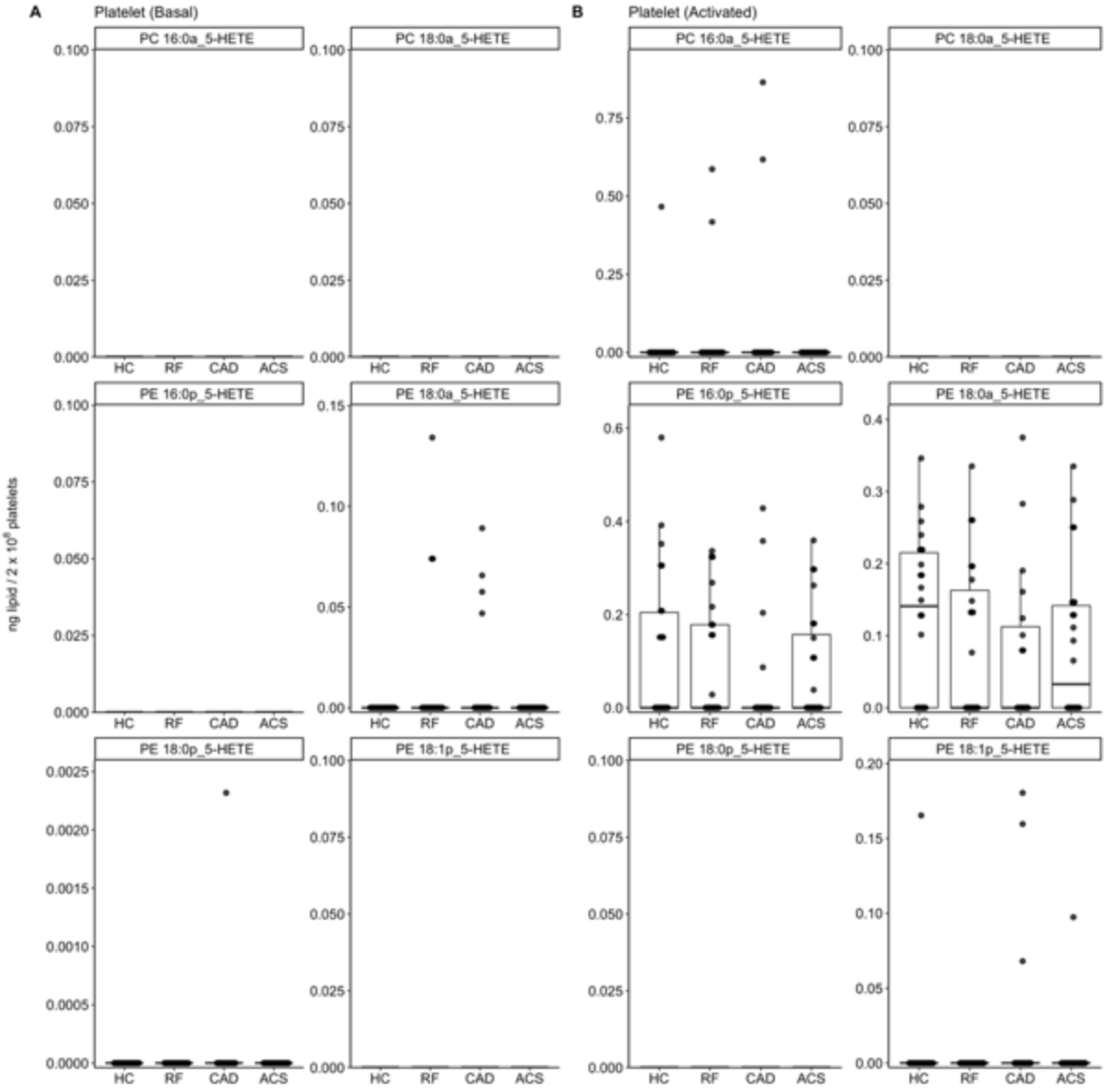

Figure 6.7. Minimal amounts of 5-HETE-PL were formed upon stimulating platelets with thrombin.

Lipids were extracted from platelets (2 x 10^8) in resting conditions (Panel A) or following activation with thrombin (0.2 U/ml, Panel B) as in Materials and Methods. Lipids amounts (ng) were calculated by LC-MS/MS and plotted as a box plot with the ggplot2 R package. Box edges indicate the interquartile range (IQR) with the median line inside the box. Whiskers indicate 1.5 times the IQR. Statistical significance was tested with Mann-Whitney-Wilcoxon test, and where significant differences exist, they are indicated by stars (*: $p < 0.05$, **: $p < 0.01$, ***: $p < 0.001$). ACS: acute coronary syndrome (n=24), CAD: coronary artery disease but no ACS (n=19), RF: Risk factors with no significant coronary artery disease (n=23), HC: Healthy control (n=24).

6.2.2 Aspirin use is associated with higher 12-HETE-PL and lower 15- and 11-HETE-PL generation in thrombin-stimulated platelets

In the previous **Chapter 3**, I showed that thrombin-activated platelets from participants on aspirin supplementation generated higher amounts of 12-HETE-PL compared with those who were not taking aspirin. To investigate this in the clinical cohort, 12-HETE-PL levels from thrombin-activated platelets were re-analysed by aspirin use. The RF and CAD groups were compared since they include patients both on and off aspirin, unlike HC (none taking aspirin) or ACS (all taking aspirin). Here, I found that 12-HETE-PL levels are higher when patients in the same clinical group (RF or CAD) when taking aspirin (**Figure 6.8A**). When I analysed samples from patients not on aspirin, there were no differences in 12-HETE-PLs in thrombin-activated platelets between HC, RF and CAD groups (**Figure 6.8B**).

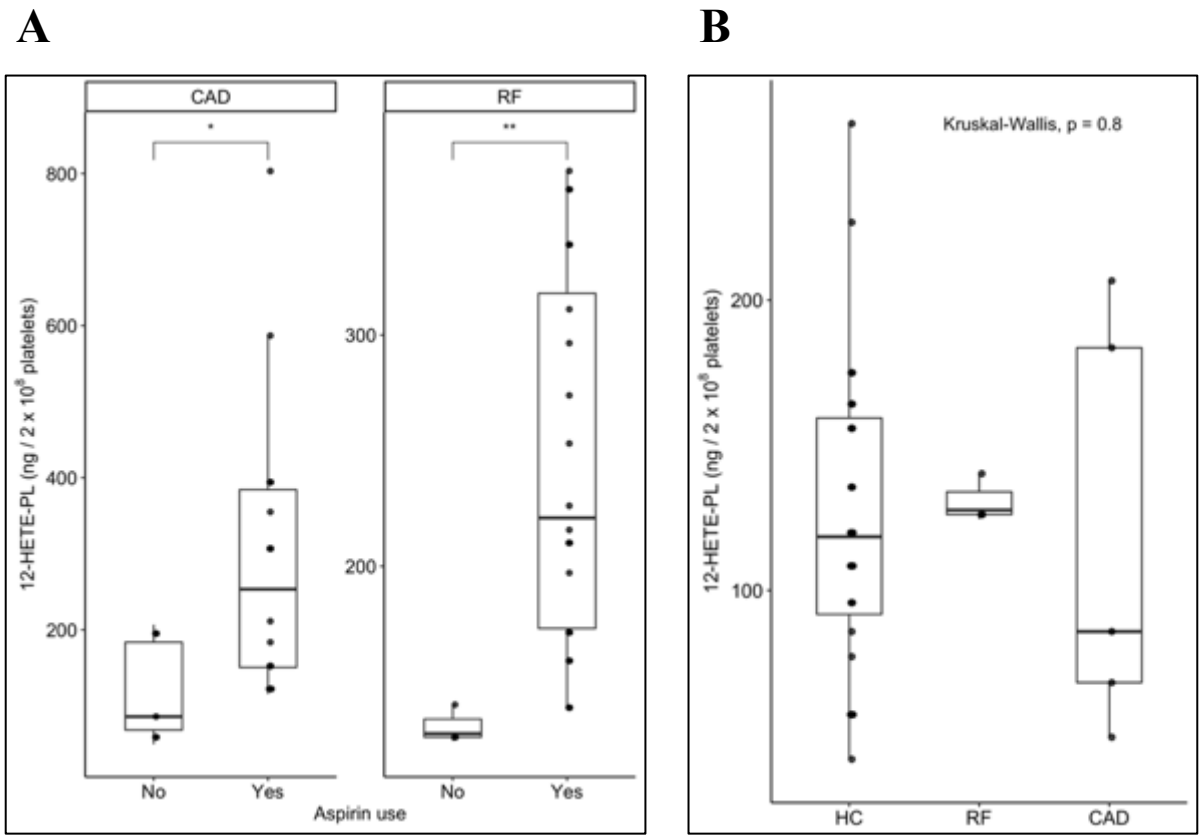

Figure 6.8. Levels of 12-HETE-PL in thrombin-activated platelets were higher in patients on aspirin compared to no aspirin. Panel A: The amounts of 12-HETE-PL generated from thrombin-activated platelets from CAD and RF patients by aspirin use. Panel B: Analysis of 12-HETE-PL levels in thrombin-activated platelets from HC, RF and CAD patients not supplemented with aspirin. Lipids were extracted from platelets (2 x 10^8) following activation with thrombin (0.2 U/ml) as in Materials and Methods. Lipids amounts (ng) were calculated by LC-MS/MS for 6 lipids for each HETE-PL positional isomer (including 4 PE and 2 PC, as in Materials and Methods) and combined by *sn2* fatty acid. This was then plotted as a box plot with the ggplot2 R package. Box edges indicate the interquartile range (IQR) with the median line inside the box. Whiskers indicate 1.5 times the IQR. Statistical significance was tested with Mann-Whitney-Wilcoxon test for pairwise comparison (Panel A, ns: not significant, *: $p < 0.05$, **: $p < 0.01$, ***:$p < 0.001$) or Kruskal-Wallis test for non-parametric analysis of variance on rank (Panel B). CAD: coronary artery disease (but no acute coronary syndrome, ACS), RF: Risk factors with no significant coronary artery disease, HC: Healthy control.

To determine which 12-HETE-PLs were responsible for the impact of aspirin, I next analysed individual lipid species. Acyl 12-HETE-PC lipids were significantly higher in thrombin-activated platelets from patients on aspirin, with an upward trend noticed for diacyl 12-HETE-PE species (**Figure 6.9**A). Pooling 12-HETE-PL lipids by head group maintains the significant difference observed with 12-HETE-PC, but demonstrates a non-significant upward trend with 12-HETE-PE (**Figure 6.9**B). When I analysed samples from patients not on aspirin, there were no differences in the amounts of individual 12-HETE-PL species in thrombin-activated platelets between HC, RF and CAD (**Figure 6.10**). Therefore, it is likely that the higher 12-HETE-PL levels seen in platelets from ACS patients are due to the impact of aspirin as will be addressed the discussion.

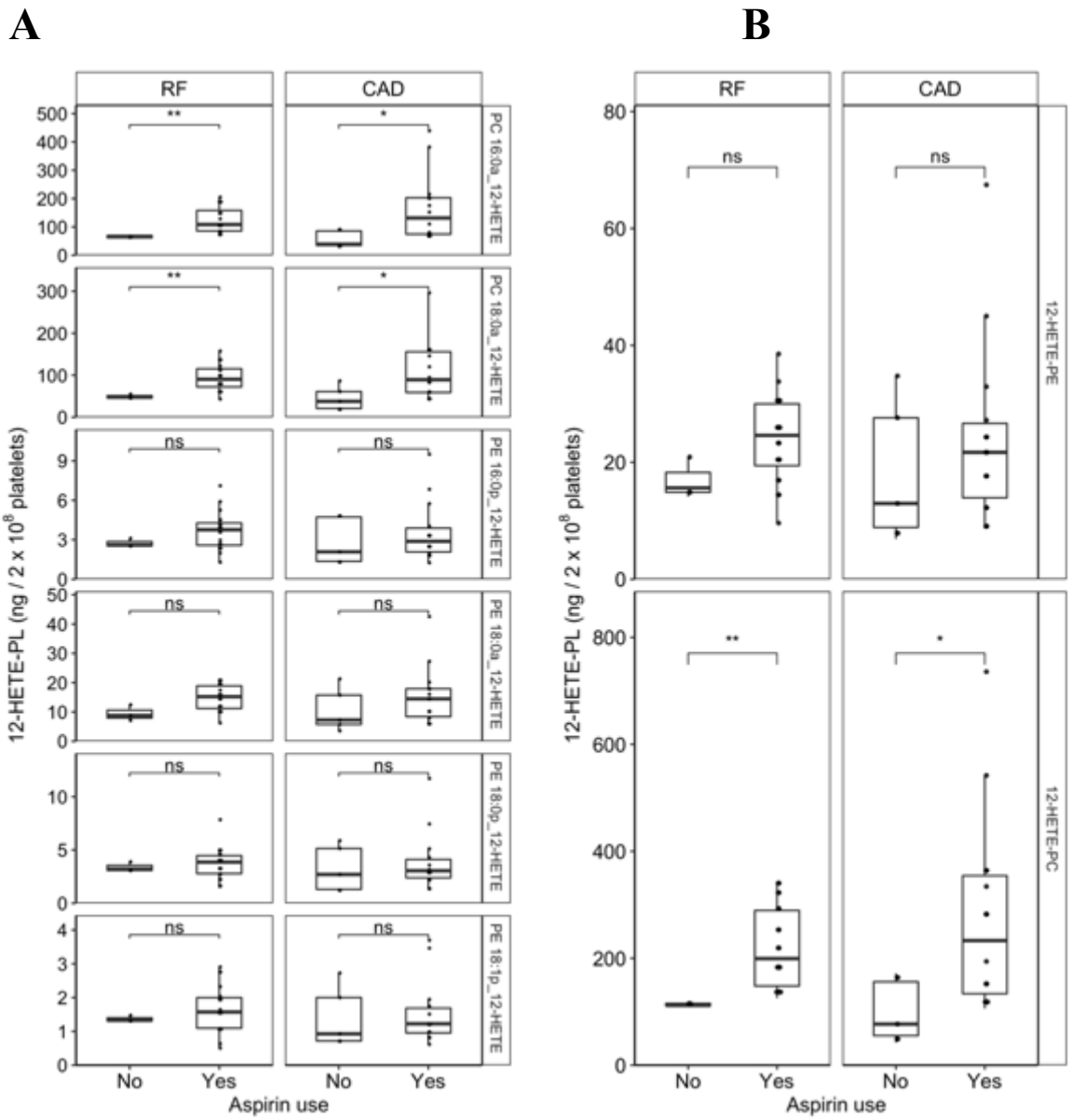

Figure 6.9. Higher levels of thrombin generated platelet 12-HETE-PL in diacyl PC lipids with an upward trend in diacyl PE lipids.

Panel A: The amounts of individual 12-HETE-PL species generated in thrombin-activated platelets from CAD and RF patients by aspirin use. Panel B: Analysis of 12-HETE-PL levels pooled by headgroup in thrombin-activated platelets from RF and CAD patients by aspirin use. Lipids were extracted from platelets (2 x 10^8) following activation with thrombin (0.2 U/ml) as in Materials and Methods. Lipids amounts (ng) were calculated by LC-MS/MS and plotting them as a box plot with the ggplot2 R package. Box edges indicate the interquartile range (IQR) with the median line inside the box. Whiskers indicate 1.5 times the IQR. Combined PE/PE were calculated as the sum of the individual lipids by headgroup (All PE or All PC). Statistical significance was tested with Mann-Whitney-Wilcoxon test (ns: not significant, *: $p < 0.05$, **: $p < 0.01$, ***:$p < 0.001$). CAD: coronary artery disease (but no acute coronary syndrome, ACS), RF: Risk factors with no significant coronary artery disease.

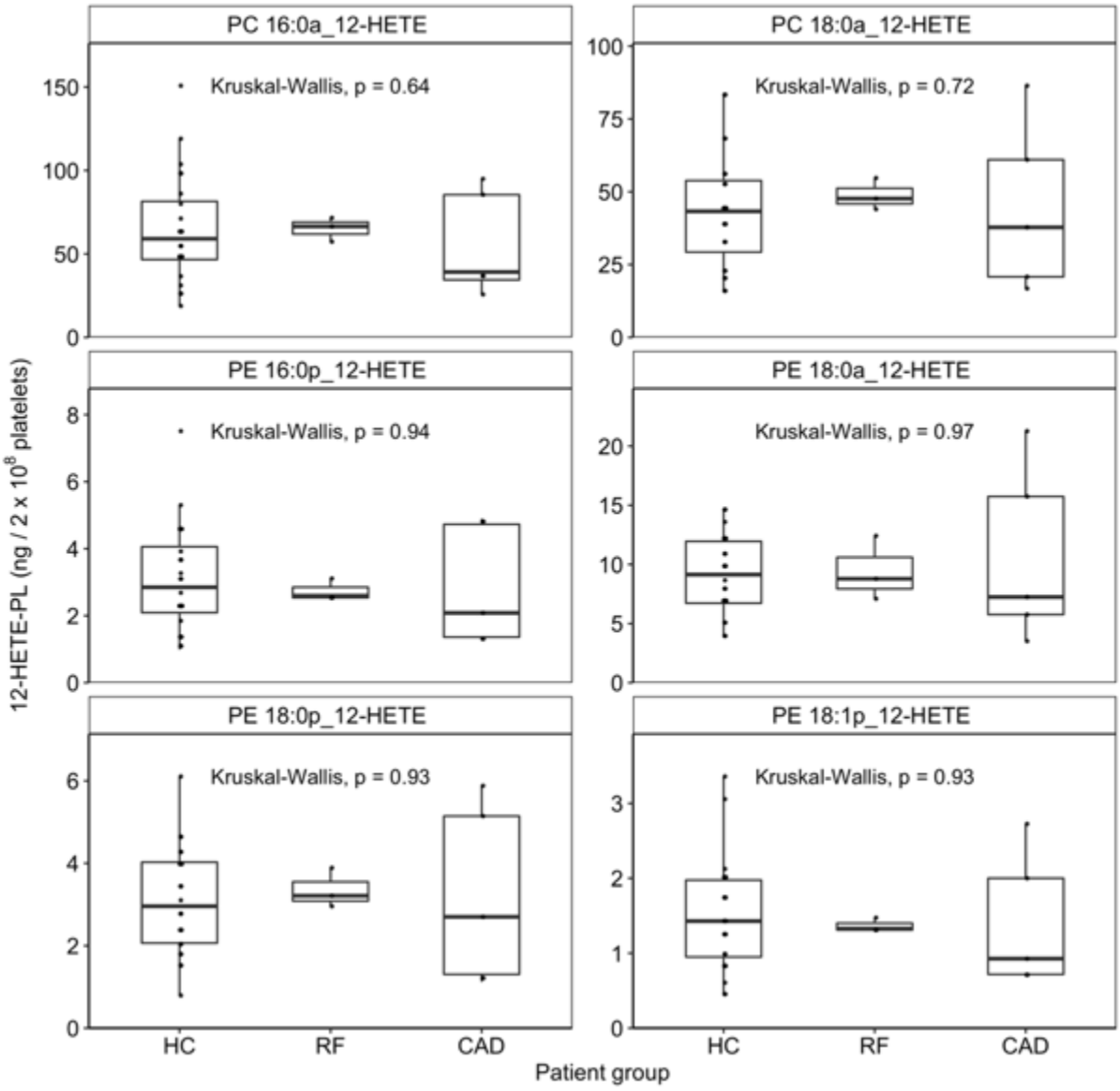

Figure 6.10. Patients not on aspirin had similar levels of platelet 12-HETE-PL in thrombin-activated platelets between groups irrespective of headgroup or *sn1* fatty acid.

Lipids were extracted from platelets (2 x 10^8) following thrombin stimulation (0.2 U/ml) as in Materials and Methods. Lipids amounts (ng) were calculated by LC-MS/MS for 6 lipids for each HETE-PL positional isomer and potting them as a box plot with the ggplot2 R package. Box edges indicate the interquartile range (IQR) with the median line inside the box. Whiskers indicate 1.5 times the IQR. Statistical significance was tested with the Kruskal-Wallis test for non-parametric analysis of variance on rank. CAD: coronary artery disease (but no acute coronary syndrome, ACS), RF: Risk factors with no significant coronary artery disease, HC: Healthy control.

Next, to test the effect of aspirin on COX-1 generated 15-HETE-PL and 11-HETE-PL, I compared the levels of these lipids in the RF/CAD patient groups by aspirin use. As expected, activated platelets from patients taking aspirin generated lower amounts of 15-HETE-PL and 11-HETE-PL (**Figure 6.11**).

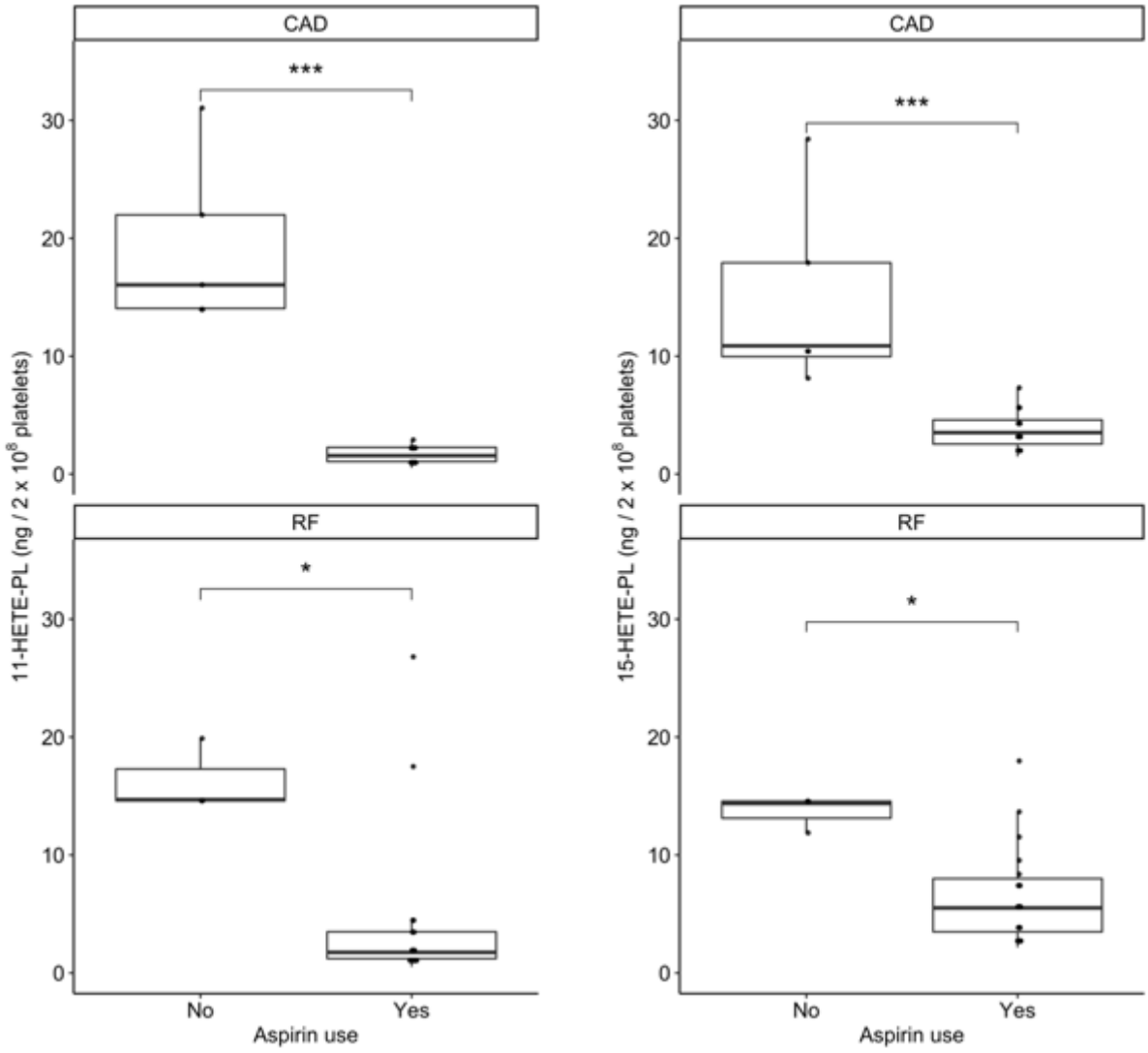

Figure 6.11. The amount of 15- and 11-HETE-PL in thrombin-activated platelets is lower in patients on aspirin.

Lipids were extracted from platelets (2 x 10^8) following activation with thrombin (0.2 U/ml) as in Materials and Methods. Lipids amounts (ng) were calculated by LC-MS/MS for 6 lipids for each HETE-PL positional isomer (including 4 PE and 2 PC, as in Materials and Methods) and combined by *sn2* fatty acid. This was then plotted as a box plot with the ggplot2 R package. Box edges indicate the interquartile range (IQR) with the median line inside the box. Whiskers indicate 1.5 times the IQR. Statistical significance was tested with Mann-Whitney-Wilcoxon test for pairwise comparison (*: $p < 0.05$, **: $p < 0.01$, ***:$p < 0.001$). CAD: coronary artery disease (but no acute coronary syndrome, ACS), RF: Risk factors with no significant coronary artery disease

In a previous **Chapter 3**, I showed that the higher amounts of diacyl 12-HETE-PL in thrombin-activated platelets from healthy participants on aspirin were only observed in males. Thus, I next tested the impact of gender on HETE-PL levels in thrombin-activated platelets from patients on aspirin versus patients off aspirin. The CAD/RF group did not have sufficient number of males and females on/off aspirin to allow for a comparison within the same clinical group, and therefore I opted to examine ACS (all on aspirin) versus HC (none on aspirin) by gender, acknowledging that any observed differences may also relate to the disease process.

I found there were significantly higher diacyl 12-HETE-PL levels in ACS (all on aspirin) versus HC (none on aspirin) in both men and women (**Figure 6.12**). This gender consistency was also observed for all 12-HETE-PL species irrespective of headgroup (PC/PE) or *sn1* fatty acid (**Figure 6.13**). These findings suggest that aspirin supplementation is associated with higher diacyl 12-HETE-PL generation compared with no aspirin in thrombin-activated platelets in both men and women of the clinical cohort.

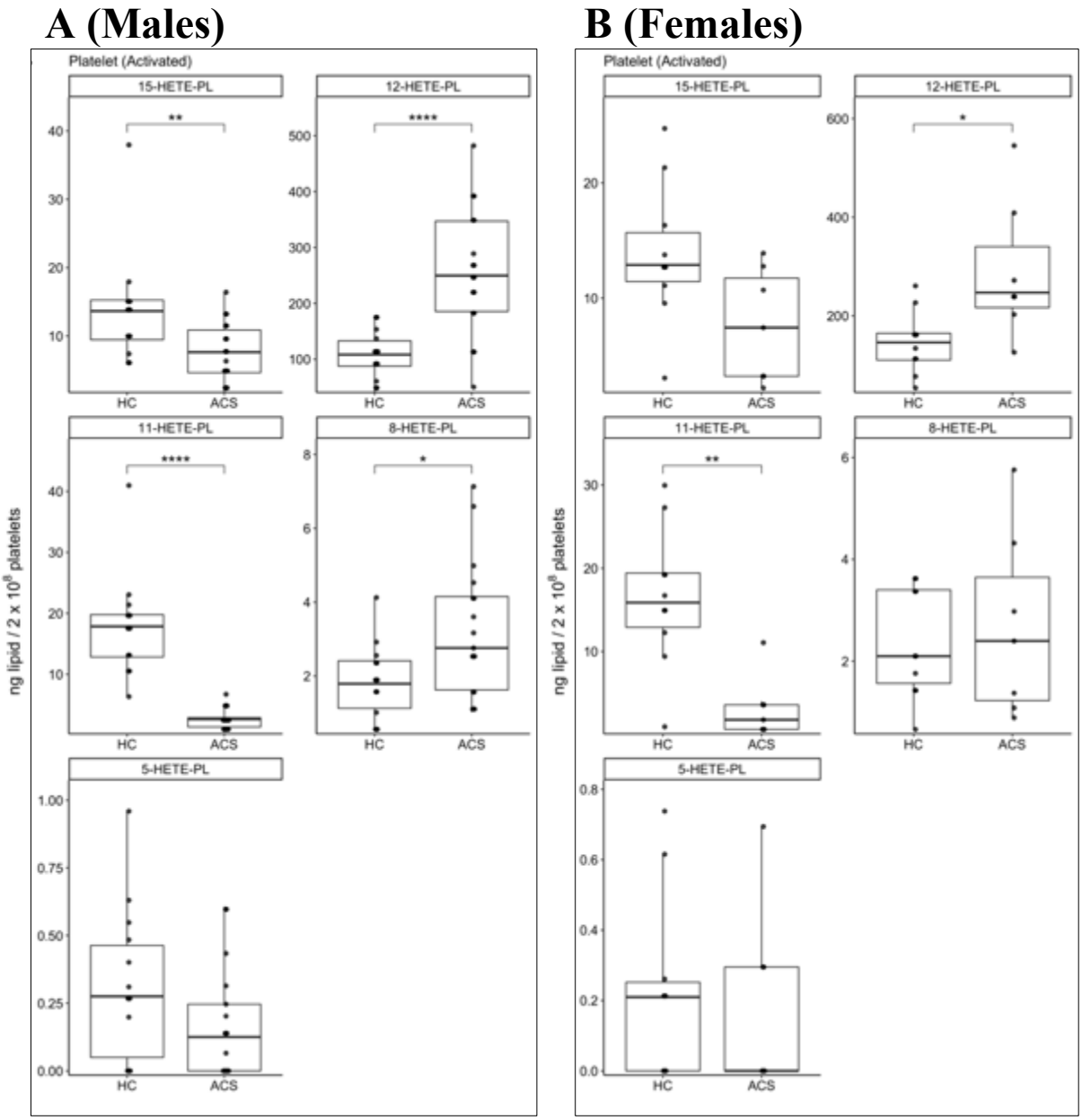

Figure 6.12. Gender-specific analysis of HETE-PL (pooled by *sn2* fatty acid) in thrombin-activated platelets demonstrated a consistent pattern between ACS (all on aspirin) and HC (none on aspirin) in both males (Panel A) and females (Panel B).

Lipids were extracted from platelets (2 x 10^8) following activation with thrombin (0.2 U/ml) as in Materials and Methods. Lipids amounts (ng) were calculated by LC-MS/MS for 6 lipids for each HETE-PL positional isomer (including 4 PE and 2 PC, as in Materials and Methods) and combined by *sn2* fatty acid. This was then plotted as a box plot with the ggplot2 R package. Box edges indicate the interquartile range (IQR) with the median line inside the box. Whiskers indicate 1.5 times the IQR. Statistical significance was tested with Mann-Whitney-Wilcoxon test, and where significant differences exist, they are indicated by stars (*: $p < 0.05$, **: $p < 0.01$, ***: $p < 0.001$). ACS: acute coronary syndrome, HC: healthy control.

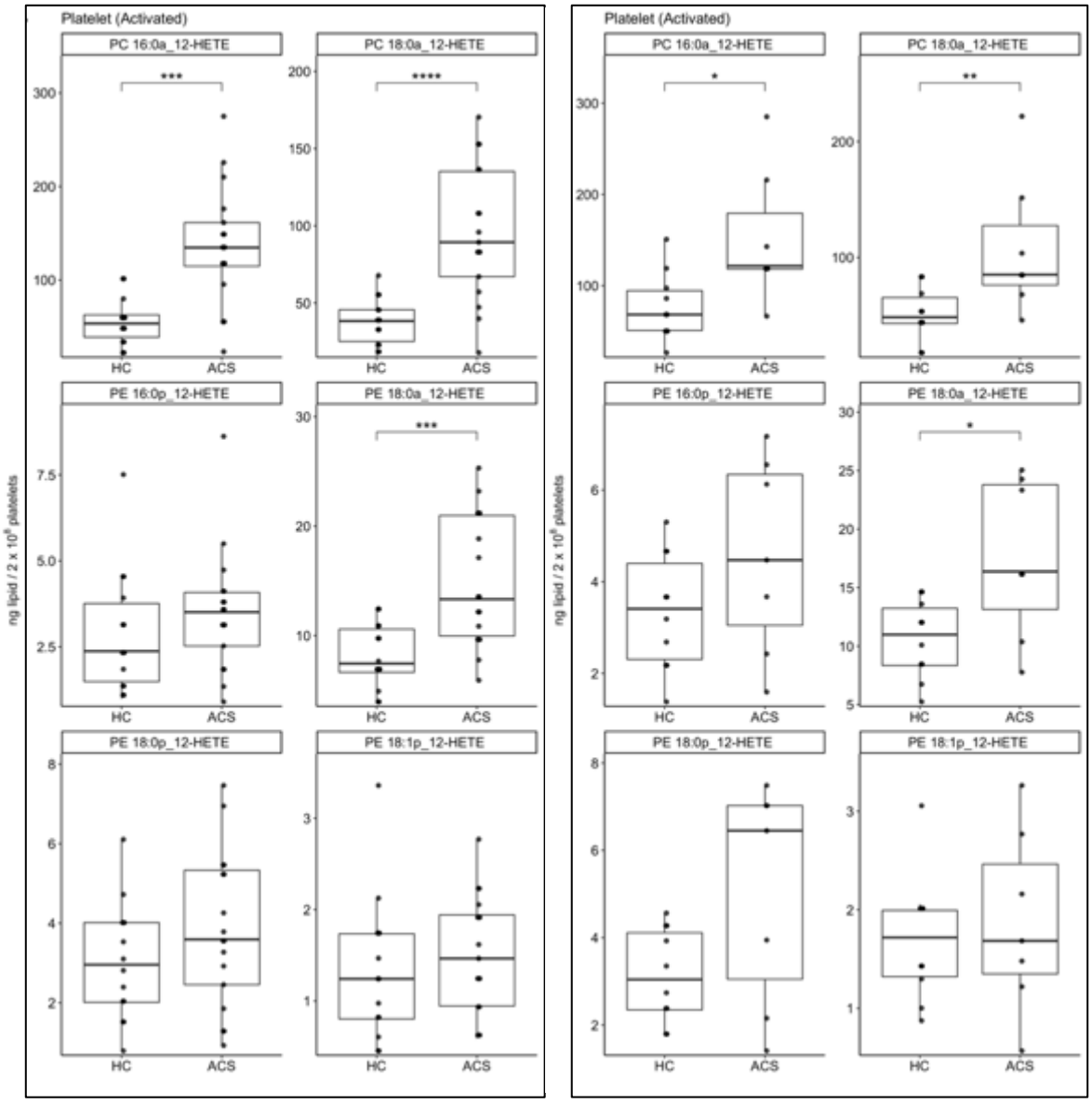

Figure 6.13. Gender-specific analysis of individual 12-HETE-PL species in thrombin-activated platelets demonstrated a consistent pattern between ACS (all on aspirin) and HC (none on aspirin) in both men and women irrespective of headgroup or *sn1* fatty acid.

Panel A: Males; Panel B: Females. Lipids were extracted from platelets (2 x 10^8) following activation with thrombin (0.2 U/ml, Panel B) as in Materials and Methods. Lipids amounts (ng) were calculated by LC-MS/MS and plotting them as a box plot with the ggplot2 R package. Box edges indicate the interquartile range (IQR) with the median line inside the box. Whiskers indicate 1.5 times the IQR. Statistical significance was tested with Mann-Whitney-Wilcoxon test, and where significant differences exist, they are indicated by stars (*: $p < 0.05$, **: $p < 0.01$, ***: $p < 0.001$). ACS: acute coronary syndrome, HC: healthy control.

6.2.3 There were no differences in resting leukocyte HETE-PL amounts between clinical groups

Next, HETE-PL were measured in leukocytes from patients both in resting states and following activation with A23817. The reason why A23817 was chosen as an agonist is to ensure activation of all leukocyte subpopulations in the sample irrespective of differences in receptors and response to agonists. Whilst this does not reflect physiological activation of leukocytes, it quantifies the capacity of these cells to generate HETE-PL upon stimulation, and ensures that the sample contains viable leukocytes capable of lipid synthesis.

To visualise differences in leukocyte HETE-PL generation across the clinical groups, I initially plotted the data on a heatmap (**Figure 6.14**). HETE-PL were detected in very low amounts in resting leukocytes. A23817-activated leukocytes generated higher levels of 15-, 11-, 5- and 12-HETE-PL species compared with resting cells. The non-enzymatically generated 8-HETE-PL was absent or found at low levels in A23817-activated leukocytes. Hierarchical clustering was performed to examine for grouping between lipids based on common patterns across samples (**Figure 6.14**). This demonstrated grouping by *sn2* fatty acid with 12-, 11-, 5- and 15-HETE-PL clustering together whereas 8-HETE-PL species clustered separately. This clustering likely reflects the difference between enzymatic versus non-enzymatic origin of the described HETE-PL groups.

The amounts HETE-PL (both PC and PE) in A23817-activated leukocytes were generally lower in ACS samples compared with HC. This was seen for both PC and PE phospholipids, and was not related to FA composition. This suggests that leukocytes from ACS may have altered and less potent signalling machinery upstream of and including LOX enzymes in response to A23817.

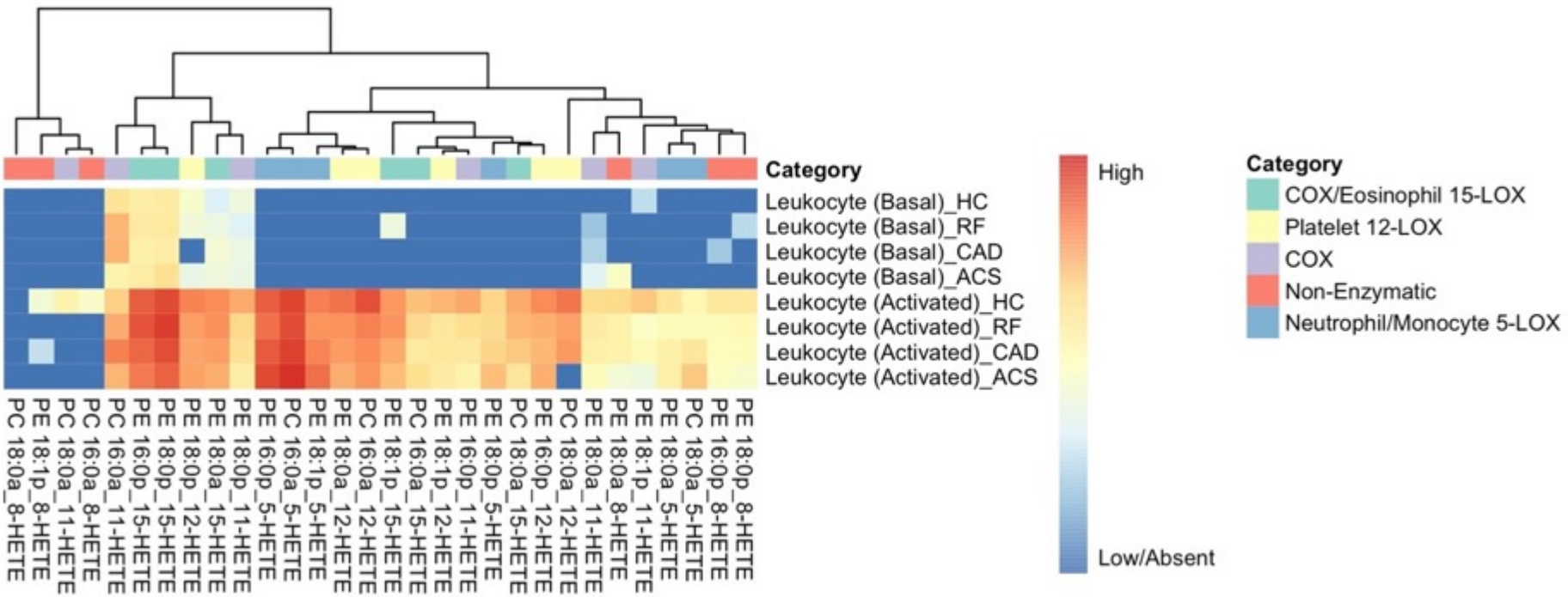

Figure 6.14. Heatmap of HETE-PL lipids in leukocytes from patients with arterial thrombosis revealed influence of ionophore-stimulation and differences between groups.

Lipids were extracted from human leukocytes (4 x 10^6) in resting conditions or following activation with A23817 (10μM) as in Materials and Methods. Lipids amounts (ng) were calculated by LC-MS/MS and averaged by patient group and activation status. Following this, the data was log10 transformed and plotted on the heatmap with hierarchical clustering using the pheatmap R package. Category is the proposed enzymatic origin of HETE-PL species. ACS: acute coronary syndrome (n=24), CAD: coronary artery disease but no ACS (n=19), RF: Risk factors with no significant coronary artery disease (n=23), HC: Healthy control (n=24).

Next, to obtain an overview of differences in leukocyte HETE-PL between clinical groups and test for statistical significance, box plots for were charted for measured lipids combined by HETE positional isomer. This has the advantage of identifying changes in families of lipids specific to the different LOX isoforms.

There were no differences in resting leukocyte HETE-PL amounts between groups (HC, RF, CAD and ACS), as seen in **Figure 6.15**A. Following A23187 activation, levels of all HETE-PL isomers increased with significant differences between groups seen (**Figure 6.15**B).

Specifically, 15-HETE-PL were significantly lower in ACS compared with HC, RF and CAD. This may relate to aspirin supplementation of all ACS patients, and its inhibition of COX-1 primarily (low dose aspirin) with a possible effect on COX-2. For 11-, 12- and 8-HETE-PL, the levels decreased in a stepwise fashion from HC through to RF, CAD and then ACS. Whilst COX-1/COX-2 inhibition by aspirin could explain the finding with 15- and 11-HETE-PL, it leaves 12-HETE-PL unexplained. Finally, levels of 5-HETE-PL were significantly higher in ACS vs RF, and demonstrated an upward trend between ACS vs HC ($p=0.085$). This demonstrates that the different HETE-PL isomers, with the exception of 5-HETE-PL, share a similar pattern by increasing upon A23817 activation from resting levels, but with a decreasing amount going from HC through to RF, CAD and ACS. This may indicate that A23817 is affecting similar pathways upstream of LOX non-selectively.

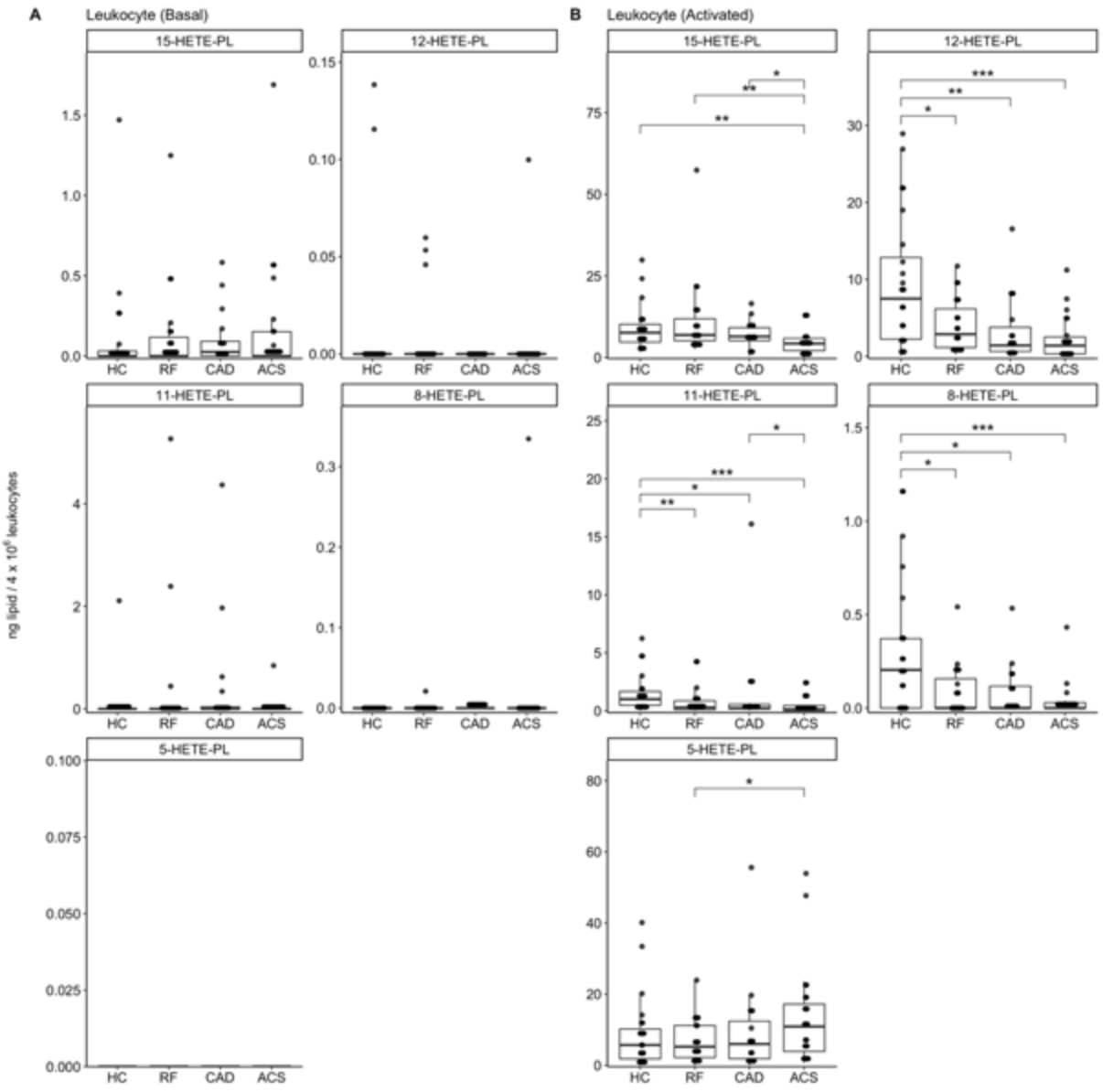

Figure 6.15. Pooling of leukocyte HETE-PL by *sn2* fatty acid confirmed lower HETE-PL levels in ionophore-activated leukocytes from patients with ACS compared with HC, with the exception of 5-HETE-PL.Lipids were extracted from leukocytes (4 x 10^6) in resting conditions (Panel A) or following activation with A23817 (10μM, Panel B) as in Materials and Methods. Lipids amounts (ng) were calculated by LC-MS/MS for 6 lipids for each HETE-PL positional isomer (including 4 PE and 2 PC, as in Materials and Methods) and combined by *sn2* fatty acid. This was then plotted as a box plot with the ggplot2 R package. Box edges indicate the interquartile range (IQR) with the median line inside the box. Whiskers indicate 1.5 times the IQR. Statistical significance was tested with Mann-Whitney-Wilcoxon test, and where significant differences exist, they are indicated by stars (*: p <0.05, **: p <0.01, ***: p <0.001). ACS: acute coronary syndrome (n=24), CAD: coronary artery disease but no ACS (n=19), RF: Risk factors with no significant coronary artery disease (n=23), HC: Healthy control (n=24). Next, I expanded on the overview presented above in leukocytes by going on

to examine individual lipid species which may drive the patterns observed with the combined HETE-PL positional isomers. To start with, 15-HETE-PL species, which may be generated by COX-1, COX-2 or 15-LOX in leukocytes, were low in resting states but increased upon activation with A23187 by 60-fold (**Figure 6.16**). Whilst there were no significant differences in any of the 15-HETE-PL species in resting leukocytes between clinical groups (**Figure 6.16**A), there were significantly lower levels of 15-HETE-PE species in A23817-activated leukocytes from ACS versus HC and/or RF. In contrast, 15-HETE-PCs were formed in much lower levels overall (**Figure 6.16**B). As with platelets, this may be explained by the inhibitory effect on COX-1 and COX-2 caused by aspirin.

Whilst 12-HETE-PL species were mostly undetected in resting leukocytes (**Figure 6.17**A), stimulation with A23187 led to an increase in the amount of these lipids (**Figure 6.17**B). There were significantly lower levels of 12-HETE-PL species in A23817-activated leukocytes from ACS patients compared with HC for all 12-HETE-PL (**Figure 6.17**B). This was the case for both PE and PC forms of 12-HETE-PL, with the exception being PE 18:0p_12-HETE which showed a similar, but non-significant, trend.

11-HETE-PL species (most likely generated by COX-1 or COX-2 in leukocytes) were detected in very low levels in resting leukocytes with no significant differences observed between patient groups (**Figure 6.18**A). Upon A23817 activation, 11-HETE-PE lipid levels increased in all clinical groups. However, 11-HETE-PC was very low or undetected even after stimulation increasing by only around 4-fold (**Figure 6.18**B). There were significantly lower levels of 11-HETE-PL in A23817-activated leukocytes from ACS/CAD compared with HC.

8-HETE-PL were undetected in resting leukocytes across all clinical groups (**Figure 6.19**A). Following A23817-activation, 8-HETE-PE (but not -PC) were detected in small amounts in all groups, with significantly lower levels in ACS versus HC (**Figure 6.19**B).

5-HETE-PL were undetectable in resting leukocytes, but were present in A23817-stimulated leukocytes (**Figure 6.20**). There was a trend towards higher levels of 5-HETE-PL lipids in A23817-activated leukocytes from patients with ACS versus RF/HC. This however only reached statistical significance for PE 16:0p_5-HETE and PE 18:1p_5-HETE in ACS vs RF.

In summary, there were no differences in resting leukocyte HETE-PL amounts between groups for lipid species from all positional isomers. On activation, HETE-PL increase, which is expected given the mobilisation of PLA_2 and calcium within the cells. Lower levels of COX-1/COX-2 derived lipids (15- and 11-HETE-PL) are seen in ACS v HC, likely related to aspirin supplementation. The findings for 12-HETE-PL, which was lower in leukocytes from ACS v HC, will be further explored in section **0** below.

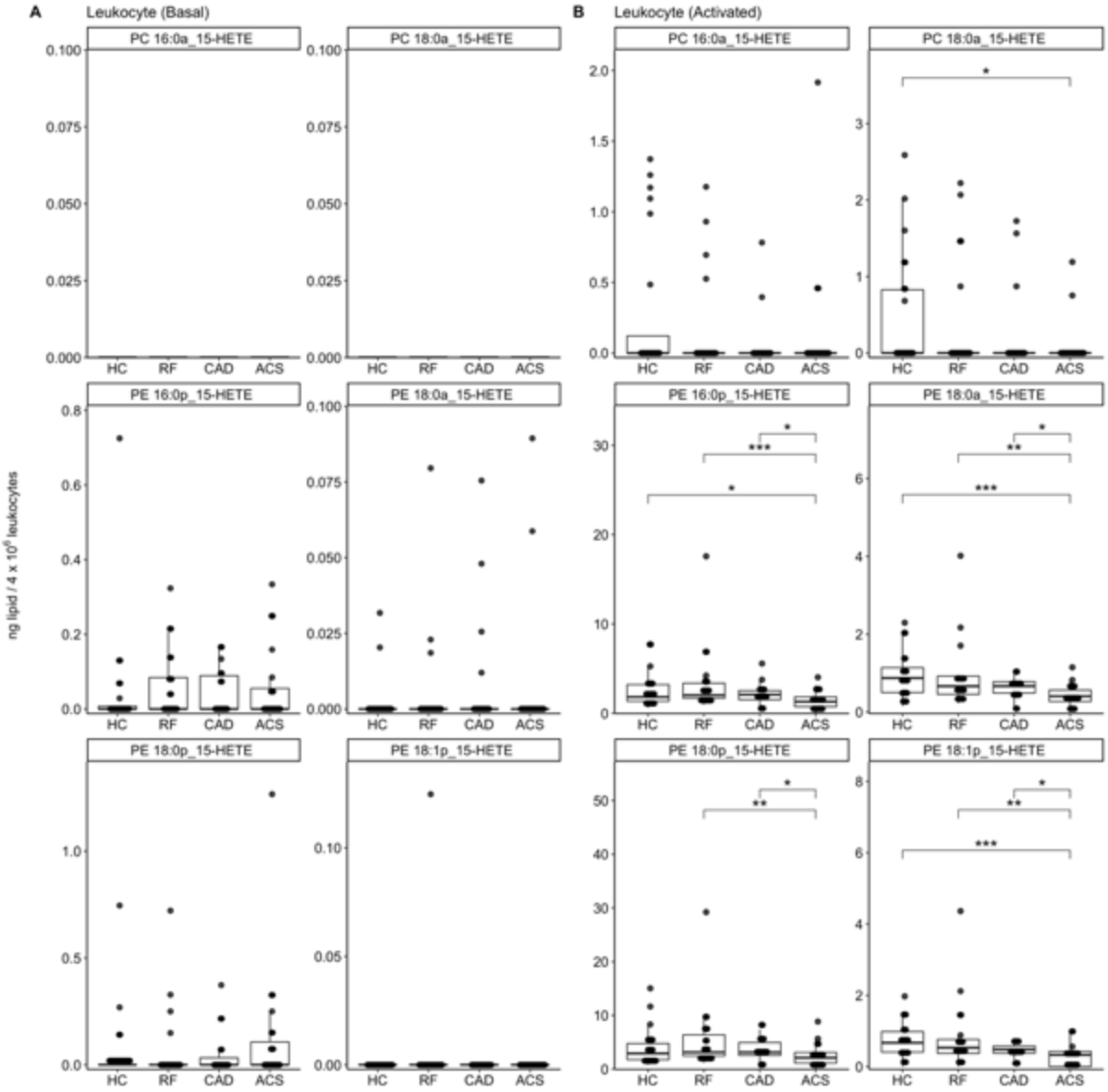

Figure 6.16. Levels of 15-HETE-PL in ionophore-stimulated leukocytes were lower in patients with arterial thrombosis compared with healthy controls.

Lipids were extracted from leukocytes (4 x 10^6) in resting conditions (Panel A) or following activation with A23817 (10μM, Panel B) as in Materials and Methods. Lipids amounts (ng) were calculated by LC-MS/MS and plotted as a box plot with the ggplot2 R package. Box edges indicate the interquartile range (IQR) with the median line inside the box. Whiskers indicate 1.5 times the IQR. Statistical significance was tested with Mann-Whitney-Wilcoxon test, and where significant differences exist, they are indicated by stars (*: $p < 0.05$, **: $p < 0.01$, ***: $p < 0.001$). ACS: acute coronary syndrome (n=24), CAD: coronary artery disease but no ACS (n=19), RF: Risk factors with no significant coronary artery disease (n=23), HC: Healthy control (n=24).

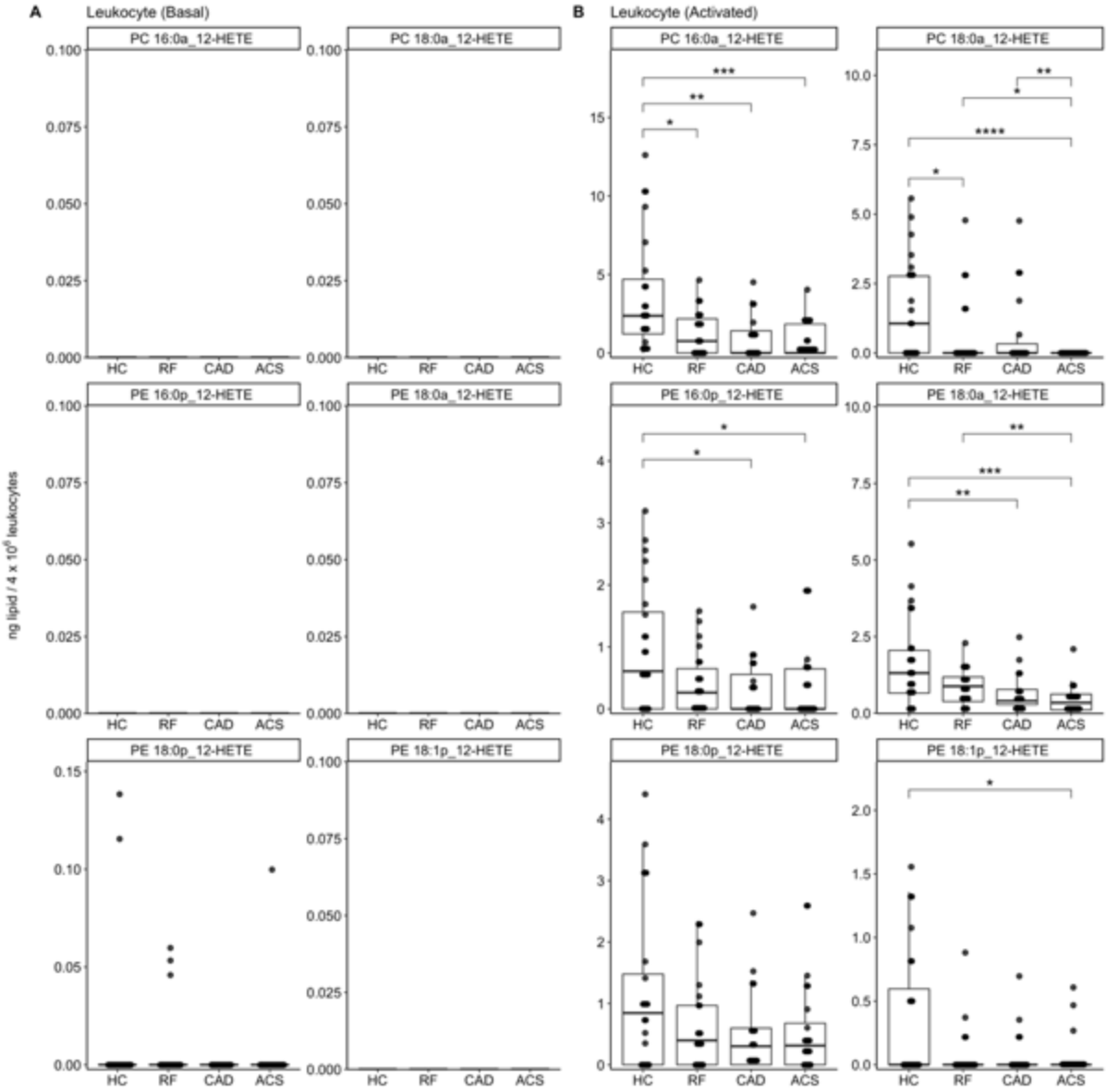

Figure 6.17. Levels of 12-HETE-PL in ionophore-stimulated leukocytes were lower in patients with arterial thrombosis compared with healthy controls.

Lipids were extracted from leukocytes (4 x $10^{6)}$ in resting conditions (Panel A) or following activation with A23817 (10μM, Panel B) as in Materials and Methods. Lipids amounts (ng) were calculated by LC-MS/MS and plotted as a box plot with the ggplot2 R package. Box edges indicate the interquartile range (IQR) with the median line inside the box. Whiskers indicate 1.5 times the IQR. Statistical significance was tested with Mann-Whitney-Wilcoxon test, and where significant differences exist, they are indicated by stars (*: $p < 0.05$, **: $p < 0.01$, ***: $p < 0.001$). ACS: acute coronary syndrome (n=24), CAD: coronary artery disease but no ACS (n=19), RF: Risk factors with no significant coronary artery disease (n=23), HC: Healthy control (n=24).

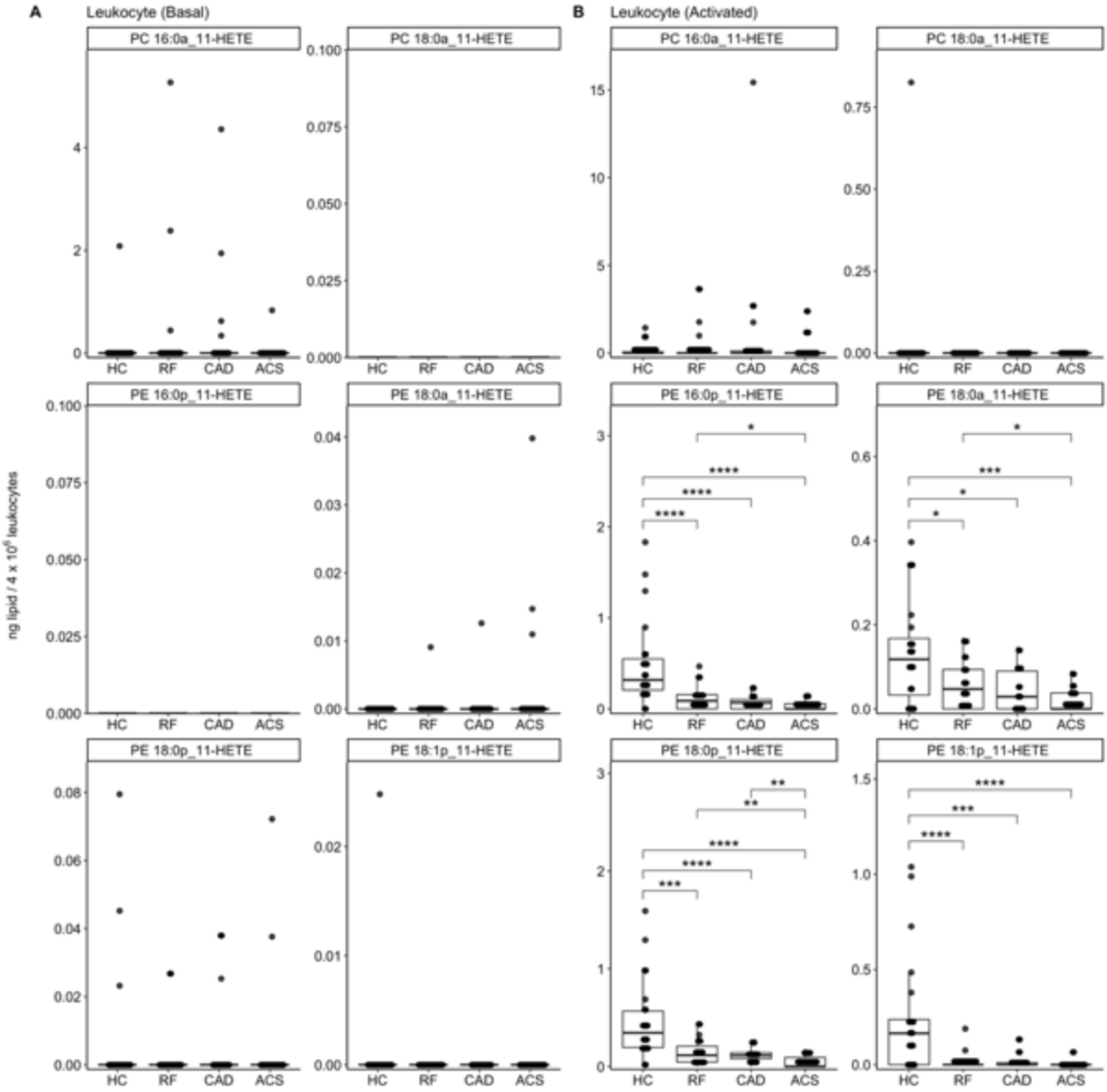

Figure 6.18. Levels of 11-HETE-PL in ionophore-stimulated leukocytes were lower in patients with arterial thrombosis compared with healthy controls.

Lipids were extracted from leukocytes (4 x 10^6) in resting conditions (Panel A) or following activation with A23817 (10μM, Panel B) as in Materials and Methods. Lipids amounts (ng) were calculated by LC-MS/MS and plotted as a box plot with the ggplot2 R package. Box edges indicate the interquartile range (IQR) with the median line inside the box. Whiskers indicate 1.5 times the IQR. Statistical significance was tested with Mann-Whitney-Wilcoxon test, and where significant differences exist, they are indicated by stars (*: p <0.05, **: p <0.01, ***: p <0.001). ACS: acute coronary syndrome (n=24), CAD: coronary artery disease but no ACS (n=19), RF: Risk factors with no significant coronary artery disease (n=23), HC: Healthy control (n=24).

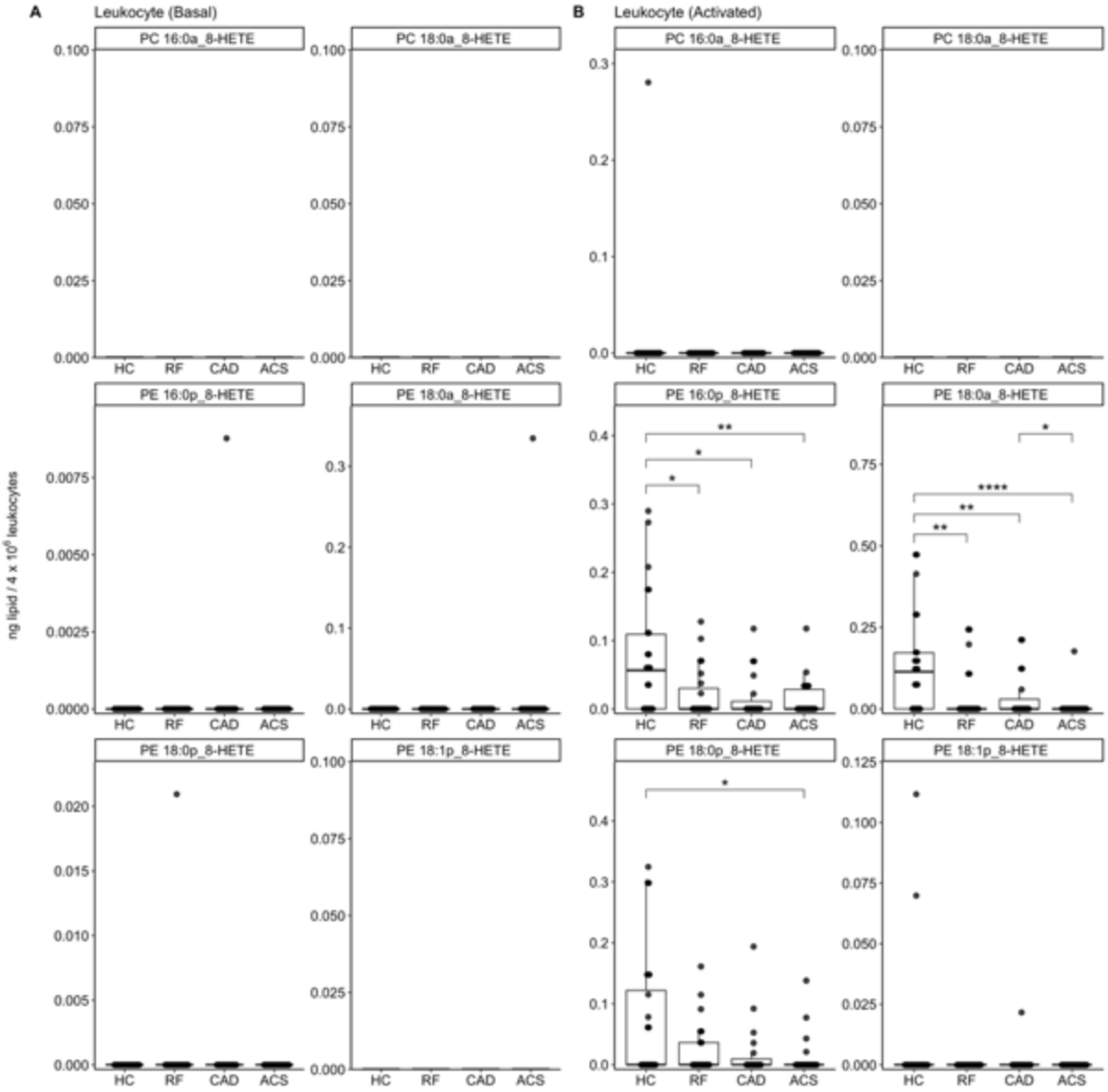

Figure 6.19. Non-enzymatic 8-HETE-PL were detected in small amounts in ionophore-stimulated leukocytes with lower levels in patients with arterial thrombosis compared with healthy controls.

Lipids were extracted from leukocytes (4 x 10^6) in resting conditions (Panel A) or following activation with A23817 (10μM, Panel B) as in Materials and Methods. Lipids amounts (ng) were calculated by LC-MS/MS and plotted as a box plot with the ggplot2 R package. Box edges indicate the interquartile range (IQR) with the median line inside the box. Whiskers indicate 1.5 times the IQR. Statistical significance was tested with Mann-Whitney-Wilcoxon test, and where significant differences exist, they are indicated by stars (*: $p < 0.05$, **: $p < 0.01$, ***: $p < 0.001$). ACS: acute coronary syndrome (n=24), CAD: coronary artery disease but no ACS (n=19), RF: Risk factors with no significant coronary artery disease (n=23), HC: Healthy control (n=24).

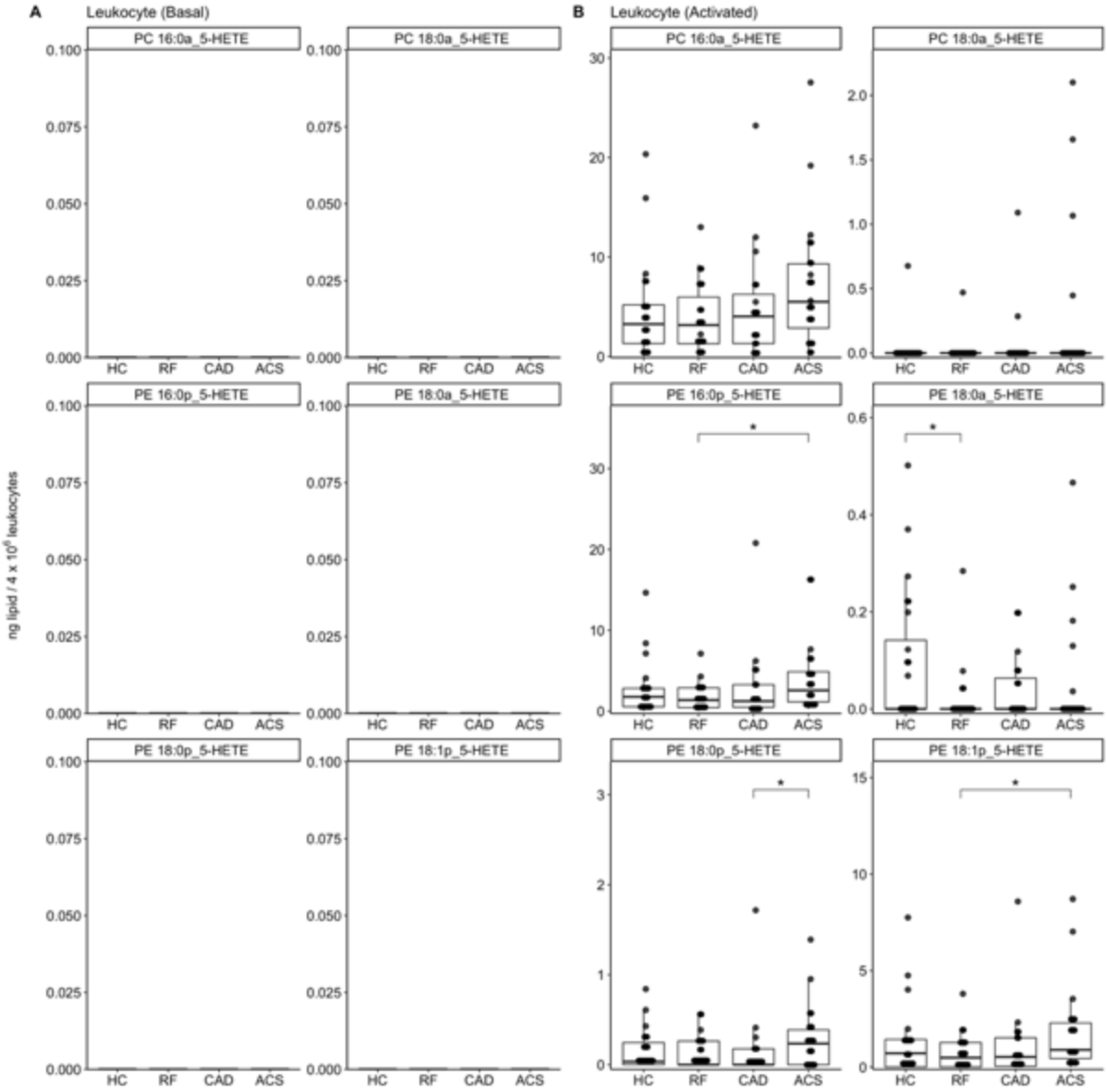

Figure 6.20. Levels of 5-HETE-PL in ionophore-stimulated leukocytes demonstrated a mostly non-significant trend of higher levels in patients with ACS compared with HC.

Lipids were extracted from leukocytes (4 x 10^6) in resting conditions (Panel A) or following activation with A23817 (10μM, Panel B) as in Materials and Methods. Lipids amounts (ng) were calculated by LC-MS/MS and plotted as a box plot with the ggplot2 R package. Box edges indicate the interquartile range (IQR) with the median line inside the box. Whiskers indicate 1.5 times the IQR. Statistical significance was tested with Mann-Whitney-Wilcoxon test, and where significant differences exist, they are indicated by stars (*: $p < 0.05$, **: $p < 0.01$, ***: $p < 0.001$). ACS: acute coronary syndrome (n=24), CAD: coronary artery disease but no ACS (n=19), RF: Risk factors with no significant coronary artery disease (n=23), HC: Healthy control (n=24).

6.2.4 P2Y12 inhibitors may interfere with 12-HETE-PL generation in A23817-activated leukocyte samples

In the previous section (**6.2.3**), the levels of 12-HETE-PL generated by A23817-activated leukocytes were seen to be lower in patients with ACS/CAD/RF compared with HC. Given that 12-HETE-PL is a product of platelet 12-LOX, it is possible that leukocyte samples contain some platelets or platelet-derived EVs either as part of platelet:leukocyte aggregates or as contaminants. It is recognized that P2Y12 inhibitors (clopidogrel, prasugrel or ticagrelor) can impair the ability of platelet:leukocyte aggregates to form[330,331]. This led me to hypothesize that the lower 12-HETE-PL seen in ACS vs HC may be due to lower amounts of platelet:leukocyte aggregates due to P2Y12 supplementation of all ACS patients, some of the RF/CAD patients, but none of the HC participants.

To test this, I analysed the amount of 12-HETE-PL generated by A23817-activated leukocytes samples by P2Y12 inhibitor use. As described previously, the RF and CAD groups were selected for this analysis as they included patients both on and off P2Y12 inhibitors. This analysis demonstrated that 12-HETE-PL generation in A23817-activated leukocytes was significantly lower when patients were taking P2Y12 inhibitors (**Figure 6.21**A). Further analysis of individual 12-HETE-PL species demonstrated lower levels in samples of A23817-stimulated leukocytes from patients on P2Y12 inhibitors for acyl (18:0a, 16:0a), but not ether (plasmalogen: 18:0p, 18:1p, 16:0p) linked 12-HETE-PL at the *sn1* position (**Figure 6.21**B). This suggests that P2Y12 inhibitor use may also have an effect on 12-HETE re-esterification pathways to acyl lysoPL in A23817-activated leukocytes. These findings will be addressed in the discussion section for this chapter.

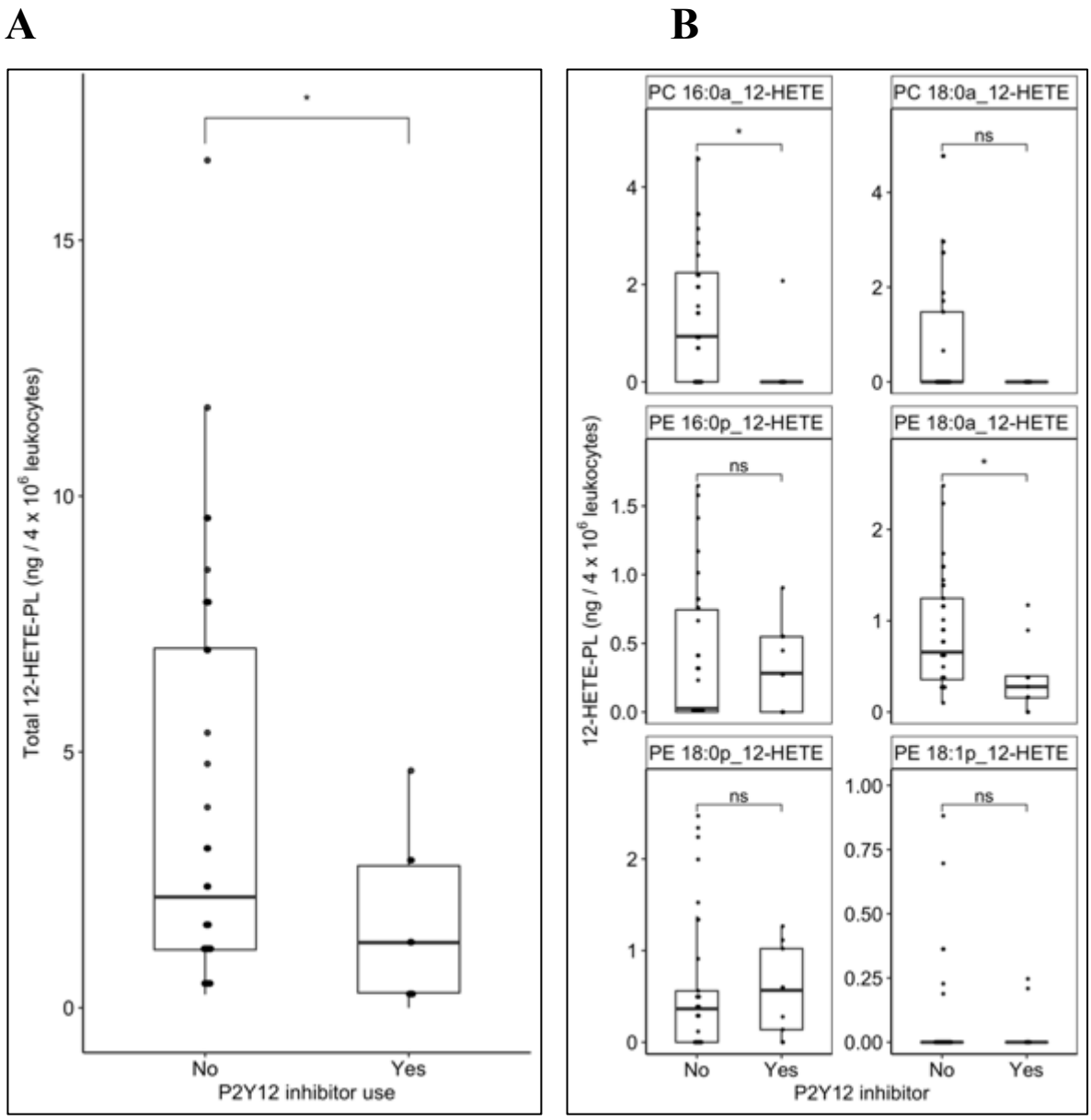

Figure 6.21. Levels of diacyl 12-HETE-PL in ionophore-stimulated leukocytes were lower in patients on P2Y12 inhibitors.

Panel A: The amount of total 12-HETE-PL (the sum of all species) from A23817-activated leukocytes of RF/CAD patients by P2Y12 inhibitor use. Panel B: Examining individual 12-HETE-PL lipid species in RF/CAD patients by P2Y12 inhibitor use. Lipids were extracted from leukocytes (4 x 10^6) following stimulation with A23187 (10μM) as in Materials and Methods. Lipids amounts (ng) were calculated by LC-MS/MS for 6 lipids for each 12-HETE-PL positional isomer (including 4 PE and 2 PC) and combined by *sn2* fatty acid for the total 12-HETE-PL. This was then plotted as a box plot with the ggplot2 R package. Box edges indicate the interquartile range (IQR) with the median line inside the box. Whiskers indicate 1.5 times the IQR. Statistical significance was tested with Mann-Whitney-Wilcoxon test (ns: not significant, *: p <0.05, **: p <0.01, ***:p <0.001). CAD: coronary artery disease (but no acute coronary syndrome, ACS), RF: Risk factors with no significant coronary artery disease.

6.2.5 HETE-PL lipids were not detected in plasma EV samples

To investigate whether plasma EV samples contain HETE-PL, I measured these lipids and demonstrated that they were not detected in the majority of plasma EV samples (>90%) across all patient groups. Where HETE-PL were detected, the total average amounts (ng, pooled by *sn2* fatty acid) were very small (0.06 ng/EV sample for 15-HETE-PL and 0.01 ng/EV sample for 11- and 12-HETE-PL) with no significant differences between clinical groups (**Figure 6.22**). This suggests that unlike activated platelets and leukocytes, HETE-PL are not a major constituent of plasma EV membranes.

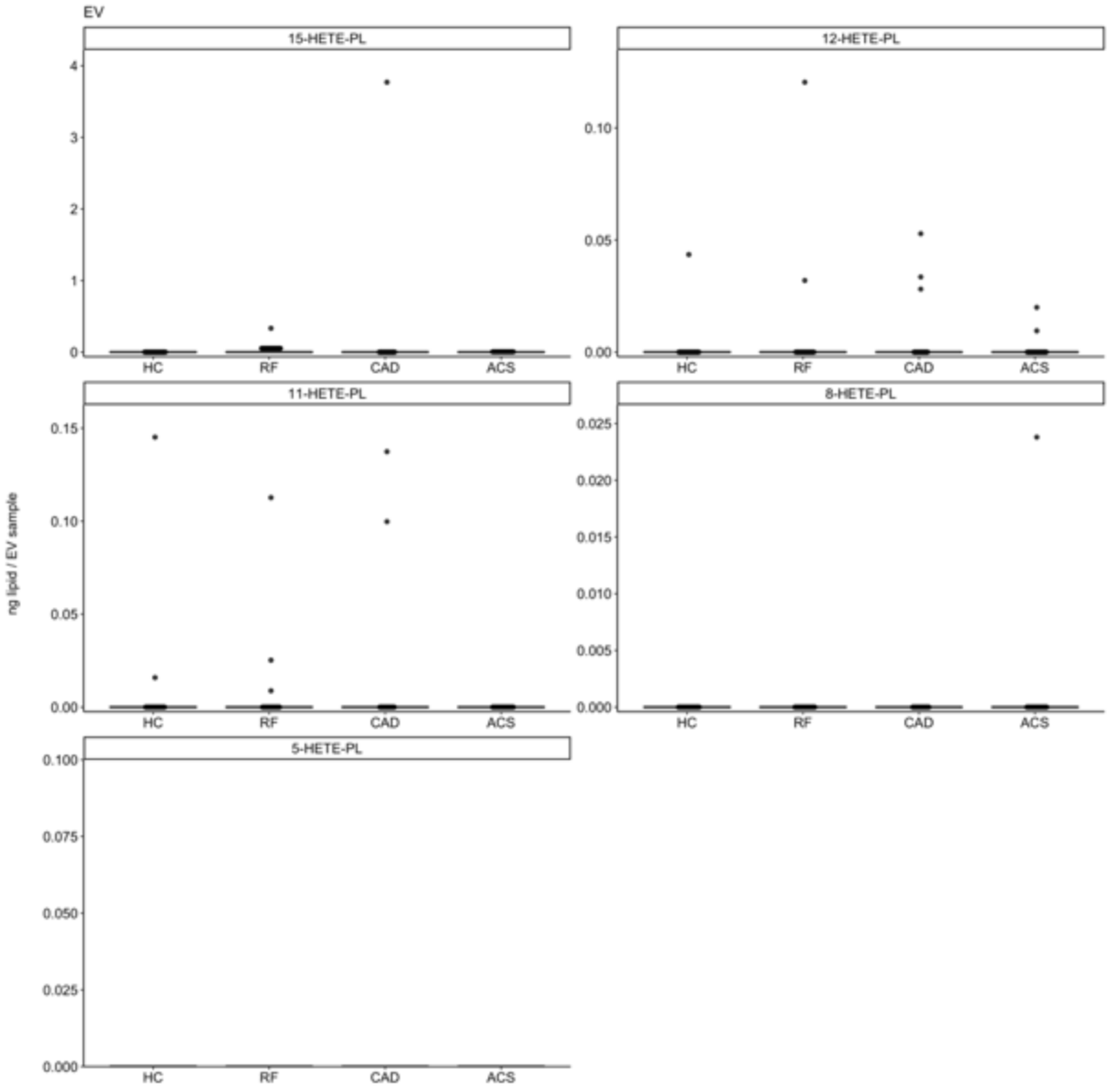

Figure 6.22. HETE-PL lipids were undetectable in plasma EV for the majority of patients.

Extracellular vesicles (EV) were isolated from 6 ml of plasma (as in Materials and Methods) and underwent lipid extraction. Analysis by LC-MS/MS was carried out to determine lipid amounts (ng) for 6 lipids for each HETE-PL positional isomer (including 4 PE and 2 PC, as in Materials and Methods) and combined by *sn2* fatty acid. This was then plotted as a box plot with the ggplot2 R package. Box edges indicate the interquartile range (IQR) with the median line inside the box. Whiskers indicate 1.5 times the IQR. Statistical significance was tested with Mann-Whitney-Wilcoxon test, and where significant differences exist, they are indicated by stars (*: $p < 0.05$, **: $p < 0.01$, ***: $p < 0.001$). ACS: acute coronary syndrome (n=24), CAD: coronary artery disease but no ACS (n=19), RF: Risk factors with no significant coronary artery disease (n=23), HC: Healthy control (n=24).

6.2.6 Diacyl HETE-PL lipids are the main drivers for differences between clinical groups in activated platelets, but not leukocytes

In section **6.2.1**, I showed that the amount of total 12-HETE-PL in thrombin-activated platelets was higher in ACS vs HC (**Figure 6.4B**). This was only seen for 12-HETE-PL with an acyl bond at *sn1*, and not ether (plasmalogen) forms. In this section, I explored this further in all HETE-PL positional isomers, carrying out a subgroup analysis by *sn1* bond type on both platelets and leukocytes

In resting platelets, no differences were seen for HETE-PLs between clinical groups for diacyl and plasmalogen forms (**Figure 6.23**A). However, in thrombin-activated platelets, the previously described increase in 12-HETE-PL between HC and ACS was again only observed when an acyl, not ether (plasmalogen), bond was present at the *sn1* position (**Figure 6.23**B). This was also observed for 8-HETE-PL which had significantly higher amounts in ACS vs HC in diacyls, but not plasmalogens. This pattern was not seen for other HETE-PL positional isomers which had similar profiles for both diacyls and plasmalogens.

In leukocytes, the profiles for 15-, 5- and 8-HETE-PL generated with A23817 stimulation were similar for both diacyl and plasmalogen lipids (**Figure 6.24**B). The lower levels of 12-HETE-PL in ACS vs HC were only statistically significant for acyl 12-HETE-PLs. The opposite pattern was seen for 11-HETE-PL which demonstrated lower levels in ACS vs HC in plasmalogens, but not diacyls. The latter finding however may be limited by the low overall diacyl 11-HETE-PL levels across the groups which may statistically inflate small differences.

Taken together, these findings demonstrate that HETE-PL differences between patient groups may be specific to the type of *sn1* bond.

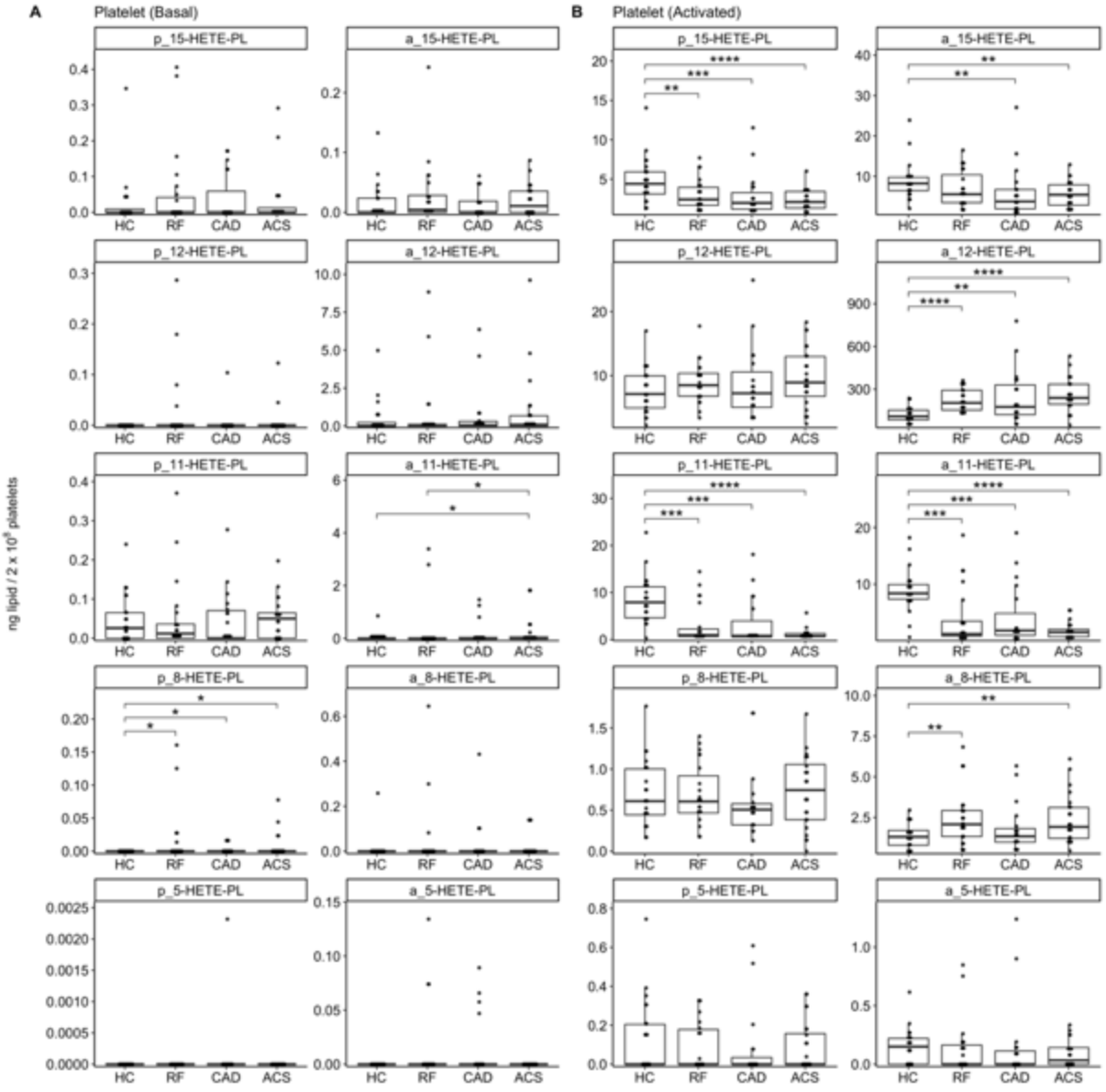

Figure 6.23. Subgrouping platelet HETE-PL by *sn1* bond demonstrates higher levels of diacyl (but not plasmalogen) 12-HETE-PL in thrombin-activated platelets from patients with ACS vs HC.

Lipids were extracted from platelets (2 x 10^8) in resting conditions (Panel A) or following activation with thrombin (0.2 U/ml, Panel B) as in Materials and Methods. Lipids amounts (ng) were calculated by LC-MS/MS for 6 lipids for each HETE-PL positional isomer (including 4 PE [3 plasmalogens, 1 diacyl] and 2 PC [both diacyls]) and combined by *sn1* (acyl – indicated by prefix 'a_'; plasmalogen – indicated by 'p_') and *sn2* (positional isomer) fatty acid. This was plotted as a box plot with edges indicating the IQR, whiskers 1.5x IQR and median line inside the box. Statistical significance was tested with Mann-Whitney-Wilcoxon test, and where significant differences exist, they are indicated by stars (*: p <0.05, **: p <0.01, ***: p <0.001). ACS: acute coronary syndrome, CAD: coronary artery disease (but no ACS), RF: Risk factors with no significant coronary artery disease, HC: Healthy controls.

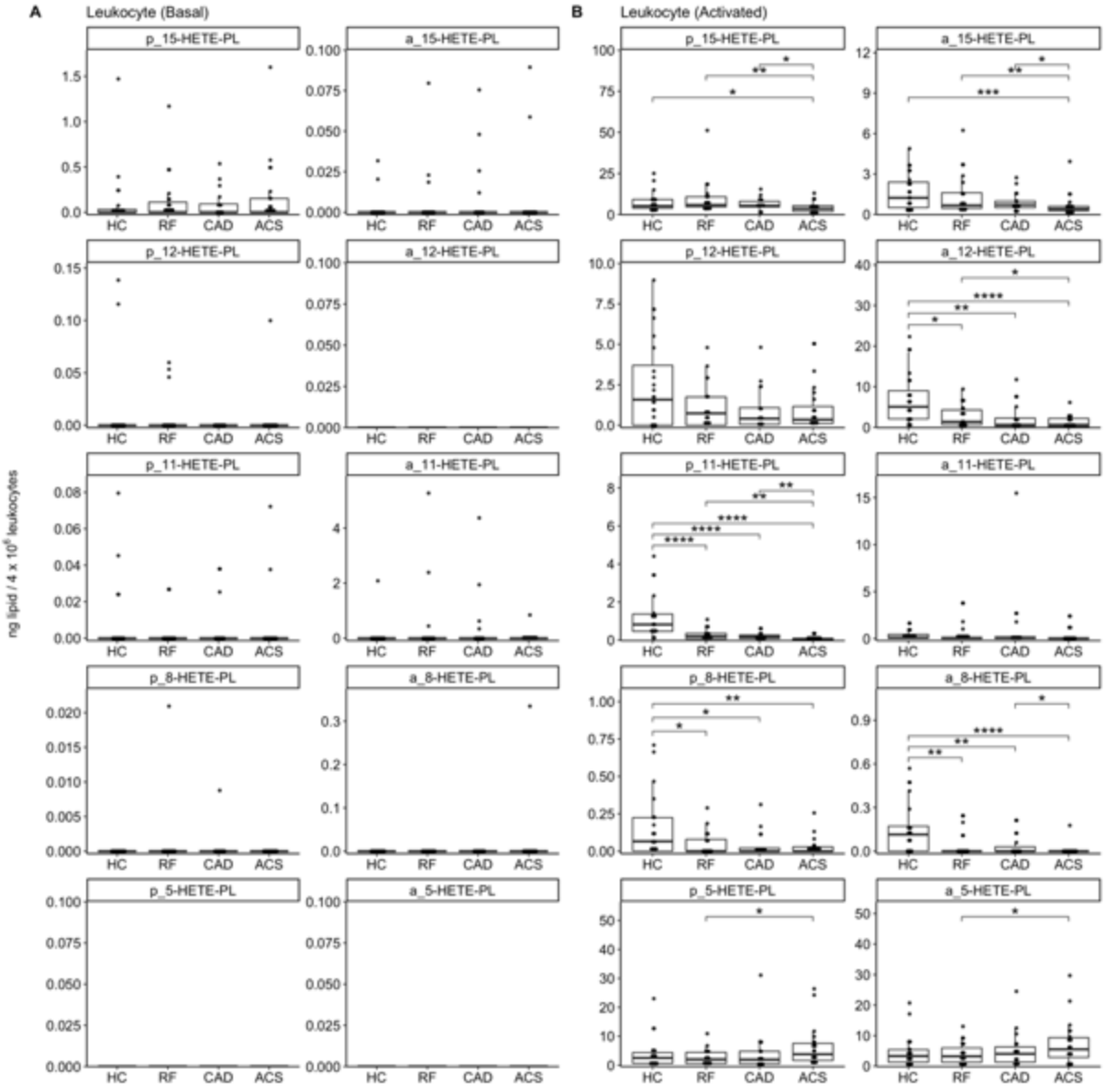

Figure 6.24. Leukocyte HETE-PL trends were similar for diacyls and plasmalogens.

Lipids were extracted from leukocytes (4 x 10^6) in resting conditions (Panel A) or following activation with A23817 (10μM, Panel B) as in Materials and Methods. Lipids amounts (ng) were calculated by LC-MS/MS for 6 lipids for each HETE-PL positional isomer (including 4 PE [3 plasmalogens, 1 diacyl] and 2 PC [both diacyls]) and combined by *sn1* (acyl – indicated by prefix 'a_'; plasmalogen – indicated by 'p_') and *sn2* (positional isomer) fatty acid. This was plotted as a box plot with edges indicating the IQR, whiskers 1.5x IQR and median line inside the box. Statistical significance was tested with Mann-Whitney-Wilcoxon test, and where significant differences exist, they are indicated by stars (*: p <0.05, **: p <0.01, ***: p <0.001). ACS: acute coronary syndrome, CAD: coronary artery disease (but no ACS), RF: Risk factors with no significant coronary artery disease, HC: Healthy controls.

6.2.7 HETE-PL amounts positively correlate with thrombin generation in platelets, but not leukocytes or plasma EV.

To investigate the relationship of HETE-PL levels with coagulation capacity of plasma membranes, correlation plots were generated (**Figure 6.25**). These examined the relationship between HETE-PL species pooled by *sn2* positional isomer described in this chapter with thrombin generation on the surface of resting platelets, resting leukocytes and plasma EV, as shown in **Chapter 5**.

This analysis demonstrated positive correlation between some HETE-PL species and thrombin generation on the surface of resting platelets, but not resting leukocytes or plasma EV. Specifically, the only significant correlations were between thrombin generation on the surface of resting platelets and the levels of 15-, 5- and 8-HETE-PL. These however were weak with R values ranging from 0.22 – 0.40.

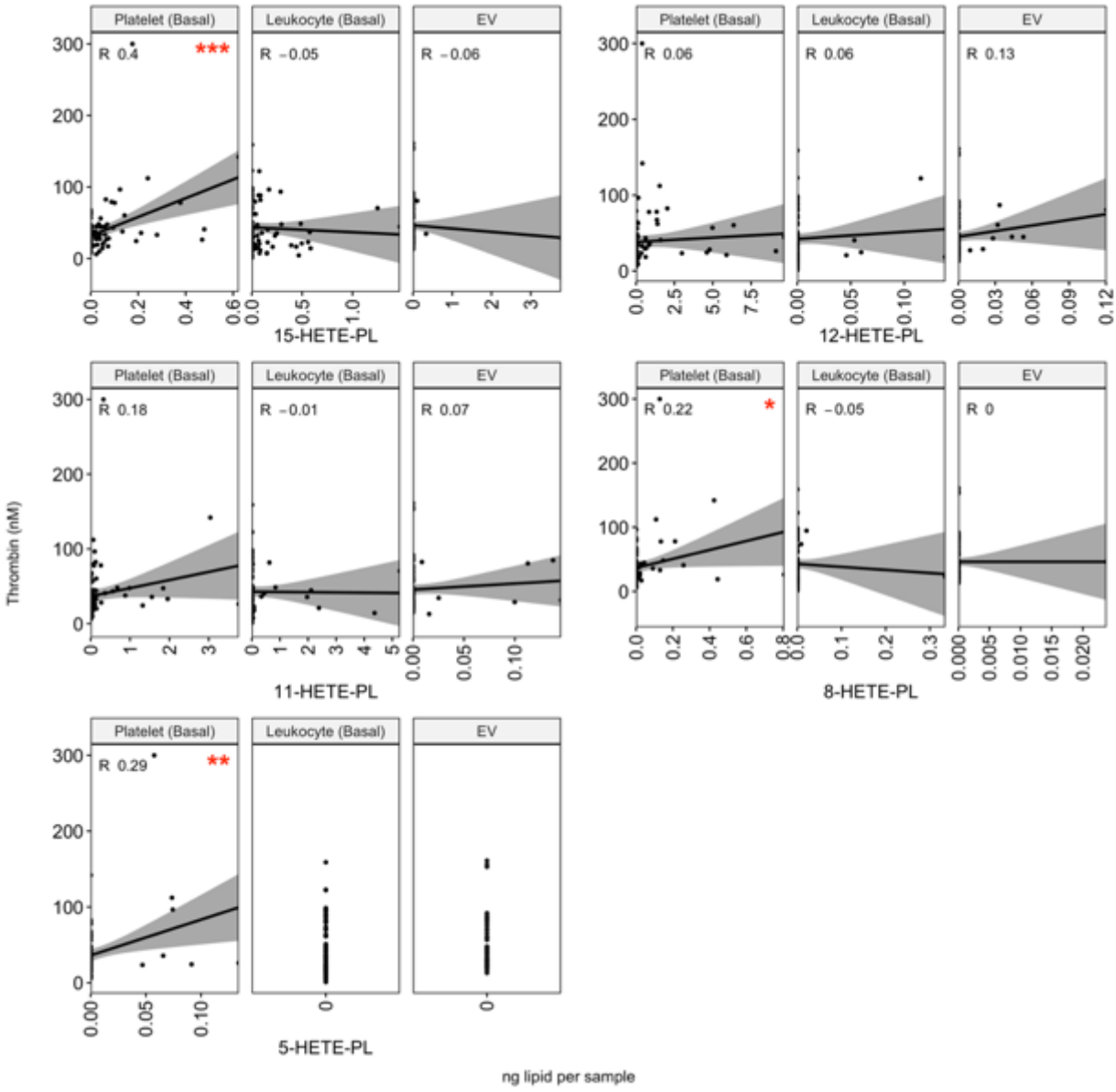

Figure 6.25. There is correlation between some HETE-PL species and thrombin generation on the surface of resting platelets, but not resting leukocytes or plasma EV.

A correlation analysis of thrombin generation on the surface of resting platelets, resting leukocytes and plasma EV with HETE-PL lipid species pooled by *sn2* fatty acid is shown in this diagram. The correlated data was generated from the prothrombinase assay and HETE-PL lipid quantification for all patients (as in Materials and Methods), Pearson's R correlation coefficients and significance was calculated and graphs plotted with the ggplot2 R package. *: $p < 0.05$, **: $p < 0.01$, ***: $p < 0.001$.

6.3 DISCUSSION

In this chapter, characterisation of the HETE-PL composition of platelets, leukocytes and plasma EV using LC-MS/MS techniques was carried out in patients with ACS and CAD compared with RF and HC. This demonstrated that HETE-PL lipids were detected in low amounts in resting platelets, resting leukocytes and in plasma EV samples across all patient groups with no significant differences between patients with ACS/CAD and HC/RF in resting states. As predicted, the levels of HETE-PL increased upon activation of platelets (thrombin) and leukocytes (A23817), which is consistent with previous studies and relates to their agonist-induced enzymatic generation[40]. Here, differences were noted between clinical groups in the amounts of HETE-PL generated by platelets and leukocytes, which seemed to be driven by the use of aspirin and P2Y12 inhibitors.

Since all ACS patients were taking aspirin, and none of the HC patients were, the finding of higher 12-HETE-PL levels in thrombin-activated platelet from ACS patients are likely explained by use of aspirin. This is driven by higher amounts of diacyl species of 12-HETE-PL, since the levels of plasmalogen species did not differ between groups (**Figure 6.9**). These findings may potentially suggest that aspirin affects the re-esterification process of platelet 12-HETE based on the *sn1* composition of lysoPL. This is consistent with findings described previously in **Chapter 3**, where paired platelet samples from the same individuals on/off aspirin demonstrated more diacyl 12-HETE-PL generation on aspirin which was not related to the amount of free 12-HETE. The exact location in the HETE-PL synthesis pathway where aspirin acts remains unknown, but based on current findings and those demonstrated in **Chapter 3**, aspirin is likely acting downstream of free oxylipin formation and therefore may relate to the functionality or expression profile of the platelet LPAT family of enzymes responsible for the re-esterification of oxylipin-CoAs. LPAT enzymes acylate multiple, but

distinct, lysoPL lipids due to varying specificity and may also make a distinction between FA-CoA based on chair length and saturation status. Examples include LPCAT-3, which is present in the platelet proteome, and has been described to favour acyl lysoPL over 1-O-alkyl lysoPL[332,333]. It is possible therefore that aspirin, either directly or indirectly through TxA_2 signalling, is promoting the activity of LPATs that utilise lysoPL with an acyl bond at *sn1*, but not ether bonds (alkyl and alkenyl lysoPL).

In **Chapter 3**, the higher levels of 12-HETE-PL in thrombin-activated platelets from patients on aspirin (versus not) were seen in men, but not women. This was not observed in the current chapter where 12-HETE-PL profiles in thrombin-activated platelets were consistently higher in ACS (all on aspirin) vs HC (none of aspirin) irrespective of gender (**Figure 6.13**). Subgrouping by both aspirin and gender was not possible for RF/CAD as there were fewer participants than statistically acceptable in some sub-groups. Nevertheless, the absence of a gender influence on the effect that aspirin has on 12-HETE-PL in this chapter raises the possibility that ACS and its associated inflammatory state may affect 12-HETE-PL levels by directly interfering with platelet behaviour irrespective of gender or aspirin. However, it is important to note the difference in age between participants in the two cohorts, who were older (mean age 65 years) in the current clinical cohort than the previously studied healthy cohort (age range 20-50 years) in **Chapter 3**. This age difference makes the two cohorts less comparable, but may suggest age-specific/hormone-related differences (e.g. post-menopause) in the effect aspirin has on eoxPL generation, which remains unknown.

The detection of 12-HETE-PL in A23817-activated leukocytes likely reflects the presence of platelets or platelet-derived EV in the samples, since human leukocytes do not possess the 12-LOX isoform and the ability to generate 12-HETE-PL. This was previously described in a

paper published by our group utilising the same methods for leukocyte isolation from patients with antiphospholipid syndrome and healthy controls. In that study, leukocyte samples contained 12-HETE-PE which increased upon stimulation with A23817 and thus this was thought to be derived from platelets or platelet-derived EVs present in the samples[69]. These may be present as contaminants, or in the form of platelet-leukocyte aggregates. Such aggregates are well known to result from interactions and adhesions between platelets and a variety of leukocytes including neutrophils and monocytes[334]. Whilst present physiologically in low levels, these heterotypic aggregates often positively correlate with the degree of inflammation[334]. This goes against my observed trend of lower 12-HETE-PL in A23817-activated leukocytes from ACS, an inflamed state, compared with HC. Nevertheless, one factor which reduces platelet-leukocyte aggregates is the use of P2Y12 inhibitors[330,331,334]. Indeed, in our samples, we noted that the levels of 12-HETE-PL in A23817-activated leukocyte samples were lower in patients on P2Y12 inhibitors compared with those who were not (**Figure 6.21**). This observation however was only seen for 12-HETE-PL with an acyl, but not an ether (plasmalogen), bond at *sn1*. This argues against platelet:leukocyte aggregates as the source, as one would expect lower overall 12-HETE-PL with P2Y12 inhibitors irrespective of *sn1* bond. Nevertheless, platelet-leukocyte aggregates must still be considered as one of the possible sources of 12-HETE-PL which are affected by P2Y12 inhibitors as described earlier. Indeed, it is worth noting that all ACS patients, but none of the HC participants, received P2Y12 inhibitors prior to sample collection which is compatible with the findings of lower 12-HETE-PL in A23817-activated leukocyte samples from ACS patients (v HC) seen in **Figure 6.17**. Overall, these findings suggest a complex interaction between HETE-PL, disease state and pharmacotherapy (P2Y12 inhibitors).

The very low levels of HETE-PL in resting cells (platelets and leukocytes) and EV suggests that they are not the main drivers of the *in vitro* prothrombinase activity described on the surface of these cells in **Chapter 5**. In fact, the only HETE-PL which was significantly higher in resting cells from CAD/ACS (v HC) was the non-enzymatically generated 8-HETE-PL in platelets (**Figure 6.2**). However, 8-HETE-PL levels were very low and likely reflect an underlying oxidative stress state in patients with advanced atherosclerosis. Whilst 8-HETE-PL correlated weakly (but significantly) with the amount of thrombin generation on the surface of resting platelets (**Figure 6.25**), there were no significant differences between groups in prothrombinase activity on the surface of platelets. The fact that the prothrombinase assay is designed to examine thrombin generation on the surface of unstimulated platelets and leukocytes does not account for the complex feedback loops between activated cell membranes and the coagulation system. This is particularly important to address as the differences in HETE-PL profiles described in this chapter occurred mainly in activated cells (platelets/leukocytes), which would not have taken part in the prothrombinase assay. This point of course is not relevant to EV which are acellular particles studied in their resting state. Whilst oxPL have been reported in plasma EV, these were non-enzymatically generated oxPC secondary to oxidative stress and not enzymatically generated HETE-PLs being examined here[194,335].

The majority of the literature on oxPL in ACS focuses on lipoproteins, specifically oxLDL which is characterised by the presence of oxidized proteins and lipids[336,337]. These studies have focused mainly on the atherogenic potential of oxPL (predominantly non-enzymatically generated oxPC) in facilitating macrophage uptake of OxLDL, subsequent foam cell formation, inflammation and atherosclerosis progression[336,338]. Differences in the platelet oxidized lipidome in ACS/CAD have been described recently by Chatterjee et al, demonstrating higher

levels of platelet oxPC in ACS/CAD compared to matched controls[68]. However, the oxPC species described in that publication were predominantly generated non-enzymatically or truncated from larger lipids, in contrast to HETE-PLs which were the focus of this work. They describe a possible mechanism for formation of oxPL based on platelet uptake of LDL, and subsequent generation of oxidized and peroxidised lipids by reactive oxygen species (ROS). Beyond this, there have been no studies to date examining the platelet or leukocyte lipidome in ACS as it relates to enzymatic pathways of eoxPL generation, highlighting the novelty of my current study.

6.4 CONCLUSION

In conclusion, this chapter demonstrates a complex interaction between HETE-PL, coronary artery disease and pharmacotherapy (aspirin with platelets/P2Y12 inhibitors with leukocytes). Platelets generated higher levels of 12-HETE-PL upon thrombin-activation in patients with ACS compared with HC. A similar phenomenon was observed in CAD/RF patients on aspirin compared to those not taking aspirin. These observations were unique to 12-HETE-PL that contain an acyl, not ether (plasmalogen), bond at the *sn1* position in both PE/PC headgroups. This may, at least in part, be due to a possible differential effect that aspirin has on diacyl vs plasmalogen 12-HETE-PL generation and re-esterification, which remains untested. Leukocytes demonstrated overall lower levels of 12-HETE-PL in ACS patients after A23817 activation, which may be related to P2Y12 inhibitor use. The amounts of HETE-PL in resting cells and plasma EV were very low, making them unlikely to contribute to differences in membrane thrombotic potential described in previous chapters with plasma EV and leukocytes.

CHAPTER 7 CHARACTERISING THE APL COMPOSITION OF PLATELETS, LEUKOCYTES AND EV IN AN ARTERIAL THROMBOSIS COHORT.

7.1 INTRODUCTION

The presence of aPL on the external leaflet of the plasma membrane is critical for initiating coagulation reactions[22,339]. The negatively charged head groups on PS allow the calcium-mediated binding and assembly of coagulation factors on the surface of activated cells and EV which is enhanced by the presence of PE[22,24,279]. In resting cells, aPL are maintained on the internal leaflet of the plasma membrane via the action of the ATP-consuming 'flippase/floppase' enzymes. This asymmetry is lost upon cell stress or activation by virtue of 'scramblase' activity. This exposes aPL to the external leaflet of the membrane and enables coagulation reactions to take place[22,24]. The other group of membrane-bound structures which contain aPL are EV, defined by aPL positivity as traditionally detected by annexin V or lactadherin binding[22,340]. Whether the aPL composition and amount varies in prothrombotic disease states, such as ACS, is largely unstudied and will form the focus of this chapter.

The majority of the literature on aPL trafficking and detection utilises a flow cytometry-based method which relies on aPL-binding fluorescent probes[341-343]. The commonest of these is annexin V-FITC, which can bind to either PS or PE in the presence of calcium [342,343]. There are a number of limitations to this method, the main one being its non-quantitative nature. The binding of annexin V probes to cells and EV during flow cytometry exhibits rapidly saturated kinetics, likely as a result of steric hindrance preventing additional aPL from binding to this large protein[20]. Consequently, whilst it is feasible to count annexin V^{+ve} cells and EV using this method, it is not possible to quantify how much aPL is on the surface, distinguish between PS and PE or know what molecular species are exposed. This is relevant since recent studies have shown that the procoagulant activity of aPL is influenced by fatty acyl composition, with an impaired ability of PE comprising shorter FA chains to support coagulation [20]. Mass spectrometry with biotin derivatisation allows the quantitative analysis of aPL molecular

species, distinguishing between external and total aPL amounts [117]. To date, no studies have reported on externalisation of aPL species in blood cells from patients with ACS, or their contribution to procoagulant reactions in this thrombotic condition.

In a previous **Chapter 5**, I demonstrated that thrombin generation on the surface of leukocytes and EV was higher in patients with ACS compared with HC. In addition, there was more thrombin generation on the surface of plasma EV from CAD/RF patients compared with HC. One possible contributor to this enhanced thrombin generation could be differing aPL composition of the cell surface. As discussed previously, patients with ACS demonstrate higher levels of circulating TAT/FDP indicating endogenous activation of coagulation is higher[288]. Whilst this is likely to be multifactorial, there is some evidence of higher numbers of circulating cells and EV with externalised aPL, as detected by annexin V binding, in ACS[344]. However, there are no studies quantifying the amount or proportion of aPL externalised on the surface of circulating cells and EV in ACS, nor any analysis of the different PS and PE molecular species on the surface.

In this chapter, I will analyse aPL in platelets, leukocytes and plasma EV in patients with ACS, CAD, RF and HC. Using LC-MS/MS, quantitative profiling of PS and PE species will be undertaken for both total and externalised lipids. The aim is to establish whether patients with coronary disease (ACS/CAD) have different aPL profiles from those without (RF/HC). In addition, using the clinical cohort, prothrombinase data generated in **Chapter 5**, correlations between aPL species and the ability of membranes to support coagulation reactions will be carried out to establish the relevance of aPL species to coagulation.

7.2 RESULTS

7.2.1 Platelet aPL lipids cluster by *sn2* fatty acid

To visualise the amounts of total (throughout the membrane) and externalised (on outer leaflet only) platelet aPL lipids across the clinical groups, I initially plotted the data on a heatmap (**Figure 7.1**A). Platelets from all clinical groups externalised more aPL in thrombin-activated samples compared with resting levels. This is consistent with the expected activation of 'scramblase' enzymes and loss of membrane asymmetry[20]. Platelets from RF patients had a lower amount (ng per 2 x 10^8 platelets) of externalised aPL species compared to the other groups, both in resting and thrombin-activated states. Thrombin-activated platelets contained similar or slightly lower levels of total aPL compared to resting platelets (**Figure 7.1**B), presumably secondary to phospholipase activation and hydrolysis of membrane aPL[26,345]. Of note however, higher amounts of total PE and PS were seen in the CAD group compared to other groups in both resting and thrombin-activated platelets.

Hierarchical clustering of the dataset shows grouping of externalised aPL by *sn2* fatty acid irrespective of head group, with lipids containing AA grouping separately from lipids containing oleic acid (**Figure 7.1**A). A similar clustering pattern by *sn2* fatty acid was seen with total aPL lipids (**Figure 7.1**B). This may be due to a higher abundance of AA-containing aPL compared to those containing oleic acid.

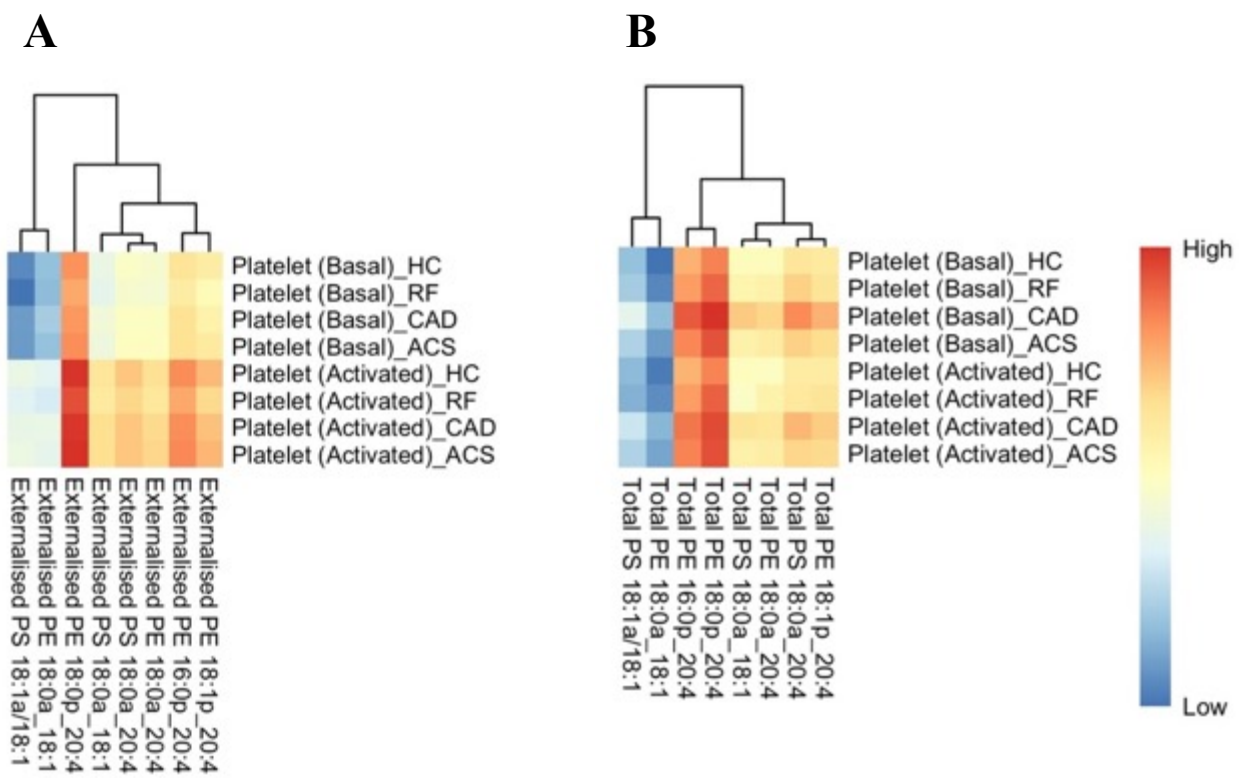

Figure 7.1. Heatmap of aPL lipids in platelets from patients with arterial thrombosis demonstrates higher externalisation with thrombin-activation, with clustering by *sn2* fatty acid.

Panel A: Externalised aPL. Panel B: Total aPL. Lipids were extracted from resting platelets (2 x 10^8) or following activation with thrombin (0.2 U/ml) as in Materials and Methods. Lipids amounts (ng per 2 x 10^8 platelets) were calculated by LC-MS/MS, log10 transformed and plotted as a heatmap with hierarchical clustering using the pheatmap R package. ACS: acute coronary syndrome (n=24), CAD: coronary artery disease but no ACS (n=19), RF: Risk factors with no significant coronary artery disease (n=23), HC: healthy control (n=24).

7.2.2 Quantitative analysis of platelet aPL demonstrates more external PS 18:0a_18:1 and PE 18:0a_20:4 in ACS vs HC, but no differences in fraction (%) aPL externalised

To quantify differences between clinical groups and test for statistical significance, box plots were generated. Platelet aPL lipids were summed by head group (PS or PE) in order to obtain an overview of differences between clinical groups and test for statistical significance (**Figure 7.2**). On thrombin-activation of platelets, the average amount of externalised aPL increased by approximately 4-fold for PE and 6-fold for PS compared with resting platelets. For both resting and thrombin-activated platelets, there were significantly higher levels of total PS and PE in CAD compared with HC. Externalised PS and PE were significantly higher in resting platelets from ACS and CAD compared with RF, whereas thrombin-activated platelets had significantly higher externalised PE, but not PS, in ACS compared with RF (**Figure 7.2**). These findings are consistent with a thrombin-induced aPL externalisation expected in platelets from mobilising 'scramblase' enzymes[26], and showed that the pattern of differences between groups seen in resting states is also observed in thrombin-activated platelets.

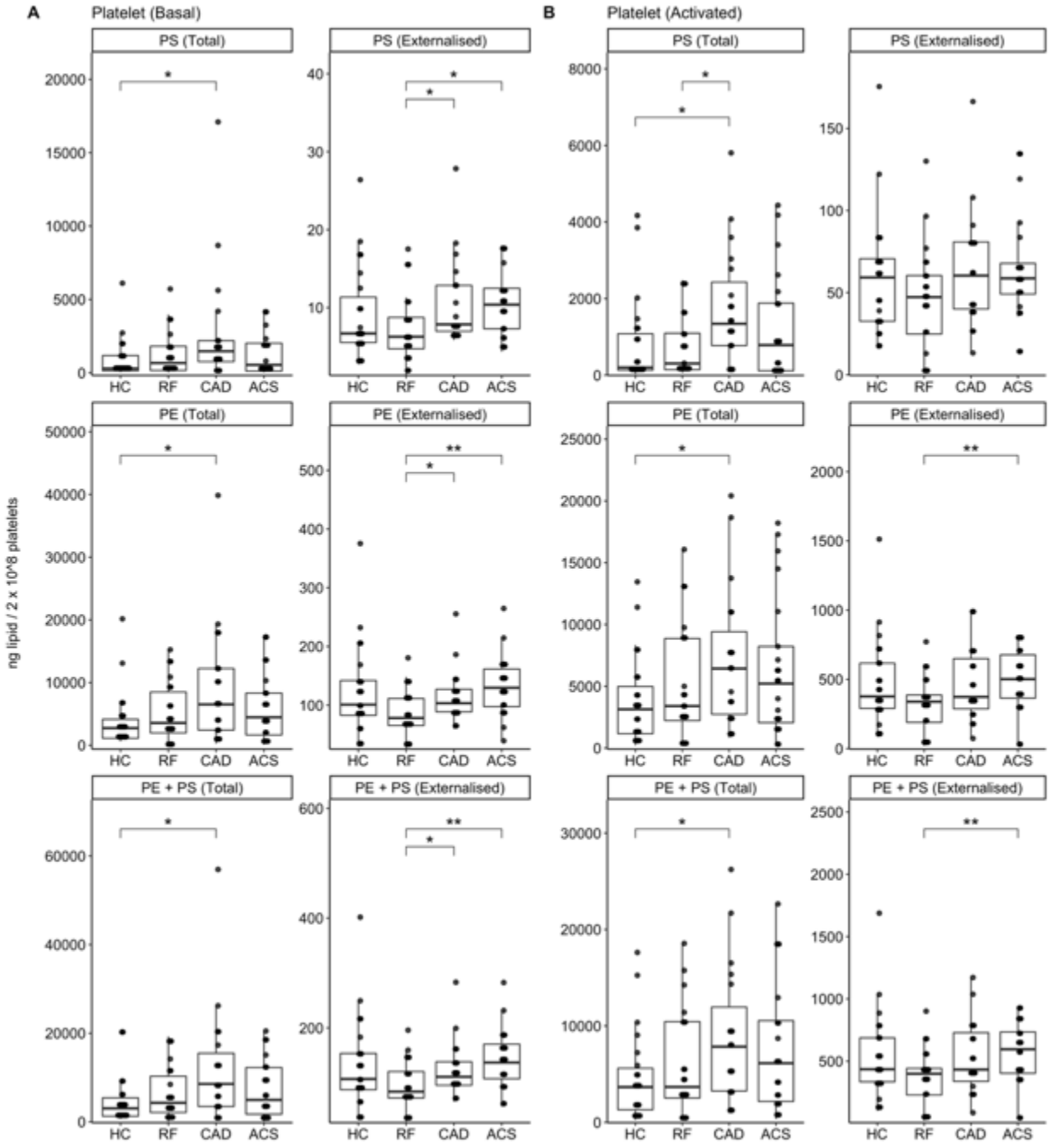

Figure 7.2. Summing platelet aPL lipids by headgroup demonstrates more PS/PE externalisation in ACS and CAD (v RF) in resting conditions.

Lipids were extracted from resting platelets (2 x 10^8) (Panel A) or following activation with thrombin (0.2 U/ml, Panel B) as in Materials and Methods. Lipids amounts (ng) were calculated by LC-MS/MS, summed by head group and plotted as a box plot with the ggplot2 R package. Box edges indicate the interquartile range (IQR) with the median line inside the box. Whiskers indicate 1.5 times the IQR. Statistical significance was tested with Mann-Whitney-Wilcoxon test, and where significant differences exist, they are indicated by stars (*: $p < 0.05$, **: $p < 0.01$, ***: $p < 0.001$). ACS: acute coronary syndrome (n=24), CAD: coronary artery disease but no ACS (n=19), RF: Risk factors with no significant coronary artery disease (n=23), HC: healthy control (n=24).

Next, I expanded on the overview presented above by examining aPL species which may drive the patterns observed with the summed PS/PE lipids. Starting with total (throughout the membrane) aPL, the levels of total PE were similar between ACS compared with other groups for all PE species in both resting and thrombin-activated platelets (**Figure 7.3**). There were however significantly higher levels of total PE species in the CAD group compared to HC in resting and thrombin-activated platelets. This was observed for all PE species studied. Likewise, the levels of total PS in platelets were similar between ACS and other groups including HC (**Figure 7.4**). However, the CAD group demonstrated higher levels of total PS compared with HC in both resting and thrombin-activated platelets for all PS species examined. Overall, these data indicate no difference in total aPL between ACS and HC, but higher levels in CAD v HC, for both resting and thrombin-activated platelets.

The levels of most externalised PE species in resting platelets were higher in ACS patients compared to HC and/or RF groups (**Figure 7.5**). Specifically, there were significantly higher levels of externalised PE 16:0p_20:4 (v RF), PE 18:1p_20:4 (v RF), PE 18:0p_20:4 (v RF) and PE 18:0a_20:4 (v HC/RF). Patients with CAD had higher levels of externalised PE 18:0a_18:1 (v HC/RF) and a similar pattern to ACS for externalised PE 16:0p_20:4, PE 18:1p_20:4 and PE 18:0a_20:4. In thrombin-activated platelets, similar patterns to resting conditions were observed in ACS for externalised PE 16:0p_20:4, PE 18:1p_20:4, PE 18:0p_20:4 and PE 18:0a_20:4 (v RF only). Externalised PS species were also detected in higher levels in resting platelets from ACS patients compared to HC and/or RF. Specifically, there were significantly higher levels of externalised PS 18:0a_18:1 (v HC/RF) and PS 18:0a_20:4 (v RF). Patients with CAD also had higher levels of externalised PS 18:0a_18:1 compared with HC/RF. In thrombin-activated platelets, similar patterns were observed in ACS for externalised PS 18:0a_18:1 (higher in ACS vs RF only), with the addition of a significantly higher externalised PS 18:1a/18:1 (v RF). Overall, the amount

of externalised aPL was higher in ACS v HC/RF on the surface of both resting and thrombin-activated platelets.

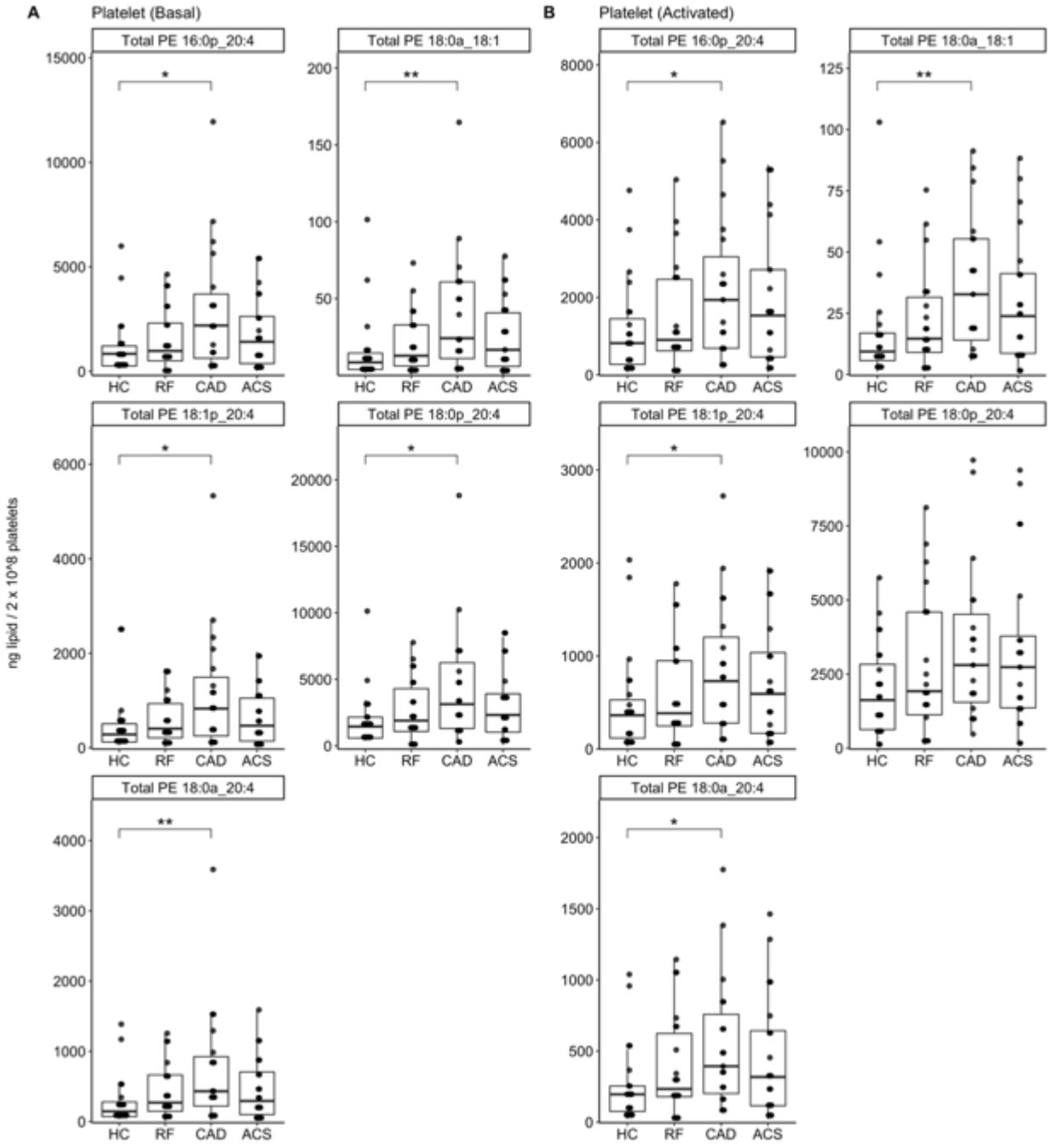

Figure 7.3. Higher levels of total platelet PE were noted in platelets from CAD, but not ACS, compared with HC.

Lipids were extracted from platelets (2 x 10^8) in resting conditions (Panel A) or following activation with thrombin (0.2 U/ml, Panel B) as in Materials and Methods. Lipids amounts (ng) were calculated by LC-MS/MS and plotted as a box plot with the ggplot2 R package. Box edges indicate the interquartile range (IQR) with the median line inside the box. Whiskers indicate 1.5 times the IQR. Statistical significance was tested with Mann-Whitney-Wilcoxon test, and where significant differences exist, they are indicated by stars (*: p <0.05, **: p <0.01, ***: p <0.001). ACS: acute coronary syndrome (n=24), CAD: coronary artery disease but no ACS (n=19), RF: Risk factors with no significant coronary artery disease (n=23), HC: healthy control (n=24).

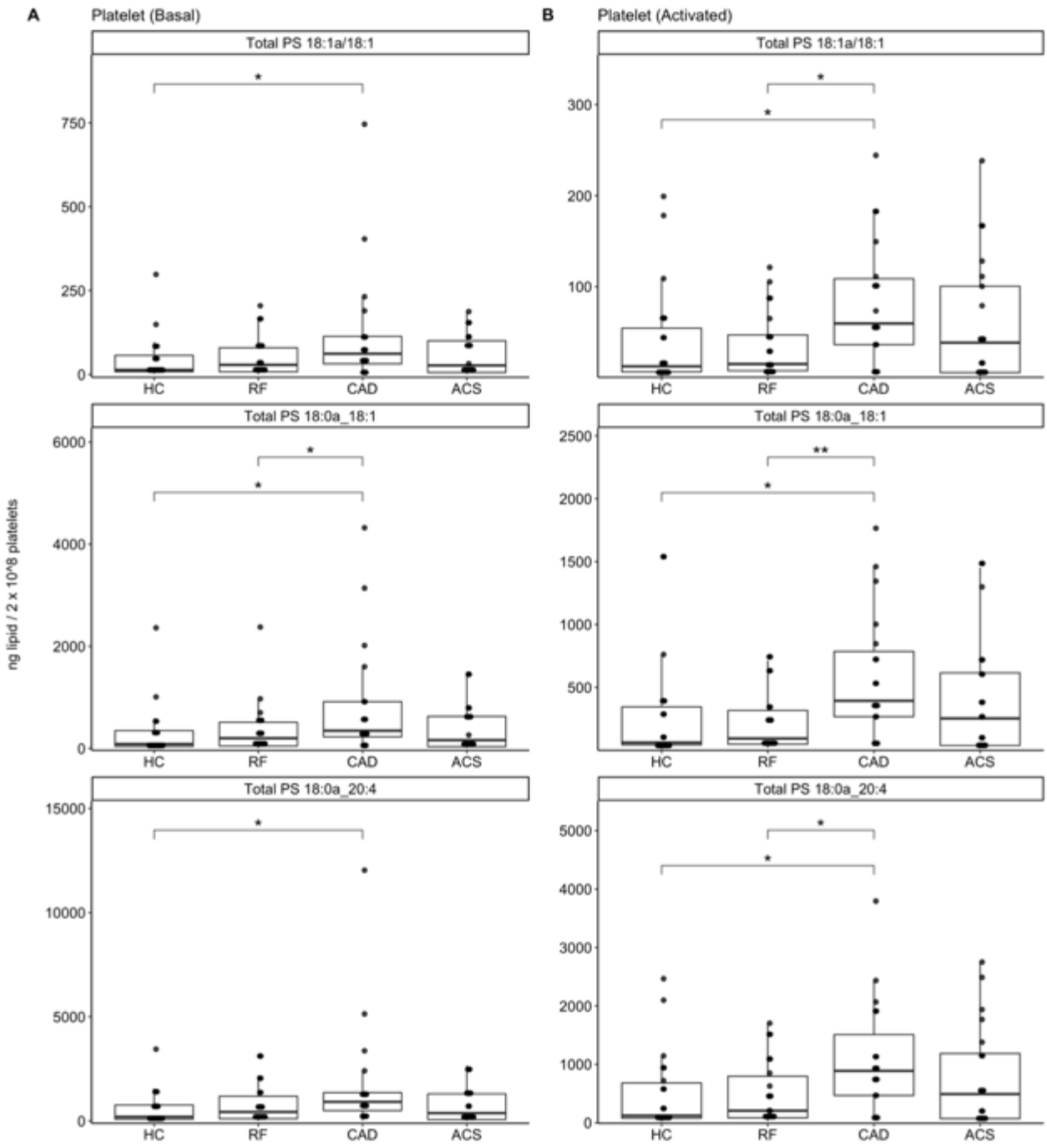

Figure 7.4. Higher levels of total platelet PS were noted in platelets from CAD, but not ACS, compared with HC.

Lipids were extracted from platelets (2 x 10^8) in resting conditions (Panel A) or following activation with thrombin (0.2 U/ml, Panel B) as in Materials and Methods. Lipids amounts (ng) were calculated by LC-MS/MS and plotted as a box plot with the ggplot2 R package. Box edges indicate the interquartile range (IQR) with the median line inside the box. Whiskers indicate 1.5 times the IQR. Statistical significance was tested with Mann-Whitney-Wilcoxon test, and where significant differences exist, they are indicated by stars (*: $p < 0.05$, **: $p < 0.01$, ***: $p < 0.001$). ACS: acute coronary syndrome (n=24), CAD: coronary artery disease but no ACS (n=19), RF: Risk factors with no significant coronary artery disease (n=23), HC: healthy control (n=24).

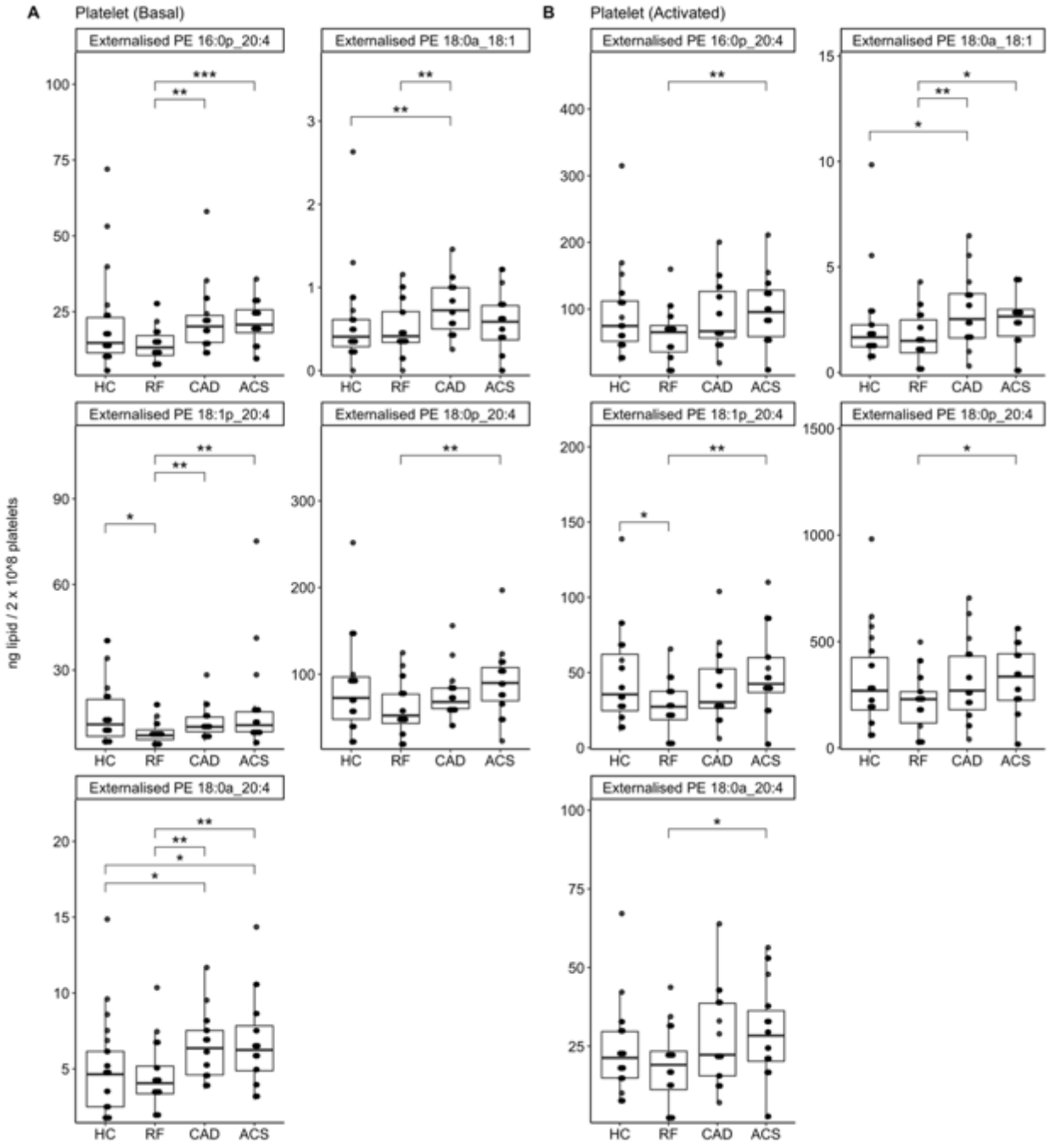

Figure 7.5. Higher levels of externalised PE in platelets from ACS patients compared to HC/RF.

Lipids were extracted from platelets (2 x 10^8) in resting conditions (Panel A) or following activation with thrombin (0.2 U/ml, Panel B) as in Materials and Methods. Lipids amounts (ng) were calculated by LC-MS/MS and plotted as a box plot with the ggplot2 R package. Box edges indicate the interquartile range (IQR) with the median line inside the box. Whiskers indicate 1.5 times the IQR. Statistical significance was tested with Mann-Whitney-Wilcoxon test, and where significant differences exist, they are indicated by stars (*: p <0.05, **: p <0.01, ***: p <0.001). ACS: acute coronary syndrome (n=24), CAD: coronary artery disease but no ACS (n=19), RF: Risk factors with no significant coronary artery disease (n=23), HC: healthy control (n=24).

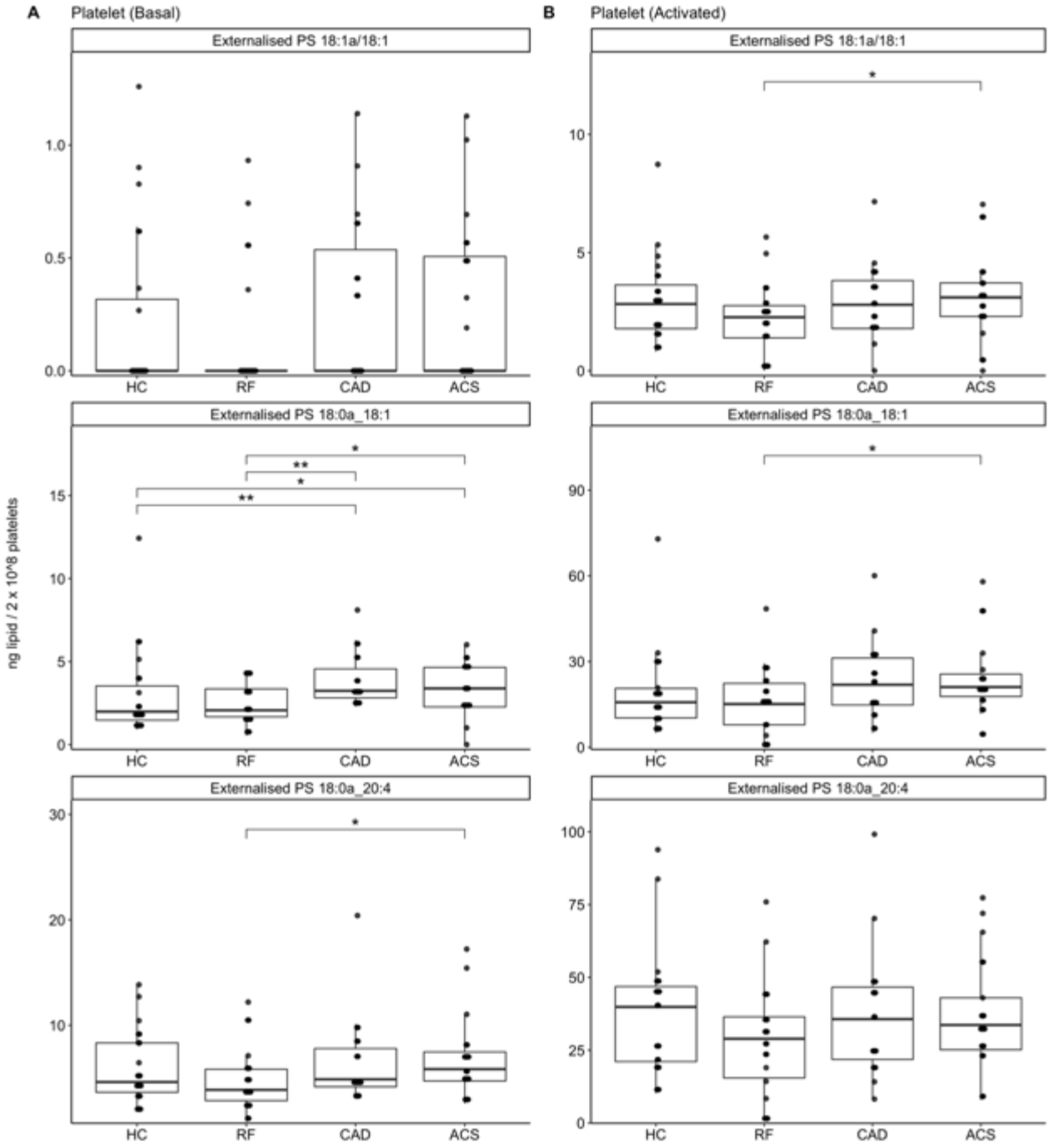

Figure 7.6. Higher levels of externalised PS in platelets from ACS patients compared to HC/RF.

Lipids were extracted from resting platelets (2 x 10^8) (Panel A) or following activation with thrombin (0.2 U/ml, Panel B) as in Materials and Methods. Lipids amounts (ng) were calculated by LC-MS/MS and plotted as a box plot with the ggplot2 R package. Box edges indicate the interquartile range (IQR) with the median line inside the box. Whiskers indicate 1.5 times the IQR. Statistical significance was tested with Mann-Whitney-Wilcoxon test, and where significant differences exist, they are indicated by stars (*: $p < 0.05$, **: $p < 0.01$, ***: $p < 0.001$). ACS: acute coronary syndrome (n=24), CAD: coronary artery disease but no ACS (n=19), RF: Risk factors with no significant coronary artery disease (n=23), HC: healthy control (n=24).

The relationship of outer to inner membrane leaflet aPL may have an impact on membrane biophysical properties such as curvature and enzymatic binding[346-348]. Therefore, I investigated differences between the groups in the fraction (percentage) of aPL externalised, calculated as ng externalised (outer leaflet) ÷ ng total (throughout membrane) × 100%.

To start with, I studied differences in the fraction (%) of PE externalised across the clinical groups for all lipid species (**Figure 7.7**). In resting platelets, there were no significant differences between ACS and HC/RF. However, there was significantly lower % PE externalised in CAD compared with HC, particularly for PE 18:1p_20:4 and PE 18:0p_20:4. In thrombin-activated platelets, there was significantly lower % PE externalised in CAD and RF compared with HC for all species, and lower % PE 18:0a_18:1 externalised in ACS compared with HC.

To examine for differences in the fraction (percentage) of PS externalised for all lipid species, I carried out a similar analysis as demonstrated in **Figure 7.8**. Similar to fraction of PE externalised, there were no significant differences in % PS externalised between ACS and HC/RF in resting cells. In thrombin-activated platelets, there was significantly lower % PS externalised in CAD/RF compared with HC for all species (borderline p-values for PS 18:0a_18:1 in RF compared with HC).

In summary, these data suggest no differences in % aPL externalisation in platelets from ACS vs HC.

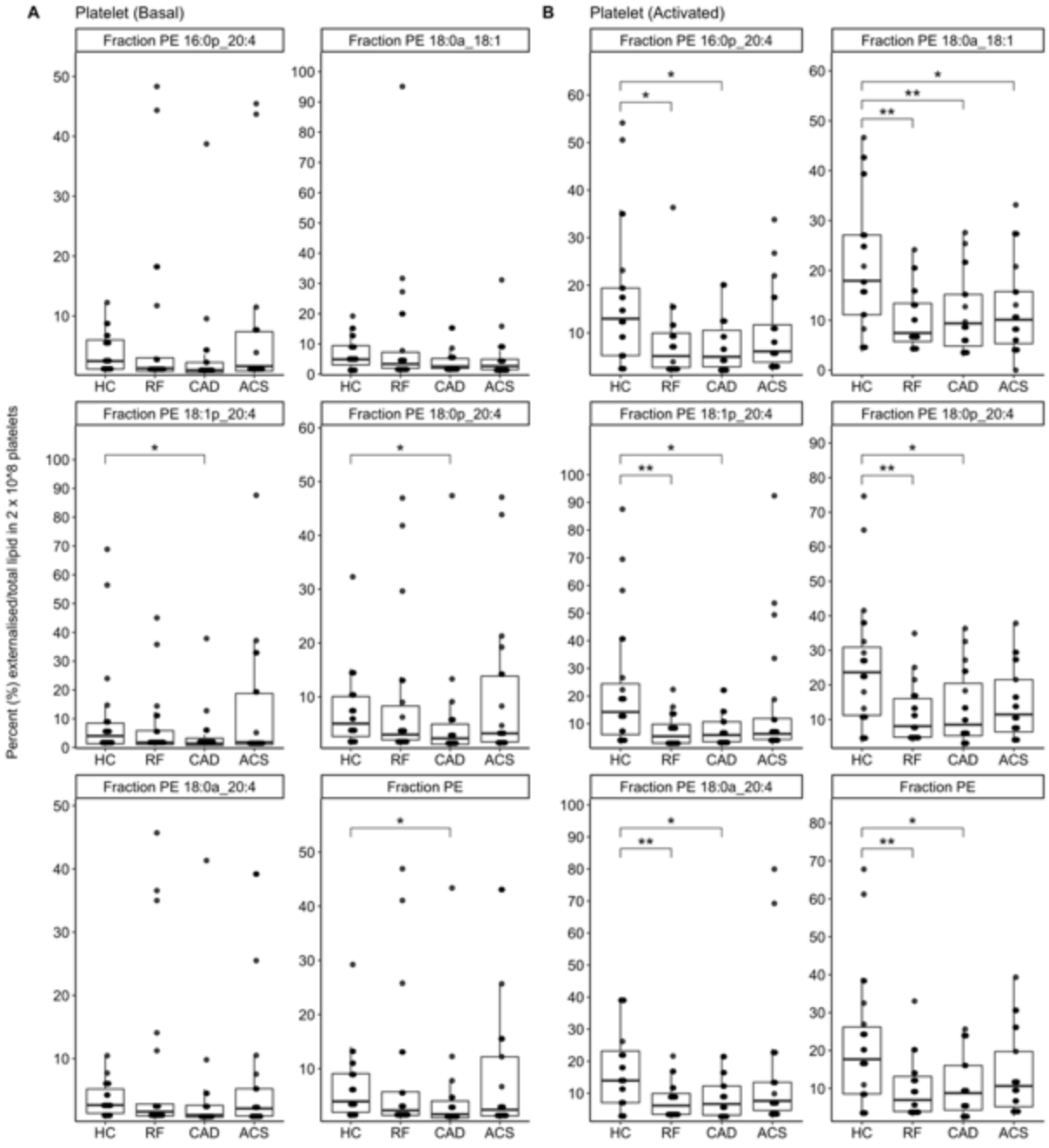

Figure 7.7. Fraction of PE externalised in platelets is largely similar between ACS and HC.

The fraction of externalised PE was calculated for each sample and expressed as a percentage (ng externalised ÷ ng total × 100%). Lipids were extracted from resting platelets (2 x 10^8, Panel A) or following activation with thrombin (0.2 U/ml, Panel B) as in Materials and Methods. Lipids amounts (ng) were calculated by LC-MS/MS, fraction externalised calculated as described above and plotted as a box plot with the ggplot2 R package. Box edges indicate the interquartile range (IQR) with the median line inside the box. Whiskers indicate 1.5 times the IQR. Statistical significance was tested with Mann-Whitney-Wilcoxon test, and where significant differences exist, they are indicated by stars (*: $p < 0.05$, **: $p < 0.01$, ***: $p < 0.001$). ACS: acute coronary syndrome (n=24), CAD: coronary artery disease but no ACS (n=19), RF: Risk factors with no significant coronary artery disease (n=23), HC: healthy control (n=24).

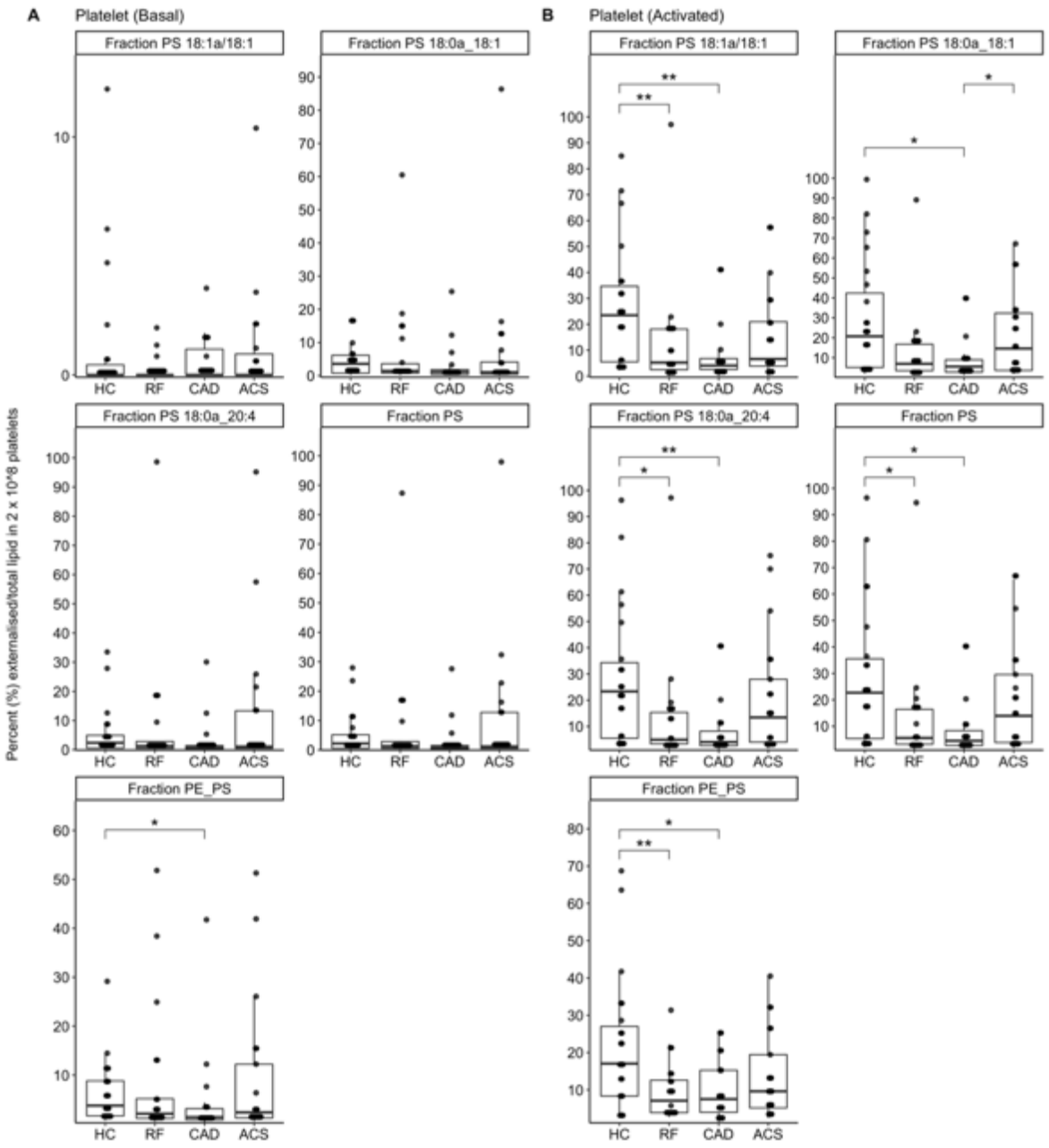

Figure 7.8. Fraction of PS externalised in platelets is similar between ACS and RF/HC.

The fraction of externalised PS was calculated for each sample and expressed as a percentage (ng externalised ÷ ng total × 100%). Lipids were extracted from resting platelets (2 x 10^8, Panel A) or following activation with thrombin (0.2 U/ml, Panel B) as in Materials and Methods. Lipids amounts (ng) were calculated by LC-MS/MS, fraction externalised calculated as described above and plotted as a box plot with the ggplot2 R package. Fraction PE_PS indicated the sum of all PS/PE fractions. Box edges indicate the interquartile range (IQR) with the median line inside the box. Whiskers indicate 1.5 times the IQR. Statistical significance was tested with Mann-Whitney-Wilcoxon test, and where significant differences exist, they are indicated by stars (*: p <0.05, **: p <0.01, ***: p <0.001). ACS: acute coronary syndrome (n=24), CAD: coronary artery disease but no ACS (n=19), RF: Risk factors with no significant coronary artery disease (n=23), HC: healthy control (n=24).

7.2.3 Leukocyte aPL cluster by *sn1* fatty acid

Next, the levels of aPL were measured in both resting and A23817-activated leukocytes from all patients. A23817 was chosen as an agonist to ensure activation of all leukocyte subpopulations in the sample irrespective of differences in receptors and response to agonists. Whilst this does not reflect physiological activation of leukocytes, it quantifies the capacity of these cells to mobilise aPL upon stimulation, and ensures that the sample contains viable leukocytes capable of scrambling lipids to the outer leaflet.

To visualise the amount of total (throughout the membrane) and externalised (on outer leaflet only) leukocyte aPL lipids across the clinical groups, I initially plotted the data on a heatmap (**Figure 7.9**). A23817-activated leukocytes showed higher amounts of externalised aPL lipids in all clinical groups compared with resting leukocytes, consistent with activation of scramblases[22,339]. The amount of externalised aPL was lower for all species in resting and activated leukocytes from RF patients compared to other groups. A23817 activation of leukocyte samples did not change total aPL amounts from resting states (**Figure 7.9**B). Of note, leukocytes from CAD patients had higher amounts of total aPL species in both resting and activated states, although there was no difference in total or externalised aPL between ACS and HC.

Column wise hierarchical clustering demonstrated grouping of leukocyte externalised aPL lipids by *sn1* fatty acid irrespective of head group, with plasmalogen lipids generally clustering separately from diacyl lipids (**Figure 7.9**). A similar clustering pattern by *sn1* fatty acid was seen in leukocyte total aPL and is likely driven by the higher abundance of plasmalogen lipids compared to diacyls.

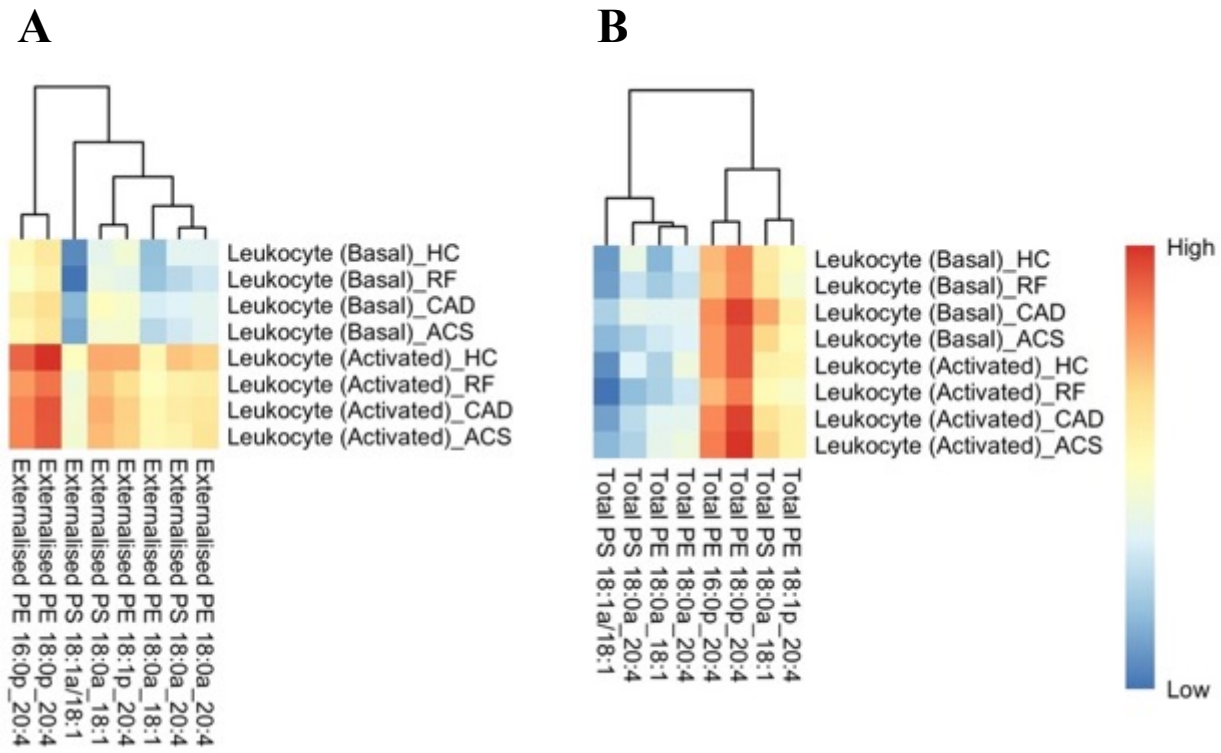

Figure 7.9. Heatmap of aPL lipids in leukocytes from patients with arterial thrombosis demonstrate increased externalisation with A23817 stimulation, with aPL clustering by *sn1* fatty acid.

Panel A: Externalised aPL. Panel B: Total aPL. Lipids were extracted from resting leukocytes (4 x 10^6) or following activation with A23817 (10 μM) as in Materials and Methods. Lipids amounts (ng) were calculated by LC-MS/MS, log10 transformed and plotted as a heatmap with hierarchical clustering using the pheatmap R package. ACS: acute coronary syndrome (n=24), CAD: coronary artery disease but no ACS (n=19), RF: Risk factors with no significant coronary artery disease (n=23), HC: healthy control (n=24).

7.2.4 Quantitative analysis of leukocyte aPL demonstrates more external PS 18:0a_18:1 in ACS vs HC, but no differences in fraction (%) aPL externalised

To obtain an overview of differences in leukocyte aPL between clinical groups and test for statistical significance, box plots were generated for aPL lipids combined by headgroup (**Figure 7.10**). In resting leukocytes, there were significantly higher levels of externalised PE in CAD and ACS compared with RF. However, examining external PS demonstrated no significant differences. Additionally, there were no significant differences in total (throughout the membrane) PS and PE between clinical groups. Upon A23817-activation of leukocytes, the amount of externalised aPL increased by approximately 7-fold for both PE and PS compared with resting leukocytes, with no differences between ACS/CAD compared with HC or RF (**Figure 7.10**B). The amounts of externalised PE in A23817-activated leukocytes were lower in RF compared with HC, and total PS was higher in A23817-activated leukocytes from CAD compared with RF.

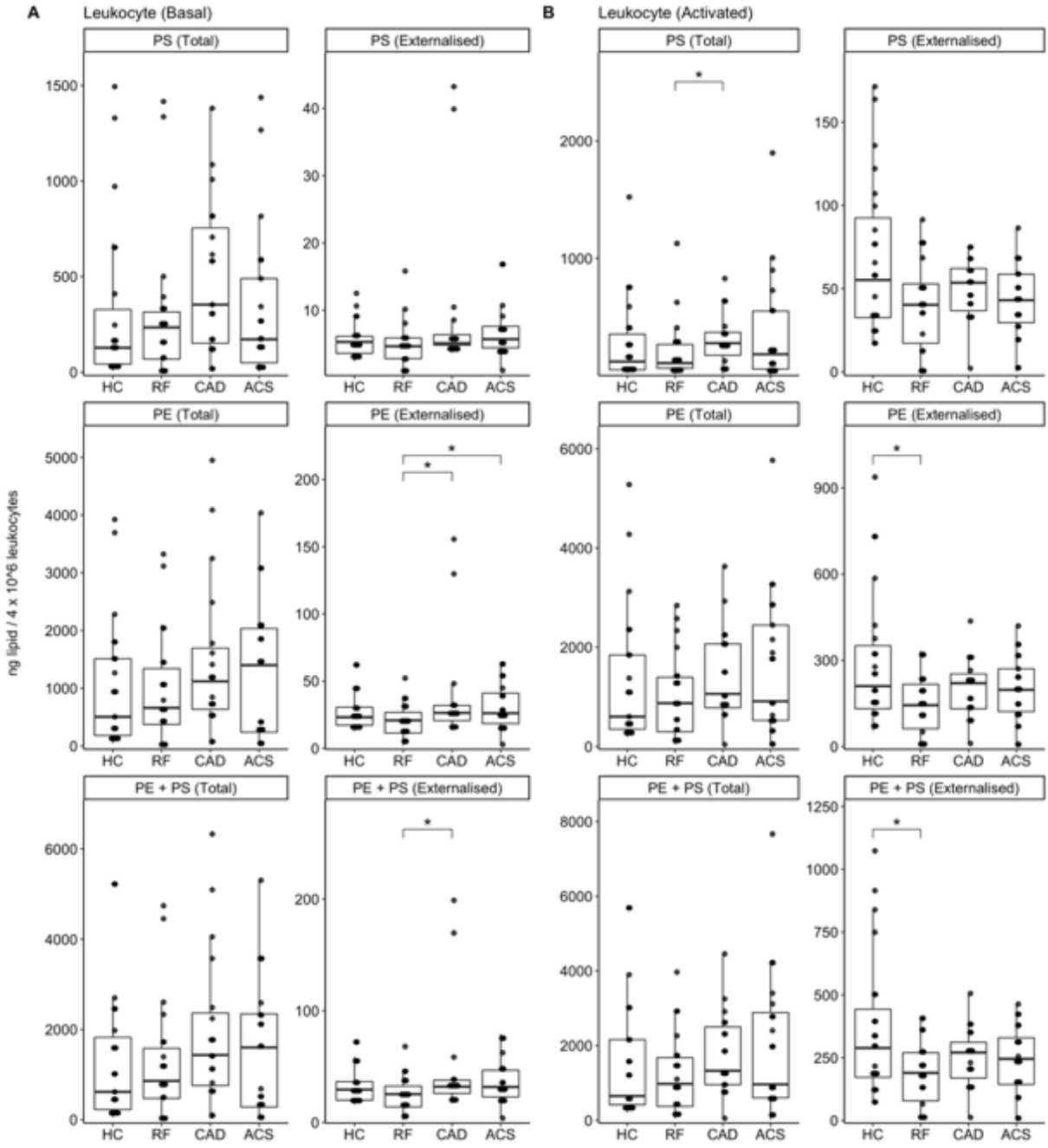

Figure 7.10. Consolidating leukocyte aPL lipids by headgroup demonstrates more externalised PE in ACS/CAD vs RF in resting samples.

Lipids were extracted from leukocytes (4 x 10^6) in resting conditions (Panel A) or following activation with A23817 (10 μM, Panel B) as in Materials and Methods. Lipids amounts (ng) were calculated by LC-MS/MS, summed by headgroup and plotted as a box plot with the ggplot2 R package. Box edges indicate the interquartile range (IQR) with the median line inside the box. Whiskers indicate 1.5 times the IQR. Statistical significance was tested with Mann-Whitney-Wilcoxon test, and where significant differences exist, they are indicated by stars (*: $p < 0.05$, **: $p < 0.01$, ***: $p < 0.001$). ACS: acute coronary syndrome (n=24), CAD: coronary artery disease but no ACS (n=19), RF: Risk factors with no significant coronary artery disease (n=23), HC: healthy control (n=24).

Similar to the analysis of aPL in platelets, I expanded on the overview presented above in leukocytes by going on to examine individual PS/PE species which may drive the patterns observed above. To start with total (throughout the membrane) aPL, PE species in resting and A23817-activated leukocytes were similar between ACS and other groups including HC for all PE species studied (**Figure 7.11**). There were however significantly higher levels of PE 18:0a_18:1 in the CAD group compared to HC in resting and A23817-activated leukocytes. Similarly, the levels of total PS in resting and A23817-activated leukocytes were similar for all PS species studied between ACS and other groups including HC (**Figure 7.12**). However, the CAD group demonstrated higher levels of total PS 18:0a_18:1 compared with HC, both in resting and activated leukocytes. A23817-activated leukocytes contained similar or slightly lower levels of total aPL compared to resting platelets, presumably secondary to phospholipase activation and hydrolysis of membrane aPL[13]. Overall therefore, aPL species measured throughout the membrane (i.e. 'total') were similar between ACS and HC, but higher PE and PS 18:0a_18:1 in CAD compared with HC.

There were no differences in the amounts of externalised PE species in resting leukocytes from ACS vs HC. In contrast, the levels of externalised PE species in resting leukocytes were higher in CAD patients compared to HC and/or RF groups (**Figure 7.13**). Specifically, resting leukocytes from CAD patients had significantly higher levels of externalised PE 18:0a_18:1 (compared with HC/RF), PE 18:0p_20:4 (compared with RF) and PE 16:0p_20:4 (compared with RF). Upon A23817-activation, no differences were seen in externalised PE amounts in leukocytes from ACS/CAD patients compared with RF/HC. In terms of externalised PS species, leukocytes from patients with ACS and CAD had significantly higher amounts of PS 18:0a_18:1 compared to HC/RF in resting states, and significantly lower amounts of externalised PS 18:0a_20:4 compared to HC on A23817 activation (**Figure 7.14**). In summary therefore, whilst resting

leukocytes from CAD patients contained higher levels of most externalised aPL species studied, only PS 18:0a_18:1 was higher in ACS vs HC.

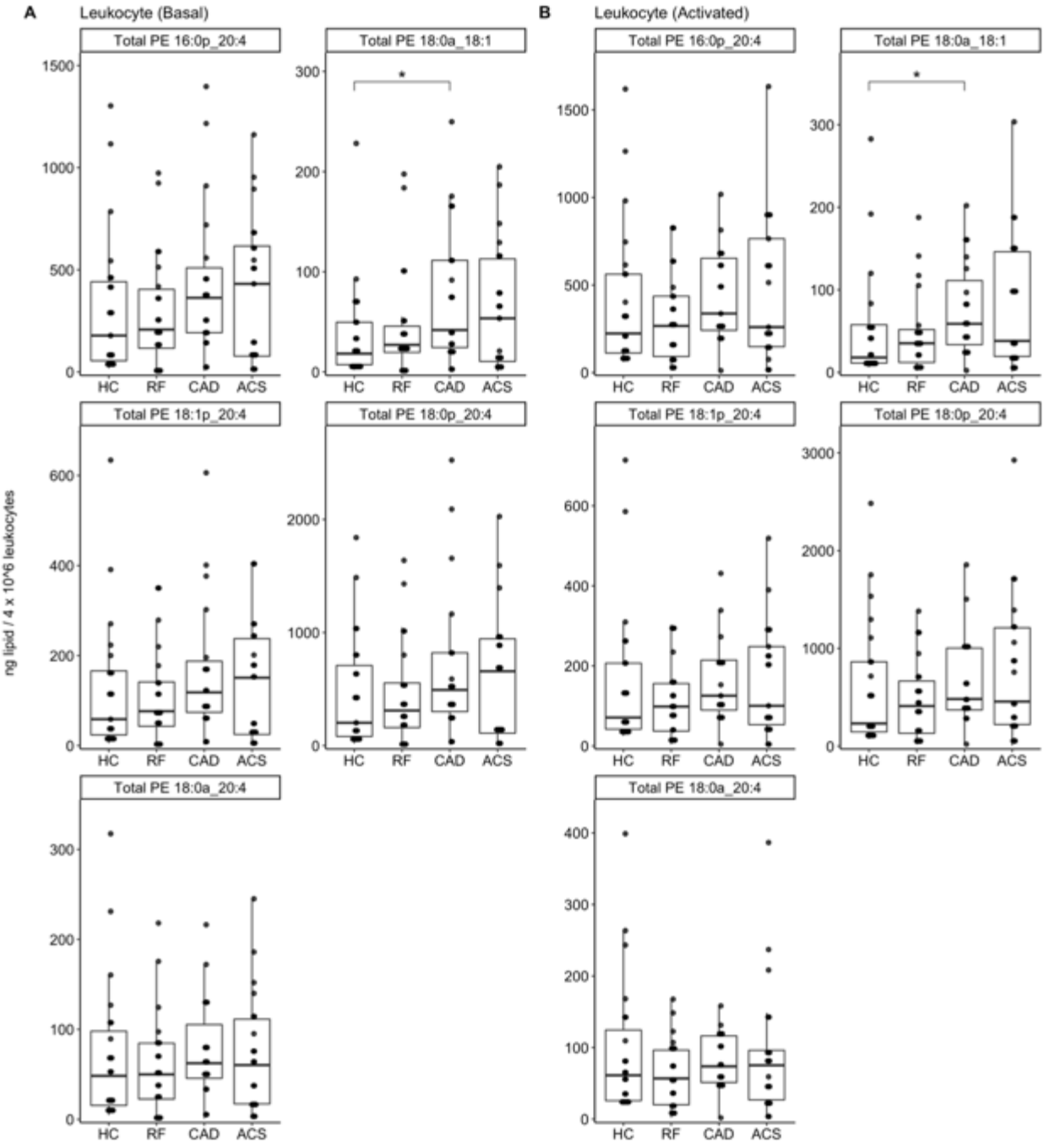

Figure 7.11. No differences detected in leukocyte total PE amounts between ACS and HC, though CAD patients had higher PE 18:0a_18:1 (compared with HC).

Lipids were extracted from resting leukocytes (4 x 10^6, Panel A) or following activation with A23817 (10 μM, Panel B) as in Materials and Methods. Lipids amounts (ng) were calculated by LC-MS/MS and plotted as a box plot with the ggplot2 R package. Box edges indicate the interquartile range (IQR) with the median line inside the box. Whiskers indicate 1.5 times the IQR. Statistical significance was tested with Mann-Whitney-Wilcoxon test, and where significant differences exist, they are indicated by stars (*: $p < 0.05$, **: $p < 0.01$, ***: $p < 0.001$). ACS: acute coronary syndrome (n=24), CAD: coronary artery disease but no ACS (n=19), RF: Risk factors with no significant coronary artery disease (n=23), HC: healthy control (n=24).

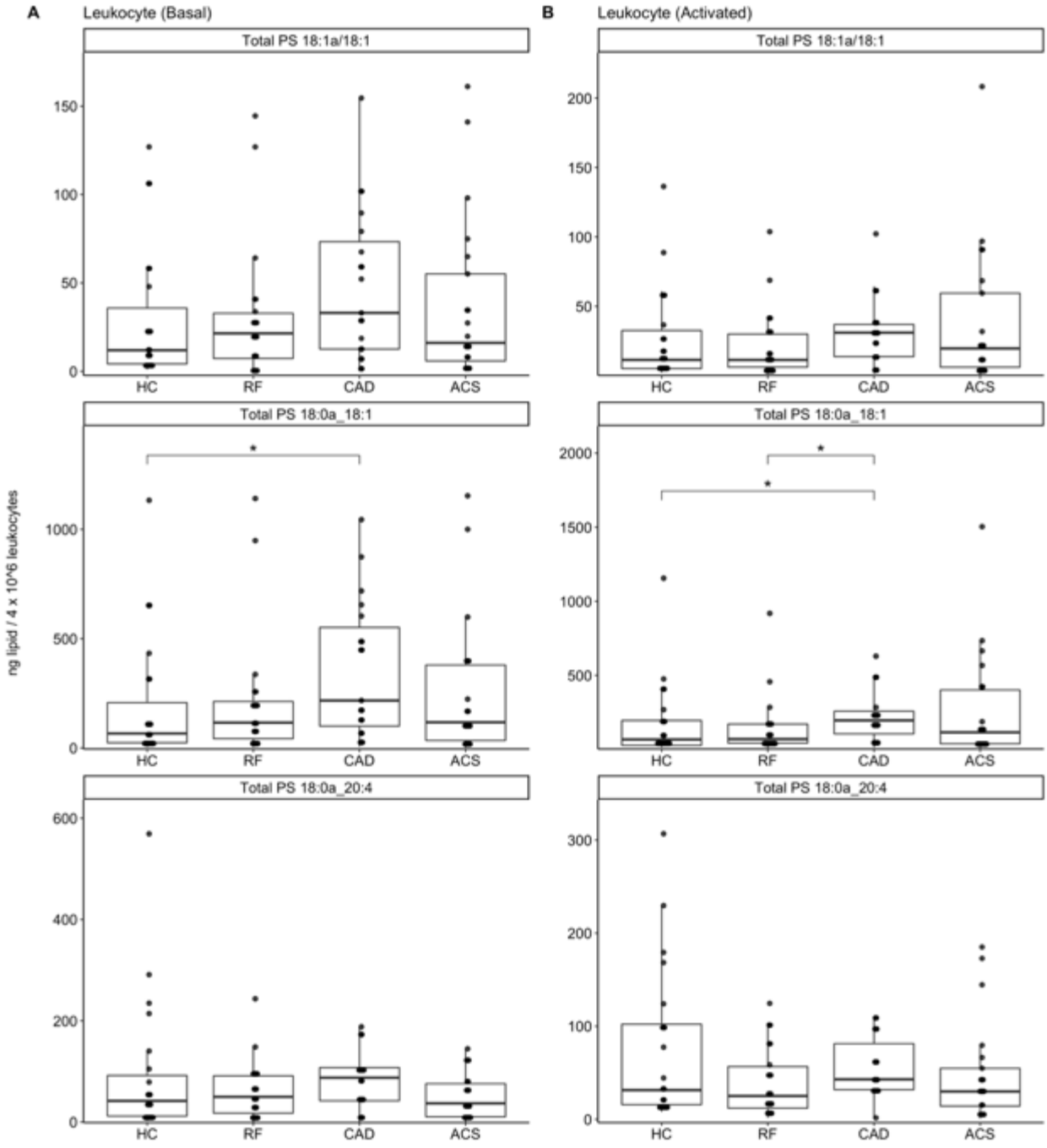

Figure 7.12. No differences detected in leukocyte total PS amounts between ACS and HC, though CAD patients had higher PS 18:0a_18:1 (compared with HC).

Lipids were extracted from resting leukocytes (4 x 10^6, Panel A) or following activation with A23817 (10 μM, Panel B) as in Materials and Methods. Lipids amounts (ng) were calculated by LC-MS/MS and plotted as a box plot with the ggplot2 R package. Box edges indicate the interquartile range (IQR) with the median line inside the box. Whiskers indicate 1.5 times the IQR. Statistical significance was tested with Mann-Whitney-Wilcoxon test, and where significant differences exist, they are indicated by stars (*: $p < 0.05$, **: $p < 0.01$, ***: $p < 0.001$). ACS: acute coronary syndrome (n=24), CAD: coronary artery disease but no ACS (n=19), RF: Risk factors with no significant coronary artery disease (n=23), HC: healthy control (n=24).

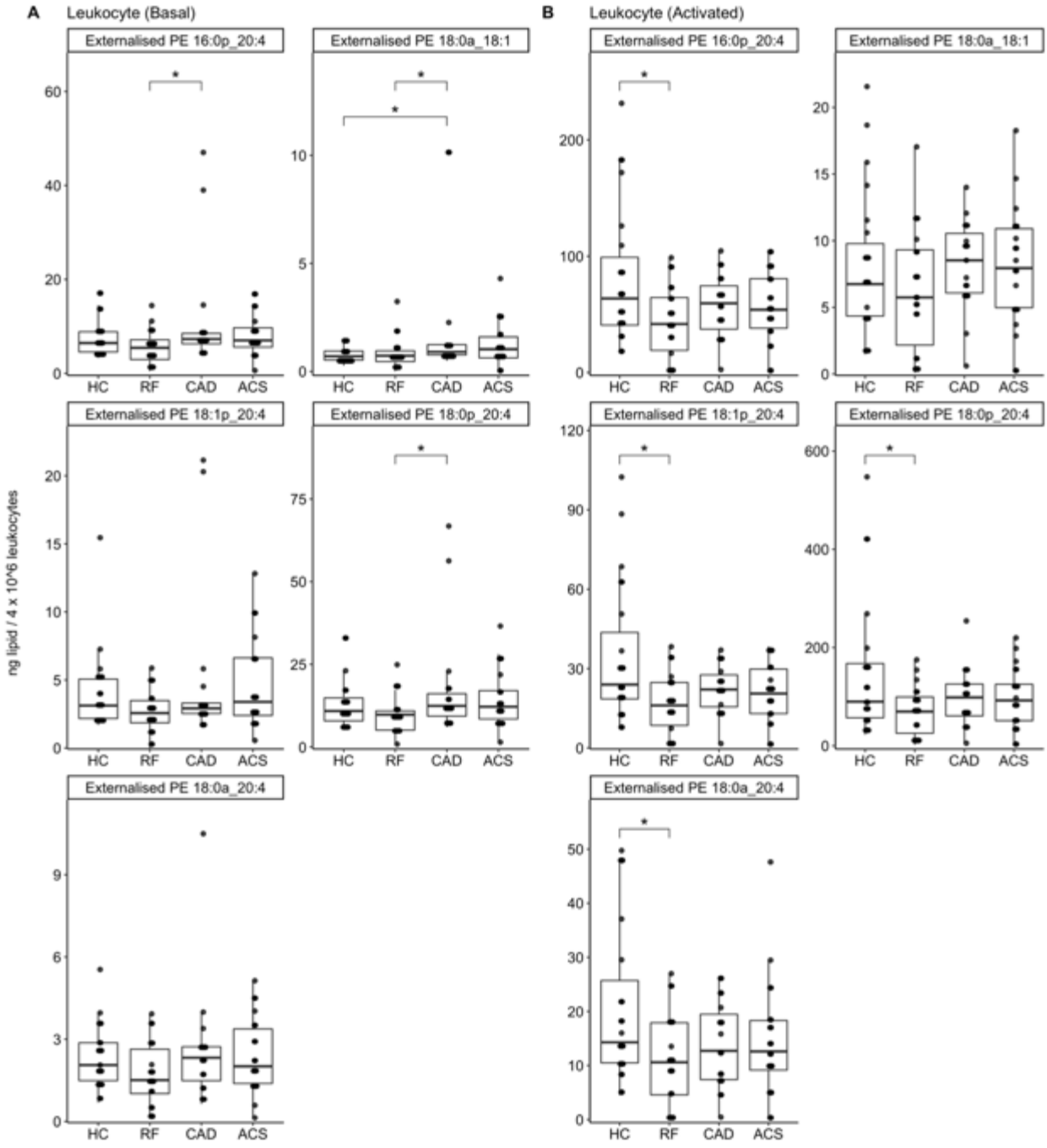

Figure 7.13. Resting leukocytes externalise more PE 16:0p_20:4, PE 18:0a_18:1 and PE 18:0p_20:4 in patients with CAD compared with HC and/or RF.

Lipids were extracted from resting leukocytes (4 x 10^6, Panel A) or following activation with A23817 (10 μM, Panel B) as in Materials and Methods. Lipids amounts (ng) were calculated by LC-MS/MS and plotted as a box plot with the ggplot2 R package. Box edges indicate the interquartile range (IQR) with the median line inside the box. Whiskers indicate 1.5 times the IQR. Statistical significance was tested with Mann-Whitney-Wilcoxon test, and where significant differences exist, they are indicated by stars (*: $p < 0.05$, **: $p < 0.01$, ***: $p < 0.001$). ACS: acute coronary syndrome (n=24), CAD: coronary artery disease but no ACS (n=19), RF: Risk factors with no significant coronary artery disease (n=23), HC: healthy control (n=24).

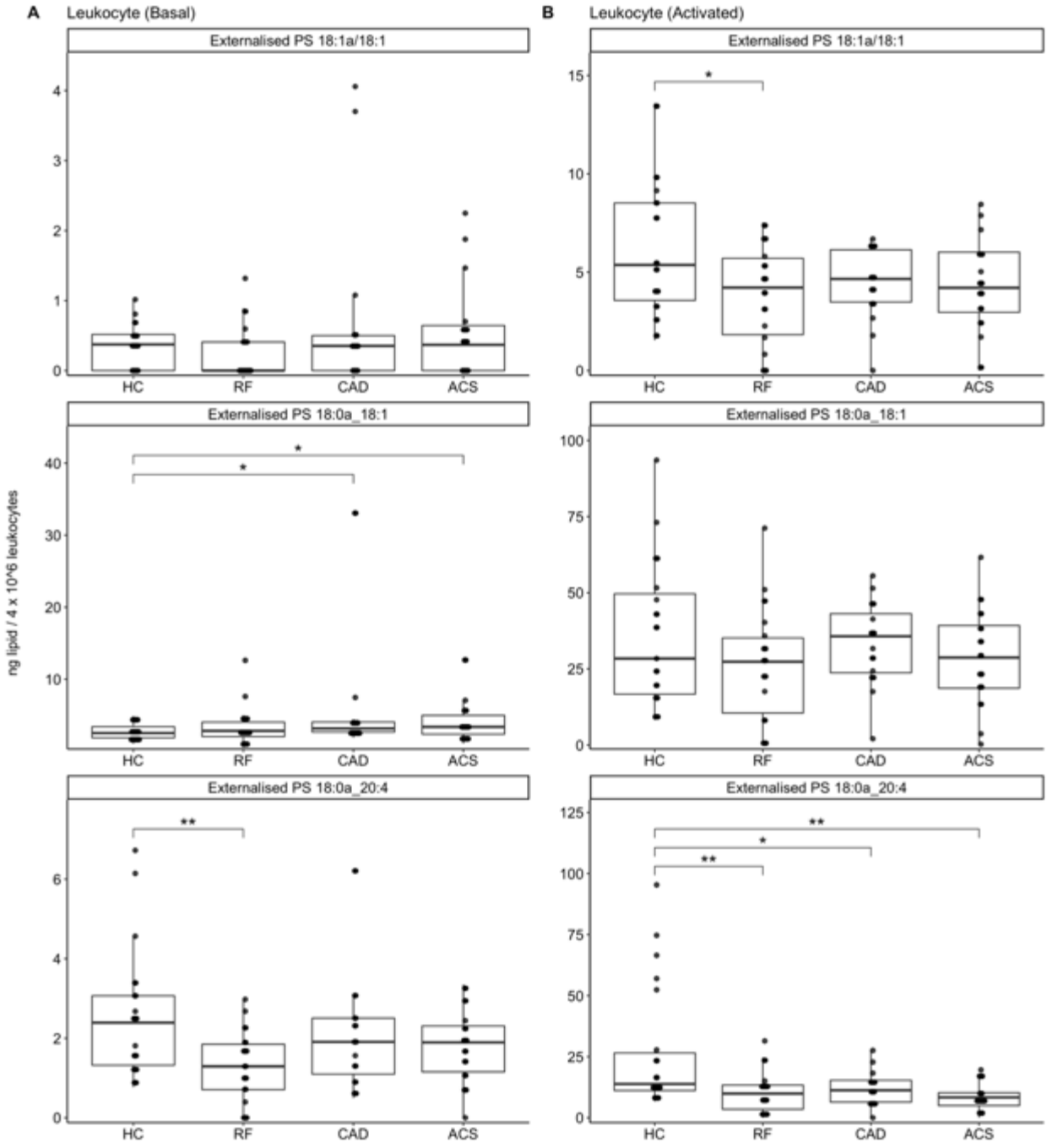

Figure 7.14. Leukocytes externalise more PS 18:0a_18:1 (in resting states), but less PS 18:0a_20:4 (on A23817 activation), in patients with ACS/CAD compared with HC.

Lipids were extracted from leukocytes (4 x 10^6) in resting conditions (Panel A) or following activation with calcium (10 μM, Panel B) as in Materials and Methods. Lipids amounts (ng) were calculated by LC-MS/MS and plotted as a box plot with the ggplot2 R package. Box edges indicate the interquartile range (IQR) with the median line inside the box. Whiskers indicate 1.5 times the IQR. Statistical significance was tested with Mann-Whitney-Wilcoxon test, and where significant differences exist, they are indicated by stars (*: p <0.05, **: p <0.01, ***: p <0.001). ACS: acute coronary syndrome (n=24), CAD: coronary artery disease but no ACS (n=19), RF: Risk factors with no significant coronary artery disease (n=23), HC: healthy control (n=24).

Next, I examined the fraction (percentage) of PE externalised, calculated as ng externalised (outer leaflet) ÷ ng total (throughout membrane) × 100%, across the clinical groups for all leukocyte PE lipid species (**Figure 7.15**). In resting leukocytes, there were no significant differences between clinical groups. However, upon activation of leukocytes with A23817, there was significantly lower % PE externalised in ACS/CAD/RF compared with HC for all species. The fraction (percentage) of PS externalised is demonstrated in **Figure 7.16**. For resting leukocytes, there were no significant differences in the fraction of PS externalised between ACS/CAD compared with HC for all PS species. However, there were significantly higher % PS 18:0a_20:4 externalised in ACS when compared with RF. In A23817-activated leukocytes, there was significantly lower % PS externalised in ACS/CAD/RF compared HC for all PS species.

Taken together, these figures demonstrate no differences in resting leukocyte aPL between clinical groups, with the exception of higher % PS 18:0a_18:1 in ACS v RF. Whilst % externalised aPL in A23817-activated leukocytes were higher than resting states, the interpretation of differences between groups is unlikely to be of physiological or clinical relevance given the nature of the agonist chosen.

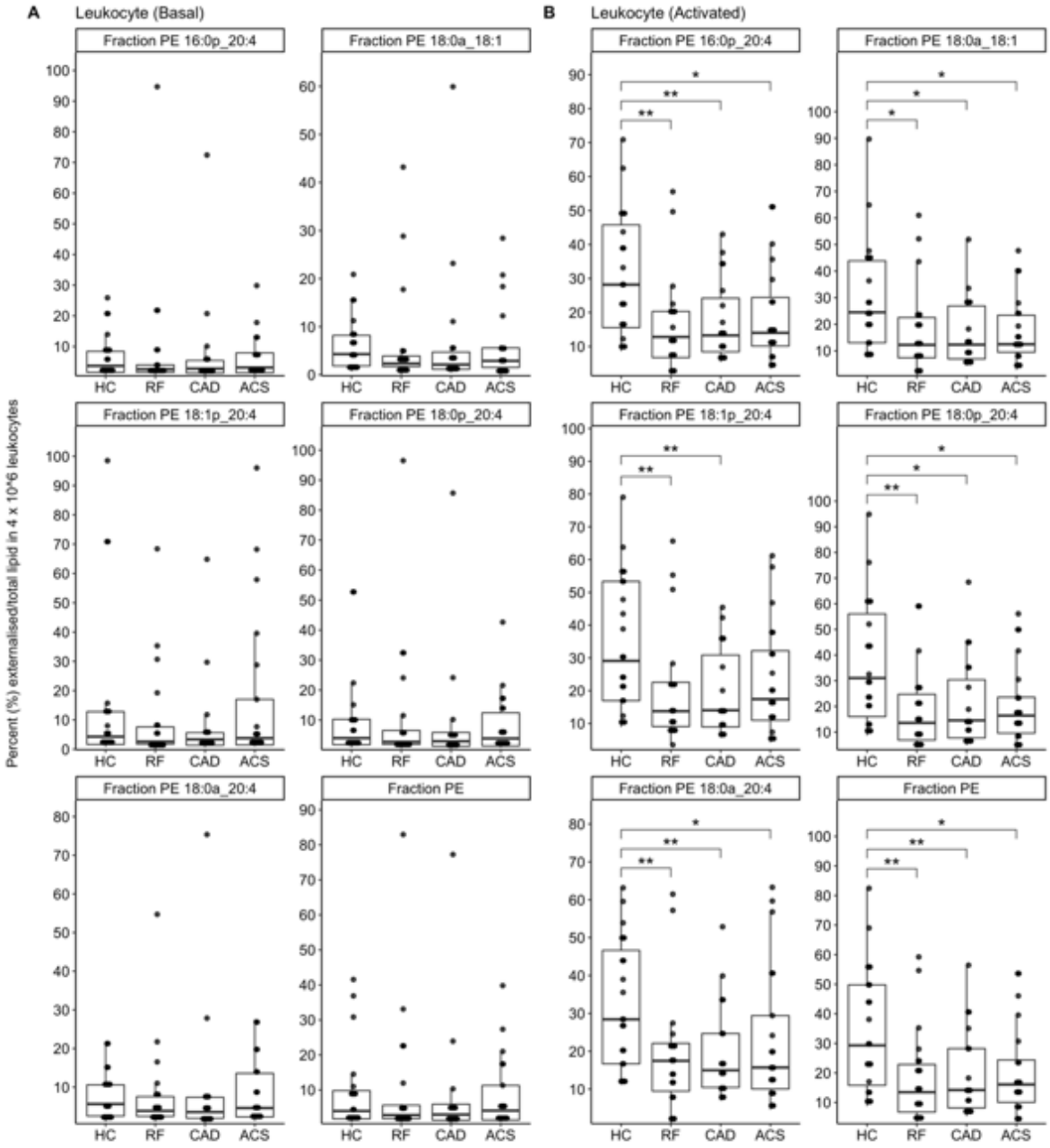

Figure 7.15. Fraction of PE externalised in resting leukocytes is similar between groups.

The fraction of externalised PE was calculated for each sample and expressed as a percentage (ng externalised ÷ ng total × 100%) for individual species or the sum thereof (Fraction_PE). Lipids were extracted from leukocytes (4 x 10^6) in resting conditions (Panel A) or following activation with A23817 (10 μM, Panel B) as in Materials and Methods. Lipids amounts (ng) were calculated by LC-MS/MS with fractions calculated as above and plotted as a box plot with the ggplot2 R package. Box edges indicate the interquartile range (IQR) with the median line inside the box. Whiskers indicate 1.5 times the IQR. Statistical significance was tested with Mann-Whitney-Wilcoxon test, and where significant differences exist, they are indicated by stars (*: $p < 0.05$, **: $p < 0.01$, ***: $p < 0.001$). ACS: acute coronary syndrome (n=24), CAD: coronary artery disease but no ACS (n=19), RF: Risk factors with no significant coronary artery disease (n=23), HC: healthy control (n=24).

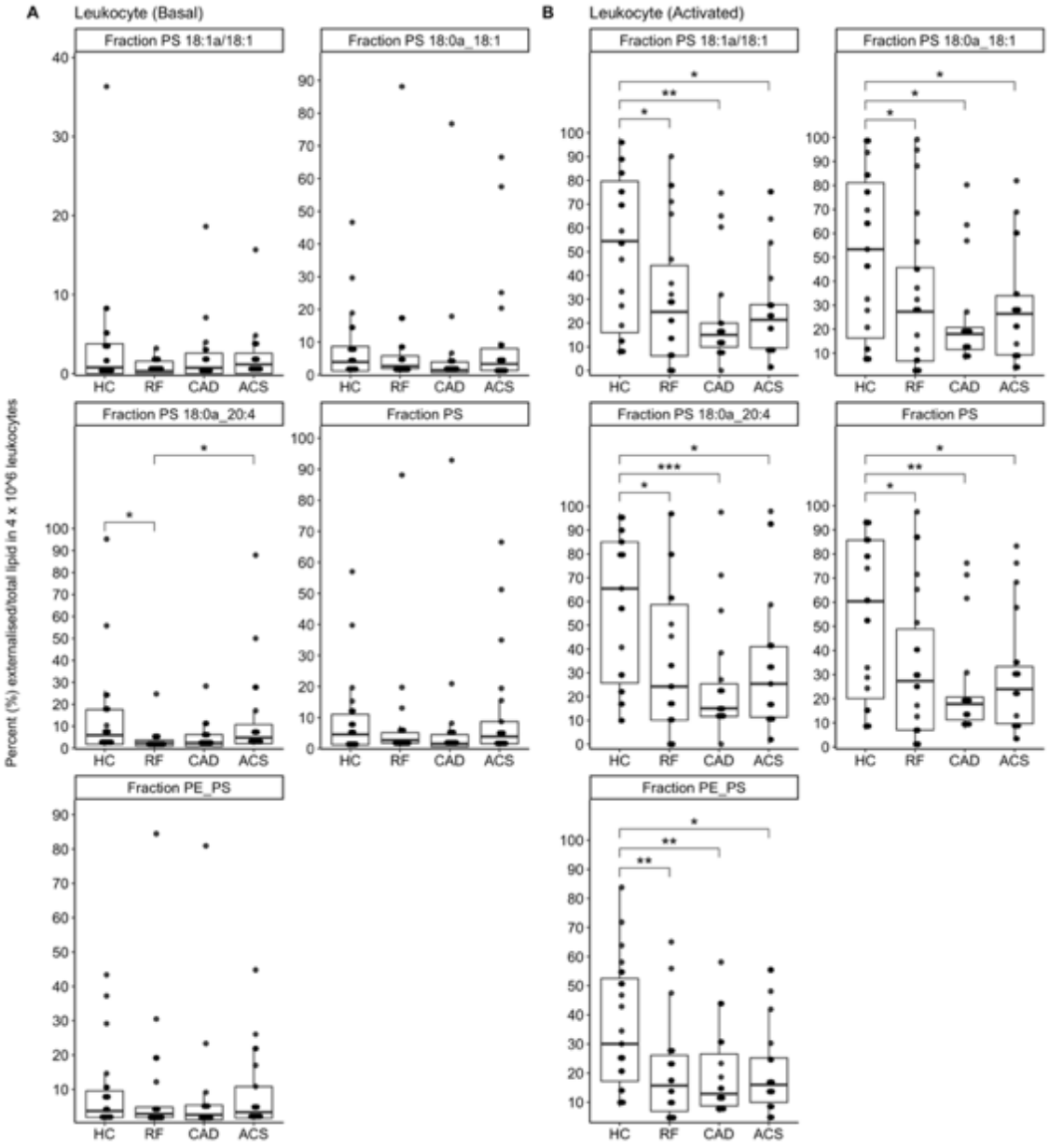

Figure 7.16. Fraction of PS externalised in resting leukocytes is similar between ACS and HC, but higher in ACS (vs RF) for PS 18:0a_20:4.

The fraction of externalised PS was calculated for each sample and expressed as a percentage (ng externalised ÷ ng total × 100%) for individual species or the sum thereof (Fraction_PS). Lipids were extracted from leukocytes (4 x 10^6) in resting conditions (Panel A) or following activation with A23817 (10 μM, Panel B) as in Materials and Methods. Lipids amounts (ng) were calculated by LC-MS/MS with fractions calculated as above and plotted as a box plot with the ggplot2 R package. Fraction PE_PS indicated the sum of all PS/PE fractions. Box edges indicate the interquartile range (IQR) with the median line inside the box. Whiskers indicate 1.5 times the IQR. Statistical significance was tested with Mann-Whitney-Wilcoxon test, and where significant differences exist, they are indicated by stars (*: p <0.05, **: p <0.01, ***: p <0.001). ACS: acute coronary syndrome (n=24), CAD: coronary artery disease but no ACS (n=19), RF: Risk factors with no significant coronary artery disease (n=23), HC: healthy control (n=24)

7.2.5 EV aPL cluster by both *sn1* and *sn2* fatty acids

Next, I analysed washed EV-rich fractions obtained from plasma samples, as per Materials and Methods, for aPL lipids. These samples were processed in the LC-MS/MS without any count adjustment, as EV characterisation was performed later from frozen PFP aliquots. Nevertheless, where indicated in this chapter, I carried out mathematical adjustment of aPL amounts per 1 x 10^9 EV as characterised with SEC/NTA and reported previously in **Chapter 5**.

I plotted the unadjusted EV lipid data on a heatmap to visualise differences in total (throughout the membrane) and externalised (on outer leaflet only) aPL lipids across the clinical groups and between lipid species (**Figure 7.17**). There were higher amounts of externalised plasmalogen aPL in plasma EV compared to diacyl aPL with minimal apparent differences between clinical groups (**Figure 7.17**A). Column-wise hierarchical clustering demonstrated grouping by both *sn1* and *sn2* fatty acids, with lipids containing both a plasmalogen (*sn1*) and arachidonate (*sn2*) forming a separate cluster to lipids containing an acyl (*sn1*) and oleic acid (*sn2*). The observed clustering is likely driven by a high abundance of aPL with a plasmalogen *sn1* and an arachidonate at *sn2*.

There were higher amounts of total aPL in the RF, CAD and ACS group compared to HC (**Figure 7.17**B). The profile of total aPL species in plasma EV consistently showed higher levels of plasmalogen lipids compared with diacyls in all clinical groups. Similar to externalised aPL in EV, column-wise hierarchical clustering of total aPL demonstrated grouping by *sn1* and *sn2* FA, with distinct clusters for plasmalogens (*sn1*) containing arachidonate (*sn2*), and for acyls (*sn1*) containing oleic acid (*sn2*). Once more, this clustering pattern is likely due to the high abundance of plasmalogens in the EV membrane.

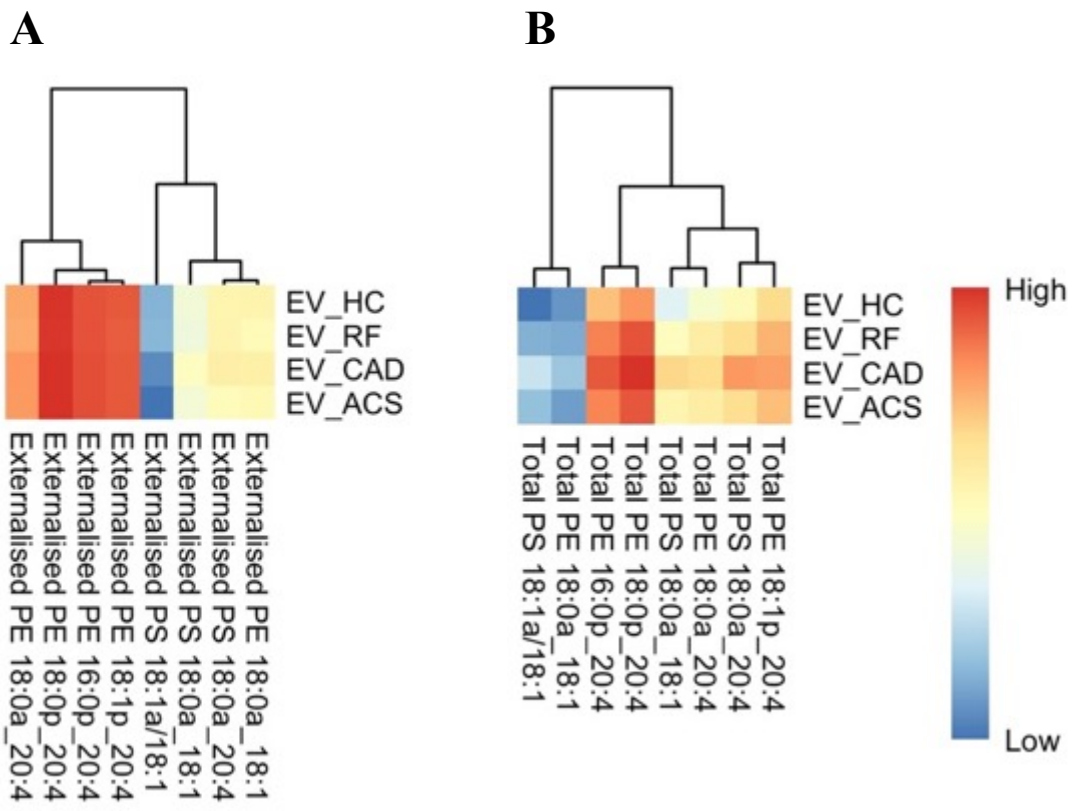

Figure 7.17. Heatmap of aPL lipids in plasma EV from patients with arterial thrombosis demonstrate clustering by both *sn1* bond (acyl vs plasmalogen) and *sn2* fatty acid (20:4 vs 18:1).

Panel A: Externalised aPL from plasma EV. Panel B: Total aPL from plasma EV. Lipids were extracted from EV samples isolated from 6 ml of plasma as in Materials and Methods. Lipids amounts (ng) were calculated by LC-MS/MS, log10 transformed and plotted as a heatmap with hierarchical clustering using the pheatmap R package. ACS: acute coronary syndrome (n=24), CAD: coronary artery disease but no ACS (n=19), RF: Risk factors with no significant coronary artery disease (n=23), HC: healthy control (n=24).

7.2.6 Quantitative analysis of plasma EV aPL demonstrates significantly lower fraction (%) aPL externalised in ACS vs HC

EV-derived aPL lipids were summed by headgroup (PS/PE) and plotted on a boxplot to give an overview of any differences between clinical groups (**Figure 7.18**). Plasma EV isolated from patients with ACS and CAD had significantly higher levels of total PS and total PE compared with HC, which normalised once adjusted by EV counts. The levels of externalised PE and PS demonstrated no significant difference between ACS and HC, with the only detectable difference being higher externalised PS in CAD vs HC/RF which disappeared following adjustment.

Next, I analysed individual PS/PE lipid species detected in plasma EV. The levels of most measured EV-derived total (through the membrane) PE species were higher in plasma from patients with ACS and CAD compared with HC (**Figure 7.19**A). Specifically, ACS/CAD patients had higher levels of total PE 16:0p_20:4 (v HC), PE 18:1p_20:4 (v HC), PE 18:0p_20:4 (v HC) and PE 18:0a_20:4 (v HC) in plasma EV. Additionally, CAD patients had higher levels of total PE 18:0a_18:1 compared with RF. Once adjusted by EV counts however (**Figure 7.19**B), these differences disappear suggesting that they are likely related to the higher EV counts in ACS/CAD vs HC, as seen in **Chapter 5**.

The levels of total PS species in plasma EV were higher in ACS/CAD compared with HC (**Figure 7.20**A). Specifically, patients with ACS/CAD had higher levels of total PS 18:1a/18:1 (v HC), PS 18:0a_18:1 (v HC) and PS 18:0a_20:4 (v HC) in plasma EV. Once adjusted by EV counts however (**Figure 7.20**B), these differences disappear indicating that they relate to the higher EV counts in ACS/CAD vs HC, as seen in **Chapter 5**.

There were no significant differences in the levels of EV-derived externalised (outer leaflet only) PE species from plasma between clinical groups (**Figure 7.21**A). Once adjusted by EV counts however, a trend towards lower levels of externalised PE is noted for EV from RF, CAD and ACS compared with HC (**Figure 7.21**B). EV-derived externalised PS species from plasma were similar between ACS and HC (**Figure 7.22**A), although plasma from patients with CAD had significantly higher levels of externalised PS 18:0a_20:4 (v HC) and PS 18:0a_18:1 (v HC). Once adjusted by EV counts, these differences disappeared (**Figure 7.22**B), indicating that they were driven by higher EV counts in CAD v HC patients.

Overall, these data demonstrate that differences in EV-derived aPL amounts between groups are likely driven by inherent variations in EV counts which were higher in the RF, CAD and ACS group compared with HC.

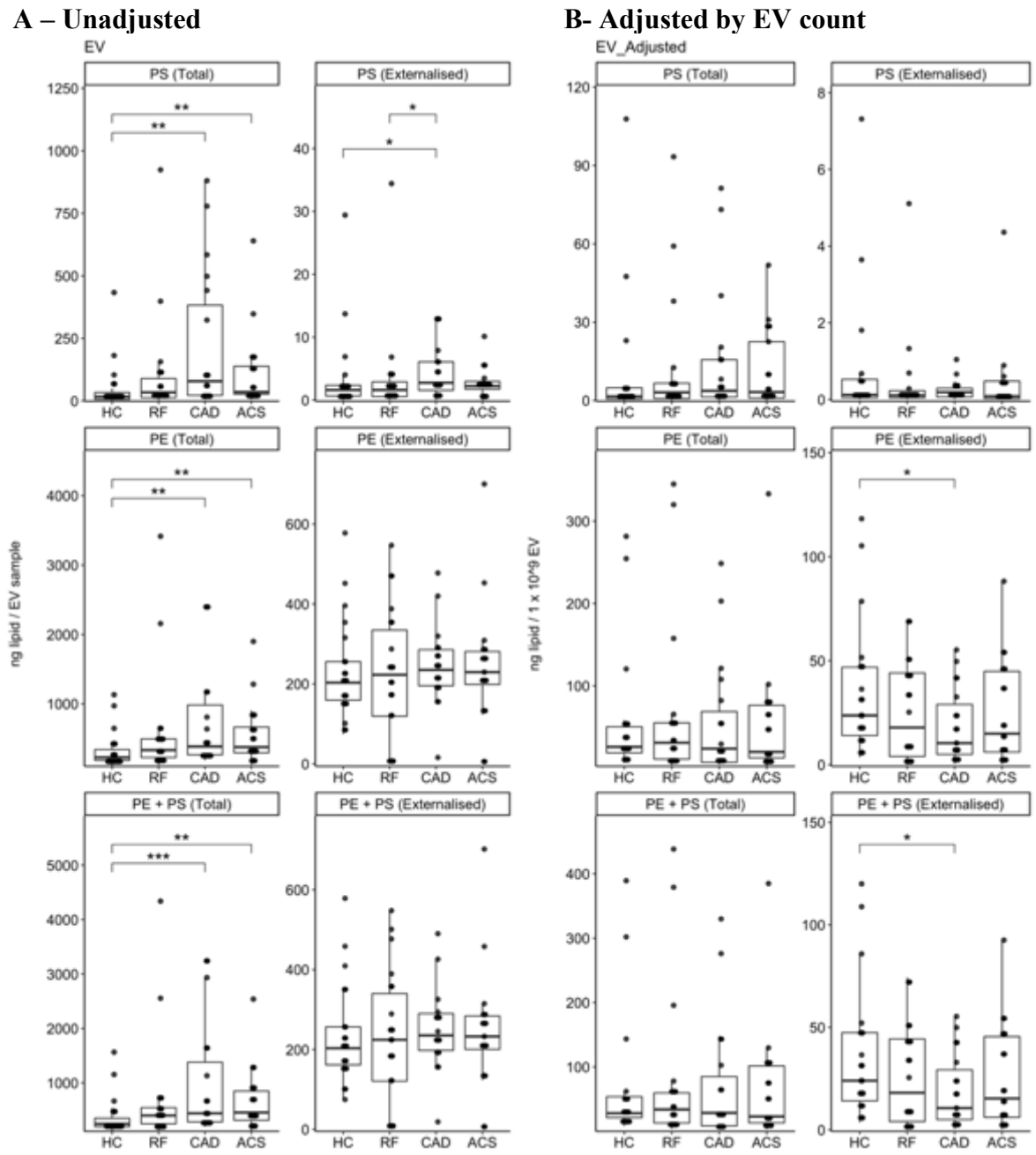

Figure 7.18. Consolidating EV-derived aPL lipids by headgroups demonstrates higher amounts in ACS vs HC for total, but not externalised, aPL.

Lipids were extracted from EV samples isolated from 6 ml of plasma as in Materials and Methods. Lipids amounts (ng) were calculated by LC-MS/MS, summed by headgroup and plotted as a box plot with the ggplot2 R package unadjusted (A) or after adjustment by EV counts (B). Box edges indicate the interquartile range (IQR) with the median line inside the box. Whiskers indicate 1.5 times the IQR. Statistical significance was tested with Mann-Whitney-Wilcoxon test, and where significant differences exist, they are indicated by stars (*: $p < 0.05$, **: $p < 0.01$, ***: $p < 0.001$). ACS: acute coronary syndrome (n=24), CAD: coronary artery disease but no ACS (n=19), RF: Risk factors with no significant coronary artery disease (n=23), HC: healthy control (n=24).

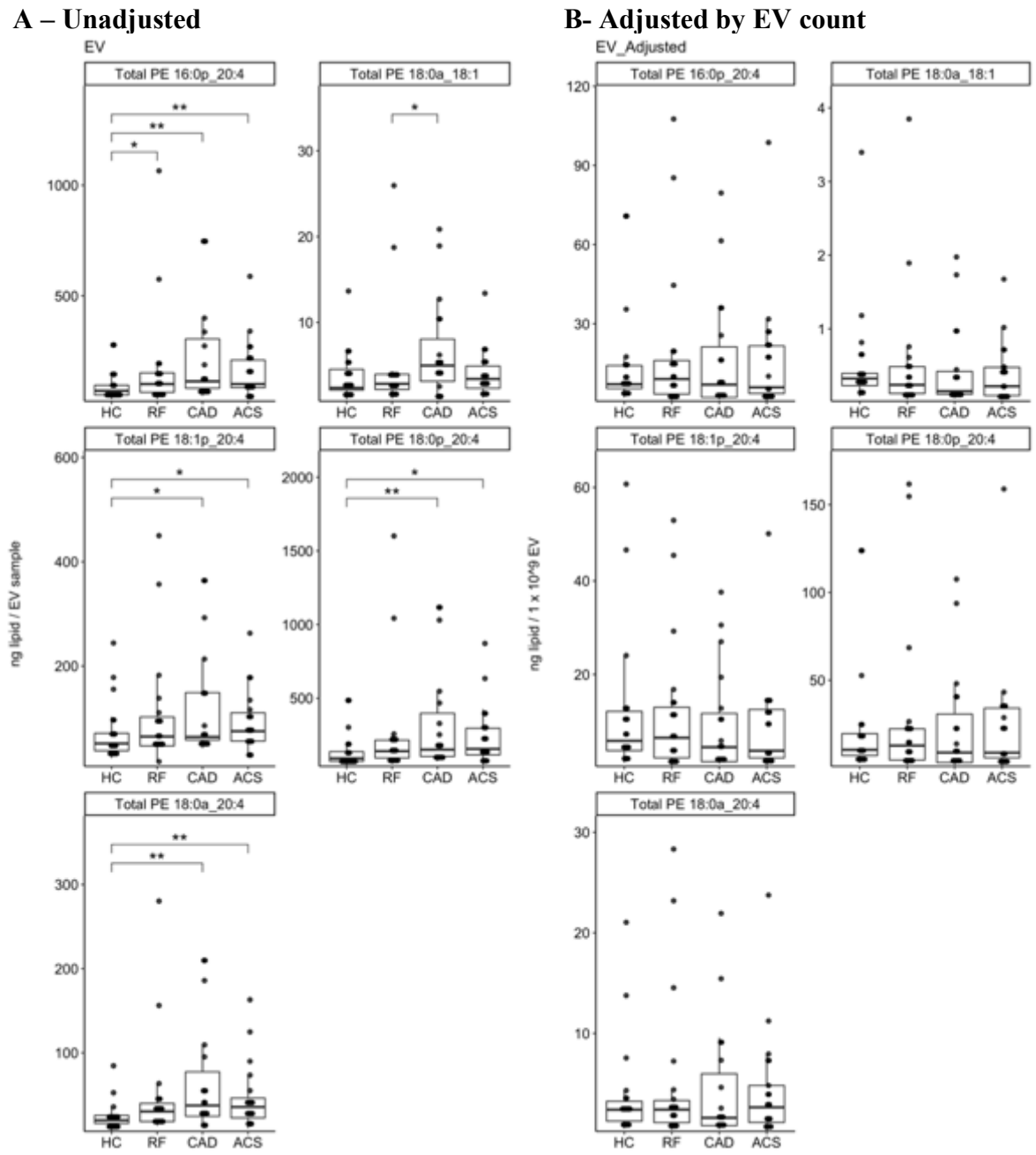

Figure 7.19. Higher levels of EV-derived total PE species in ACS and CAD patients compared with HC, which normalise once adjusted by EV count.

Lipids were extracted from EV samples isolated from 6 ml of plasma as in Materials and Methods. Lipids amounts (ng) were calculated by LC-MS/MS and plotted as a box plot with the ggplot2 R package unadjusted (A) or after adjustment by EV counts (B). Box edges indicate the interquartile range (IQR) with the median line inside the box. Whiskers indicate 1.5 times the IQR. Statistical significance was tested with Mann-Whitney-Wilcoxon test, and where significant differences exist, they are indicated by stars (*: $p < 0.05$, **: $p < 0.01$, ***: $p < 0.001$). ACS: acute coronary syndrome (n=24), CAD: coronary artery disease but no ACS (n=19), RF: Risk factors with no significant coronary artery disease (n=23), HC: healthy control (n=24).

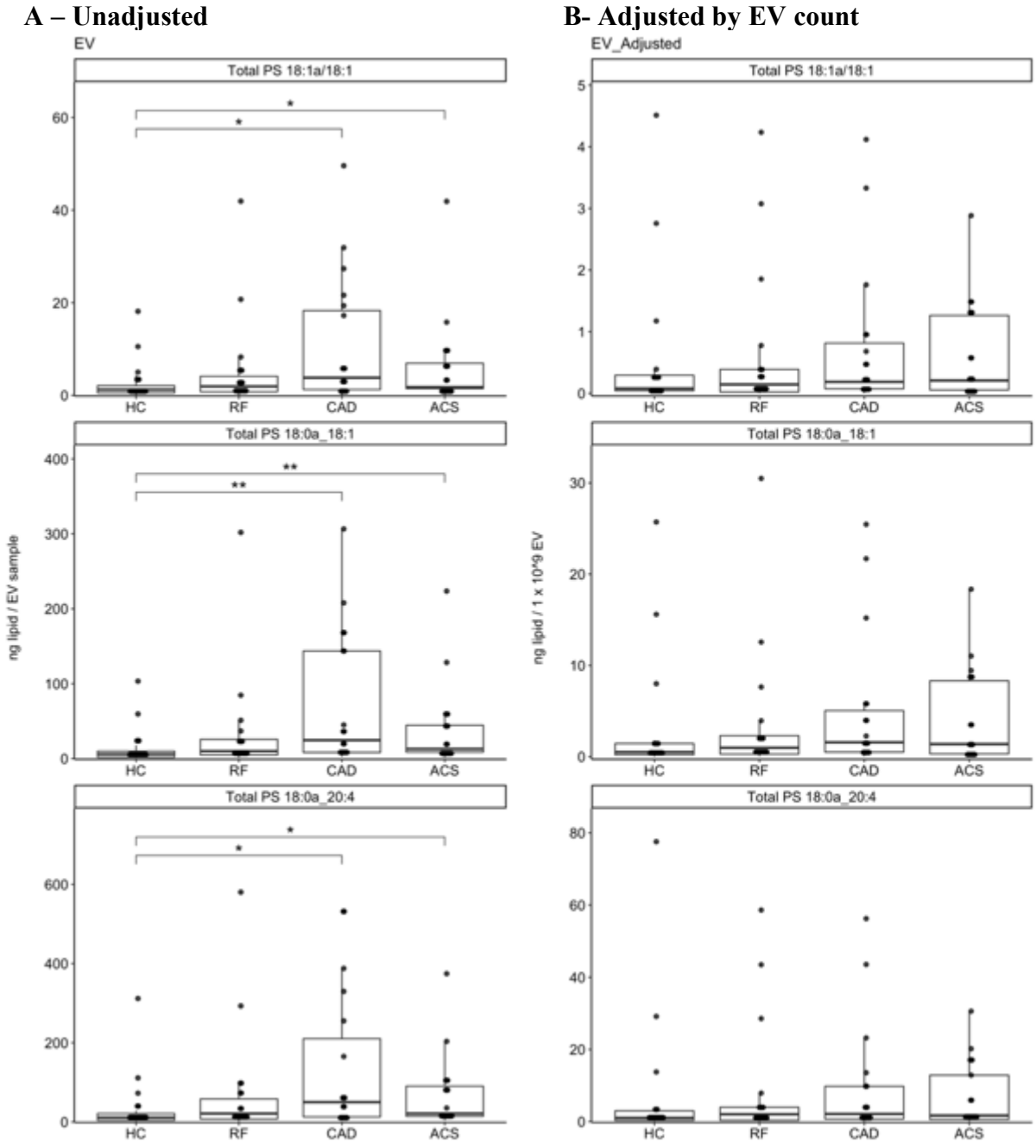

Figure 7.20. Higher levels of EV-derived total PE species in ACS and CAD patients compared with HC, which is normalised once adjusted by EV count.

Lipids were extracted from EV samples isolated from 6 ml of plasma as in Materials and Methods. Lipids amounts (ng) were calculated by LC-MS/MS and plotted as a box plot with the ggplot2 R package unadjusted (A) or after adjustment by EV counts (B). Box edges indicate the interquartile range (IQR) with the median line inside the box. Whiskers indicate 1.5 times the IQR. Statistical significance was tested with Mann-Whitney-Wilcoxon test, and where significant differences exist, they are indicated by stars (*: $p < 0.05$, **: $p < 0.01$, ***: $p < 0.001$). ACS: acute coronary syndrome (n=24), CAD: coronary artery disease but no ACS (n=19), RF: Risk factors with no significant coronary artery disease (n=23), HC: healthy control (n=24).

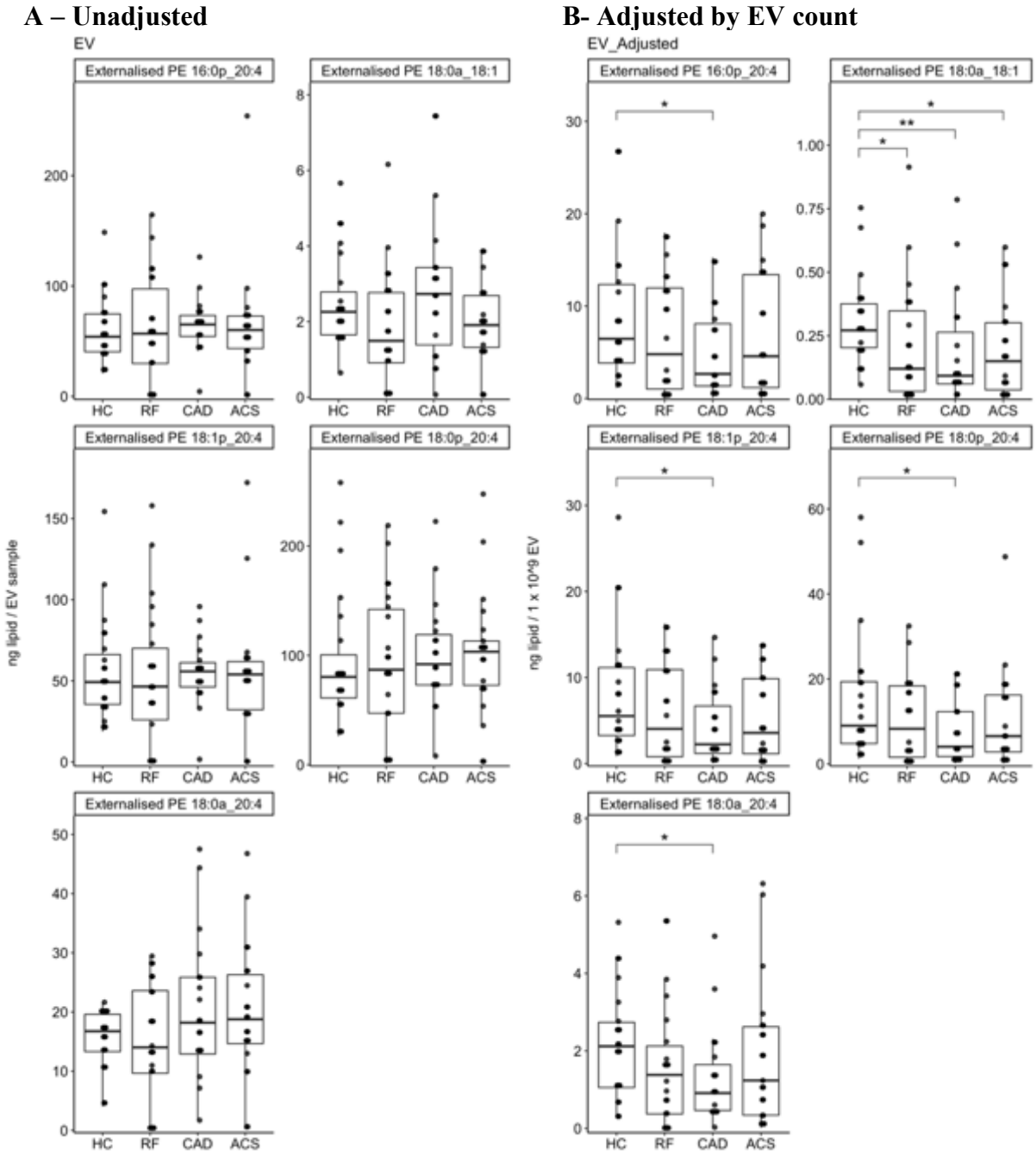

Figure 7.21. The levels of EV-derived externalised PE species were similar across all clinical groups.

Lipids were extracted from EV samples isolated from 6 ml of plasma as in Materials and Methods. Lipids amounts (ng) were calculated by LC-MS/MS and plotted as a box plot with the ggplot2 R package unadjusted (A) or after adjustment by EV counts (B). Box edges indicate the interquartile range (IQR) with the median line inside the box. Whiskers indicate 1.5 times the IQR. Statistical significance was tested with Mann-Whitney-Wilcoxon test, and where significant differences exist, they are indicated by stars (*: $p < 0.05$, **: $p < 0.01$, ***: $p < 0.001$). ACS: acute coronary syndrome (n=24), CAD: coronary artery disease but no ACS (n=19), RF: Risk factors with no significant coronary artery disease (n=23), HC: healthy control (n=24).

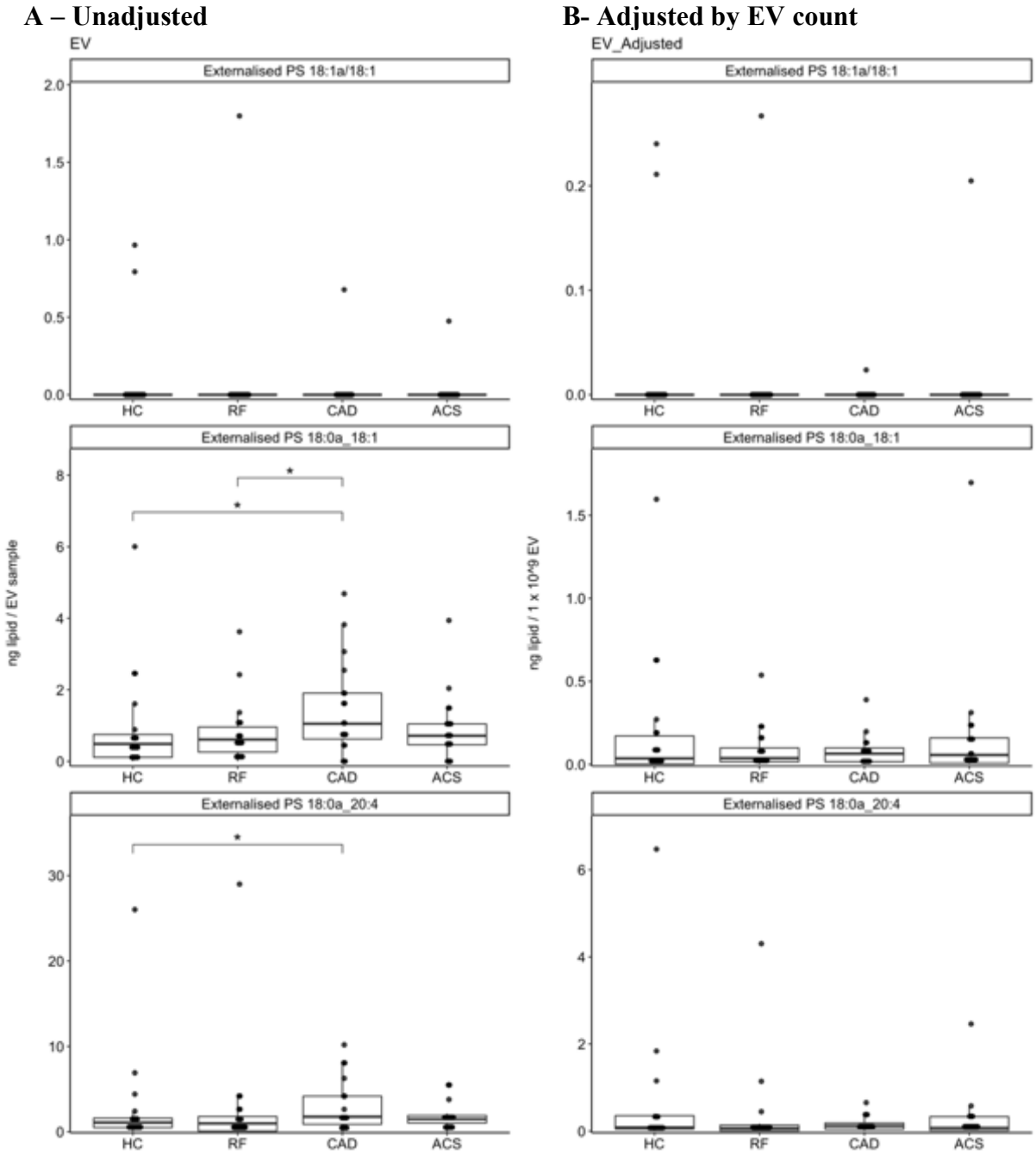

Figure 7.22. The levels of EV-derived externalised PS species were higher in CAD, but not ACS, compared with HC; but normalise after adjustment by EV count.

Lipids were extracted from EV samples isolated from 6 ml of plasma as in Materials and Methods. Lipids amounts (ng) were calculated by LC-MS/MS and plotted as a box plot with the ggplot2 R package unadjusted (A) or after adjustment by EV counts (B). Box edges indicate the interquartile range (IQR) with the median line inside the box. Whiskers indicate 1.5 times the IQR. Statistical significance was tested with Mann-Whitney-Wilcoxon test, and where significant differences exist, they are indicated by stars (*: $p < 0.05$, **: $p < 0.01$, ***: $p < 0.001$). ACS: acute coronary syndrome (n=24), CAD: coronary artery disease but no ACS (n=19), RF: Risk factors with no significant coronary artery disease (n=23), HC: healthy control (n=24).

Next, I examined EV samples for differences in the fraction (percentage) of PE externalised, calculated as ng externalised (outer leaflet) ÷ ng total (throughout membrane) × 100%, across the clinical groups for all PE lipid species in plasma EV (**Figure 7.23**). This demonstrated that significantly lower % PE externalised were detected in plasma EV from patients with ACS/CAD/RF compared with HC. This was the case for all PE species. The fraction (%) PS externalised in plasma EV was similar between ACS and CAD patients compared with HC/RF (**Figure 7.24**). This was the case for all PS species.

Taken together, the plasma EV aPL data demonstrate that despite no differences in unadjusted externalised (outer leaflet) aPL in ACS patients compared with HC, the fraction (%) aPL externalised in plasma EV from ACS patients was lower than HC. Of note is the high fraction % aPL externalised in EV which was in the order of 50-80%, contrasting with activated platelets and leukocytes which were in the order of 10-30% seen in sections **7.2.2** and **7.2.4**. The association between % aPL and thrombin generation was explored below in section **7.2.7**.

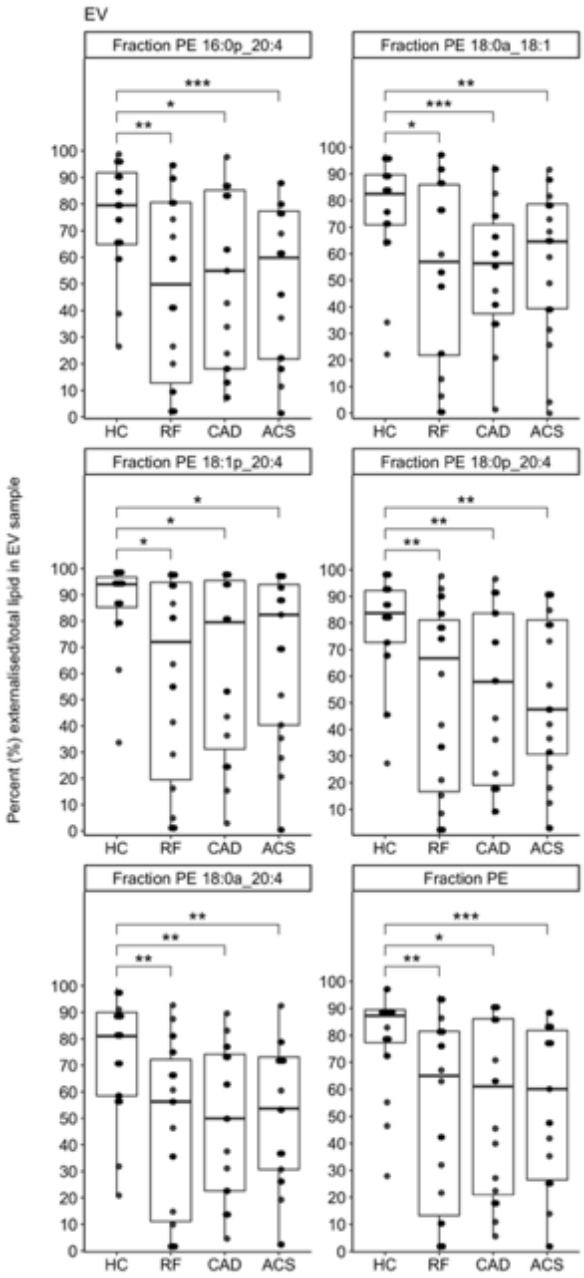

Figure 7.23. Fraction of PE externalised in plasma EV is lower in ACS/CAD/RF compared with HC.

The fraction of externalised PE was calculated for each sample and expressed as a percentage (ng externalised ÷ ng total × 100%). Lipids were extracted from EV samples isolated from 6 ml of plasma as in Materials and Methods. Lipids amounts (ng) were calculated by LC-MS/MS with fractions calculated as above and plotted as a box plot with the ggplot2 R package. Box edges indicate the interquartile range (IQR) with the median line inside the box. Whiskers indicate 1.5 times the IQR. Statistical significance was tested with Mann-Whitney-Wilcoxon test, and where significant differences exist, they are indicated by stars (*: $p < 0.05$, **: $p < 0.01$, ***: $p < 0.001$). ACS: acute coronary syndrome (n=24), CAD: coronary artery disease but no ACS (n=19), RF: Risk factors with no significant coronary artery disease (n=23), HC: healthy control (n=24).

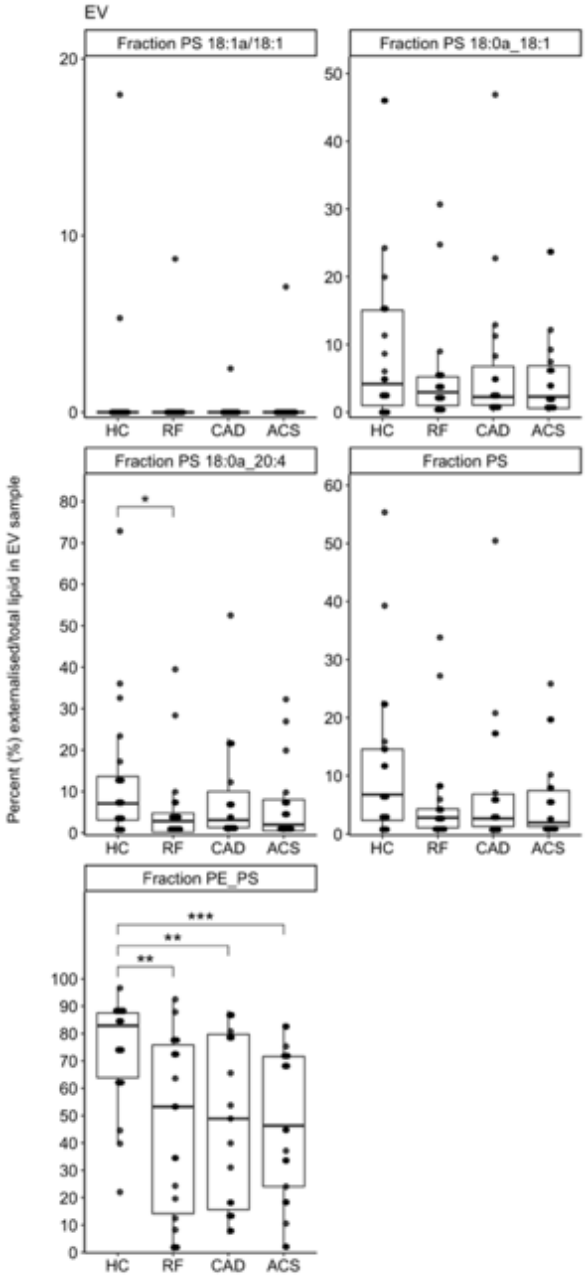

Figure 7.24. Fraction of PS externalised in plasma EV is similar between ACS and CAD patients and HC.

The fraction of externalised PS was calculated for each sample and expressed as a percentage (ng externalised ÷ ng total × 100%). Lipids were extracted from EV samples isolated from 6 ml of plasma as in Materials and Methods. Lipids amounts (ng) were calculated by LC-MS/MS with fractions calculated as above and plotted as a box plot with the ggplot2 R package. Box edges indicate the interquartile range (IQR) with the median line inside the box. Whiskers indicate 1.5 times the IQR. Statistical significance was tested with Mann-Whitney-Wilcoxon test, and where significant differences exist, they are indicated by stars (*: $p < 0.05$, **: $p < 0.01$, ***: $p < 0.001$). ACS: acute coronary syndrome (n=24), CAD: coronary artery disease but no ACS (n=19), RF: Risk factors with no significant coronary artery disease (n=23), HC: healthy control (n=24).

7.2.7 Thrombin generation on membrane surfaces correlates positively with resting platelet and leukocyte % aPL externalised, but negatively with plasma EV % aPL externalised.

Next, I wanted to investigate the relationship of aPL amounts with the coagulation capacity of plasma membranes, to understand whether platelets, leukocytes and EV differ in their contribution to coagulation reactions via aPL lipids. To do this, I carried out correlation analyses to examine the dependence between the amounts of aPL species described in this chapter and the amount of thrombin generated on the surface of resting platelets, resting leukocytes and plasma EV reported in **Chapter 5**. It is worth specifying that no count adjustment for EV data was used for this correlation analysis, so as to provide a more direct measure of the relationship between membrane aPL and thrombin generation capacity in the EV preparations.

Thrombin generation correlated positively with some total (throughout the membrane) PE species in plasma EV and leukocytes, but not platelets (**Figure 7.25**). Specifically, weak, but significant, positive correlations were noted for thrombin generation with total PE 18:0a_18:1 in leukocytes and EV, and with PE 16:0p_20:4, PE 18:1p_20:4 , PE 18:0p_20:4 and PE 18:0a_20:4 in EV. There was no correlation seen for thrombin generation with total PS 18:1a/18:1, PS 18:0a_18:1 or PS 18:0a_20:4 in platelets, leukocytes or EV.

In terms of externalised aPL, there was no correlation observed for thrombin generation with any platelet aPL species. However, thrombin generation correlated positively with some externalised aPL species in leukocytes, but negatively with externalised PE in EV (**Figure 7.26**). Specifically, there was weak (yet significant) positive correlation of thrombin generation

with externalised PS 18:0a_18:1 and PE 18:0a_18:1 in resting leukocytes. In EV, whilst there was no correlation with externalised PS species, thrombin generation was negatively correlated with externalised PE 16:0p_20:4 and PE 18:1p_20:4.

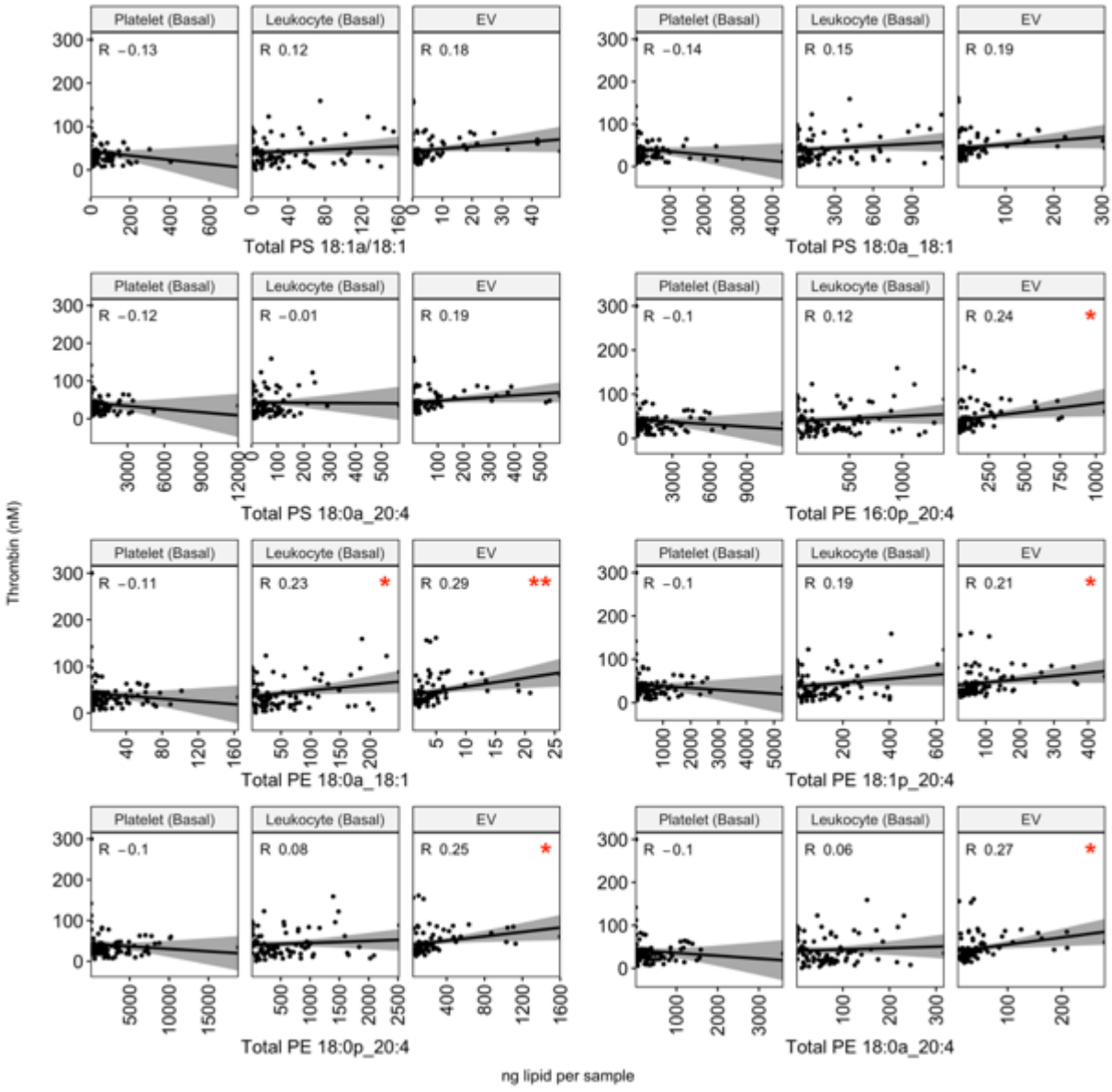

Figure 7.25. Thrombin generation correlated positively with total PE species in EV (all species), leukocytes (PE 18:0a_18:1) but not platelets.

A correlation analysis of thrombin generation on the surface of resting platelets, resting leukocytes and plasma EV with total (throughout the membrane) aPL species is shown in this diagram. The correlated data was generated from the prothrombinase assay and aPL lipid quantification for all patients (as in Materials and Methods), Pearson's R correlation coefficients and significance was calculated and graphs plotted with the ggplot2 R package. Significant correlations indicated by a red star(s) as follows *: $p < 0.05$, **: $p < 0.01$, ***: $p < 0.001$.

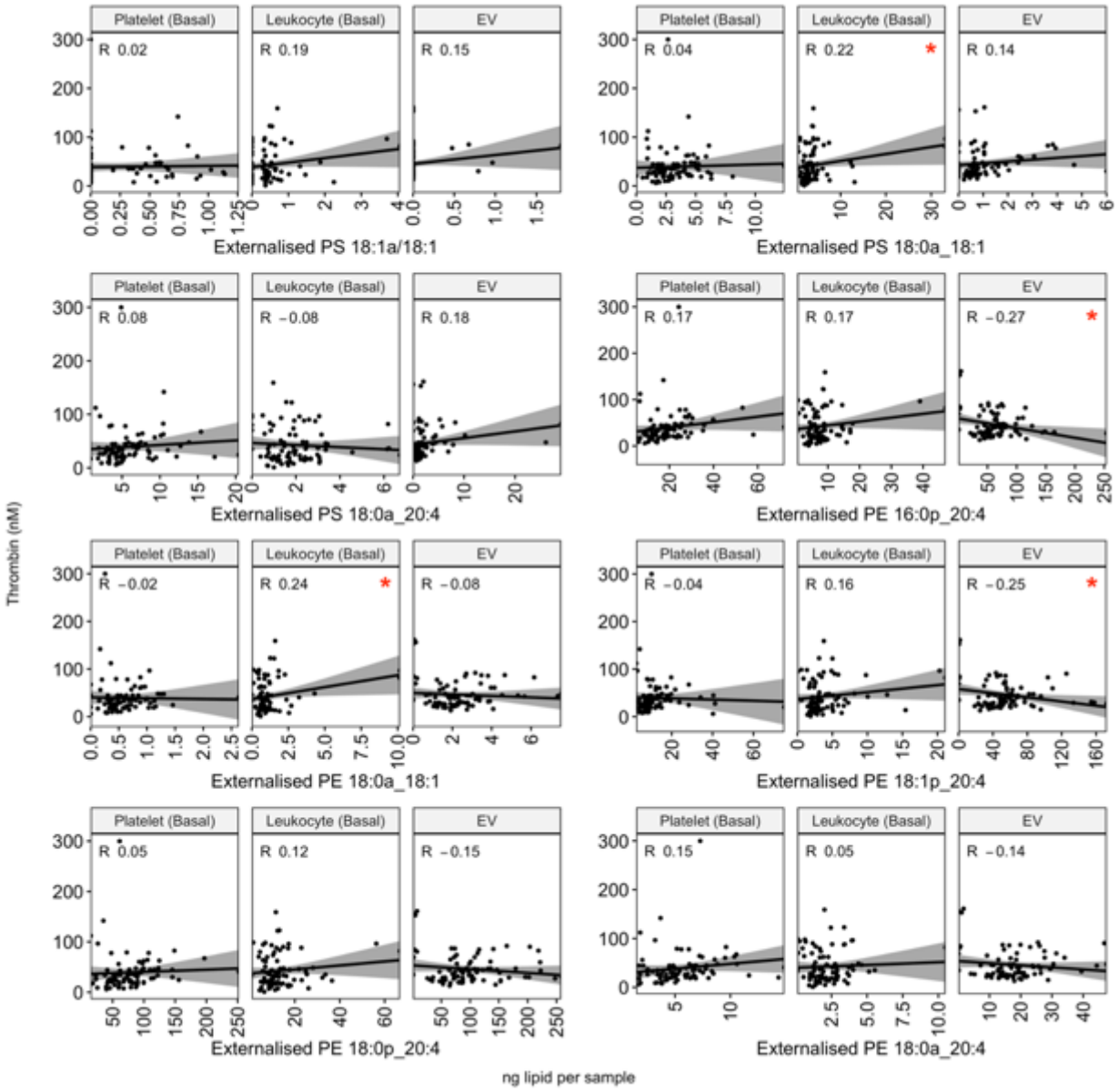

Figure 7.26. Thrombin generation correlates positively with externalised aPL species in leukocytes (PE 18:0a_18:1), but negatively with externalised PE in EV (PE 16:0p_20:4, PE 18:1p_20:4).

A correlation analysis of thrombin generation on the surface of resting platelets, resting leukocytes and plasma EV with externalised (outer leaflet) aPL species is shown in this diagram. The correlated data was generated from the prothrombinase assay and aPL lipid quantification for all patients (as in Materials and Methods), Pearson's R correlation coefficients and significance was calculated and graphs plotted with the ggplot2 R package. Significant correlations indicated by a red star(s) as follows *: $p < 0.05$, **: $p < 0.01$, ***: $p < 0.001$.

Next, to investigate whether there is a relationship between thrombin generation and fraction (%) externalised aPL species in resting platelets, resting leukocytes and plasma EV, I carried out a correlation analysis. This demonstrated a positive correlation between % aPL externalised in resting platelets and leukocytes, but a negative correlation in plasma EV (**Figure 7.27**). Specifically, significant positive correlations with thrombin generation were noted for all PE and PS species in resting platelets. In resting leukocytes, significant positive correlations were seen for PS 18:0a_18:1, PE 16:0p_20:4, PE 18:0a_18:1, PE 18:0p_20:4 and PE 18:0a_20:4. In plasma EV, no correlation was noted with PS, but there was a significant negative correlation for all PE species with an R value of -0.68 to -0.65.

Pooling of aPL lipids by head group demonstrated that thrombin generation correlates positively with the fraction of externalised PS/PE in platelets and leukocytes, but negatively with externalised PE and fraction of externalised PE in plasma EV (**Figure 7.28**). Specifically, significant positive correlations were noted in platelets and leukocytes for thrombin generation and all fraction (%) externalised PE, PS and sum of all aPL (PE plus PS). In plasma EV, a positive correlation was noted between thrombin generation and total PS and PE, but a negative correlation was noted with externalised PE and fraction (%) of externalised PE.

Taken together, these data are consistent with the accepted role of aPL in mediating coagulation reactions upon cell activation and increased aPL externalisation[20,27]. Unexpectedly however, plasma EV, which were demonstrated by this thesis to have much higher fraction (%) PE externalised on the surface (in the order of >50%, **Figure 7.24**) compared with activated platelets and leukocytes (in the order of <25%, **Figure 7.8** and **Figure 7.16**), demonstrate a negative correlation with thrombin generation. In other words, a higher fraction (%) PE on the

EV surface was associated with lower thrombin generation. Possible implications and mechanisms of this will be addressed in the discussion section of this chapter.

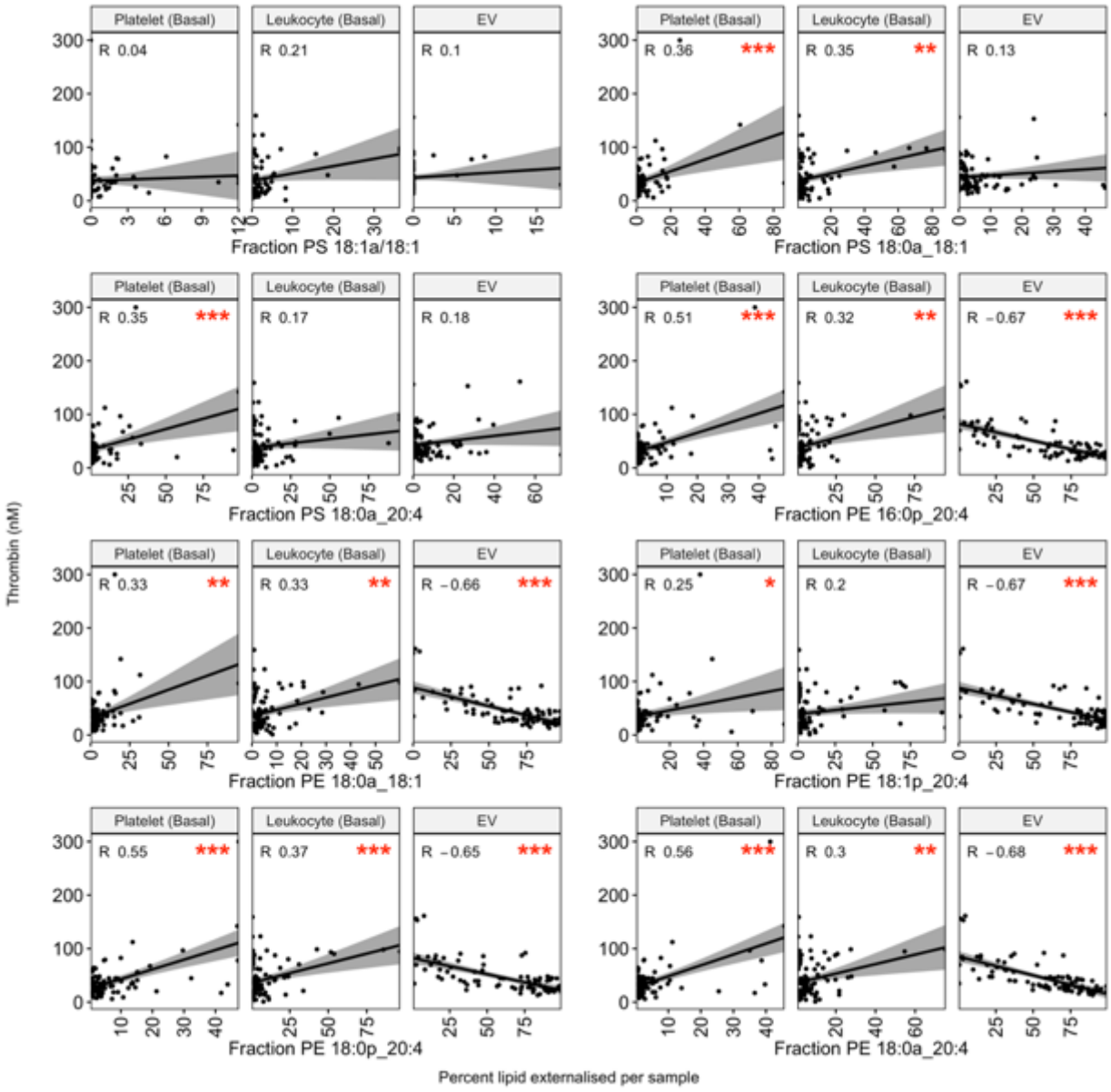

Figure 7.27. Thrombin generation correlates with fraction (%) externalised aPL positively in platelets and leukocytes, but negatively in EV.

A correlation analysis of thrombin generation on the surface of resting platelets, resting leukocytes and plasma EV with fraction (%) externalised aPL species is shown in this diagram. The correlated data was generated from the prothrombinase assay and aPL lipid quantification for all patients (as in Materials and Methods), the fraction of externalised aPL was calculated as a percentage (ng externalised ÷ ng total × 100%), Pearson's R correlation coefficients and significance was calculated and graphs plotted with the ggplot2 R package. Significant correlations indicated by a red star(s) as follows *: $p < 0.05$, **: $p < 0.01$, ***: $p < 0.001$.

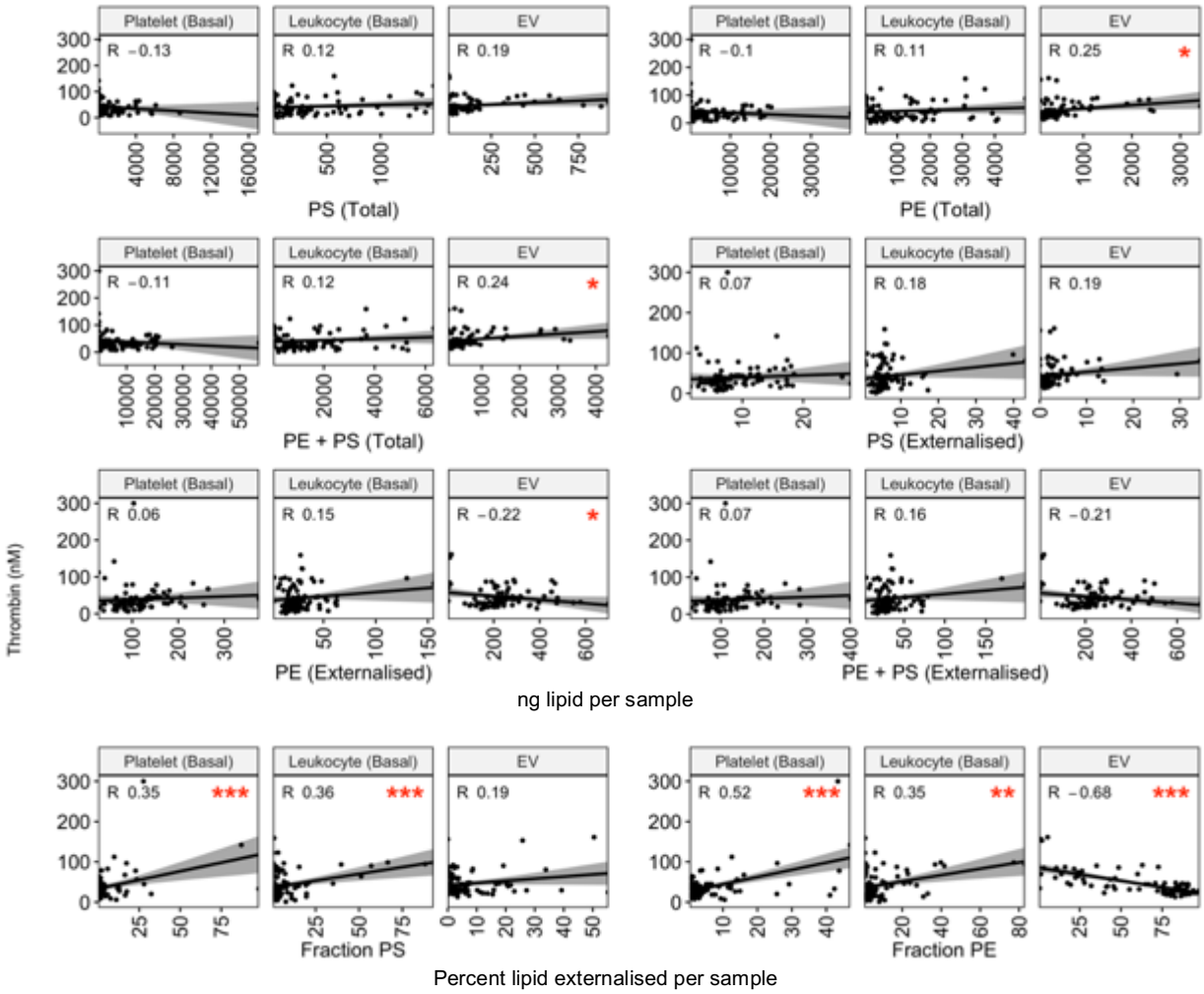

Figure 7.28. Combining aPL species by head group demonstrates that thrombin generation correlates positively with fraction (%) externalised PS/PE in platelets and leukocytes, but negatively with externalised PE and fraction (%) externalised PE in plasma EV.

A correlation analysis of thrombin generation on the surface of resting platelets, resting leukocytes and plasma EV with total, externalised and fraction (%) externalised aPL pooled by headgroup (PS/PE) is shown in this diagram. The correlated data was generated from the prothrombinase assay and aPL lipid quantification for all patients (as in Materials and Methods), the fraction of externalised aPL was calculated as a percentage (ng externalised ÷ ng total × 100%), Pearson's R correlation coefficients and significance was calculated and graphs plotted with the ggplot2 R package. Significant correlations indicated by a red star(s) as follows *: $p < 0.05$, **: $p < 0.01$, ***: $p < 0.001$.

7.3 DISCUSSION

Throughout this chapter, I studied the lipid profiles from platelets and leukocytes in both resting and *in vitro* activated conditions. Whilst it was important to study activated cells to examine their capacity to mobilise and externalise aPL[20,90], resting states are perhaps more relevant in human disease as they reflect the nature of circulating membranes in patients following an ACS event. Variations to the resting circulating PL membranes may therefore affect coagulation reactions in ACS, and play some part in the increased thrombin generation described in the literature[288]. In this chapter, I demonstrated that patients with ACS have more ng externalised aPL on the surface of their resting platelets and leukocytes, but a similar fraction (%) aPL externalised, compared with HC. In contrast, plasma EV from ACS patients had similar amounts of externalised aPL to HC, but higher total PE which led to a lower fraction (%) PE externalised. This may suggest that the proportion of outer/inner leaflet aPL is more relevant in driving differences in coagulation reactions between clinical groups than ng externalised as will be discussed below. Indeed, thrombin generation was better correlated with fraction (%) aPL (positive in platelets and leukocytes, and negative in EV) than ng externalised. Seeing as differences in thrombin generation between groups seen in **Chapter 5** were mainly seen with EV, my findings in this chapter suggest a potential role for circulating EV in mediating procoagulant activity in arterial thrombosis driven by % PE composition on their membrane surfaces as will be discussed below.

Platelets from patients with ACS had higher levels of externalised aPL compared with HC/RF in both resting and activated conditions (**Figure 7.2**). This is consistent with a recent paper by Wang et al where a higher number of PS^{+ve} platelets, as labelled with lactadherin and measured with flow cytometry, was detected in patients with ACS compared with controls with

cardiovascular risk factors[344]. However, it is unclear whether these higher external aPL levels are a cause or a consequence of the acute inflammation caused by ACS. Whilst having higher levels of external-facing aPL may suggest that platelets from ACS patients have more procoagulant activity, this was not found to be the case in **Chapter 5** where thrombin generation on the surface of resting platelets was similar across all groups. Indeed, externalised aPL (ng) was not correlated with thrombin generation on the surface of resting platelets as seen in **Figure 7.26**. However, there was a positive correlation noted between fraction (%) of aPL externalised and the amount of thrombin generation on the surface of resting platelets (**Figure 7.27**). This is consistent with the known essential role of aPL externalisation in mediating haemostasis, as seen in patients with Scott syndrome who lack this ability[26]. This suggests that the fraction (%) aPL externalised is more relevant to coagulation reactions than pure amount of ng external-facing aPL in platelets. The reason for this may relate to the influence of the PL composition of both the inner and outer leaflets on membrane curvature and therefore potentially on enzymatic kinetics[347]. Specifically, it is recognized that PE lipids impose a negative membrane curvature due to their inverted conical shape owing to a smaller headgroup relative to FA tail (**Figure 7.29**)[347]. It is also reported that membranes with a negative curvature may allosterically regulate enzymatic activity, as reported for diacylglycerol kinase ϵ bound to *in-vitro* generated liposomes varying in PE/PC amounts[346]. Therefore, it is conceivable that the ratio of outer:inner PE may be more influential than pure amount (ng) of outer PE in allosterically regulating coagulation complex activity, which remains untested.

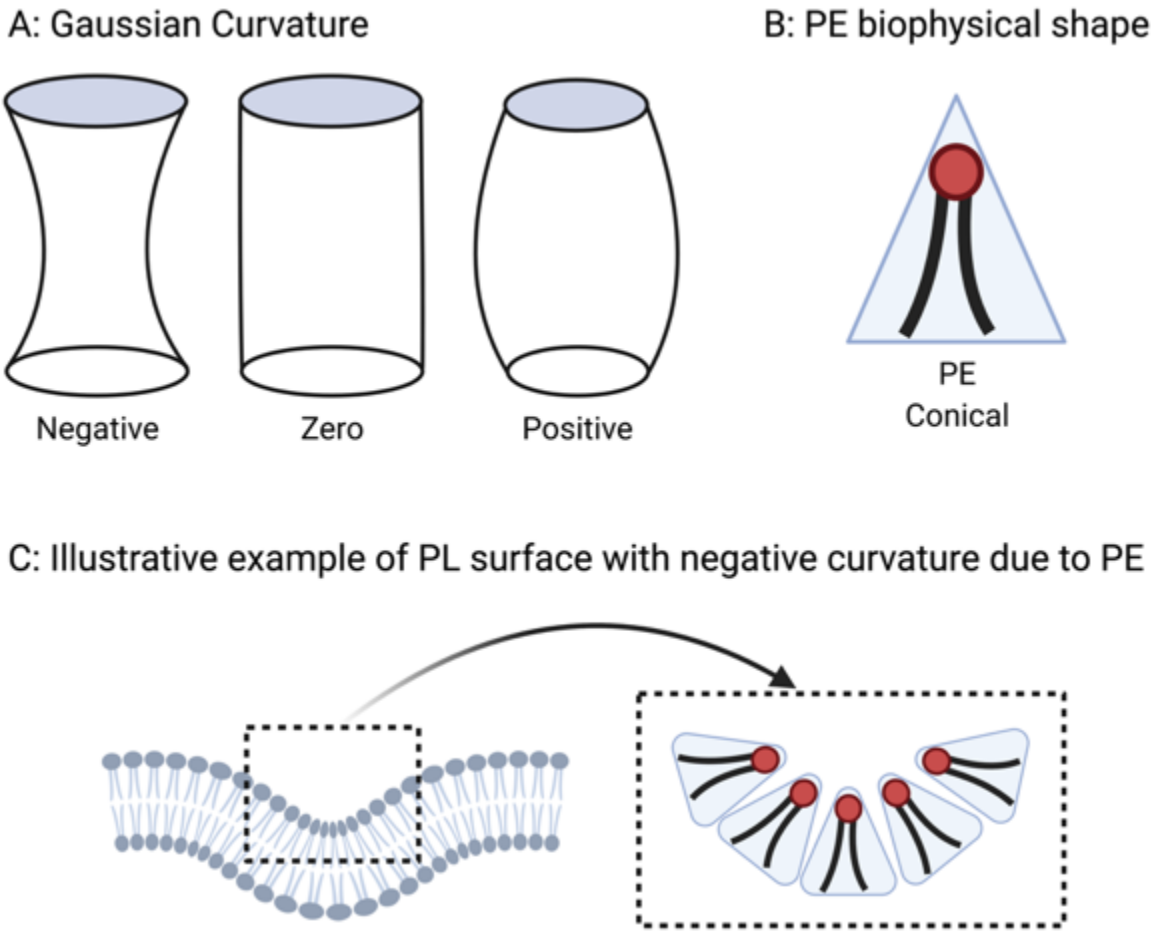

Figure 7.29. The influence of PE on the curvature of cell membranes.

A) Cell membranes exhibit Gaussian curvature due to the biophysical properties of lipid and protein components. B) Phosphatidylethanolamine (PE) has an inverted conical biophysical shape due to the relatively small headgroup compared to the lipid tail. C) The presence of inverted conical lipids, such as PE, in the outer leaflet of the phospholipid membrane results in a negative curvature[347].

Unlike platelets, leukocytes from ACS generated more thrombin on their surface compared with HC as seen previously in **Chapter 5**. Additionally, externalized PS 18:0a_18:1 was higher in resting leukocytes from ACS patients compared with HC (**Figure 7.14**) and correlated positively with thrombin generation in leukocytes (**Figure 7.26**). Unlike the conical shape seen with lipids containing a PE head group, PS lipids have a cylindrical shape. This may suggest that their impact on membrane curvature is less than PE and therefore ng PS external may be more important than the ratio between outer and inner PS. The mechanism by which external facing PS affects coagulation reactions may be solely through its negative charge in physiological pH, and not related to the membrane curvature. Taken together, it is possible that the higher thrombin generation on the surface of resting leukocytes in ACS vs HC described in **Chapter 5** is related to the higher external PS 18:0a_18:1 observed in this chapter. This is consistent with similar observations reported in the literature, where a higher number of PS^{+ve} leukocytes correlated to more thrombin and FXa generation on the surface of leukocytes from ACS patients compared with controls[344].

The higher amounts of total PE seen in EV samples from ACS, CAD and RF patients compared with HC (**Figure 7.19**) is likely related to the higher number of circulating EV seen in these patient groups compared with HC as shown in **Chapter 5** and previously reported in the literature[349]. As described earlier, recognizing that the biophysical properties of the membrane curvature may be influenced by both external and total aPL, the fraction (%) aPL externalised was calculated, showing lower % PE externalised in EV samples from ACS compared with HC (**Figure 7.23**). Unlike platelets and leukocytes however, the fraction (%) PE in EV samples correlated negatively with thrombin generation (**Figure 7.27**). This is despite the observation that EV have a very high amount of fraction % PE externalised (>50%, **Figure 7.24**) compared with platelets and leukocytes (<25%, even following activation, **Figure 7.8**

and **Figure 7.16**). Indeed, when I plotted the amount of thrombin generated against the fraction % PE from all samples, I observed an inverted-U relationship as shown below in **Figure 7.30**. In other words, the amount of thrombin generation increases with rising fraction % PE externalised until a point (around 40-50% external:total membrane PE), when it takes a turn downwards with lower thrombin generation at very high % PE externalisation (>50%) (**Figure 7.30**). The mechanism for this is unknown, but possible factors influencing this interaction may relate to the different curvature between blood cells and EV. The smaller diameter of EVs compared with blood cells makes them have a higher curvature[348]. When this is combined with the very high fraction % PE externalised (inverted cone shape), it may lead to a much more negative curvature on the surface of EV compared with platelets and leukocytes[346,347,350]. This very high curvature in turn may allosterically modify coagulation factor assembly on the EV membrane surface leading to possible factor sequestration or inhibition of prothrombinase activity[346,347,350]. The observation of higher membrane procoagulant ability at lower negatively charged PL concentration was also observed by previous studies examining procoagulant HETE-PE containing liposomes *in vitro*[81]. This was hypothesized to be a consequence of lower lipid content enabling coagulation proteins to co-localize in smaller areas at higher concentrations[81]. This hypothesis remains untested but highlights a new perspective on the role of the aPL-rich EV in influencing procoagulant reactions through high % PE externalisation and membrane curvature[81].

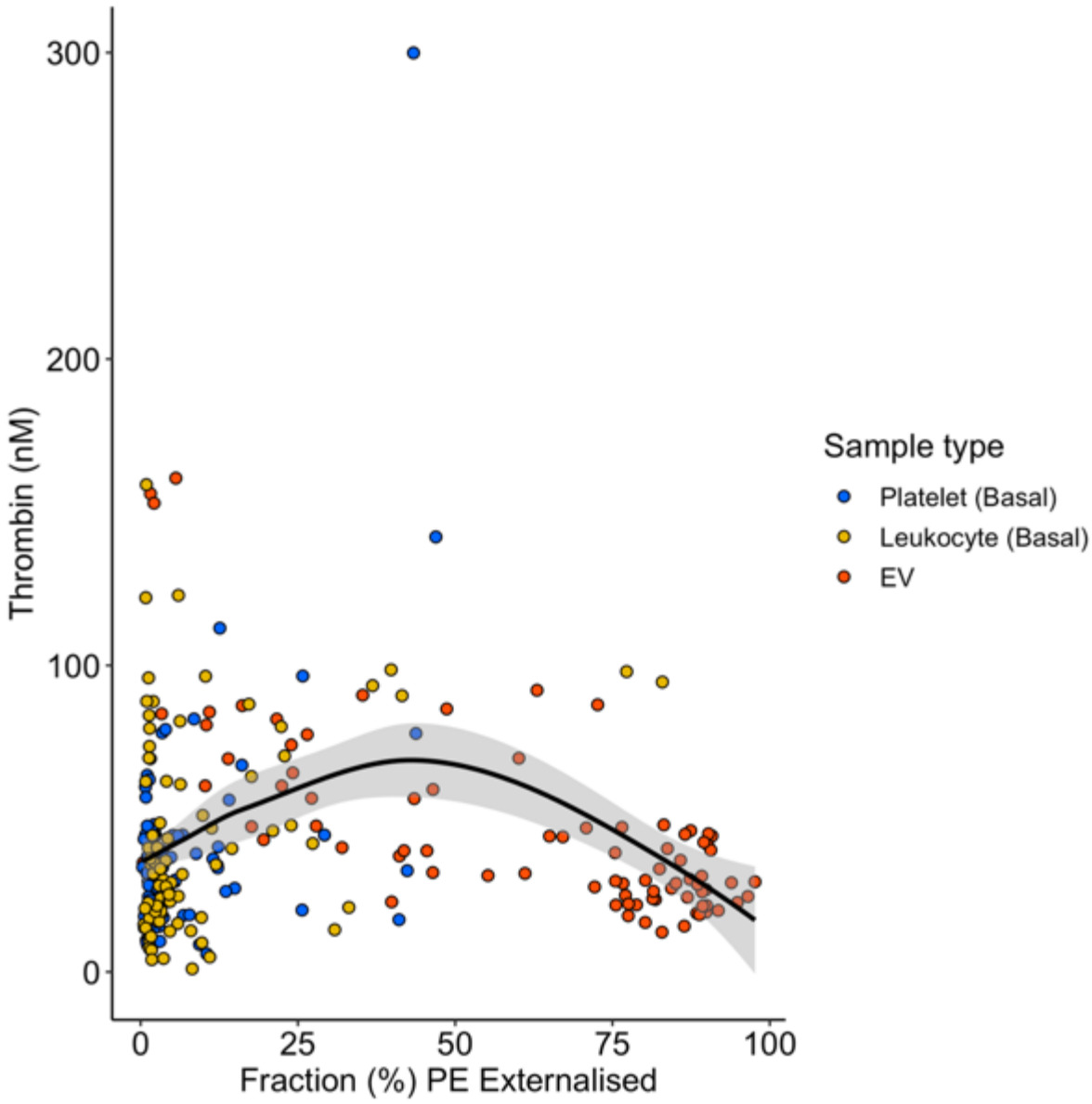

Figure 7.30. Thrombin generation exhibits an inverted-U relationship with the fraction % PE externalised on membrane surfaces.

A scatter plot of thrombin generation on the surface of resting platelets, resting leukocytes and plasma EV with fraction (%) externalised PE species is shown in this diagram. A curve of best fit was drawn using Local Polynomial Regression Fitting ('loess' function in R) and plotted with 95% confidence intervals (shaded grey). Data was generated from the prothrombinase assay and aPL lipid quantification for all patients (as in Materials and Methods), the fraction of externalised PE was calculated as a percentage (ng externalised ÷ ng total × 100%). Graphs plotted with the ggplot2 R package and samples labelled by type (platelets, leukocytes or EV).

It is generally accepted that annexin V^{+ve} EV (containing externalised aPL) are procoagulant. Many studies have concluded that a higher number of EVs implies more PS exposure in the circulation which in turn could lead to a more procoagulant phenotype[213,229,351]. This was observed in a study by Liu et al, where ACS patients were noted to have more PS^{+ve} EV compared with healthy controls. In the same study, the authors demonstrated that *in-vitro* tenase and prothrombinase activity on EV-rich plasma fractions correlated positively with EV counts and was significantly reduced upon blocking PS-binding sites with lactadherin[351]. However, methods used in the literature to study PS^{+ve} EV are limited to flow cytometry-based assays that rely on the use of annexin V. This marker is used to label EV with externalised aPL, but does not allow for the accurate quantification of external aPL amounts nor for determining the total aPL content within the membranes. Therefore, any conclusions from such study may be due to the impact of EV count on thrombin generation as opposed to altered EV membrane aPL amounts. To complicate matters, recent advances in cryo-transmission electron microscopy have demonstrated that almost half of EV released by platelets were not labelled by annexin V[352,353]. This raises doubts as to the sensitivity of annexin V probes in detecting EV which by definition must contain aPL on their outer leaflet, compromising the quantitative accuracy of methods employing this probe to detect aPL[217,349]. To tackle the limitations with annexin V-based aPL quantification, this chapter utilises the only technique published to date to quantify aPL with a high degree of accuracy distinguishing between external and total membrane aPL using LC-MS/MS and biotin derivatisation[117]. Furthermore, whilst this method has been used before in platelets and leukocytes, this chapter represents a novel description of applying this technique to plasma EV[20], demonstrating that the fraction % PE externalised may influence EV procoagulant activity given its correlation with thrombin generation on the surface of plasma EV samples.

7.4 CONCLUSION

In conclusion, despite positively correlating with thrombin generation across the cohort, the fraction (%) aPL on platelets and leukocytes from ACS patients was similar to samples from HC participants, suggesting that the aPL lipidome of these cells is unlikely to contribute to systemic activation of the coagulation system that follows ACS.

Unlike platelets and leukocytes however, the distribution of aPL in plasma EV was predominantly on the outer leaflet of the membrane. Furthermore, there was a lower fraction (%) aPL externalised in plasma EV from ACS patients compared to HC participants. This was accompanied by a negative correlation between the fraction (%) externalised PE and thrombin generation on the surface of plasma EV. Taken together, this suggests an inverted-U relationship between aPL externalisation and thrombin generation. This in turn highlights a possible new role for plasma EV in mediating coagulation reactions, where ‘less is more’ when it comes to the proportion of external:total aPL and coagulation reactions.

CHAPTER 8 GENERAL DISCUSSION

The overarching aim of this thesis was to characterise the inflammatory procoagulant lipidome within arterial clots and circulating blood cells and EV from patients with arterial thrombosis, as well as investigate variations in the healthy eoxPL platelet lipidome in response to aspirin, gender and thrombin. The hypothesis being that an altered procoagulant surface in circulating blood cells contributes to the underlying mechanisms of thrombosis in ACS. To this end, I demonstrated the presence of HETE-PL lipids within three groups of human arterial thrombi, established that thrombin generation on the surface of EV is higher in ACS compared to HC correlating negatively with % PE externalized, and found that aspirin leads to more diacyl 12-LOX derived eoxPL generation in thrombin activated platelets (**Figure 8.1**). These findings are novel and provide new evidence to suggest that inflammatory procoagulant phospholipids may be associated with arterial thrombosis, building on the the increasing acceptance of the 'inflammatory hypothesis' behind arterial thrombosis, and representing possible new targets for consideration of further studies.

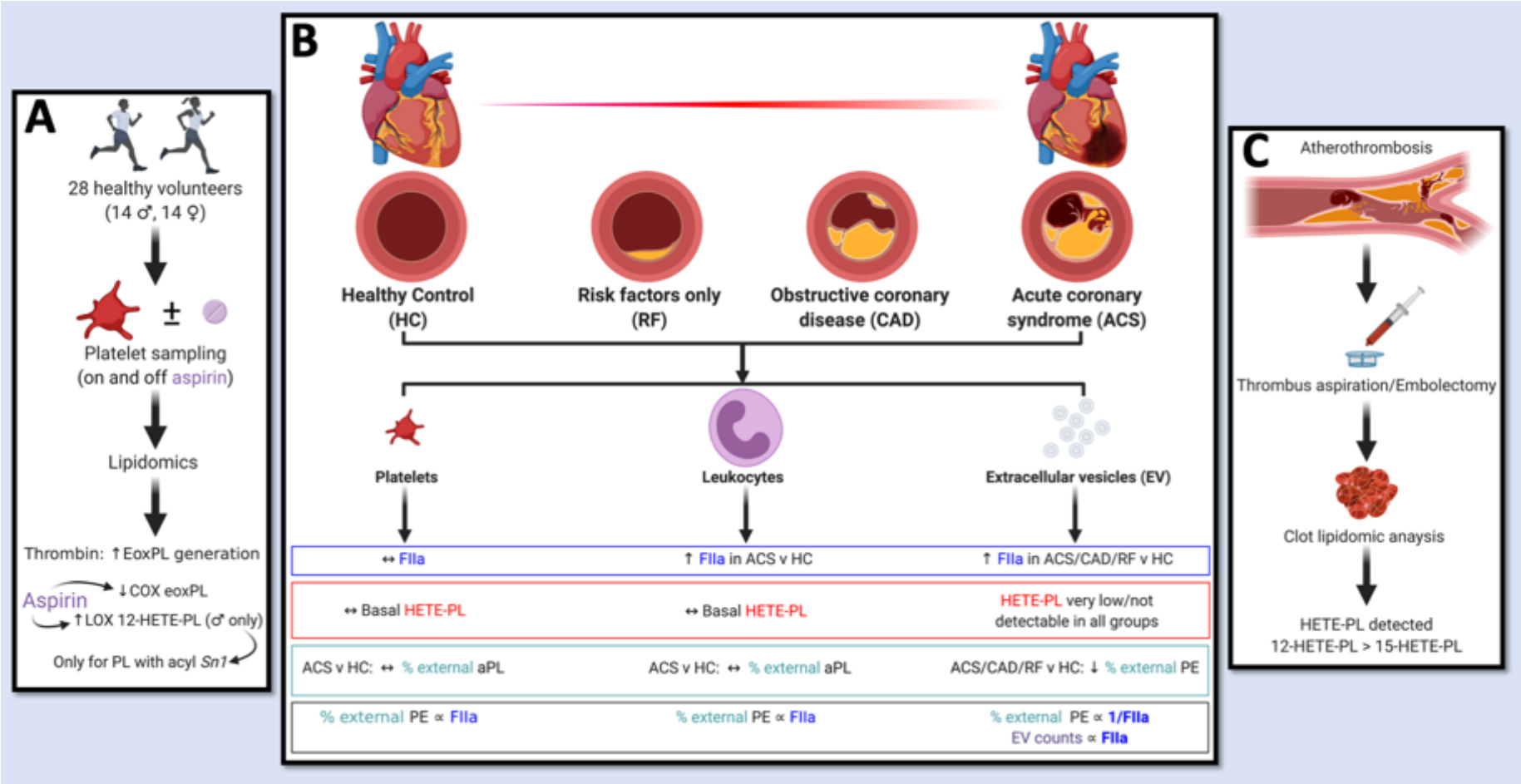

Figure 8.1. Graphical summary of findings from this thesis.

A: the first part of this thesis examined platelet eoxPL profiles in a 'healthy cohort' with the key finding of an increase in diacyl 12-HETE-PL in thrombin-activated platelets from donors on aspirin . B: the larger part of this thesis examined a 'clinical cohort' representing a spectrum of coronary disease, investigating membrane procoagulant properties and the HETE-PL and aPL lipidomes from platelets, leukocytes and plasma EV. The key findings from this section are higher thrombin generation on the surface of plasma EV from ACS/CAD/RF v HC, with an inverse association between thrombin and % external PE. C: The HETE-PL lipidomes from arterial thrombi was investigated as part of this thesis, with the key finding being the presence of HETE-PL lipids within the clot architecture.

8.1 PLATELET EOXPL IN HEALTHY DONORS

Prior to this thesis, the largest study of healthy human platelet eoxPLs included only three participants, which limited any conclusions on how the platelet lipidome varies in response to thrombin and aspirin supplementation[70]. Nevertheless, these studies demonstrated that thrombin, a potent platelet agonist, led to the elevation of almost 900 lipids by more than two-fold, the majority of which were not present in resting state. In addition, the study demonstrated that approximately 45% of the lipids generated in response to thrombin decreased by at least 50% with aspirin supplementation, indicating an important role for COX-1 in their formation[70]. Nevertheless, there was a large degree of variation between the three genetically unrelated participants both in their response to thrombin and aspirin, with one donor demonstrating more lipid generation (amount and number) in response to thrombin, whereas another demonstrating less inhibition of the lipid pool in response to aspirin. Additionally, the study was not powered to detected differences in how 12-LOX generation of eoxPL was affected by aspirin. Given the importance of eoxPL in driving coagulation and inflammatory reactions, the first part of this PhD thesis (**Chapter 3**) examined platelet lipid extracts from a previously recruited healthy cohort of 28 genetically unrelated adults to investigate variation in eoxPL in platelets in response to thrombin, aspirin and gender (**Figure 8.1**A). This is the largest cohort to date to examine the platelet eoxPL lipidome, demonstrating that the levels of eoxPL increase in response to thrombin and cluster by their enzymatic origin. Aspirin supplementation consistently reduced the amounts of COX-1 generated eoxPL in thrombin-activated platelets, but also increased the amounts of 12-LOX generated eoxPL associated with an acyl group at the *sn1* position. This finding was replicated in the clinical cohort platelet HETE-PL profiles described in **Chapter 6**. The likely mechanism for this is unclear, but seems to be downstream of 12-LOX activity since the levels of free 12-HETE were unaffected by aspirin supplementation (**Figure 3.14**), suggesting that the likely mechanism for the higher diacyl

12-HETE-PL amounts relates to the re-acetylation process of free 12-HETE to acyl lysoPL. It is therefore possible that aspirin affects the LPAT/MBOAT enzymes directly by modifying their structure and activity. Whilst no studies to date have demonstrated such a direct effect of aspirin on LPATs, it is known that aspirin-induced acetylation of lysine and/or serine residues contained within enzyme structures other than COX may alter their function[354]. In fact, aspirin has been shown to acetylate numerous biomolecules such as albumin, RNA and histones, which has given rise to interest in studying the COX-independent aspirin activity in fields such as cancer research where aspirin has demonstrated a promising role[354-356]. This widespread aspirin activity may cause an indirect effect on LPAT/MBOAT by interfering with upstream pathways such as mitogen activated protein kinases (MAPK)[53,357]. Alternatively, by interfering with COX-1 eicosanoid synthesis, the effect of aspirin on HETE-PL synthesis may be an indirect consequence of reducing TxA_2-mediated platelet function[358]. In all proposed cases, the findings from this thesis suggest that aspirin leads to more re-esterification of free HETE to acyl lysoPL, but the exact mechanism for this, and whether it is a direct or indirect aspirin effect, remains unclear and may require further studies as will be suggested in section **8.7**.

The clinical implication of more 12-HETE-PL in the membranes of thrombin-activated platelets, caused by aspirin supplementation, is unknown. Studies from our group demonstrated that increasing the amount of 12-HETE-PL in PL membranes enhances the negative surface charge and promotes the assembly of coagulation factors in a dose-dependent manner[69,81]. This may therefore suggest that the aspirin-related increase in procoagulant eoxPL on the surface of thrombin activated platelets could lead to more thrombin generation. However, studies examining thrombin generation on the surface of liposomes with increasing proportions of HETE-PL demonstrated an inverted U relationship, whereby higher levels of eoxPL generated less thrombin than lower levels[81]. This was thought to be related to a possible colocalization of

coagulation factors in smaller areas at higher concentrations on the liposomal surface, although this mechanism remains untested. It is possible therefore that the higher levels of 12-HETE-PL that are induced by aspirin on the surface of thrombin-activated platelets may lead to an additional anti-thrombotic phenotype by reducing the amount of thrombin formed. Exploring this *in-vivo* would be limited by difficulties in examining thrombin generation on the surface of activated platelet aggregates and the lack of assays to do so.

8.2 HETE-PL IN ARTERIAL THROMBI

Although HETE-PL were shown to be essential to coagulation in murine models of venous thrombosis[69,72], there's limited evidence to show that they are present within human clot architecture. Only one study to date has carried out LC-MS/MS on human thrombi showing their presence in clots extracted from patients with AAA[119]. In these patients, an atherosclerotic process takes place in the abdominal aorta leading to aneurysms that contain intramural thrombi[150,359]. Subsequent murine studies of AAA demonstrated that genetic deletion of *Alox12* and *Alox15*, which results in the absence of 12- and 15-HETE-PL, were protective against the development of AAA[119]. Beyond this study, no others have shown the presence the HETE-PL within arterial thrombi. For this reason, a lipidomic analysis of arterial thrombi was carried out as part of this thesis (**Figure 8.1**C) to investigate the presence of HETE-PL in human coronary, peripheral and carotid clots (**Chapter 4**). This demonstrated the presence of HETE-PL lipids in all isolated clots, with higher levels in the coronary clots. Of the different positional isomers detected, 12-HETE-PL accounted for most of the variance between the different types of clots. This probably relates to the contribution of platelets, where most of circulating 12-HETE-PL is generated, to the thrombotic process. What is lacking from this thesis however is a mechanistic explanation of the role of these lipids in human arterial thrombotic disease. Given the procoagulant role these lipids play, one could hypothesize that interfering with their

formation may affect arterial thrombus formation. Whilst testing this would not be possible in humans, due to the absence of specific LOX inhibitors, it may be tested in mice. This could be in the form of utilizing arterial thrombosis models, such as ferric chloride carotid artery injury, in *Alox15* and *Alox12* knockout mice compared to wildtype, as will be suggested in section **8.7**. If this demonstrates a protective phenotype, it could spark interest in developing agents that block LOX function which could serve as anticoagulants.

8.3 THROMBIN GENERATION ON CIRCULATING MEMBRANES FROM PATIENTS WITH ACS

Patients who suffer from an acute ischaemic event, such as ACS or stroke, are at a significantly higher risk of experiencing recurrent ACS, stroke or die from cardiovascular causes compared to those without ACS. This is thought to be related to residual inflammation which correlates positively with sustained activation of the coagulation system in the months that follow, although no mechanisms for this activation have been proposed[360-362]. Given that phospholipids play a major role in mediating coagulation reactions, I tested whether the membrane surfaces of platelets, leukocytes and plasma EV were more coagulant in patients with ACS compared to healthy controls (**Figure 8.1**B). This was described in **Chapter 5** and demonstrated that PL membranes from plasma EV and leukocytes, but not platelets, support higher thrombin generations in patients with ACS compared with HC in a TF-independent fashion. These findings could contribute to the sustained activation of the coagulation system described in the literature for patients with a recent history of ACS. Whilst platelets have traditionally been viewed as the main drivers of thrombosis in ACS, it was leukocytes and plasma EV which demonstrated higher procoagulant membrane phenotypes compared to HC. Current therapies do not target leukocytes or plasma EV in the management of arterial thrombosis, which could represent an unaddressed therapeutic area to reduce the residual

thrombotic burden of ACS patients. Additionally, the findings of higher procoagulant membrane properties could present a case for targeting PL membranes in patients with ACS with the aim of reducing the prothrombotic burden. However, the timing of any such intervention requires more characterisation of this observation. For instance, in this thesis, all ACS samples were taken within 48 of the acute event, and therefore the findings reflect the acute phase. This immediate stage is known to be prothrombotic and is the reason why patients may receive more intensive anti-thrombotic treatment in the first few days after ACS such as the addition of a low molecular-weight heparin[363]. It is unclear however whether the phenotype of more procoagulant membrane properties continue in the weeks or months after the acute event where persistent activation of the coagulation system have been described in ACS[361]. To test this, patients with a history of ACS in the last 12 months could be studied at various stages. In fact, longitudinal studies of patients with ACS in the acute (48 hours), intermediate (6 weeks) and distant (6 months) phase could shed more information on the variation of procoagulant membrane properties over time.

8.4 THE PROCOAGULANT LIPIDOME ON CIRCULATING MEMBRANES IN ACS PATIENTS

After investigating membrane procoagulant abilities on the surface of resting platelets, resting leukocytes and plasma EV in ACS vs HC, as described above, I proceeded to characterise the procoagulant lipidome from these samples. The HETE-PL lipidome was described in **Chapter 6** demonstrating very low levels of HETE-PL in resting platelets, leukocytes and plasma EV with no differences between groups (**Figure 8.1**B). This suggests that the procoagulant activity noted in ACS patients on the surface of resting leukocytes and plasma EV is unlikely to be caused by increased activation of the LOX/eoxPL pathways. Whilst this thesis is the first study investigating differences in HETE-PLs in arterial

thrombosis, recent studies examining the oxidized lipidome have been reported on different human thrombotic conditions. In 2017, a study on patients with APLS and history of venous (but not arterial) thrombosis reported higher resting levels of HETE-PL compared with healthy controls[69]. In fact, the study went on to demonstrate higher levels of plasma immunoglobulin G (IgG) against HETE-PL, suggesting that exposure to the higher resting levels had triggered an immune response in APLS patients. Other studies on arterial thrombosis have demonstrated higher levels of non-enzymatically formed oxPL in patients with ACS compared to controls, although the procoagulant role of that group of lipids was not tested[68]. The findings of this thesis therefore suggest that HETE-PL may be associated with acute thrombus formation, as evidenced by their presence within arterial thrombi, but are unlikely to contributed to the residual risk of thrombosis given that they are not elevated in resting states on circulating membrane surfaces.

Another major group of PL which could contribute to the procoagulant activity of circulating membrane surfaces are native aPL. These lipids were characterised in **Chapter 7** and the data was analysed in tandem with the amount of thrombin generated on the surface of these membranes (**Figure 8.1**B). Across all samples irrespective of clinical groups, there was a positive correlation between the fraction (%) aPL externalised and the amount of thrombin generated on the surface of resting platelets and leukocytes. This is consistent with the accepted role of aPL on the surface of these cells as procoagulant molecules, whereby more externalisation leads to more coagulation reactions[20]. Platelets from ACS patients had similar fraction (%) aPL externalised compared with HC, which fits with the lack of difference noted in the amount of thrombin generation. Leukocytes on the other hand had higher thrombin generation in ACS vs HC, despite having a similar fraction (%) aPL externalised between the two groups. This could be due to differences in sensitivity between assays, whereby small non-

significant lipidomic differences result in a detectable difference in thrombin generation. Alternatively, there could be unmeasured lipids at play which are yet to be identified as part of the coagulation reactions. Nevertheless, the use of LC-MS/MS to characterise aPL on plasma membranes is an underutilised tool in this area of research which has traditionally relied on non-quantitative techniques with Annexin V/Lactadherin based markers of surface aPL.

Thrombin generation on the surface of plasma EV samples from ACS, CAD and RF was significantly higher compared to HC. Whilst HETE-PL were undetectable in plasma EV, aPL were abundant. This is consistent with the definition of EV as aPL-rich vesicles irrespective of whether they are ectosomes, exosomes or apoptotic bodies. Unlike platelets and leukocytes however, the proportion of externalised aPL was much higher in plasma EV (~75% externalised in EV, compared to ~5% in resting platelets and leukocytes). Additionally, thrombin generation demonstrated an inverse correlation with the fraction (%) aPL externalised on the surface of plasma EV. Indeed, patients with ACS had higher thrombin generation, but lower fraction (%) PE externalised compared with HC. This novel finding suggests that coagulation reactions are regulated differently by EV compared to platelets and leukocytes, where 'less aPL is more thrombin'. One possibility could relate to the biophysical properties of EV membranes which would have higher curvature owing to their small diameters (<1000 nm). This could enable coagulation proteins to colocalize in smaller areas at higher concentrations, leading to less thrombin generation due to possible factor sequestration. This hypothesis however requires testing, but has been proposed previously with procoagulant lipids on the surface of liposomes measuring around 150-200nm[81]. Nevertheless, this thesis provides the first description of targeted LC-MS/MS measurement of aPL in EV using biotin derivatisation to distinguish external and total aPL amounts. Given the importance of aPL in mediating haemostatic reactions, as demonstrated in Scott syndrome, and EV formation, it

could be hypothesized that targeting these negatively charged lipids with an inhibitor, as will be suggested in section **8.7**. could serve as a potential therapeutic application to block the prothrombinase activity seen on the surface of EV in patients with ACS.

8.5 LIMITATIONS

There are a number of limitations to the work presented in this thesis. Firstly, the cross-sectional nature of the study on the 'clinical cohort' may be confounded by inter-individual variations which may limit their interpretation. Secondly, whilst studying patients with ACS may reveal some underlying lipidomic and functional differences, it is difficult to disentangle what is a cause or a consequence of the index event. This difficulty is widespread in the field due to the inability of researchers to predict when an ACS event will take place and therefore when sampling should occur[153]. Whilst prospective cohort studies such as the Framingham and the Northwick Park heart studies attempted to circumvent that by regular sampling of patients before, during and beyond cardiovascular events, it is impractical to do this when fresh cell samples are required for the laborious lipidomic processing employed in this thesis[364,365]. Finally, despite meeting initial criteria and power calculations to detect a difference at 5% alpha with 80% power, the sample size of this study is considered small and further validation and replication in a larger cohort would be necessary.

8.6 CONCLUSION

In conclusion, the body of work presented in this thesis set out to characterise the procoagulant lipidome in arterial thrombosis and test whether it varies in states of health and disease using LC-MS/MS and TF-independent coagulation assays. To this end, it was evident that procoagulant lipids are detected within arterial thrombi, have a differing profile between ACS and HC in circulating cells and plasma EV, and may explain a higher surface procoagulant ability in this disease state. Expanding on the findings of this thesis, and testing whether

interference with the procoagulant lipidome alters the observed incidence of arterial thrombosis may move the field closer towards utilising PL as therapeutic targets for the treatment of thrombosis.

8.7 Future Directions

8.7.1 Confirming cellular origin of HETE-PL in arterial thrombi, and understanding the dynamics of clot formation under shear.

To confirm the cellular origin of HETE-PL isomers found within arterial thrombi, further studies may utilise MALDI imaging in combination with immunohistochemistry imaging of tissue to localise products to their origin. For this, more arterial clots will need to be collected under a new ethical approval, and collaborations established with research groups that have the MALDI set up.

8.7.2 Exploring the role of *Alox15* and *Alox12* on murine models of arterial thrombosis.

Unlike venous thrombosis, the effect of *Alox15* and *Alox12* on arterial thrombosis has not been investigated. I plan to utilise our mouse colonies to carry out carotid artery ferric chloride injury to compare the content and the size/weight of the generated clot. I hypothesize that *Alox15*$^{-/-}$ and *Alox12*$^{-/-}$ will form smaller clots, which would add to the evidence of their mechanistic role in arterial thrombosis.

8.7.3 Interfering with thrombin generation using PL and EV inhibitory agents

Given the correlations noted between aPL, eoxPL and thrombin generation, and in combination with their established role in contributing to coagulation reactions, it would be interesting to study the effects of interfering with the procoagulant membrane, using existing or novel molecules, in altering the thrombin generation ability of cells. This could provide an avenue for developing therapeutic agents. It would require a combination of *in vitro* and *in vivo* studies to confirm potential efficacy of any such molecule. These ideas are currently in the planning stage, and I will likely take them forward after the PhD.

Equally, interfering with procoagulant EV formation from activated cells may offset the observed higher incidence of thrombosis in ACS and may provide a target for intervention. This however is an evolving field, and would require collaborations with an expert EV group to targeting modulators of EV formation and release. Currently, most studies on EV have focused on their role as biomarkers, which could be utilised to predict which patients are at a higher risk of thrombotic sequelae to aid decisions on personalised anti-thrombotic therapy.

8.7.4 Characterising the role of aspirin in modifying eoxPL re-esterification pathways

The differential effect that aspirin has on diacyl vs plasmalogen 12-HETE-PL generation in activated platelets merits further investigation. It is likely related to LPAT activity or expression. To study LPAT expression, perhaps transcriptomic analysis of platelets and megakaryocytes to determine which LPAT enzymes are present in platelets, followed by examining the effects of aspirin on their expression at an RNA level would form a reasonable

starting point to investigate this phenomenon. LPAT activity may be studied through international collaborations with groups that have genetically modified mice that lack one of more of the LPAT enzymes.

8.7.5 Understanding the physical interaction of aPL on the surface of EV with thrombin generation

It is possible that the negative correlation between fraction (%) PE in plasma EV and thrombin generation on their surface is a manifestation of plasma EV acting as a 'sink' for coagulation factors by virtue of biophysical properties including membrane curvature. This may be investigated further using in silico biophysical modelling and/or in vitro experiments utilising liposomes with varying fraction (%) aPL composition.

CHAPTER 9 REFERENCES

1 Nichols, M., Townsend, N., Scarborough, P. & Rayner, M. Cardiovascular disease in Europe: epidemiological update. *Eur Heart J* **34**, 3028-3034, doi:10.1093/eurheartj/eht356 (2013).

2 Luengo-Fernandez, R., Leal, J., Gray, A., Petersen, S. & Rayner, M. Cost of cardiovascular diseases in the United Kingdom. *Heart* **92**, 1384-1389, doi:10.1136/hrt.2005.072173 (2006).

3 Mensah, G. A. *et al*. Decline in Cardiovascular Mortality: Possible Causes and Implications. *Circ Res* **120**, 366-380, doi:10.1161/CIRCRESAHA.116.309115 (2017).

4 Institute of Medicine (US) Committee on Social Security Cardiovascular Disability Criteria. *Cardiovascular Disability: Updating the Social Security Listings*, <https://www.ncbi.nlm.nih.gov/pubmed/24983036> (2010).

5 Lusis, A. J. Atherosclerosis. *Nature* **407**, 233-241, doi:10.1038/35025203 (2000).

6 Spronk, H. M. H. *et al*. Atherothrombosis and Thromboembolism: Position Paper from the Second Maastricht Consensus Conference on Thrombosis. *Thromb Haemost* **118**, 229-250, doi:10.1160/TH17-07-0492 (2018).

7 Bata, I. R., Gregor, R. D., Wolf, H. K. & Brownell, B. Trends in five-year survival of patients discharged after acute myocardial infarction. *Can J Cardiol* **22**, 399-404, doi:10.1016/s0828-282x(06)70925-4 (2006).

8 Wallentin, L. *et al*. Ticagrelor versus clopidogrel in patients with acute coronary syndromes. *N Engl J Med* **361**, 1045-1057, doi:10.1056/NEJMoa0904327 (2009).

9 O'Donnell, V. B., Murphy, R. C. & Watson, S. P. Platelet lipidomics: modern day perspective on lipid discovery and characterization in platelets. *Circ Res* **114**, 1185-1203, doi:10.1161/CIRCRESAHA.114.301597 (2014).

10 Burdge, G. C. & Calder, P. C. Introduction to fatty acids and lipids. *World Rev Nutr Diet* **112**, 1-16, doi:10.1159/000365423 (2015).

11 Vance, D. E. & Vance, J. E. *Biochemistry of lipids, lipoproteins, and membranes*. 5th edn, (Elsevier, 2008).

12 Liebisch, G. *et al*. Shorthand notation for lipid structures derived from mass spectrometry. *J Lipid Res* **54**, 1523-1530, doi:10.1194/jlr.M033506 (2013).

13 O'Donnell, V. B., Rossjohn, J. & Wakelam, M. J. Phospholipid signaling in innate immune cells. *J Clin Invest* **128**, 2670-2679, doi:10.1172/JCI97944 (2018).

14 O'Donnell, V. B., Aldrovandi, M., Murphy, R. C. & Kronke, G. Enzymatically oxidized phospholipids assume center stage as essential regulators of innate immunity and cell death. *Sci Signal* **12**, doi:10.1126/scisignal.aau2293 (2019).

15 Singer, S. J. & Nicolson, G. L. The fluid mosaic model of the structure of cell membranes. *Science* **175**, 720-731, doi:10.1126/science.175.4023.720 (1972).

16 Braverman, N. E. & Moser, A. B. Functions of plasmalogen lipids in health and disease. *Biochim Biophys Acta* **1822**, 1442-1452, doi:10.1016/j.bbadis.2012.05.008 (2012).

17 Takamura, H., Tanaka, K., Matsuura, T. & Kito, M. Ether phospholipid molecular species in human platelets. *J Biochem* **105**, 168-172, doi:10.1093/oxfordjournals.jbchem.a122634 (1989).

18 Leray, C., Cazenave, J. P. & Gachet, C. Platelet phospholipids are differentially protected against oxidative degradation by plasmalogens. *Lipids* **37**, 285-290, doi:10.1007/s11745-002-0892-4 (2002).

19 Zoeller, R. A. *et al*. Plasmalogens as endogenous antioxidants: somatic cell mutants reveal the importance of the vinyl ether. *Biochem J* **338 (Pt 3)**, 769-776 (1999).

20 Clark, S. R. *et al*. Characterization of platelet aminophospholipid externalization reveals fatty acids as molecular determinants that regulate coagulation. *Proc Natl Acad Sci U S A* **110**, 5875-5880, doi:10.1073/pnas.1222419110 (2013).

21 Boesze-Battaglia, K. & Schimmel, R. Cell membrane lipid composition and distribution: implications for cell function and lessons learned from photoreceptors and platelets. *J Exp Biol* **200**, 2927-2936 (1997).

22 Zwaal, R. F. & Schroit, A. J. Pathophysiologic implications of membrane phospholipid asymmetry in blood cells. *Blood* **89**, 1121-1132 (1997).

23 Fadeel, B. & Xue, D. The ins and outs of phospholipid asymmetry in the plasma membrane: roles in health and disease. *Crit Rev Biochem Mol Biol* **44**, 264-277, doi:10.1080/10409230903193307 (2009).

24 Daleke, D. L. Regulation of transbilayer plasma membrane phospholipid asymmetry. *J Lipid Res* **44**, 233-242, doi:10.1194/jlr.R200019-JLR200 (2003).

25 Sivagnanam, U., Palanirajan, S. K. & Gummadi, S. N. The role of human phospholipid scramblases in apoptosis: An overview. *Biochim Biophys Acta Mol Cell Res* **1864**, 2261-2271, doi:10.1016/j.bbamcr.2017.08.008 (2017).

26 Lhermusier, T., Chap, H. & Payrastre, B. Platelet membrane phospholipid asymmetry: from the characterization of a scramblase activity to the identification of an essential protein mutated in Scott syndrome. *J Thromb Haemost* **9**, 1883-1891, doi:10.1111/j.1538-7836.2011.04478.x (2011).

27 van Geffen, J. P., Swieringa, F. & Heemskerk, J. W. Platelets and coagulation in thrombus formation: aberrations in the Scott syndrome. *Thromb Res* **141 Suppl 2**, S12-16, doi:10.1016/S0049-3848(16)30355-3 (2016).

28 Robinson, A., McCarty, D. & Douglas, J. Novel oral anticoagulants for acute coronary syndrome. *Ther Adv Cardiovasc Dis*, doi:10.1177/1753944716671484 (2016).

29 Evans, J. H., Spencer, D. M., Zweifach, A. & Leslie, C. C. Intracellular calcium signals regulating cytosolic phospholipase A2 translocation to internal membranes. *J Biol Chem* **276**, 30150-30160, doi:10.1074/jbc.M100943200 (2001).

30 Dennis, E. A., Cao, J., Hsu, Y. H., Magrioti, V. & Kokotos, G. Phospholipase A2 enzymes: physical structure, biological function, disease implication, chemical inhibition, and therapeutic intervention. *Chem Rev* **111**, 6130-6185, doi:10.1021/cr200085w (2011).

31 Linkous, A. & Yazlovitskaya, E. Cytosolic phospholipase A2 as a mediator of disease pathogenesis. *Cell Microbiol* **12**, 1369-1377, doi:10.1111/j.1462-5822.2010.01505.x (2010).

32 Morita, I. Distinct functions of COX-1 and COX-2. *Prostaglandins Other Lipid Mediat* **68-69**, 165-175, doi:10.1016/s0090-6980(02)00029-1 (2002).

33 Huang, J. S., Ramamurthy, S. K., Lin, X. & Le Breton, G. C. Cell signalling through thromboxane A2 receptors. *Cell Signal* **16**, 521-533, doi:10.1016/j.cellsig.2003.10.008 (2004).

34 Veldink, G. A. & Vliegenthart, J. F. Lipoxygenases, nonheme iron-containing enzymes. *Adv Inorg Biochem* **6**, 139-161 (1984).

35 Hammond, V. J. & O'Donnell, V. B. Esterified eicosanoids: generation, characterization and function. *Biochim Biophys Acta* **1818**, 2403-2412, doi:10.1016/j.bbamem.2011.12.013 (2012).

36 Brash, A. R. Lipoxygenases: occurrence, functions, catalysis, and acquisition of substrate. *J Biol Chem* **274**, 23679-23682, doi:10.1074/jbc.274.34.23679 (1999).

37 Dobrian, A. D. *et al*. Functional and pathological roles of the 12- and 15-lipoxygenases. *Prog Lipid Res* **50**, 115-131, doi:10.1016/j.plipres.2010.10.005 (2011).

38 Kuhn, H., Walther, M. & Kuban, R. J. Mammalian arachidonate 15-lipoxygenases structure, function, and biological implications. *Prostaglandins Other Lipid Mediat* **68-69**, 263-290, doi:10.1016/s0090-6980(02)00035-7 (2002).

39 Rai, G. *et al*. Potent and selective inhibitors of human reticulocyte 12/15-lipoxygenase as anti-stroke therapies. *J Med Chem* **57**, 4035-4048, doi:10.1021/jm401915r (2014).

40 Thomas, C. P. *et al*. Phospholipid-esterified eicosanoids are generated in agonist-activated human platelets and enhance tissue factor-dependent thrombin generation. *J Biol Chem* **285**, 6891-6903, doi:10.1074/jbc.M109.078428 (2010).

41 Conrad, D. J., Kuhn, H., Mulkins, M., Highland, E. & Sigal, E. Specific inflammatory cytokines regulate the expression of human monocyte 15-lipoxygenase. *Proc Natl Acad Sci U S A* **89**, 217-221, doi:10.1073/pnas.89.1.217 (1992).

42 Bailey, J. M., Bryant, R. W., Whiting, J. & Salata, K. Characterization of 11-HETE and 15-HETE, together with prostacyclin, as major products of the cyclooxygenase pathway in cultured rat aorta smooth muscle cells. *J Lipid Res* **24**, 1419-1428 (1983).

43 Setty, B. N., Stuart, M. J. & Walenga, R. W. Formation of 11-hydroxyeicosatetraenoic acid and 15-hydroxyeicosatetraenoic acid in human umbilical arteries is catalyzed by cyclooxygenase. *Biochim Biophys Acta* **833**, 484-494, doi:10.1016/0005-2760(85)90106-7 (1985).

44 Schneider, C. *et al*. Control of prostaglandin stereochemistry at the 15-carbon by cyclooxygenases-1 and -2. A critical role for serine 530 and valine 349. *J Biol Chem* **277**, 478-485, doi:10.1074/jbc.M107471200 (2002).

45 Thuresson, E. D., Lakkides, K. M. & Smith, W. L. Different catalytically competent arrangements of arachidonic acid within the cyclooxygenase active site of prostaglandin endoperoxide H synthase-1 lead to the formation of different oxygenated products. *J Biol Chem* **275**, 8501-8507, doi:10.1074/jbc.275.12.8501 (2000).

46 Maskrey, B. H. *et al*. Activated platelets and monocytes generate four hydroxyphosphatidylethanolamines via lipoxygenase. *J Biol Chem* **282**, 20151-20163, doi:10.1074/jbc.M611776200 (2007).

47 Clark, S. R. *et al*. Esterified eicosanoids are acutely generated by 5-lipoxygenase in primary human neutrophils and in human and murine infection. *Blood* **117**, 2033-2043, doi:10.1182/blood-2010-04-278887 (2011).

48 Grevengoed, T. J., Klett, E. L. & Coleman, R. A. Acyl-CoA metabolism and partitioning. *Annu Rev Nutr* **34**, 1-30, doi:10.1146/annurev-nutr-071813-105541 (2014).

49 Klett, E. L., Chen, S., Yechoor, A., Lih, F. B. & Coleman, R. A. Long-chain acyl-CoA synthetase isoforms differ in preferences for eicosanoid species and long-chain fatty acids. *J Lipid Res* **58**, 884-894, doi:10.1194/jlr.M072512 (2017).

50 Rossi Sebastiano, M. & Konstantinidou, G. Targeting Long Chain Acyl-CoA Synthetases for Cancer Therapy. *Int J Mol Sci* **20**, doi:10.3390/ijms20153624 (2019).

51 Morgan, L. T., Thomas, C. P., Kuhn, H. & O'Donnell, V. B. Thrombin-activated human platelets acutely generate oxidized docosahexaenoic-acid-containing phospholipids via 12-lipoxygenase. *Biochem J* **431**, 141-148, doi:10.1042/BJ20100415 (2010).

52 Hishikawa, D., Hashidate, T., Shimizu, T. & Shindou, H. Diversity and function of membrane glycerophospholipids generated by the remodeling pathway in mammalian cells. *J Lipid Res* **55**, 799-807, doi:10.1194/jlr.R046094 (2014).

53 Shindou, H., Hishikawa, D., Harayama, T., Yuki, K. & Shimizu, T. Recent progress on acyl CoA: lysophospholipid acyltransferase research. *J Lipid Res* **50 Suppl**, S46-51, doi:10.1194/jlr.R800035-JLR200 (2009).

54 Masumoto, N. *et al*. Membrane bound O-acyltransferases and their inhibitors. *Biochem Soc Trans* **43**, 246-252, doi:10.1042/BST20150018 (2015).

55 Chang, C. C. Y., Sun, J. & Chang, T. Membrane-bound O-acyltransferases (MBOATs). *Front. Biol.* **6**, doi:10.1007/s11515-011-1149-z (2011).

56 Shindou, H., Hishikawa, D., Harayama, T., Eto, M. & Shimizu, T. Generation of membrane diversity by lysophospholipid acyltransferases. *J Biochem* **154**, 21-28, doi:10.1093/jb/mvt048 (2013).

57 Gijon, M. A., Riekhof, W. R., Zarini, S., Murphy, R. C. & Voelker, D. R. Lysophospholipid acyltransferases and arachidonate recycling in human neutrophils. *J Biol Chem* **283**, 30235-30245, doi:10.1074/jbc.M806194200 (2008).

58 Zarini, S., Gijon, M. A., Folco, G. & Murphy, R. C. Effect of arachidonic acid reacylation on leukotriene biosynthesis in human neutrophils stimulated with granulocyte-macrophage colony-stimulating factor and formyl-methionyl-leucyl-phenylalanine. *J Biol Chem* **281**, 10134-10142, doi:10.1074/jbc.M510783200 (2006).

59 Morgan, A. H. *et al*. Phosphatidylethanolamine-esterified eicosanoids in the mouse: tissue localization and inflammation-dependent formation in Th-2 disease. *J Biol Chem* **284**, 21185-21191, doi:10.1074/jbc.M109.021634 (2009).

60 Hutchins, P. M. & Murphy, R. C. Cholesteryl ester acyl oxidation and remodeling in murine macrophages: formation of oxidized phosphatidylcholine. *J Lipid Res* **53**, 1588-1597, doi:10.1194/jlr.M026799 (2012).

61 Liu, X., Moon, S. H., Jenkins, C. M., Sims, H. F. & Gross, R. W. Cyclooxygenase-2 Mediated Oxidation of 2-Arachidonoyl-Lysophospholipids Identifies Unknown Lipid Signaling Pathways. *Cell Chem Biol* **23**, 1217-1227, doi:10.1016/j.chembiol.2016.08.009 (2016).

62 Liu, X. *et al*. 12-LOX catalyzes the oxidation of 2-arachidonoyl-lysolipids in platelets generating eicosanoid-lysolipids that are attenuated by iPLA2gamma knockout. *J Biol Chem* **295**, 5307-5320, doi:10.1074/jbc.RA119.012296 (2020).

63 Liu, G. Y. *et al*. Synthesis of oxidized phospholipids by sn-1 acyltransferase using 2-15-HETE lysophospholipids. *J Biol Chem* **294**, 10146-10159, doi:10.1074/jbc.RA119.008766 (2019).

64 Bochkov, V. N. *et al*. Generation and biological activities of oxidized phospholipids. *Antioxid Redox Signal* **12**, 1009-1059, doi:10.1089/ars.2009.2597 (2010).

65 Subbanagounder, G. *et al*. Determinants of bioactivity of oxidized phospholipids. Specific oxidized fatty acyl groups at the sn-2 position. *Arterioscler Thromb Vasc Biol* **20**, 2248-2254, doi:10.1161/01.atv.20.10.2248 (2000).

66 Berliner, J. A., Subbanagounder, G., Leitinger, N., Watson, A. D. & Vora, D. Evidence for a role of phospholipid oxidation products in atherogenesis. *Trends Cardiovasc Med* **11**, 142-147, doi:10.1016/s1050-1738(01)00098-6 (2001).

67 Serbulea, V., DeWeese, D. & Leitinger, N. The effect of oxidized phospholipids on phenotypic polarization and function of macrophages. *Free Radic Biol Med* **111**, 156-168, doi:10.1016/j.freeradbiomed.2017.02.035 (2017).

68 Chatterjee, M. *et al*. Regulation of oxidized platelet lipidome: implications for coronary artery disease. *Eur Heart J* **38**, 1993-2005, doi:10.1093/eurheartj/ehx146 (2017).

69 Lauder, S. N. *et al*. Networks of enzymatically oxidized membrane lipids support calcium-dependent coagulation factor binding to maintain hemostasis. *Sci Signal* **10**, doi:10.1126/scisignal.aan2787 (2017).

70 Slatter, D. A. *et al*. Mapping the Human Platelet Lipidome Reveals Cytosolic Phospholipase A2 as a Regulator of Mitochondrial Bioenergetics during Activation. *Cell Metab* **23**, 930-944, doi:10.1016/j.cmet.2016.04.001 (2016).

71 Dioszeghy, V. *et al*. 12/15-Lipoxygenase regulates the inflammatory response to bacterial products in vivo. *J Immunol* **181**, 6514-6524, doi:10.4049/jimmunol.181.9.6514 (2008).

72 Uderhardt, S. *et al*. Enzymatic lipid oxidation by eosinophils propagates coagulation, hemostasis, and thrombotic disease. *J Exp Med* **214**, 2121-2138, doi:10.1084/jem.20161070 (2017).

73 Hammond, V. J. *et al*. Novel keto-phospholipids are generated by monocytes and macrophages, detected in cystic fibrosis, and activate peroxisome proliferator-activated receptor-gamma. *J Biol Chem* **287**, 41651-41666, doi:10.1074/jbc.M112.405407 (2012).

74 Cook-Moreau, J. M. *et al*. Expression of 5-lipoxygenase (5-LOX) in T lymphocytes. *Immunology* **122**, 157-166, doi:10.1111/j.1365-2567.2007.02621.x (2007).

75 Crofford, L. J. COX-1 and COX-2 tissue expression: implications and predictions. *J Rheumatol Suppl* **49**, 15-19 (1997).

76 Aldrovandi, M. *et al*. Human platelets generate phospholipid-esterified prostaglandins via cyclooxygenase-1 that are inhibited by low dose aspirin supplementation. *J Lipid Res* **54**, 3085-3097, doi:10.1194/jlr.M041533 (2013).

77 Hinz, C. *et al*. Human Platelets Utilize Cycloxygenase-1 to Generate Dioxolane A3, a Neutrophil-activating Eicosanoid. *J Biol Chem* **291**, 13448-13464, doi:10.1074/jbc.M115.700609 (2016).

78 Kornilov, A. *et al*. Revising the structure of a new eicosanoid from human platelets to 8,9-11,12-diepoxy-13-hydroxyeicosadienoic acid. *J Biol Chem* **294**, 9225-9238, doi:10.1074/jbc.RA119.008915 (2019).

79 Aldrovandi, M. *et al*. DioxolaneA3-phosphatidylethanolamines are generated by human platelets and stimulate neutrophil integrin expression. *Redox Biol* **11**, 663-672, doi:10.1016/j.redox.2017.01.001 (2017).

80 Hajeyah, A. A., Griffiths, W. J., Wang, Y., Finch, A. J. & O'Donnell, V. B. The Biosynthesis of Enzymatically Oxidized Lipids. *Frontiers in Endocrinology* **11**, doi:10.3389/fendo.2020.591819 (2020).

81 Slatter, D. A. *et al*. Enzymatically oxidized phospholipids restore thrombin generation in coagulation factor deficiencies. *JCI Insight* **3**, doi:10.1172/jci.insight.98459 (2018).

82 Gale, A. J. Continuing education course #2: current understanding of hemostasis. *Toxicol Pathol* **39**, 273-280, doi:10.1177/0192623310389474 (2011).

83 Clemetson, K. J. Platelets and primary haemostasis. *Thromb Res* **129**, 220-224, doi:10.1016/j.thromres.2011.11.036 (2012).

84 van der Meijden, P. E. J. & Heemskerk, J. W. M. Platelet biology and functions: new concepts and clinical perspectives. *Nat Rev Cardiol* **16**, 166-179, doi:10.1038/s41569-018-0110-0 (2019).

85 Holinstat, M. Normal platelet function. *Cancer Metastasis Rev* **36**, 195-198, doi:10.1007/s10555-017-9677-x (2017).

86 Koupenova, M., Clancy, L., Corkrey, H. A. & Freedman, J. E. Circulating Platelets as Mediators of Immunity, Inflammation, and Thrombosis. *Circ Res* **122**, 337-351, doi:10.1161/CIRCRESAHA.117.310795 (2018).

87 Clemetson, K. J. Platelet receptors and their role in diseases. *Clin Chem Lab Med* **41**, 253-260, doi:10.1515/CCLM.2003.039 (2003).

88 Ramasamy, I. Inherited bleeding disorders: disorders of platelet adhesion and aggregation. *Crit Rev Oncol Hematol* **49**, 1-35 (2004).

89 Mann, K. G., Brummel, K. & Butenas, S. What is all that thrombin for? *J Thromb Haemost* **1**, 1504-1514 (2003).

90 Hoffman, M. & Monroe, D. M., 3rd. A cell-based model of hemostasis. *Thromb Haemost* **85**, 958-965 (2001).

91 Nelsestuen, G. L., Kisiel, W. & Di Scipio, R. G. Interaction of vitamin K dependent proteins with membranes. *Biochemistry* **17**, 2134-2138 (1978).

92 Rao, L. V. & Pendurthi, U. R. Regulation of tissue factor coagulant activity on cell surfaces. *J Thromb Haemost* **10**, 2242-2253, doi:10.1111/jth.12003 (2012).

93 Mackman, N. The role of tissue factor and factor VIIa in hemostasis. *Anesth Analg* **108**, 1447-1452, doi:10.1213/ane.0b013e31819bceb1 (2009).

94 Mandal, S. K., Iakhiaev, A., Pendurthi, U. R. & Rao, L. V. Acute cholesterol depletion impairs functional expression of tissue factor in fibroblasts: modulation of tissue factor activity by membrane cholesterol. *Blood* **105**, 153-160, doi:10.1182/blood-2004-03-0990 (2005).

95 Rao, L. V., Kothari, H. & Pendurthi, U. R. Tissue factor: mechanisms of decryption. *Front Biosci (Elite Ed)* **4**, 1513-1527, doi:10.2741/477 (2012).

96 Bach, R. R. Tissue factor encryption. *Arterioscler Thromb Vasc Biol* **26**, 456-461, doi:10.1161/01.ATV.0000202656.53964.04 (2006).

97 Bach, R. R. & Moldow, C. F. Mechanism of tissue factor activation on HL-60 cells. *Blood* **89**, 3270-3276 (1997).

98 Burnier, L., Fontana, P., Kwak, B. R. & Angelillo-Scherrer, A. Cell-derived microparticles in haemostasis and vascular medicine. *Thromb Haemost* **101**, 439-451 (2009).

99 Giesen, P. L. *et al*. Blood-borne tissue factor: another view of thrombosis. *Proc Natl Acad Sci U S A* **96**, 2311-2315, doi:10.1073/pnas.96.5.2311 (1999).

100 Nemerson, Y. & Esnouf, M. P. Activation of a proteolytic system by a membrane lipoprotein: mechanism of action of tissue factor. *Proc Natl Acad Sci U S A* **70**, 310-314, doi:10.1073/pnas.70.2.310 (1973).

101 Nemerson, Y. & Repke, D. Tissue factor accelerates the activation of coagulation factor VII: the role of a bifunctional coagulation cofactor. *Thromb Res* **40**, 351-358 (1985).

102 Seligsohn, U., Osterud, B., Brown, S. F., Griffin, J. H. & Rapaport, S. I. Activation of human factor VII in plasma and in purified systems: roles of activated factor IX, kallikrein, and activated factor XII. *J Clin Invest* **64**, 1056-1065, doi:10.1172/JCI109543 (1979).

103 Nakagaki, T., Foster, D. C., Berkner, K. L. & Kisiel, W. Initiation of the extrinsic pathway of blood coagulation: evidence for the tissue factor dependent autoactivation of human coagulation factor VII. *Biochemistry* **30**, 10819-10824 (1991).

104 Palta, S., Saroa, R. & Palta, A. Overview of the coagulation system. *Indian J Anaesth* **58**, 515-523, doi:10.4103/0019-5049.144643 (2014).

105 Heemskerk, J. W., Bevers, E. M. & Lindhout, T. Platelet activation and blood coagulation. *Thromb Haemost* **88**, 186-193 (2002).

106 Zwaal, R. F., Comfurius, P. & Bevers, E. M. Lipid-protein interactions in blood coagulation. *Biochim Biophys Acta* **1376**, 433-453 (1998).

107 Falls, L. A., Furie, B. C., Jacobs, M., Furie, B. & Rigby, A. C. The omega-loop region of the human prothrombin gamma-carboxyglutamic acid domain penetrates anionic phospholipid membranes. *J Biol Chem* **276**, 23895-23902, doi:10.1074/jbc.M008332200 (2001).

108 Tavoosi, N. *et al*. Molecular determinants of phospholipid synergy in blood clotting. *J Biol Chem* **286**, 23247-23253, doi:10.1074/jbc.M111.251769 (2011).

109 Hansen, J. B., Olsen, R. & Webster, P. Association of tissue factor pathway inhibitor with human umbilical vein endothelial cells. *Blood* **90**, 3568-3578 (1997).

110 Iversen, N., Sandset, P. M., Abildgaard, U. & Torjesen, P. A. Binding of tissue factor pathway inhibitor to cultured endothelial cells-influence of glycosaminoglycans. *Thromb Res* **84**, 267-278 (1996).

111 Kasthuri, R. S., Glover, S. L., Boles, J. & Mackman, N. Tissue factor and tissue factor pathway inhibitor as key regulators of global hemostasis: measurement of their levels in coagulation assays. *Semin Thromb Hemost* **36**, 764-771, doi:10.1055/s-0030-1265293 (2010).

112 Esmon, C. T., Vigano-D'Angelo, S., D'Angelo, A. & Comp, P. C. Anticoagulation proteins C and S. *Adv Exp Med Biol* **214**, 47-54 (1987).

113 Norstrom, E. A., Steen, M., Tran, S. & Dahlback, B. Importance of protein S and phospholipid for activated protein C-mediated cleavages in factor Va. *J Biol Chem* **278**, 24904-24911, doi:10.1074/jbc.M303829200 (2003).

114 Shi, J. *et al*. Lactadherin detects early phosphatidylserine exposure on immortalized leukemia cells undergoing programmed cell death. *Cytometry A* **69**, 1193-1201, doi:10.1002/cyto.a.20345 (2006).

115 Hou, J. *et al*. Lactadherin functions as a probe for phosphatidylserine exposure and as an anticoagulant in the study of stored platelets. *Vox Sang* **100**, 187-195, doi:10.1111/j.1423-0410.2010.01375.x (2011).

116 Tait, J. F., Smith, C. & Wood, B. L. Measurement of phosphatidylserine exposure in leukocytes and platelets by whole-blood flow cytometry with annexin V. *Blood Cells Mol Dis* **25**, 271-278, doi:10.1006/bcmd.1999.0254 (1999).

117 Thomas, C. P. *et al*. Identification and quantification of aminophospholipid molecular species on the surface of apoptotic and activated cells. *Nat Protoc* **9**, 51-63, doi:10.1038/nprot.2013.163 (2014).

118 Elia, G. Biotinylation reagents for the study of cell surface proteins. *Proteomics* **8**, 4012-4024, doi:10.1002/pmic.200800097 (2008).

119 Allen-Redpath, K. *et al*. Phospholipid membranes drive abdominal aortic aneurysm development through stimulating coagulation factor activity. *Proc Natl Acad Sci U S A* **116**, 8038-8047, doi:10.1073/pnas.1814409116 (2019).

120 Libby, P. *et al*. Atherosclerosis. *Nat Rev Dis Primers* **5**, 56, doi:10.1038/s41572-019-0106-z (2019).

121 Goldstein, J. L. & Brown, M. S. A century of cholesterol and coronaries: from plaques to genes to statins. *Cell* **161**, 161-172, doi:10.1016/j.cell.2015.01.036 (2015).

122 Hopstock, L. A. *et al*. Longitudinal and secular trends in total cholesterol levels and impact of lipid-lowering drug use among Norwegian women and men born in 1905-1977 in the population-based Tromso Study 1979-2016. *BMJ Open* **7**, e015001, doi:10.1136/bmjopen-2016-015001 (2017).

123 Schreiner, P. J., Jacobs, D. R., Jr., Wong, N. D. & Kiefe, C. I. Twenty-Five Year Secular Trends in Lipids and Modifiable Risk Factors in a Population-Based Biracial Cohort: The Coronary Artery Risk Development in Young Adults (CARDIA) Study, 1985-2011. *J Am Heart Assoc* **5**, doi:10.1161/JAHA.116.003384 (2016).

124 Ference, B. A. *et al*. Low-density lipoproteins cause atherosclerotic cardiovascular disease. 1. Evidence from genetic, epidemiologic, and clinical studies. A consensus statement from the European Atherosclerosis Society Consensus Panel. *Eur Heart J* **38**, 2459-2472, doi:10.1093/eurheartj/ehx144 (2017).

125 Boren, J. & Williams, K. J. The central role of arterial retention of cholesterol-rich apolipoprotein-B-containing lipoproteins in the pathogenesis of atherosclerosis: a triumph of simplicity. *Curr Opin Lipidol* **27**, 473-483, doi:10.1097/MOL.0000000000000330 (2016).

126 Miller, Y. I. *et al*. Oxidation-specific epitopes are danger-associated molecular patterns recognized by pattern recognition receptors of innate immunity. *Circ Res* **108**, 235-248, doi:10.1161/CIRCRESAHA.110.223875 (2011).

127 Navab, M. *et al*. The oxidation hypothesis of atherogenesis: the role of oxidized phospholipids and HDL. *J Lipid Res* **45**, 993-1007, doi:10.1194/jlr.R400001-JLR200 (2004).

128 Parthasarathy, S., Raghavamenon, A., Garelnabi, M. O. & Santanam, N. Oxidized low-density lipoprotein. *Methods Mol Biol* **610**, 403-417, doi:10.1007/978-1-60327-029-8_24 (2010).

129 Singh, R. B., Mengi, S. A., Xu, Y. J., Arneja, A. S. & Dhalla, N. S. Pathogenesis of atherosclerosis: A multifactorial process. *Exp Clin Cardiol* **7**, 40-53 (2002).

130 Badimon, L., Padro, T. & Vilahur, G. Atherosclerosis, platelets and thrombosis in acute ischaemic heart disease. *Eur Heart J Acute Cardiovasc Care* **1**, 60-74, doi:10.1177/2048872612441582 (2012).

131 Cunningham, K. S. & Gotlieb, A. I. The role of shear stress in the pathogenesis of atherosclerosis. *Lab Invest* **85**, 9-23, doi:10.1038/labinvest.3700215 (2005).

132 Alexander, R. W. Theodore Cooper Memorial Lecture. Hypertension and the pathogenesis of atherosclerosis. Oxidative stress and the mediation of arterial inflammatory response: a new perspective. *Hypertension* **25**, 155-161, doi:10.1161/01.hyp.25.2.155 (1995).

133 Nakazono, K. *et al*. Does superoxide underlie the pathogenesis of hypertension? *Proc Natl Acad Sci U S A* **88**, 10045-10048, doi:10.1073/pnas.88.22.10045 (1991).

134 Messner, B. & Bernhard, D. Smoking and cardiovascular disease: mechanisms of endothelial dysfunction and early atherogenesis. *Arterioscler Thromb Vasc Biol* **34**, 509-515, doi:10.1161/ATVBAHA.113.300156 (2014).

135 Avogaro, A., Albiero, M., Menegazzo, L., de Kreutzenberg, S. & Fadini, G. P. Endothelial dysfunction in diabetes: the role of reparatory mechanisms. *Diabetes Care* **34 Suppl 2**, S285-290, doi:10.2337/dc11-s239 (2011).

136 Gimbrone, M. A., Jr. & Garcia-Cardena, G. Endothelial Cell Dysfunction and the Pathobiology of Atherosclerosis. *Circ Res* **118**, 620-636, doi:10.1161/CIRCRESAHA.115.306301 (2016).

137 Chatzizisis, Y. S. *et al*. Role of endothelial shear stress in the natural history of coronary atherosclerosis and vascular remodeling: molecular, cellular, and vascular behavior. *J Am Coll Cardiol* **49**, 2379-2393, doi:10.1016/j.jacc.2007.02.059 (2007).

138 Bennett, M. R., Sinha, S. & Owens, G. K. Vascular Smooth Muscle Cells in Atherosclerosis. *Circ Res* **118**, 692-702, doi:10.1161/CIRCRESAHA.115.306361 (2016).

139 Geng, Y. J. & Libby, P. Evidence for apoptosis in advanced human atheroma. Colocalization with interleukin-1 beta-converting enzyme. *Am J Pathol* **147**, 251-266 (1995).

140 Clarke, M. C., Talib, S., Figg, N. L. & Bennett, M. R. Vascular smooth muscle cell apoptosis induces interleukin-1-directed inflammation: effects of hyperlipidemia-mediated inhibition of phagocytosis. *Circ Res* **106**, 363-372, doi:10.1161/CIRCRESAHA.109.208389 (2010).

141 Tabas, I., Garcia-Cardena, G. & Owens, G. K. Recent insights into the cellular biology of atherosclerosis. *J Cell Biol* **209**, 13-22, doi:10.1083/jcb.201412052 (2015).

142 Yurdagul, A., Jr., Doran, A. C., Cai, B., Fredman, G. & Tabas, I. A. Mechanisms and Consequences of Defective Efferocytosis in Atherosclerosis. *Front Cardiovasc Med* **4**, 86, doi:10.3389/fcvm.2017.00086 (2017).

143 Ruiz, J. L., Hutcheson, J. D. & Aikawa, E. Cardiovascular calcification: current controversies and novel concepts. *Cardiovasc Pathol* **24**, 207-212, doi:10.1016/j.carpath.2015.03.002 (2015).

144 Ruiz, J. L., Weinbaum, S., Aikawa, E. & Hutcheson, J. D. Zooming in on the genesis of atherosclerotic plaque microcalcifications. *J Physiol* **594**, 2915-2927, doi:10.1113/JP271339 (2016).

145 Wilcox, J. N., Smith, K. M., Schwartz, S. M. & Gordon, D. Localization of tissue factor in the normal vessel wall and in the atherosclerotic plaque. *Proc Natl Acad Sci U S A* **86**, 2839-2843, doi:10.1073/pnas.86.8.2839 (1989).

146 Wilcox, J. N., Noguchi, S. & Casanova, J. Extrahepatic synthesis of factor VII in human atherosclerotic vessels. *Arterioscler Thromb Vasc Biol* **23**, 136-141, doi:10.1161/01.atv.0000043418.84185.3c (2003).

147 Macfarlane, S. R., Seatter, M. J., Kanke, T., Hunter, G. D. & Plevin, R. Proteinase-activated receptors. *Pharmacol Rev* **53**, 245-282 (2001).

148 Rana, R. *et al*. Noncanonical Matrix Metalloprotease 1-Protease-Activated Receptor 1 Signaling Drives Progression of Atherosclerosis. *Arterioscler Thromb Vasc Biol* **38**, 1368-1380, doi:10.1161/ATVBAHA.118.310967 (2018).

149 Jones, S. M. *et al*. PAR2 (Protease-Activated Receptor 2) Deficiency Attenuates Atherosclerosis in Mice. *Arterioscler Thromb Vasc Biol* **38**, 1271-1282, doi:10.1161/ATVBAHA.117.310082 (2018).

150 Piechota-Polanczyk, A. *et al*. The Abdominal Aortic Aneurysm and Intraluminal Thrombus: Current Concepts of Development and Treatment. *Front Cardiovasc Med* **2**, 19, doi:10.3389/fcvm.2015.00019 (2015).

151 Badimon, J. J. *et al*. Local inhibition of tissue factor reduces the thrombogenicity of disrupted human atherosclerotic plaques: effects of tissue factor pathway inhibitor on

plaque thrombogenicity under flow conditions. *Circulation* **99**, 1780-1787, doi:10.1161/01.cir.99.14.1780 (1999).

152 Libby, P. Mechanisms of acute coronary syndromes and their implications for therapy. *N Engl J Med* **368**, 2004-2013, doi:10.1056/NEJMra1216063 (2013).

153 Bentzon, J. F., Otsuka, F., Virmani, R. & Falk, E. Mechanisms of plaque formation and rupture. *Circ Res* **114**, 1852-1866, doi:10.1161/CIRCRESAHA.114.302721 (2014).

154 Libby, P. & Pasterkamp, G. Requiem for the 'vulnerable plaque'. *Eur Heart J* **36**, 2984-2987, doi:10.1093/eurheartj/ehv349 (2015).

155 Pasterkamp, G., den Ruijter, H. M. & Libby, P. Temporal shifts in clinical presentation and underlying mechanisms of atherosclerotic disease. *Nat Rev Cardiol* **14**, 21-29, doi:10.1038/nrcardio.2016.166 (2017).

156 Yonetsu, T. & Jang, I. K. Advances in Intravascular Imaging: New Insights into the Vulnerable Plaque from Imaging Studies. *Korean Circ J* **48**, 1-15, doi:10.4070/kcj.2017.0182 (2018).

157 Amento, E. P., Ehsani, N., Palmer, H. & Libby, P. Cytokines and growth factors positively and negatively regulate interstitial collagen gene expression in human vascular smooth muscle cells. *Arterioscler Thromb* **11**, 1223-1230, doi:10.1161/01.atv.11.5.1223 (1991).

158 Galis, Z. S., Sukhova, G. K., Lark, M. W. & Libby, P. Increased expression of matrix metalloproteinases and matrix degrading activity in vulnerable regions of human atherosclerotic plaques. *J Clin Invest* **94**, 2493-2503, doi:10.1172/JCI117619 (1994).

159 Galis, Z. S., Sukhova, G. K., Kranzhofer, R., Clark, S. & Libby, P. Macrophage foam cells from experimental atheroma constitutively produce matrix-degrading proteinases. *Proc Natl Acad Sci U S A* **92**, 402-406, doi:10.1073/pnas.92.2.402 (1995).

160 Quillard, T., Franck, G., Mawson, T., Folco, E. & Libby, P. Mechanisms of erosion of atherosclerotic plaques. *Curr Opin Lipidol* **28**, 434-441, doi:10.1097/MOL.0000000000000440 (2017).

161 Owens, A. P., 3rd & Mackman, N. Tissue factor and thrombosis: The clot starts here. *Thromb Haemost* **104**, 432-439, doi:10.1160/TH09-11-0771 (2010).

162 Asada, Y., Yamashita, A., Sato, Y. & Hatakeyama, K. Pathophysiology of atherothrombosis: Mechanisms of thrombus formation on disrupted atherosclerotic plaques. *Pathol Int* **70**, 309-322, doi:10.1111/pin.12921 (2020).

163 Jamasbi, J. *et al*. Platelet receptors as therapeutic targets: Past, present and future. *Thromb Haemost* **117**, 1249-1257, doi:10.1160/TH16-12-0911 (2017).

164 Gachet, C., Leon, C. & Hechler, B. The platelet P2 receptors in arterial thrombosis. *Blood Cells Mol Dis* **36**, 223-227, doi:10.1016/j.bcmd.2005.12.024 (2006).

165 Silvain, J. *et al*. Composition of coronary thrombus in acute myocardial infarction. *J Am Coll Cardiol* **57**, 1359-1367, doi:10.1016/j.jacc.2010.09.077 (2011).

166 Chernysh, I. N. *et al*. The distinctive structure and composition of arterial and venous thrombi and pulmonary emboli. *Sci Rep* **10**, 5112, doi:10.1038/s41598-020-59526-x (2020).

167 Kranzhofer, R., Browatzki, M., Schmidt, J. & Kubler, W. Angiotensin II activates the proinflammatory transcription factor nuclear factor-kappaB in human monocytes. *Biochem Biophys Res Commun* **257**, 826-828, doi:10.1006/bbrc.1999.0543 (1999).

168 McMaster, W. G., Kirabo, A., Madhur, M. S. & Harrison, D. G. Inflammation, immunity, and hypertensive end-organ damage. *Circ Res* **116**, 1022-1033, doi:10.1161/CIRCRESAHA.116.303697 (2015).

169 Ketelhuth, D. F. & Hansson, G. K. Adaptive Response of T and B Cells in Atherosclerosis. *Circ Res* **118**, 668-678, doi:10.1161/CIRCRESAHA.115.306427 (2016).

170 Rocha, V. Z. & Libby, P. Obesity, inflammation, and atherosclerosis. *Nat Rev Cardiol* **6**, 399-409, doi:10.1038/nrcardio.2009.55 (2009).

171 Despres, J. P. Body fat distribution and risk of cardiovascular disease: an update. *Circulation* **126**, 1301-1313, doi:10.1161/CIRCULATIONAHA.111.067264 (2012).

172 Libby, P. *et al*. Inflammation, Immunity, and Infection in Atherothrombosis: JACC Review Topic of the Week. *J Am Coll Cardiol* **72**, 2071-2081, doi:10.1016/j.jacc.2018.08.1043 (2018).

173 Libby, P., Nahrendorf, M. & Swirski, F. K. Leukocytes Link Local and Systemic Inflammation in Ischemic Cardiovascular Disease: An Expanded "Cardiovascular Continuum". *J Am Coll Cardiol* **67**, 1091-1103, doi:10.1016/j.jacc.2015.12.048 (2016).

174 Martinod, K. & Wagner, D. D. Thrombosis: tangled up in NETs. *Blood* **123**, 2768-2776, doi:10.1182/blood-2013-10-463646 (2014).

175 Franck, G. *et al*. Roles of PAD4 and NETosis in Experimental Atherosclerosis and Arterial Injury: Implications for Superficial Erosion. *Circ Res* **123**, 33-42, doi:10.1161/CIRCRESAHA.117.312494 (2018).

176 Folco, E. J. *et al*. Neutrophil Extracellular Traps Induce Endothelial Cell Activation and Tissue Factor Production Through Interleukin-1alpha and Cathepsin G. *Arterioscler Thromb Vasc Biol* **38**, 1901-1912, doi:10.1161/ATVBAHA.118.311150 (2018).

177 Mackman, N. Eosinophils, atherosclerosis, and thrombosis. *Blood* **134**, 1781-1782, doi:10.1182/blood.2019003027 (2019).

178 Marx, C. *et al*. Eosinophil-platelet interactions promote atherosclerosis and stabilize thrombosis with eosinophil extracellular traps. *Blood* **134**, 1859-1872, doi:10.1182/blood.2019000518 (2019).

179 Ridker, P. M. A Test in Context: High-Sensitivity C-Reactive Protein. *J Am Coll Cardiol* **67**, 712-723, doi:10.1016/j.jacc.2015.11.037 (2016).

180 Blankenberg, S. & Yusuf, S. The inflammatory hypothesis: any progress in risk stratification and therapeutic targets? *Circulation* **114**, 1557-1560, doi:10.1161/CIRCULATIONAHA.106.652081 (2006).

181 Tardif, J. C. *et al*. Efficacy and Safety of Low-Dose Colchicine after Myocardial Infarction. *N Engl J Med* **381**, 2497-2505, doi:10.1056/NEJMoa1912388 (2019).

182 Ridker, P. M. *et al*. Antiinflammatory Therapy with Canakinumab for Atherosclerotic Disease. *N Engl J Med* **377**, 1119-1131, doi:10.1056/NEJMoa1707914 (2017).

183 Jy, W. *et al*. Measuring circulating cell-derived microparticles. *J Thromb Haemost* **2**, 1842-1851, doi:10.1111/j.1538-7836.2004.00936.x (2004).

184 Morel, O. *et al*. [The significance of circulating microparticles in physiology, inflammatory and thrombotic diseases]. *Rev Med Interne* **26**, 791-801, doi:10.1016/j.revmed.2005.03.015 (2005).

185 Zwaal, R. F., Comfurius, P. & Bevers, E. M. Platelet procoagulant activity and microvesicle formation. Its putative role in hemostasis and thrombosis. *Biochim Biophys Acta* **1180**, 1-8, doi:10.1016/0925-4439(92)90019-j (1992).

186 Pilzer, D., Gasser, O., Moskovich, O., Schifferli, J. A. & Fishelson, Z. Emission of membrane vesicles: roles in complement resistance, immunity and cancer. *Springer Semin Immunopathol* **27**, 375-387, doi:10.1007/s00281-005-0004-1 (2005).

187 Raposo, G. *et al*. B lymphocytes secrete antigen-presenting vesicles. *J Exp Med* **183**, 1161-1172, doi:10.1084/jem.183.3.1161 (1996).

188 Kastelowitz, N. & Yin, H. Exosomes and microvesicles: identification and targeting by particle size and lipid chemical probes. *Chembiochem* **15**, 923-928, doi:10.1002/cbic.201400043 (2014).

189 Basse, F., Gaffet, P. & Bienvenue, A. Correlation between inhibition of cytoskeleton proteolysis and anti-vesiculation effect of calpeptin during A23187-induced activation of human platelets: are vesicles shed by filopod fragmentation? *Biochim Biophys Acta* **1190**, 217-224, doi:10.1016/0005-2736(94)90077-9 (1994).

190 Fox, J. E., Austin, C. D., Boyles, J. K. & Steffen, P. K. Role of the membrane skeleton in preventing the shedding of procoagulant-rich microvesicles from the platelet plasma membrane. *J Cell Biol* **111**, 483-493, doi:10.1083/jcb.111.2.483 (1990).

191 Fox, J. E., Austin, C. D., Reynolds, C. C. & Steffen, P. K. Evidence that agonist-induced activation of calpain causes the shedding of procoagulant-containing microvesicles from the membrane of aggregating platelets. *J Biol Chem* **266**, 13289-13295 (1991).

192 McLaughlin, P. J., Gooch, J. T., Mannherz, H. G. & Weeds, A. G. Structure of gelsolin segment 1-actin complex and the mechanism of filament severing. *Nature* **364**, 685-692, doi:10.1038/364685a0 (1993).

193 Weerheim, A. M., Kolb, A. M., Sturk, A. & Nieuwland, R. Phospholipid composition of cell-derived microparticles determined by one-dimensional high-performance thin-layer chromatography. *Anal Biochem* **302**, 191-198, doi:10.1006/abio.2001.5552 (2002).

194 Huber, J. *et al*. Oxidized membrane vesicles and blebs from apoptotic cells contain biologically active oxidized phospholipids that induce monocyte-endothelial interactions. *Arterioscler Thromb Vasc Biol* **22**, 101-107, doi:10.1161/hq0102.101525 (2002).

195 Horstman, L. L. & Ahn, Y. S. Platelet microparticles: a wide-angle perspective. *Crit Rev Oncol Hematol* **30**, 111-142, doi:10.1016/s1040-8428(98)00044-4 (1999).

196 Flaumenhaft, R. Formation and fate of platelet microparticles. *Blood Cells Mol Dis* **36**, 182-187, doi:10.1016/j.bcmd.2005.12.019 (2006).

197 Fourcade, O. *et al*. Secretory phospholipase A2 generates the novel lipid mediator lysophosphatidic acid in membrane microvesicles shed from activated cells. *Cell* **80**, 919-927, doi:10.1016/0092-8674(95)90295-3 (1995).

198 Wu, Y., Tibrewal, N. & Birge, R. B. Phosphatidylserine recognition by phagocytes: a view to a kill. *Trends Cell Biol* **16**, 189-197, doi:10.1016/j.tcb.2006.02.003 (2006).

199 Skeppholm, M., Mobarrez, F., Malmqvist, K. & Wallen, H. Platelet-derived microparticles during and after acute coronary syndrome. *Thromb Haemost* **107**, 1122-1129, doi:10.1160/TH11-11-0779 (2012).

200 Wolf, P. The nature and significance of platelet products in human plasma. *Br J Haematol* **13**, 269-288, doi:10.1111/j.1365-2141.1967.tb08741.x (1967).

201 George, J. N., Thoi, L. L., McManus, L. M. & Reimann, T. A. Isolation of human platelet membrane microparticles from plasma and serum. *Blood* **60**, 834-840 (1982).

202 B.A., W. & O., V. The adhesive dendritic pseudopodium of the platelet and the release reaction. *Microvasc Res* **4**, 159-178 (1972).

203 Holme, P. A. *et al*. Shear-induced platelet activation and platelet microparticle formation at blood flow conditions as in arteries with a severe stenosis. *Arterioscler Thromb Vasc Biol* **17**, 646-653, doi:10.1161/01.atv.17.4.646 (1997).

204 Reininger, A. J. *et al*. Mechanism of platelet adhesion to von Willebrand factor and microparticle formation under high shear stress. *Blood* **107**, 3537-3545, doi:10.1182/blood-2005-02-0618 (2006).

205 Sinauridze, E. I. *et al*. Platelet microparticle membranes have 50- to 100-fold higher specific procoagulant activity than activated platelets. *Thromb Haemost* **97**, 425-434 (2007).

206 Falati, S. *et al*. Accumulation of tissue factor into developing thrombi in vivo is dependent upon microparticle P-selectin glycoprotein ligand 1 and platelet P-selectin. *J Exp Med* **197**, 1585-1598, doi:10.1084/jem.20021868 (2003).

207 Gross, P. L., Furie, B. C., Merrill-Skoloff, G., Chou, J. & Furie, B. Leukocyte-versus microparticle-mediated tissue factor transfer during arteriolar thrombus development. *J Leukoc Biol* **78**, 1318-1326, doi:10.1189/jlb.0405193 (2005).

208 Bouchard, B. A., Gissel, M. T., Whelihan, M. F., Mann, K. G. & Butenas, S. Platelets do not express the oxidized or reduced forms of tissue factor. *Biochim Biophys Acta* **1840**, 1188-1193, doi:10.1016/j.bbagen.2013.11.024 (2014).

209 Rauch, U. *et al*. Transfer of tissue factor from leukocytes to platelets is mediated by CD15 and tissue factor. *Blood* **96**, 170-175 (2000).

210 Castaman, G., Yu-Feng, L., Battistin, E. & Rodeghiero, F. Characterization of a novel bleeding disorder with isolated prolonged bleeding time and deficiency of platelet microvesicle generation. *Br J Haematol* **96**, 458-463, doi:10.1046/j.1365-2141.1997.d01-2072.x (1997).

211 Castaman, G., Yu-Feng, L. & Rodeghiero, F. A bleeding disorder characterised by isolated deficiency of platelet microvesicle generation. *Lancet* **347**, 700-701, doi:10.1016/s0140-6736(96)91259-3 (1996).

212 Sims, P. J., Wiedmer, T., Esmon, C. T., Weiss, H. J. & Shattil, S. J. Assembly of the platelet prothrombinase complex is linked to vesiculation of the platelet plasma membrane. Studies in Scott syndrome: an isolated defect in platelet procoagulant activity. *J Biol Chem* **264**, 17049-17057 (1989).

213 Ridger, V. C. *et al*. Microvesicles in vascular homeostasis and diseases. Position Paper of the European Society of Cardiology (ESC) Working Group on Atherosclerosis and Vascular Biology. *Thromb Haemost* **117**, 1296-1316, doi:10.1160/TH16-12-0943 (2017).

214 Toti, F., Satta, N., Fressinaud, E., Meyer, D. & Freyssinet, J. M. Scott syndrome, characterized by impaired transmembrane migration of procoagulant phosphatidylserine and hemorrhagic complications, is an inherited disorder. *Blood* **87**, 1409-1415 (1996).

215 Williamson, P. *et al*. Phospholipid scramblase activation pathways in lymphocytes. *Biochemistry* **40**, 8065-8072, doi:10.1021/bi001929z (2001).

216 Stormorken, H. *et al*. Studies on the haemostatic defect in a complicated syndrome. An inverse Scott syndrome platelet membrane abnormality? *Thromb Haemost* **74**, 1244-1251 (1995).

217 Zara, M. *et al*. Biology and Role of Extracellular Vesicles (EVs) in the Pathogenesis of Thrombosis. *Int J Mol Sci* **20**, doi:10.3390/ijms20112840 (2019).

218 Ghosh, A. *et al*. Platelet CD36 mediates interactions with endothelial cell-derived microparticles and contributes to thrombosis in mice. *J Clin Invest* **118**, 1934-1943, doi:10.1172/JCI34904 (2008).

219 Furlan-Freguia, C., Marchese, P., Gruber, A., Ruggeri, Z. M. & Ruf, W. P2X7 receptor signaling contributes to tissue factor-dependent thrombosis in mice. *J Clin Invest* **121**, 2932-2944, doi:10.1172/JCI46129 (2011).

220 Ramacciotti, E. *et al*. Leukocyte- and platelet-derived microparticles correlate with thrombus weight and tissue factor activity in an experimental mouse model of venous thrombosis. *Thromb Haemost* **101**, 748-754 (2009).

221 Biro, E. *et al*. Human cell-derived microparticles promote thrombus formation in vivo in a tissue factor-dependent manner. *J Thromb Haemost* **1**, 2561-2568, doi:10.1046/j.1538-7836.2003.00456.x (2003).

222 Davila, M. *et al*. Tissue factor-bearing microparticles derived from tumor cells: impact on coagulation activation. *J Thromb Haemost* **6**, 1517-1524, doi:10.1111/j.1538-7836.2008.02987.x (2008).

223 Lima, L. G., Chammas, R., Monteiro, R. Q., Moreira, M. E. & Barcinski, M. A. Tumor-derived microvesicles modulate the establishment of metastatic melanoma in a phosphatidylserine-dependent manner. *Cancer Lett* **283**, 168-175, doi:10.1016/j.canlet.2009.03.041 (2009).

224 Preston, R. A. *et al*. Effects of severe hypertension on endothelial and platelet microparticles. *Hypertension* **41**, 211-217, doi:10.1161/01.hyp.0000049760.15764.2d (2003).

225 Min, C., Kang, E., Yu, S. H., Shinn, S. H. & Kim, Y. S. Advanced glycation end products induce apoptosis and procoagulant activity in cultured human umbilical vein endothelial cells. *Diabetes Res Clin Pract* **46**, 197-202, doi:10.1016/s0168-8227(99)00094-7 (1999).

226 Sabatier, F. *et al*. Type 1 and type 2 diabetic patients display different patterns of cellular microparticles. *Diabetes* **51**, 2840-2845, doi:10.2337/diabetes.51.9.2840 (2002).

227 Llorente-Cortes, V., Otero-Vinas, M., Camino-Lopez, S., Llampayas, O. & Badimon, L. Aggregated low-density lipoprotein uptake induces membrane tissue factor procoagulant activity and microparticle release in human vascular smooth muscle cells. *Circulation* **110**, 452-459, doi:10.1161/01.CIR.0000136032.40666.3D (2004).

228 Boulanger, C. M., Amabile, N. & Tedgui, A. Circulating microparticles: a potential prognostic marker for atherosclerotic vascular disease. *Hypertension* **48**, 180-186, doi:10.1161/01.HYP.0000231507.00962.b5 (2006).

229 Mallat, Z. *et al*. Elevated levels of shed membrane microparticles with procoagulant potential in the peripheral circulating blood of patients with acute coronary syndromes. *Circulation* **101**, 841-843, doi:10.1161/01.cir.101.8.841 (2000).

230 Werner, N., Wassmann, S., Ahlers, P., Kosiol, S. & Nickenig, G. Circulating CD31+/annexin V+ apoptotic microparticles correlate with coronary endothelial function in patients with coronary artery disease. *Arterioscler Thromb Vasc Biol* **26**, 112-116, doi:10.1161/01.ATV.0000191634.13057.15 (2006).

231 Barry, O. P., Pratico, D., Savani, R. C. & FitzGerald, G. A. Modulation of monocyte-endothelial cell interactions by platelet microparticles. *J Clin Invest* **102**, 136-144, doi:10.1172/JCI2592 (1998).

232 Mallat, Z. *et al*. Shed membrane microparticles with procoagulant potential in human atherosclerotic plaques: a role for apoptosis in plaque thrombogenicity. *Circulation* **99**, 348-353, doi:10.1161/01.cir.99.3.348 (1999).

233 Bernal-Mizrachi, L. *et al*. Endothelial microparticles correlate with high-risk angiographic lesions in acute coronary syndromes. *Int J Cardiol* **97**, 439-446, doi:10.1016/j.ijcard.2003.10.029 (2004).

234 Valgimigli, M. The remarkable story of a wonder drug, which now comes to an end in the primary prevention setting: say bye-bye to aspirin! *Eur Heart J* **40**, 618-620, doi:10.1093/eurheartj/ehy872 (2019).

235 Elwood, P. C. *et al*. A randomized controlled trial of acetyl salicylic acid in the secondary prevention of mortality from myocardial infarction. *Br Med J* **1**, 436-440 (1974).

236 Antithrombotic Trialists, C. *et al*. Aspirin in the primary and secondary prevention of vascular disease: collaborative meta-analysis of individual participant data from randomised trials. *Lancet* **373**, 1849-1860, doi:10.1016/S0140-6736(09)60503-1 (2009).

237 Patrono, C. Aspirin and human platelets: from clinical trials to acetylation of cyclooxygenase and back. *Trends Pharmacol Sci* **10**, 453-458, doi:10.1016/S0165-6147(89)80010-0 (1989).

238 Fiore, L. D. *et al*. Department of Veterans Affairs Cooperative Studies Program Clinical Trial comparing combined warfarin and aspirin with aspirin alone in survivors of acute myocardial infarction: primary results of the CHAMP study. *Circulation* **105**, 557-563, doi:10.1161/hc0502.103329 (2002).

239 Randomised double-blind trial of fixed low-dose warfarin with aspirin after myocardial infarction. Coumadin Aspirin Reinfarction Study (CARS) Investigators. *Lancet* **350**, 389-396 (1997).

240 Rothberg, M. B., Celestin, C., Fiore, L. D., Lawler, E. & Cook, J. R. Warfarin plus aspirin after myocardial infarction or the acute coronary syndrome: meta-analysis with estimates of risk and benefit. *Ann Intern Med* **143**, 241-250, doi:10.7326/0003-4819-143-4-200508160-00005 (2005).

241 Protty, M. B. & Hayes, J. Dawn of the direct-acting oral anticoagulants: trends in oral anticoagulant prescribing in Wales 2009-2015. *J Clin Pharm Ther* **42**, 132-134, doi:10.1111/jcpt.12481 (2017).

242 Mega, J. L. *et al*. Rivaroxaban in patients with a recent acute coronary syndrome. *N Engl J Med* **366**, 9-19, doi:10.1056/NEJMoa1112277 (2012).

243 Johnson, J. V., Yost, R. A., Kelley, P. E. & Bradford, D. C. Tandem-in-space and tandem-in-time mass spectrometry: triple quadrupoles and quadrupole ion traps. *Anal Chem* **62**, 2162-2172 (1990).

244 Murphy, R. C. *et al*. Electrospray ionization and tandem mass spectrometry of eicosanoids. *Anal Biochem* **346**, 1-42, doi:10.1016/j.ab.2005.04.042 (2005).

245 Neumann, F. J. *et al*. 2018 ESC/EACTS Guidelines on myocardial revascularization. *Eur Heart J* **40**, 87-165, doi:10.1093/eurheartj/ehy394 (2019).

246 Hurt, L. *et al*. Cohort profile: HealthWise Wales. A research register and population health data platform with linkage to National Health Service data sets in Wales. *BMJ Open* **9**, e031705, doi:10.1136/bmjopen-2019-031705 (2019).

247 Morgan, A. H. *et al*. Quantitative assays for esterified oxylipins generated by immune cells. *Nat Protoc* **5**, 1919-1931, doi:10.1038/nprot.2010.162 (2010).

248 Berckmans, R. J., Lacroix, R., Hau, C. M., Sturk, A. & Nieuwland, R. Extracellular vesicles and coagulation in blood from healthy humans revisited. *J Extracell Vesicles* **8**, 1688936, doi:10.1080/20013078.2019.1688936 (2019).

249 Coumans, F. A. W. *et al*. Methodological Guidelines to Study Extracellular Vesicles. *Circ Res* **120**, 1632-1648, doi:10.1161/CIRCRESAHA.117.309417 (2017).

250 Hong, S. H. *et al*. Quantitative determination of 12-hydroxyeicosatetraenoic acids by chiral liquid chromatography tandem mass spectrometry in a murine atopic dermatitis model. *J Vet Sci* **16**, 307-315, doi:10.4142/jvs.2015.16.3.307 (2015).

251 Nelson, R. J. Seasonal immune function and sickness responses. *Trends Immunol* **25**, 187-192, doi:10.1016/j.it.2004.02.001 (2004).

252 Dopico, X. C. *et al*. Widespread seasonal gene expression reveals annual differences in human immunity and physiology. *Nat Commun* **6**, 7000, doi:10.1038/ncomms8000 (2015).

253 Persson, R. *et al*. Seasonal variation in human salivary cortisol concentration. *Chronobiol Int* **25**, 923-937, doi:10.1080/07420520802553648 (2008).

254 Maree, A. O. *et al*. Cyclooxygenase-1 haplotype modulates platelet response to aspirin. *J Thromb Haemost* **3**, 2340-2345, doi:10.1111/j.1538-7836.2005.01555.x (2005).

255 Kyrle, P. A., Westwick, J., Scully, M. F., Kakkar, V. V. & Lewis, G. P. Investigation of the interaction of blood platelets with the coagulation system at the site of plug formation in vivo in man--effect of low-dose aspirin. *Thromb Haemost* **57**, 62-66 (1987).

256 Szczeklik, A. *et al*. Inhibition of thrombin generation by simvastatin and lack of additive effects of aspirin in patients with marked hypercholesterolemia. *J Am Coll Cardiol* **33**, 1286-1293 (1999).

257 Butenas, S. *et al*. Antiplatelet agents in tissue factor-induced blood coagulation. *Blood* **97**, 2314-2322 (2001).

258 Hemker, H. C. & Beguin, S. Phenotyping the clotting system. *Thromb Haemost* **84**, 747-751 (2000).

259 Hemker, H. C. *et al*. Calibrated automated thrombin generation measurement in clotting plasma. *Pathophysiol Haemost Thromb* **33**, 4-15, doi:10.1159/000071636 (2003).

260 Undas, A., Brummel-Ziedins, K. E. & Mann, K. G. Antithrombotic properties of aspirin and resistance to aspirin: beyond strictly antiplatelet actions. *Blood* **109**, 2285-2292, doi:10.1182/blood-2006-01-010645 (2007).

261 Ben Freedman, S., Gersh, B. J. & Lip, G. Y. Misperceptions of aspirin efficacy and safety may perpetuate anticoagulant underutilization in atrial fibrillation. *Eur Heart J* **36**, 653-656, doi:10.1093/eurheartj/ehu494 (2015).

262 Patti, G. *et al*. Platelet function and long-term antiplatelet therapy in women: is there a gender-specificity? A 'state-of-the-art' paper. *Eur Heart J* **35**, 2213-2223b, doi:10.1093/eurheartj/ehu279 (2014).

263 Asada, Y., Yamashita, A., Sato, Y. & Hatakeyama, K. Pathophysiology of atherothrombosis: Mechanisms of thrombus formation on disrupted atherosclerotic plaques. *Pathol Int*, doi:10.1111/pin.12921 (2020).

264 Willerson, J. T., Golino, P., Eidt, J., Campbell, W. B. & Buja, L. M. Specific platelet mediators and unstable coronary artery lesions. Experimental evidence and potential clinical implications. *Circulation* **80**, 198-205, doi:10.1161/01.cir.80.1.198 (1989).

265 Antithrombotic Trialists, C. Collaborative meta-analysis of randomised trials of antiplatelet therapy for prevention of death, myocardial infarction, and stroke in high risk patients. *BMJ* **324**, 71-86, doi:10.1136/bmj.324.7329.71 (2002).

266 Jernberg, T. *et al*. Cardiovascular risk in post-myocardial infarction patients: nationwide real world data demonstrate the importance of a long-term perspective. *Eur Heart J* **36**, 1163-1170, doi:10.1093/eurheartj/ehu505 (2015).

267 Fox, K. A. *et al*. Underestimated and under-recognized: the late consequences of acute coronary syndrome (GRACE UK-Belgian Study). *Eur Heart J* **31**, 2755-2764, doi:10.1093/eurheartj/ehq326 (2010).

268 Rentrop, K. P. Thrombi in acute coronary syndromes : revisited and revised. *Circulation* **101**, 1619-1626, doi:10.1161/01.cir.101.13.1619 (2000).

269 Hatakeyama, K. *et al*. Localization and activity of tissue factor in human aortic atherosclerotic lesions. *Atherosclerosis* **133**, 213-219, doi:10.1016/s0021-9150(97)00132-9 (1997).

270 Owens, A. P., 3rd & Mackman, N. Role of tissue factor in atherothrombosis. *Curr Atheroscler Rep* **14**, 394-401, doi:10.1007/s11883-012-0269-5 (2012).

271 Bogdanov, V. Y. & Versteeg, H. H. "Soluble Tissue Factor" in the 21st Century: Definitions, Biochemistry, and Pathophysiological Role in Thrombus Formation. *Semin Thromb Hemost* **41**, 700-707, doi:10.1055/s-0035-1556049 (2015).

272 Bode, M. & Mackman, N. Regulation of tissue factor gene expression in monocytes and endothelial cells: Thromboxane A2 as a new player. *Vascul Pharmacol* **62**, 57-62, doi:10.1016/j.vph.2014.05.005 (2014).

273 Hoshiba, Y., Hatakeyama, K., Tanabe, T., Asada, Y. & Goto, S. Co-localization of von Willebrand factor with platelet thrombi, tissue factor and platelets with fibrin, and consistent presence of inflammatory cells in coronary thrombi obtained by an aspiration device from patients with acute myocardial infarction. *J Thromb Haemost* **4**, 114-120, doi:10.1111/j.1538-7836.2005.01701.x (2006).

274 Grant, S. G. The molecular evolution of the vertebrate behavioural repertoire. *Philos Trans R Soc Lond B Biol Sci* **371**, 20150051, doi:10.1098/rstb.2015.0051 (2016).

275 Naruko, T. *et al*. Neutrophil infiltration of culprit lesions in acute coronary syndromes. *Circulation* **106**, 2894-2900, doi:10.1161/01.cir.0000042674.89762.20 (2002).

276 Mazzone, A. *et al*. Increased expression of neutrophil and monocyte adhesion molecules in unstable coronary artery disease. *Circulation* **88**, 358-363, doi:10.1161/01.cir.88.2.358 (1993).

277 Biasucci, L. M. *et al*. Intracellular neutrophil myeloperoxidase is reduced in unstable angina and acute myocardial infarction, but its reduction is not related to ischemia. *J Am Coll Cardiol* **27**, 611-616, doi:10.1016/0735-1097(95)00524-2 (1996).

278 Neri Serneri, G. G. *et al*. Acute T-cell activation is detectable in unstable angina. *Circulation* **95**, 1806-1812, doi:10.1161/01.cir.95.7.1806 (1997).

279 Falls, L. A., Furie, B. & Furie, B. C. Role of phosphatidylethanolamine in assembly and function of the factor IXa-factor VIIIa complex on membrane surfaces. *Biochemistry* **39**, 13216-13222, doi:10.1021/bi0009789 (2000).

280 Waddington, E., Sienuarine, K., Puddey, I. & Croft, K. Identification and quantitation of unique fatty acid oxidation products in human atherosclerotic plaque using high-performance liquid chromatography. *Anal Biochem* **292**, 234-244, doi:10.1006/abio.2001.5075 (2001).

281 Kuhn, H., Heydeck, D., Hugou, I. & Gniwotta, C. In vivo action of 15-lipoxygenase in early stages of human atherogenesis. *J Clin Invest* **99**, 888-893, doi:10.1172/JCI119253 (1997).

282 Ong, S. B. *et al*. Inflammation following acute myocardial infarction: Multiple players, dynamic roles, and novel therapeutic opportunities. *Pharmacol Ther* **186**, 73-87, doi:10.1016/j.pharmthera.2018.01.001 (2018).

283 Mukhopadhyay, S. *et al*. Fibrinolysis and Inflammation in Venous Thrombus Resolution. *Front Immunol* **10**, 1348, doi:10.3389/fimmu.2019.01348 (2019).

284 Goto, Y. *et al*. Degradation of phospholipid molecular species during experimental cerebral ischemia in rats. *Stroke* **19**, 728-735, doi:10.1161/01.str.19.6.728 (1988).

285 Sakai, T. *et al*. Eosinophils may be involved in thrombus growth in acute coronary syndrome. *Int Heart J* **50**, 267-277, doi:10.1536/ihj.50.267 (2009).

286 Kubavat, A. H. *et al*. A randomized, comparative, multicentric clinical trial to assess the efficacy and safety of zileuton extended-release tablets with montelukast sodium tablets in patients suffering from chronic persistent asthma. *Am J Ther* **20**, 154-162, doi:10.1097/MJT.0b013e318254259b (2013).

287 Lazarus, S. C. *et al*. Safety and clinical efficacy of zileuton in patients with chronic asthma. *Am J Manag Care* **4**, 841-848 (1998).

288 van der Putten, R. F., Glatz, J. F. & Hermens, W. T. Plasma markers of activated hemostasis in the early diagnosis of acute coronary syndromes. *Clin Chim Acta* **371**, 37-54, doi:10.1016/j.cca.2006.03.005 (2006).

289 Gao, C. *et al*. Procoagulant activity of erythrocytes and platelets through phosphatidylserine exposure and microparticles release in patients with nephrotic syndrome. *Thromb Haemost* **107**, 681-689, doi:10.1160/TH11-09-0673 (2012).

290 Tan, X. *et al*. Role of erythrocytes and platelets in the hypercoagulable status in polycythemia vera through phosphatidylserine exposure and microparticle generation. *Thromb Haemost* **109**, 1025-1032, doi:10.1160/TH12-11-0811 (2013).

291 Yang, C. *et al*. Contributions of phosphatidylserine-positive platelets and leukocytes and microparticles to hypercoagulable state in gastric cancer patients. *Tumour Biol* **37**, 7881-7891, doi:10.1007/s13277-015-4667-5 (2016).

292 Chen, D. & Dorling, A. Critical roles for thrombin in acute and chronic inflammation. *J Thromb Haemost* **7 Suppl 1**, 122-126, doi:10.1111/j.1538-7836.2009.03413.x (2009).

293 De Caterina, R. & Goto, S. Targeting thrombin long-term after an acute coronary syndrome: Opportunities and challenges. *Vascul Pharmacol* **81**, 1-14, doi:10.1016/j.vph.2016.03.003 (2016).

294 Brambilla, M. *et al*. Tissue factor in patients with acute coronary syndromes: expression in platelets, leukocytes, and platelet-leukocyte aggregates. *Arterioscler Thromb Vasc Biol* **28**, 947-953, doi:10.1161/ATVBAHA.107.161471 (2008).

295 Mackman, N. Role of tissue factor in hemostasis, thrombosis, and vascular development. *Arterioscler Thromb Vasc Biol* **24**, 1015-1022, doi:10.1161/01.ATV.0000130465.23430.74 (2004).

296 Owens, A. P., 3rd & Mackman, N. Microparticles in hemostasis and thrombosis. *Circ Res* **108**, 1284-1297, doi:10.1161/CIRCRESAHA.110.233056 (2011).

297 Loeffen, R. *et al*. Factor XIa and Thrombin Generation Are Elevated in Patients with Acute Coronary Syndrome and Predict Recurrent Cardiovascular Events. *PLoS One* **11**, e0158355, doi:10.1371/journal.pone.0158355 (2016).

298 Mulvihill, N. T. & Foley, J. B. Inflammation in acute coronary syndromes. *Heart* **87**, 201-204, doi:10.1136/heart.87.3.201 (2002).

299 Altman, R. Risk factors in coronary atherosclerosis athero-inflammation: the meeting point. *Thromb J* **1**, 4, doi:10.1186/1477-9560-1-4 (2003).

300 Eckel, R. H. *et al*. Prevention Conference VI: Diabetes and Cardiovascular Disease: Writing Group II: pathogenesis of atherosclerosis in diabetes. *Circulation* **105**, e138-143, doi:10.1161/01.cir.0000013954.65303.c5 (2002).

301 Han, Y., Runge, M. S. & Brasier, A. R. Angiotensin II induces interleukin-6 transcription in vascular smooth muscle cells through pleiotropic activation of nuclear factor-kappa B transcription factors. *Circ Res* **84**, 695-703, doi:10.1161/01.res.84.6.695 (1999).

302 Kianoush, S. *et al*. Associations of Cigarette Smoking With Subclinical Inflammation and Atherosclerosis: ELSA-Brasil (The Brazilian Longitudinal Study of Adult Health). *J Am Heart Assoc* **6**, doi:10.1161/JAHA.116.005088 (2017).

303 Rodriguez-Iturbe, B., Pons, H. & Johnson, R. J. Role of the Immune System in Hypertension. *Physiol Rev* **97**, 1127-1164, doi:10.1152/physrev.00031.2016 (2017).

304 Mihai, S. *et al*. Inflammation-Related Mechanisms in Chronic Kidney Disease Prediction, Progression, and Outcome. *J Immunol Res* **2018**, 2180373, doi:10.1155/2018/2180373 (2018).

305 Guasti, L. *et al*. Neutrophils and clinical outcomes in patients with acute coronary syndromes and/or cardiac revascularisation. A systematic review on more than 34,000 subjects. *Thromb Haemost* **106**, 591-599, doi:10.1160/TH11-02-0096 (2011).

306 Thomas, M. R. *et al*. Prognostic impact of baseline inflammatory markers in patients with acute coronary syndromes treated with ticagrelor and clopidogrel. *Eur Heart J Acute Cardiovasc Care*, 2048872619878075, doi:10.1177/2048872619878075 (2019).

307 Kannel, W. B., Anderson, K. & Wilson, P. W. White blood cell count and cardiovascular disease. Insights from the Framingham Study. *JAMA* **267**, 1253-1256 (1992).

308 van Niel, G., D'Angelo, G. & Raposo, G. Shedding light on the cell biology of extracellular vesicles. *Nat Rev Mol Cell Biol* **19**, 213-228, doi:10.1038/nrm.2017.125 (2018).

309 Kockx, M. M. Apoptosis in the atherosclerotic plaque: quantitative and qualitative aspects. *Arterioscler Thromb Vasc Biol* **18**, 1519-1522, doi:10.1161/01.atv.18.10.1519 (1998).

310 Leroyer, A. S. *et al*. Cellular origins and thrombogenic activity of microparticles isolated from human atherosclerotic plaques. *J Am Coll Cardiol* **49**, 772-777, doi:10.1016/j.jacc.2006.10.053 (2007).

311 Kolodgie, F. D. *et al*. Localization of apoptotic macrophages at the site of plaque rupture in sudden coronary death. *Am J Pathol* **157**, 1259-1268, doi:10.1016/S0002-9440(10)64641-X (2000).

312 Tans, G. *et al*. Comparison of anticoagulant and procoagulant activities of stimulated platelets and platelet-derived microparticles. *Blood* **77**, 2641-2648 (1991).

313 Horstman, L. L., McCauley, R. F., Jy, W. & Ahn, Y. S. Tissue Factor-Negative Cell-Derived Microparticles Play a Distinctive Role in Hemostasis: A Viewpoint Review. *Semin Thromb Hemost* **45**, 509-513, doi:10.1055/s-0039-1688570 (2019).

314 Panes, O. *et al*. Human platelets synthesize and express functional tissue factor. *Blood* **109**, 5242-5250, doi:10.1182/blood-2006-06-030619 (2007).

315 Bouchard, B. A., Mann, K. G. & Butenas, S. No evidence for tissue factor on platelets. *Blood* **116**, 854-855, doi:10.1182/blood-2010-05-285627 (2010).

316 Wang, Y. *et al*. Platelet-derived microparticles regulates thrombin generation via phophatidylserine in abdominal sepsis. *J Cell Physiol* **233**, 1051-1060, doi:10.1002/jcp.25959 (2018).

317 Tripisciano, C. *et al*. Different Potential of Extracellular Vesicles to Support Thrombin Generation: Contributions of Phosphatidylserine, Tissue Factor, and Cellular Origin. *Sci Rep* **7**, 6522, doi:10.1038/s41598-017-03262-2 (2017).

318 Ayers, L., Harrison, P., Kohler, M. & Ferry, B. Procoagulant and platelet-derived microvesicle absolute counts determined by flow cytometry correlates with a measurement of their functional capacity. *J Extracell Vesicles* **3**, doi:10.3402/jev.v3.25348 (2014).

319 Lacroix, R. *et al*. Impact of pre-analytical parameters on the measurement of circulating microparticles: towards standardization of protocol. *J Thromb Haemost* **10**, 437-446, doi:10.1111/j.1538-7836.2011.04610.x (2012).

320 Boulanger, C. M. *et al*. Circulating microparticles from patients with myocardial infarction cause endothelial dysfunction. *Circulation* **104**, 2649-2652, doi:10.1161/hc4701.100516 (2001).

321 Omoto, S. *et al*. Detection of monocyte-derived microparticles in patients with Type II diabetes mellitus. *Diabetologia* **45**, 550-555, doi:10.1007/s00125-001-0772-7 (2002).

322 Ryu, A. R., Kim, D. H., Kim, E. & Lee, M. Y. The Potential Roles of Extracellular Vesicles in Cigarette Smoke-Associated Diseases. *Oxid Med Cell Longev* **2018**, 4692081, doi:10.1155/2018/4692081 (2018).

323 Karpman, D., Stahl, A. L. & Arvidsson, I. Extracellular vesicles in renal disease. *Nat Rev Nephrol* **13**, 545-562, doi:10.1038/nrneph.2017.98 (2017).

324 Catalano, M. & O'Driscoll, L. Inhibiting extracellular vesicles formation and release: a review of EV inhibitors. *J Extracell Vesicles* **9**, 1703244, doi:10.1080/20013078.2019.1703244 (2020).

325 Furman, D. *et al*. Chronic inflammation in the etiology of disease across the life span. *Nat Med* **25**, 1822-1832, doi:10.1038/s41591-019-0675-0 (2019).

326 Huang, M. J. *et al*. Blood coagulation system in patients with chronic kidney disease: a prospective observational study. *BMJ Open* **7**, e014294, doi:10.1136/bmjopen-2016-014294 (2017).

327 Morel, O., Jesel, L., Abbas, M. & Morel, N. Prothrombotic changes in diabetes mellitus. *Semin Thromb Hemost* **39**, 477-488, doi:10.1055/s-0033-1343888 (2013).

328 Spronk, H. M., van der Voort, D. & Ten Cate, H. Blood coagulation and the risk of atherothrombosis: a complex relationship. *Thromb J* **2**, 12, doi:10.1186/1477-9560-2-12 (2004).

329 Armstrong, E. J., Morrow, D. A. & Sabatine, M. S. Inflammatory biomarkers in acute coronary syndromes: part I: introduction and cytokines. *Circulation* **113**, e72-75, doi:10.1161/CIRCULATIONAHA.105.595520 (2006).

330 Braun, O. O. *et al*. Greater reduction of platelet activation markers and platelet-monocyte aggregates by prasugrel compared to clopidogrel in stable coronary artery disease. *Thromb Haemost* **100**, 626-633 (2008).

331 Klinkhardt, U. *et al*. Clopidogrel but not aspirin reduces P-selectin expression and formation of platelet-leukocyte aggregates in patients with atherosclerotic vascular disease. *Clin Pharmacol Ther* **73**, 232-241, doi:10.1067/mcp.2003.13 (2003).

332 Jain, S. *et al*. Characterization of human lysophospholipid acyltransferase 3. *J Lipid Res* **50**, 1563-1570, doi:10.1194/jlr.M800398-JLR200 (2009).

333 Lewandrowski, U. *et al*. Platelet membrane proteomics: a novel repository for functional research. *Blood* **114**, e10-19, doi:10.1182/blood-2009-02-203828 (2009).

334 Ed Rainger, G. *et al*. The role of platelets in the recruitment of leukocytes during vascular disease. *Platelets* **26**, 507-520, doi:10.3109/09537104.2015.1064881 (2015).

335 Yeang, C. *et al*. Reduction of myocardial ischaemia-reperfusion injury by inactivating oxidized phospholipids. *Cardiovasc Res* **115**, 179-189, doi:10.1093/cvr/cvy136 (2019).

336 Tsimikas, S. *et al*. Oxidized phospholipids, Lp(a) lipoprotein, and coronary artery disease. *N Engl J Med* **353**, 46-57, doi:10.1056/NEJMoa043175 (2005).

337 Solati, Z. & Ravandi, A. Lipidomics of Bioactive Lipids in Acute Coronary Syndromes. *Int J Mol Sci* **20**, doi:10.3390/ijms20051051 (2019).

338 Tsimikas, S. *et al*. Oxidized phospholipids predict the presence and progression of carotid and femoral atherosclerosis and symptomatic cardiovascular disease: five-year prospective results from the Bruneck study. *J Am Coll Cardiol* **47**, 2219-2228, doi:10.1016/j.jacc.2006.03.001 (2006).

339 Kodigepalli, K. M., Bowers, K., Sharp, A. & Nanjundan, M. Roles and regulation of phospholipid scramblases. *FEBS Lett* **589**, 3-14, doi:10.1016/j.febslet.2014.11.036 (2015).

340 Morel, O., Jesel, L., Freyssinet, J. M. & Toti, F. Cellular mechanisms underlying the formation of circulating microparticles. *Arterioscler Thromb Vasc Biol* **31**, 15-26, doi:10.1161/ATVBAHA.109.200956 (2011).

341 Andree, H. A. *et al*. Binding of vascular anticoagulant alpha (VAC alpha) to planar phospholipid bilayers. *J Biol Chem* **265**, 4923-4928 (1990).

342 Koopman, G. *et al*. Annexin V for flow cytometric detection of phosphatidylserine expression on B cells undergoing apoptosis. *Blood* **84**, 1415-1420 (1994).

343 Meers, P. & Mealy, T. Phospholipid determinants for annexin V binding sites and the role of tryptophan 187. *Biochemistry* **33**, 5829-5837, doi:10.1021/bi00185a022 (1994).

344 Wang, L. *et al*. Microparticles and blood cells induce procoagulant activity via phosphatidylserine exposure in NSTEMI patients following stent implantation. *Int J Cardiol* **223**, 121-128, doi:10.1016/j.ijcard.2016.07.260 (2016).

345 Beckett, C. S., Kell, P. J., Creer, M. H. & McHowat, J. Phospholipase A2-catalyzed hydrolysis of plasmalogen phospholipids in thrombin-stimulated human platelets. *Thromb Res* **120**, 259-268, doi:10.1016/j.thromres.2006.09.005 (2007).

346 Bozelli, J. C., Jr. *et al*. Membrane curvature allosterically regulates the phosphatidylinositol cycle, controlling its rate and acyl-chain composition of its lipid intermediates. *J Biol Chem* **293**, 17780-17791, doi:10.1074/jbc.RA118.005293 (2018).

347 McMahon, H. T. & Boucrot, E. Membrane curvature at a glance. *J Cell Sci* **128**, 1065-1070, doi:10.1242/jcs.114454 (2015).

348 Middleton, E. R. & Rhoades, E. Effects of curvature and composition on alpha-synuclein binding to lipid vesicles. *Biophys J* **99**, 2279-2288, doi:10.1016/j.bpj.2010.07.056 (2010).

349 Dickhout, A. & Koenen, R. R. Extracellular Vesicles as Biomarkers in Cardiovascular Disease; Chances and Risks. *Front Cardiovasc Med* **5**, 113, doi:10.3389/fcvm.2018.00113 (2018).

350 Lee, S. R., Park, Y. & Park, J. W. Curvature Effect of a Phosphatidylethanolamine-Included Membrane on the Behavior of Cinnamycin on the Membrane. *J Phys Chem B* **124**, 8984-8988, doi:10.1021/acs.jpcb.0c06029 (2020).

351 Liu, Y. *et al*. Dissimilarity of increased phosphatidylserine-positive microparticles and associated coagulation activation in acute coronary syndromes. *Coron Artery Dis* **27**, 365-375, doi:10.1097/MCA.0000000000000368 (2016).

352 Brisson, A. R., Tan, S., Linares, R., Gounou, C. & Arraud, N. Extracellular vesicles from activated platelets: a semiquantitative cryo-electron microscopy and immuno-gold labeling study. *Platelets* **28**, 263-271, doi:10.1080/09537104.2016.1268255 (2017).

353 Tait, J. F., Gibson, D. F. & Smith, C. Measurement of the affinity and cooperativity of annexin V-membrane binding under conditions of low membrane occupancy. *Anal Biochem* **329**, 112-119, doi:10.1016/j.ab.2004.02.043 (2004).

354 Alfonso, L. F., Srivenugopal, K. S. & Bhat, G. J. Does aspirin acetylate multiple cellular proteins? (Review). *Mol Med Rep* **2**, 533-537, doi:10.3892/mmr_00000132 (2009).

355 Alfonso, L., Ai, G., Spitale, R. C. & Bhat, G. J. Molecular targets of aspirin and cancer prevention. *Br J Cancer* **111**, 61-67, doi:10.1038/bjc.2014.271 (2014).

356 Nam, M. H. *et al*. Aspirin inhibits TGFbeta2-induced epithelial to mesenchymal transition of lens epithelial cells: selective acetylation of K56 and K122 in histone H3. *Biochem J* **477**, 75-97, doi:10.1042/BCJ20190540 (2020).

357 Nixon, A. B., O'Flaherty, J. T., Salyer, J. K. & Wykle, R. L. Acetyl-CoA:1-O-alkyl-2-lyso-sn-glycero-3-phosphocholine acetyltransferase is directly activated by p38 kinase. *J Biol Chem* **274**, 5469-5473, doi:10.1074/jbc.274.9.5469 (1999).

358 Smyth, E. M. Thromboxane and the thromboxane receptor in cardiovascular disease. *Clin Lipidol* **5**, 209-219, doi:10.2217/clp.10.11 (2010).

359 Behr-Rasmussen, C., Grondal, N., Bramsen, M. B., Thomsen, M. D. & Lindholt, J. S. Mural thrombus and the progression of abdominal aortic aneurysms: a large population-based prospective cohort study. *Eur J Vasc Endovasc Surg* **48**, 301-307, doi:10.1016/j.ejvs.2014.05.014 (2014).

360 Moon, J. Y., Nagaraju, D., Franchi, F., Rollini, F. & Angiolillo, D. J. The role of oral anticoagulant therapy in patients with acute coronary syndrome. *Ther Adv Hematol* **8**, 353-366, doi:10.1177/2040620717733691 (2017).

361 Reganon, E., Vila, V., Martinez-Sales, V., Vaya, A. & Aznar, J. Inflammation, fibrinogen and thrombin generation in patients with previous myocardial infarction. *Haematologica* **87**, 740-745; discussion 745 (2002).

362 Weitz, J. I. Insights into the role of thrombin in the pathogenesis of recurrent ischaemia after acute coronary syndrome. *Thromb Haemost* **112**, 924-931, doi:10.1160/TH14-03-0265 (2014).

363 Schiele, F. Fondaparinux and acute coronary syndromes: update on the OASIS 5-6 studies. *Vasc Health Risk Manag* **6**, 179-187, doi:10.2147/vhrm.s6099 (2010).

364 Ten Cate, H. & Meade, T. The Northwick Park Heart Study: evidence from the laboratory. *J Thromb Haemost* **12**, 587-592, doi:10.1111/jth.12545 (2014).

365 Mahmood, S. S., Levy, D., Vasan, R. S. & Wang, T. J. The Framingham Heart Study and the epidemiology of cardiovascular disease: a historical perspective. *Lancet* **383**, 999-1008, doi:10.1016/S0140-6736(13)61752-3 (2014).

CHAPTER 10 APPENDICES

10.1 APPENDIX 10.1 – PATIENT INFORMATION LEAFLET (ACS)

The information leaflet for patients with ACS as part of the 'clinical cohort'.

GIG CYMRU NHS WALES
Bwrdd Iechyd Prifysgol Caerdydd a'r Fro
Cardiff and Vale University Health Board

Patient Information Leaflet

Title of Study: A pilot, exploratory study to investigate procoagulant phospholipids in arterial thrombosis

Thank you for expressing an interest in this study. Before deciding whether you wish to take part, it is important that you understand why the study is being done and what it involves. Please take time to read this information carefully and consider discussing it with family or friends. This study is being undertaken as part of an educational project.

What is the purpose of the study?

Clots form on the surfaces of cells in the blood such as platelets and white cells. Fatty molecules (phospholipids) in the membrane of these cells bind to clotting factors and help to control the formation of a clot. When cells become active, they release small packages of membranes (microparticles) which also contribute to clot formation. Different fatty molecules may help to control how thick or thin the blood is. If the blood is too thick, clots can form where they are not wanted leading to heart attacks. The aim of this study is to find out which phospholipids are present on the surface of cells and microparticles in people who have clotting disease and compare them with individuals who don't. This may help explain why some people are prone to clotting.

Why have I been chosen?

We are looking for volunteers to help try to identify whether certain phospholipids cause increased clotting. You have been invited to take part in the study because you have recently experienced a heart attack.

Do I have to take part?

No, taking part is entirely your decision. If you decide to participate, we will discuss the study and go through the information leaflet with you. We will then request that you sign a consent form to show that you have agreed to take part. You can decide to withdraw from the study at any time, even if you have signed the consent form. This will not affect any of your current treatment or future care in any way.

Version 2.0 date (Cardiac) 02 January 2019 IRAS Project ID: 243701

What will the study involve?

A member of the research team will explain the study and answer any questions that you have. You will be asked to sign a consent form but you should only do this if you are happy to take part.

A blood sample will be taken by a trained member of the research team in a designated clinical area in the cardiology department, or if you are receiving in-patient treatment, the sample will be taken on the ward.

The total amount of blood that will be taken is 75ml (equivalent to just over 4 tablespoons).

As part of the study, we want to identify any risk factors in your medical background that contribute to clot formation. Clinical data related to your thrombotic condition will be recorded by the study team, however this will be kept confidential and no identifiable data will be shared outside of the study.

Will I be required to re-attend?

No, will not need to attend for further testing.

Can I withdraw from the study at a later date?

Yes, all participants have the right to withdraw from the study at any time by contacting the study team (details below). If you withdraw from the study, data collected up to the point of withdrawal will be kept. Any unanalysed tissue collected up to the point of withdrawal will be destroyed. No further data or tissue would be collected or any other research procedures carried out on or in relation to you.

What will happen to the blood samples that are taken?

The blood for the specialised tests on phospholipids and microparticles will be processed on the day the sample is taken. Most tests will be done that day although some will be performed and analysed later on samples which will be kept securely in the Infection and Immunity laboratory in the Sir Geraint Evans Cardiovascular Research Building at the School of Medicine Cardiff University. The samples that are stored will be labelled by a pseudo-anonymized study number. We will be able to link the study number to you so the laboratory results and clinical details can be linked. All samples will be processed on the day in accordance to the Human Tissue Act 2004 and will be deemed "non-relevant" as it would have been "treated, processed or lysed through a process intended to render them acellular.". These "non-relevant" material will be stored by the research team in the School of Medicine Cardiff University for up to 5 years for research governance purposes, and will be destroyed thereafter.

What information will be collected about me?

We will record your age and gender as well as clinical information related to your clotting disorder on a database identified by a study number. We will be able to link the study number to your name and hospital records through a separate database.

Cardiff and Vale Health Board will collect information from you and your medical records for this research study in accordance with our instructions. The site will keep your name, NHS number, Date of Birth and contact details confidential and will not pass this information to Cardiff and Vale UHB. [NHS/other site] will use this information as needed, to contact you about the research study, and make sure that relevant information about the study is recorded for your care, and to oversee the quality of the study. Certain individuals from Cardiff and Vale UHB and regulatory organisations may look at your medical and research records to check the accuracy of the research study. Cardiff and Vale UHB will only receive information without any identifying information. The people who analyse the information will not be able to identify you and will not be able to find out your name, NHS number, Date of Birth or contact details.

Cardiff and Vale Health Board will keep identifiable information about you from this study for 5 years after the study has finished.

What are the risks of taking part in the study?

We require a blood sample at study entry. The risks associated with blood taking include mild pain and bruising. The total volume of blood taken (approximately 4 tablespoons in total) is small when compared to the total amount of blood in the body. We would therefore not expect this to cause any harm. We will not be changing your treatment in any way.

Will the study benefit me directly?

It is unlikely that the study will provide information that helps you directly but it may help us to better understand why some people get clots. If the results of the study may be beneficial to your care we will discuss this with you.

How will my information be kept secure?

Cardiff and Vale UHB is the sponsor for this study based in the United Kingdom. We will be using information from you and your medical records in order to undertake this study and will act as the data controller for this study. This means that we are responsible for looking after your information and using it properly. Cardiff and Vale UHB will keep identifiable information about you for 5 years after the study has finished. The study team will store study data securely without any identifiable data in an encrypted and password protected database which complies with the General Data Protection Regulation (GDPR) and Data Protection Act 2018. These data will be held by the study team for up to 5 years.

Your rights to access, change or move your information are limited, as we need to manage your information in specific ways in order for the research to be reliable and accurate. If you withdraw from the study, we will keep the information about you that we have already obtained. To safeguard your rights, we will use the minimum personally-identifiable information possible. You can find out more about how we use your information by contacting cav.ig.dept@wales.nhs.uk.

What will happen to the results of the study?

The results may be submitted for publication in a journal that is accessible to the public. They will also contribute to a research project funded by the Wellcome Trust. Your data will be

anonymised and therefore you cannot be personally identified. Access to a summary of the study results may be obtained by directly contacting the study team by email on ProttyM3@cardiff.ac.uk. It is anticipated that the first such summary will be available from early 2020 onwards.

Will my GP or other health care professional be informed that I am taking part in the study?

This study will not affect your care in any way and so we will not notify your GP or other health care professional unless you ask us to.

What if there is a problem?

If you have any concerns about any aspect of this study, you should ask to speak to the researchers who will do their best to answer your questions (contact details at the end). If you remain unhappy and wish to complain formally, you can do this by using the NHS complaints procedure. Details can be found on the NHS website or ask a member of staff.

In the unlikely event that something does go wrong, and you are harmed during the research study there are no special compensation arrangements. If you are harmed and this is due to someone's negligence, then you may have grounds for a legal action for compensation against your local Trust/Health Board but you may have to pay your legal costs. The normal National Health Service complaints mechanisms will still be available to you.

Who funds and supervises the study?

The study is being funded by the Wellcome Trust. The study has been reviewed by the Yorkshire & The Humber - Leeds East independent ethics committee.

If I am interested in the study, how do I enrol?

If you are interested in taking part, please contact the research team by email: ProttyM3@cardiff.ac.uk.

Contact details for researchers:-

Prof Zaheer Yousef, Consultant Cardiologist, Department of Cardiology, University Hospital of Wales, Heath Park, Cardiff, CF14 4XN. Telephone: 029207 42972

Dr Majd Protty, Cardiology Registrar, Sir Geraint Evans Cardiovascular Research Building, Cardiff University School of Medicine, Heath Park, Cardiff, CF14 4XN. Telephone: 029206 87309.

Contact details for independent contact:-

Dr Steve Knapper, Department of Haematology, Cardiff University School of Medicine, Heath Park, Cardiff, CF14 4XN. Telephone: 02920 745379.

Local site details:

Principal Investigator and their contact details: Dr Majd Protty, Cardiology Registrar, Sir Geraint Evans Cardiovascular Research Building, Cardiff University School of Medicine, Heath Park, Cardiff, CF14 4XN. Telephone: 029206 87309.

Version 2.0 date (Cardiac) 02 January 2019 IRAS Project ID: 243701

10.2 Appendix 10.2 – Consent form (ACS Patients)

The consent form for patients with acute coronary syndrome as part of the 'clinical cohort'.

Consent Form v2.0

Title of Study: A pilot, exploratory study to investigate procoagulant phospholipids in arterial thrombosis.

Patient Identification Number for this study: _____

	INITIALS
Please initial the boxes	
1. I confirm that I have read and understand the information sheet dated 02 Jan 2019 for the above study. I have had the opportunity to consider the information, ask questions and have had these answered satisfactorily.	☐
2. I understand that my participation is voluntary and that I am free to withdraw at any time without giving any reason, without my medical care or legal rights being affected.	☐
3. I understand that relevant sections of my medical notes and data collected during the study may be looked at by individuals from regulatory authorities, Cardiff & Vale UHB or NHS Health Board overseeing the research. I give permission for these individuals to have access to my records.	☐
4. I agree to take part in the above study and I understand that a total of **75** ml (just over 4 tablespoonfuls) of blood will be taken for research purposes.	☐
5. I agree that my data will be stored securely for up to 5 years before being destroyed.	☐

Name of Patient (printed): …… Date:……

Signature: ……

Name of Person taking consent: …… Date: ……

Signature: ……

When completed, 1 for patient; 1 for researcher site file; 1 (original) to be kept in medical notes

Version 2.0 (cardiac) date 02/01/2019 IRAS Project ID: 243701

10.3 Appendix 10.3 – Patient information leaflet (HC, RF and CAD)

The information leaflet for control patients as part of the 'clinical cohort'.

GIG CYMRU NHS WALES
Bwrdd Iechyd Prifysgol Caerdydd a'r Fro
Cardiff and Vale University Health Board

Patient Information Leaflet

Title of Study: A pilot, exploratory study to investigate procoagulant phospholipids in arterial thrombosis

Thank you for expressing an interest in this study. Before deciding whether you wish to take part, it is important that you understand why the study is being done and what it involves. Please take time to read this information carefully and consider discussing it with family or friends. This study is being undertaken as part of an educational project.

What is the purpose of the study?

Clots form on the surfaces of cells in the blood such as platelets and white cells. Fatty molecules (phospholipids) in the membrane of these cells bind to clotting factors and help to control the formation of a clot. When cells become active, they release small packages of membranes (microparticles) which also contribute to clot formation. Different fatty molecules may help to control how thick or thin the blood is. If the blood is too thick, clots can form where they are not wanted leading to heart attacks. The aim of this study is to find out which phospholipids are present on the surface of cells and microparticles in people who have clotting disease and **compare them with individuals who don't**. This may help explain why some people are prone to clotting.

Why have I been chosen?

We are looking for volunteers to help try to identify whether certain phospholipids cause increased clotting. You have been invited to take part in the study because you have not had a heart attack, but you fall into 1 of the 3 categories that we are interested in studying as controls:

- Patients with significant coronary artery disease without a heart attack, Or
- Patients without significant coronary artery disease, but with risk factors for ischaemic heart disease, Or
- Healthy volunteer (no history of coronary artery disease and no risk factors for ischaemic heart disease)

Do I have to take part?

No, taking part is entirely your decision. If you decide to participate, we will discuss the study and go through the information leaflet with you. We will then request that you sign a consent form to show that you have agreed to take part. You can decide to withdraw from the study at any time, even if you have signed the consent form. This will not affect any of your current treatment or future care in any way.

Version 1.0 date (Controls) 02 January 2019 IRAS Project ID: 243701

What will the study involve?

A member of the research team will explain the study and answer any questions that you have. You will be asked to sign a consent form but you should only do this if you are happy to take part.

A blood sample will be taken by a trained member of the research team in a designated clinical area in the cardiology department, or if you are receiving in-patient treatment, the sample will be taken on the ward.

The total amount of blood that will be taken is 75ml (equivalent to just over 4 tablespoons).

As part of the study, we want to identify any risk factors in your medical background that contribute to clot formation. Clinical data related to your thrombotic condition will be recorded by the study team, however this will be kept confidential and no identifiable data will be shared outside of the study.

Will I be required to re-attend?

No, will not need to attend for further testing.

Can I withdraw from the study at a later date?

Yes, all participants have the right to withdraw from the study at any time by contacting the study team (details below). If you withdraw from the study, data collected up to the point of withdrawal will be kept. Any unanalysed tissue collected up to the point of withdrawal will be destroyed. No further data or tissue would be collected or any other research procedures carried out on or in relation to you.

What will happen to the blood samples that are taken?

The blood for the specialised tests on phospholipids and microparticles will be processed on the day the sample is taken. Most tests will be done that day although some will be performed and analysed later on samples which will be kept securely in the Infection and Immunity laboratory in the Sir Geraint Evans Cardiovascular Research Building at the School of Medicine Cardiff University. The samples that are stored will be labelled by a pseudo-anonymized study number. We will be able to link the study number to you so the laboratory results and clinical details can be linked. All samples will be processed on the day in accordance to the Human Tissue Act 2004 and will be deemed "non-relevant" as it would have been "treated, processed or lysed through a process intended to render them acellular.". These "non-relevant" material will be stored by the research team in the School of Medicine Cardiff University for up to 5 years for research governance purposes, and will be destroyed thereafter.

What information will be collected about me?

We will record your age and gender as well as clinical information related to your clotting disorder on a database identified by a study number. We will be able to link the study number to your name and hospital records through a separate database.

Cardiff and Vale UHB will collect information from you and your medical records for this research study in accordance with our instructions. The site will keep your name, NHS number, Date of Birth and contact details confidential and will not pass this information to Cardiff and Vale UHB. [NHS/other site] will use this information as needed, to contact you about the research study, and make sure that relevant information about the study is recorded for your care, and to oversee the quality of the study. Certain individuals from Cardiff and Vale UHB and regulatory organisations may look at your medical and research records to check the accuracy of the research study. Cardiff and Vale UHB will only receive information without any identifying information. The people who analyse the information will not be able to identify you and will not be able to find out your name, NHS number, Date of Birth or contact details.

Cardiff and Vale UHB will keep identifiable information about you from this study for 5 years after the study has finished.

What are the risks of taking part in the study?

We require a blood sample at study entry. The risks associated with blood taking include mild pain and bruising. The total volume of blood taken (approximately 4 tablespoons in total) is small when compared to the total amount of blood in the body. We would therefore not expect this to cause any harm. We will not be changing your treatment in any way.

Will the study benefit me directly?

It is unlikely that the study will provide information that helps you directly but it may help us to better understand why some people get clots. If the results of the study may be beneficial to your care we will discuss this with you.

How will my information be kept secure?

Cardiff and Vale UHB is the sponsor for this study based in the United Kingdom. We will be using information from you and your medical records in order to undertake this study and will act as the data controller for this study. This means that we are responsible for looking after your information and using it properly. Cardiff and Vale UHB will keep identifiable information about you for 5 years after the study has finished. The study team will store study data securely without any identifiable data in an encrypted and password protected database which complies with the General Data Protection Regulation (GDPR) and Data Protection Act 2018. These data will be held by the study team for up to 5 years.

Your rights to access, change or move your information are limited, as we need to manage your information in specific ways in order for the research to be reliable and accurate. If you withdraw from the study, we will keep the information about you that we have already obtained. To safeguard your rights, we will use the minimum personally-identifiable information possible. You can find out more about how we use your information by contacting cav.ig.dept@wales.nhs.uk.

What will happen to the results of the study?

The results may be submitted for publication in a journal that is accessible to the public. They will also contribute to a research project funded by the Wellcome Trust. Your data will be

anonymised and therefore you cannot be personally identified. Access to a summary of the study results may be obtained by directly contacting the study team by email on ProttyM3@cardiff.ac.uk. It is anticipated that the first such summary will be available from early 2020 onwards.

Will my GP or other health care professional be informed that I am taking part in the study?

This study will not affect your care in any way and so we will not notify your GP or other health care professional unless you ask us to.

What if there is a problem?

If you have any concerns about any aspect of this study, you should ask to speak to the researchers who will do their best to answer your questions (contact details at the end). If you remain unhappy and wish to complain formally, you can do this by using the NHS complaints procedure. Details can be found on the NHS website or ask a member of staff.

In the unlikely event that something does go wrong, and you are harmed during the research study there are no special compensation arrangements. If you are harmed and this is due to someone's negligence, then you may have grounds for a legal action for compensation against your local Trust/Health Board but you may have to pay your legal costs. The normal National Health Service complaints mechanisms will still be available to you.

Who funds and supervises the study?

The study is being funded by the Wellcome Trust. The study has been reviewed by the Yorkshire & The Humber - Leeds East independent ethics committee.

If I am interested in the study, how do I enrol?

If you are interested in taking part, please contact the research team by email: ProttyM3@cardiff.ac.uk.

Contact details for researchers:-

Prof Zaheer Yousef, Consultant Cardiologist, Department of Cardiology, University Hospital of Wales, Heath Park, Cardiff, CF14 4XN. Telephone: 029207 42972

Dr Majd Protty, Cardiology Registrar, Sir Geraint Evans Cardiovascular Research Building, Cardiff University School of Medicine, Heath Park, Cardiff, CF14 4XN. Telephone: 029206 87309.

Contact details for independent contact:-

Dr Steve Knapper, Department of Haematology, Cardiff University School of Medicine, Heath Park, Cardiff, CF14 4XN. Telephone: 02920 745379.

Local site details:

Principal Investigator and their contact details: Dr Majd Protty, Cardiology Registrar, Sir Geraint Evans Cardiovascular Research Building, Cardiff University School of Medicine, Heath Park, Cardiff, CF14 4XN. Telephone: 029206 87309.

Version 1.0 date (Controls) 02 January 2019 IRAS Project ID: 243701

10.4 Appendix 10.4 – Consent form (HC, RF and CAD)

The consent form for control patients as part of the 'clinical cohort'.

Consent Form v1.0

Title of Study: A pilot, exploratory study to investigate procoagulant phospholipids in arterial thrombosis.

Patient Identification Number for this study: _____

	INITIALS
Please initial the boxes	
1. I confirm that I have read and understand the information sheet dated 02 Jan 2019 for the above study. I have had the opportunity to consider the information, ask questions and have had these answered satisfactorily.	☐
2. I understand that my participation is voluntary and that I am free to withdraw at any time without giving any reason, without my medical care or legal rights being affected.	☐
3. I understand that relevant sections of my medical notes and data collected during the study may be looked at by individuals from regulatory authorities, Cardiff & Vale UHB or NHS Health Board overseeing the research. I give permission for these individuals to have access to my records.	☐
4. I agree to take part in the above study and I understand that a total of **75** ml (just over 4 tablespoonfuls) of blood will be taken for research purposes.	☐
5. I agree that my data will be stored securely for up to 5 years before being destroyed.	☐

Name of Patient (printed): …… Date:……

Signature: ……

Name of Person taking consent: …… Date: ……

Signature: ……

When completed, 1 for patient; 1 for researcher site file; 1 (original) to be kept in medical notes

Version 1.0 (controls) date 02/01/2019 IRAS Project ID: 243701

10.5 Appendix 10.5 – Patient information leaflet (Clots)

The information leaflet for patients arterial thrombosis as part of the 'clots cohort'.

GIG CYMRU NHS WALES
Bwrdd Iechyd Prifysgol Caerdydd a'r Fro
Cardiff and Vale University Health Board

Patient Information Leaflet

Title of Study: A pilot, exploratory study to investigate procoagulant phospholipids in arterial thrombosis

Thank you for expressing an interest in this study. Before deciding whether you wish to take part, it is important that you understand why the study is being done and what it involves. Please take time to read this information carefully and consider discussing it with family or friends. This study is being undertaken as part of an educational project.

What is the purpose of the study?

Clots form on the surfaces of cells in the blood such as platelets and white cells. Fatty molecules (phospholipids) in the membrane of these cells bind to clotting factors and help to control the formation of a clot. When cells become active, they release small packages of membranes (microparticles) which also contribute to clot formation. Different fatty molecules may help to control how thick or thin the blood is. If the blood is too thick, clots can form where they are not wanted leading to emergencies that threaten the blood supply to the limbs, brain or heart. The aim of this study is to find out which phospholipids are present in diseased tissue (clots or vessels) in people who have clotting disease. This may help explain why some people are prone to clotting.

Why have I been chosen?

We are looking for volunteers to help try to identify whether certain phospholipids cause increased clotting. You have been invited to take part in the study because you will be undergoing (or have undergone) a vascular procedure to remove this diseased tissue (clot or vessel).

Do I have to take part?

No, taking part is entirely your decision. If you decide to participate, we will discuss the study and go through the information leaflet with you. We will then request that you sign a consent form to show that you have agreed to take part. You can decide to withdraw from the study at any time, even if you have signed the consent form. This will not affect any of your current treatment or future care in any way.

Version 2.0 date (Vascular) 02 January 2019 IRAS Project ID: 243701

What will the study involve?

A member of the research team will explain the study and answer any questions that you have. You will be asked to sign a consent form but you should only do this if you are happy to take part.

As part of your vascular procedure, the diseased tissue (e.g clot) will be/has been removed to restore healthy blood flow to your organs/body. This diseased tissue is normally discarded. We propose to use it for medical research. There will be no change to your clinical management whether you participate or not.

As part of the study, we want to identify any risk factors in your medical background that contribute to clot formation. Clinical data related to your thrombotic condition will be recorded by the study team, however this will be kept confidential and no identifiable data will be shared outside of the study.

Will I be required to re-attend?

No, will not need to attend for further testing.

Can I withdraw from the study at a later date?

Yes, all participants have the right to withdraw from the study at any time by contacting the study team (details below). If you withdraw from the study, data collected up to the point of withdrawal will be kept. Any unanalysed tissue collected up to the point of withdrawal will be destroyed. No further data or tissue would be collected or any other research procedures carried out on or in relation to you.

What will happen to the samples that are taken?

The samples will be frozen using dry ice and transported to the laboratory at Cardiff University where they will undergo specialised tests on phospholipids. Most tests will be performed and analysed later on samples which will be stored securely in the Infection and Immunity laboratory in the Sir Geraint Evans Cardiovascular Research Building at the School of Medicine Cardiff University. The samples that are stored will be labelled by a pseudo-anonymized study number. We will be able to link the study number to you so the laboratory results and clinical details can be linked. All samples will be processed in accordance to the Human Tissue Act 2004 and will be deemed “non-relevant” as it would have been “treated, processed or lysed through a process intended to render them acellular.”. These “non-relevant” material will be stored by the research team in the School of Medicine Cardiff University for up to 5 years for research governance purposes, and will be destroyed thereafter.

What information will be collected about me?

We will record your age and gender as well as clinical information related to your clotting disorder on a database identified by a study number. We will be able to link the study number to your name and hospital records through a separate database.

Cardiff and Vale Health Board will collect information from you and your medical records for this research study in accordance with our instructions. The site will keep your name, NHS number, Date

of Birth and contact details confidential and will not pass this information to Cardiff and Vale UHB. Cardiff and Vale Health Board will use this information as needed, to contact you about the research study, and make sure that relevant information about the study is recorded for your care, and to oversee the quality of the study. Certain individuals from Cardiff and Vale UHB and regulatory organisations may look at your medical and research records to check the accuracy of the research study. Cardiff and Vale UHB will only receive information without any identifying information. The people who analyse the information will not be able to identify you and will not be able to find out your name, NHS number, Date of Birth or contact details.

Cardiff and Vale Health Board will keep identifiable information about you from this study for 5 years after the study has finished.

What are the risks of taking part in the study?

There will be no change to your clinical management and therefore no additional risks.

Will the study benefit me directly?

It is unlikely that the study will provide information that helps you directly but it may help us to better understand why some people get clots. If the results of the study may be beneficial to your care we will discuss this with you.

How will my information be kept secure?

Cardiff and Vale UHB is the sponsor for this study based in the United Kingdom. We will be using information from you and your medical records in order to undertake this study and will act as the data controller for this study. This means that we are responsible for looking after your information and using it properly. Cardiff and Vale UHB will keep identifiable information about you for 5 years after the study has finished. The study team will store study data securely without any identifiable data in an encrypted and password protected database which complies with the General Data Protection Regulation (GDPR) and Data Protection Act 2018. These data will be held by the study team for up to 5 years.

Your rights to access, change or move your information are limited, as we need to manage your information in specific ways in order for the research to be reliable and accurate. If you withdraw from the study, we will keep the information about you that we have already obtained. To safeguard your rights, we will use the minimum personally-identifiable information possible. You can find out more about how we use your information by contacting cav.ig.dept@wales.nhs.uk.

What will happen to the results of the study?

The results may be submitted for publication in a journal that is accessible to the public. They will also contribute to a research project funded by the Wellcome Trust. Your data will be anonymised and therefore you cannot be personally identified. Access to a summary of the study results may be obtained by directly contacting the study team by email on ProttyM3@cardiff.ac.uk. It is anticipated that the first such summary will be available from early 2020 onwards.

Will my GP or other health care professional be informed that I am taking part in the study?

This study will not affect your care in any way and so we will not notify your GP or other health care professional unless you ask us to.

What if there is a problem?

If you have any concerns about any aspect of this study, you should ask to speak to the researchers who will do their best to answer your questions (contact details at the end). If you remain unhappy and wish to complain formally, you can do this by using the NHS complaints procedure. Details can be found on the NHS website or ask a member of staff.

In the unlikely event that something does go wrong, and you are harmed during the research study there are no special compensation arrangements. If you are harmed and this is due to someone's negligence, then you may have grounds for a legal action for compensation against your local Trust/Health Board but you may have to pay your legal costs. The normal National Health Service complaints mechanisms will still be available to you.

Who funds and supervises the study?

The study is being funded by the Wellcome Trust. The study has been reviewed by the Yorkshire & The Humber - Leeds East independent ethics committee.

If I am interested in the study, how do I enrol?

If you are interested in taking part, please contact the research team by email: ProttyM3@cardiff.ac.uk.

Contact details for researchers:-

Prof Zaheer Yousef, Consultant Cardiologist, Department of Cardiology, University Hospital of Wales, Heath Park, Cardiff, CF14 4XN. Telephone: 029207 42972

Dr Majd Protty, Cardiology Registrar, Sir Geraint Evans Cardiovascular Research Building, Cardiff University School of Medicine, Heath Park, Cardiff, CF14 4XN. Telephone: 029206 87309.

Contact details for independent contact:-

Dr Steve Knapper, Department of Haematology, Cardiff University School of Medicine, Heath Park, Cardiff, CF14 4XN. Telephone: 02920 745379.

Local site details:

Principal Investigator and their contact details: Dr Majd Protty, Cardiology Registrar, Sir Geraint Evans Cardiovascular Research Building, Cardiff University School of Medicine, Heath Park, Cardiff, CF14 4XN. Telephone: 029206 87309.

Version 2.0 date (Vascular) 02 January 2019 IRAS Project ID: 243701

10.6 Appendix 10.6 – Consent form (Clots)

The consent form for patients with arterial thrombosis as part of the 'clots cohort'.

Consent Form v1.0

Title of Study: A pilot, exploratory study to investigate procoagulant phospholipids in arterial thrombosis

Patient Identification Number for this study:

Please initial the boxes	**INITIALS**
1. I confirm that I have read and understand the information sheet dated 02 Jan 2019 for the above study. I have had the opportunity to consider the information, ask questions and have had these answered satisfactorily.	☐
2. I understand that my participation is voluntary and that I am free to withdraw at any time without giving any reason, without my medical care or legal rights being affected.	☐
3. I understand that relevant sections of my medical notes and data collected during the study may be looked at by individuals from regulatory authorities, Cardiff & Vale UHB or NHS Health Board overseeing the research. I give permission for these individuals to have access to my records.	☐
4. I agree to take part in the above study and I understand that diseased tissue (clots and/or vessels) that are extracted as part of my vascular procedure/intervention will be taken for research purposes.	☐
5. I agree that my data will be stored securely for up to 5 years before being destroyed.	☐

Name of Patient (printed): …… Date:……

Signature: ……

Name of Person taking consent: …… Date: ……

Signature: ……

When completed, 1 for patient; 1 for researcher site file; 1 (original) to be kept in medical notes

Version 1.0 (vascular) date 06 December 2018 IRAS Project ID: 243701

10.7 APPENDIX 10.7 – REPRESENTATIVE CHROMATOGRAMS FOR LIPIDS MEASURED

Chromatograms for the lipids measured in this thesis.

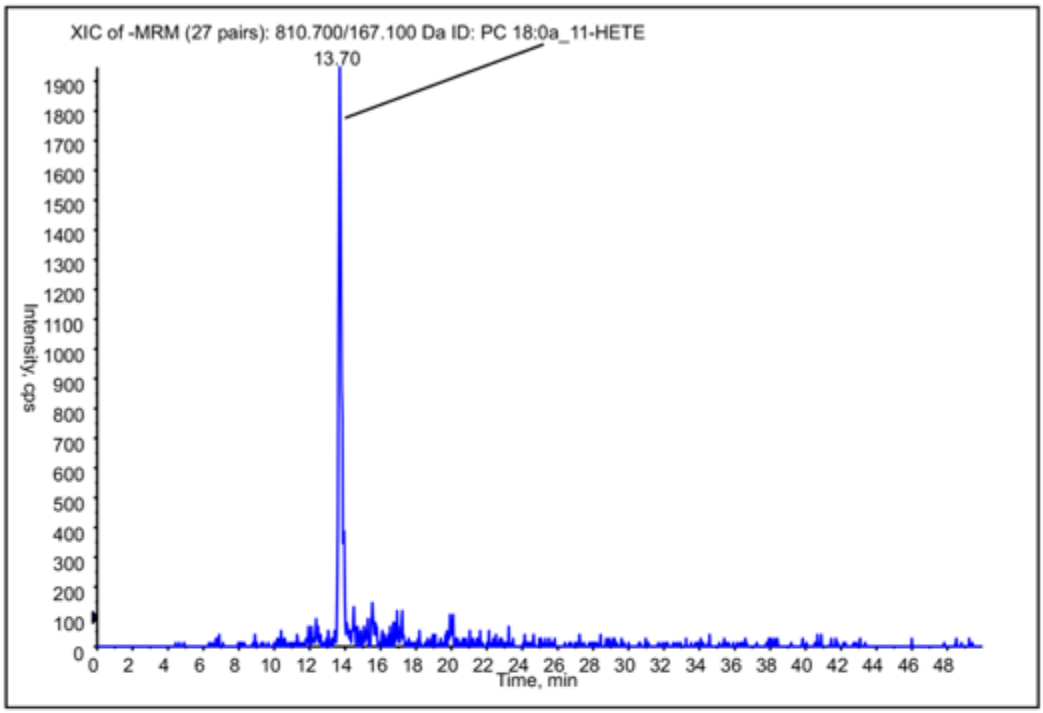

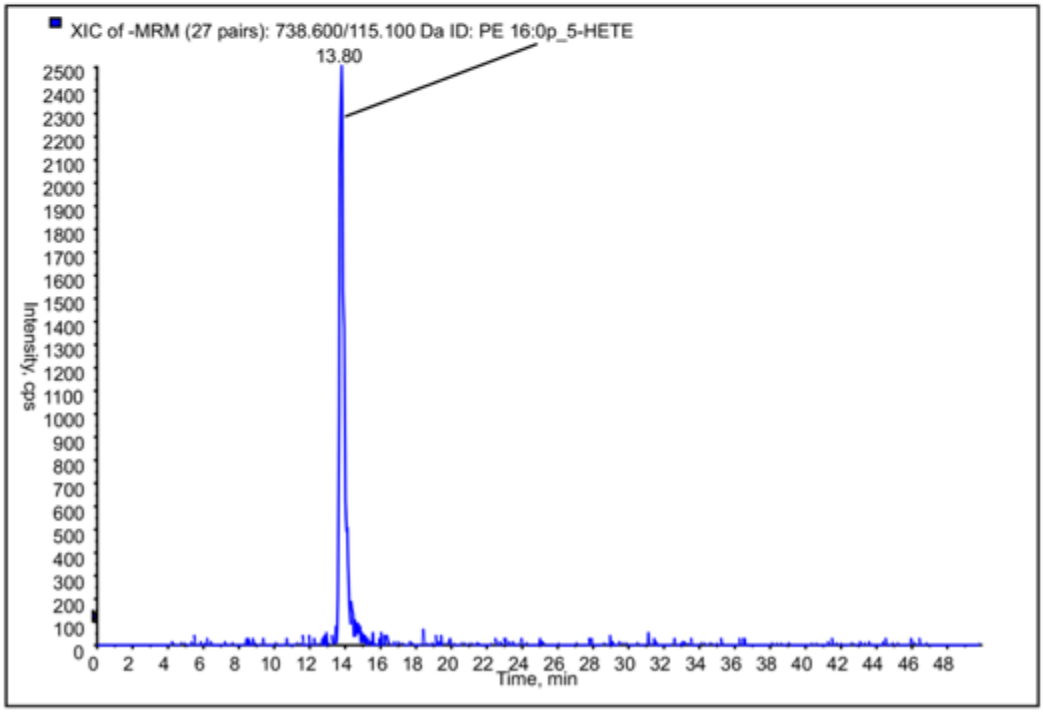

Appendix 10.7 continued…

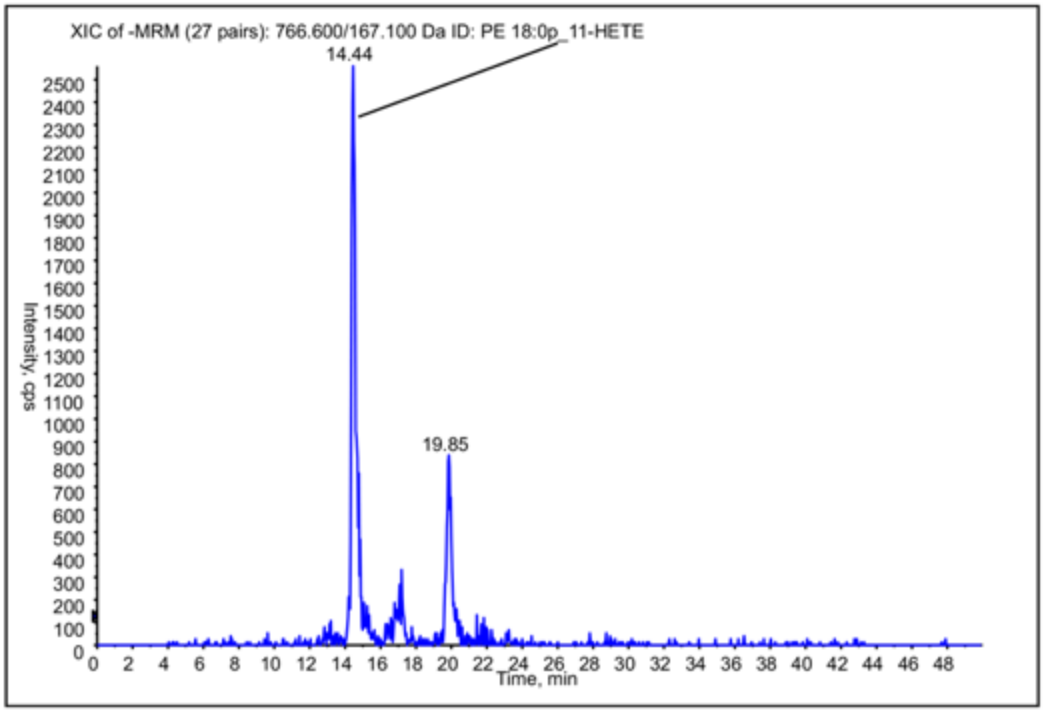

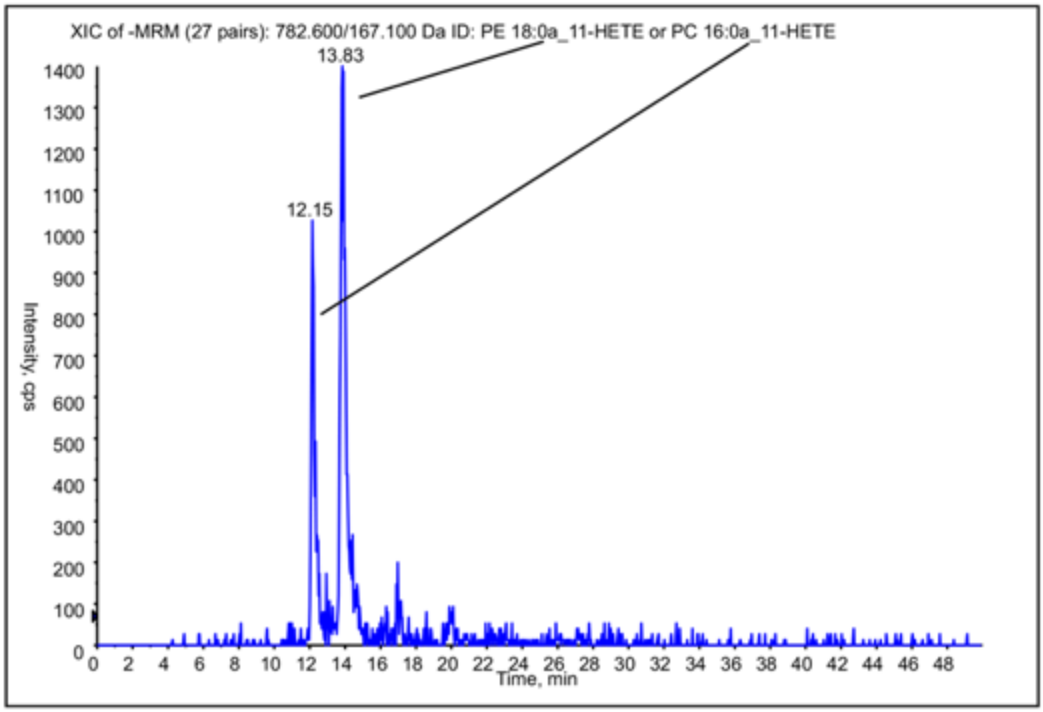

Appendix 10.7 continued…

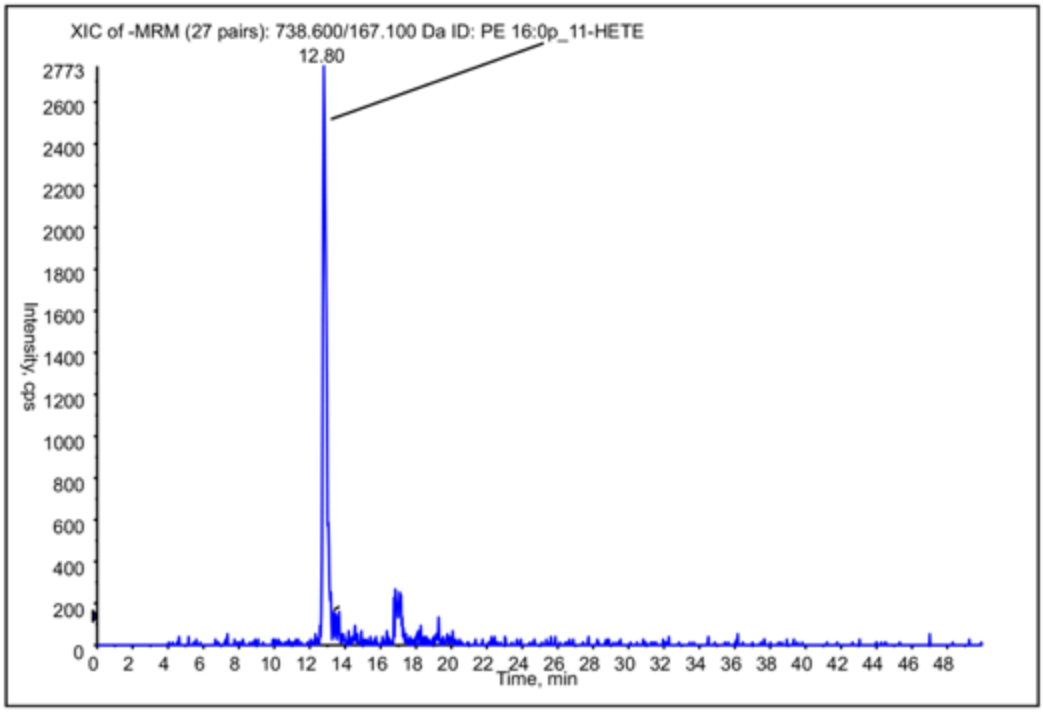

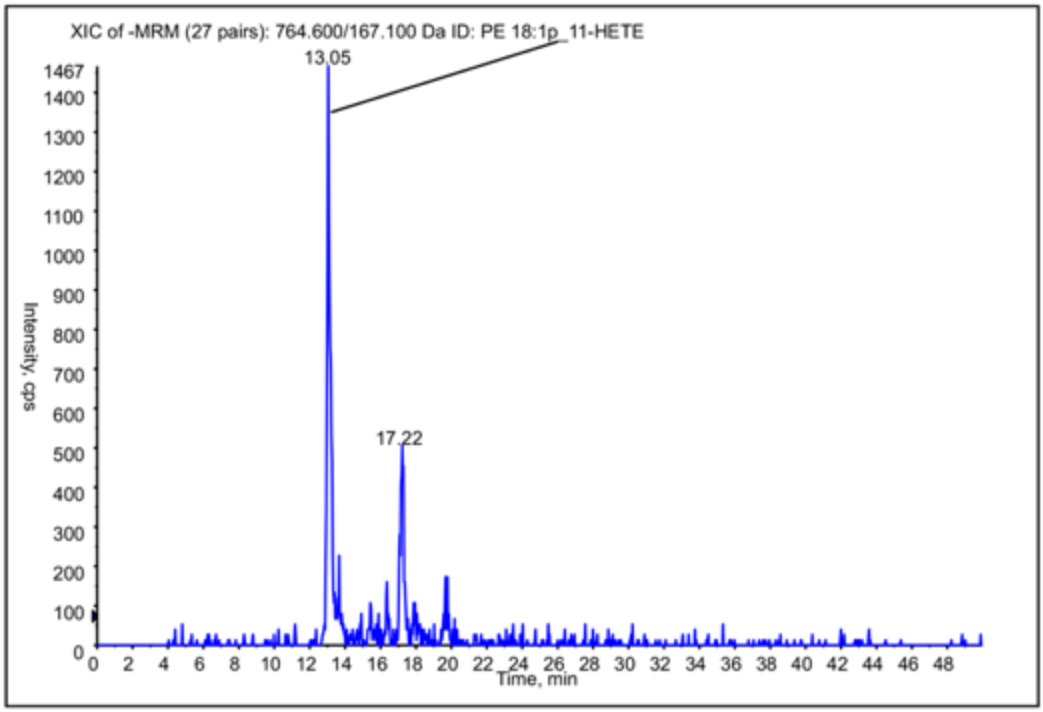

Appendix 10.7 continued…

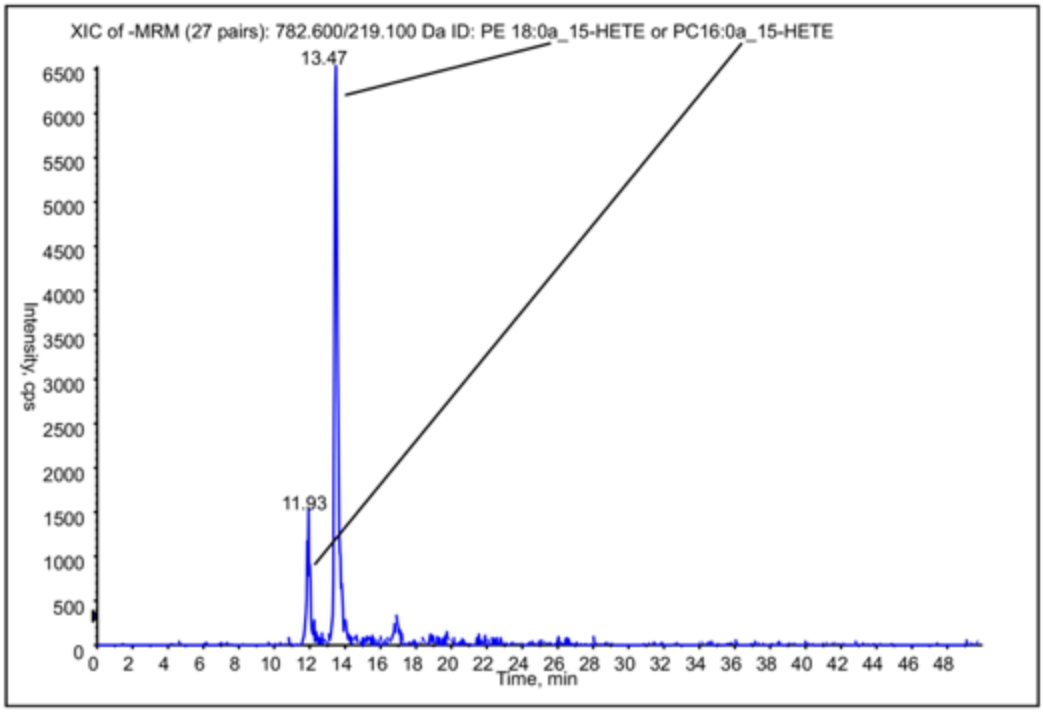

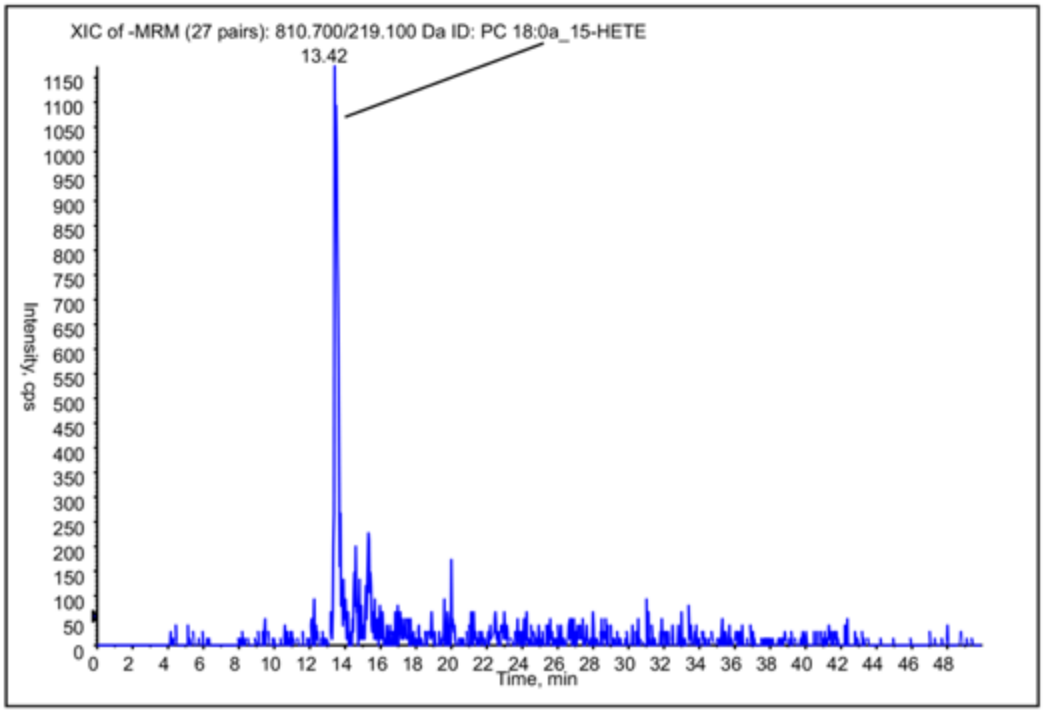

Appendix 10.7 continued…

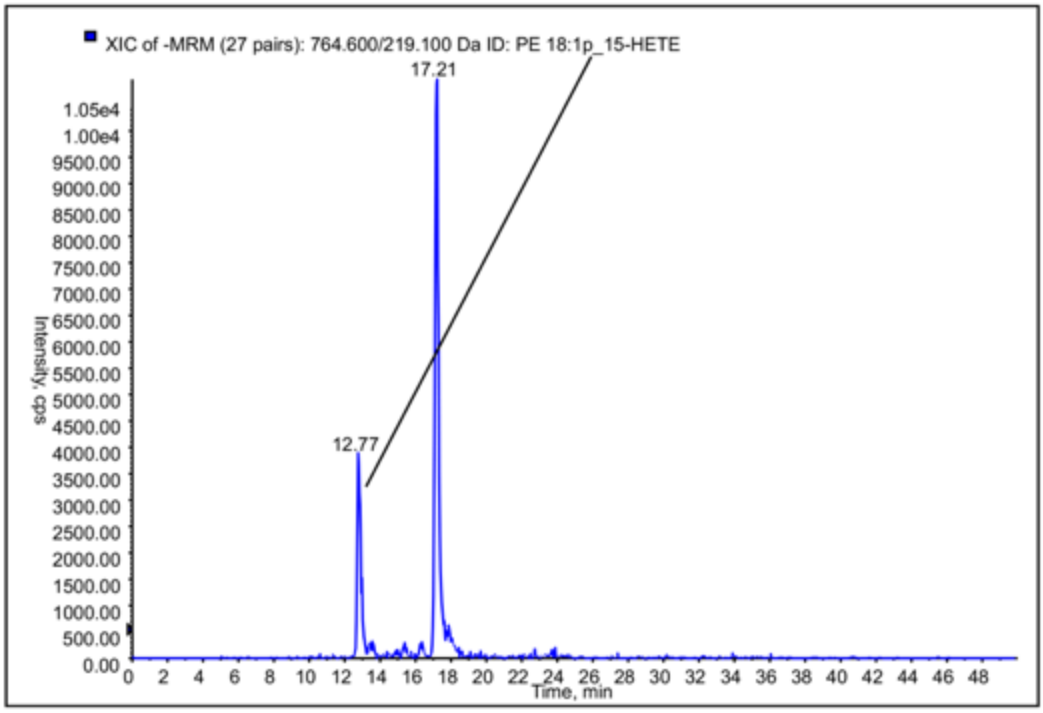

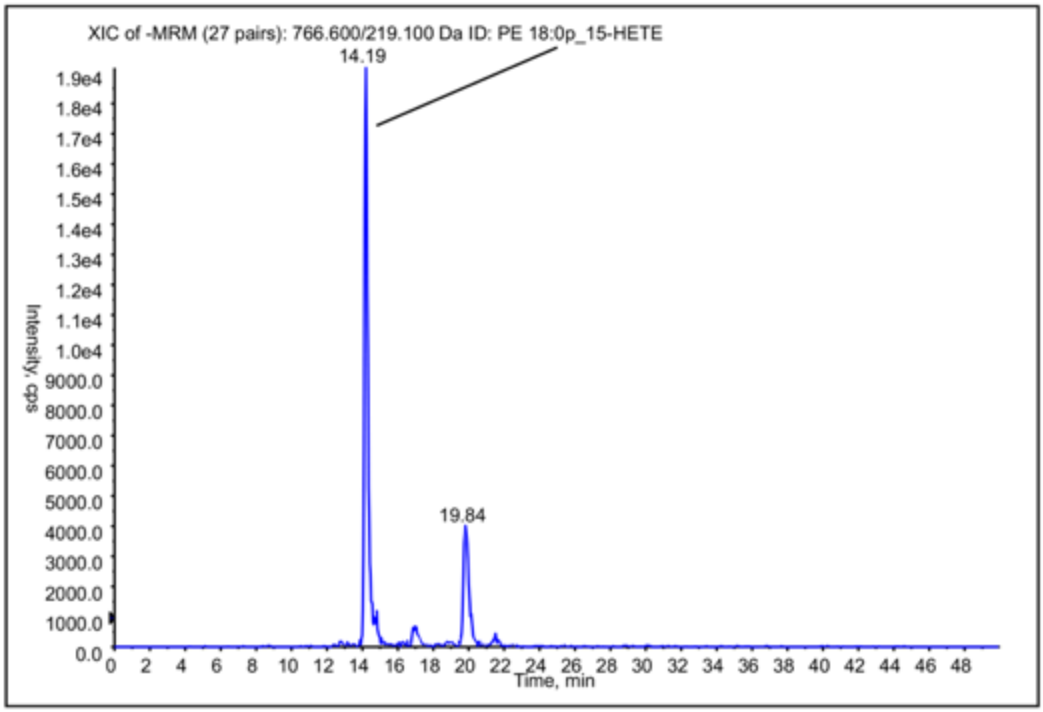

Appendix 10.7 continued…

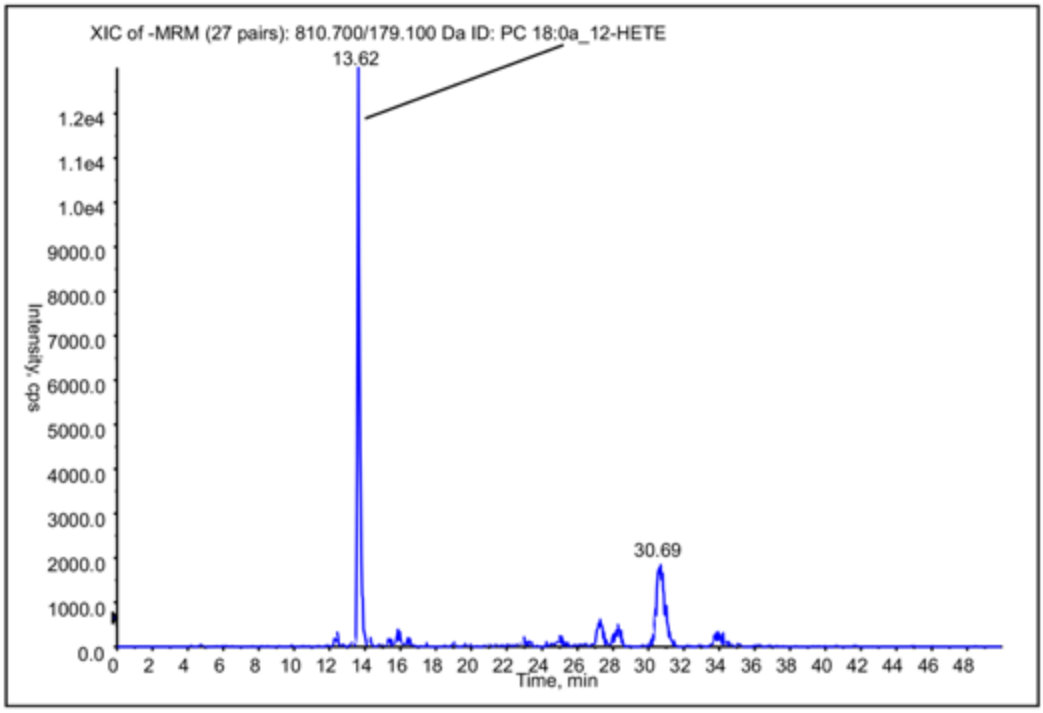

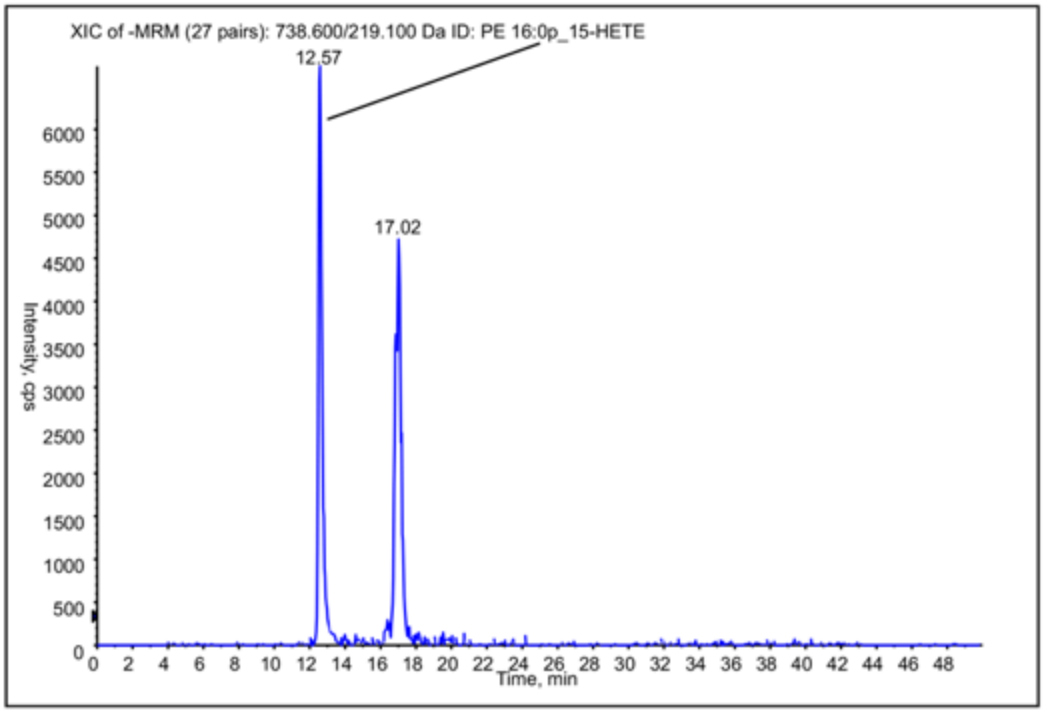

Appendix 10.7 continued…

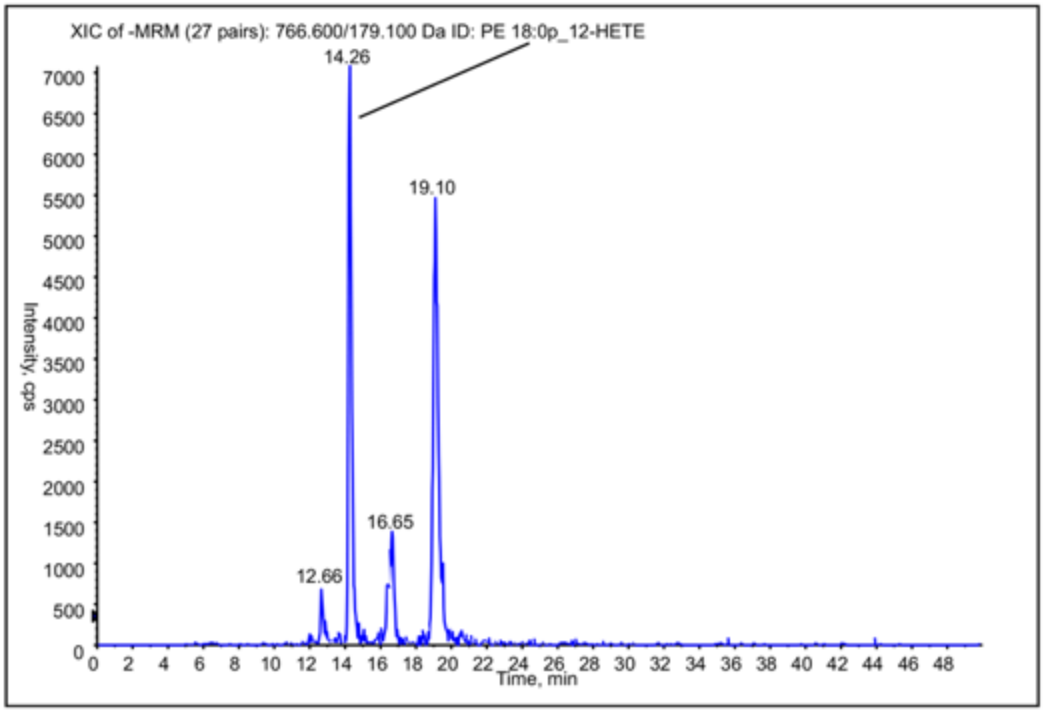

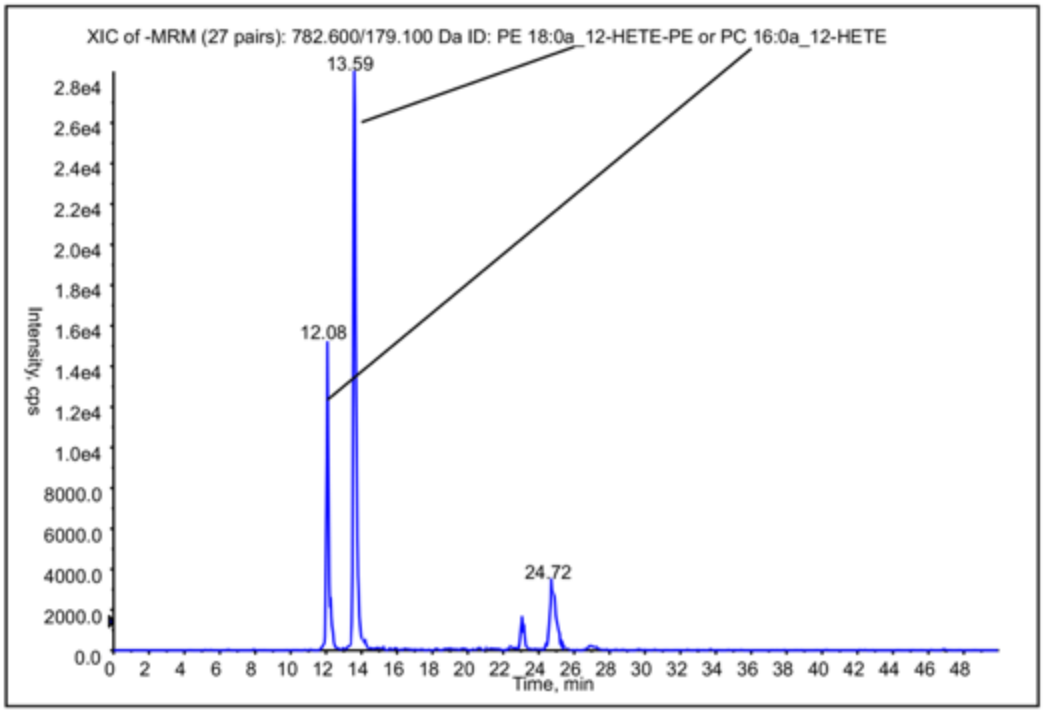

Appendix 10.7 continued…

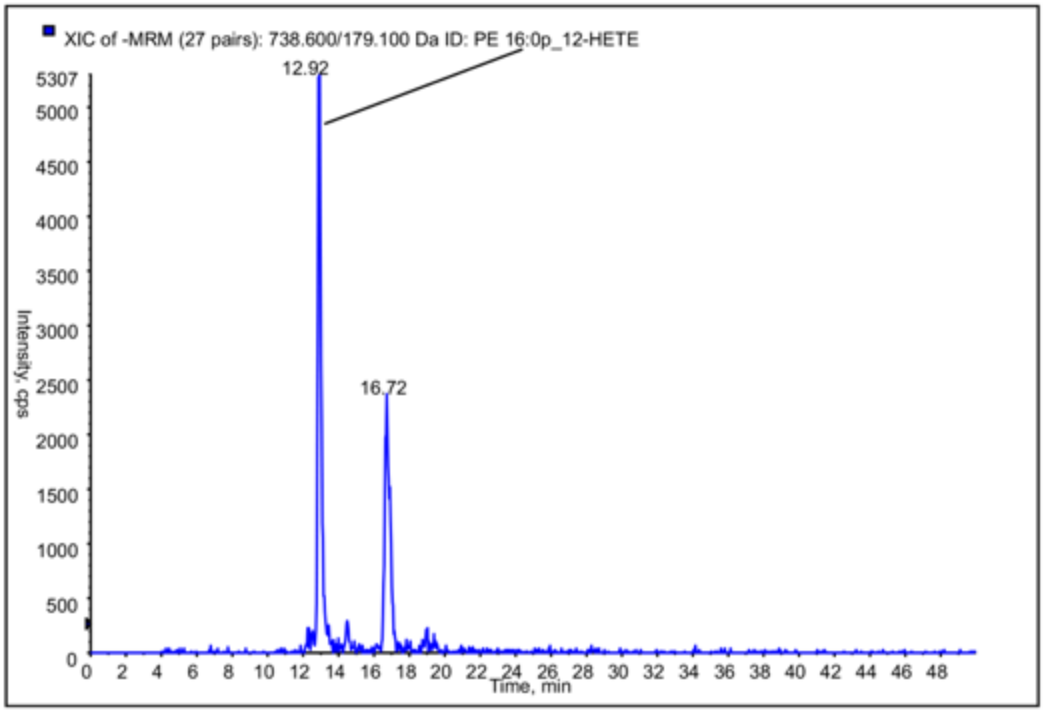

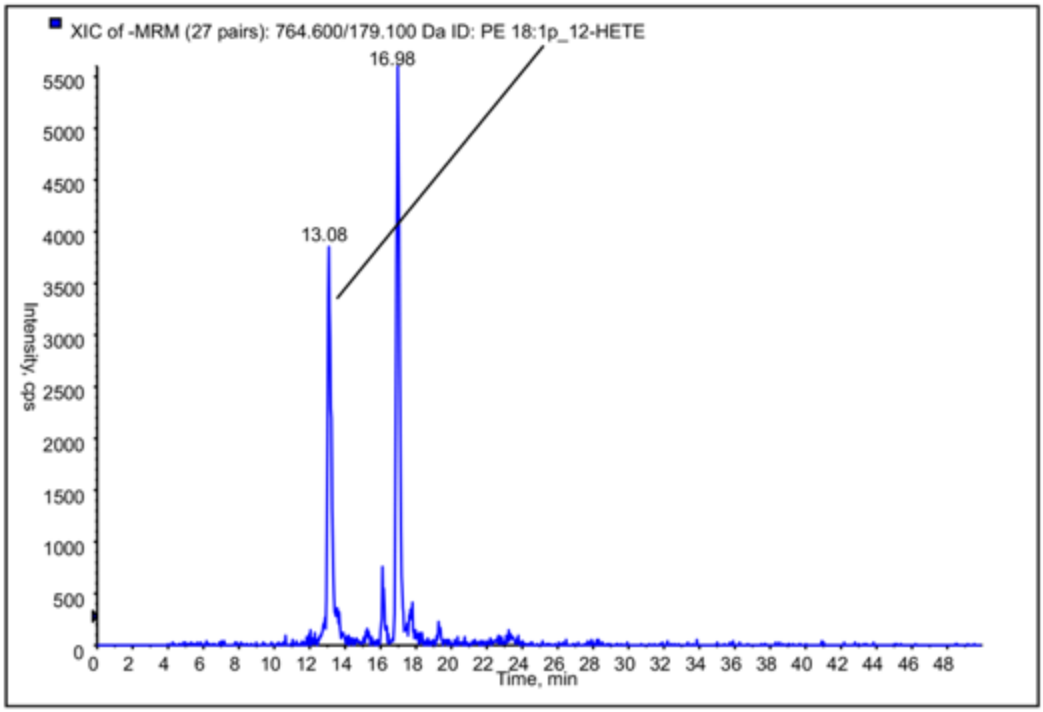

Appendix 10.7 continued…

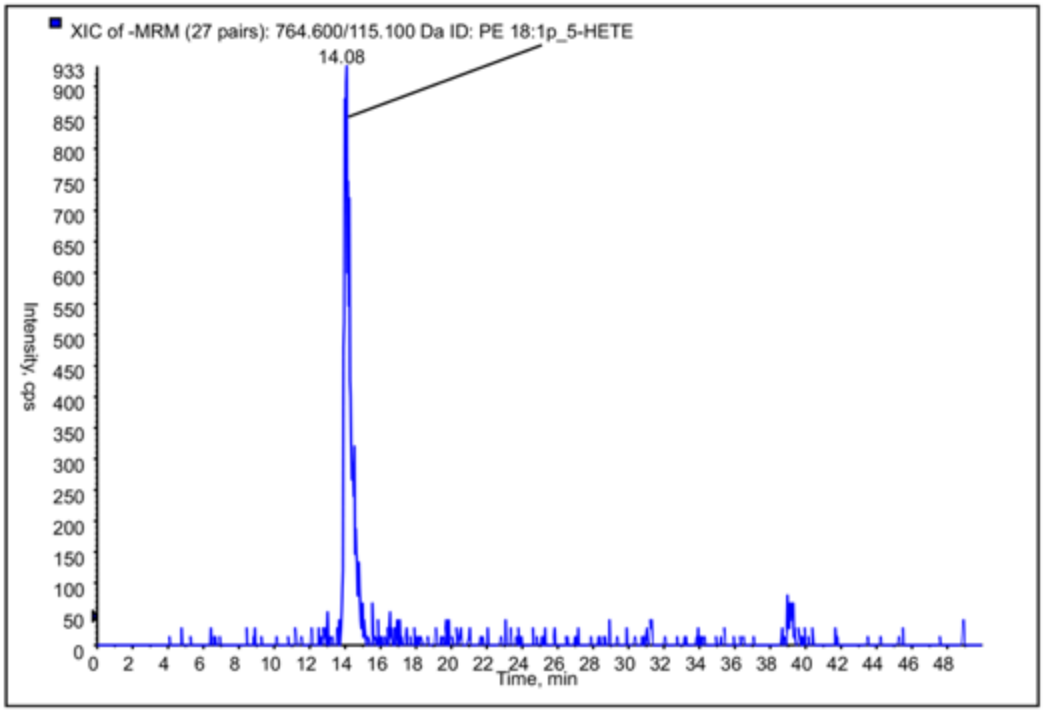

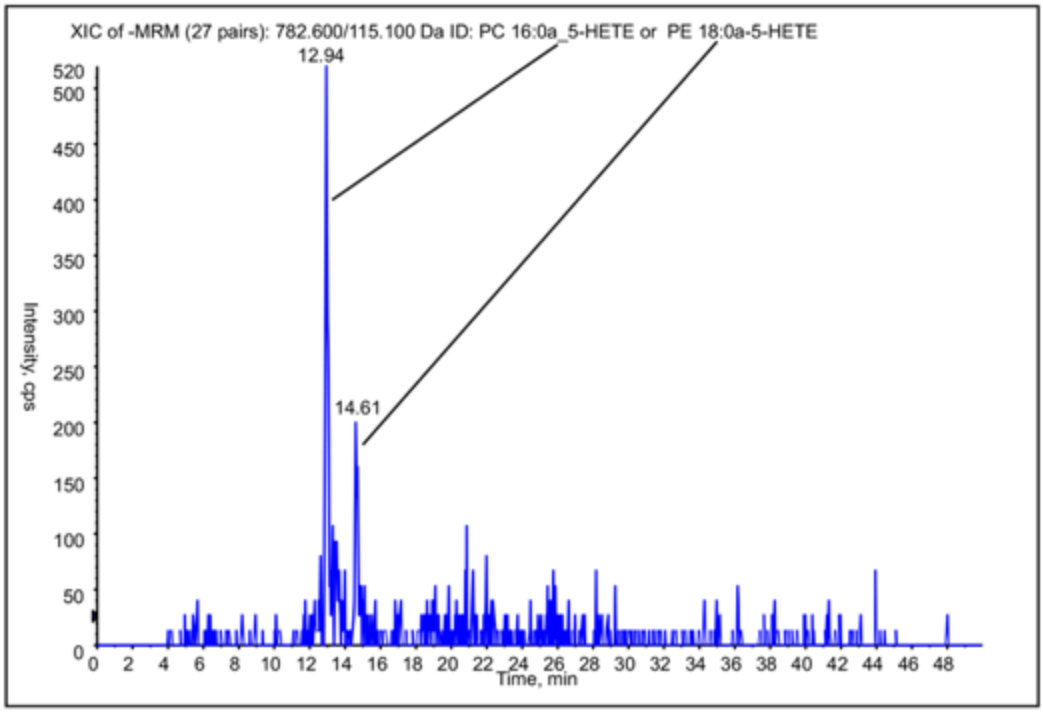

Appendix 10.7 continued…

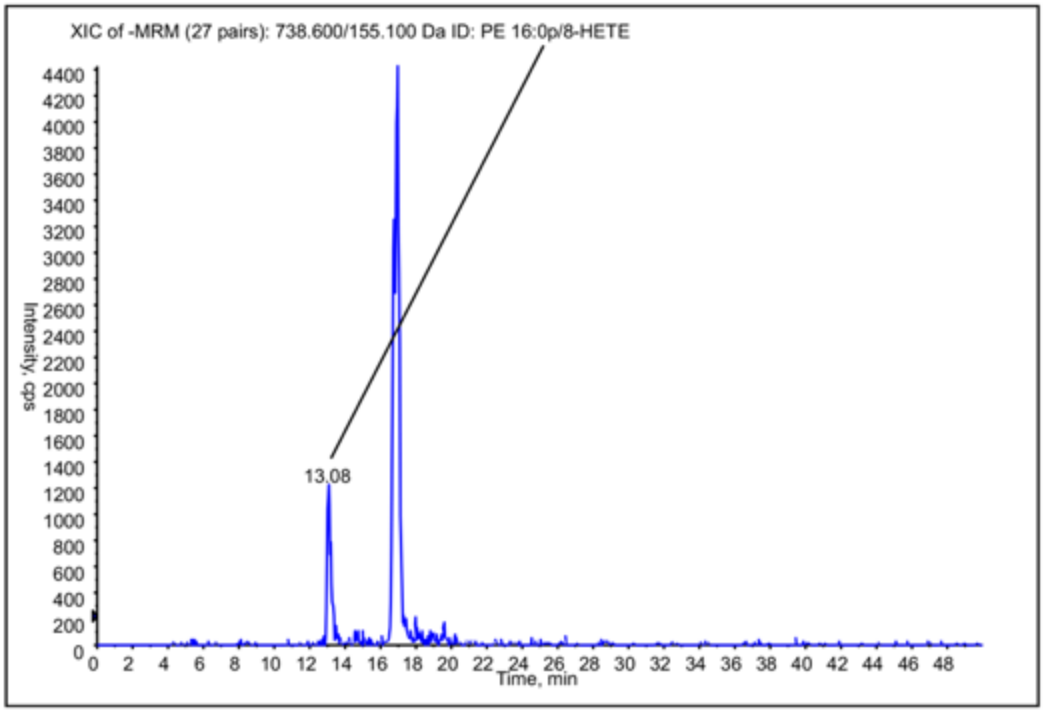

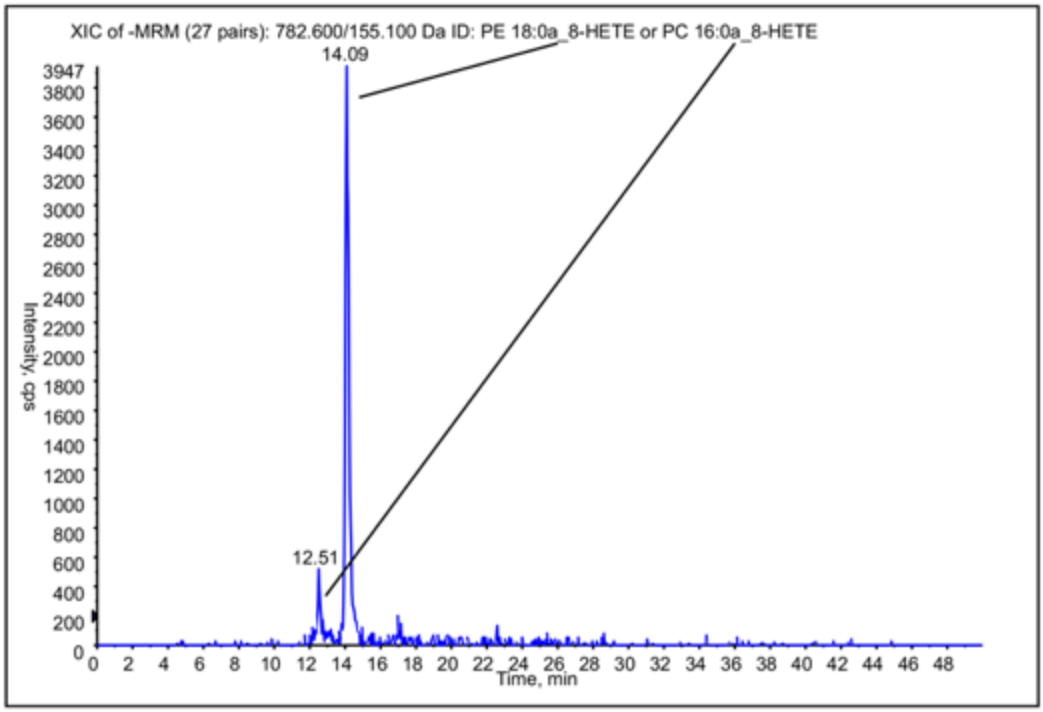

Appendix 10.7 continued…

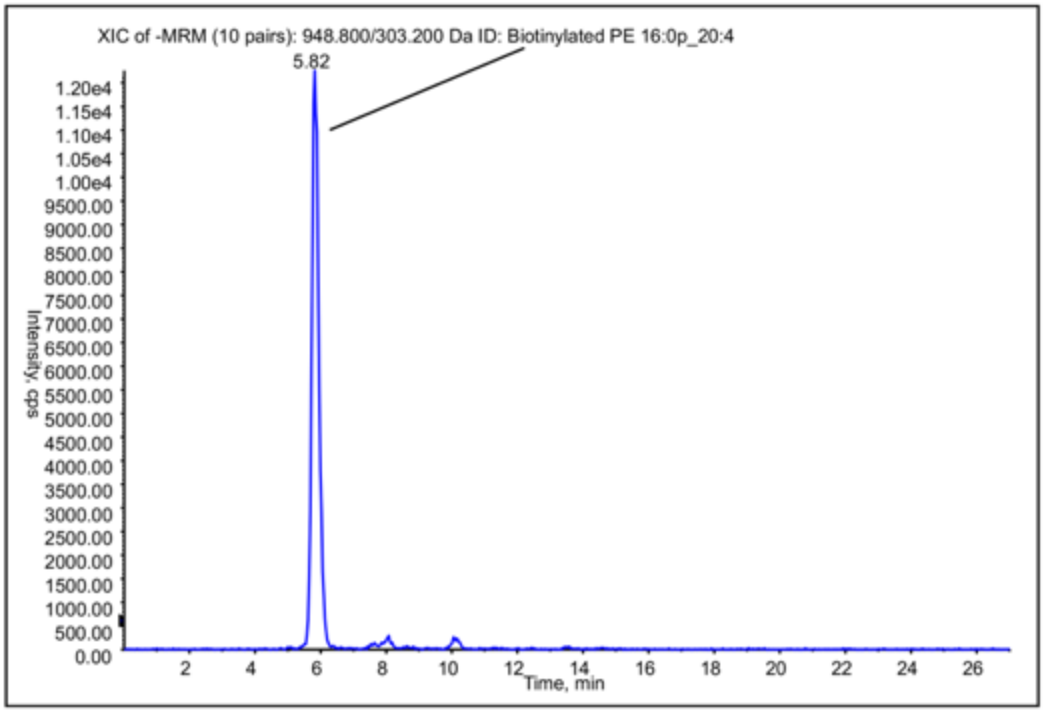

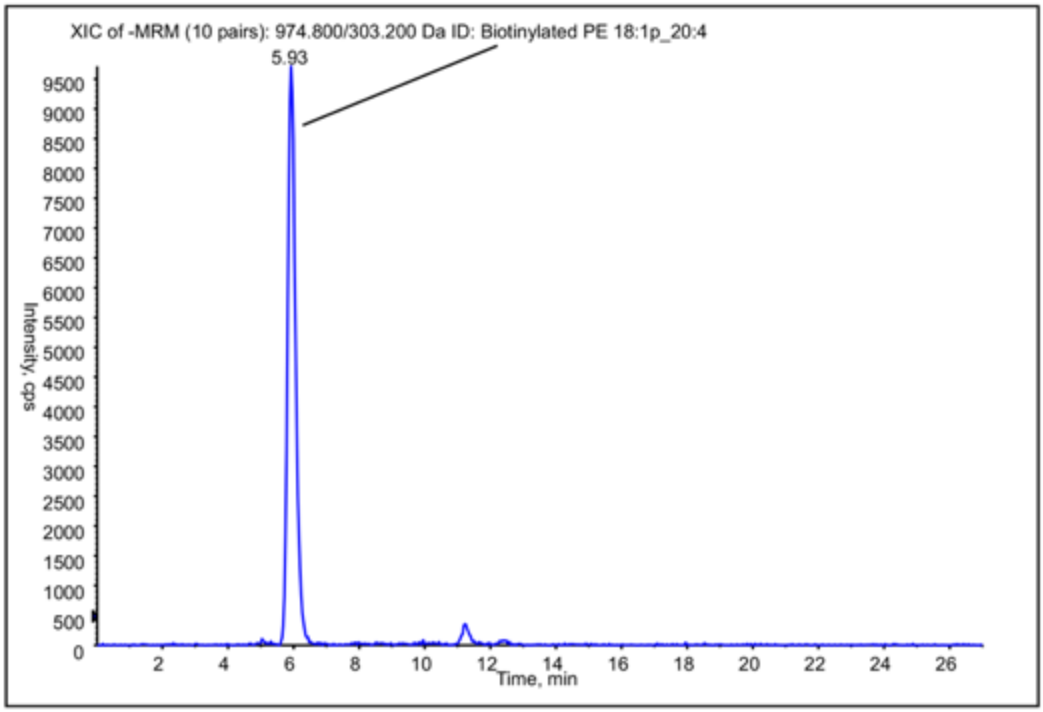

Appendix 10.7 continued…

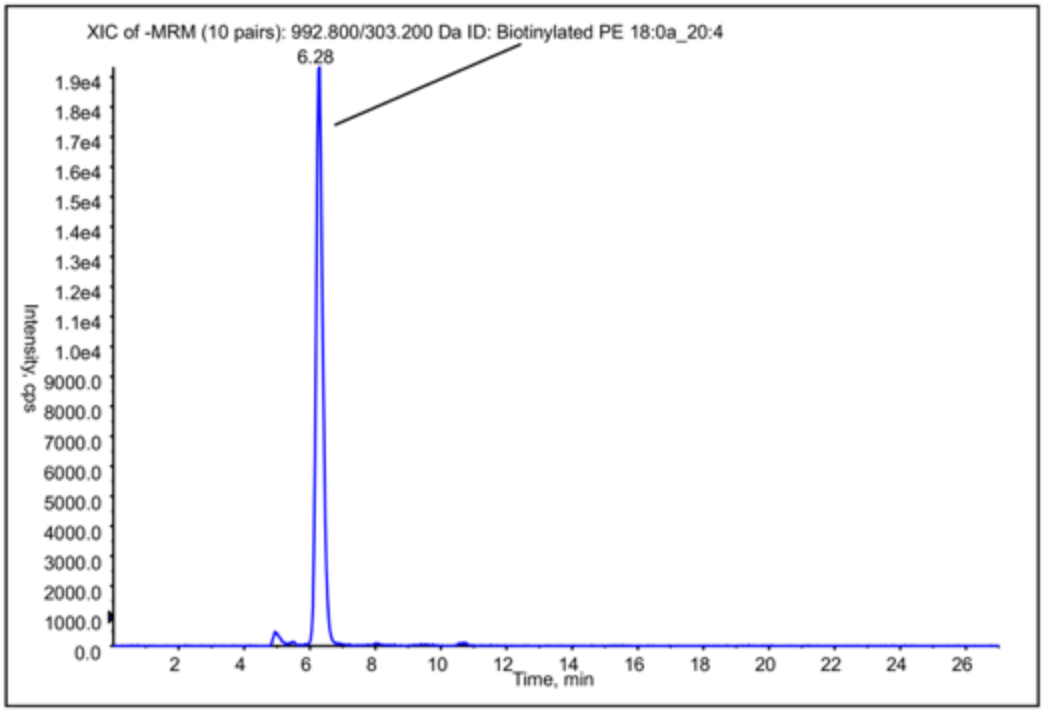

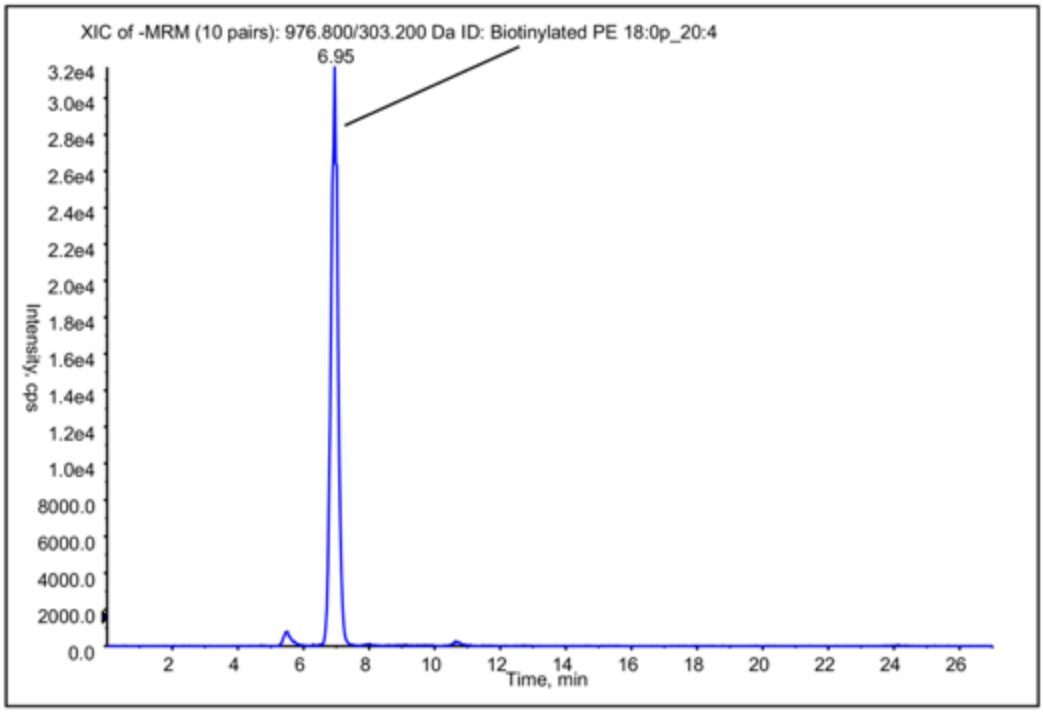

Appendix 10.7 continued…

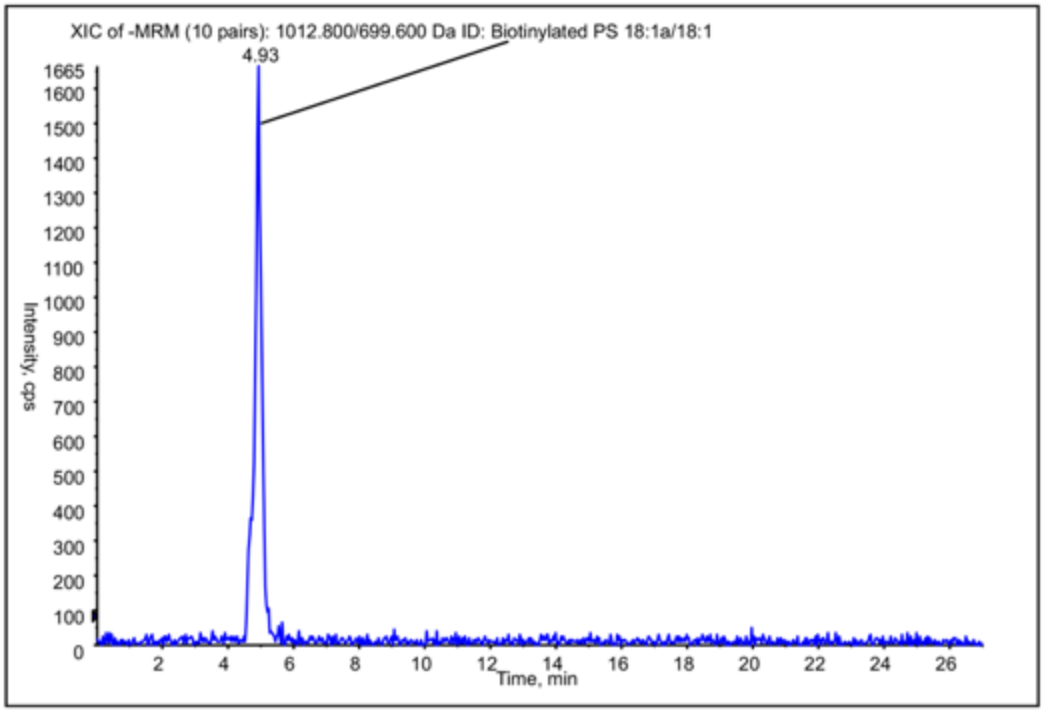

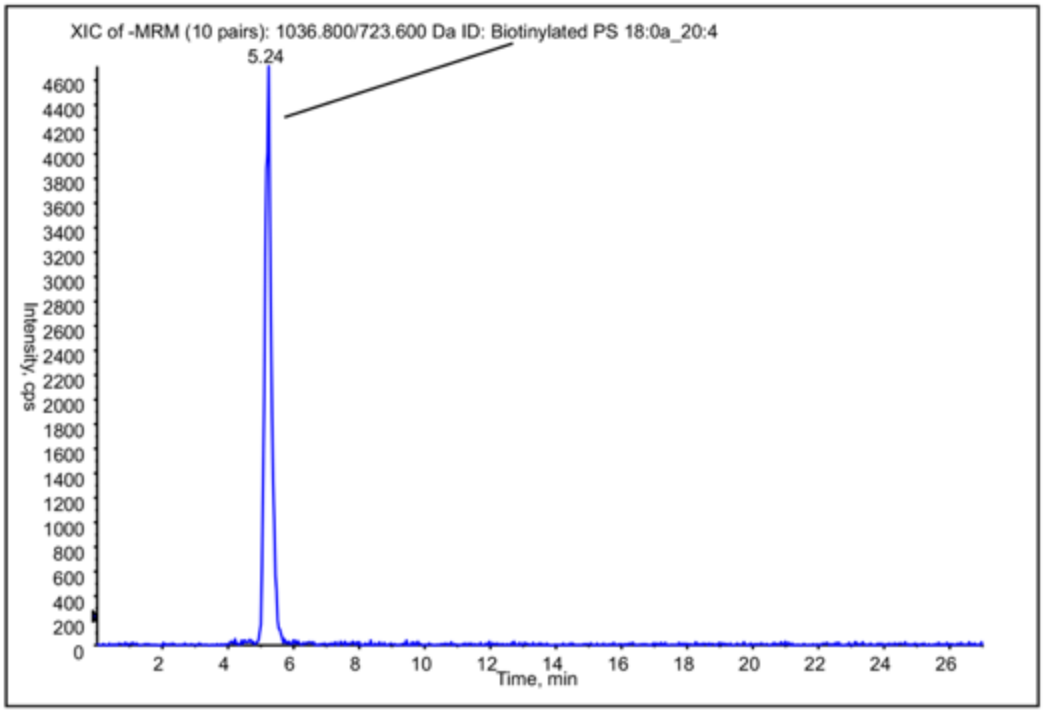

Appendix 10.7 continued…